



日中笹川医学奨学金制度  
第41期（学位取得コース）

報 告 書

2019年4月～2021年3月

公益財団法人 日中医学協会

# 目 次

No.	氏名	所属機関	研究先	指導責任者	頁数
G1	趙 申 チヨウ シン (課程博士)	上海交通大学医学院附属第九人民医院	北海道大学大学院歯学研究院	鄭 漢忠	……P1
		研修医	口腔顎顔面外科学教室	教授	
研究テーマ：PTH間欠投与による骨血管の組織学的変化					
G2	常 立甲 ジョウ リツカ (課程博士)	石家荘市第四医院	千葉大学	橋本 謙二	……P49
		主管技師	社会精神保健教育研究センター	教授	
研究テーマ：精神疾患の病因解明と新規治療法の開発					
G3	朱 俊 シュ シュン (論文博士)	江蘇省蘇北人民医院	順天堂大学大学院医学研究科	村上 晶	……P285
		主治医師	眼科学	教授	
研究テーマ：骨髄由来免疫制御細胞のマウス角膜移植に及ぼす影響					
G4	孟 雪 モウ セツ (論文博士)	中国医科大学附属盛京医院	順天堂大学大学院医学研究科	池田 勝久	……P298
		主治医師	耳鼻咽喉科学	主任教授	
研究テーマ：次世代シークエンサーを用いた頭頸部癌の特異的癌遺伝子の創出					
G5	蔣 元源 ショウ ゲンゲン (課程博士)	南京市口腔医院	昭和大学大学院歯学研究科	榎 宏太郎	辞退
		住院医师	歯科矯正学講座	教授	
研究テーマ：咀嚼と下顎骨軟骨組織の病理学的変化の関係について					
G6	劉 雨桐 リュウ ウトゥ (課程博士)	西安交通大学外国语学院	杏林大学大学院	宮首 弘子	……P345
		学生	国際協力研究科	教授	
研究テーマ：日本語ネイティブ医療通訳者と中国語ネイティブ医療通訳者の特性比較研究					
G7	許 婧 キョ セイ (課程博士)	貴州医科大学附属医院	金沢医科大学	古家 大祐	……P378
		主治医師	糖尿病・内分泌内科	教授	
研究テーマ：SGLT-2 阻害薬と糖尿病性腎臓病					
G8	盧 雪婧 ロ セツセイ (課程博士)	京都大学大学院医学研究科	京都大学大学院医学研究科	稲垣 暢也	……P400
		学生	糖尿病・内分泌・栄養内科学	教授	
研究テーマ：脂肪摂食後GIP分泌のメカニズム					
G9	張 含鳳 チヨウ ガンフウ (課程博士)	四川省腫瘤医院	広島大学大学院医系科学研究科	宮下 美香	……P418
		主管護師	保健学分野	教授	
研究テーマ：中国の生殖年齢にある男性がん患者の妊娠性温存をめざした支援サービス：患者と医療専門職者の視点からの定性研究					
G10	崔 力萌 サイ リキモ (課程博士)	北京市予防医学研究中心	長崎大学	高村 昇	……P448
		研究員	原爆後障害医療研究所	教授	
研究テーマ：福島県富岡町における環境放射能モニタリングと住民の被ばく線量評価					

# 日中笹川医学奨学金制度(学位取得コース)評価書

## 課程博士：指導教官用



第 41 期


研究者番号： G4101

作成日：2021年1月26日

氏名	趙 申	ZHAO SHEN	性別	M	生年月日	1989.07.07
所属機関(役職)	上海交通大学医学院附属第九人民医院歯内療法学科(研修医)					
研究先(指導教官)	北海道大学大学院歯学研究院口腔病態学分野口腔顎顔面外科学教室(鄭 漢忠教授)					
研究テーマ	PTH 間欠投与による骨血管の組織学的変化 Histological alternation of blood vessel in bone by intermittent PTH administration					
専攻種別	<input type="checkbox"/> 論文博士			<input checked="" type="checkbox"/> 課程博士		

### 研究者評価(指導教官記入欄)

成績状況	優	取得単位数
		取得単位数/取得すべき単位数総数
学生本人が行った研究の概要	6週齢のマウスを用いてPTHの間欠的投与が骨造成に大きな影響を及ぼす骨血管の新生にどのような影響を及ぼすかを組織学的、遺伝子学的に検討した。その結果、PTHの間欠的投与を行った群ではendomucin-positive/EphB4陽性の血管が造成し、血管径も著明に拡大していることが明らかになった。このことからPTHの間欠投与は骨芽細胞だけではなく、骨特異的な血管の増生に影響を及ぼすことが明らかになった。	
総合評価	【良かった点】 endomucin-positive/EphB4陽性の血管の増生を組織学的、遺伝子学的に明らかにしたこと。	
	【改善すべき点】 今回の研究ではPTHの投与期間を2週間としたが、4週、6週などの長期投与での結果が今後期待される場所である。	
	【今後の展望】 骨粗鬆症患者への新薬の開発などにこれまでと異なる視点を与えたことは大いに評価される。	

学位取得見込	2020年3月学位取得済みである。	
評価者（指導教官名） 鄭 漢忠		

# 日中笹川医学奨学金制度(学位取得コース)報告書 研究者用



第41期                      研究者番号: G4101                      作成日: 2021年3月      日

氏名	Zhao Shen	趙 申	性別	M	生年月日 1989. 07. 07
所属機関(役職)	上海交通大学医学院附属第九人民医院歯内療法学科(研修医)				
研究先(指導教官)	北海道大学大学院歯学研究院 口腔病態学分野 口腔顎顔面外科学教室(鄭 漢忠教授)				
研究テーマ	PTH間欠投与による骨血管の組織学的変化 Histological alternation of blood vessel in bone by intermittent PTH administration				
専攻種別	論文博士	<input type="checkbox"/>	課程博士	<input checked="" type="checkbox"/>	
1. 研究概要(1)					
1) 目的(Goal) & 戦略(Approach) Intermittent administration of parathyroid hormone (PTH) promotes preosteoblastic proliferation and differentiation into osteoblasts, which are coupled with osteoclasts, finally resulting in enhanced bone formation. Endomucin-high-positive bone-specific blood vessels have been reported to interact with osteoblastic cells to form new bones. However, it is still veiled whether PTH can affect the distribution of bone-specific blood vessels and other cell-types which surround the blood vessels.					
2) 材料と方法(Materials and methods) In this study, we have attempted to histologically examine bone-specific blood vessels after the intermittent PTH administration. Six weeks-old C57BL/6J mice received vehicle (control group) or 20 µg/kg/day of human PTH [1-34] (hPTH; PTH group) for 2 weeks. Mice were fixed with aldehyde solution, and the femora and tibiae were used for immunohistochemical analyses. Gene expression of the control and PTH-administered bone was examined by RT-PCR.					
4) 実験結果(Results) In the control group, numbers of endomucin-positive/EphB4-positive blood vessels were observed, while few numbers of αSMA-reactive blood vessels were seen. After PTH administration, the numbers of endomucin-positive/EphB4-positive blood vessels increased, and the vascular diameters were markedly-expanded when compared to the control group. Of note, numbers of blood vessels which accompany αSMA-positive cells were increased in the PTH group, and were divided into two histologically distinct types: the blood vessels surrounded by ALP-reactive/αSMA-positive cells that were closed to the bone surface, and the blood vessels associated only with αSMA-positive cells that showed a long cell shape with extending thin cytoplasmic processes.					
5) 考察(Discussion) In this study, we have attempted to histologically demonstrate the altered distribution of bone-specific blood vessels in murine bone after intermittent PTH administration. Our main histological findings can be summarized as follows: ① Intermittent PTH administration increased the number of endomucin-positive blood vessels and significantly expanded their diameter. ② The numbers of αSMA-positive, ephrinB2-positive, and EphB4-positive blood vessels also increased after PTH administration. ③ αSMA-positive cells were markedly-increased in number and can be distinctively divided into the first type, αSMA-positive vascular smooth muscle cells closely surrounding the endomucin-reactive vascular endothelial cells, the second type, αSMA/ALP double-positive cells close but not adjacent to blood vessels, and the third type, αSMA-positive but ALP-negative cells extending their straightly extending cytoplasmic processes. In summary, the intermittent administration of PTH may affect both osteoblastic cells and bone-specific blood vessels.					
6) 参考文献(References) 1. Schweser KM, Crist BD (2017) Osteoporosis: a discussion on the past 5 years. Curr Rev Musculoskelet Med 10: 265 - 274 2. Kim SC, Kim DH, Mogun H, Eddings W, Polinski JM, Franklin JM Solomon DH (2016) Impact of the U.S. food and drug administration's safety-related announcements on the use of bisphosphonates after hip fracture. J Bone Miner Res 31: 1536 - 1540 3. Orwoll E, Scheele W, Paul S, Adami S, Syversen U, Diez-Perez A, Kaufman JM, Clancy AD, Gaich GA (2003) The effect of teriparatide [human parathyroid hormone (1-34)] therapy on bone density in men with osteoporosis. J Bone Miner Res 18: 9 - 17 4. Skripitz R, Aspenberg P (2004) Parathyroid hormone—a drug for orthopedic surgery? Acta Orthop Scand 75: 654 - 662					

1. 研究概要 (2) 5. Luiz de Freitas PH, Li M, Ninomiya T, Nakamura M, Ubaidus S, Oda K, Udagawa N, Maeda T, Takagi R, Amizuka N (2009) Intermittent PTH administration stimulates pre-osteoblastic proliferation without leading to enhanced bone formation in osteoclast-less c-fos(-/-) mice. *J Bone Miner Res* 24: 1586 - 1597
6. Yamamoto T, Hasegawa T, Sasaki M, Hongo H, Tsuboi K, Shimizu T, Ohta M, Haraguchi M, Takahata T, Oda K, Freitas PHL, Takakura A, Takao-Kawabata R, Isogai Y, Amizuka N (2016) Frequency of teriparatide administration affects the histological pattern of bone formation in young adult male mice. *Endocrinology* 157: 2604 - 2620
7. Kusumbe AP, Ramasamy SK, Adams RH (2014) Coupling of angiogenesis and osteogenesis by a specific vessel subtype in bone. *Nature* 507: 323 - 328
8. Ramasamy SK, Kusumbe AP, Wang L, Adams RH (2014) Endothelial Notch activity promotes angiogenesis and osteogenesis in bone. *Nature* 507: 376 - 380
9. Sivaraj KK, Adams RH (2016) Blood vessel formation and function in bone. *Development* 143: 2706 - 2715
10. Armulik A, Genove G, Betsholtz C (2011) Pericytes: developmental, physiological, and pathological perspectives, problems, and promises. *Dev Cell* 21: 193 - 215
11. Aizman I, Holland WS, Yang C, Bates D (2016) alphaSMA Expression in Large Colonies of Colony-Forming Units-Fibroblast as an Early Predictor of Bone Marrow MSC Expandability. *Cell Med* 8: 79 - 85
12. Ramasamy SK (2017) Structure and functions of blood vessels and vascular niches in bone. *Stem Cells Int* 2017: 5046953
13. Matthews BG, Grcevic D, Wang L, Hagiwara Y, Roguljic H, Joshi P, Shin DG, Adams DJ, Kalajzic I (2014) Analysis of alphaSMA-labeled progenitor cell commitment identifies notch signaling as an important pathway in fracture healing. *J Bone Miner Res* 29: 1283 - 1294
14. Kusumbe AP, Ramasamy SK, Itkin T, Mae MA, Langen UH, Betsholtz C, Lapidot T, Adams RH (2016) Age-dependent modulation of vascular niches for haematopoietic stem cells. *Nature* 532: 380 - 384
15. Kunisaki Y, Bruns I, Scheiermann C, Ahmed J, Pinho S, Zhang D, Mizoguchi T, Wei Q, Lucas D, Ito K, Mar JC, Bergman A, Frenette PS (2013) Arteriolar niches maintain haematopoietic stem cell quiescence. *Nature* 502: 637 - 643
16. Mendez-Ferrer S, Michurina TV, Ferraro F, Mazloom AR, Macarthur BD, Lira SA, Scadden DT, Ma'ayan A, Enikolopov GN, Frenette PS (2010) Mesenchymal and haematopoietic stem cells form a unique bone marrow niche. *Nature* 466: 829 - 834
17. Rundle CH, Xing W, Lau KW, Mohan S (2016) Bidirectional ephrin signaling in bone. *Osteoporos Sarcopenia* 2: 65 - 76
18. Zhao C, Irie N, Takada Y, Shimoda K, Miyamoto T, Nishiwaki T, Suda T, Matsuo K (2006) Bidirectional ephrinB2-EphB4 signaling controls bone homeostasis. *Cell Metab* 4: 111 - 121
19. Ng YS, Ramsauer M, Loureiro RM, D'Amore PA (2004) Identification of genes involved in VEGF-mediated vascular morphogenesis using embryonic stem cell-derived cystic embryoid bodies. *Lab Invest* 84: 1209 - 1218
20. Allan EH, Hausler KD, Wei T, Gooi JH, Quinn JM, Crimmins-Irwin B, Pompolo S, Sims NA, Gillespie MT, Onyia JE, Martin TJ (2008) EphrinB2 regulation by PTH and PTHrP revealed by molecular profiling in differentiating osteoblasts. *J Bone Miner Res* 23: 1170 - 1181
21. Du JH, Lin SX, Wu XL, Yang SM, Cao LY, Zheng A, Wu JN, Jiang XQ (2019) The function of Wnt ligands on osteocyte and bone remodeling. *J Dent Res* 98: 930 - 938.
22. Baron R, Hesse E (2012) Update on bone anabolics in osteoporosis treatment: rationale, current status, and perspectives. *J Clin Endocrinol Metab* 97: 311 - 325
23. Portal-Nunez S, Lozano D, Esbrit P (2012) Role of angiogenesis on bone formation. *Histol Histopathol* 27: 559 - 566
24. Grüneboom A, Hawwari I, Weidner D, Culemann S, Müller S, Henneberg S, Henneberg S, Brenzel A, Merz S, Bornemann L, Zec K, Wuelling M, Kling L, Hasenberg M, Voortmann S, Lang S, Baum W, Ohs A, Kraff O, Quick HH, Jäger M, Landgraaber S, Dudda M, Danuser R, Stein JV, Rohde M, Gelse K, Garbe AI, Adamczyk A, Westendorf AM, Hoffmann D, Christiansen S, Engel DR, Vortkamp A, Krönke G, Herrmann M, Kamradt T, Schett G, Hasenberg A, Gunzer M (2019) A network of trans-cortical capillaries as mainstay for blood circulation in long bones. *Nature Metabolism* 1:236 - 250
25. Jiang L, Zhang W, Wei L, Zhou Q, Yang G, Qian N, Tang Y, Gao Y, Jiang X (2018) Early effects of parathyroid hormone on vascularized bone regeneration and implant osseointegration in aged rats. *Biomaterials* 179:15 - 28
26. Rey A, Manen D, Rizzoli R, Ferrari SL, Caverzasio J (2007) Evidences for a role of p38 MAP kinase in the stimulation of alkaline phosphatase and matrix mineralization induced by parathyroid hormone in osteoblastic cells. *Bone* 41: 59 - 67
27. Nakajima A, Shimoji N, Shiomi K, Shimizu S, Moriya H, Einhorn TA, Yamazaki M (2002) Mechanisms for the enhancement of fracture healing in rats treated with intermittent low-dose human parathyroid hormone (1-34). *J Bone Miner Res* 17: 2038 - 2047
28. Hirota S, Takaoka K, Hashimoto J, Nakase T, Takemura T, Morii E, Fukuyama A, Morihana K, Kitamura Y, Nomura S (1994) Expression of mRNA of murine bone-related proteins in ectopic bone induced by murine bone morphogenetic protein-4. *Cell and tissue research* 277: 27 - 32
29. Marini M, Rosa I, Ibbá-Manneschi L, Manetti M (2018) Telocytes in skeletal, cardiac and smooth muscle interstitium: morphological and functional aspects. *Histol Histopathol* 33:1151 - 1165

3. 学会発表 Conference presentation ※筆頭演者として総会・国際学会を含む主な学会で発表したものを記載

※Describe your presentation as the principal presenter in major academic meetings including general meetings or

学会名 Conference	日本解剖学会第65回東北・北海道連合支部学術集会		
演題 Topic	The biological effect of bone-specific blood vessels by intermittent PTH administration in mice.		
開催日 date	2019 年 9 月 8 日	開催地 venue	北海道江別市
形式 method	<input checked="" type="checkbox"/> 口頭発表 Oral	<input type="checkbox"/> ポスター発表 Post	言語 Language <input type="checkbox"/> 日本語 <input checked="" type="checkbox"/> 英語 <input type="checkbox"/> 中国語
共同演者名 Co-presenter	Zhao S., Hasegawa T., Tei K., Amizuka N		
学会名 Conference			
演題 Topic			
開催日 date	年 月 日	開催地 venue	
形式 method	<input type="checkbox"/> 口頭発表 Oral	<input type="checkbox"/> ポスター発表 Post	言語 Language <input type="checkbox"/> 日本語 <input type="checkbox"/> 英語 <input type="checkbox"/> 中国語
共同演者名 Co-presenter			
学会名 Conference			
演題 Topic			
開催日 date	年 月 日	開催地 venue	
形式 method	<input type="checkbox"/> 口頭発表 Oral	<input type="checkbox"/> ポスター発表 Post	言語 Language <input type="checkbox"/> 日本語 <input type="checkbox"/> 英語 <input type="checkbox"/> 中国語
共同演者名 Co-presenter			
学会名 Conference			
演題 Topic			
開催日 date	年 月 日	開催地 venue	
形式 method	<input type="checkbox"/> 口頭発表 Oral	<input type="checkbox"/> ポスター発表 Post	言語 Language <input type="checkbox"/> 日本語 <input type="checkbox"/> 英語 <input type="checkbox"/> 中国語
共同演者名 Co-presenter			

4. 受賞（研究業績 Award (Research achievement)

名称 Award name			
	国名 Country		受賞年 Year of 年 月
名称 Award name			
	国名 Country		受賞年 Year of 年 月

## 2. 執筆論文 Publication of thesis ※記載した論文を添付してください。Attach all of the papers listed below.

論文名 1 Title	Intermittent PTH Administration Increases Bone-Specific Blood Vessels and Surrounding Stromal Cells in Murine Long Bones				
掲載誌名 Published journal	Calcified Tissue International				
	2020 年 11 月	Epub ahead of print		言語 Language	English
第 1 著者名 First author	Shen Zhao	第 2 著者名 Second author	Tomoka Hasegawa	第 3 著者名 Third author	Hiromi Hongo
その他著者名 Other authors	Tomomaya Yamamoto, Miki Abe, Taiji Yoshida, Mai Haraguchi, Paulo Henrique Luiz de Freitas, Mingi Li, Kanchu Tei, Norio Amizuka				
論文名 2 Title					
掲載誌名 Published journal					
	年 月	巻(号)	頁 ~	頁	言語 Language
第 1 著者名 First author		第 2 著者名 Second author		第 3 著者名 Third author	
その他著者名 Other authors					
論文名 3 Title					
掲載誌名 Published journal					
	年 月	巻(号)	頁 ~	頁	言語 Language
第 1 著者名 First author		第 2 著者名 Second author		第 3 著者名 Third author	
その他著者名 Other authors					
論文名 4 Title					
掲載誌名 Published journal					
	年 月	巻(号)	頁 ~	頁	言語 Language
第 1 著者名 First author		第 2 著者名 Second author		第 3 著者名 Third author	
その他著者名 Other authors					
論文名 5 Title					
掲載誌名 Published journal					
	年 月	巻(号)	頁 ~	頁	言語 Language
第 1 著者名 First author		第 2 著者名 Second author		第 3 著者名 Third author	
その他著者名 Other authors					



5. 本研究テーマに関わる他の研究助成金受給 Other research grants concerned with your resarc

受給実績 Receipt record	<input type="checkbox"/> 有 <input type="checkbox"/> 無
助成機関名称 Funding agency	
助成金名称 Grant name	
受給期間 Supported	年 月 ~ 年 月
受給額 Amount received	円
受給実績 Receipt record	<input type="checkbox"/> 有 <input type="checkbox"/> 無
助成機関名称 Funding agency	
助成金名称 Grant name	
受給期間 Supported	年 月 ~ 年 月
受給額 Amount received	円

6. 他の奨学金受給 Another awarded scholarship

受給実績 Receipt record	<input type="checkbox"/> 有 <input type="checkbox"/> 無
助成機関名称 Funding agency	
奨学金名称 Scholarship	
受給期間 Supported	年 月 ~ 年 月
受給額 Amount received	円

7. 研究活動に関する報道発表 Press release concerned with your research activities

※記載した記事を添付してください。 Attach a copy of the article described below

報道発表 Press release	<input type="checkbox"/> 有 <input type="checkbox"/> 無	発表年月日 Date of release	
発表機関 Released medium			
発表形式 Release method	・新聞 ・雑誌 ・Web site ・記者発表 ・その他 ( )		
発表タイトル Released title			

8. 本研究テーマに関する特許出願予定 Patent application concerned with your research theme

出願予定 Scheduled	<input type="checkbox"/> 有 <input type="checkbox"/> 無	出願国 Application	
出願内容(概要) Application contents			

9. その他 Others

--

指導責任者(署名)

鄭 漢 忠





# Intermittent PTH Administration Increases Bone-Specific Blood Vessels and Surrounding Stromal Cells in Murine Long Bones

Shen Zhao<sup>1,2,3</sup> · Tomoka Hasegawa<sup>2</sup> · Hiromi Hongo<sup>2</sup> · Tomomaya Yamamoto<sup>4</sup> · Miki Abe<sup>2</sup> · Taiji Yoshida<sup>2</sup> · Mai Haraguchi<sup>2</sup> · Paulo Henrique Luiz de Freitas<sup>5</sup> · Minqi Li<sup>6</sup> · Kanchu Tei<sup>3</sup> · Norio Amizuka<sup>2</sup>

Received: 7 July 2020 / Accepted: 29 October 2020 / Published online: 10 November 2020  
© Springer Science+Business Media, LLC, part of Springer Nature 2020

## Abstract

To verify whether PTH acts on bone-specific blood vessels and on cells surrounding these blood vessels, 6-week-old male mice were subjected to vehicle (control group) or hPTH [1–34] (20 µg/kg/day, PTH group) injections for 2 weeks. Femoral metaphyses were used for histochemical and immunohistochemical studies. In control metaphyses, endomucin-positive blood vessels were abundant, but αSMA-reactive blood vessels were scarce. In the PTH-administered mice, the lumen of endomucin-positive blood vessels was markedly enlarged. Moreover, many αSMA-positive cells were evident near the blood vessels, and seemed to derive from those vessels. These αSMA-positive cells neighboring the blood vessels showed features of mesenchymal stromal cells, such as immunopositivity for c-kit and tissue nonspecific alkaline phosphatase (TNALP). Thus, PTH administration increased the population of perivascular/stromal cells positive for αSMA and c-kit, which were likely committed to the osteoblastic lineage. To understand the cellular events that led to increased numbers and size of bone-specific blood vessels, we performed immunohistochemical studies for PTH/PTHrP receptor and VEGF. After PTH administration, PTH/PTHrP receptor, VEGF and its receptor flk-1 were consistently identified in both osteoblasts and blood vessels (endothelial cells and surrounding perivascular cells). Our findings suggest that exogenous PTH increases the number and size of bone-specific blood vessels while fostering perivascular/stromal cells positive for αSMA/TNALP/c-kit.

**Keywords** Blood vessel · Bone · Parathyroid hormone (PTH) · Endomucin · Vascular smooth muscle cell

## Introduction

Teriparatide, a recombinant form of the human parathyroid hormone (PTH), and more recently, abaloparatide, a recombinant analog to PTH-related peptide (PTHrP),

are gradually becoming the preferred drugs for the treatment of osteoporosis [1–3]. The anabolic action of PTH and PTHrP has been demonstrated in clinical trials showing increased bone mass and reduced fracture rates in osteoporotic subjects receiving these drugs [3–5]. The earlier studies of our group showed that intermittent PTH administration promotes preosteoblastic proliferation and osteoblastic bone formation—with both processes being finely mediated by the cell coupling between osteoblasts

**Electronic supplementary material** The online version of this article (<https://doi.org/10.1007/s00223-020-00776-2>) contains supplementary material, which is available to authorized users.

✉ Tomoka Hasegawa  
hasegawa@den.hokudai.ac.jp

<sup>1</sup> National Clinical Research Center of Stomatology, Department of Endodontics, School of Medicine, Shanghai Key Laboratory of Stomatology & Shanghai Research Institute of Stomatology, Ninth People's Hospital, Shanghai Jiaotong University, Shanghai, China

<sup>2</sup> Developmental Biology of Hard Tissue, Graduate School of Dental Medicine, Faculty of Dental Medicine, Hokkaido University, Kita 13 Nishi 7 Kita-ku, Sapporo 060-8586, Japan

<sup>3</sup> Oral and Maxillofacial Surgery, Graduate School of Dental Medicine, Faculty of Dental Medicine, Hokkaido University, Sapporo, Japan

<sup>4</sup> Section of Dentistry, Camp Asaka, Japan Ground Self-Defense Forces, Tokyo, Japan

<sup>5</sup> Department of Dentistry, Federal University of Sergipe, Lagarto, Brazil

<sup>6</sup> Shandong Provincial Key Laboratory of Oral Biomedicine, The School of Stomatology, Shandong University, Jinan, China

and osteoclasts [6, 7]. Other studies have demonstrated the effect of PTH on blood vessels during bone healing. For instance, PTH-enhanced structural allograft healing has been linked to decreases in angiopoietin-2-mediated arteriogenesis [8]. Similarly, PTH1-34 treatment and/or increases in mesenchyme stem cells increased the number of vascular vessels, resulting in the stabilization of a femur fracture model in mice [9]. Therefore, PTH appears to not only affect bone cells but also blood vessels during bone healing. However, current studies have not determined whether PTH affects vascular endothelial cells in bone tissue without fracture healing or bone grafting, which may provide important insights into the osteo-vascular interactions associated with PTH treatment.

Recently, Kusumbe and Ramasamy's team characterized two subtypes of bone-specific endothelial cells, type H and type L [10]. While the type H cell is strongly positive for both CD31 and endomucin and is found near the metaphyseal growth plate, the type L cell has weak positivity for CD31 and endomucin and populates long bone's diaphyses [10, 11]. Interestingly, some degree of crosstalk between endomucin<sup>high</sup>-positive bone-specific blood vessels and osteoblastic cells seems to take place [10]: endomucin<sup>high</sup>-positive endothelial cells would secrete noggin, affecting both osteoblasts and chondrocytes, which in turn secrete vascular endothelial growth factor (VEGF) to sustain angiogenesis [10, 11]. Other studies have unveiled crosstalk involving endothelial cells, whereby vascular endothelial cells in arteries and arterioles expressed ephrinB2, whereas endothelial cells in veins expressed EphB4, a receptor for ephrinB2 [12]. Evidence on the interactions between EphB4 and ephrinB2 in the skeleton [13, 14] is growing, and since others have suggested that EphB4/ephrinB2 signaling acts as a coupling factor in bone cells [13, 14], it may be that EphB4-positive veins and ephrinB2-reactive arteries can stimulate osteoblastic cells in one way or another. Taken together, these findings hint to an important and yet relatively neglected role for blood vessels in bone metabolism.

This putative role for the blood vessels in bone metabolism is supported by two related insights, the first being the gradual disappearance of perivascular cells in areas of accelerated bone modeling and remodeling. Considering a normal, homeostatic state, periosteal nutrient arteries and arterioles surrounded by vascular smooth muscle cells make their way toward a long bone's diaphyseal marrow [15]. These peripheral vascular smooth muscle cells gradually disappear to form sinusoidal capillaries that extend to the metaphyseal chondro-osseous junction; there, the peripheral vascular smooth muscle cell sheath is lost and discontinuous basement membranes are present [16]. Thus—and perivascular cells and vascular smooth muscle cells are normally not seen near vascular endothelial cells in

the metaphyses—especially close to the growth plate, a site of endochondral ossification.

The second insight is the likely potential for transdifferentiation of vascular smooth muscle cells. Blood vessels are made of different cell types, roughly divided into inner, vascular endothelial cells and outer, perivascular cells [17]. A vascular smooth muscle cell is a type of perivascular cell that always covers arteries, veins, arterioles and venules and regulates vessel caliber [16].  $\alpha$ -Smooth muscle actin ( $\alpha$ SMA) is a marker of vascular smooth muscle cells and myofibroblasts [18], but is also a hallmark of undifferentiated mesenchymal cells in calcified tissues [19]. It is plausible, therefore, that vascular smooth muscle cells may still have some potential for transdifferentiation [16, 18, 20]. Bone arteries are in fact reportedly covered with  $\alpha$ SMA-positive cells that have the potential to differentiate into one of many mesenchymal lineages including osteoblasts [21–24].

Thus, the biological effects of PTH on bone-specific blood vessels and their constituent cells are yet to be fully explored. In this study, we have tried to determine whether intermittent PTH administration (1) affects the distribution and size of endomucin-positive, bone-specific blood vessels specific to bone, and (2) influences the population of stromal cells between osteoblasts and bone-specific blood vessels in mice.

## Materials and Methods

### Animals

Six-week-old male C57BL/6 J mice ( $n = 12$ , Japan CLEA, Tokyo, Japan) were handled according to Hokkaido University's guidelines for animal care and research use (approved study protocol #15-0032). Mice were allocated to a control group receiving vehicle only (0.9% saline,  $n = 12$ ) or to a PTH group receiving hPTH [1–34] (Sigma-Aldrich Co., LLC., St. Louis, MO,  $n = 12$ ). As previously described [6, 7], mice received 20  $\mu$ g/kg/day of hPTH [1–34] every 12 h for 2 weeks.

### Specimen Preparation

Before fixation, mice were anesthetized with an intraperitoneal injection of pentobarbital for body weight determination. Afterward, all mice were perfused with 4% paraformaldehyde diluted in 0.1 M cacodylate buffer (pH 7.4) through the cardiac left ventricle 6 h after receiving the last vehicle or hPTH [1–34] injection, as previously reported [7]. After perfusion with 4% paraformaldehyde, the femora and tibiae were extracted and immediately immersed in the same solution for 24 h at 4 °C. Then, specimens were washed in

phosphate-buffered saline (PBS) for 3 days before decalcification with 10% or 4.13% EDTA-2Na for paraffin and epoxy-resin embedding, respectively. For paraffin embedding, samples were dehydrated in ascending ethanol solutions, soaked in xylene, and finally embedded in paraffin. For epoxy-resin embedding, samples were post-fixed with 1% osmium tetroxide in 0.1 M cacodylate buffer for 8 h at 4 °C, dehydrated in ascending acetone solutions, and finally embedded in epoxy-resin (Epon 812).

### Single Immunohistochemical Studies

Paraffin-embedded histological sections were used for an immunohistochemical panel of the following antigens: endomucin,  $\alpha$ SMA, c-kit, PTH/PTH-related peptide (PTHrP) receptor, vascular endothelial growth factor (VEGF) and Flk-1. Especially, the immunohistochemistry of PTH/PTHrP receptor, VEGF, and Flk-1 were performed on serial sections. After deparaffinization, standardized procedures for immunostaining were followed [25]. In brief, sections were treated for endogenous peroxidase inhibition with 0.3% H<sub>2</sub>O<sub>2</sub> in PBS for 30 min, and subsequently for nonspecific stain blocking with 1% bovine serum albumin (BSA; Serologicals Proteins Inc. Kankakee, IL) in PBS (1% BSA-PBS) for 20 min at room temperature. After that, sections were incubated with the corresponding pair of antibodies according to the antigen of interest (primary/secondary), as follows: (1) endomucin, rat antibody against endomucin (Santa Cruz Biotechnology, Inc., Dallas, TX, diluted 1:100)/horseradish peroxidase (HRP)-conjugated anti-rat IgG (Zymed Laboratories Inc., South San Francisco, CA, diluted 1:100); (2)  $\alpha$ SMA, mouse antibody against  $\alpha$ SMA (Thermo Fisher Scientific Inc., Cheshire, UK, diluted 1:400)/HRP-conjugated rabbit anti-mouse IgG (Bethyl Laboratories, Inc., Montgomery, TX); (3) c-kit, goat antibody against c-kit (R&D Systems Inc., Minneapolis, MN, diluted 1:25)/HRP-conjugated anti-goat IgG (American Qualex Scientific Products, Inc., San Clemente, CA, diluted 1:100); (4) PTH/PTHrP receptor, rabbit antibody against PTH/PTHrP receptor (Assay Biotechnology Company, Inc., Sunnyvale, CA, diluted 1:50)/HRP-conjugated anti-rabbit IgG (Dako Denmark A/S, Produktionsvej, Denmark); (5) VEGF, rabbit antibody against VEGF (Santa Cruz Biotechnology, Inc., diluted 1:100)/HRP-conjugated anti-rabbit IgG (Zymed, diluted 1:100); (6) Flk-1, mouse antibody against Flk-1 (Santa Cruz, diluted 1:10)/HRP-conjugated rabbit anti-mouse IgG (Bethyl) (See Supple Table 1).

Reactions were assessed using 3, 3'-diaminobenzidine tetrahydrochloride (Dojindo Laboratories, Kumamoto, Japan). Then, specimens were observed under a Nikon Eclipse Ni microscope (Nikon Instruments Inc. Tokyo, Japan) and light microscopic images were acquired with a digital camera (Nikon DXM1200C, Nikon).

### Double Immunohistochemical Studies

For endomucin/ $\alpha$ SMA double immunohistochemical staining, dewaxed paraffin sections were incubated with 1% BSA-PBS, and then with mouse antibody against  $\alpha$ SMA (Thermo Fisher), and subsequently with HRP-conjugated secondary antibody as described above. The immunostained sections were reacted with anti-endomucin antibody (Santa Cruz), followed by incubation with ALP-conjugated goat anti-rat IgG (Jackson Immuno Research Laboratories, Inc., West Grovew, PA). HRP visualization was described above, and ALP envision was performed by slide immersion in an aqueous solution containing 2.5 mg of naphthol AS-BI phosphate (Sigma) and 18 mg of Fast Blue RR salt (Sigma) diluted in 30 mL of a 0.1 M Tris-HCl buffer (pH 8.5) for 15 min at 37 °C until immunoreactivity could be seen.

For immunofluorescent detection of endomucin/ $\alpha$ SMA, sections were incubated with mouse antibody against  $\alpha$ SMA, and then with FITC-conjugated goat anti-mouse IgG (MP Biomedicals. LLC., Solon, OH) diluted 1:100 with 1% BSA-PBS. The sections were subsequently incubated with rat antibody against endomucin, and subsequently reacted with Alexa 594-conjugated rabbit anti-rat IgG (Thermo Fisher) diluted 1:100. All sections were embedded by VECTASHIELD hard-set mounting medium with DAPI (Vector Laboratories, Inc. Burlingame, CA) and observed under light microscopy.

As with the immunofluorescent detection of endomucin/ephrinB2 and endomucin/EphB4, the sections immunostained for endomucin, which were followed with Alexa 594-labeling, were reacted with goat antibody against mouse ephrinB2 (R&D Systems) diluted 1:50, or with goat antibody against mouse EphB4 (R&D Systems) diluted 1:50 at 4 °C overnight. After several washings in PBS, they were incubated with Alex 488-conjugated donkey anti-goat IgG (Abcam PLC., Cambridge, UK) for 1 h.

For the detection of tissue nonspecific alkaline phosphatase (TNALP)/  $\alpha$ SMA, dewaxed paraffin sections were incubated with mouse antibody against  $\alpha$ SMA (Thermo Fisher), and then labeled with HRP-conjugated secondary antibody as described. The immuno-labeled sections were reacted with rabbit polyclonal antisera against TNALP diluted 1:300 with 1% BSA-PBS [26]; then, they were incubated with ALP-conjugated goat anti-rabbit antibody (Jackson).

### Transmission Electron Microscopy Studies

Semi-thin sections of epoxy-resin embedding specimens were cut with an ultramicrotome (Sorvall MT-5000; Ivan Sorvall, Inc., Norwalk, CT), stained with toluidine blue staining and observed under a Nikon Eclipse E800 microscope (Nikon Instruments Inc. Tokyo, Japan). Ultra-thin

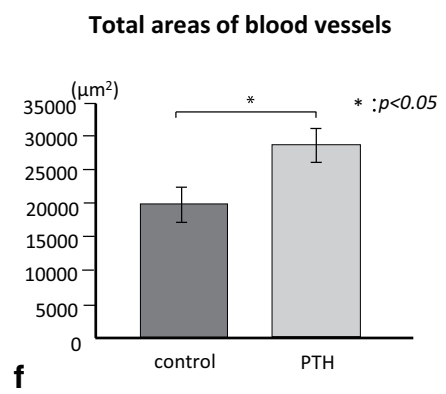
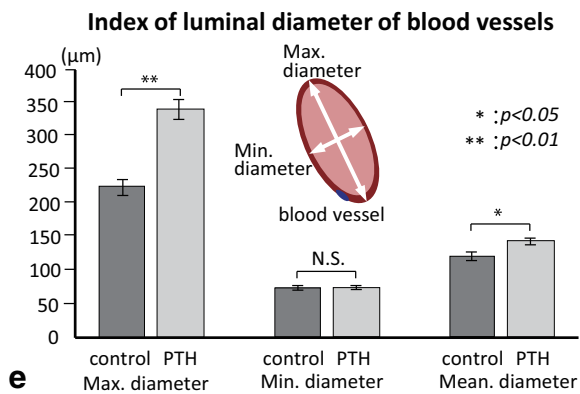
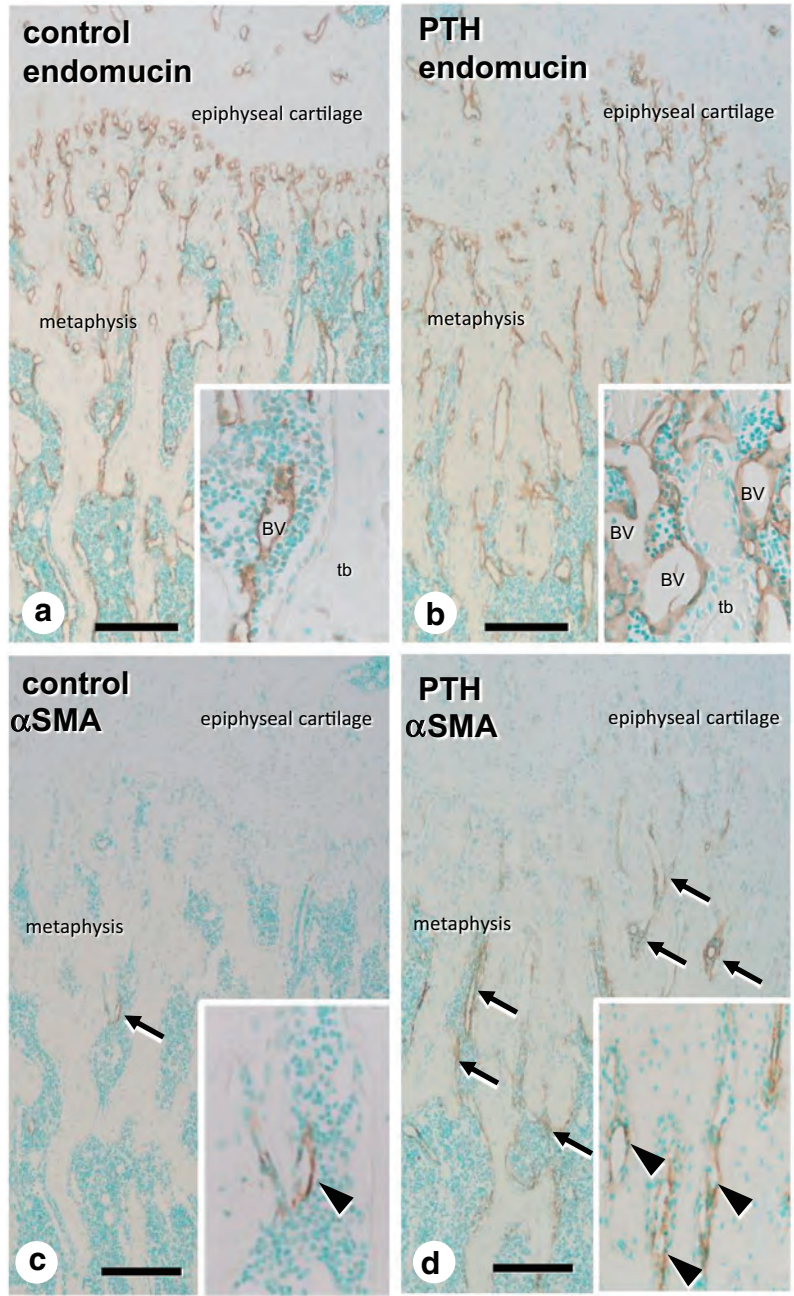


**Fig. 1** Increased diameters of bone-specific blood vessels and immunodetection of  $\alpha$ SMA-positive blood vessels after intermittent PTH administration. **a–d** show the immunoreactivity of endomucin (brown color, **a** and **b**) and  $\alpha$ SMA (brown color, **c** and **d**) in control (**a**, **c**) and PTH-treated (**b**, **d**) specimens, respectively. Note the enlarged endomucin-positive blood vessels (BV) in the PTH group (**b** see the inset) compared with the control specimens (**a** see the inset).  $\alpha$ SMA-immunopositive blood vessels were markedly increased after PTH administration (**d** see the arrows), while only a few  $\alpha$ SMA-positive blood vessels were seen in control specimens (**c**). **e** shows the statistical analysis of the maximum, minimum, and mean diameters of endomucin-reactive blood vessels in the ROI of control and PTH-treated specimens. There were significant differences in the maximum and mean diameter of endomucin-immunoreactive blood vessels between control and PTH-treated mice. **f** verifies the area occupied by endomucin-reactive blood vessels in the control and PTH-treated groups. Notably, significantly increased indices were observed in the PTH-treated specimens. *tb* trabecular bone. Bar, **a–d** 300  $\mu$ m

sections obtained with an ultramicrotome were stained with uranyl acetate and lead citrate. These specimens were subjected to TEM observation (Hitachi H-7100, Hitachi Co., Tokyo, Japan) at 80 kV.

#### Quantification of the Numbers of Endomucin-Positive, $\alpha$ SMA-Positive, and EphB4-Positive Blood Vessels, Diameters and Areas of Blood Vessels, and Bone Volume/Tissue Volume (BV/TV), Osteoblast Surface/Bone Surface (Ob.S/BS), TNALP(+)areas/TV, and VEGF(+)cell Areas/TV Ratios

A boxed area with 800  $\mu$ m (width)  $\times$  1000  $\mu$ m (length), the region of interest (ROI), located directly below the central bottom of the proximal femoral growth plate in the control and PTH-treated groups ( $n = 6$  for each group) was used to quantify endomucin-positive,  $\alpha$ SMA-positive, and EphB4-positive blood vessels, as well as blood vessel diameter and area indices, and bone volume/tissue volume (BV/TV), osteoblast surface/bone surface (Ob.S/BS), TNALP(+)areas/TV, and VEGF(+)areas/TV ratios. Additionally, our study also determined the maximum diameter (length of the longest line joining two points within a blood vessel's outline and passing through its centroid), minimum diameter (length of the shortest line joining two points within the blood vessel's outline and passing through centroid), and mean diameter (average length of diameters measured at 2-degree intervals and passing through the blood vessel's centroid) of endomucin-immunopositive blood vessels. Four images of different regions in the ROI at  $\times 200$  magnification were acquired to create a composite ROI image in order to obtain a sufficiently high-resolution image to determine the aforementioned indices with the Image-Pro Plus 6.2 software (Media Cybernetics, Inc., Bethesda MD).

#### RT-PCR and Real-Time PCR Assessment

Total RNA was extracted from femora to evaluate *Gapdh*, *Endomucin*,  *$\alpha$ Sma*, *Ephb4*, *ephrinb2*, and *PTH/PTHrP receptor* gene expression. The specimens were homogenized in 10 mL TRIzol reagent (Life Technologies Co. Carlsbad, CA) per 1 g of tissue to extract total RNAs. The mixture was centrifuged at 15,000 rpm for 5 min at 4  $^{\circ}$ C to remove small debris. The supernatant was then transferred to a new tube, which was vortexed for 15 s after the addition of 2 mL of chloroform. The lysate was then transferred to a new tube and incubated for 5 min at RT. After phase separation, the aqueous phase containing the RNA was transferred to a fresh new tube, after which the RNA was precipitated by adding 5 mL of isopropyl alcohol per 10 mL TRIzol reagent. After 10 min of incubation at RT, the mixture was centrifuged for 60 min at 15,000 rpm at 4  $^{\circ}$ C. The resulting RNA pellet was washed with 1 mL 75% ethanol and briefly air-dried. The RNA was then dissolved in 30  $\mu$ L DEPC-treated water. First-strand cDNA was synthesized from 2 mg of total RNA with the SuperScript VILO cDNA Synthesis Kit (Life Technologies). The primer sequences used for RT-PCR are detailed in the Supplementary Information (Suppl. Table 2). PCR was performed using a thermal cycler using the following thermal profile: denaturation at 94  $^{\circ}$ C for 30 s, annealing at 60  $^{\circ}$ C (for *Gapdh*) or 55  $^{\circ}$ C (for *Endomucin*,  *$\alpha$ Sma*, *Ephb4*, *ephrinb2*, and *PTH/PTHrP receptor*) for 30 s, extension at 72  $^{\circ}$ C for 30 s, and a final incubation at 72  $^{\circ}$ C for 10 min. The RT-PCR products were electrophoresed on a 2% agarose gel containing ethidium bromide and visualized with the E-Gel Imager software (Life Technologies). Real-time PCR assays were performed using Taqman probes (Applied Biosystems) to assess the expressions of the *Endomucin* (Mm00497495\_m1),  *$\alpha$ Sma* (Mm00725412\_s1), *Ephb4* (Mm01201157\_m1), *Ephrinb2* (Mm00438670\_m1), and *Pth1r* (Mm00441046\_m1) genes. This step was conducted using a StepOne Real-Time PCR System (Applied Biosystems) and gene expression profiles were normalized to *Gapdh* (Mm99999915\_g1) expression using the  $2^{-\Delta\Delta C_t}$  method.

#### Statistical Analysis

All statistical analyses were carried out using SPSS version 18.0.0 and analyzed for statistical significance by Student's t-test with significance set to  $p < 0.05$ . Numerical data were presented as mean  $\pm$  SD.

## Results

### Increased Lumen Diameters of Bone-Specific Blood Vessels and the Appearance of $\alpha$ SMA-Positive Blood Vessels After Intermittent PTH Administration

Despite the increased trabecular thickness and the consequent reduced intertrabecular space, endomucin-positive blood vessels appeared wider in diameter in the PTH group (Fig. 1a, b). We then measured the maximum, minimum and mean diameters of endomucin-reactive blood vessels in the ROI of control and PTH-treated specimens (Fig. 1e). The maximum diameter of endomucin-immunoreactive blood vessels were significantly larger in PTH-treated animals ( $224.53 \pm 10.06 \mu\text{m}$  vs.  $339.22 \pm 14.58 \mu\text{m}$ ,  $p < 0.01$ ). Likewise, the mean diameter too was larger in the PTH group ( $121.37 \pm 4.76 \mu\text{m}$  vs.  $144.01 \pm 4.63 \mu\text{m}$ ,  $p < 0.05$ ) (Fig. 1e). The minimum vessel diameter was similar in specimens from the control and the PTH groups ( $73.16 \pm 2.94 \mu\text{m}$  vs.  $73.26 \pm 2.32 \mu\text{m}$ , with no significance). In parallel with the increased lumen diameter, the area occupied by endomucin-reactive blood vessels was larger in the PTH-treated group ( $19,841.02 \pm 2585.61 \mu\text{m}^2$  vs.  $28,652.31 \pm 2413.11 \mu\text{m}^2$ ,  $p < 0.05$ ) (Fig. 1f).

Interestingly, cell number and area of  $\alpha$ SMA-immunopositive cells were markedly increased after PTH administration, while only few  $\alpha$ SMA-positive blood vessels were seen in control specimens (Fig. 1c, d).

### Immunolocalization of Endomucin-Positive Blood Vessels and $\alpha$ SMA-Immunoreactive Cell After PTH Administration

In PTH-administered metaphyses,  $\alpha$ SMA-positive cells extended from endomucin-reactive blood vessels and occupied the periphery of such vessels (Fig. 2b, d). In control specimens, on the other hand, a small number of  $\alpha$ SMA-positive cells surrounded few endomucin-positive blood vessels (Fig. 2a, c). On higher magnification, some  $\alpha$ SMA-positive cells lied close to endomucin-positive blood vessels, while other such cells were more distant from these vessels, showing a linear fibroblastic profile at the intertrabecular region (Fig. 2e).

### Distribution of EphrinB2-Positive and EphB4-Reactive Cells After PTH Administration

In the PTH group, endomucin-positive blood vessels seemed closer to ephrinB2-reactive osteoblasts (Fig. 3a, b). After PTH treatment, most  $\alpha$ SMA-positive fibroblastic cells extending from the blood vessels reached the nearby

ephrinB2-reactive osteoblastic layers. In contrast, control specimens featured scarce  $\alpha$ SMA-reactive cells around the blood vessels, without the pattern of cellular extension/migration toward the ephrinB2-positive osteoblastic layers (compare Fig. 3c and d). Meanwhile, EphB4 immunoreactivity was detected on endomucin-positive blood vessels from both control and PTH groups, which suggests that these endomucin-positive blood vessels are veins and venules (Fig. 4a–f).

The histochemical observations on the distribution of EphB4-positive,  $\alpha$ SMA-positive, endomucin-positive blood vessels were verified in quantitative terms (Fig. 4g). The number of EphB4-positive,  $\alpha$ SMA-positive, endomucin-positive blood vessels were  $50.17 \pm 18.45$  vs  $82.33 \pm 14.63$  ( $p < 0.01$ ),  $3.50 \pm 2.17$  vs  $26.67 \pm 7.58$  ( $p < 0.01$ ),  $63.00 \pm 18.01$  vs  $147 \pm 42.37$  ( $p < 0.01$ ) in the ROIs of the control and the PTH group, respectively. *Endomucin*,  *$\alpha$ Sma*, *ephrinb2*, and *Ephb4* expressions were found to be significantly upregulated after PTH administration according to RT-PCR and real-time PCR analyses (*endomucin*:  $1.23 \pm 0.07$  in the control group and  $1.78 \pm 0.07$  in the PTH group,  $p < 0.001$ ;  *$\alpha$ Sma*:  $0.65 \pm 0.08$  in the control group and  $2.48 \pm 0.37$  in the PTH group,  $p < 0.001$ ; *ephrinb2*:  $0.90 \pm 0.07$  in the control group and  $2.39 \pm 0.56$  in the PTH group,  $p < 0.001$ ; *Ephb4*:  $1.42 \pm 0.09$  in the control group and  $1.80 \pm 0.07$  in the PTH group,  $p < 0.001$ ) (Fig. 4h–l).

### Histochemical Characteristics of $\alpha$ SMA-Positive Stromal Cells Extending from Bone-Specific Blood Vessels

We have examined the co-immunolocalization of TNALP and  $\alpha$ SMA, as well as the ultrastructure of fibroblastic stromal cells located between the blood vessels and osteoblasts. In control specimens,  $\alpha$ SMA-positive cells surrounded the blood vessels and did not show TNALP-reactivity (Fig. 5a). After PTH administration, however, the  $\alpha$ SMA-positive cells that extended from the blood vessels were TNALP-positive (Fig. 5b). Still, TNALP-positive cells occupied a broader area than did  $\alpha$ SMA-positive cells between blood vessels and osteoblasts. In the control metaphyses, some bone marrow cells and few fibroblastic cells were positive for c-kit, a marker of mesenchymal stem cell [27] (Fig. 5c). After PTH administration, c-kit-reactive interstitial stromal cells occupied the same areas of the metaphyseal intertrabecular region as did  $\alpha$ SMA-positive cells (Fig. 5d).

We also compared the control and PTH-treated bone TNALP(+)-areas/TV and Ob.S/BS ratios in the ROI. Notably, both the TNALP(+)-areas/TV and Ob.S/BS ratios were significantly elevated in the ROI where bone-specific blood vessels had significantly larger diameters and total luminal areas (please see Fig. 1). The TNALP(+)-areas/TV ratio was  $1.75 \pm 0.15\%$  in the control group and  $9.67 \pm 0.36\%$  in

**Fig. 2** Immunolocalization of endomucin-positive blood vessels and  $\alpha$ SMA-immunoreactive cells after PTH administration. **a, b** show the double detection of endomucin (blue-purple color) and  $\alpha$ SMA (brown color) via immunohistochemistry in control (**a**) and PTH-treated (**b**) specimens. The control specimens exhibited a small number of  $\alpha$ SMA-positive cells (indicated with an arrow in **a**) surrounded by blood vessels (BV), while PTH-treated specimens exhibited many  $\alpha$ SMA-positive cells (arrows, brown color in **b**) extended from endomucin-reactive blood vessels (indicated with an asterisk in **b**). **c–e** Immunofluorescent microscopic images of the double detection of endomucin (red color) and  $\alpha$ SMA (green color, white arrowheads) in control (**c**) and the PTH-treated specimens (**d**). When the PTH-treated metaphyses were examined at a higher magnification, many  $\alpha$ SMA-positive cells (green color, white arrows) were localized away from the blood vessels and featured a linear fibroblastic profile (**e**). *tb* trabecular bone. Bar, **a–d** 50  $\mu$ m, **e** 10  $\mu$ m

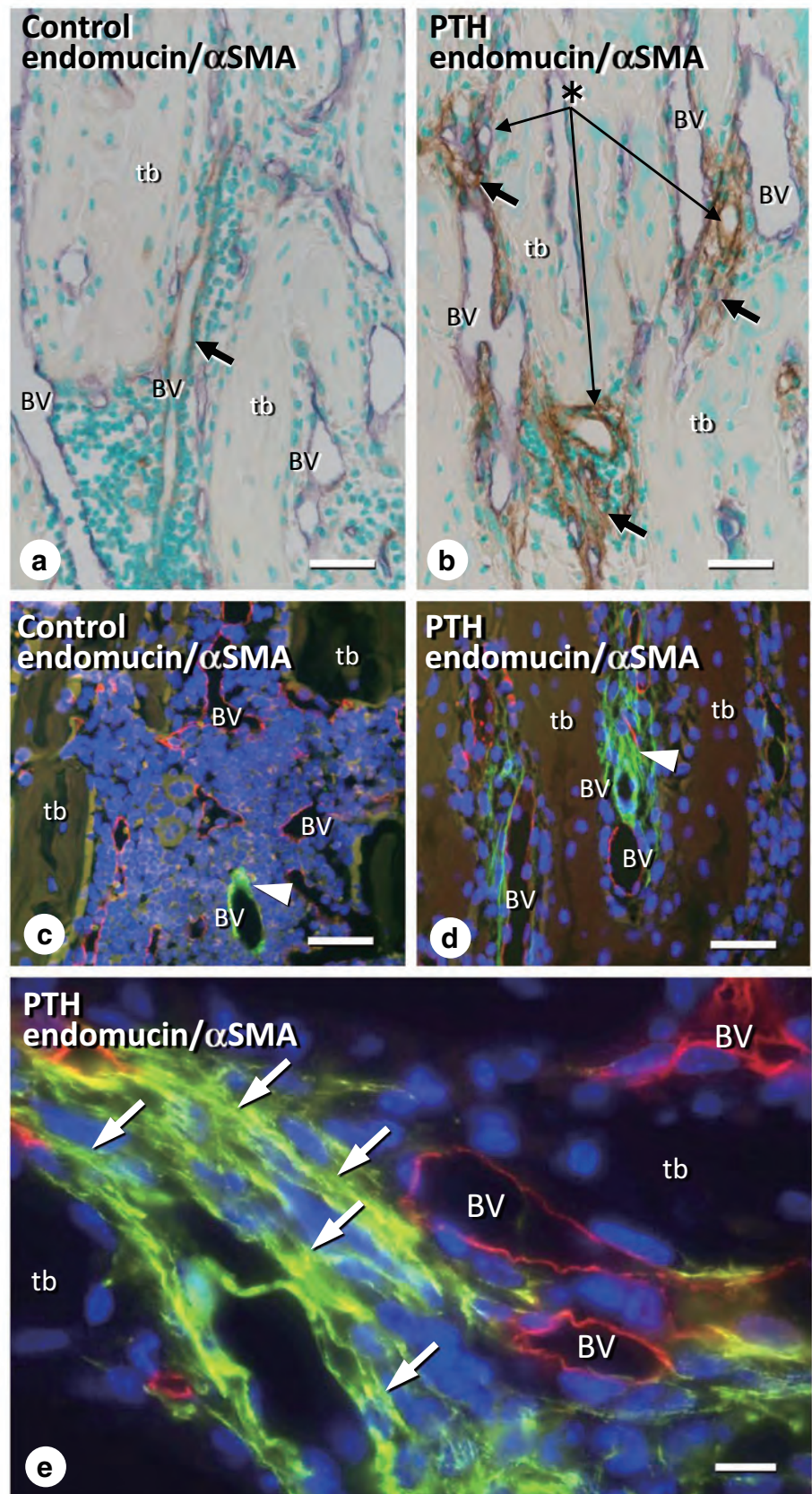
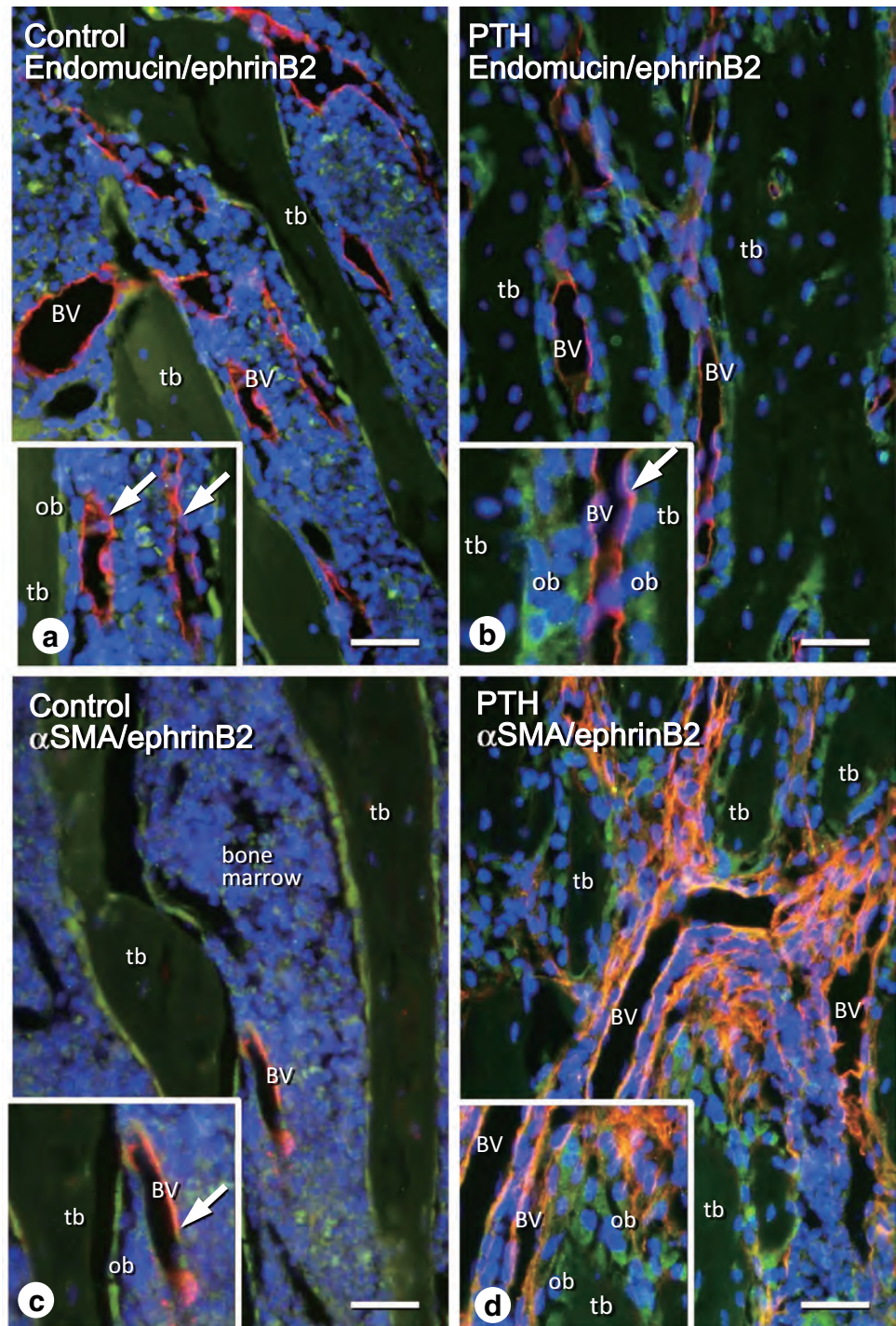




**Fig. 3** Distribution of ephrinB2-positive cells after PTH administration. **a** and **b** show the double immunofluorescent detection of endomucin (red color) and ephrinB2 (green color) in control (**a**) and PTH-treated (**b**) specimens. Moreover, **c** and **d** represent the double immunofluorescent staining of  $\alpha$ SMA (red color) and ephrinB2 (green color) in control (**c**) and PTH-treated (**d**) samples. In both the control and PTH groups, ephrinB2 reactivity can be seen in osteoblasts (“ob” in insets, **a**, **b**). In the PTH group, endomucin-positive blood vessels (red color, BV) were localized closer to ephrinB2-reactive osteoblasts (see inset in **b**). After PTH treatment, most  $\alpha$ SMA-positive fibroblastic cells (red color) extending from the blood vessels intervened the cell layer of ephrinB2-reactive osteoblasts (green color) (see inset in **d**). In contrast, control specimens displayed only a few  $\alpha$ SMA-reactive cells (red color, an arrow in the inset), which were restricted to the blood vessels (**c**). *tb* trabecular bone. Bar, **a–d** 30  $\mu$ m



the PTH group ( $p < 0.001$ ) (Fig. 5e), whereas Ob.S/BS was  $27.4 \pm 1.5\%$  in the control group and  $56.9 \pm 2.1\%$  in the PTH group ( $p < 0.001$ ) (Fig. 5f).

Histologically, PTH-treated metaphyses showed blood vessels with walls thicker than those in control specimens (Compare Fig. 6a–c). A variety of cell type was found among blood vessels and osteoblasts: some had long bodies with thin cytoplasmic processes and were distant from

bone surfaces, while others had a transparent cell bodies different from mature osteoblasts (Fig. 6c). Under TEM, it was possible to see that the elongated cytoplasmic processes of the interstitial cells made contact with osteoblastic cells. Moreover, there were blood vessels surrounded by vascular smooth muscle cells that made contact with osteoblasts (Fig. 6d–g).

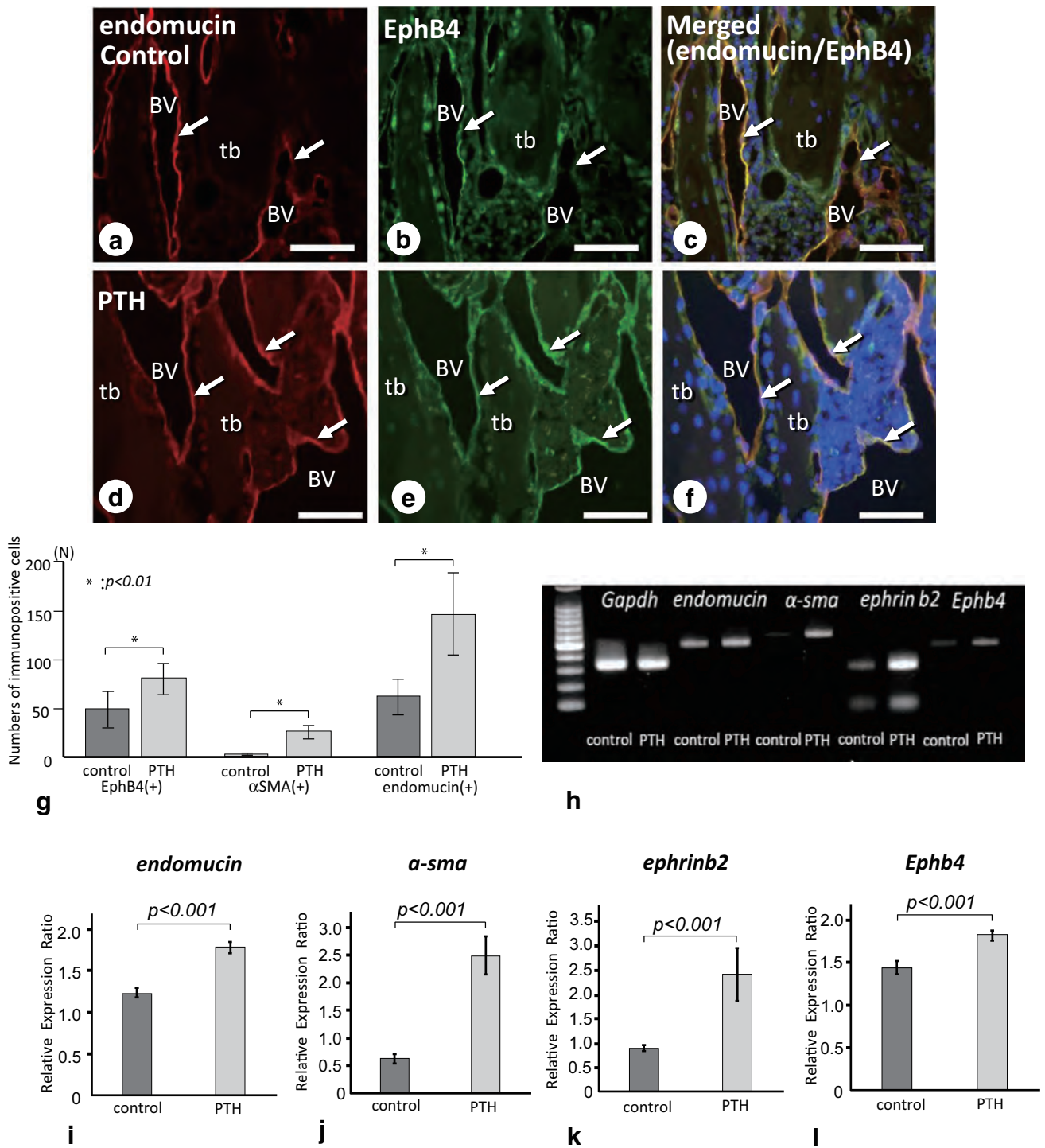


**Fig. 4** Immunolocalization of EphB4 and statistical analyses of the numbers and gene expression of EphB4-, αSMA-, or endomucin-positive blood vessels. **a-f** represent the immunofluorescent detection of endomucin (red color, **a, d**), EphB4 (green color, **b, e**), and merged images of endomucin and EphB4 (**c, f**) in control (**a-c**) and PTH-treated (**d-f**) specimens. EphB4 immunoreactivity (white arrows, **a, d**) can be seen mainly on endomucin-positive blood vessels (BV, white arrows in **b, e**) from both the control (**a, b**) and PTH (**d, e**) groups. The merged image shows the same localization of endomu-

cin and EphB4 on blood vessels (white arrows, yellow color in **c, f**) in both the control (**c**) and PTH groups (**f**). **g** A statistical analysis of the number of EphB4-positive, αSMA-positive, and endomucin-positive blood vessels in the ROI of the control (dark gray bars) and PTH (light gray bars) groups. **h** Presents the RT-PCR results of the *Gapdh*, *endomucin*, *α-sma*, *ephrinb2*, and *Ephb4* genes between the control and PTH groups. **i-l** represent the real-time PCR analyses of *endomucin*, *α-sma*, *ephrinb2*, and *Ephb4* gene expression after PTH administration. *tb* trabecular bone. Bar, **a-d** 50 μm

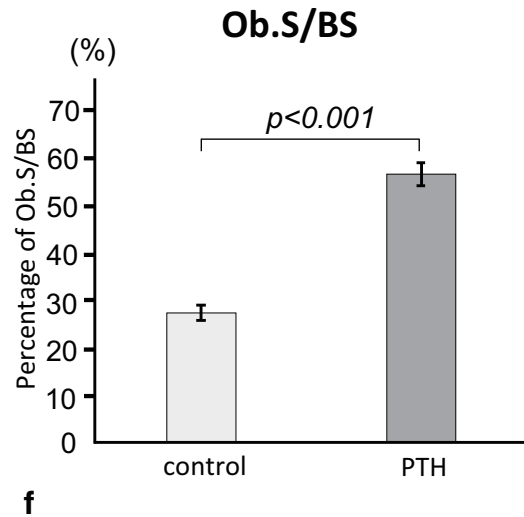
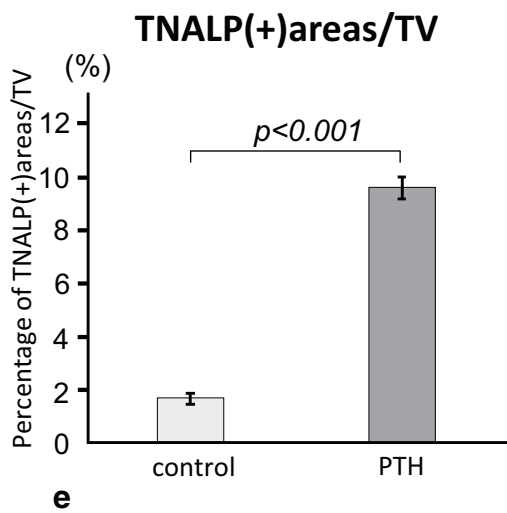
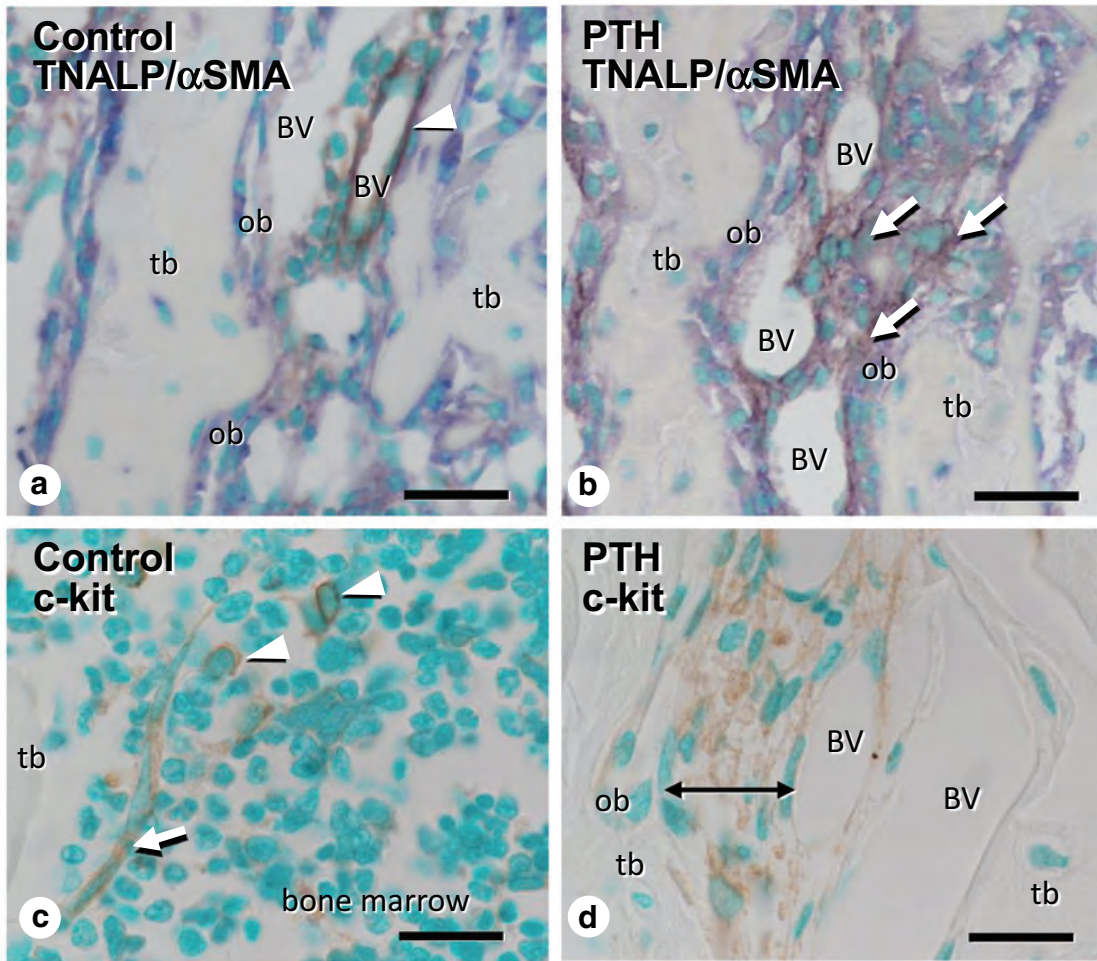


**Fig. 5** Immunohistochemistry of TNALP,  $\alpha$ SMA, and c-kit in the control and PTH-treated metaphyses. **a, b** show the double detection of TNALP (blue-purple color) and  $\alpha$ SMA (brown color) in control (**a**) and PTH-treated (**b**) specimens. In the control specimens,  $\alpha$ SMA-positive cells were tightly associated with blood vessels (BV) (indicated with a white arrowhead in **a**), but not with TNALP-reactive osteoblasts (ob). After PTH administration,  $\alpha$ SMA-positive cells (brown color, white arrows in **b**) extended from the blood vessels and appeared to intermingle with TNALP-reactive cells (blue-purple color), which are more broadly associated with the intertrabecular region (**b**). **c** and **d** illustrate the immunodetection of c-kit (brown color) in control (**c**) and PTH-treated (**d**) specimens. In the control metaphyses, a few fibroblastic cells (indicated with a white arrow) and bone marrow cells (white arrowheads) were positive for c-kit (**c**). After PTH administration, however, c-kit-reactive interstitial stromal cells (the arrow indicates the c-kit-positive cell area) were observed between the osteoblasts and blood vessels in the metaphyseal intertrabecular region (**d**). **e** and **f** represent the statistical analyses of the TNALP(+)/areas/TV and Ob.S/BS ratios, respectively. *tb* trabecular bone. Bar, **a–d** 50  $\mu$ m

### Immunolocalization of the PTH/PTHrP Receptor, VEGF, and Flk-1 in PTH-Treated Metaphyses

As shown in Fig. 7, the control specimens mainly exhibited PTH/PTHrP receptors in the osteoblasts (Fig. 7a), whereas the PTH-treated specimens exhibited PTH/PTHrP receptor immunopositivity not only in the osteoblasts but also in blood vessels and neighboring cells (Fig. 7b). Consistent with these results, PTH treatment significantly increased PTH/PTHrP receptor mRNA in the PTH group (the gene expression ratios were  $0.80 \pm 0.05$  in the control group and  $2.07 \pm 0.27$  in PTH group,  $p < 0.001$ ) (Fig. 7g, h). The control metaphyses hardly exhibited either VEGF or Flk-1 immunoreactivity (Fig. 7c, e). After PTH administration, however, VEGF and Flk-1 immunopositivity was detectable mainly in osteoblasts and blood vessels/nearby cells (Fig. 7d, f). Additionally, PTH-treated metaphyses had significantly higher VEGF(+)/areas/TV ratios than the controls (Fig. 7i).

## Discussion

In this study, we have demonstrated that intermittent PTH administration affects bone-specific blood vessels and cells neighboring the blood vessels. We have reported elsewhere that intermittent PTH administration fostered osteoblastic bone formation and proliferation of Runx2-positive/

TNALP-reactive preosteoblasts [6, 7]. Our current observations suggest that  $\alpha$ SMA-positive cells surrounding the blood vessels are affected by exogenous PTH—presumably increasing the number of such cell type. This suggestion is strengthened by our finding of intense PTH/PTHrP receptor immunoreactivity in blood vessels following PTH administration, which ratified our earlier report on the expression of PTH/PTHrP receptor by vascular endothelial cells in the kidney [28]. Additional support to our conjecture comes from the study by Jiang et al., who showed that PTH treatment promotes vascularized bone regeneration by improving blood vessel formation and increasing the osteogenic potential of aged bone marrow mesenchymal stem cells [29]. Taken together, these evidences suggest a biological effect of PTH on blood vessels.

An exciting finding of this study is the increase in the number and in the diameter of blood vessels after PTH treatment, along with the growth in the population  $\alpha$ SMA-positive/c-kit-reactive cells—which not only surrounded the blood vessels, but extended from the vicinity of these blood vessels toward the osteoblastic cell layer. Even though the intertrabecular space became narrower as consequence of PTH-driven increased bone formation, the diameter of bone-specific blood vessels was enlarged (Fig. 1). It is known that teriparatide causes a temporary drop in blood pressure, which is likely due to decreased arterial pressure. Studies with rats, dogs and rabbits showed that their aortas relaxed after PTH administration, thus inducing temporary blood hypotension [30]. Similarly, PTH reportedly induced the relaxation of cultured rat aorta vascular smooth muscle cells by increasing intracellular cyclic AMP [31, 32]. In contrast to this PTH-driven relaxation of vascular smooth muscle cells, most metaphyseal blood vessels in our study formed EphB4-reactive venous sinusoids lacking tunica media coverage and continuous basement membranes. Therefore, the enlarged blood vessels seen in PTH-treated bones did not seem to be directly involved with PTH-driven arterial relaxation.

The movement of  $\alpha$ SMA-positive stromal cells away from the blood vessels may “pull” vascular endothelial cells with them, thus widening the lumen of the blood vessels. Moreover, we have registered the increased number of endomucin-immunoreactive/EphB4-positive blood vessels in the metaphysis. Dhillon et al. demonstrated that intermittent treatment with recombinant PTH-enhanced structural allograft healing via two processes: (1) anabolic

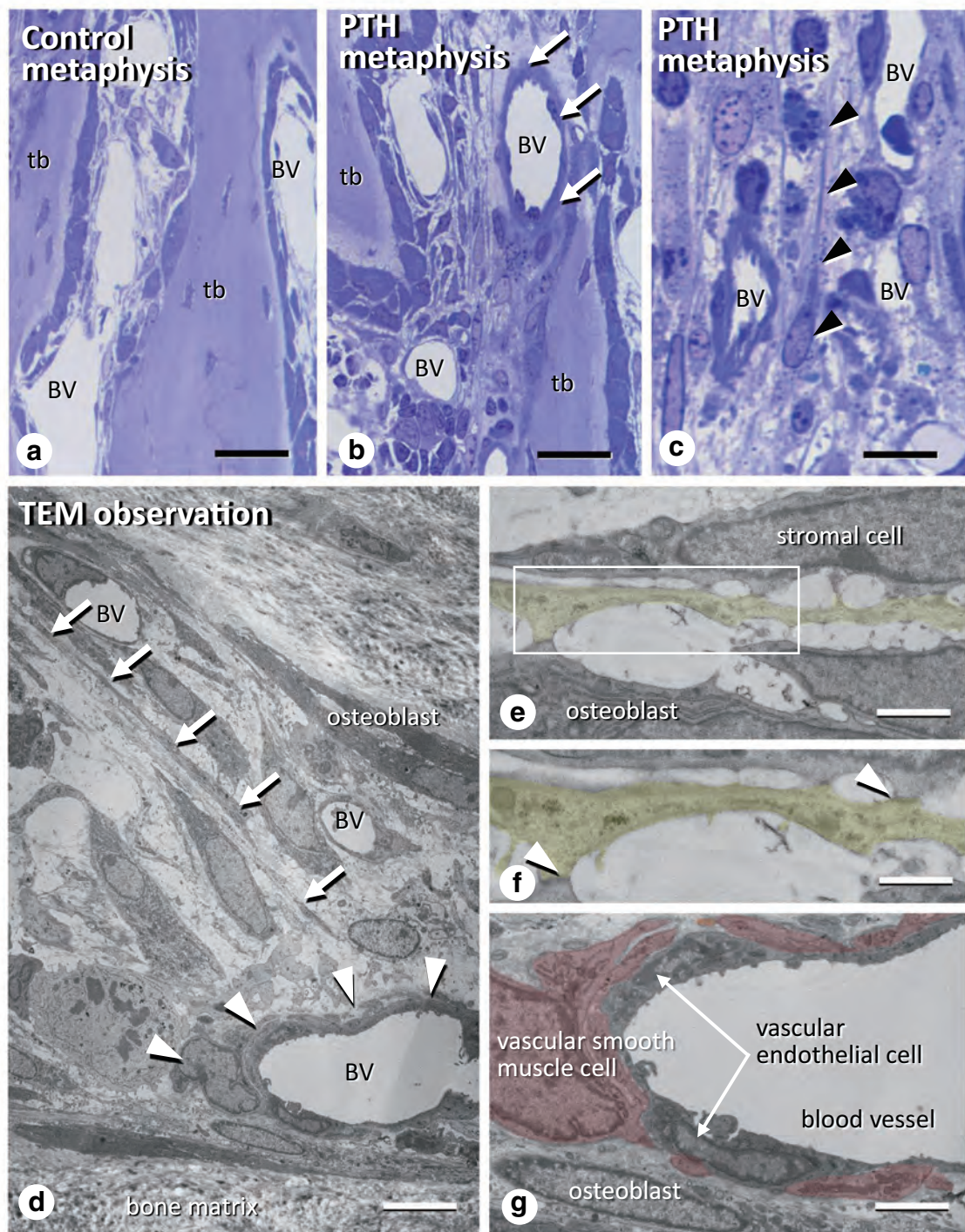


**Fig. 6** Ultrastructure of interstitial stromal cells between blood vessels and osteoblasts in the intertrabecular region after PTH administration. **a–c** Semi-thin sections of control (**a**) and PTH-treated (**b**, **c**) metaphyses stained with toluidine blue. Note that PTH-treated blood vessels (BV, white arrows in **b**) exhibited thicker walls than those of the control blood vessels (**a**). At a higher magnification, spindle cell types with long straight cytoplasmic processes (arrowheads in **c**) can be seen close to the blood vessels (BV, **c**). The TEM images show the elongated cytoplasmic processes of the interstitial cells (white

arrows in **d**) and blood vessels surrounded with smooth muscle cells (white arrowheads in **d**). The long cytoplasmic processes (yellow color) of the interstitial cells show cell-to-cell contact with other stromal cells and osteoblasts (**e**). A highly magnified image reveals the direct contact between the membranes of these cells (white arrowheads, **f**). **g** A highly magnified image of the blood vessel shown in **d**. Vascular endothelial cells and vascular smooth muscle cells (red color) appeared to make partial contact with the bone surface. Bar, **a**, **b** 30  $\mu\text{m}$ , **c**, **d** 10  $\mu\text{m}$ , **e** 3  $\mu\text{m}$ , **f** 2  $\mu\text{m}$ , **g** 5  $\mu\text{m}$

effects on new bone formation by inducing small vessel angiogenesis, and (2) inhibition of large vessels by arteriogenesis [8]. Intermittent PTH administration reportedly stimulates angiopoietin-1 gene expression but reduces the expression of the angiopoietin-2 gene, indicating that downregulation of angiopoietin-2-mediated arteriogenesis is a critical therapeutic mechanism of PTH for bone repair. In our study, the increases in blood vessels in PTH-treated metaphyses appeared to be consistent with Dhillon's observation. The numbers of  $\alpha$ SMA-positive blood vessels were increased after PTH administration; however, many  $\alpha$ SMA-positive cells migrated from the blood vessels instead of forming mature blood vessels with the tunica media of  $\alpha$ SMA-positive vascular smooth muscles (*i.e.*, arteriogenesis). Our study did not employ a bone repair model; however, our mouse model results largely support those of Dhillon et al.

It is also interesting that  $\alpha$ SMA-positive cells formed thick tunica media in metaphyseal blood vessels while spreading among osteoblasts and blood vessels in the intertrabecular spaces. The  $\alpha$ SMA-positive stromal cells extending from the blood vessels toward the osteoblastic layer seem to be undifferentiated mesenchymal cells that also expressed c-kit and TNALP. A recent report suggested that c-kit was expressed by fetal, but not by postnatal skeletal progenitors [33]. Consistently, we hardly detected c-kit-reactive stromal cells in control specimens (Fig. 5). Jiang et al. reported that PTH directly facilitated the proliferation of vascular endothelial cells and indirectly enhanced angiogenesis by promoting mesenchymal stem cell angiogenic differentiation [9]. Based on our observations, the cells positive for  $\alpha$ SMA/TNALP/c-kit that extend from the PTH-treated blood vessels may include mesenchymal stem cells, which could then differentiate into vascular endothelial cells. In contrast, another study demonstrated the occurrence of transcortical perivascular cells near blood vessels in cortical bone and their osteogenic potential contributed to new osteoblast formation [24]. Therefore, the cells positive for  $\alpha$ SMA/TNALP/c-kit derived from the PTH-treated blood vessels may differentiate into both vascular endothelial cells and osteoprogenitor cells. However, given that both osteoblastic cells and vascular

endothelial cells possess the PTH/PTHrP receptor, it seems necessary to determine whether PTH acts predominantly from bone to blood vessels or vice versa to recruit the cells positive for  $\alpha$ SMA/TNALP/c-kit between the blood vessels and osteoblasts.

The intimate connection between blood vessels and bone tissues has been subjected to scientific scrutiny [34]. Since the bone matrix is highly vascularized, the assumption was that blood vessels were delivery channels for oxygen, nutrients, growth factors, and hormones, all the while taking part in hematopoiesis at the neighboring bone marrow [17]. That may not be the case: recently, it has been demonstrated that there is a network of transcortical capillaries that acts as a mainstay for blood circulation in long bones [35]. In addition, Kusumbe, Ramasamy et al. reported on a bone-specific, CD31<sup>high</sup>/endomucin<sup>high</sup> subtype of blood vessels and proposed that angiogenesis also plays an important role in bone development and remodeling [10, 11].

The putative site for osteo-vascular interaction may be the region filled with the  $\alpha$ SMA-positive/c-kit-reactive interstitial stromal cells between the blood vessels and the bone surfaces. In fact, many cell types were identified in that area under higher magnification (Fig. 6). Some of these cells extended long cytoplasmic processes linearly and parallel to the bone surfaces. Judging from the cell shape and the long cytoplasmic processes, this cell may well be the telocyte discovered in 2003 [36]. Telocytes are fibroblast-like cells with extremely long but thin cellular processes. However, telocytes have not been described in bone so far and, therefore, further examination is mandatory.

Considering our present findings and the supporting literature, we postulate that PTH, apart from affecting the number and the size of bone-specific blood vessels, also promotes the proliferation of  $\alpha$ SMA-positive cells surrounding the blood vessels. Once proliferated, these  $\alpha$ SMA-positive/c-kit-reactive interstitial stromal cells may differentiate into vascular smooth muscle cells or into a less differentiated cell type that is possibly committed to the osteogenic lineage. The wide distribution of PTH/PTHrP receptor expression and the variety of cell type among the blood vessels and bone surfaces—at least in part—makes this postulation plausible.

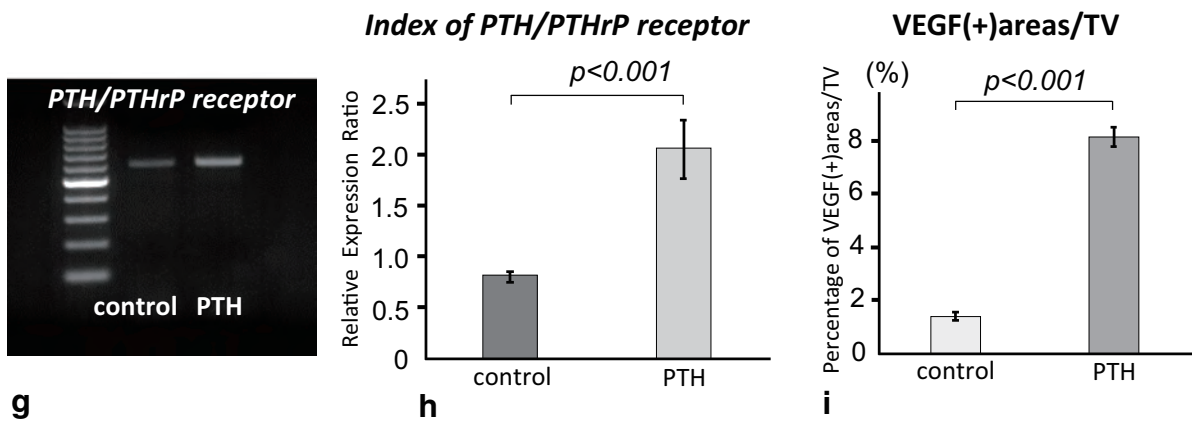
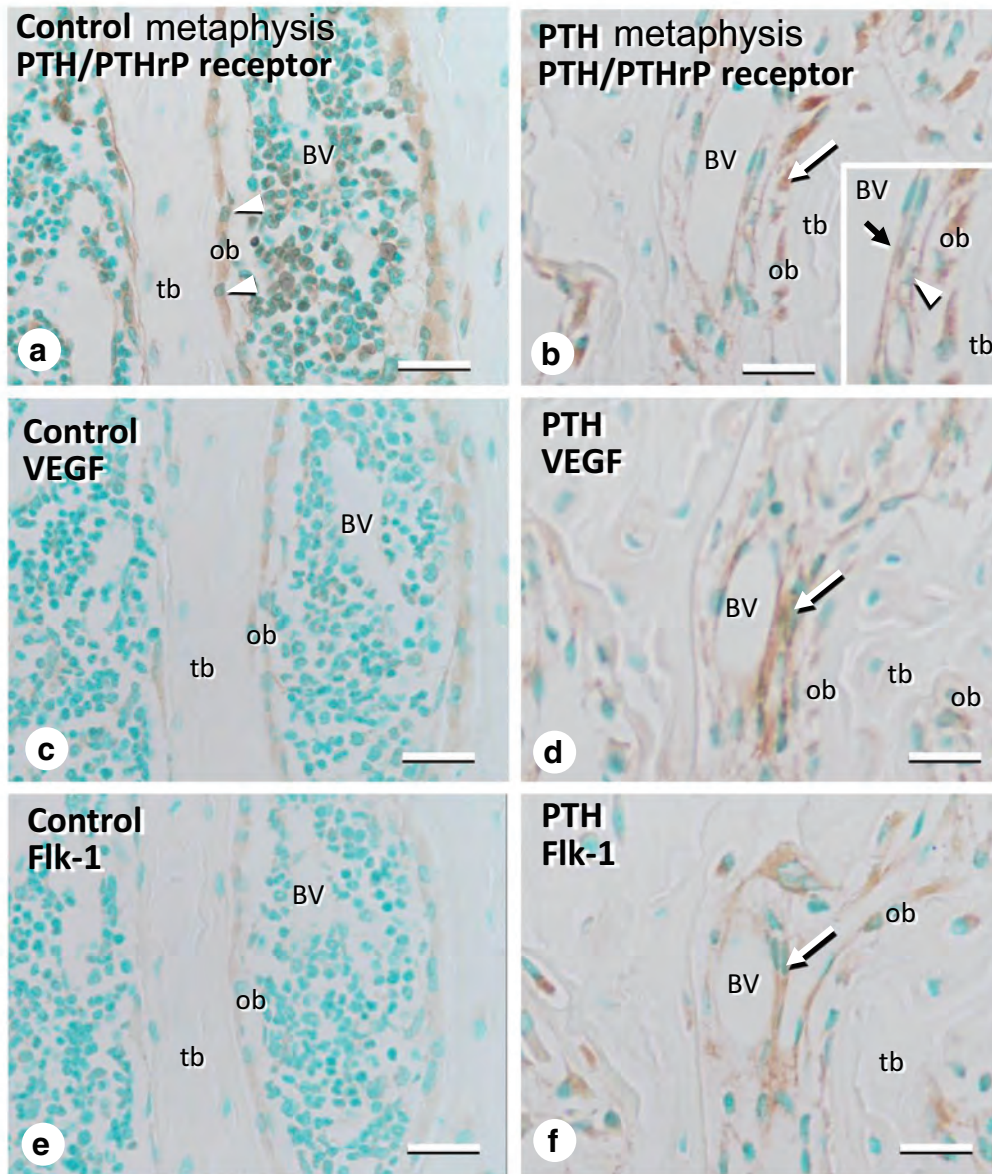


**Fig. 7** Immunolocalization of PTH/PTHrP receptor, VEGF, and Flk-1 in PTH-treated metaphyses. **a–f** represent the immunolocalization of the PTH/PTHrP receptor (**a, b**), VEGF (**c, d**), and Flk-1 (**e, f**) on the serial sections of control (**a, c, e**) and PTH-treated (**b, d, f**) metaphyses. Notice that PTH/PTHrP receptor immunopositivity can be observed not only in osteoblasts on trabeculae (tb) but also in blood vessels (BV, indicated with a black arrow) and surrounding cells (indicated with a white arrowhead) in PTH-treated metaphysis (**b**), whereas the immunoreactivity was restricted to osteoblasts (arrowheads in **a**). The control metaphyses exhibited very faint VEGF-positivity (**c**) and Flk-1 immunoreactivity (**e**), whereas the PTH-treated metaphyses exhibited a relatively intense VEGF-positivity (indicated with a white arrow, **d**) and Flk-1 immunopositivity (indicated with a white arrow, **f**) mainly in blood vessels (BV) and nearby cells (white arrows), as well as osteoblasts (ob). **g** and **h** represent the RT-PCR results and statistical analyses of PTH/PTHrP receptor expression estimated by real-time PCR. **i** presents the statistical analyses of the VEGF(+)/areas/TV indices. *Tb* trabecular bone. Bar, **a–f** 20  $\mu$ m

**Author Contributions** TH designed the study and prepared the first draft of the paper as a corresponding author. SZ is the researcher mainly in charge of this work, including RT-PCR, immunohistochemistry and TEM observation experiments. HH, MA, TY contributed to the experimental work including the preparation of paraffin samples of PTH-administered mice. TY was responsible for statistics. PHLF, ML, KT and NA participated in the discussion, editing and formatting of the manuscript. All authors revised the paper for intellectual content and approved its final version.

**Funding** This study was partially supported by grants from Japanese Society for the Promotion of Science (JSPS, 19K10040 to Hasegawa T) and partially supported by a grant-in-aid for young scientists provided by the Japanese Association for Oral Biology and Kazato Research Foundation (Hasegawa T) and by Japan China Sasakawa Medical Fellowship (Zhao S).

## Compliance with Ethical Standards

**Conflict of interest** Shen Zhao, Tomoka Hasegawa, Hiromi Hongo, Tomomaya Yamamoto, Miki Abe, Taiji Yoshida, Mai Haraguchi, Paulo Henrique Luiz de Freitas, Minqi Li, Kanchu Tei, and Norio Amizuka declare no competing interests.

**Animal Rights and Informed Consent** All animal experiments in this study were conducted under the Hokkaido University Guidelines for Animal Experimentation. The experimental protocol was approved by the Hokkaido University Animal Care and Use Committee which is accredited by the Association for Assessment and Accreditation of Laboratory Animal Care (approved research proposal #15-0032).

## References

- Schweser KM, Crist BD (2017) Osteoporosis: a discussion on the past 5 years. *Curr Rev Musculoskelet Med* 10:265–274
- Orwoll E, Scheele W, Paul S, Adami S, Syversen U, Diez-Perez A, Kaufman JM, Clancy AD, Gaich GA (2003) The effect of teriparatide [human parathyroid hormone (1–34)] therapy on bone density in men with osteoporosis. *J Bone Miner Res* 18:9–17
- Cosman F, Hattersley G, Hu MY, Williams GC, Fitzpatrick LA, Black DM (2017) Effects of abaloparatide-SC on fractures and bone mineral density in subgroups of postmenopausal women with osteoporosis and varying baseline risk factors. *J Bone Miner Res* 32(1):17–23
- Skriptitz R, Aspenberg P (2004) Parathyroid hormone—a drug for orthopedic surgery? *Acta Orthop Scand* 75:654–662
- Moreira CA, Fitzpatrick LA, Wang Y, Recker RR (2017) Effects of abaloparatide-SC (BA058) on bone histology and histomorphometry: the ACTIVE phase 3 trial. *Bone* 97:314–319
- Luiz de Freitas PH, Li M, Ninomiya T, Nakamura M, Ubaidus S, Oda K, Udagawa N, Maeda T, Takagi R, Amizuka N (2009) Intermittent PTH administration stimulates pre-osteoblastic proliferation without leading to enhanced bone formation in osteoclast-less c-fos(-/-) mice. *J Bone Miner Res* 24:1586–1597
- Yamamoto T, Hasegawa T, Sasaki M, Hongo H, Tsuboi K, Shimizu T, Ohta M, Haraguchi M, Takahata T, Oda K, Freitas PHL, Takakura A, Takao-Kawabata R, Isogai Y, Amizuka N (2016) Frequency of teriparatide administration affects the histological pattern of bone formation in young adult male mice. *Endocrinology* 157:2604–2620
- Dhillon RS, Xie C, Tyler W, Calvi LM, Awad HA, Zuscik MJ, O’Keefe RJ, Schwarz EM (2013) PTH-enhanced structural allograft healing is associated with decreased angiotensin-2-mediated arteriogenesis, mast cell accumulation, and fibrosis. *J Bone Miner Res* 28(3):586–597
- Jiang X, Xu C, Shi H, Cheng Q (2019) PTH 1–34 improves bone healing by promoting angiogenesis and facilitating MSCs migration and differentiation in a stabilized fracture mouse model. *PLoS ONE* 14(12):e0226163
- Kusumbe AP, Ramasamy SK, Adams RH (2014) Coupling of angiogenesis and osteogenesis by a specific vessel subtype in bone. *Nature* 507:323–328
- Ramasamy SK, Kusumbe AP, Wang L, Adams RH (2014) Endothelial Notch activity promotes angiogenesis and osteogenesis in bone. *Nature* 507:376–380
- Wang HU, Chen ZF, Anderson DJ (1998) Molecular distinction and angiogenic interaction between embryonic arteries and veins revealed by ephrin-B2 and its receptor Eph-B4. *Cell* 93(5):741–753
- Rundle CH, Xing W, Lau KW, Mohan S (2016) Bidirectional ephrin signaling in bone. *Osteoporos Sarcopenia* 2:65–76
- Zhao C, Irie N, Takada Y, Shimoda K, Miyamoto T, Nishiwaki T, Suda T, Matsuo K (2006) Bidirectional ephrinB2-EphB4 signaling controls bone homeostasis. *Cell Metab* 4:111–121
- Ramasamy SK (2017) Structure and functions of blood vessels and vascular niches in bone. *Stem Cells Int* 2017:5046953
- Armulik A, Genove G, Betsholtz C (2011) Pericytes: developmental, physiological, and pathological perspectives, problems, and promises. *Dev Cell* 21:193–215
- Sivaraj KK, Adams RH (2016) Blood vessel formation and function in bone. *Development* 143:2706–2715
- Aizman I, Holland WS, Yang C, Bates D (2016) alphaSMA expression in large colonies of colony-forming units-fibroblast as an early predictor of bone marrow MSC expandability. *Cell Med* 8:79–85
- Hosoya A, Nakamura H, Ninomiya T, Yoshida K, Yoshida N, Nakaya H, Wakitani S, Yamada H, Kasahara E, Ozawa H (2006) Immunohistochemical localization of alpha-smooth muscle actin during rat molar tooth development. *J Histochem Cytochem* 54(12):1371–1378
- Matthews BG, Grcevic D, Wang L, Hagiwara Y, Roguljic H, Joshi P, Shin DG, Adams DJ, Kalajzic I (2014) Analysis of alphaSMA-labeled progenitor cell commitment identifies notch signaling as an important pathway in fracture healing. *J Bone Miner Res* 29:1283–1294
- Kusumbe AP, Ramasamy SK, Itkin T, Mae MA, Langen UH, Betsholtz C, Lapidot T, Adams RH (2016) Age-dependent



- modulation of vascular niches for haematopoietic stem cells. *Nature* 532:380–384
22. Kunisaki Y, Bruns I, Scheiermann C, Ahmed J, Pinho S, Zhang D, Mizoguchi T, Wei Q, Lucas D, Ito K, Mar JC, Bergman A, Frenette PS (2013) Arteriolar niches maintain haematopoietic stem cell quiescence. *Nature* 502:637–643
  23. Mendez-Ferrer S, Michurina TV, Ferraro F, Mazloom AR, MacArthur BD, Lira SA, Scadden DT, Ma'ayan A, Enikolopov GN, Frenette PS (2010) Mesenchymal and haematopoietic stem cells form a unique bone marrow niche. *Nature* 466:829–834
  24. Root SH, Wee NK-Y, Novak S, Rosen CJ, Baron R, Matthews BG, Kalajzic I (2020) Perivascular osteoprogenitors are associated with transcortical channels of long bones. *Stem Cell* 38:769–781
  25. Hasegawa T, Yamamoto T, Sakai S, Miyamoto Y, Hongo H, Qiu Z, Abe M, Takeda S, Oda K, de Freitas PHL, Li M, Endo K, Amizuka N (2019) Histological effects of the combined administration of eldcalcitol and a parathyroid hormone in the metaphyseal trabeculae of ovariectomized rats. *J Histochem Cytochem* 67(3):169–184
  26. Oda K, Amaya Y, Fukushi-Irié M, Kinameri Y, Ohsuye K, Kubota I, Fujimura S, Kobayashi J (1999) A general method for rapid purification of soluble versions of glycosylphosphatidylinositol-anchored proteins expressed in insect cells: an application for human tissue-nonspecific alkaline phosphatase. *J Biochem* 126:694–699
  27. Deng W (2010) Mesenchymal stem cells express C-kit. *Circ Res* 107(10):e17
  28. Amizuka N, Lee HS, Kwan MY, Arazani A, Warshawsky H, Hendy GN, Ozawa H, White JH, Goltzman D (1997) Cell-specific expression of the parathyroid hormone (PTH)/PTH-related peptide receptor gene in kidney from kidney-specific and ubiquitous promoters. *Endocrinology* 138(1):469–481
  29. Jiang L, Zhang W, Wei L, Zhou Q, Yang G, Qian N, Tang Y, Gao Y, Jiang X (2018) Early effects of parathyroid hormone on vascularized bone regeneration and implant osseointegration in aged rats. *Biomaterials* 179:15–28
  30. Pang PK, Tenner TE Jr, Yee JA, Yang M, Janssen HF (1980) Hypotensive action of parathyroid hormone preparations on rats and dogs. *Proc Natl Acad Sci USA* 77(1):675–678
  31. Nickols GA (1985) Increased cyclic AMP in cultured vascular smooth muscle cells and relaxation of aortic strips by parathyroid hormone. *Eur J Pharmacol* 116(1–2):137–144
  32. Nickols GA, Metz MA, Cline WH Jr (1986) Endothelium-independent linkage of parathyroid hormone receptors of rat vascular tissue with increased adenosine 3',5'-monophosphate and relaxation of vascular smooth muscle. *Endocrinology* 119(1):349–356
  33. He DD, Tang XT, Dong W, Cui G, Peng G, Yin X, Chen Y, Jing N, Zhou BO (2020) C-kit expression distinguishes fetal from postnatal skeletal progenitors. *Stem Cell Rep* 14(4):614–630
  34. Portal-Nunez S, Lozano D, Esbrit P (2012) Role of angiogenesis on bone formation. *Histol Histopathol* 27:559–566
  35. Grüneboom A, Hawwari I, Weidner D, Culemann S, Müller S, Henneberg S, Henneberg S, Brenzel A, Merz S, Bornemann L, Zec K, Wuelling M, Kling L, Hasenberg M, Voortmann S, Lang S, Baum W, Ohs A, Kraff O, Quick HH, Jäger M, Landgraeber S, Dudda M, Danuser R, Stein JV, Rohde M, Gelse K, Garbe AI, Adamczyk A, Westendorf AM, Hoffmann D, Christiansen S, Engel DR, Vortkamp A, Krönke G, Herrmann M, Kamradt T, Schett G, Hasenberg A, Gunzer M (2019) A network of transcortical capillaries as mainstay for blood circulation in long bones. *Nat Metab* 1:236–250
  36. Marini M, Rosa I, Ibba-Manneschi L, Manetti M (2018) Telocytes in skeletal, cardiac and smooth muscle interstitium: morphological and functional aspects. *Histol Histopathol* 33:1151–1165

**Publisher's Note** Springer Nature remains neutral with regard to jurisdictional claims in published maps and institutional affiliations.

# 博士論文

---

**Histological alteration of bone specific-blood vessels in murine long  
bones with intermittent PTH administration**

(PTH 間歇投与によるマウス長管骨における骨特異  
的血管の組織学的変化)

---

令和2年3月申請

北海道大学  
大学院歯学研究科口腔医学専攻

趙 申

**Histological alteration of bone specific-blood vessels in murine long bones with intermittent PTH administration**

Zhao Shen

Oral and Maxillofacial Surgery, Graduate School of Dental Medicine, Hokkaido University, Sapporo, Japan

**Abbreviated Title: *Blood vessels in PTH-administered bone***

**#Address for correspondence:**

Zhao Shen

Oral and Maxillofacial Surgery,  
Graduate School of Dental Medicine, Hokkaido University

Kita 13 Nishi 7 Kita-ku

Sapporo, 060-8586, Japan

Tel/Fax: +81-11-706-4283

E-mail: [zhaoshen@den.hokudai.ac.jp](mailto:zhaoshen@den.hokudai.ac.jp)

## **Abstract**

It is well known that the intermittent administration of parathyroid hormone (PTH) promotes bone formation, but it remains to be unveiled if PTH could affect the distribution of bone-specific blood vessels and other cell-types surrounding the blood vessels. In this study, we have attempted to histologically examine bone-specific blood vessels after intermittent PTH administration. Six-week-old C57BL/6J mice received vehicle (control group) or 20 µg/kg/day of hPTH [1–34] (PTH group) for two weeks. The mice were then fixed and their femora and tibiae were examined for the immunohistochemical profile. The gene expression of bone was also examined by RT-PCR. In the control femoral metaphysis, there were many endomucin-positive/EphB4-positive blood vessels and few  $\alpha$ SMA-reactive blood vessels. In the PTH administered femoral metaphysis, the numbers of endomucin-positive/EphB4-positive blood vessels and their diameters were significantly expanded when compared to those of the control groups. Interestingly, blood vessels accompanied with  $\alpha$ SMA-positive cells were significantly increased in number in the PTH group, and were histochemically divided into two distinct types: the one surrounded by ALP-reactive/ $\alpha$ SMA-positive cells close to the bone surface, and the others accompanied merely with  $\alpha$ SMA-positive cells that showed a long cell shape extending thin cytoplasmic processes. In summary, the intermittent administration of PTH may affect both osteoblastic cells and bone-specific blood vessels.

**210 words**

**Keywords:** *blood vessel, bone, parathyroid hormone (PTH), endomucin, vascular smooth muscle cell*

## Introduction

Osteoporosis is a typical symptom in geriatric disease. For years, the first-line drug in therapy for osteoporosis has remained bisphosphonates [1]. However, it has been reported that bisphosphonates could be associated with severe complications such as osteonecrosis of the jaw or atypical femur fractures [2]. Over the last decade, teriparatide, which is a recombinant form of parathyroid hormone (PTH), has become the preferred drug for the treatment of osteoporosis [1, 3]. The anabolic action of PTH has also been demonstrated in clinical trials: PTH increased bone mass and reduced the fracture rate in patients with osteoporosis [4]. In our previous study, we have demonstrated that intermittent PTH administration promotes preosteoblastic proliferation and osteoblastic bone formation, both of which are finely tuned by cell coupling with osteoclasts, and finally induced new bone formation [5, 6].

Recently, Kusumbe and Ramasamy demonstrated two new disparate subtypes of endothelial cells in bone according to distribution and function: type H and type L [7]. The type H bone-specific subtype is a blood vessel that features CD31 and endomucin double strong positivity located underneath the growth plate in the metaphysis, while the type L subtype showed CD31 and endomucin low positivity in diaphysis [7, 8]. Endomucin<sup>high</sup>-positive bone-specific blood vessels have been shown to reciprocally interact with osteoblastic cells [7]. Endomucin<sup>high</sup>-positive endothelial cells have been reported to secrete noggin, supporting osteoblasts and chondrocytes, which secrete vascular endothelial growth factor (VEGF) sustaining angiogenesis in reverse [7, 8]. This may implicate the reciprocal interaction of blood vessels and osteoblastic cells in bone in a normal state.

It is well-known that blood vessels consist of various cell-types, being roughly divided into inner vascular endothelial cells and outer perivascular cells [9]. A vascular smooth muscle cell is a type of perivascular cell that always covers arteries/veins including arterioles and venules and appears to regulate vessel caliber [10].  $\alpha$ -Smooth muscle actin ( $\alpha$ SMA) is a specific marker of vascular smooth muscle cells and myofibroblasts [11]. The nutrient arteries and arterioles surrounded by vascular smooth muscle cells invade from the periosteum into the bone and run in the inner bone marrow region of the diaphyses of long bones [12]. However, the peripheral vascular smooth muscle cells gradually disappear to form sinusoidal capillaries that extend from the sinusoidal capillaries toward the chondro-osseous

junctions, where they are not covered by peripheral vascular smooth muscle cells and are sometimes surrounded by discontinuous basement membranes [10]. Therefore, perivascular cells including vascular smooth muscle cells will not always be adjacent to vascular endothelial cells, depending on the micro-circumstance of the blood vessels. It is assumed that perivascular cells such as vascular smooth muscle cells may not be fully differentiated but still possess the potential to differentiate into other cell types [10, 11, 13]. Indeed, it has been reported that arteries in bone are covered by  $\alpha$ SMA-positive smooth muscle cells that have the potential to differentiate into different mesenchymal lineages [14–16].

Recently, considerable reports have supported the importance of the interactions between EphB4 and ephrinB2 in the cardiovascular system and skeletal system [17, 18]. EphB4 is a marker for veins, while ephrinB2 is a marker for arteries. Since previous reports have suggested EphB4/ephrinB2 action as a coupling factor in bone [17], it may be possible for EphB4-positive veins/ephrinB2-reactive arteries to affect the activities of osteoblastic cells. Thus, PTH-driven anabolic effects may affect both osteoblastic cells and vascular endothelial cells and the surrounding perivascular cells including vascular smooth muscle cells. Alternately, it might be possible that PTH would directly affect vascular endothelial cells of bone-specific blood vessels and surrounding vascular smooth muscle cells. However, the biological effects of PTH on bone-specific blood vessels including vascular endothelial cells and surrounding vascular smooth muscle cells remain unknown.

Therefore, in this study we have attempted to histochemically examine the bone-specific blood vessels in long bone after intermittent PTH administration *in vivo*.

## **Materials and methods**

### ***Animals***

Six-week-old male C57BL/6J mice (n = 12, Japan CLEA, Tokyo, Japan) were divided into a control group and PTH group following the principles for animal care and research use set by Hokkaido University (approved No: 15-0032). The control group received vehicle (0.9% saline) while the PTH group received hPTH [1–34] (Sigma-Aldrich Co., LLC., St. Louis, MO). According to our previous report [6], the mice received 20 µg/kg/day of hPTH [1–34] twice per day. Intraperitoneal injections were performed at 8:00 am and 8:00 pm for two weeks. Mice were kept under standard conditions.

### ***Specimen preparation***

Before fixation, mice were anesthetized with an intraperitoneal injection of chloral hydrate for bodyweight determination. Then, all mice were perfused with 4% paraformaldehyde diluted in 0.1 M cacodylate buffer (pH 7.4) through the cardiac left ventricle. After perfusion with 4% paraformaldehyde solution, the femora and tibiae were extracted promptly and immersed in the same solution for 24 hours at 4°C. After washing in phosphate-buffered saline (PBS) for three days, all the samples were decalcified with 10% or 4.13% EDTA-2Na for paraffin-specimens and epoxy resin-specimens, respectively. For paraffin-embedded specimens, samples were dehydrated in ascending ethanol solutions, soaked in xylene, and finally embedded in paraffin. For epoxy resin-embedded specimens, samples were post-fixed with 1% osmium tetroxide in a 0.1 M cacodylate buffer for eight hours at 4°C, dehydrated in ascending acetone solutions, and finally embedded with epoxy resin (Epon 812).

### ***Histological and immunohistochemical detection***

Dewaxed paraffin sections were examined for endomucin, αSMA, EphB4 and ephrin B2 as previously examined [5]. The sections were treated for endogenous peroxidase inhibition with 0.3% H<sub>2</sub>O<sub>2</sub> in PBS for 30 mins, and subsequently for nonspecific staining blocking by 1% bovine serum albumin (BSA; Serologicals Proteins Inc. Kankakee, IL) in PBS (1% BSA-PBS) for 20 mins at room temperature. Then, sections were incubated with rat antibody against endomucin (Santa Cruz Biotechnology, Inc., Dallas, TX) at a dilution of 1:100 and 4°C overnight. Following

several washings in PBS, they were incubated with horseradish peroxidase (HRP)-conjugated anti-rat IgG (Zymed Laboratories Inc., South San Francisco, CA) at a dilution of 1:100. To detect  $\alpha$ SMA, the dewaxed sections treated with 1% BSA–PBS were incubated with mouse antibody against  $\alpha$ SMA (Thermo Fisher Scientific Inc., Cheshire, UK) at a dilution of 1:400 and 4°C overnight. Then, the sections were incubated with HRP-conjugated rabbit anti-mouse IgG (Bethyl Laboratories, Inc., Montgomery, TX). For the detection of EphB4 and ephrinB2, the dewaxed sections were reacted with goat antibody against mouse EphB4 (R&D Systems Inc., Minneapolis, MN) at a dilution of 1:50 or with goat antibody against mouse ephrinB2 (R&D Systems Inc., Minneapolis, MN) at a dilution of 1:50 and 4°C overnight. After several washings in PBS, they were incubated with HRP-conjugated rabbit anti-goat IgG (American Qualex Scientific Products, Inc., San Clemente, CA) for 1 h. Immune complexes of all sections were visualized using 3, 3'-diaminobenzidine tetrahydrochloride (Dojindo Laboratories, Kumamoto, Japan). Then, specimens were observed under a Nikon Eclipse Ni microscope (Nikon Instruments Inc. Tokyo, Japan), and light microscopic images were acquired with a digital camera (Nikon DXM1200C, Nikon).

#### ***Double immunohistochemical and immunofluorescence staining***

For  $\alpha$ SMA/endomucin double immunohistochemical staining procedures, dewaxed paraffin sections were incubated with 1% BSA–PBS and then with mouse antibody against  $\alpha$ SMA (Thermo Fisher Scientific Inc.) at a dilution of 1:400 with 1% BSA–PBS. After that, they were incubated with fluorescein (FITC)-conjugated goat anti-mouse IgG (MP Biomedicals. LLC., Solon, OH) at a dilution of 1:100 with 1% BSA–PBS and then incubated with rat antibody against endomucin at a dilution of 1:100 at 4°C after washing with PBS. Sections were subsequently reacted with Alexa 594-conjugated rabbit anti-rat IgG (Thermo Fisher Scientific Inc., Cheshire, UK) at a dilution of 1: 100. For the detection of  $\alpha$ SMA and ALP, dewaxed paraffin sections were incubated with 1% BSA–PBS and then with mouse antibody against  $\alpha$ SMA (Thermo Fisher Scientific Inc.) at a dilution of 1:400 with 1% BSA–PBS; then, they were incubated with fluorescein (FITC)-conjugated goat anti-mouse IgG (MP Biomedicals. LLC., Solon, OH) at a dilution of 1:100. After PBS washing, the sections were reacted with rabbit polyclonal antisera against TNALP at a dilution of 1:300 with 1% BSA–PBS; then, they were incubated with Alexa Fluor



594-conjugated goat anti-rabbit IgG (Thermo Fisher Scientific, Inc, Waltham, MA) at a dilution of 1:100 with 1% BSA-PBS for 1 h. All sections were embedded by VECTASHIELD hard-set mounting medium with DAPI (Vector Laboratories, Inc. Burlingame, CA) and observed under light microscopy.

### ***Toluidine blue staining***

Semi-thin sections were prepared with an ultramicrotome and were then stained with toluidine blue staining and observed under a Nikon microscope. Light microscopy images were acquired with a digital camera.

### ***Static parameters for bone histomorphometry***

A 800×1000 µm Region of Interest (ROI) located underneath the growth plate of femoral metaphysis was employed to assess the following static parameters: number of endomucin-positive, αSMA-positive, EphB4-positive, and ephrinB2-positive blood vessels, maximum diameter (length of longest line joining two points of blood vessel's outline and passing through the centroid)/minimum diameter (length of the shortest line joining two points in the blood vessel's outline and passing through the centroid)/mean diameter (average length of diameters measured at 2 degree intervals and passing through the blood vessel's centroid) of the endomucin-immunopositive blood vessels, area of the endomucin-reactive blood vessels. Images of the ROI stained for endomucin/αSMA, EphB4, ephrinB2 from the control groups and PTH groups (n = 6 for each group) were used to determine the number of each kind of vessel and the external diameter of the endomucin-immunoreactive blood vessel within the ROI were measured with Image-Pro Plus 6.2 (Media Cybernetics, Inc., Bethesda MD); the results were later statistically analyzed as follows.

### ***RT-PCR assessment***

Total RNA was extracted from fresh frozen femora and tibiae using TRIzol reagent (Life Technologies Co., Carlsbad, CA). For RT-PCR, total RNA was reverse transcribed to cDNA using SuperScript VILO cDNA Synthesis Kit (Life Technologies). For PCR amplification, the following primer sets were used: (forward) 5'- TGTCTTCACCACCATGGAGAAGG -3' and (reverse) 5'- GTGGATGCAGGGATGATGTTCTG -3' for GAPDH, (forward) 5'- CTATGAAAATAACAGTGCCAAATACTCCAA -3' and (reverse) 5'-

AGGATCCATCACGATGTCAGTTCTTGGTTT -3' for endomucin, and (forward) 5'-  
GTATGTGGCTATTCAGGCTG -3' and (reverse) 5'-  
CTTCTGCATCCTGTCAGCAA -3' for  $\alpha$ -SMA, (forward) 5'-  
CCCAAATAGGAGACGAGTCC -3' and (reverse) 5'-  
CTCAAAAGGAGGTGGTCCAG -3' for EphB4, and (forward) 5'-  
TCCAGGAGGGACTCTGTGTGGAAG -3' and (reverse)  
5'-CGGGGTATTCTCCTTCTTAATTGT -3' for ephrinB2. PCR products were  
electrophoresed on a 2% agarose gel containing ethidium bromide and visualized with  
UV light.

### *Statistical analysis*

All statistical analyses were carried out using SPSS version 18.0.0 and analyzed for statistical significance by Student's t-test. Data values were presented as mean  $\pm$  SE. For the study, any p-value of 0.05 was considered statistically significant.

## Results

### *Altered distribution of bone specific-blood vessels after intermittent PTH administration*

Metaphyseal trabeculae and the trabecular bone mass were increased in femora of the PTH group compared with the control group (**Figure 1A–B**). After PTH administration, the number of endomucin-positive blood vessels appeared to increase histologically and their diameters seemed to expand compared to the control groups (**Figure 1C–D**). Therefore, we measured the cross-sectioned maximum diameter, the minimum diameter, and the mean diameter of the endomucin-reactive blood vessels in the ROI of 800  $\mu\text{m}$  x 1,000  $\mu\text{m}$  (**Figure 1E**). One consequence of intermittent PTH administration is that the indices of the maximum and mean diameter of the endomucin-immunoreactive blood vessels were significantly higher than those of the control specimens. The average maximum diameter of the endomucin-immunoreactive blood vessels in the control group were  $224.53 \pm 10.06$   $\mu\text{m}$  and the average mean diameter of the endomucin-reactive blood vessels was  $121.37 \pm 4.76$   $\mu\text{m}$ . In the PTH group, the average maximum diameter and mean diameter of the endomucin-reactive blood vessels were  $339.22 \pm 14.58$   $\mu\text{m}$  ( $p < 0.01$  vs. control) and  $144.01 \pm 4.63$   $\mu\text{m}$  ( $p < 0.05$  vs. control), respectively. There was no significant difference in the minimum diameter of the endomucin-positive blood vessels between the control group and the PTH group as shown in **Figure 1E**. The average minimum diameter of the endomucin-reactive blood vessels was  $73.16 \pm 2.94$   $\mu\text{m}$  in the control group and  $73.26 \pm 2.32$   $\mu\text{m}$  in the PTH group. Additionally, we examined the cross-section areas of the endomucin-immunopositive blood vessels in the ROI (**Figure 1F**). After intermittent PTH administration, the area of the endomucin-reactive blood vessels had significantly increased: The cross-sectioned areas of the endomucin-immunopositive blood vessels were  $19,841.02 \pm 2,585.61$   $\mu\text{m}^2$  in the control group and  $28,652.31 \pm 2,413.11$   $\mu\text{m}^2$  in the PTH group ( $p < 0.05$ ).

### *Immunolocalization of $\alpha\text{SMA}$ -immunoreactive, EphB4-immunoreactive and ephrinB2-immunoreactive cells in PTH-administrated blood vessels*

The number of  $\alpha\text{SMA}$ -immunopositive cells was markedly-increased in the vicinity of endomucin-reactive blood vessels after PTH administration. There was a huge number of  $\alpha\text{SMA}$ -reactive blood vessels in the metaphyses by PTH administration,

while there seemed a few  $\alpha$ SMA-positive blood vessels in the control counterparts (**Figure 2A–C**). In addition, the numbers of EphB4-positive blood vessels and ephrinB2-positive arteries increased in PTH-treated metaphyses when compared with those in the control specimens (**Figure 2 D–I**).

Using the immunostained sections, we counted the number of each type of blood vessel in the ROI underneath the growth plate. After intermittent PTH administration, the numbers of endomucin-positive,  $\alpha$ SMA-positive, EphB4-positive, and ephrinB2-positive blood vessels were significantly increased (**Figure 2J**). The numbers of endomucin-positive,  $\alpha$ SMA-positive, EphB4-positive, and ephrinB2-positive blood vessels in the control group were  $50.17 \pm 18.45$ ,  $3.50 \pm 2.17$ ,  $63.00 \pm 18.01$ , and  $4.00 \pm 1.55$ , respectively. The numbers of endomucin-positive,  $\alpha$ SMA-positive, EphB4-positive, and ephrinB2-positive blood vessels in the PTH group were  $82.33 \pm 14.63$ ,  $26.67 \pm 7.58$ ,  $147 \pm 42.37$ , and  $21.5 \pm 4.84$ , respectively ( $p < 0.01$  vs. control). When examined by RT-PCR, the gene expressions of endomucin,  $\alpha$ SMA, EphB4, and ephrinB2 in the femora consistently appeared elevated after PTH administration (**Figure 2K**).

*The distribution of  $\alpha$ SMA-immunoreactive cells surrounding endomucin-immunoreactive blood vessels in PTH-administered metaphyses*

Some  $\alpha$ SMA-immunopositive cells seemed closely associated with endomucin-positive vascular endothelial cells, being identical to vascular smooth muscle cells. However, the others were located somewhat apart from the blood vessels, and therefore appeared to be cell-types other than vascular smooth muscle cells (**Figure 3A–D**). To define the characteristics of  $\alpha$ SMA-positive cells not identical to vascular smooth muscle cells, we examined the double immunodetection of ALP and  $\alpha$ SMA, and consequently divided them into two distinct cell-types (**Figure 3E–H**): the  $\alpha$ SMA-positive cells bearing ALP-reactivity located in close proximity to the blood vessels in the intertrabecular regions (**Figure 3E and G**), and the  $\alpha$ SMA-positive but ALP-negative cells that extend long cell bodies and thin cytoplasmic processes (**Figure 3F and H**). Taken together, three  $\alpha$ SMA-positive cell-types appeared after PTH administration:  $\alpha$ SMA-positive vascular smooth muscle cells,  $\alpha$ SMA/ALP double-positive cells close but not adjacent to blood vessels, and  $\alpha$ SMA-positive/ALP-negative cells that extend their straightly extending cytoplasmic processes. Thus, it appears that the cellular population surrounding the

blood vessels changes after PTH administration. Therefore, we examined the corresponding region using semi-thin sections (**Figure 4**). Two distinct cell-types were shown to be located around blood vessels in the femoral metaphysis of the PTH-administered mice (**Figure 4B–D**). One was the cells revealing a long cell-shape with thin cytoplasmic processes distant from bone, and the other was the cells containing several cell organelles in the somehow translucent cytoplasm.

## Discussion

In this study, we have attempted to histologically demonstrate the altered distribution of bone-specific blood vessels in murine bone after intermittent PTH administration. Our main histological findings can be summarized as follows:

- 1) Intermittent PTH administration increased the number of endomucin-positive blood vessels and significantly expanded their diameter.
- 2) The numbers of  $\alpha$ SMA-positive, ephrinB2-positive, and EphB4-positive blood vessels also increased after PTH administration.
- 3)  $\alpha$ SMA-positive cells were markedly-increased in number and can be distinctively divided into the first type,  $\alpha$ SMA-positive vascular smooth muscle cells closely surrounding the endomucin-reactive vascular endothelial cells, the second type,  $\alpha$ SMA/ALP double-positive cells close but not adjacent to blood vessels, and the third type,  $\alpha$ SMA-positive but ALP-negative cells extending their straightly extending cytoplasmic processes.

To our knowledge, this is the first report to suggest that the intermittent administration of PTH affects bone-specific blood vessels in bone.

One may wonder why we have employed regimens of two- and four-times administration of PTH each day. Using murine models, we have recently demonstrated that the high frequency of intermittent PTH administration (two or four times per day) promotes bone remodeling by stimulating both bone resorption and formation, while low-frequency PTH administration (once a day or per two days) caused both remodeling-based/mini-modeling-based bone formation [6]. In addition, we have reported that high-frequency PTH administration stimulated preosteoblastic proliferation and subsequent osteoblastic differentiation by mediating cell coupling with osteoclasts [5]. Therefore, the anabolic effects of PTH appear to be based on accelerated preosteoblastic proliferation and finely-tuned cell coupling with osteoclasts.

These cellular events take place in the region of mature osteoblasts including preosteoblastic cells, bone marrow-stromal cells, and blood vessels rather than in the region of the osteocytic network embedded in bone, although many investigators have suggested that PTH-driven anabolic action is reportedly mediated by the sclerostin/Wnt pathway of osteocytes [21, 22]. In accordance with our previous

reports, we decided to employ high-frequency PTH administration in this study rather than low-frequency to ensure adequate regimens to examine the bone specific-blood vessels and the surrounding cells; consequently, we were able to observe the significant alteration of bone specific-blood vessels by PTH.

Regarding the biological actions of blood vessels in bone, many studies have paid close attention to the intimate connection between blood vessels and bone tissues [23]. Since bone is highly vascularized tissue, it has been previously assumed that blood vessels serve as a tunnel by which to transmit oxygen, nutrition, growth factors, and hormones into the bone and take part in the hematopoiesis of neighboring bone marrow [9]. Recently, it has been demonstrated that there is a network of trans-cortical capillaries as a mainstay for blood circulation in long bone [24]. Literally, Kusumbe and Ramasamy et al. reported a bone-specific subtype of blood vessels featuring CD31<sup>high</sup>/endomucin<sup>high</sup>, and illuminated that angiogenesis also plays an important role in bone development and remodeling [7, 8]. Endomucin<sup>high</sup>-positive blood vessels in the metaphyses of long bone have been shown to reciprocally interact with osteoblastic cells requiring various cytokines, microRNA, and signaling pathways. Thus, while recent studies on bone/blood vessel interaction have progressed, few reports have elucidated the biological action of PTH on bone-specific blood vessels.

In the present study, intermittent PTH administration increased the number of endomucin-immunoreactive/EphB4-positive blood vessels and the maximum/mean diameters and area of endomucin-positive blood vessels in the metaphyses of murine femora and tibiae. Since most blood vessels in this area are capillaries that are not surrounded by vascular smooth muscle cells, the enlargement of blood vessels in this area seems non-ascribable to the relaxation of vascular smooth muscle cells but is rather probably due to morphological changes in the capillaries. In addition, we assume that the reason why blood vessels increased in number might be due to angiogenesis stimulated by PTH. Another interpretation may be that PTH mainly reacts to the development and remodeling of bone by the classical Wnt/ $\beta$ -catenin pathway [22], which might be able to react to the angiogenesis by the VEGF-relevant pathway. However, further investigation is necessary to define the cellular mechanism of the increased numbers and diameters of capillaries after PTH administration.

We have observed that three  $\alpha$ SMA-positive cell-types appear after PTH administration: the first is  $\alpha$ SMA-positive vascular smooth muscle cells closely

surrounding the endomucin-reactive vascular endothelial cells, the second is  $\alpha$ SMA/ALP double-positive cells close but not adjacent to blood vessels, and the third is  $\alpha$ SMA-positive but ALP-negative cells extending their straightly extending cytoplasmic processes. The first appears to be vascular smooth muscle cells, but the other two might be other cell-types. Since the control vascular endothelial cells were hardly accompanied by  $\alpha$ SMA-positive vascular smooth muscle cells in the metaphyses, it seems likely that undifferentiated perivascular cells might differentiate into vascular smooth muscle cells by PTH administration.  $\alpha$ SMA-positive/ALP-reactive cells that were located close but not adjacent to endomucin-positive/ $\alpha$ SMA-reactive blood vessels seem different to vascular smooth muscle cells even though they showed  $\alpha$ SMA-immunoreactivity. It has been previously reported that arteries in bone were covered by  $\alpha$ SMA-positive/NG2-reactive vascular smooth muscle cells [14], possessing the potential to differentiate into other mesenchymal lineages [7, 8]. Therefore,  $\alpha$ SMA-positive/ALP-reactive cells close to the blood vessels might be derived from vascular smooth muscle cells that have differentiated from perivascular cells. Alternately, perivascular cells may have directly differentiated into  $\alpha$ SMA-positive/ALP-reactive cells. A previous study indicated that PTH may promote vascularized bone regeneration and directly improve blood vessel formation and the osteogenic potential of aged bone marrow mesenchymal stem cells [25]. Since ALP is an important bone metabolic marker expressed in the osteoblastic lineage [26–28] that also comes from bone marrow mesenchymal cells, these cells may be able to differentiate into preosteoblasts/osteoblasts. Taken together, it may be possible for PTH to stimulate perivascular cells to differentiate into either vascular smooth muscle cells or an ALP-positive osteoblastic lineage.

Regarding  $\alpha$ SMA-positive/ALP-negative cells with long cell bodies and thin cytoplasmic processes located in middle of the intertrabecular region, this cell-type extends long cytoplasmic processes linearly parallel to the bone surface. Judging from the cell shape and long cytoplasmic processes, this may be a kind of telocyte that was discovered in 2003 [29]. Telocytes are fibroblast-like cells extending extremely long but thin prolongations. There has not yet been any report of the discovery of telocytes in bone and further examination is warranted. Taken together, bone specific-blood vessels may play an important role in the bone formation process.

In summary, the intermittent administration of PTH may affect both osteoblastic



cells and bone-specific blood vessels.

## References

1. Schweser KM, Crist BD (2017) Osteoporosis: a discussion on the past 5 years. *Curr Rev Musculoskelet Med* 10: 265–274
2. Kim SC, Kim DH, Mogun H, Eddings W, Polinski JM, Franklin JM, Solomon DH (2016) Impact of the U.S. food and drug administrations safety-related announcements on the use of bisphosphonates after hip fracture. *J Bone Miner Res* 31: 1536–1540
3. Orwoll E, Scheele W, Paul S, Adami S, Syversen U, Diez-Perez A, Kaufman JM, Clancy AD, Gaich GA (2003) The effect of teriparatide [human parathyroid hormone (1–34)] therapy on bone density in men with osteoporosis. *J Bone Miner Res* 18: 9–17
4. Skripitz R, Aspenberg P (2004) Parathyroid hormone--a drug for orthopedic surgery? *Acta Orthop Scand* 75: 654–662
5. Luiz de Freitas PH, Li M, Ninomiya T, Nakamura M, Ubaidus S, Oda K, Udagawa N, Maeda T, Takagi R, Amizuka N (2009) Intermittent PTH administration stimulates pre-osteoblastic proliferation without leading to enhanced bone formation in osteoclast-less c-fos(-/-) mice. *J Bone Miner Res* 24: 1586–1597
6. Yamamoto T, Hasegawa T, Sasaki M, Hongo H, Tsuboi K, Shimizu T, Ohta M, Haraguchi M, Takahata T, Oda K, Freitas PHL, Takakura A, Takao-Kawabata R, Isogai Y, Amizuka N (2016) Frequency of teriparatide administration affects the histological pattern of bone formation in young adult male mice. *Endocrinology* 157: 2604–2620
7. Kusumbe AP, Ramasamy SK, Adams RH (2014) Coupling of angiogenesis and osteogenesis by a specific vessel subtype in bone. *Nature* 507: 323–328
8. Ramasamy SK, Kusumbe AP, Wang L, Adams RH (2014) Endothelial Notch activity promotes angiogenesis and osteogenesis in bone. *Nature* 507: 376–380
9. Sivaraj KK, Adams RH (2016) Blood vessel formation and function in bone. *Development* 143: 2706–2715
10. Armulik A, Genove G, Betsholtz C (2011) Pericytes: developmental, physiological, and pathological perspectives, problems, and promises. *Dev Cell* 21: 193–215

11. Aizman I, Holland WS, Yang C, Bates D (2016) alphaSMA Expression in Large Colonies of Colony-Forming Units-Fibroblast as an Early Predictor of Bone Marrow MSC Expandability. *Cell Med* 8: 79–85
12. Ramasamy SK (2017) Structure and functions of blood vessels and vascular niches in bone. *Stem Cells Int* 2017: 5046953
13. Matthews BG, Greecevic D, Wang L, Hagiwara Y, Roguljic H, Joshi P, Shin DG, Adams DJ, Kalajzic I (2014) Analysis of alphaSMA-labeled progenitor cell commitment identifies notch signaling as an important pathway in fracture healing. *J Bone Miner Res* 29: 1283–1294
14. Kusumbe AP, Ramasamy SK, Itkin T, Mae MA, Langen UH, Betsholtz C, Lapidot T, Adams RH (2016) Age-dependent modulation of vascular niches for haematopoietic stem cells. *Nature* 532: 380–384
15. Kunisaki Y, Bruns I, Scheiermann C, Ahmed J, Pinho S, Zhang D, Mizoguchi T, Wei Q, Lucas D, Ito K, Mar JC, Bergman A, Frenette PS (2013) Arteriolar niches maintain haematopoietic stem cell quiescence. *Nature* 502: 637–643
16. Mendez-Ferrer S, Michurina TV, Ferraro F, Mazloom AR, Macarthur BD, Lira SA, Scadden DT, Maayan A, Enikolopov GN, Frenette PS (2010) Mesenchymal and haematopoietic stem cells form a unique bone marrow niche. *Nature* 466: 829–834
17. Rundle CH, Xing W, Lau KW, Mohan S (2016) Bidirectional ephrin signaling in bone. *Osteoporos Sarcopenia* 2: 65–76
18. Zhao C, Irie N, Takada Y, Shimoda K, Miyamoto T, Nishiwaki T, Suda T, Matsuo K (2006) Bidirectional ephrinB2-EphB4 signaling controls bone homeostasis. *Cell Metab* 4: 111–121
19. Ng YS, Ramsauer M, Loureiro RM, D'Amore PA (2004) Identification of genes involved in VEGF-mediated vascular morphogenesis using embryonic stem cell-derived cystic embryoid bodies. *Lab Invest* 84: 1209–1218
20. Allan EH, Hausler KD, Wei T, Gooi JH, Quinn JM, Crimeen-Irwin B, Pompolo S, Sims NA, Gillespie MT, Onyia JE, Martin TJ (2008) EphrinB2 regulation by PTH and PTHrP revealed by molecular profiling in differentiating osteoblasts. *J Bone Miner Res* 23: 1170–1181
21. Du JH, Lin SX, Wu XL, Yang SM, Cao LY, Zheng A, Wu JN, Jiang XQ (2019) The function of Wnt ligands on osteocyte and bone remodeling. *J Dent Res* 98:

930–938.

22. Baron R, Hesse E (2012) Update on bone anabolics in osteoporosis treatment: rationale, current status, and perspectives. *J Clin Endocrinol Metab* 97: 311–325
23. Portal-Nunez S, Lozano D, Esbrit P (2012) Role of angiogenesis on bone formation. *Histol Histopathol* 27: 559–566
24. Grüneboom A, Hawwari I, Weidner D, Culemann S, Müller S, Henneberg S, Henneberg S, Brenzel A, Merz S, Bornemann L, Zec K, Wuelling M, Kling L, Hasenberg M, Voortmann S, Lang S, Baum W, Ohs A, Kraff O, Quick HH, Jäger M, Landgraeber S, Dudda M, Danuser R, Stein JV, Rohde M, Gelse K, Garbe AI, Adamczyk A, Westendorf AM, Hoffmann D, Christiansen S, Engel DR, Vorkamp A, Krönke G, Herrmann M, Kamradt T, Schett G, Hasenberg A, Gunzer M (2019) A network of trans-cortical capillaries as mainstay for blood circulation in long bones. *Nature Metabolism* 1:236–250
25. Jiang L, Zhang W, Wei L, Zhou Q, Yang G, Qian N, Tang Y, Gao Y, Jiang X (2018) Early effects of parathyroid hormone on vascularized bone regeneration and implant osseointegration in aged rats. *Biomaterials* 179:15–28
26. Rey A, Manen D, Rizzoli R, Ferrari SL, Caverzasio J (2007) Evidences for a role of p38 MAP kinase in the stimulation of alkaline phosphatase and matrix mineralization induced by parathyroid hormone in osteoblastic cells. *Bone* 41: 59–67
27. Nakajima A, Shimoji N, Shiomi K, Shimizu S, Moriya H, Einhorn TA, Yamazaki M (2002) Mechanisms for the enhancement of fracture healing in rats treated with intermittent low-dose human parathyroid hormone (1-34). *J Bone Miner Res* 17: 2038–2047
28. Hirota S, Takaoka K, Hashimoto J, Nakase T, Takemura T, Morii E, Fukuyama A, Morihana K, Kitamura Y, Nomura S (1994) Expression of mRNA of murine bone-related proteins in ectopic bone induced by murine bone morphogenetic protein-4. *Cell and tissue research* 277: 27–32
29. Marini M, Rosa I, Ibbá-Manneschi L, Manetti M (2018) Telocytes in skeletal, cardiac and smooth muscle interstitium: morphological and functional aspects. *Histol Histopathol* 33:1151–1165

## Figure legends

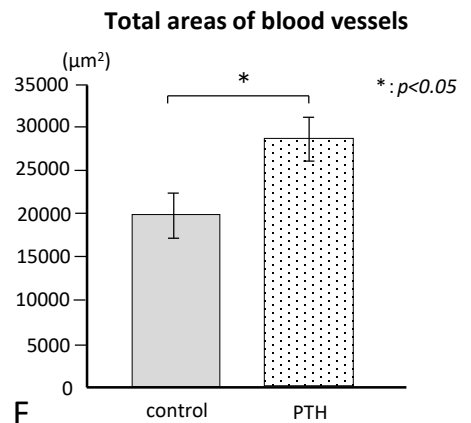
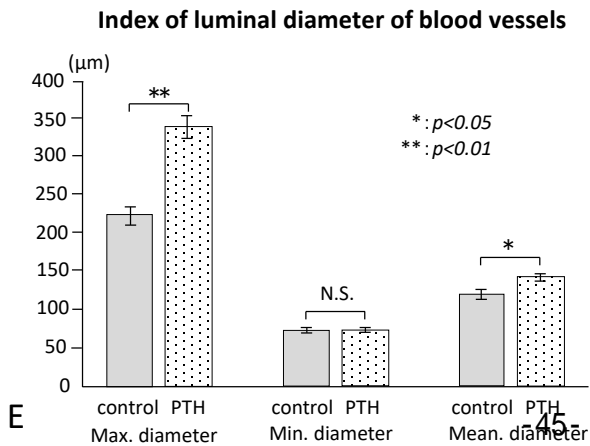
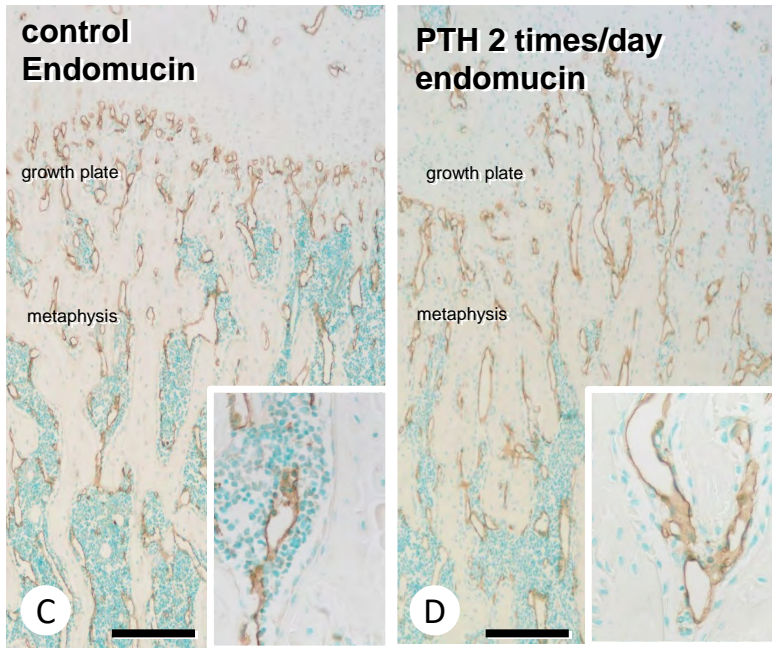
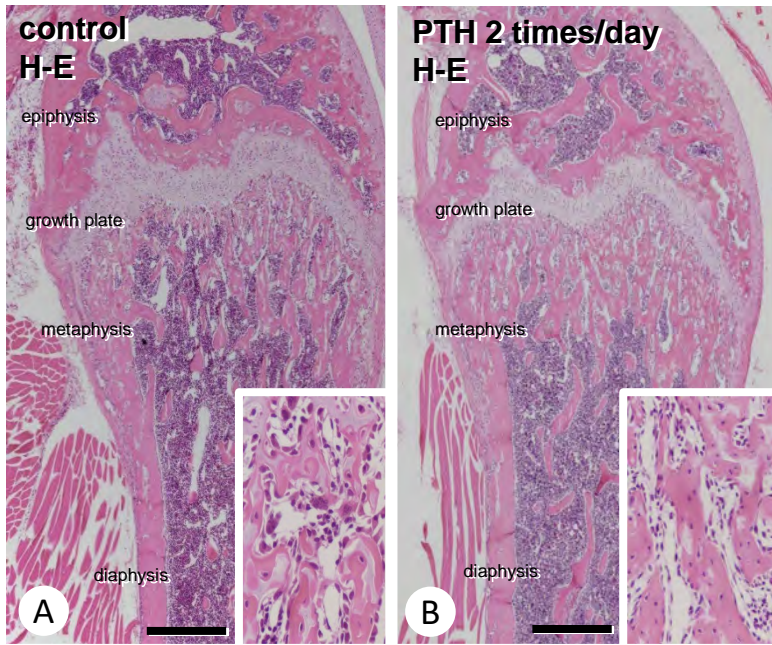
**Fig. 1** HE staining of the control mice's femora (A) and PTH-administered mice's femora (B). The bone mass increased in the PTH-administered mice (B) compared to the control groups (A). In the metaphysis of the femora, the diameter of the endomucin-positive blood vessels (brown color) tended to expand in PTH mice (D) compared to control mice (C). Graph E showed the index of the luminal diameter of endomucin-positive blood vessels. After PTH administration, the maximum and mean diameter of the endomucin-positive blood vessels were significantly increased compared to the control group (\*  $p < 0.05$ , \*\*  $p < 0.01$ ). Graph F demonstrated the total areas of the endomucin-positive blood vessels in the ROI. The area of the endomucin-positive blood vessels was significantly expanded after PTH injection ( $p < 0.05$ ). Bars: A, B: 500  $\mu\text{m}$  C, D: 200  $\mu\text{m}$

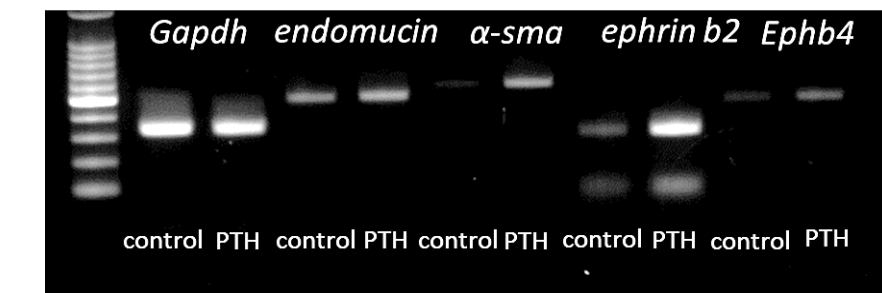
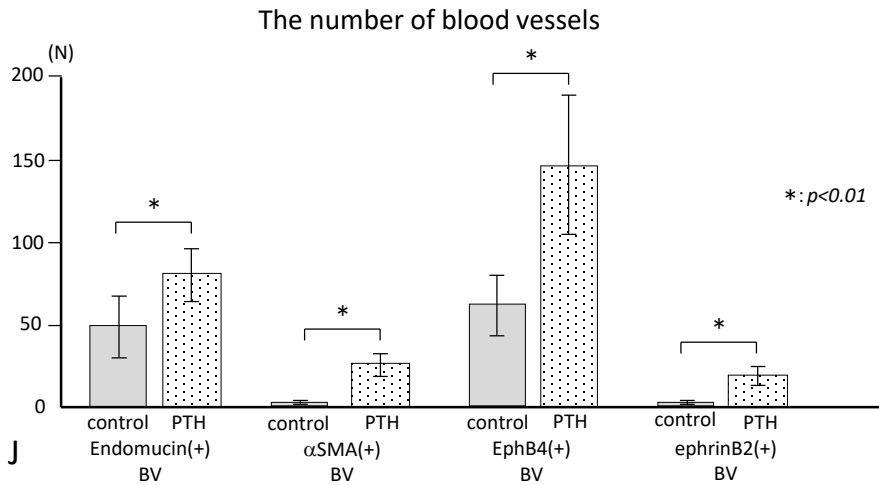
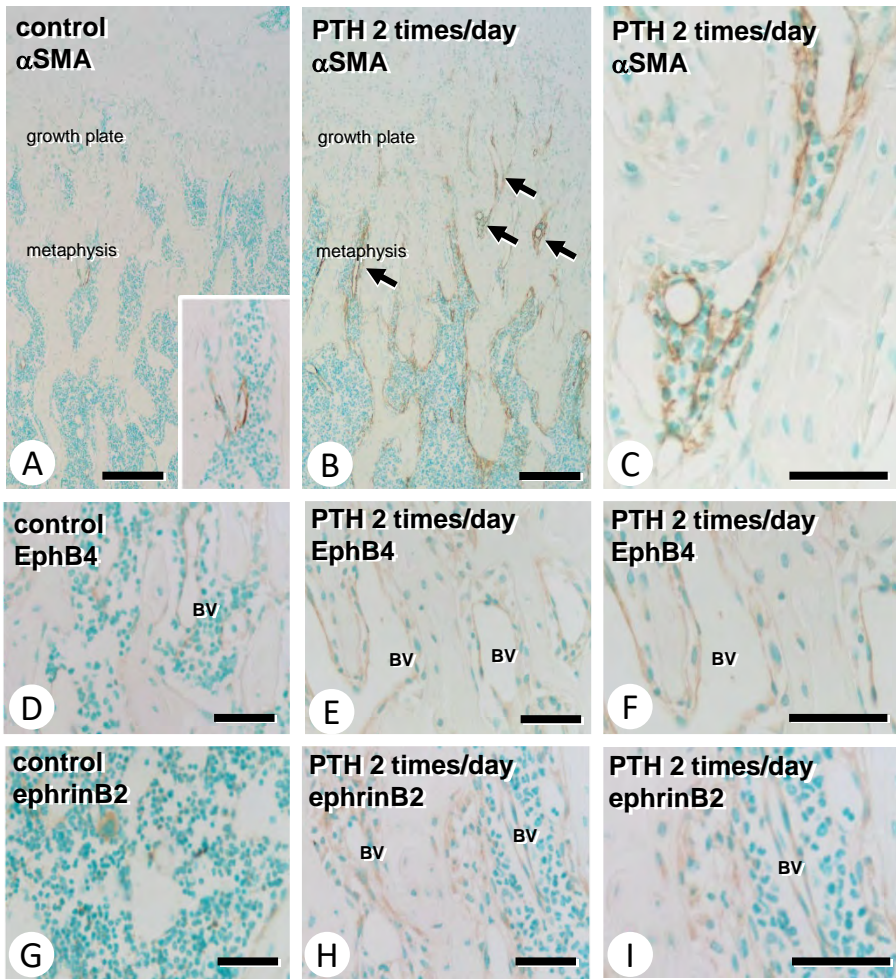
**Fig. 2** In the metaphysis, both  $\alpha\text{SMA}$ -positive blood vessels (brown color) and  $\alpha\text{SMA}$ -immunopositive cells close to the endomucin-reactive blood vessels tended to increase in PTH-administered groups (B and C) compared to the control group (A). Figures D–F demonstrated the immunolocalization of EphB4 (brown color) and Figures G–I showed the immunolocalization of ephrinB2 (brown color) in the control and PTH-administered groups. The number of endomucin-,  $\alpha\text{SMA}$ -, EphB4-, and ephrinB2-positive blood vessels were significantly increased in PTH mice, respectively (J,  $p < 0.01$ ). The gene expressions of *Endomucin*,  *$\alpha$ -sma*, *Ephrinb2*, and *Ephb4* were also increased by RT-PCR analysis (K). BV: blood vessel  
Bars: A, B: 200  $\mu\text{m}$  C–I: 50  $\mu\text{m}$

**Fig. 3** After PTH administration,  $\alpha\text{SMA}$ -immunoreactivity (brown color: A and B; green color: C and D) were localized on the vascular smooth muscle cells associated with endomucin-positive vascular endothelial cells and other types of cells other than the blood vessels (arrows: B and D). ALP (blue color: E and F; red color: G and H) and  $\alpha\text{SMA}$  (brown color: E and F; green color: G and H) double staining demonstrated 1) ALP-positive/ $\alpha\text{SMA}$ -positive cells close to the blood vessels (G), and 2) ALP-negative/ $\alpha\text{SMA}$ -positive cells extending long cell bodies and thin cytoplasmic

processes in the PTH-administered groups (arrows, H). BV: blood vessel  
Bars: A, B: 200  $\mu\text{m}$  C–I: 50  $\mu\text{m}$

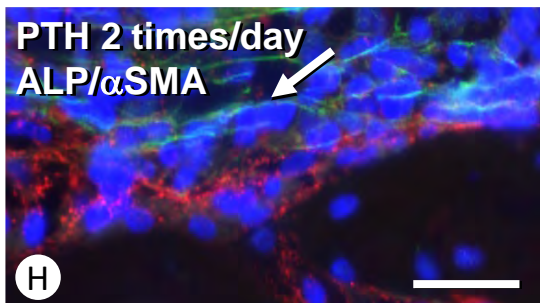
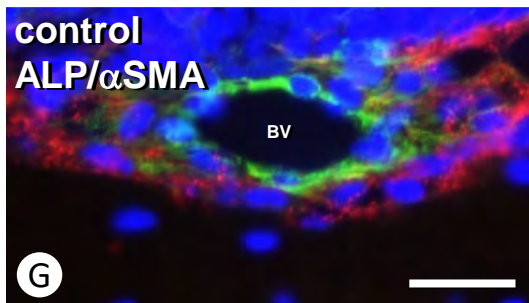
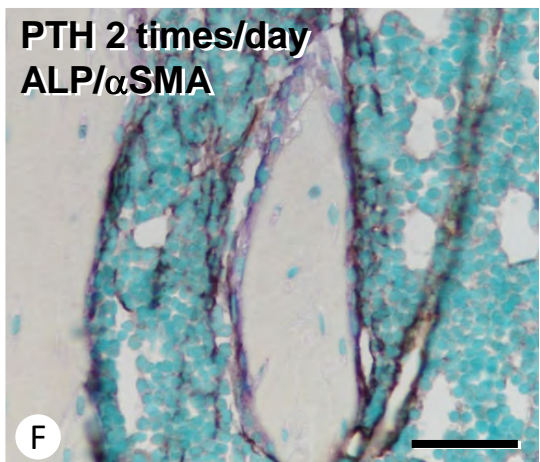
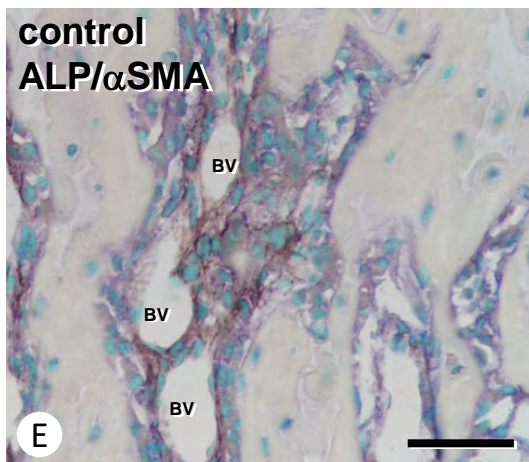
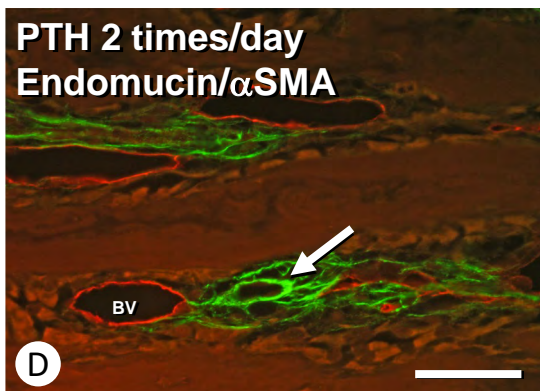
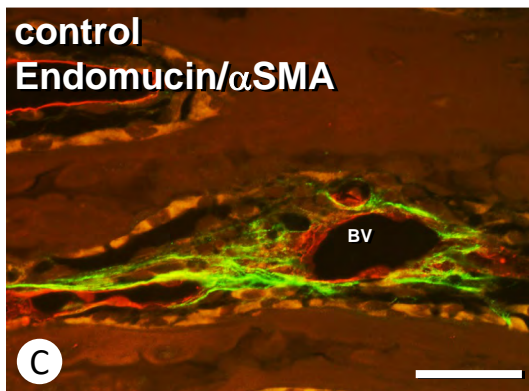
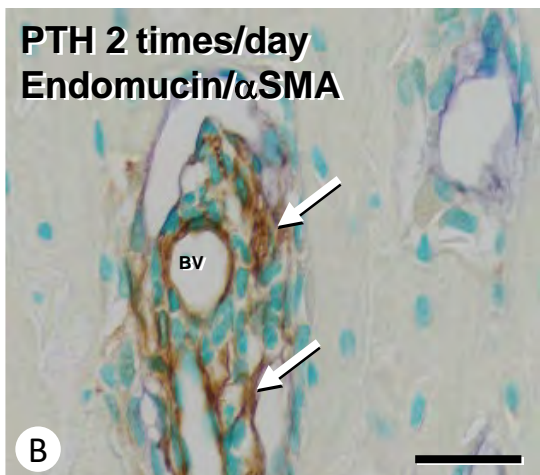
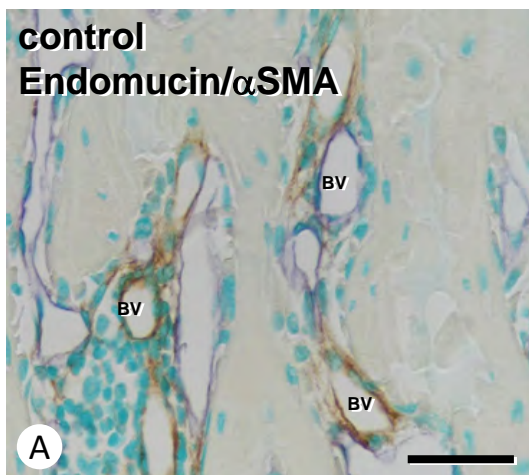
**Fig. 4** The semi-thin section obtained from the PTH group demonstrated two different type of cells in the bone marrow region over the osteoblasts (C–D). One is the spindle cell that reveals a long shape with thin cytoplasmic processes distant from the bone (inset, D), and the other is cuboidal cells that appeared to contain several cell organelles (arrows, D). ob: osteoblast; BV: blood vessel.  
Bars: A, B: 50  $\mu\text{m}$  C, D: 20  $\mu\text{m}$

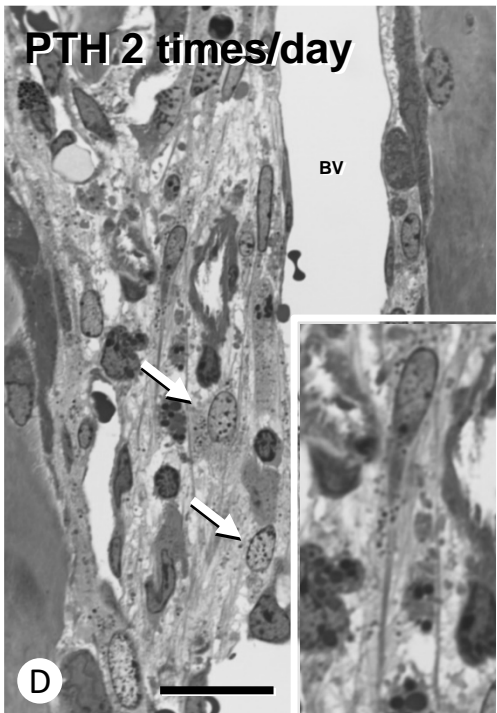
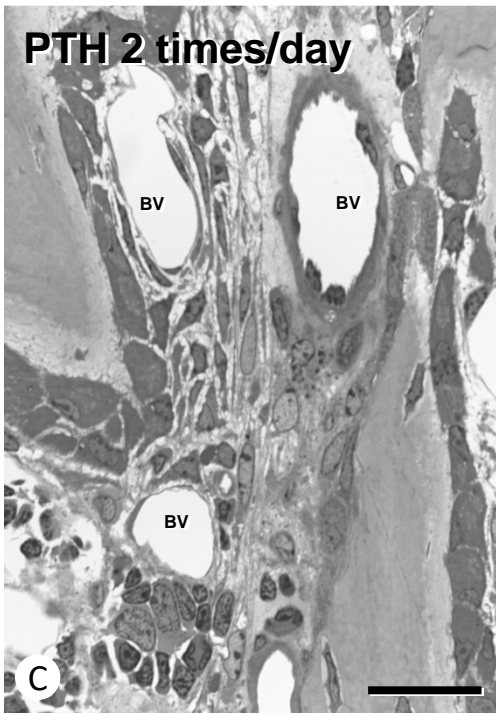
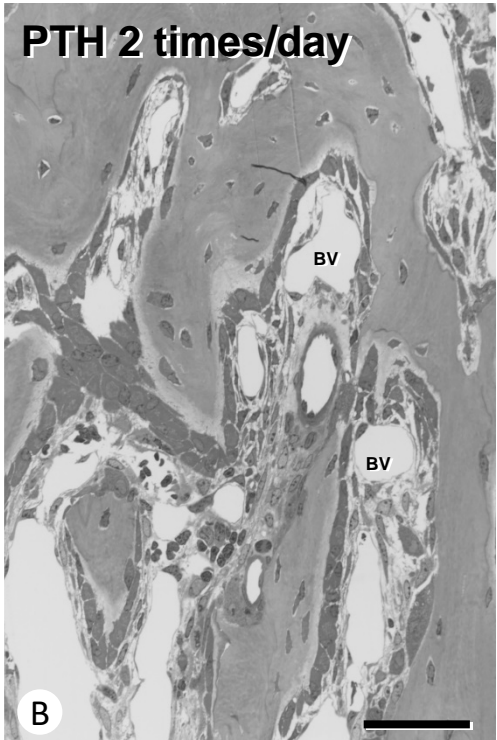
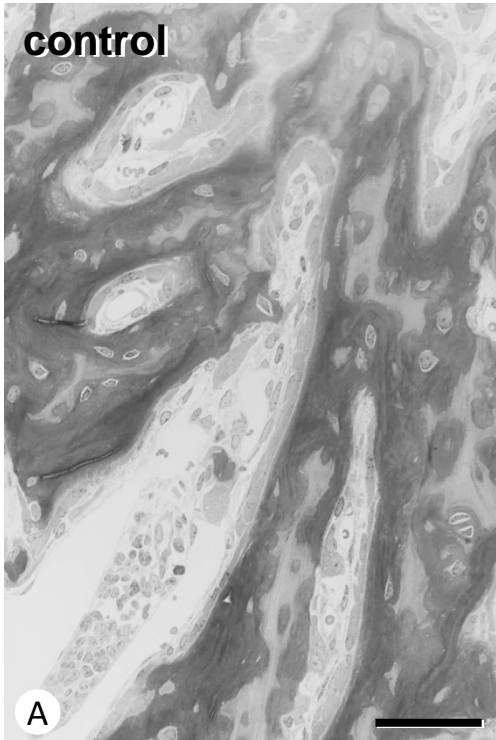




K







# 日中笹川医学奨学金制度(学位取得コース)評価書

## 課程博士：指導教官用



第 41 期

研究者番号： G4102

作成日： 2021 年 3 月 8 日

氏名	常立甲	CHANG LIJIA	性別	M	生年月日	1984.08.28
所属機関(役職)	石家庄市第四医院産前診断センター(主管技師)					
研究先(指導教官)	千葉大学社会精神保健教育研究センター病態解析研究部門(橋本 謙二教授)					
研究テーマ	精神疾患の病因解明と新規治療法の開発 Study of pathogenesis of psychiatric disorders and the development of novel therapeutic methods					
専攻種別	<input type="checkbox"/> 論文博士			<input checked="" type="checkbox"/> 課程博士		

### 研究者評価(指導教官記入欄)

成績状況	優 良 可 不可 学業成績係数=3.94	取得単位数
		取得単位数 33 / 取得すべき単位数 30
学生本人が行った研究の概要	千葉大学で開発した新規抗うつ薬アルケタミンの分子機序に関わる研究成果を数多く論文発表した。またうつ病の病因における迷走神経を介する脳-腸相関の重要性を見出し、論文発表した。またストレス後のレジリエンスおよび漸弱性の機序における、IL-6 と相互作用する Arid5 遺伝子の役割を見出した。	
総合評価	【良かった点】 日夜、休日も研究室に来て実験するほど、研究熱心であった。また研究室の他の大学院生や研究員(中国からの留学生など)の実験も積極的に協力し、研究室内で良い人間関係を築いた。	
	【改善すべき点】 現時点では、特に改善する点はない。	
	【今後の展望】 中国に帰国後、中国において活躍する人材になると共に、日中の学術交流に貢献していく人材になるであろう。	
学位取得見込	2020 年 9 月末に学位(医学博士)を取得した。	

評価者(指導教官名) 橋本謙二

# 日中笹川医学奨学金制度(学位取得コース)報告書

## 研究者用



第41期

研究者番号: G4102

作成日: 2021年3月3日

氏名	Chang Lijia	常立甲	性別	M	生年月日 1984. 08. 28
所属機関(役職)	石家庄市第四医院産前診断センター(主管技師)				
研究先(指導教官)	千葉大学社会精神保健教育研究センター 病態解析研究部門(橋本 謙二教授)				
研究テーマ	精神疾患の病因解明と新規治療法の開発 Study of pathogenesis of psychiatric disorders and the development of novel therapeutic methods				
専攻種別	論文博士	<input type="checkbox"/>	課程博士	<input checked="" type="checkbox"/>	
1. 研究概要(1)					
<p>1) 目的 (Goal) : The N-methyl-D-aspartate receptor (NMDAR) antagonist (R,S)-ketamine produces rapid and sustained antidepressant effects in treatment-resistant patients with depression although intranasal use of (R,S)-ketamine in ketamine abusers is popular. On March 5, 2019, the US Food Drug Administration (FDA) approved Janssen Pharmaceutical Inc.'s (S)-ketamine nasal spray for treatment-resistant depression[1]. However, there are no reports showing the direct comparison of intranasal administration of (R,S)-ketamine and its two enantiomers for antidepressant and side effects in rodents. The purpose of this study is to compare the antidepressant and side effects of intranasal administration of (R,S)-ketamine and its two enantiomers (R)-ketamine and (S)-ketamine.</p> <p>2) 戦略 (Approach) : In a chronic social defeat stress (CSDS) model of depression, the antidepressant effects of intranasal administration of (R,S)-ketamine and its two enantiomers (R)-ketamine and (S)-ketamine will be evaluated by the behavior tests of locomotion, tail suspension test (TST), forced swimming test (FST) and 1% sucrose preference test (SPT). The side effects of these three compounds in mice will be assessed by the locomotion test, prepulse inhibition (PPI) test and conditioned place preference (CPP) test.</p> <p>3) 材料と方法 (Materials and methods) : ① Animals, Male adult C57BL/6 mice and male adult CD1 (ICR) mice were used. ② Materials, (R)-Ketamine hydrochloride and (S)-ketamine hydrochloride were prepared by recrystallization of (R,S)-ketamine. ③ Chronic social defeat stress (CSDS) model: The C57BL/6 mice were exposed to a different CD1 aggressor mouse for 10 min per day for consecutive 10 days. ④ Treatment and behavioral tests, the CSDS susceptible mice were divided to four groups. Subsequently, saline (0.5 ml/kg), (R,S)-ketamine (10 mg/kg), (R)-ketamine (10 mg/kg), or (S)-ketamine (10 mg/kg) was administered intranasally into CSDS susceptible mice. Behavioral tests, including locomotion test (LMT), tail suspension test (TST), forced swimming test (FST) and 1% sucrose preference test (SPT). ⑤ Side effects of behavioral tests, including Locomotion, Prepulse inhibition (PPI) test, Conditioned place preference (CPP) test. ⑥ Analysis was performed using PASW Statistics 20.</p> <p>4) 実験結果 (Results) : ① The order of potency of antidepressant effects in a CSDS model was (R)-ketamine &gt; (R,S)-ketamine &gt; (S)-ketamine. ② The order of potencies of side effects (i.e., psychosis, abuse liability) in mice after intranasal administration was (S)-ketamine &gt; (R,S)-ketamine &gt; (R)-ketamine. Detail results were attached in the published paper.</p> <p>5) 考察 (Discussion) : ① In the present study, we compared (R,S)-ketamine, and its two enantiomers in CSDS susceptible mice (for antidepressant effects) and control mice (for side effects). The order of potency of antidepressant effects after a single intranasal administration to CSDS susceptible mice is (R)-ketamine &gt; (R,S)-ketamine &gt; (S)-ketamine. Furthermore, the order of potency of side effects (i.e., psychosis and abuse liability) after intranasal administration is (S)-ketamine &gt; (R,S)-ketamine &gt; (R)-ketamine. Collectively, it is likely that (R)-ketamine would be a rapid-acting and sustained antidepressant without side effects compared to (R,S)-ketamine and (S)-ketamine. ② In this study, we found that antidepressant effects of (R,S)-ketamine and its two enantiomers in CSDS susceptible mice after a single intranasal administration may be less potent than those of a single i.p. administration[2-5]. Lower bioavailability of intranasal administration of (R,S)-ketamine and its two enantiomers may contribute to lower efficacy of intranasal administration compared to i.p. administration. Interestingly, the potency of antidepressant effects of (R,S)-ketamine and its two enantiomers was not correlated with the potencies of these compounds at the NMDAR, suggesting that NMDAR inhibition may not play a key role in the antidepressant effects of (R,S)-ketamine and its enantiomers[6]. ③ Due to its</p>					

## 1. 研究概要 (2)

serious side effects, clinical use of ketamine has remained limited[7-9], although it has been used as an off-label antidepressant in the USA[10]. In this study, we found that locomotion after a single intranasal administration of (R)-ketamine is lower than those of (R,S)-ketamine and (S)-ketamine, consistent with the previous reports[3]. Furthermore, we found that a single intranasal administration of (R)-ketamine did not cause PPI deficits in mice compared to (R,S)-ketamine and (S)-ketamine, consistent with the previous reports of i.p. administration[3]. Finally, we found that repeated intranasal administration of (R)-ketamine did not increase CPP scores in mice although (R,S)-ketamine and (S)-ketamine increased CPP scores, in a dose dependent manner, consistent with the previous reports of i.p. administration[2,11]. Unlike (R,S)-ketamine and (S)-ketamine, it seems that intranasal infusion of (R)-ketamine does not appear to cause psychotomimetic effects or have abuse potential in humans, based on the lack of behavioral abnormalities (e.g., PPI deficits, CPP) observed in mice after single or repeated intranasal administration[12]. Taken all together, it seems likely that (S)-ketamine contributes to the acute psychotomimetic and dissociative effects of (R,S)-ketamine, whereas (R)-ketamine may not be associated with these side effects [13]. ④ On March 5, 2019, the US FDA approved nasal spray of (S)-ketamine for treatment-resistant depression[1]. Due to the risk of serious adverse outcomes from sedation and dissociation caused by administration of (S)-ketamine, as well as the potential for abuse and misuse of the drug, FDA said that the drug will only be available through a restricted distribution system, under a Risk Evaluation and Mitigation Strategy (REMS). Patients will self-administer (S)-ketamine under the supervision of a health care provider in a certified doctor's office or clinic; the nasal spray cannot be taken home [1]. Given the lack of adverse side effects of (R)-ketamine, it is possible that patients may take (R)-ketamine to their home.

## 6) 参考文献 (References)

- [1] FDA News Release on March 5, 2019. FDA Approves New Nasal Spray Medication for Treatment-resistant Depression; Available Only at a Certified Doctor's Office or Clinic. <https://www.fda.gov/NewsEvents/Newsroom/PressAnnouncements/ucm632761.htm>
- [2] Yang, C., Shirayama, Y., Zhang, J.C., Ren, Q., Yao, W., Ma, M., Dong, C., Hashimoto, K., 2015. R-ketamine: a rapid-onset and sustained antidepressant without psychotomimetic side effects. *Transl. Psychiatry* 5, e632.
- [3] Yang, C., Qu, Y., Abe, M., Nozawa, D., Chaki, S., Hashimoto, K., 2017a. (R)-ketamine shows greater potency and longer lasting antidepressant effects than its metabolite (2R,6R)-hydroxynorketamine. *Biol. Psychiatry* 82, e43-e44.
- [4] Yang, C., Qu, Y., Fujita, Y., Ren, Q., Ma, M., Dong, C., Hashimoto, K., 2017b. Possible role of the gut microbiota-brain axis in the antidepressant effects of (R)-ketamine in a social defeat stress model. *Transl. Psychiatry* 7, 1294.
- [5] Yang, C., Ren, Q., Qu, Y., Zhang, J.C., Ma, M., Dong, C., Hashimoto, K., 2018a. Mechanistic target of rapamycin-independent antidepressant effects of (R)-ketamine in a social defeat stress model. *Biol. Psychiatry* 83, 18-28.
- [6] Ebert, B., Mikkelsen, S., Thorkildsen, C., Borgbjerg, F.M., 1997. Norketamine, the main metabolite of ketamine, is a non-competitive NMDA receptor antagonist in the rat cortex and spinal cord. *Eur. J. Pharmacol.* 333, 99-104.
- [7] Domino, E.F., 2010. Taming the ketamine tiger. 1965. *Anesthesiology* 113, 678-684.
- [8] Sanacora, G., Frye, M.A., McDonald, W., Mathew, S.J., Turner, M.S., Schatzberg, A.F., Summergrad, P., Nemeroff, C.B., American Psychiatric Association (APA) Council of Research Task Force on Novel Biomarkers and Treatments, 2017. A consensus statement on the use of ketamine in the treatment of mood disorders. *JAMA Psychiatry* 74, 399-405.
- [9] Singh, I., Morgan, C., Curran, V., Nutt, D., Schlag, A., McShane, R., 2017. Ketamine treatment for depression: opportunities for clinical innovation and ethical foresight. *Lancet Psychiatry* 4, 419-426.
- [10] Wilkinson, S.T., Toprak, M., Turner, M.S., Levine, S.P., Katz, R.B., Sanacora, G., 2017. A survey of the clinical, off-label use of ketamine as a treatment for psychiatric disorders. *Am. J. Psychiatry* 174, 695-696.
- [11] Yang, C., Kobayashi, S., Nakao, K., Dong, C., Han, M., Qu, Y., Ren, Q., Zhang, J.C., Ma, M., Toki, H., Yamaguchi, J.I., Chaki, S., Shirayama, Y., Nakazawa, K., Manabe, T., Hashimoto, K., 2018b. AMPA receptor activation-independent antidepressant actions of ketamine metabolite (S)-norketamine. *Biol. Psychiatry* 84, 591-600.
- [12] Hashimoto, K., 2016a. R-ketamine: a rapid-onset and sustained antidepressant without risk of brain toxicity. *Psychol. Med.* 46, 2449-2451.
- [13] Zanos, P., Moaddel, R., Morris, P.J., Riggs, L.M., Highland, J.N., Georgiou, P., Pereira, E.F.R., Albuquerque, E.X., Thomas, C.J., Zarate Jr., C.A., Gould, T.D., 2018. Ketamine and ketamine metabolite pharmacology: insights into therapeutic mechanisms. *Pharmacol. Rev.* 70, 621-660.

## 2. 執筆論文 Publication of thesis ※記載した論文を添付してください。

Attach all of the papers listed below.

論文名 1 Title	Comparison of antidepressant and side effects in mice after intranasal administration of (R,S)-ketamine, (R)-ketamine, and (S)-ketamine					
掲載誌名 Published journal	Pharmacology Biochemistry and Behavior					
	2019 年 6 月	181 巻 (号)	53 頁 ~	59 頁	言語 Language	English
第1著者名 First author	Lijia Chang	第2著者名 Second author	Kai Zhang	第3著者名 Third author	Yaoyu Pu	
その他著者名 Other authors	Youge Qu, Si-ming Wang, Zhongwei Xiong, Qian Ren, Chao Dong, Yuko Fujita, Kenji Hashimoto					
論文名 2 Title	Lack of dopamine D1 receptors in the antidepressant actions of (R)-ketamine in a chronic social defeat stress model					
掲載誌名 Published journal	European Archives of Psychiatry and Clinical Neuroscience					
	2020 年 3 月	270 (2) 巻 (号)	271 頁 ~	275 頁	言語 Language	English
第1著者名 First author	Lijia Chang	第2著者名 Second author	Kai Zhang	第3著者名 Third author	Yaoyu Pu	
その他著者名 Other authors	Youge Qu, Si-ming Wang, Zhongwei Xiong, Yukihiro Shirayama, Kenji Hashimoto					
論文名 3 Title	Antidepressant Actions of Ketamine and Its Two Enantiomers (Chapter Title)					
掲載誌名 Published journal	Ketamine from Abused Drug to Rapid-acting Antidepressant (Book Title)					
	2020 年 1 月	巻 (号)	105 頁 ~	125 頁	言語 Language	English
第1著者名 First author	Lijia Chang	第2著者名 Second author	Yan Wei	第3著者名 Third author	Kenji Hashimoto	
その他著者名 Other authors						
論文名 4 Title	Abnormalities of the composition of the gut microbiota and short-chain fatty acids in mice after splenectomy					
掲載誌名 Published journal	Brain, Behavior, & Immunity - Health					
	2021 年 2 月	11 巻 (号)	100198		言語 Language	English
第1著者名 First author	Yan Wei/Lijia Chang	第2著者名 Second author	Tamaki Ishima	第3著者名 Third author	Xiayun Wan	
その他著者名 Other authors	Li Ma, Gerile Wuyun, Yaoyu Pu, Kenji Hashimoto					
論文名 5 Title	A historical review of antidepressant effects of ketamine and its enantiomers					
掲載誌名 Published journal	Pharmacology Biochemistry and Behavior					
	2020 年 2 月	190 巻 (号)	172870		言語 Language	English
第1著者名 First author	Yan Wei	第2著者名 Second author	Lijia Chang	第3著者名 Third author	Kenji Hashimoto	
その他著者名 Other authors						

2. 執筆論文 Publication of thesis ※記載した論文を添付してください。  
Attach all of the papers listed below.

論文名 6 Title	Antibiotic-induced microbiome depletion protects against MPTP-induced dopaminergic neurotoxicity in the brain					
掲載誌名 Published journal	Aging (Albany NY)					
	2019 年 9 月	11(17) 巻(号)	6915 頁 ~ 6929 頁	言語 Language	English	
第1著者名 First author	Yaoyu Pu	第2著者名 Second author	Lijia Chang	第3著者名 Third author	Youge Qu	
その他著者名 Other authors	Siming Wang, Kai Zhang, Kenji Hashimoto					
論文名 7 Title	Glyphosate exposure exacerbates the dopaminergic neurotoxicity in the mouse brain after repeated administration of MPTP					
掲載誌名 Published journal	Neuroscience letters					
	2020 年 1 月	730 巻(号)	135032	言語 Language	English	
第1著者名 First author	Yaoyu Pu	第2著者名 Second author	Lijia Chang	第3著者名 Third author	Youge Qu	
その他著者名 Other authors	Siming Wang, Yunfei Tan, Xingming Wang, Jiancheng Zhang, Kenji Hashimoto					
論文名 8 Title	Neuronal brain injury after cerebral ischemic stroke is ameliorated after subsequent administration of (R)-ketamine, but not (S)-ketamine					
掲載誌名 Published journal	Pharmacology Biochemistry and Behavior					
	2020 年 4 月	191 巻(号)	172904	言語 Language	English	
第1著者名 First author	Zhongwei Xiong	第2著者名 Second author	Lijia Chang	第3著者名 Third author	Youge Qu	
その他著者名 Other authors	Yaoyu Pu, Siming Wang, Yuko Fujita, Tamaki Ishima, Jincao Chen, Kenji Hashimoto					
論文名 9 Title	Abnormal expression of colony stimulating factor 1 receptor (CSF1R) and transcription factor PU.1 (SP11) in the spleen from patients with major psychiatric disorders: A role of brain-spleen axis					
掲載誌名 Published journal	Journal of Affective Disorders					
	2020 年 7 月	272 巻(号)	110 頁 ~ 115 頁	言語 Language	English	
第1著者名 First author	Jiancheng Zhang	第2著者名 Second author	Lijia Chang	第3著者名 Third author	Yaoyu Pu	
その他著者名 Other authors	Kenji Hashimoto					
論文名 10 Title	Abnormal composition of gut microbiota is associated with resilience versus susceptibility to inescapable electric stress					
掲載誌名 Published journal	Translational Psychiatry					
	2019 年 9 月	190 巻(号)	231 頁 ~ 頁	言語 Language	English	
第1著者名 First author	Kai Zhang	第2著者名 Second author	Yuko Fujita	第3著者名 Third author	Lijia Chang	
その他著者名 Other authors	Youge Qu, Yaoyu Pu, Siming Wang, Yukihiko Shirayama, Kenji Hashimoto					

## 2. 執筆論文 Publication of thesis ※記載した論文を添付してください。

Attach all of the papers listed below.

論文名 11 Title	Dietary intake of glucoraphanin prevents the reduction of dopamine transporter in the mouse striatum after repeated administration of MPTP					
掲載誌名 Published journal	Neuropsychopharmacology Reports					
	2019 年 9 月	39(3) 巻(号)	247 頁 ~	251 頁	言語 Language	English
第1著者名 First author	Yaoyu Pu	第2著者名 Second author	Younge Qu	第3著者名 Third author	Lijia Chang	
その他著者名 Other authors	Si-Ming Wang, Kai Zhang, Yusuke Ushida, Hiroyuki Sukanuma, Kenji Hashimoto					
論文名 12 Title	Antibiotic-induced microbiome depletion is associated with resilience in mice after chronic social defeat stress					
掲載誌名 Published journal	Antibiotic-induced microbiome depletion is associated with resilience in mice after chronic social defeat stress					
	2020 年 1 月	260 巻(号)	448 頁 ~	457 頁	言語 Language	English
第1著者名 First author	Siming Wang	第2著者名 Second author	Younge Qu	第3著者名 Third author	Lijia Chang	
その他著者名 Other authors	Yaoyu Pu, Kai Zhang, Kenji Hashimoto					
論文名 13 Title	Phencyclidine-induced cognitive deficits in mice are ameliorated by subsequent repeated intermittent administration of (R)-ketamine, but not (S)-ketamine: Role of BDNF-TrkB signaling					
掲載誌名 Published journal	Pharmacology Biochemistry and Behavior					
	2020 年 1 月	188 巻(号)	172839 頁 ~	頁	言語 Language	English
第1著者名 First author	Yunfei Tan	第2著者名 Second author	Yuko Fujita	第3著者名 Third author	Younge Qu	
その他著者名 Other authors	Lijia Chang, Yaoyu Pu, Siming Wang, Xingming Wang, Kenji Hashimoto					
論文名 14 Title	Essential role of microglial transforming growth factor- $\beta$ 1 in antidepressant actions of (R)-ketamine and the novel antidepressant TGF- $\beta$ 1					
掲載誌名 Published journal	Transl Psychiatry					
	2020 年 1 月	10(1) 巻(号)	32 頁 ~	頁	言語 Language	English
第1著者名 First author	Kai Zhang	第2著者名 Second author	Chun Yang	第3著者名 Third author	Lijia Chang	
その他著者名 Other authors	Akemi Sakamoto, Toru Suzuki, Yuko Fujita, Youge Qu, Siming Wang, Yaoyu Pu, Yunfei Tan, Xingming Wang, Tamaki Ishima, Yukihiko Shirayama, Masahiko Hatano, Kenji F Tanaka, Kenji Hashimoto					
論文名 15 Title	Maternal glyphosate exposure causes autism-like behaviors in offspring through increased expression of soluble epoxide hydrolase					
掲載誌名 Published journal	Proceedings of the National Academy of Sciences of the United States of America					
	2020 年 5 月	117(21) 巻(号)	11753 頁 ~	11759 頁	言語 Language	English
第1著者名 First author	Yaoyu Pu	第2著者名 Second author	Jun Yang	第3著者名 Third author	Lijia Chang	
その他著者名 Other authors	Younge Qu, Siming Wang, Kai Zhang, Zhongwei Xiong, Jiancheng Zhang, Yunfei Tan, Xingming Wang, Yuko Fujita, Tamaki Ishima, Debin Wang, Sung Hae Hong, Bruce D Hammock, Kenji Hashimoto					



## 2. 執筆論文 Publication of thesis ※記載した論文を添付してください。

Attach all of the papers listed below.

論文名 16 Title	A key role of the subdiaphragmatic vagus nerve in the depression-like phenotype and abnormal composition of gut microbiota in mice after lipopolysaccharide administration					
掲載誌名 Published journal	Transl Psychiatry					
	2019 年 6 月	10(1) 巻(号)	186 頁 ~	頁	言語 Language	English
第1著者名 First author	Jiancheng Zhang	第2著者名 Second author	Li Ma	第3著者名 Third author	Lijia Chang	
その他著者名 Other authors	Yaoyu Pu, Youge Qu, Kenji Hashimoto					
論文名 17 Title	Betaine supplementation is associated with the resilience in mice after chronic social defeat stress: a role of brain-gut-microbiota axis					
掲載誌名 Published journal	Journal of Affective Disorders					
	2020 年 7 月	272 巻(号)	66 頁 ~	76 頁	言語 Language	English
第1著者名 First author	Youge Qu	第2著者名 Second author	Kai Zhang	第3著者名 Third author	Yaoyu Pu	
その他著者名 Other authors	Lijia Chang, Siming Wang, Yunfei Tan, Xingming Wang, Jiancheng Zhang, Tetsuo Ohnishi, Takeo Yoshikawa, Kenji Hashimoto					
論文名 18 Title	Ingestion of Lactobacillus intestinalis and Lactobacillus reuteri causes depression- and anhedonia-like phenotypes in antibiotic-treated mice via the vagus nerve					
掲載誌名 Published journal	Journal of Neuroinflammation					
	2020 年 8 月	17(1) 巻(号)	241 頁 ~	頁	言語 Language	English
第1著者名 First author	Siming Wang	第2著者名 Second author	Tamaki Ishima	第3著者名 Third author	Jiancheng Zhang	
その他著者名 Other authors	Youge Qu, Lijia Chang, Yaoyu Pu, Yuko Fujita, Yunfei Tan, Xingming Wang, Kenji Hashimoto					
論文名 19 Title	Rapid-acting and long-lasting antidepressant-like action of (R)-ketamine in Nrf2 knock-out mice: a role of TrkB signaling					
掲載誌名 Published journal	European Archives of Psychiatry and Clinical Neuroscience					
	2020 年 11 月	巻(号)	頁 ~	頁	言語 Language	English
第1著者名 First author	Youge Qu	第2著者名 Second author	Jiajing Shan	第3著者名 Third author	Siming Wang	
その他著者名 Other authors	Lijia Chang, Yaoyu Pu, Xingming Wang, Yunfei Tan, Masayuki Yamamoto, Kenji Hashimoto					
論文名 20 Title	A role of the subdiaphragmatic vagus nerve in depression-like phenotypes in mice after fecal microbiota transplantation from Chrna7 knock-out mice with depression-like phenotypes					
掲載誌名 Published journal	Brain, Behavior, and Immunity					
	2021 年 1 月	巻(号)	頁 ~	頁	言語 Language	English
第1著者名 First author	Yaoyu Pu/Yunfei Tan	第2著者名 Second author	Youge Qu	第3著者名 Third author	Lijia Chang	
その他著者名 Other authors	Siming Wang, Yan Wei, Xingming Wang, Kenji Hashimoto					

2. 執筆論文 Publication of thesis ※記載した論文を添付してください。  
Attach all of the papers listed below.

論文名 21 Title	Dextran sulfate sodium-induced inflammation and colitis in mice are ameliorated by (R)-ketamine, but not (S)-ketamine: A role of TrkB signaling						
掲載誌名 Published journal	European Journal of Pharmacology						
	2021 年 2 月	897 卷(号)	173954 頁 ~	頁	言語 Language	English	
第1著者名 First author	Yuko Fujita	第2著者名 Second author	Yaeko Hashimoto	第3著者名 Third author	Hiroyo Hashimoto		
その他著者名 Other authors	Lijia Chang, Kenji Hashimoto						
論文名 22 Title							
掲載誌名 Published journal							
	年 月	卷(号)	頁 ~	頁	言語 Language		
第1著者名 First author		第2著者名 Second author		第3著者名 Third author			
その他著者名 Other authors							
論文名 23 Title							
掲載誌名 Published journal							
	年 月	卷(号)	頁 ~	頁	言語 Language		
第1著者名 First author		第2著者名 Second author		第3著者名 Third author			
その他著者名 Other authors							
論文名 24 Title							
掲載誌名 Published journal							
	年 月	卷(号)	頁 ~	頁	言語 Language		
第1著者名 First author		第2著者名 Second author		第3著者名 Third author			
その他著者名 Other authors	Xiayun Wan, Li Ma, Gerile Wuyun, Yaoyu Pu, Kenji Hashimoto						
論文名 25 Title							
掲載誌名 Published journal							
	年 月	卷(号)	頁 ~	頁	言語 Language		
第1著者名 First author		第2著者名 Second author		第3著者名 Third author			
その他著者名 Other authors							

3. 学会発表 Conference presentation ※筆頭演者として総会・国際学会を含む主な学会で発表したものを記載

※Describe your presentation as the principal presenter in major academic meetings including general meetings or

学会名 Conference	The Chiba-Otawa Joint Session of Pharmacology 2019			
演題 Topic	"Antidepressant actions of ketamine enantiomers"			
開催日 date	2019 年 7 月 24 日	開催地 venue	Chiba University Graduate School of Medicine	
形式 method	<input type="checkbox"/> 口頭発表 Oral <input type="checkbox"/> ポスター発表 Poster	言語 Language	<input type="checkbox"/> 日本語 <input type="checkbox"/> 英語 <input type="checkbox"/> 中国語	
共同演者名 Co-presenter				
学会名 Conference				
演題 Topic				
開催日 date	年 月 日	開催地 venue		
形式 method	<input type="checkbox"/> 口頭発表 Oral <input type="checkbox"/> ポスター発表 Poster	言語 Language	<input type="checkbox"/> 日本語 <input type="checkbox"/> 英語 <input type="checkbox"/> 中国語	
共同演者名 Co-presenter				
学会名 Conference				
演題 Topic				
開催日 date	年 月 日	開催地 venue		
形式 method	<input type="checkbox"/> 口頭発表 Oral <input type="checkbox"/> ポスター発表 Poster	言語 Language	<input type="checkbox"/> 日本語 <input type="checkbox"/> 英語 <input type="checkbox"/> 中国語	
共同演者名 Co-presenter				
学会名 Conference				
演題 Topic				
開催日 date	年 月 日	開催地 venue		
形式 method	<input type="checkbox"/> 口頭発表 Oral <input type="checkbox"/> ポスター発表 Poster	言語 Language	<input type="checkbox"/> 日本語 <input type="checkbox"/> 英語 <input type="checkbox"/> 中国語	
共同演者名 Co-presenter				

4. 受賞 (研究業績 Award (Research achievement))

名称 Award name	国名 Country		受賞年 Year of	年 月
	国名 Country		受賞年 Year of	年 月

5. 本研究テーマに関わる他の研究助成金受給 Other research grants concerned with your research

受給実績 Receipt record	<input type="checkbox"/> 有 <input checked="" type="checkbox"/> 無
助成機関名称 Funding agency	
助成金名称 Grant name	
受給期間 Supported	年 月 ~ 年 月
受給額 Amount received	円
受給実績 Receipt record	<input type="checkbox"/> 有 <input checked="" type="checkbox"/> 無
助成機関名称 Funding agency	
助成金名称 Grant name	
受給期間 Supported	年 月 ~ 年 月
受給額 Amount received	円

6. 他の奨学金受給 Another awarded scholarship

受給実績 Receipt record	<input type="checkbox"/> 有 <input checked="" type="checkbox"/> 無
助成機関名称 Funding agency	
奨学金名称 Scholarship	
受給期間 Supported	年 月 ~ 年 月
受給額 Amount received	円

7. 研究活動に関する報道発表 Press release concerned with your research activities

※記載した記事を添付してください。 Attach a copy of the article described below


報道発表 Press release	<input type="checkbox"/> 有 <input checked="" type="checkbox"/> 無	発表年月日 Date of release	
発表機関 Released medium			
発表形式 Release method	・新聞 ・雑誌 ・Web site ・記者発表 ・その他 ( )		
発表タイトル Released title			

8. 本研究テーマに関する特許出願予定 Patent application concerned with your research theme

出願予定 Scheduled	<input type="checkbox"/> 有 <input checked="" type="checkbox"/> 無	出願国 Application	
出願内容(概要) Application contents			

9. その他 Others

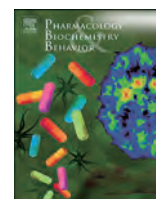
--

指導責任者(署名) 橋本謙二 



Contents lists available at ScienceDirect

## Pharmacology, Biochemistry and Behavior

journal homepage: [www.elsevier.com/locate/pharmbiochembeh](http://www.elsevier.com/locate/pharmbiochembeh)

## Comparison of antidepressant and side effects in mice after intranasal administration of (*R,S*)-ketamine, (*R*)-ketamine, and (*S*)-ketamine

Lijia Chang, Kai Zhang, Yaoyu Pu, Youge Qu, Si-ming Wang, Zhongwei Xiong, Qian Ren, Chao Dong, Yuko Fujita, Kenji Hashimoto\*

Division of Clinical Neuroscience, Chiba University Center for Forensic Mental Health, Chiba 260-8670, Japan



## ARTICLE INFO

## Keywords:

Antidepressant  
(*R*)-ketamine  
(*R,S*)-ketamine  
(*S*)-ketamine  
Side effects

## ABSTRACT

The *N*-methyl-D-aspartate receptor (NMDAR) antagonist (*R,S*)-ketamine produces rapid and sustained antidepressant effects in treatment-resistant patients with depression although intranasal use of (*R,S*)-ketamine in ketamine abusers is popular. In March 5, 2019, nasal spray of (*S*)-ketamine for treatment-resistant depression was approved as a new antidepressant by the US Food Drug Administration. Clinical study of (*R*)-ketamine is underway. In a chronic social defeat stress (CSDS) model, we compared the antidepressant effects of (*R,S*)-ketamine, (*R*)-ketamine, and (*S*)-ketamine after a single intranasal administration. Furthermore, we also compared the side effects (i.e., locomotion, prepulse inhibition (PPI), abuse liability) of these three compounds in mice. The order of potency of antidepressant effects after a single intranasal administration was (*R*)-ketamine > (*R,S*)-ketamine > (*S*)-ketamine. In contrast, the order of locomotor activity and prepulse inhibition (PPI) deficits after a single intranasal administration was (*S*)-ketamine > (*R,S*)-ketamine > (*R*)-ketamine. In the conditioned place preference (CPP) test, both (*S*)-ketamine and (*R,S*)-ketamine increased CPP scores in mice after repeated intranasal administration, in a dose dependent manner. In contrast, (*R*)-ketamine did not increase CPP scores in mice. These findings suggest that intranasal administration of (*R*)-ketamine would be a safer antidepressant than (*R,S*)-ketamine and (*S*)-ketamine.

### 1. Introduction

In 2000, Berman et al. (2000) reported a first double-blind, placebo-controlled study of the *N*-methyl-D-aspartate receptor (NMDAR) antagonist (*R,S*)-ketamine, demonstrating that (*R,S*)-ketamine exhibits rapid antidepressant effects in treatment-resistant patients with major depressive disorder (MDD). Subsequently, a number of groups replicated robust antidepressant effects of (*R,S*)-ketamine in treatment-resistant patients with MDD (Murrough et al., 2013; Su et al., 2017; Zarate et al., 2006;). Interestingly, (*R,S*)-ketamine could produce anti-suicidal effects in treatment-resistant patients with MDD (Grunebaum et al., 2018; Larkin and Beautrais, 2011; Murrough et al., 2015; Price et al., 2009). Several meta-analyses showed that (*R,S*)-ketamine exhibits rapid antidepressant and anti-suicidal ideation effects in treatment-resistant patients with MDD or bipolar disorder (Kishimoto et al., 2016; Newport et al., 2015; Wilkinson et al., 2018; Xu et al., 2016). Off-label use of (*R,S*)-ketamine (i.e., intravenous and intranasal administration) for antidepressant effects is increasing in the United State of America (USA) although the common adverse effects (e.g.,

psychotomimetic effects and dissociative effects) of (*R,S*)-ketamine are not resolved (Singh et al., 2017; Wilkinson et al., 2017; Zhu et al., 2016). Thus, although (*R,S*)-ketamine is the most attractive antidepressant in the treatment of severe depression, the precise mechanisms underlying its antidepressant actions remain elusive (Abdallah et al., 2018; Chaki, 2017a, 2017b; Duman, 2018; Gould et al., 2019; Hashimoto, 2016a, 2016b; Krystal et al., 2019; Monteggia and Zarate Jr, 2015; Murrough et al., 2017; Zanos et al., 2018; Zhang and Hashimoto, 2019a).

(*R,S*)-ketamine ( $K_i = 0.53 \mu\text{M}$  for NMDAR) is a racemic mixture containing equal parts of (*R*)-ketamine (or arketamine) ( $K_i = 1.4 \mu\text{M}$  for NMDAR) and (*S*)-ketamine (or esketamine) ( $K_i = 0.30 \mu\text{M}$  for NMDAR) (Ebert et al., 1997). (*R*)-ketamine is reported to show greater potency and longer-lasting antidepressant effects than (*S*)-ketamine in several animal models of depression (Fukumoto et al., 2017; Yang et al., 2015, 2017a, 2017b, 2018a; Zanos et al., 2016; Zhang et al., 2014). Unlike (*S*)-ketamine, (*R*)-ketamine might not induce psychotomimetic side effects or exhibit abuse potential in rodents (Yang et al., 2015, 2016). In addition, unlike (*R,S*)-ketamine and (*S*)-ketamine, (*R*)-ketamine did not

\* Corresponding author.

E-mail address: [hashimoto@faculty.chiba-u.jp](mailto:hashimoto@faculty.chiba-u.jp) (K. Hashimoto).

<https://doi.org/10.1016/j.pbb.2019.04.008>

Received 2 April 2019; Received in revised form 25 April 2019; Accepted 25 April 2019

Available online 26 April 2019

0091-3057/ © 2019 Elsevier Inc. All rights reserved.

cause the expression of heat shock protein HSP-70 (a marker for neuronal injury) in the rat retrosplenial cortex after a single intraperitoneal (i.p.) administration (Tian et al., 2018). A positron emission tomography (PET) study showed a marked reduction of dopamine D<sub>2/3</sub> receptor binding in conscious monkey striatum after a single intravenous (i.v.) infusion of (S)-ketamine but not that of (R)-ketamine, suggesting that (S)-ketamine-induced dopamine release might be associated with acute psychotomimetic and dissociative side effects in humans (Hashimoto et al., 2017). Therefore, it seems that (R)-ketamine could be a safer antidepressant in humans than (R,S)-ketamine and (S)-ketamine (Hashimoto, 2014, 2016a, 2016b, 2016c).

Fukumoto et al. (2017) reported that (R,S)-ketamine (10 mg/kg) and (R)-ketamine (10 mg/kg), but not (S)-ketamine (3 and 10 mg/kg), significantly reversed the depressive-like behavior induced by repeated treatments with corticosterone in rats at 24 h after a single i.p. administration, indicating that (S)-ketamine's antidepressant effects are less potent than (R,S)-ketamine and (R)-ketamine. On March 5, 2019, the US Food Drug Administration (FDA) approved Janssen Pharmaceutical Inc.'s (S)-ketamine nasal spray for treatment-resistant depression (FDA 2019). It is well known that bioavailability (17–29%) of intranasal administration of (R,S)-ketamine in humans is markedly lower than i.v. (100%) and intramuscular (i.m.) administration (93%) (Li and Vlisides, 2016; Peltoniemi et al., 2016; Zhang and Hashimoto, 2019a), suggesting lower efficacy and higher individual difference of intranasal administration compared to i.v. and i.m. administration. However, there are no reports showing the direct comparison of intranasal administration of (R,S)-ketamine and its two enantiomers for antidepressant and side effects in rodents.

The purpose of this study is to compare the antidepressant and side effects of intranasal administration of (R,S)-ketamine and its two enantiomers (R)-ketamine and (S)-ketamine. First, we compared the antidepressant effects of a single intranasal administration of (R,S)-ketamine, (R)-ketamine and (S)-ketamine in susceptible mice after chronic social defeat stress (CSDS). Second, we compared the side effects [i.e., locomotion, prepulse inhibition (PPI), conditioned place preference (CPP)] of intranasal administration of (R,S)-ketamine, (R)-ketamine and (S)-ketamine in mice.

## 2. Methods and Materials

### 2.1. Animals

Male adult C57BL/6 mice ( $n = 400$ ), aged 8 weeks (body weight 20–25 g, Japan SLC, Inc., Hamamatsu, Japan) and male adult CD1 (ICR) mice ( $n = 40$ ), aged 13–15 weeks (body weight > 40 g, Japan SLC, Inc., Hamamatsu, Japan) were used. Animals were housed under controlled temperatures and 12h/dark cycles (lights on between 07:00 and 19:00 h), with ad libitum food (CE-2; CLEA Japan, Inc., Tokyo, Japan) and water. The protocol was approved by the Chiba University Institutional Animal Care and Use Committee (Permission number: 29-420). This study was carried out in strict accordance with the recommendations in the Guide for the Care and Use of Laboratory Animals of the National Institutes of Health, USA. Animals were deeply anesthetized with isoflurane before being killed by cervical dislocation. All efforts were made to minimize suffering.

### 2.2. Materials

(R)-Ketamine hydrochloride and (S)-ketamine hydrochloride were prepared by recrystallization of (R,S)-ketamine (Ketalar®, ketamine hydrochloride, Daiichi Sankyo Pharmaceutical Ltd., Tokyo, Japan) and D-(–)-tartaric acid and L-(+)-tartaric acid, respectively (Zhang et al., 2014). The dose (10, 20 or 40 mg/kg as hydrochloride) of (R,S)-ketamine and its enantiomers dissolved in the physiological saline was used as previously reported (Chang et al., 2019; Yang et al., 2015, 2017a, 2017b, 2018a; Zhang et al., 2018). Other reagents were purchased

commercially.

### 2.3. Chronic social defeat stress (CSDS) model

The procedure of CSDS was performed as previously reported (Chang et al., 2019; Dong et al., 2017; Golden et al., 2011; Yang et al., 2015, 2017a, 2017b, 2018a; Xiong et al., 2018a, 2018b; Zhang et al., 2018). The C57BL/6 mice were exposed to a different CD1 aggressor mouse for 10 min per day for consecutive 10 days. When the social defeat session ended, the resident CD1 mouse and the intruder mouse were housed in one half of the cage separated by a perforated Plexiglas divider to allow visual, olfactory, and auditory contact for the remainder of the 24-h period. At 24 h after the last session, all mice were housed individually. On day 11, a social interaction test (SIT) was performed to identify subgroups of mice that were susceptible and unsusceptible to social defeat stress. This was accomplished by placing mice in an interaction test box (42 × 42 cm) with an empty wire-mesh cage (10 × 4.5 cm) located at one end. The movement of the mice was tracked for 2.5 min, followed by 2.5 min in the presence of an unfamiliar aggressor confined in the wire-mesh cage. The duration of the subject's presence in the “interaction zone” (defined as the 8-cm-wide area surrounding the wire-mesh cage) was recorded by a stopwatch. The interaction ratio was calculated as time spent in an interaction zone with an aggressor/time spent in an interaction zone without an aggressor. An interaction ratio of 1 was set as the cutoff: mice with scores < 1 were defined as “susceptible” to social defeat stress and those with scores ≥ 1 were defined as “resilient”. Approximately 70–80% of mice were susceptible after CSDS. Susceptible mice were randomly divided in the subsequent experiments. Control C57BL/6 mice without CSDS were housed in the cage before the behavioral tests.

### 2.4. Treatment and behavioral tests

The CSDS susceptible mice were divided to four groups. Subsequently, saline (0.5 ml/kg), (R,S)-ketamine (10 mg/kg), (R)-ketamine (10 mg/kg), or (S)-ketamine (10 mg/kg) was administered intranasally into CSDS susceptible mice (Fig. 1A). Mice were restrained by hand, and saline or ketamine was administered intranasally into awake mice using Eppendorf micropipette (Eppendorf Japan, Tokyo, Japan). Behavioral tests, including locomotion test (LMT), tail suspension test (TST), forced swimming test (FST) and 1% sucrose preference test (SPT), were performed as reported previously (Dong et al., 2017; Yang et al., 2015, 2017a, 2017b, 2018a; Xiong et al., 2018a, 2018b; Zhang et al., 2018). LMT and TST were performed 2 and 4 h after a single injection, respectively. FST was performed 1 day after injection. SPT was performed 2, and 7 days after a single injection (Fig. 1A).

#### 2.4.1. Locomotion

The locomotor activity was measured by an animal movement analysis system SCANETMV-40 (MELQUEST Co., Ltd., Toyama, Japan). The mice were placed in experimental cages (length × width × height: 560 × 560 × 330 mm). The cumulative locomotor activity counts were recorded for 60 min. Cages were cleaned between testing session.

#### 2.4.2. TST

A small piece of adhesive tape placed approximately 2 cm from the tip of the tail for mouse. A single hole was punched in the tape and mice were hung individually, on a hook. The immobility time was recorded for 10 min. Mice were considered immobile only when they hung passively and completely motionless.

#### 2.4.3. FST

The FST was conducted using an automated forced-swim apparatus (SCANET MV-40; MELQUEST Co., Ltd., Toyama, Japan). Mice were placed individually in a cylinder (diameter: 23 cm; height: 31 cm) containing 15 cm of water maintained at a temperature of

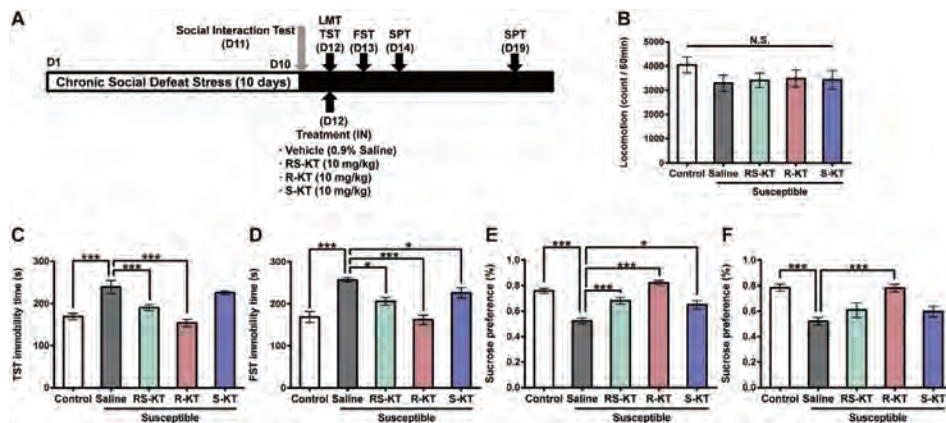


Fig. 1. Schedule of a CSDS model, treatment, and behavioral tests.

(A): CSDS was performed from day 1 to day 10, and the social interaction test (SIT) was performed on day 11. Saline (0.5 ml/kg), (R,S)-ketamine (10 mg/kg), (R)-ketamine (10 mg/kg), or (S)-ketamine (10 mg/kg) was administered intranasally into the susceptible mice on day 12. LMT and TST were performed 2 and 4 h after a single injection, respectively. SPT was performed 2, and 7 days after a single injection. (B): LMT (day 12). (C): TST (day 12). (D): FST (day 13). (E): SPT (day 14). (F): SPT (day 19). The values represent the mean  $\pm$  S.E.M. ( $n = 15$  or  $16$ ). \* $P < 0.05$ , \*\* $P < 0.01$ , \*\*\* $P < 0.001$  compared with saline-treated susceptible mice. N.S.: not significant. LMT: locomotion test. TST: tail suspension test. FST: forced swimming test. SPT: 1% sucrose preference test. R-KT: (R)-ketamine. RS-KT: (R,S)-ketamine. S-KT: (S)-ketamine.

$23^{\circ}\text{C} \pm 1^{\circ}\text{C}$ . The immobility time was calculated using the activity time as (total) – (active) time by the apparatus analysis software. The immobility time of each mouse was recorded for a period of 6 min.

#### 2.4.4. SPT

Mice were exposed to water and 1% sucrose solution for 48 h, followed by 4 h of water and food deprivation and a 1-hour exposure to two identical bottles (water and 1% sucrose solution). The bottles containing water and sucrose were weighed before and at the end of this period. The sucrose preference was calculated as a percentage of sucrose solution consumption to the total liquid consumption.

### 2.5. Side effects

#### 2.5.1. Locomotion

After habituation (60 min) in the cage, saline (0.5 ml/kg), (R,S)-ketamine (10, 20 or 40 mg/kg), (R)-ketamine (10, 20 or 40 mg/kg), or (S)-ketamine (10, 20 or 40 mg/kg) was injected intranasally into male C57BL/6 mice. Locomotor activity was measured using an animal movement analysis system (SCANET MV-40, Melquest, Toyama, Japan). The system consisted of a rectangular enclosure (560  $\times$  560 mm). The side walls (height, 60 mm) of the enclosure were equipped with 144 pairs of photosensors located at 6-mm intervals at a height of 30 mm from the bottom edge. An animal was placed in the observation cage 60 min from a single dose of saline or compounds. A pair of photosensors was scanned every 0.1 s to detect the animal's movements. The intersection of paired photosensors (10 mm apart) in the enclosure was counted as one unit of locomotor activity. Data collected for 60 min after a single injection were used in this study.

#### 2.5.2. Prepulse inhibition (PPI) test

Male C57BL/6 mice were tested for their acoustic startle reactivity (ASR) in a startle chamber (SR-LAB; San Diego Instruments, San Diego, CA, USA) using the standard methods described previously (Matsuura et al., 2015; Yang et al., 2015; Yang et al., 2018b). The test sessions were begun after an initial 10-min acclimation period in the chamber. The mice were subjected to one of six trials: (1) pulse alone, as a 40 ms broadband burst; a pulse (40 ms broadband burst) preceded by 100 ms with a 20 ms prepulse that was (2) 4 dB, (3) 8 dB, (4) 12 dB, or (5) 16 dB over background (65 dB); and (6) background only (no stimulus). The amount of PPI was expressed as the percentage decrease in the amplitude of the startle reactivity caused by presentation of the prepulse (% PPI). Saline (0.5 ml/kg), or (R,S)-ketamine (10, 20 or 40 mg/kg) [or (R)-ketamine (10, 20 or 40 mg/kg), (S)-ketamine (10, 20 or 40 mg/kg)] was administered intranasally 20 min (including the 10-min acclimation period) before the machine records. The PPI test lasted 20 min in

total.

#### 2.5.3. Conditioned place preference (CPP) test

The place conditioning paradigm (Brain Science Idea Inc., Osaka, Japan) was used for studying ketamine-induced rewarding effects, as reported previously (Yang et al., 2015; Yang et al., 2018b). Male C57BL/6 mouse was allowed to move freely between transparent and black boxes for a 15 min session once a day, for 3 days (days 1–3) as preconditioning. On day 3, the time spent in each box was measured. There was no significant difference between time spent in the black compartment with a smooth floor and the white compartment with a textured floor, indicating that there was no place preference before conditioning. On days 4, 6, and 8, saline (0.5 ml/kg), or (R,S)-ketamine (10, 20 or 40 mg/kg) [or (R)-ketamine (10, 20 or 40 mg/kg), (S)-ketamine (10, 20 or 40 mg/kg)] was intranasally administered, and then mice were confined to either the transparent or black box for 30 min. On days 5, 7, and 9, mice were given saline and placed in the opposite ketamine-conditioning box for 30 min. On day 10, the post-conditioning test was performed without drug treatment, and the time spent in each box was measured for 15 min. A counterbalanced protocol was used in order to nullify any initial preference by the mouse. The CPP score was designated as the time spent in the drug-conditioning sites, minus the time spent in the saline-conditioning sites.

### 2.6. Statistical analysis

The data show as the mean  $\pm$  standard error of the mean (S.E.M.). Analysis was performed using PASW Statistics 20 (formerly SPSS Statistics; SPSS, Tokyo, Japan). The data were analyzed using the one-way analysis of variance (ANOVA), followed by *post-hoc* Fisher's Least Significant Difference (LSD) test. The PPI data were also analyzed using multivariate analysis of variance, followed by *post-hoc* Fisher's LSD test. The  $P$ -values of  $< 0.05$  were considered statistically significant.

## 3. Results

### 3.1. Antidepressant effects of (R,S)-ketamine, (R)-ketamine and (S)-ketamine in CSDS susceptible mice

Locomotion showed no difference ( $F_{4,72} = 0.735$ ,  $P = 0.571$ ) among the five groups (Fig. 1B). One-way ANOVA of TST data showed a statistical significance ( $F_{4,72} = 15.23$ ,  $P < 0.001$ ) among the five groups (Fig. 1C). *Post-hoc* tests showed that (R,S)-ketamine (10 mg/kg) and (R)-ketamine (10 mg/kg) significantly attenuated the increased immobility times of TST in CSDS susceptible mice (Fig. 1C). However, (S)-ketamine (10 mg/kg) did not attenuate the increased immobility

time of TST in CSDS susceptible mice although (S)-ketamine slightly decreased the increased immobility time (Fig. 1C). One-way ANOVA of FST data showed a statistical significance ( $F_{4,72} = 13.77$ ,  $P < 0.001$ ) among the five groups (Fig. 1D). *Post-hoc* tests showed that three compounds (10 mg/kg) significantly attenuated the increased immobility times of FST in CSDS susceptible mice (Fig. 1D). One-way ANOVA of SPT data showed statistical significance (2 days after a single injection:  $F_{4,72} = 20.78$ ,  $P < 0.001$ ) among the five groups (Fig. 1E). *Post-hoc* tests showed that three compounds (10 mg/kg) significantly attenuated the decreased sucrose preference of SPT in CSDS susceptible mice (Fig. 1E). One-way ANOVA of SPT data showed statistical significance (7 days after a single injection:  $F_{4,72} = 9.311$ ,  $P < 0.001$ ) among the five groups (Fig. 1F). *Post-hoc* tests showed that sucrose preference of (R)-ketamine-treated group was significantly higher from saline-treated group. However, sucrose preference of (R,S)-ketamine-treated group and (S)-ketamine-treated group was not different from saline-treated group (Fig. 1E and F). Collectively, the order of potency of antidepressant effects in a CSDS model was (R)-ketamine > (R,S)-ketamine > (S)-ketamine.

### 3.2. Effects of (R,S)-ketamine, (R)-ketamine, and (S)-ketamine on locomotion in mice after a single intranasal administration

Effects of three compounds on locomotion of male mice were examined after a single intranasal administration. One-way ANOVA of the data showed statistical significances ( $F_{9,70} = 8.931$ ,  $P < 0.001$ ) among the ten groups (Fig. 2A). *Post-hoc* tests showed that a single intranasal administration of (R,S)-ketamine (20 and 40 mg/kg) or (S)-ketamine (10, 20 and 40 mg/kg) significantly increased locomotion compared to saline-treated group (Fig. 2A). Furthermore, locomotion of (S)-ketamine (40 mg/kg) treated mice was significantly higher than that of (R,S)-ketamine (40 mg/kg) or (R)-ketamine (40 mg/kg) treated mice. In contrast, all doses (10, 20 or 40 mg/kg) of (R)-ketamine did not alter locomotion in mice (Fig. 2A).

### 3.3. Effects of (R,S)-ketamine, (R)-ketamine, and (S)-ketamine on PPI in mice after a single intranasal administration

PPI test was performed to examine the effects of three compounds in mice. There were no changes in the acoustic startle response among the four groups for (R,S)-ketamine [Wilks lambda = 0.717,  $P = 0.589$ ], (R)-ketamine [Wilks lambda = 0.629,  $P = 0.226$ ], and (S)-ketamine [Wilks lambda = 0.588,  $P = 0.405$ ] (Fig. 3A–3C).

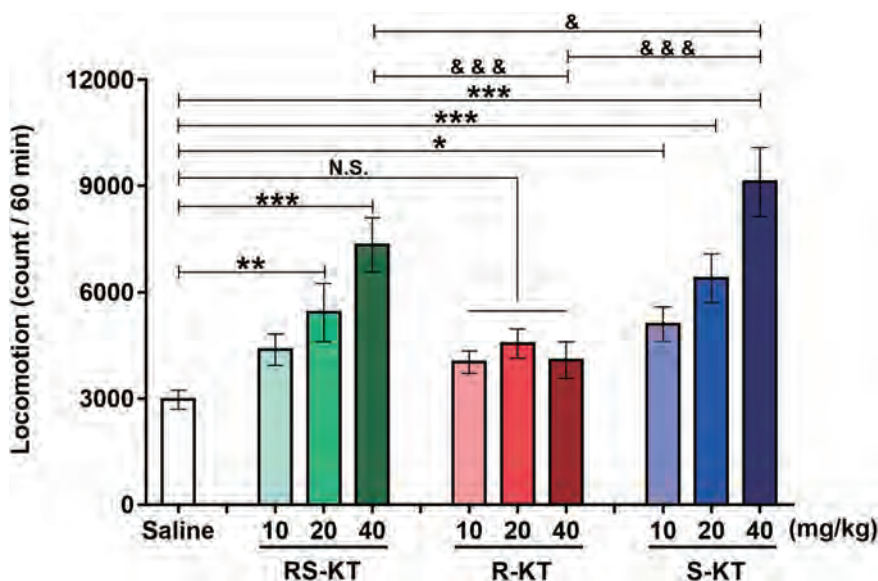


Fig. 2. Effects of (R,S)-ketamine, (R)-ketamine, and (S)-ketamine on locomotion after a single intranasal administration.

Saline (0.5 ml/kg), (R,S)-ketamine (10, 20, or 40 mg/kg), (R)-ketamine (10, 20, or 40 mg/kg), or (S)-ketamine (10, 20, or 40 mg/kg) was administered intranasally into male mice. Locomotor activity was measured 60 min after a single injection of the compounds. The values represent the mean  $\pm$  S.E.M. ( $n = 8$ ). \* $P < 0.05$ , \*\* $P < 0.01$ , \*\*\* $P < 0.001$  compared with saline-treated mice. &  $P < 0.05$  compared to RS-KT (40 mg/kg). &&& $P < 0.001$  compared to R-KT (40 mg/kg). N.S.: not significant. R-KT: (R)-ketamine. RS-KT: (R,S)-ketamine. S-KT: (S)-ketamine.

The MANOVA analysis of all PPI data of (R,S)-ketamine revealed that there was a significant effect [Wilks lambda = 0.497,  $P = 0.042$ ]. Treatment with (R,S)-ketamine (10, 20 or 40 mg/kg) decreased PPI at all dB groups, in a dose dependent manner. Subsequent *post-hoc* tests indicated significant differences in PPI between the saline group and (R,S)-ketamine (40 mg/kg) group at all dB groups (Fig. 3A). In contrast, the MANOVA analysis of all PPI data of (R)-ketamine revealed that there was not a significant effect [Wilks lambda = 0.625,  $P = 0.216$ ] (Fig. 3B). The MANOVA analysis of all PPI data of (S)-ketamine revealed that there was a significant effect [Wilks lambda = 0.299,  $P < 0.001$ ]. Treatment with (S)-ketamine (10, 20 or 40 mg/kg) decreased PPI at all dB groups, in a dose dependent manner. Subsequent *post-hoc* tests indicated significant differences in PPI deficits between the saline group and (S)-ketamine (20 and 40 mg/kg) group at all dB groups. Furthermore, (S)-ketamine (10 mg/kg) significantly decreased PPI at 73 dB (Fig. 3C).

### 3.4. Effects of (R,S)-ketamine, (R)-ketamine, and (S)-ketamine on CPP scores in mice after repeated intranasal administration

In the conditioned place preference (CPP) test (Fig. 4A), both (R,S)-ketamine and (S)-ketamine, but not (R)-ketamine, increased CPP scores, in a dose dependent manner (Fig. 4). Repeated intranasal administration of (R,S)-ketamine (40 mg/kg), but not the low doses (10 and 20 mg/kg), significantly increased CPP scores ( $F_{3,34} = 3.054$ ,  $P = 0.042$ ) (Fig. 4B). In contrast, repeated intranasal administration of (R)-ketamine (10, 20 or 40 mg/kg) did not increase CPP scores ( $F_{3,36} = 0.072$ ,  $P = 0.974$ ) (Fig. 4C). Repeated intranasal administration of (S)-ketamine (20 and 40 mg/kg), but not the low dose (10 mg/kg), significantly increased CPP scores ( $F_{3,36} = 14.0$ ,  $P < 0.001$ ) (Fig. 4D).

Collectively, the order of potencies of side effects (i.e., psychosis, abuse liability) in mice after intranasal administration was (S)-ketamine > (R,S)-ketamine > (R)-ketamine.

## 4. Discussion

In the present study, we compared (R,S)-ketamine, and its two enantiomers, in CSDS susceptible mice (for antidepressant effects) and control mice (for side effects). The order of potency of antidepressant effects after a single intranasal administration to CSDS susceptible mice is (R)-ketamine > (R,S)-ketamine > (S)-ketamine. Furthermore, the order of potency of side effects (i.e., psychosis and abuse liability) after



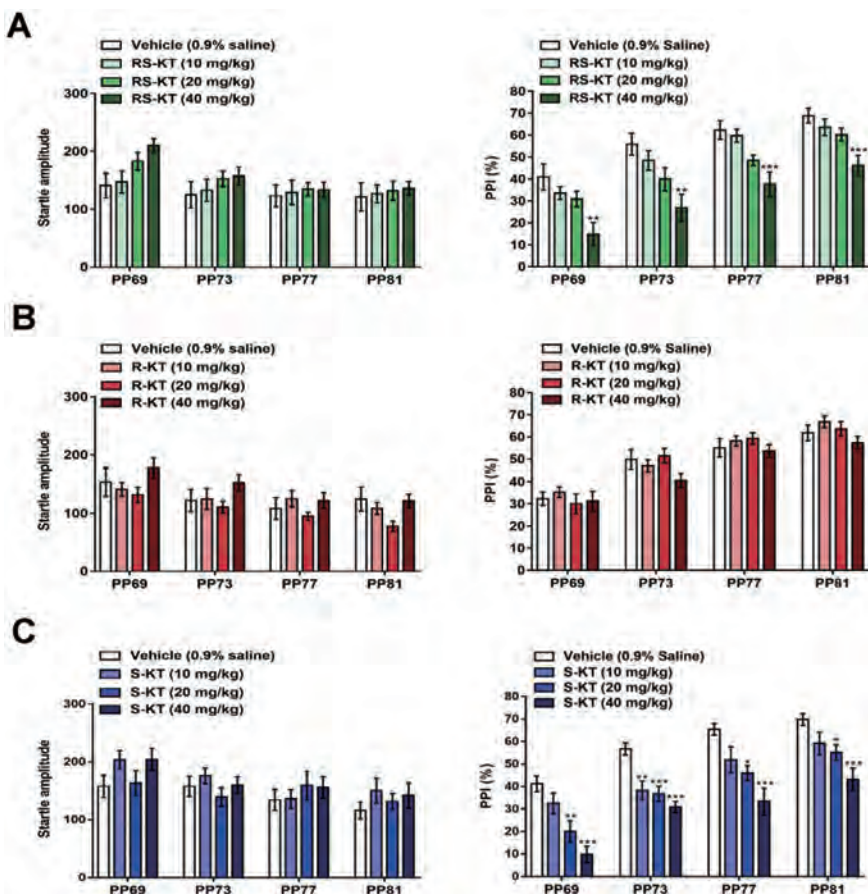


**Fig. 3.** Effects of (*R,S*)-ketamine, (*R*)-ketamine, and (*S*)-ketamine on PPI after a single intranasal administration. (A): Saline (0.5 ml/kg), or (*R,S*)-ketamine (10, 20, or 40 mg/kg) was administered intranasally into male mice. (B): Saline (0.5 ml/kg), or (*R*)-ketamine (10, 20, or 40 mg/kg) was administered intranasally into male mice. (C): Saline (0.5 ml/kg), or (*S*)-ketamine (10, 20, or 40 mg/kg) was administered intranasally into male mice. Startle response amplitude and PPI were measured as described in the [Method Section](#). The values represent the mean  $\pm$  S.E.M. ( $n = 9$  or  $10$ ). \* $P < 0.05$ , \*\* $P < 0.01$ , \*\*\* $P < 0.001$  compared with saline-treated mice. N.S.: not significant. R-KT: (*R*)-ketamine. RS-KT: (*R,S*)-ketamine. S-KT: (*S*)-ketamine.

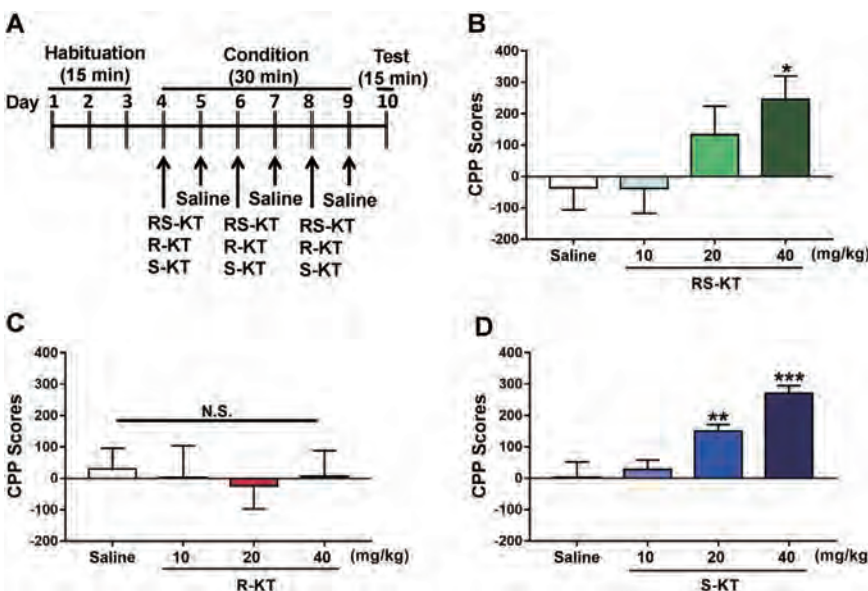


**Fig. 4.** Effects of (*R,S*)-ketamine, (*R*)-ketamine, and (*S*)-ketamine on CPP score after repeated intranasal administration. (A): Schedule of habituation, treatment, and behavioral test. (B): Saline (0.5 ml/kg), or (*R,S*)-ketamine (10, 20, or 40 mg/kg) was administered intranasally into male mice. (C): Saline (0.5 ml/kg), or (*R*)-ketamine (10, 20, or 40 mg/kg) was administered intranasally into male mice. (D): Saline (0.5 ml/kg), or (*S*)-ketamine (10, 20, or 40 mg/kg) was administered intranasally into male mice. CPP score was measured as described in the [Method Section](#). The values represent the mean  $\pm$  S.E.M. ( $n = 8-10$ ). \* $P < 0.05$ , \*\* $P < 0.01$ , \*\*\* $P < 0.001$  compared with saline-treated mice. N.S.: not significant. R-KT: (*R*)-ketamine. RS-KT: (*R,S*)-ketamine. S-KT: (*S*)-ketamine.

intranasal administration is (*S*)-ketamine > (*R,S*)-ketamine > (*R*)-ketamine. Collectively, it is likely that (*R*)-ketamine would be a rapid-acting and sustained antidepressant without side effects compared to (*R,S*)-ketamine and (*S*)-ketamine.

In this study, we found that antidepressant effects of (*R,S*)-ketamine and its two enantiomers in CSDS susceptible mice after a single intranasal administration may be less potent than those of a single i.p. administration (Dong et al., 2017; Yang et al., 2015, 2017a, 2017b, 2018a; Zhang et al., 2015; Zhang and Hashimoto, 2019b). Lower

bioavailability of intranasal administration of (*R,S*)-ketamine and its two enantiomers may contribute to lower efficacy of intranasal administration compared to i.p. administration. Interestingly, the potency of antidepressant effects of (*R,S*)-ketamine and its two enantiomers was not correlated with the potencies of these compounds at the NMDAR (Ebert et al., 1997), suggesting that NMDAR inhibition may not play a key role in the antidepressant effects of (*R,S*)-ketamine and its enantiomers. Previously, Fukumoto et al. (2017) reported that (*R,S*)-ketamine and (*R*)-ketamine, but not (*S*)-ketamine, show antidepressant

effects in rats with repeated corticosterone treatments after a single i.p. administration, consistent with our current data.

Due to its serious side effects, clinical use of ketamine has remained limited (Domino, 2010; Sanacora et al., 2017; Singh et al., 2017; Zhu et al., 2016), although it has been used as an off-label antidepressant in the USA (Reardon, 2018; Wilkinson et al., 2017). In this study, we found that locomotion after a single intranasal administration of (R)-ketamine is lower than those of (R,S)-ketamine and (S)-ketamine, consistent with the previous reports (Ryder et al., 1978; Yang et al., 2015) of subcutaneous or i.p. administration. Furthermore, we found that a single intranasal administration of (R)-ketamine did not cause PPI deficits in mice compared to (R,S)-ketamine and (S)-ketamine, consistent with the previous reports of i.p. administration (Yang et al., 2015). Interestingly, it was reported that the ED<sub>50</sub> of (R)-ketamine (6.33 mg/kg) for PPI deficits in rats was higher than that of (S)-ketamine (2.86 mg/kg), indicating that (S)-ketamine disrupts PPI with 2.5-fold higher potency than (R)-ketamine (Halberstadt et al., 2016). Finally, we found that repeated intranasal administration of (R)-ketamine did not increase CPP scores in mice although (R,S)-ketamine and (S)-ketamine increased CPP scores, in a dose dependent manner, consistent with the previous reports of i.p. administration (Yang et al., 2015, 2018b). A PET study showed that a single i.v. infusion of (S)-ketamine (0.5 mg/kg for 40-min), but not (R)-ketamine (0.5 mg/kg for 40-min), produced a marked reduction of dopamine D<sub>2/3</sub> receptor binding in conscious monkey striatum, suggesting that (S)-ketamine-induced dopamine release might be associated with acute psychotomimetic and dissociative side effects in humans (Hashimoto et al., 2017). Unlike (R,S)-ketamine and (S)-ketamine, it seems that intranasal infusion of (R)-ketamine does not appear to cause psychotomimetic effects or have abuse potential in humans, based on the lack of behavioral abnormalities (e.g., PPI deficits, CPP) observed in mice after single or repeated intranasal administration (Hashimoto, 2016a, 2016b, 2016c).

Mathisen et al. (1995) reported that the incidence of side effects (i.e., blurred vision, altered hearing, dizziness, proprioceptive disturbances, illusions) of (S)-ketamine (0.45 mg/kg, i.m.) treated group in patients with oral pain was higher than (R)-ketamine (1.8 mg/kg, i.m.) treated group, although the dose of (S)-ketamine (0.45 mg/kg) is lower than (R)-ketamine (1.8 mg/kg). Furthermore, it is also reported that experiencing illusion and alterations in hearing, vision, and proprioception is attributable to (S)-ketamine's actions (Oye et al., 1992; Vollenweider et al., 1997), whereas the feelings of relaxation are associated with (R)-ketamine's actions (Vollenweider et al., 1997; Zanos et al., 2018). Taken all together, it seems likely that (S)-ketamine contributes to the acute psychotomimetic and dissociative effects of (R,S)-ketamine, whereas (R)-ketamine may not be associated with these side effects (Zanos et al., 2018).

On March 5, 2019, the US FDA approved nasal spray of (S)-ketamine for treatment-resistant depression (FDA, 2019). Due to the risk of serious adverse outcomes from sedation and dissociation caused by administration of (S)-ketamine, as well as the potential for abuse and misuse of the drug, FDA said that the drug will only be available through a restricted distribution system, under a Risk Evaluation and Mitigation Strategy (REMS). Patients will self-administer (S)-ketamine under the supervision of a health care provider in a certified doctor's office or clinic; the nasal spray cannot be taken home (FDA, 2019). Given the lack of adverse side effects of (R)-ketamine, it is possible that patients may take (R)-ketamine to their home.

In conclusion, this study suggests that the order of potency for antidepressant effects in a CSDS model after a single intranasal administration is (R)-ketamine > (R,S)-ketamine > (S)-ketamine. In contrast, the order of potency for side effects in mice after intranasal administration is (S)-ketamine > (R,S)-ketamine > (R)-ketamine. Therefore, it is likely that (R)-ketamine could be a safer antidepressant without side effects than (R,S)-ketamine and (S)-ketamine.

## Acknowledgements

This study was supported by AMED, Japan (to K.H., JP19dm0107119). Dr. Lijia Chang was supported by the Japan China Sasakawa Medical Fellowship (Tokyo, Japan). Dr. Zhongwei Xiong (Wuhan University, China) was supported by the China Scholarship Council (China).

## Conflict of interest

Dr. Hashimoto is an inventor on a filed patent application on "The use of (R)-ketamine in the treatment of psychiatric diseases" by Chiba University. Dr. Hashimoto has received research support from Dainippon-Sumitomo, Otsuka, and Taisho. Other authors declare no conflict of interest.

## References

- Abdallah, C.G., Sanacora, G., Duman, R.S., Krystal, J.H., 2018. The neurobiology of depression, ketamine and rapid-acting antidepressants: is it glutamate inhibition or activation? *Pharmacol. Ther.* 190, 148–158.
- Berman, R.M., Cappiello, A., Anand, A., Oren, D.A., Heninger, G.R., Charney, D.S., Krystal, J.H., 2000. Antidepressant effects of ketamine in depressed patients. *Biol. Psychiatry* 47, 351–354.
- Chaki, S., 2017a. Beyond ketamine: new approaches to the development of safer antidepressants. *Curr. Neuropharmacol.* 15, 963–976.
- Chaki, S., 2017b. mGlu<sub>2/3</sub> receptor antagonists as novel antidepressants. *Trends Pharmacol. Sci.* 38, 569–580.
- Chang, L., Zhang, K., Pu, Y., Qu, Y., Wang, S.M., Xiong, Z., Shirayama, Y., Hashimoto, K., 2019. Lack of dopamine D<sub>1</sub> receptors in the antidepressant actions of (R)-ketamine in a chronic social defeat stress model. *Eur. Arch. Psychiatry Clin. Neurosci.* <https://doi.org/10.1007/s00406-019-01012-1>. 2019 Mar 29.
- Domino, E.F., 2010. Taming the ketamine tiger. 1965. *Anesthesiology* 113, 678–684.
- Dong, C., Zhang, J.C., Yao, W., Ren, Q., Ma, M., Yang, C., Chaki, S., Hashimoto, K., 2017. Rapid and sustained antidepressant action of the mGlu<sub>2/3</sub> receptor antagonist MGS0039 in the social defeat stress model: comparison with ketamine. *Int. J. Neuropsychopharmacol.* 20, 228–236.
- Duman, R.S., 2018. Ketamine and rapid-acting antidepressants: a new era in the battle against depression and suicide. *F1000Res.* 7 (pii: F1000 Faculty Rev-659).
- Ebert, B., Mikkelsen, S., Thorikildsen, C., Borgbjerg, F.M., 1997. Norketamine, the main metabolite of ketamine, is a non-competitive NMDA receptor antagonist in the rat cortex and spinal cord. *Eur. J. Pharmacol.* 333, 99–104.
- FDA News Release on March 5, 2019. FDA Approves New Nasal Spray Medication for Treatment-resistant Depression; Available Only at a Certified Doctor's Office or Clinic. <https://www.fda.gov/NewsEvents/Newsroom/PressAnnouncements/ucm632761.htm>.
- Fukumoto, K., Toki, H., Iijima, M., Hashihayata, T., Yamaguchi, J.I., Hashimoto, K., Chaki, S., 2017. Antidepressant potential of (R)-ketamine in rodent models: comparison with (S)-ketamine. *J. Pharmacol. Exp. Ther.* 361, 9–16.
- Golden, S.A., Covington III, H.E., Berton, O., Russo, S.J., 2011. A standardized protocol for repeated social defeat stress in mice. *Nat. Protoc.* 6, 1183–1191.
- Gould, T.D., Zarate Jr., C.A., Thompson, S.M., 2019. Molecular pharmacology and neurobiology of rapid-acting antidepressants. *Annu. Rev. Pharmacol. Toxicol.* 59, 213–236.
- Grunebaum, M.F., Galfalvy, H.C., Choo, T.H., Keilp, J.G., Moitra, V.K., Parris, M.S., Marver, J.E., Burke, A.K., Milak, M.S., Sublette, M.E., Oquendo, M.A., Mann, J.J., 2018. Ketamine for rapid reduction of suicidal thoughts in major depression: a midazolam-controlled randomized clinical trial. *Am. J. Psychiatry* 175, 327–335.
- Halberstadt, A.L., Slepak, N., Hyun, J., Buell, M.R., Powell, S.B., 2016. The novel ketamine analog methoxetamine produces dissociative-like behavioral effects in rodents. *Psychopharmacology* 233, 1215–1225.
- Hashimoto, K., 2014. The R-stereoisomer of ketamine as an alternative for ketamine for treatment-resistant major depression. *Clin. Psychopharmacol. Neurosci.* 12, 72–73.
- Hashimoto, K., 2016a. R-ketamine: a rapid-onset and sustained antidepressant without risk of brain toxicity. *Psychol. Med.* 46, 2449–2451.
- Hashimoto, K., 2016b. Ketamine's antidepressant action: beyond NMDA receptor inhibition. *Expert Opin. Ther. Targets* 20, 1389–1392.
- Hashimoto, K., 2016c. Detrimental side effects of repeated ketamine infusions in the brain. *Am. J. Psychiatry* 173, 1044–1045.
- Hashimoto, K., Kakiuchi, T., Ohba, H., Nishiyama, S., Tsukada, H., 2017. Reduction of dopamine D<sub>2/3</sub> receptor binding in the striatum after a single administration of es-ketamine, but not R-ketamine: a PET study in conscious monkeys. *Eur. Arch. Psychiatry Clin. Neurosci.* 267, 173–176.
- Kishimoto, T., Chawla, J.M., Hagi, K., Zarate, C.A., Kane, J.M., Bauer, M., Correll, C.U., 2016. Single-dose infusion ketamine and non-ketamine N-methyl-D-aspartate receptor antagonists for unipolar and bipolar depression: a meta-analysis of efficacy, safety and time trajectories. *Psychol. Med.* 46, 1459–1472.
- Krystal, J.H., Abdallah, C.G., Sanacora, G., Charney, D.S., Duman, R.S., 2019. Ketamine: a paradigm shift for depression research and treatment. *Neuron* 101, 774–778.
- Larkin, G.L., Beautrais, A.L., 2011. A preliminary naturalistic study of low-dose ketamine

- for depression and suicide ideation in the emergency department. *Int. J. Neuropsychopharmacol.* 14, 1127–1131.
- Li, L., Vlissides, P.E., 2016. Ketamine: 50 years of modulating the mind. *Front. Hum. Neurosci.* 10, 612.
- Mathisen, L.C., Skjelbred, P., Skoglund, L.A., Oye, I., 1995. Effect of ketamine, an NMDA receptor inhibitor, in acute and chronic orofacial pain. *Pain* 61, 215–220.
- Matsuura, A., Fujita, Y., Iyo, M., Hashimoto, K., 2015. Effects of sodium benzoate on pre-pulse inhibition deficits and hyperlocomotion in mice after administration of phen-cyclidine. *Acta. Neuropsychiatr.* 27, 159–167.
- Monteggia, L.M., Zarate Jr., C., 2015. Antidepressant actions of ketamine: from molecular mechanisms to clinical practice. *Curr. Opin. Neurobiol.* 30, 139–143.
- Murrough, J.W., Iosifescu, D.V., Chang, L.C., Al Jurdi, R.K., Green, C.E., Perez, A.M., Iqbal, S., Pillemer, S., Foulkes, A., Shah, A., Charney, D.S., Mathew, S.J., 2013. Antidepressant efficacy of ketamine in treatment-resistant major depression: a two-site randomized controlled trial. *Am. J. Psychiatry* 170, 1134–1142.
- Murrough, J.W., Soleimani, L., DeWilde, K.E., Collins, K.A., Lapidus, K.A., Iacoviello, B.M., Lener, M., Kautz, M., Kim, J., Stern, J.B., Price, R.B., Perez, A.M., Brallier, J.W., Rodriguez, G.J., Goodman, W.K., Iosifescu, D.V., Charney, D.S., 2015. Ketamine for rapid reduction of suicidal ideation: a randomized controlled trial. *Psychol. Med.* 45, 3571–3580.
- Murrough, J.W., Abdallah, C.G., Mathew, S.J., 2017. Targeting glutamate signalling in depression: progress and prospects. *Nat. Rev. Drug Discov.* 16, 472–486.
- Newport, D.J., Carpenter, L.L., McDonald, W.M., Potash, J.B., Tohen, M., Nemeroff, C.B., 2015. APA council of research task force on novel biomarkers and treatments. Ketamine and other NMDA antagonists: early clinical trials and possible mechanisms in depression. *Am. J. Psychiatry* 172, 950–966.
- Oye, I., Paulsen, O., Maurset, A., 1992. Effects of ketamine on sensory perception: evidence for a role of *N*-methyl-*D*-aspartate receptors. *J. Pharmacol. Exp. Ther.* 260, 1209–1213.
- Peltoniemi, M.A., Hagelberg, N.M., Olkkola, K.T., Saari, T., 2016. Ketamine: a review of clinical pharmacokinetics and pharmacodynamics in anesthesia and pain therapy. *Clin. Pharmacokinet.* 55, 1059–1077.
- Price, R.B., Nock, M.K., Charney, D.S., Mathew, S.J., 2009. Effects of intravenous ketamine on explicit and implicit measures of suicidality in treatment-resistant depression. *Biol. Psychiatry* 66, 522–526.
- Reardon, S., 2018. ‘Party drug’ turned antidepressant approaches approval. *Nat. Rev. Drug Discov.* 17, 773–775.
- Ryder, S., Way, W.L., Trevor, A.J., 1978. Comparative pharmacology of the optical isomers of ketamine in mice. *Eur. J. Pharmacol.* 49, 15–23.
- Sanacora, G., Frye, M.A., McDonald, W., Mathew, S.J., Turner, M.S., Schatzberg, A.F., Summergrad, P., Nemeroff, C.B., American Psychiatric Association (APA) Council of Research Task Force on Novel Biomarkers and Treatments, 2017. A consensus statement on the use of ketamine in the treatment of mood disorders. *JAMA Psychiatry* 74, 399–405.
- Singh, I., Morgan, C., Curran, V., Nutt, D., Schlag, A., McShane, R., 2017. Ketamine treatment for depression: opportunities for clinical innovation and ethical foresight. *Lancet Psychiatry* 4, 419–426.
- Su, T.P., Chen, M.H., Li, C.T., Lin, W.C., Hong, C.J., Gueorguieva, R., Tu, P.C., Bai, Y.M., Cheng, C.M., Krystal, J.H., 2017. Dose-related effects of adjunctive ketamine in Taiwanese patients with treatment-resistant depression. *Neuropsychopharmacology* 42, 2482–2492.
- Tian, Z., Dong, C., Fujita, A., Fujita, Y., Hashimoto, K., 2018. Expression of heat shock protein HSP-70 in the retrosplenial cortex of rat brain after administration of (*R,S*)-ketamine and (*S*)-ketamine, but not (*R*)-ketamine. *Pharmacol. Biochem. Behav.* 172, 17–21.
- Vollenweider, F.X., Leenders, K.L., Oye, I., Hell, D., Angst, J., 1997. Differential psychopathology and patterns of cerebral glucose utilisation produced by (*S*)- and (*R*)-ketamine in healthy volunteers using positron emission tomography (PET). *Eur. Neuropsychopharmacol.* 7, 25–38.
- Wilkinson, S.T., Toprak, M., Turner, M.S., Levine, S.P., Katz, R.B., Sanacora, G., 2017. A survey of the clinical, off-label use of ketamine as a treatment for psychiatric disorders. *Am. J. Psychiatry* 174, 695–696.
- Wilkinson, S.T., Ballard, E.D., Bloch, M.H., Mathew, S.J., Murrough, J.W., Feder, A., Sos, P., Wang, G., Zarate Jr., C.A., Sanacora, G., 2018. The effect of a single dose of intravenous ketamine on suicidal ideation: a systematic review and individual participant data meta-analysis. *Am. J. Psychiatry* 175, 150–158.
- Xiong, Z., Zhang, K., Ishima, T., Ren, Q., Chang, L., Chen, J., Hashimoto, K., 2018a. Comparison of rapid and long-lasting antidepressant effects of negative modulators of  $\alpha 5$ -containing GABA<sub>A</sub> receptors and (*R*)-ketamine in a chronic social defeat stress model. *Pharmacol. Biochem. Behav.* 175, 139–145.
- Xiong, Z., Zhang, K., Ishima, T., Ren, Q., Ma, M., Pu, Y., Chang, L., Chen, J., Hashimoto, K., 2018b. Lack of rapid antidepressant effects of Kir4.1 channel inhibitors in a chronic social defeat stress model: comparison with (*R*)-ketamine. *Pharmacol. Biochem. Behav.* 176, 57–62.
- Xu, Y., Hackett, M., Carter, G., Loo, C., Gálvez, V., Glozier, N., Glue, P., Lapidus, K., McGirr, A., Somogyi, A.A., Mitchell, P.B., Rodgers, A., 2016. Effects of low-dose and very low-dose ketamine among patients with major depression: a systematic review and meta-analysis. *Int. J. Neuropsychopharmacol.* 19 (pii: pyv124).
- Yang, C., Shirayama, Y., Zhang, J.C., Ren, Q., Yao, W., Ma, M., Dong, C., Hashimoto, K., 2015. *R*-ketamine: a rapid-onset and sustained antidepressant without psychotomimetic side effects. *Transl. Psychiatry* 5, e632.
- Yang, C., Han, M., Zhang, J.C., Ren, Q., Hashimoto, K., 2016. Loss of parvalbumin-immunoreactivity in mouse brain regions after repeated intermittent administration of esketamine, but not *R*-ketamine. *Psychiatric Res.* 239, 281–283.
- Yang, C., Qu, Y., Abe, M., Nozawa, D., Chaki, S., Hashimoto, K., 2017a. (*R*)-ketamine shows greater potency and longer lasting antidepressant effects than its metabolite (2*R,6R*)-hydroxynorketamine. *Biol. Psychiatry* 82, e43–e44.
- Yang, C., Qu, Y., Fujita, Y., Ren, Q., Ma, M., Dong, C., Hashimoto, K., 2017b. Possible role of the gut microbiota-brain axis in the antidepressant effects of (*R*)-ketamine in a social defeat stress model. *Transl. Psychiatry* 7, 1294.
- Yang, C., Ren, Q., Qu, Y., Zhang, J.C., Ma, M., Dong, C., Hashimoto, K., 2018a. Mechanistic target of rapamycin-independent antidepressant effects of (*R*)-ketamine in a social defeat stress model. *Biol. Psychiatry* 83, 18–28.
- Yang, C., Kobayashi, S., Nakao, K., Dong, C., Han, M., Qu, Y., Ren, Q., Zhang, J.C., Ma, M., Toki, H., Yamaguchi, J.I., Chaki, S., Shirayama, Y., Nakazawa, K., Manabe, T., Hashimoto, K., 2018b. AMPA receptor activation-independent antidepressant actions of ketamine metabolite (*S*)-norketamine. *Biol. Psychiatry* 84, 591–600.
- Zanos, P., Moaddel, R., Morris, P.J., Georgiou, P., Fischell, J., Elmer, G.I., Alkondon, M., Yuan, P., Pribut, H.J., Singh, N.S., Dossou, K.S., Fang, Y., Huang, X.P., Mayo, C.L., Wainer, I.W., Albuquerque, E.X., Thompson, S.M., Thomas, C.J., Zarate Jr., C.A., Gould, T.D., 2016. NMDAR inhibition-independent antidepressant actions of ketamine metabolites. *Nature* 533, 481–486.
- Zanos, P., Moaddel, R., Morris, P.J., Riggs, L.M., Highland, J.N., Georgiou, P., Pereira, E.F.R., Albuquerque, E.X., Thomas, C.J., Zarate Jr., C.A., Gould, T.D., 2018. Ketamine and ketamine metabolite pharmacology: insights into therapeutic mechanisms. *Pharmacol. Rev.* 70, 621–660.
- Zarate, C.A., Singh, J.B., Carlson, P.J., Brutsche, N.E., Ameli, R., Luckenbaugh, D.A., Charney, D.S., Manji, H.K., 2006. A randomized trial of an *N*-methyl-*D*-aspartate antagonist in treatment-resistant major depression. *Arch. Gen. Psychiatry* 63, 856–864.
- Zhang, J.C., Li, S.X., Hashimoto, K., 2014. *R*(–)-ketamine shows greater potency and longer lasting antidepressant effects than *S*(+)-ketamine. *Pharmacol. Biochem. Behav.* 116, 137–141.
- Zhang, J.C., Yao, W., Dong, C., Yang, C., Ren, Q., Ma, M., Han, M., Hashimoto, K., 2015. Comparison of ketamine, 7,8-dihydroxyflavone, and ANA-12 antidepressant effects in the social defeat stress model of depression. *Psychopharmacology* 232, 4325–4335.
- Zhang, K., Hashimoto, K., 2019a. An update on ketamine and its two enantiomers as rapid-acting antidepressants. *Expert Rev. Neurother.* 19, 83–92.
- Zhang, K., Hashimoto, K., 2019b. Lack of opioid system in the antidepressant actions of ketamine. *Biol. Psychiatry* 85, e25–e27.
- Zhang, K., Toki, H., Fujita, Y., Ma, M., Chang, L., Qu, Y., Harada, S., Nemoto, T., Mizuno-Yasuhira, A., Yamaguchi, J.I., Chaki, S., Hashimoto, K., 2018. Lack of deuterium isotope effects in the antidepressant effects of (*R*)-ketamine in a chronic social defeat stress model. *Psychopharmacology* 235, 3177–3185.
- Zhu, W., Ding, Z., Zhang, Y., Shi, J., Hashimoto, K., Lu, L., 2016. Risks associated with misuse of ketamine as a rapid-acting antidepressant. *Neurosci. Bull.* 32, 557–564.



# Lack of dopamine D<sub>1</sub> receptors in the antidepressant actions of (*R*)-ketamine in a chronic social defeat stress model

Lijia Chang<sup>1</sup> · Kai Zhang<sup>1</sup> · Yaoyu Pu<sup>1</sup> · Youge Qu<sup>1</sup> · Si-ming Wang<sup>1</sup> · Zhongwei Xiong<sup>1</sup> · Yukihiko Shirayama<sup>1,2</sup> · Kenji Hashimoto<sup>1</sup>

Received: 17 February 2019 / Accepted: 26 March 2019 / Published online: 29 March 2019  
© Springer-Verlag GmbH Germany, part of Springer Nature 2019

## Abstract

It is reported that dopamine D<sub>1</sub> receptors in the medial prefrontal cortex play a role in the antidepressant actions of (*R,S*)-ketamine. However, its role in the antidepressant actions of (*R*)-ketamine, which is more potent than (*S*)-ketamine, is unknown. In the locomotion test, tail suspension test, forced swimming test and 1% sucrose preference test, pretreatment with dopamine D<sub>1</sub> receptor antagonist SCH-23390 did not block the antidepressant effects of (*R*)-ketamine in the susceptible mice after chronic social defeat stress. These findings suggest that dopamine D<sub>1</sub> receptors may not play a major role in the antidepressant actions of (*R*)-ketamine.

**Keywords** Antidepressant · (*R*)-ketamine · Dopamine D<sub>1</sub> receptor · Social defeat stress

## Introduction

The *N*-methyl-D-aspartate receptor (NMDAR) antagonist (*R,S*)-ketamine exhibits rapid and sustained antidepressant effects in treatment-resistant patients with major depressive disorder [1–3]. (*R,S*)-ketamine is a racemic mixture containing equal parts of (*R*)-ketamine (or arketamine) and (*S*)-ketamine (or esketamine). (*R,S*)-ketamine (K<sub>i</sub> = 0.53 μM for NMDAR) is a racemic mixture containing equal parts of (*R*)-ketamine (or arketamine) (K<sub>i</sub> = 1.4 μM for NMDAR) and (*S*)-ketamine (or esketamine) (K<sub>i</sub> = 0.30 μM for NMDAR) [4]. Interestingly, (*R*)-ketamine shows greater potency and longer-lasting antidepressant effects than (*S*)-ketamine in rodents with depression-like phenotype [5–11]. Thus, it is suggested that NMDAR may not play a major role in the antidepressant effects of (*R*)-ketamine [12]. Importantly, side effects of (*R*)-ketamine are less potent than (*S*)-ketamine [7, 13–15]. Collectively, (*R*)-ketamine may be a safer antidepressant in humans than (*R,S*)-ketamine and (*S*)-ketamine.

However, the precise mechanisms underlying the antidepressant actions of (*R*)-ketamine remain unknown.

Preclinical studies suggest that medial prefrontal cortex (mPFC) plays a role in the antidepressant effects of (*R,S*)-ketamine [or (*R*)-ketamine] in rats with or without depression-like phenotype [16, 17]. A recent study demonstrated that disruption of dopamine D<sub>1</sub> receptor encoded by the *Drd1* in the mPFC blocked the rapid antidepressant effects of (*R,S*)-ketamine in control mice [18], suggesting that *Drd1* cells, and activation of dopamine D<sub>1</sub> receptors in the mPFC, are necessary for the rapid antidepressant actions of (*R,S*)-ketamine. In contrast, Li et al. [19] reported that dopamine D<sub>1</sub> receptor antagonist SCH-23390 did not block the antidepressant-like effects of ketamine in control mice, inconsistent with the report from Hare et al. [18]. Importantly, these two reports did not use rodents with depression-like phenotype [20]. At present, the role of dopamine D<sub>1</sub> receptors in the antidepressant effects of (*R*)-ketamine in animal models of depression such as a chronic social defeat stress (CSDS) model has not been reported.

This study was undertaken to examine whether the pretreatment of dopamine D<sub>1</sub> receptor antagonist SCH-23390 could influence the antidepressant effects of (*R*)-ketamine in a CSDS model.

✉ Kenji Hashimoto  
hashimoto@faculty.chiba-u.jp

<sup>1</sup> Division of Clinical Neuroscience, Chiba University Center for Forensic Mental Health, Chiba 260-8670, Japan

<sup>2</sup> Department of Psychiatry, Teikyo University Chiba Medical Center, Ichihara 299-0111, Japan

## Methods and materials

### Animals

Male adult C57BL/6 mice ( $n=60$ ), aged 8 weeks (body weight 20–25 g, Japan SLC, Inc., Hamamatsu, Japan) and male adult CD1 (ICR) mice ( $n=20$ ), aged 13–15 weeks (body weight > 40 g, Japan SLC, Inc., Hamamatsu, Japan) were used. Animals were housed under controlled temperatures and 12 h light/dark cycles (lights on between 07:00 and 19:00 h), with ad libitum food (CE-2; CLEA Japan, Inc., Tokyo, Japan) and water. The protocol was approved by the Chiba University Institutional Animal Care and Use Committee (Permission number: 30-385). This study was carried out in strict accordance with the recommendations in the Guide for the Care and Use of Laboratory Animals of the National Institutes of Health, USA. Animals were deeply anaesthetized with isoflurane before being killed by cervical dislocation. All efforts were made to minimize suffering.

### Materials

(*R*)-ketamine hydrochloride was prepared as described previously [6]. The dose (10 mg/kg as hydrochloride) of (*R*)-ketamine dissolved in the saline was used as previously reported [7–11, 21]. The dose of SCH-23390 hydrochloride (0.1 mg/kg, Sigma-Aldrich Co., St Louis, MO, USA) was used as previously reported [19].

### Chronic social defeat stress (CSDS) model, treatment and behavioral tests

The procedure of CSDS and behavioral tests were performed as previously reported [7–11, 21]. The CSDS susceptible mice were divided to four groups; saline + saline group,

saline + (*R*)-ketamine group, SCH-23390 + (*R*)-ketamine group, SCH-23390 + saline group. Saline or SCH-23390 was administered intraperitoneally (i.p.) into the susceptible mice 30 min before single i.p. administration of saline or (*R*)-ketamine (day 12). Control (no CSDS) mice received saline + saline. Behavioral tests, including locomotion test (LMT), tail suspension test (TST), forced swimming test (FST) and 1% sucrose preference test (SPT), were performed. LMT and TST were performed 2 and 4 h after a single injection of (*R*)-ketamine or saline, respectively. FST was performed 24 h after a single injection of (*R*)-ketamine or saline. SPT was performed 2 and 4 days after a single injection of (*R*)-ketamine or saline (Fig. 1).

### Statistical analysis

The data show as the mean  $\pm$  standard error of mean (S.E.M.). Analysis was performed using PASW Statistics 20 (Tokyo, Japan). The behavioral data were analyzed using the one-way analysis of variance (ANOVA), followed by post hoc Tukey test. The *P* values of less than 0.05 were considered statistically significant.

## Results

### Effects of SCH-23390 in the antidepressant effect of (*R*)-ketamine in a CSDS model

Locomotion showed no difference ( $F_{4,44} = 1.094$ ,  $P = 0.371$ ) among the five groups (Fig. 2a). One-way ANOVA of TST and FST data showed a statistical significance (TST:  $F_{4,44} = 12.08$ ,  $P < 0.001$ , FST:  $F_{4,44} = 22.58$ ,  $P < 0.001$ ) among the five groups (Fig. 2b, c). Post-hoc tests showed that (*R*)-ketamine (10 mg/kg) significantly

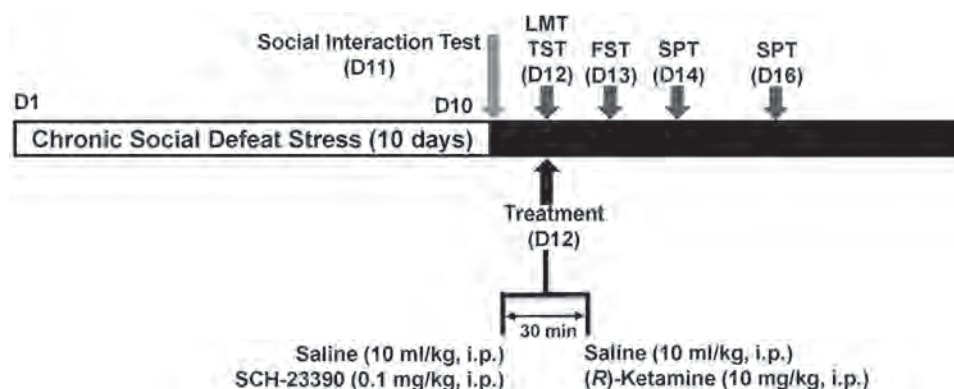


**Fig. 1** Schedule of CSDS, treatment, and behavioral tests. CSDS was performed from day 1 to day 10, and the social interaction test (SIT) was performed on day 11. Saline (10 ml/kg) or SCH-23390 (0.1 mg/kg) was administered i.p. in the susceptible mice on day 12. Saline (10 ml/kg) or (*R*)-ketamine (10 mg/kg) was administered i.p. into

mice 30 min after administration of saline or SCH-23390. LMT and TST were performed 2 and 4 h after a single injection of (*R*)-ketamine or saline, respectively. SPT was performed 2 and 4 days after single injection of (*R*)-ketamine or saline

attenuated the increased immobility times of TST and FST in susceptible mice after CSDS (Fig. 2b, c). However, there were no differences between saline + (*R*)-ketamine group and SCH-23390 + (*R*)-ketamine group in the immobility times of TST and FST (Fig. 2b, c). Furthermore, there were no differences between saline + saline group and SCH-23390 + saline group in the immobility times of TST and FST in the susceptible mice (Fig. 2b, c).

One-way ANOVA of SPT data showed statistical significances (2 days after a single injection:  $F_{4,44} = 7.561$ ,  $P < 0.001$ , 4 days after a single injection:  $F_{4,44} = 20.36$ ,  $P < 0.001$ ) among five groups (Fig. 2d, e). Post-hoc tests showed that sucrose preference of saline + (*R*)-ketamine group was significantly higher from saline + saline group (Fig. 2d, e). Furthermore, sucrose preference of saline + (*R*)-ketamine group was not different from SCH-23390 + (*R*)-ketamine group (Fig. 2d, e). Moreover, sucrose preference of saline + saline group was not different from SCH-23390 + saline group (Fig. 2d, e).

### Discussion

We demonstrated that pretreatment with SCH-23390 did not block the antidepressant effects of (*R*)-ketamine in the susceptible mice after CSDS, suggesting that dopamine  $D_1$  receptors do not play a major role in the antidepressant actions of (*R*)-ketamine.

It is reported that pretreatment with haloperidol (0.15 mg/kg, a nonselective dopamine  $D_{2/3}$  receptor antagonist), but not SCH-23390 (0.04 and 0.1 mg/kg, a selective dopamine  $D_1$  receptor antagonist), significantly prevented the antidepressant-like effects of (*R,S*)-ketamine (20 mg/kg) in control mice [19]. Moreover, administration of (*R,S*)-ketamine (10 mg/kg) in combination with pramipexole (0.3 mg/kg, a dopamine  $D_{2/3}$  receptor agonist) exerted antidepressant-like effects compared with each drug alone [19]. These results suggest that dopamine  $D_{2/3}$  receptors, but not  $D_1$  receptors, are involved in the antidepressant-like effects of ketamine in control mice [19]. In contrast, bilateral infusion (10 min before) of a selective dopamine  $D_1$  receptor antagonist SCH-39166 into the mPFC completely

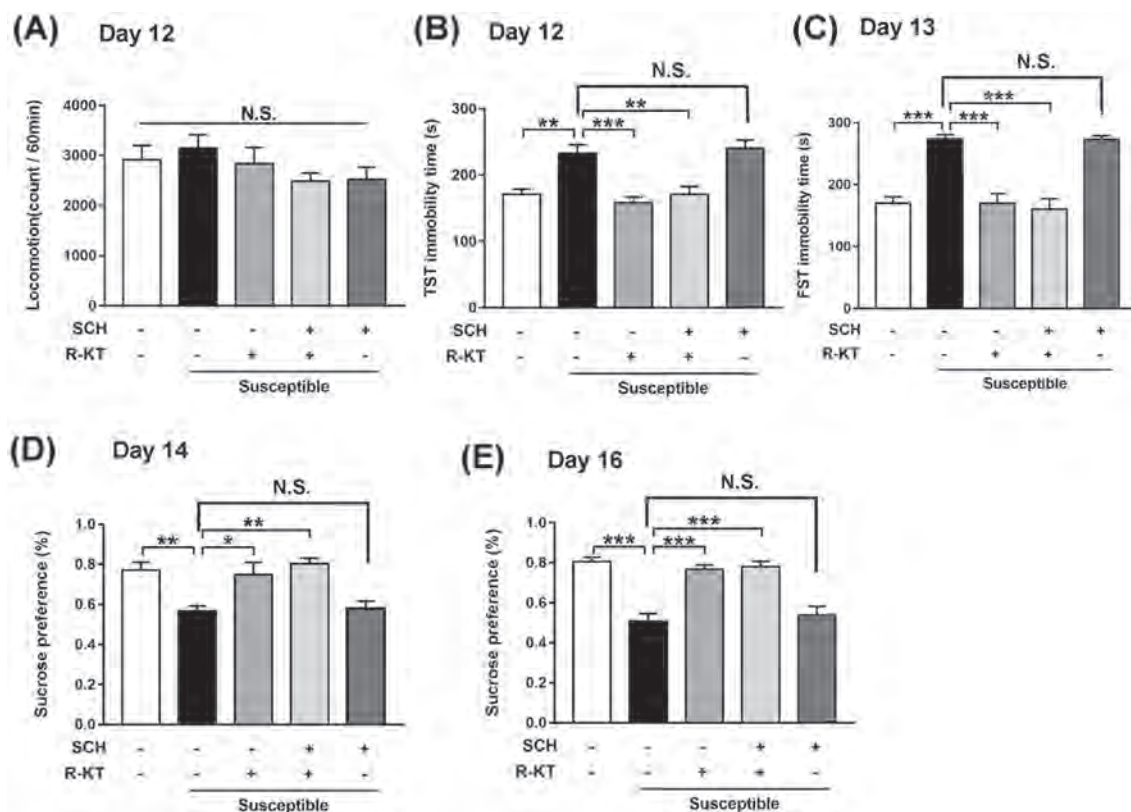


**Fig. 2** Effects of SCH-23390 in the antidepressant effects of (*R*)-ketamine in a CSDS model. **a** LMT (day 12). **b** TST (day 12). **c** FST (day 13). **d** SPT (day 14) and **e** SPT (day 16). The values represent the mean ± S.E.M. ( $n = 9$  or  $10$ ). \* $P < 0.05$ , \*\* $P < 0.01$ , \*\*\* $P < 0.001$ .

N.S. not significance, LMT locomotion test, TST tail suspension test, FST forced swimming test, R-KT (*R*)-ketamine, SCH SCH-23390, SPT 1% sucrose preference test

blocked the antidepressant-like effects of (*R,S*)-ketamine in control mice [18]. In addition, infusion of a selective dopamine D<sub>1</sub> receptor agonist SKF-81297 into the mPFC decreased the immobility time of FST in the control mice 24 h after a single dose, suggesting antidepressant-like effects of SKF-81297 in mice [18]. This paper suggests that activation at dopamine D<sub>1</sub> receptors in the mPFC may contribute to ketamine's antidepressant-like effects [18]. Although the reasons underlying these discrepancies remain unclear, variations in the experimental conditions may contribute to these discrepancies. One possibility is the difference in the route of administration (systemic administration of (*R*)-ketamine vs. direct infusion of (*R,S*)-ketamine into the mPFC). Another possibility is the use of rodents with or without depression-like phenotype. Very interestingly, healthy control subjects exhibited modest, but significant, increases in depressive symptoms for up to 1 day after a single ketamine infusion [22], suggesting that ketamine does not induce antidepressant-like effects in healthy control subjects. Collectively, the use of rodents with or without depression-like phenotypes may contribute to these discrepancies [20]. Therefore, further detailed study using rodents with depression-like phenotype is needed to confirm the role of dopamine D<sub>1</sub> receptors in the antidepressant effects of ketamine and its enantiomers.

A high dose (30 mg/kg) of ketamine rapidly increases extracellular dopamine in the mPFC of rats [23], suggesting that ketamine-induced dopamine release may play a role in ketamine's actions such as antidepressant effects [18]. A recent study demonstrated that (*S*)-ketamine caused a robust increase in dopamine release in the PFC compared with (*R*)-ketamine [24]. If ketamine-induced dopamine release in the PFC plays a key role in the antidepressant effects of ketamine, (*S*)-ketamine must be more potent than (*R*)-ketamine in animal models of depression. Nonetheless, further detailed study underlying the role of dopamine D<sub>1</sub> receptors in the antidepressant effects of ketamine and its enantiomers is needed.

In conclusion, this study showed that pretreatment with SCH-23390 did not block the acute and long-lasting antidepressant effects of (*R*)-ketamine in a CSDS model. Therefore, it is unlikely that dopamine D<sub>1</sub> receptors play a major role in the antidepressant actions of (*R*)-ketamine although this may, in part, contribute to its other pharmacological actions.

**Acknowledgements** This study was supported by AMED (to K.H., JP18dm0107119). Dr. Hashimoto is an inventor on a filed patent application on "The use of (*R*)-ketamine in the treatment of psychiatric diseases" by Chiba University. Dr. Hashimoto has received research support from Dainippon-Sumitomo, Otsuka, and Taisho.

## Compliance with ethical standards

**Conflict of interest** All authors declare that they have no conflict of interest.

## References

- Newport DJ, Carpenter LL, McDonald WM, Potash JB, Tohen M, Nemeroff CB (2015) Ketamine and other NMDA antagonists: early clinical trials and possible mechanisms in depression. *Am J Psychiatry* 172(10):950–966
- Kishimoto T, Chawla JM, Hagi K, Zarate CA, Kane JM, Bauer M, Correll CU (2016) Single-dose infusion ketamine and non-ketamine *N*-methyl-*D*-aspartate receptor antagonists for unipolar and bipolar depression: a meta-analysis of efficacy, safety and time trajectories. *Psychol Med* 46(7):1459–1472
- Zhang K, Hashimoto K (2019) An update on ketamine and its two enantiomers as rapid-acting antidepressants. *Expert Rev Neurother* 19(1):83–92
- Ebert B, Mikkelsen S, Thorkildsen C, Borgbjerg FM (1997) Nor-ketamine, the main metabolite of ketamine, is a non-competitive NMDA receptor antagonist in the rat cortex and spinal cord. *Eur J Pharmacol* 333(1):99–104
- Fukumoto K, Toki H, Iijima M, Hashihayata T, J-i Yamaguchi, Hashimoto K, Chaki S (2017) Antidepressant potential of (*R*)-ketamine in rodent models: comparison with (*S*)-ketamine. *J Pharmacol Exp Ther* 36(1):9–16
- Zhang JC, Li SX, Hashimoto K (2014) *R*(-)-ketamine shows greater potency and longer lasting antidepressant effects than *S*(+)-ketamine. *Pharmacol Biochem Behav* 116:137–141
- Yang C, Shirayama Y, Jc Zhang, Ren Q, Yao W, Ma M, Dong C, Hashimoto K (2015) *R*-ketamine: a rapid-onset and sustained antidepressant without psychotomimetic side effects. *Transl Psychiatry* 5:e632
- Yang C, Qu Y, Abe M, Nozawa D, Chaki S, Hashimoto K (2017) (*R*)-ketamine shows greater potency and longer lasting antidepressant effects than its metabolite (2*R*,6*R*)-hydroxynorketamine. *Biol Psychiatry* 82(5):e43–e44
- Yang C, Qu Y, Fujita Y, Ren Q, Ma M, Dong C, Hashimoto K (2017) Possible role of the gut microbiota-brain axis in the antidepressant effects of (*R*)-ketamine in a social defeat stress model. *Transl Psychiatry* 7(12):1294
- Yang C, Ren Q, Qu Y, Zhang J-C, Ma M, Dong C, Hashimoto K (2018) Mechanistic target of rapamycin-independent antidepressant effects of (*R*)-ketamine in a social defeat stress model. *Biol Psychiatry* 83(1):18–28
- Zhang K, Ma M, Dong C, Hashimoto K (2018) Role of inflammatory bone markers in the antidepressant actions of (*R*)-ketamine in a chronic social defeat stress model. *Int J Neuropsychopharmacol* 21(11):1025–1030
- Hashimoto K (2016) Letter to the Editor: *R*-ketamine: a rapid-onset and sustained antidepressant without risk of brain toxicity. *Psychol Med* 46(11):2449–2451
- Yang C, Han M, J-c Zhang, Ren Q, Hashimoto K (2016) Loss of parvalbumin-immunoreactivity in mouse brain regions after repeated intermittent administration of esketamine, but not *R*-ketamine. *Psychiatry Res* 239:281–283
- Hashimoto K, Kakiuchi T, Ohba H, Nishiyama S, Tsukada H (2017) Reduction of dopamine D<sub>2/3</sub> receptor binding in the striatum after a single administration of esketamine, but not *R*-ketamine: a PET study in conscious monkeys. *Eur Arch Psychiatry Clin Neurosci* 267(2):173–176

15. Tian Z, Dong C, Fujita A, Fujita Y, Hashimoto K (2018) Expression of heat shock protein HSP-70 in the retrosplenial cortex of rat brain after administration of (R, S)-ketamine and (S)-ketamine, but not (R)-ketamine. *Pharmacol Biochem Behav* 172:17–21
16. Fuchikami M, Thomas A, Liu R, Wohleb ES, Land BB, DiLeone RJ, Aghajanian GK, Duman RS (2015) Optogenetic stimulation of infralimbic PFC reproduces ketamine's rapid and sustained antidepressant actions. *Proc Natl Acad Sci USA* 112(26):8106–8111
17. Shirayama Y, Hashimoto K (2017) Effects of a single bilateral infusion of *R*-ketamine in the rat brain regions of a learned helplessness model of depression. *Eur Arch Psychiatry Clin Neurosci* 267(2):177–182
18. Hare BD, Shinohara R, Liu RJ, Pothula S, DiLeone RJ, Duman RS (2019) Optogenetic stimulation of medial prefrontal cortex *Drd1* neurons produces rapid and long-lasting antidepressant effects. *Nat Commun* 10(1):223
19. Li Y, Zhu ZR, Ou BC, Wang YQ, Tan ZB, Deng CM, Gao YY, Tang M, So JH, Mu YL, Zhang LQ (2015) Dopamine D<sub>2</sub>/D<sub>3</sub> but not dopamine D<sub>1</sub> receptors are involved in the rapid antidepressant-like effects of ketamine in the forced swim test. *Behav Brain Res* 279:100–105
20. Hashimoto K, Shirayama Y (2018) What are the causes for discrepancies of antidepressant actions of (2*R*,6*R*)-hydroxynorketamine? *Biol Psychiatry* 84(1):e7–e8
21. Chang L, Toki H, Qu Y, Fujita Y, Mizuno-Yasuhira A, Yamaguchi JI, Chaki S, Hashimoto K (2018) No sex-specific differences in the acute antidepressant actions of (*R*)-ketamine in an inflammation model. *Int J Neuropsychopharmacol* 21(10):932–937
22. Nugent AC, Ballard ED, Gould TD, Park LT, Moaddel R, Brutsche NE, Zarate CA Jr (2018) Ketamine has distinct electrophysiological and behavioral effects in depressed and healthy subjects. *Mol Psychiatry*. <https://doi.org/10.1038/s41380-018-0028-2>
23. Moghaddam B, Adams B, Verma A, Daly D (1997) Activation of glutamatergic neurotransmission by ketamine: a novel step in the pathway from NMDA receptor blockade to dopaminergic and cognitive disruptions associated with the prefrontal cortex. *J Neurosci* 17(8):2921–2927
24. Ago Y, Tanabe W, Higuchi M, Tsukada S, Hashimoto K, Hashimoto H (2018) (*R*)-ketamine, (*S*)-ketamine and their metabolites affect differentially in vivo monoamine release in the prefrontal cortex of mice: different involvement of AMPA receptor. Poster W-131 at 57th annual meeting of The American College of Neuropsychopharmacology, Hollywood, FL, 12 Dec 2018



# Antidepressant Actions of Ketamine and Its Two Enantiomers



Lijia Chang, Yan Wei, and Kenji Hashimoto

**Abstract** The *N*-methyl-D-aspartate receptor antagonist ketamine has been widely used as an off-label medication to treat depression because it elicits rapid and robust antidepressant effects in treatment-resistant patients with depression. (*R,S*)-ketamine is a racemic mixture containing equal amounts of (*R*)-ketamine (or arketamine) and (*S*)-ketamine (or esketamine). On March 5, 2019, the United States Food and Drug Administration approved an (*S*)-ketamine nasal spray for treatment-resistant depression. In contrast, (*R*)-ketamine has been reported to have a greater potency and longer-lasting antidepressant effects than (*S*)-ketamine in rodent models of depression. However, the precise mechanisms underlying the robust antidepressant effects of ketamine enantiomers remain unknown. In this chapter, we discuss recent findings on the antidepressant actions of two enantiomers of ketamine.

**Keywords** Arketamine · Ketamine · Esketamine

## 1 Introduction

Ketamine is a noncompetitive *N*-methyl-D-aspartate receptor (NMDAR) antagonist that has drawn significant attention in recent decades from scientists all over the world because of its robust antidepressant effects (Cusin 2019; Duman 2018; Hashimoto 2016b, 2017, 2019). Ketamine was first synthesized at Parke-Davis (Detroit, MI, USA) by Calvin Lee Stevens in 1962, with a study of ketamine's

---

L. Chang · K. Hashimoto (✉)

Division of Clinical Neuroscience, Chiba University Center for Forensic Mental Health,  
Chiba, Japan

e-mail: [hashimoto@faculty.chiba-u.jp](mailto:hashimoto@faculty.chiba-u.jp)

Y. Wei

Division of Clinical Neuroscience, Chiba University Center for Forensic Mental Health,  
Chiba, Japan

Key Laboratory of Medical Electrophysiology of Ministry of Education and Medical  
Electrophysiological Key Laboratory of Sichuan Province, Collaborative Innovation Center  
for Prevention and Treatment of Cardiovascular Disease, Institute of Cardiovascular Research,  
Southwest Medical University, Luzhou, Sichuan, China

dissociative anesthetics effects in the prison population quickly following in 1964 (Cohen et al. 2018; Domino 2010; Li and Vlisides 2016). Afterward, ketamine's anesthetic effects were subsequently confirmed by other investigators, and the drug began to be employed as an anesthetic in humans and animals in 1966 (Domino 2010; Stevenson 2005). In view of ketamine's unique pharmacological properties of pain relief and sedation (Gao et al. 2016), it was approved formally for use by the United States (US) Food and Drug Administration (FDA) in 1970 and was placed by the World Health Organization (WHO) in 1985 onto an essential medicines list as an intravenous anesthetic (Gowda et al. 2016; WHO 2011).

Berman et al. (2000) first conducted a placebo-controlled study of ketamine application in eight patients with major depressive disorder (MDD), who were given a dosage of 0.5 mg/kg over 40 min; their depressive symptoms significantly improved within 3 days, while feelings of perceptual disturbances or euphoria occurred in the same patients after treatment (Berman et al. 2000). More generally, in these individuals, the drug produced rapid-acting and sustained antidepressant effects although psychotomimetic effects were also reported after a single infusion of ketamine (Berman et al. 2000). Subsequent studies replicated the noted robust antidepressant effects of ketamine in treatment-resistant patients with MDD and bipolar disorder (BD) (Zarate et al. 2006; Newport et al. 2015; Kishimoto et al. 2016).

Despite ketamine's powerful antidepressant effects in humans, there are some potential drawbacks that cannot be neglected. When used as an anesthetic for anesthesia in surgical procedures, acute and chronic pain management, and critical care (Kurdi et al. 2014), side effects such as hallucinations, agitation, confusion, and psychotomimetic effects resembling schizophrenia can follow (Domino 2010; Gao et al. 2016; Krystal et al. 1994; Kurdi et al. 2014). For some patients, ketamine also brings about cognitive impairments (Molero et al. 2018; Szlachta et al. 2017), urinary tract inflammation (Sihra et al. 2018), liver enzyme abnormalities (Zhao et al. 2018), and other symptoms such as an increase in the heart rate or blood pressure (Sheth et al. 2018). Further, considering the effects reported during recreational usage or the euphoric "dissociated" state caused by higher doses, there exists a potential for abuse no matter what the drug's original intended purpose in a situation is (Heal et al. 2018; Ivan Ezquerra-Romano et al. 2018; Liao et al. 2017; Morgan

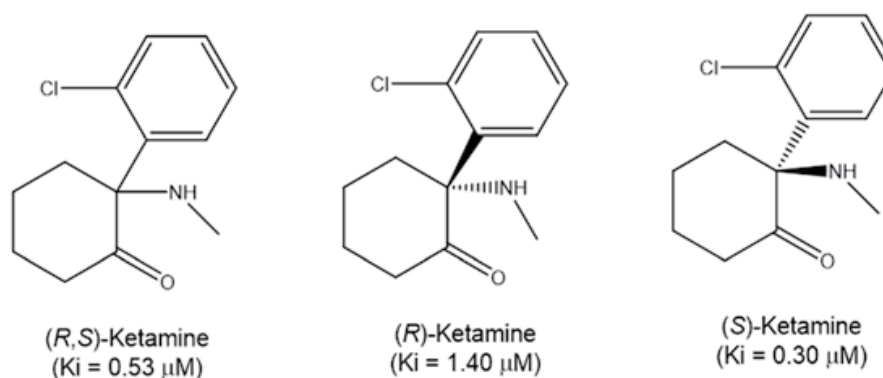


**Fig. 1** Chemical structure of ketamine and its two enantiomers. The values in the parenthesis are the  $K_i$  value for the NMDAR (Hashimoto 2019)

and Curran 2012; Tracy et al. 2017). At present, however, there are no superior antidepressants to ketamine that show robust antidepressant effects in patients with MDD (Duman 2018).

Ketamine is a racemic mixture containing equal amounts of (*R*)-ketamine (or arketamine) and (*S*)-ketamine (or esketamine) (Fig. 1) (Domino 2010). Different affinities and potencies of these two ketamine enantiomers exist. (*S*)-ketamine has about a three- to fourfold greater affinity for the NMDAR as compared with (*R*)-ketamine (Fig. 1). Conversely, (*S*)-ketamine holds approximately a three- to fourfold greater anesthetic potency and shows greater undesirable psychotomimetic side effects in comparison with (*R*)-ketamine (Domino 2010; Hashimoto 2016b, c). In prior research, (*R*)-ketamine showed a greater degree of potency and longer-lasting antidepressant effects than (*S*)-ketamine in several rodents model of depression (Fukumoto et al. 2017; Yang et al. 2015, 2018a; Zhang et al. 2014), and (*R*)-ketamine also did not present side effects on psychotomimetic actions or abuse liability in contrast with (*S*)-ketamine (Chang et al. 2019a; Yang et al. 2015). Third, (*R*)-ketamine is expected to constitute a safer choice than either (*R,S*)-ketamine or (*S*)-ketamine in consideration of its antidepressant actions (Chang et al. 2019a; Hashimoto 2016b, c). However, the precise molecular and cellular mechanisms underlying ketamine's antidepressant effects remain to be elucidated. To date, there is much debate ongoing about the molecular mechanisms underlying ketamine's antidepressant effects in humans and rodents alike. Therefore, it is necessary to summarize the current findings on ketamine's antidepressant effects to further the understanding of the neurobiology of ketamine's actions.

## 2 (*R,S*)-Ketamine's Antidepressant Effects

### 2.1 Summary of (*R,S*)-Ketamine's Antidepressant Effects

Data from the WHO indicate that more than 300 million people of all ages are suffering from depression, which is the leading cause of disability worldwide, leading to a great expenditure of medical and health resources (WHO 2017). Currently available antidepressants have a delay period of approximately 3–4 weeks before they begin working, and about 30% of patients with depression are resistant entirely to these antidepressants (Zhang and Hashimoto 2019). Moreover, other NMDAR antagonists except ketamine have failed in clinical trials (Hashimoto 2019). Therefore, it is unlikely that NMDAR inhibition plays a key role in the antidepressant actions of ketamine.

(*R,S*)-Ketamine's antidepressant effects have been studied for almost 20 years after Berman et al.'s seminal report (Berman et al. 2000). In the following decade, most studies on patients with MDD have revealed promising prospects for the use of (*R,S*)-ketamine's antidepressant effects. Furthermore, clinical trials conducted on the subjects of ketamine's administration dosage, timing, route, curative effect,

tolerability, safety, and antisuicidal effects have also been investigated. Even its use in different types of depression, including treatment-resistant depression, posttraumatic stress disorder (PTSD), and bipolar depression, has been explored in more recent studies (Bobo et al. 2016; Liriano et al. 2019; Schwartz et al. 2016; Zhang and Hashimoto 2019). Further, several rodent models of depression [i.e., the learned helplessness (LH) model, chronic unpredictable mild stress (CUMS) model, and chronic social defeat stress (CSDS) model] have been established for the purpose of testing (*R,S*)-ketamine's antidepressant effects (Krishnan and Nestler 2011). In short, an array of research modalities including original investigations, clinical trials, systematic reviews, and meta-analyses have been used to study (*R,S*)-ketamine's antidepressant effects (Krishnan and Nestler 2011; Sanacora et al. 2017; Short et al. 2018; Singh et al. 2017; Veraart et al. 2018).

## 2.2 (*R,S*)-Ketamine's Antidepressant Effects in Humans

In clinical trials, interventional studies have been adopted for evaluating the beneficial effects of (*R,S*)-ketamine. A number of randomized single-/double-blind placebo-/drug-controlled studies have been performed by many researchers to observe the antidepressant effects of (*R,S*)-ketamine in patients with MDD, who were often infused with only a single intravenous dose of 0.5 mg/kg. Berman et al. (2000) first reported the double-blinded and placebo-controlled study of (*R,S*)-ketamine. Then, Zarate et al. (2006) replicated that a high number (71%) of participants showed significant improvements in depressive symptoms within 24 h of drug administration, and 25% of the study subjects showed antidepressant effects for at least 1 week after a single dose of ketamine as part a randomized, placebo-controlled, double-blind crossover study.

A review of the [ClinicalTrials.gov](https://www.clinicaltrials.gov) database found that about 160 applications from around the world for studying (*R,S*)-ketamine's antidepressant effect on patients with depression existed by the end of June 2019. Study subjects mainly included those with MDD with or without suicide ideation, treatment-resistant depression, BD, and PTSD. Studies chiefly involved a randomized single-blind or double-blind design and were placebo-controlled or midazolam-controlled interventions. Collectively, it seems that (*R,S*)-ketamine is viewed as a promising antidepressant for the treatment of severe depression. Systematic reviews and meta-analyses have also been adopted as investigational means by scientists for evaluating the impact of the antidepressant effect of (*R,S*)-ketamine. Such meta-analyses often include treatment-resistant patients with MDD or BD, and their data are mainly a collection of those from randomized controlled trials (RCTs) (Coyle and Laws 2015; Kishimoto et al. 2016; Newport et al. 2015; Serafini et al. 2014; Wilkinson et al. 2018).

(*R,S*)-Ketamine appears to exhibit rapid antidepressant and antisuicidal ideation effects in treatment-resistant patients with depression. Two midazolam-controlled randomized clinical trials conducted in depressed patients with low levels of suicidal

ideation (Grunebaum et al. 2018; Murrough et al. 2013a) demonstrated rapid reductions in suicidal ideation and depressive symptoms within 24 h after treatment with (*R,S*)-ketamine as compared with in the midazolam treatment group (Grunebaum et al. 2018; Murrough et al. 2013a). (*R,S*)-Ketamine has similarly demonstrated early emerging evidence of having antisuicidal effects in depressed patients with suicidal ideation in other research that last from 1 day to 1 week (Bartoli et al. 2017; Reinstatler and Youssef 2015; Wilkinson et al. 2018).

In special studies on treatment-resistant depression, (*R,S*)-ketamine has been proposed as an effective antidepressant, but there is a lack of long-term data on sustained depression remission in patients (Serafini et al. 2014; Papadimitropoulou et al. 2017). When considering bipolar depression, (*R,S*)-ketamine was found to be an effective antidepressant (Parsaik et al. 2015), but there is also limited evidence to support the maintenance of a response for up to 24 h following a single intravenous dose of ketamine in bipolar depression, and (*R,S*)-ketamine did not show a statistical advantage in remission of bipolar depression (McCloud et al. 2015). Therefore, more RCT studies are needed to verify (*R,S*)-ketamine's antidepressant effect in different types of depression.

### 2.3 Routes of Administration of (*R,S*)-Ketamine

An understanding of the route of administration of (*R,S*)-ketamine is required to confirm its antidepressant effects. There exist a number of studies on routes of administration of (*R,S*)-ketamine, including intravenous, intramuscular, intranasal, subcutaneous, oral, sublingual, transmucosal, and intrarectal, and the bioavailability of these forms of administration varies widely as determined by the absorption of pharmacokinetics although the intravenous route is the most commonly used in patients with depression at this time (Andrade 2017; Hashimoto 2019; Zanos et al. 2018; Zhang and Hashimoto 2019). The bioavailability of intranasal administration of (*R,S*)-ketamine is lower than that of either intravenous or intramuscular administration (Hashimoto 2019; Zhang and Hashimoto 2019). In an effort to assess the safety and efficacy of (*R,S*)-ketamine, Andrade (2017) suggested that the infusion of ketamine by the subcutaneous, intranasal, and oral routes is worth further study based on their clinical practicability. Retrospective data from 22 patients given oral ketamine at a dose of 50 mg per 3 days, which was titrated up by 25 mg per 3 days, showed that 30% of patients with treatment-resistant depression responded to the oral (*R,S*)-ketamine and approximately 70% patients had no improvement in mood symptoms (Al Shirawi et al. 2017). Rosenblat et al. (2019) published a systematic review involving a small number of clinical studies that suggested that oral ketamine could produce significant antidepressant effects, but the drug's antisuicidal effects and efficacy remain undetermined in patients with treatment-resistant depression. Andrade (2019) suggested that oral ketamine should be evaluated by higher-quality studies in the future. Elsewhere, intranasal administration of a single dose of 50 mg of (*R,S*)-ketamine in a 2014 randomized, double-blind crossover

study led to depressive symptoms being significantly improved in 44% of patients (8/18) after 24 h, with minimal psychosis and dissociation observed in the study (Lapidus et al. 2014). Thus, multiple routes other than the intravenous infusion of ketamine are under consideration in research.

#### ***2.4 (R,S)-Ketamine's Antidepressant Effects After Repeated Infusion***

Repeated ketamine infusion is very important for maintenance therapy of patients with treatment-resistant depression (Murrough et al. 2013b; Strong and Kabbaj 2018). In a randomized controlled trial, the infusion of ketamine with three methods, including single, repeated, and maintenance, was performed to observe (*R,S*)-ketamine's antidepressant effects in treatment-resistant patients; results suggested that a single intravenous dose (0.5 mg/kg) over 40 min significantly improved depressive symptoms after 24 h of infusion. Elsewhere, six repeated infusions worked for a time in 59% of participants whose response criteria met the clinical needs, while these participants had no further benefit from weekly maintenance infusions based on the Montgomery–Åsberg Depression Rating Scale (MADRS) scores (Phillips et al. 2019). In addition, the efficiency of (*R,S*)-ketamine's antidepressant effects were also investigated in patients with PTSD treated by eight repeated ketamine infusions done over 4 weeks (Abdallah et al. 2019) and in those with unipolar and bipolar depressive disorder with current suicidal ideation treated by six repeated ketamine infusions performed during a 12-day period (Zhan et al. 2019; Zheng et al. 2018); these studies supported that the rapid and robust antidepressant effects of (*R,S*)-ketamine can be cumulative and sustained following repeated infusion. Despite ketamine's potential for abuse and psychotomimetic effects, it represents a new drug option for antidepressant treatment. Thus, further investigation of (*R,S*)-ketamine's antidepressant effects is necessary.

#### ***2.5 (R,S)-Ketamine's Antidepressant Effects in Rodents***

Animal models of depression were adopted by researchers to investigate (*R,S*)-ketamine's antidepressant effects. Animal models of depression have previously been used for the development of new antidepressants (Fernando and Robbins 2011; Pittenger et al. 2007). In a shock-induced depression model, Chaturvedi et al. (1999) reported that the antidepressant effects of (*R,S*)-ketamine at a dose range of 2.5–10 mg/kg significantly increased ambulation and rearing in the open field test and attenuated the immobility time during the forced swimming test as compared with control mice who received shock. In a rat LH model, Koike et al. (2011) reported that (*R,S*)-ketamine (10 mg/kg) exerted rapid and sustained antidepressant

effects for at least 72 h after treatment, in which the number of escape failures significantly decreased in the LH paradigm and the immobility time during the tail suspension test was significantly reduced in comparison with in the vehicle-treated group. In a CUMS model of either mice or rats, (*R,S*)-ketamine at a single dose of 10 mg/kg elicited rapid-onset and long-lasting antidepressant effects as evaluated by the behavioral tests of forced swimming, tail suspension, and sucrose preference; even the ameliorated anhedonia lasted for 8 days in this model (Ma et al. 2013; Sun et al. 2016). Hollis and Kabbaj (2014) suggested in their research that CSDS model is a valuable research tool for investigating possible causes and treatments for human depression. In a CSDS model, as compared with the TrkB agonists 7,8-dihydroxyflavone and TrkB antagonist ANA-12, (*R,S*)-ketamine showed longer-lasting antidepressant effects for 7 days (Zhang et al. 2015). In contrast, however, Donahue et al. (2014) reported that a single administration of ketamine (10 mg/kg) showed a rapid antidepressant effect in a CSDS model, attenuating social avoidance in the social interaction test but having no effect on anhedonia in the intracranial self-stimulation test (Donahue et al. 2014).

In addition, inflammation-induced mice or rat depression models, such as those using lipopolysaccharides or complete Freund's adjuvant, can also be useful in observing (*R,S*)-ketamine's antidepressant effects, in that depression-like behaviors were often determined by forced swimming test; sucrose preference test; and the pro-inflammatory cytokine levels of interleukin (IL)-1 $\beta$ , IL-6, and tumor necrosis factor- $\alpha$  (Ji et al. 2019; Remus and Dantzer 2016; Reus et al. 2017; Zhang et al. 2016). However, (*R,S*)-ketamine's potential psychotomimetic and other unwanted side effects have also been well-documented in these animal models, prompting behaviors such as hyperlocomotion, prepulse inhibition deficits, conditioned place preference, schizophrenia-like psychotic symptoms, and novel object recognition impairment (Becker et al. 2003; Chan et al. 2013; Chang et al. 2019a; Giorgetti et al. 2015; Imre et al. 2006; Lahti et al. 1995; Ma and Leung 2018; Yang et al. 2015; Zanos et al. 2017), which may pose a major barrier to further clinical study in patients with MDD.

### 3 (S)-Ketamine's Antidepressant Effects

#### 3.1 Summary of (S)-Ketamine's Antidepressant Effects

(*S*)-Ketamine is an isomer of (*R,S*)-ketamine, which was introduced for medical use in analgesia and anesthesia in the early 1990s (Esketamine 2006; Trimmel et al. 2018). The US FDA originally stated that the stereoisomers of (*R,S*)-ketamine had not received enough attention for its commercial development in 1992 (Luft and Mendes 2005). Now, (*S*)-ketamine has been brought into greater focus over (*R,S*)-ketamine for its antidepressant effects in patients with treatment-resistant depression, due to its incorporation into a nasal spray approved by the US FDA on March

5, 2019 (Canada 2019; US Food and Drug Administration 2019). The evaluation of the (*S*)-ketamine nasal spray was conducted by way of four phase III RCTs, including three short-term (4-week) clinical trials and a withdrawal maintenance-of-effect trial, where patients experienced many side effects including disassociation, dizziness, nausea, sedation, vertigo, anxiety, and lethargy (US Food and Drug Administration 2019). Therefore, there are many challenges in the study of (*S*)-ketamine, which cannot meet the needs of all patients with MDD, and even the antidepressant efficiency and the side effects of (*S*)-ketamine are still under discussion. On the other hand, the existing literature or studies concerning the use of (*S*)-ketamine in patients with MDD number far less than those on the topic of (*R,S*)-ketamine, but the latter is still not yet approved by FDA for treatment via any route of administration.

In a case report, Paslakis et al. (2010) reported their results obtained with using off-label oral (*S*)-ketamine (1.25 mg/kg) within 14 days: two patients with treatment-resistant depression showed rapid and sustained improvement in their psychopathology within the first week, while another two patients did not respond to the drug throughout the entire treatment period. In addition, several studies have concluded that (*S*)-ketamine produces similar antidepressant effects to those of (*R,S*)-ketamine (Paul et al. 2009) but is better-tolerated than (*R,S*)-ketamine, yet severe psychotomimetic effects with (*S*)-ketamine have also been reported (Correia-Melo et al. 2017; Paul et al. 2009). It is worth mentioning that a case series of repeated (*S*)-ketamine (0.25 mg/kg over 40 min) off-label use demonstrated an improvement in depressive symptoms in 50% of the patients following infusion within 1 or 2 weeks, although 25% of the patients suffered from dissociative symptoms (Segmiller et al. 2013). Another case series reported that the safety and efficacy of (*S*)-ketamine were well demonstrated in patients with treatment-resistant depression (TRD); still, the potential for associated psychotic symptoms can leave some patients out of consideration (Ajub and Lacerda 2018). Thus, additional case studies are needed to review the efficacy and psychosis effects of (*S*)-ketamine.

According to clinical trials records from [ClinicalTrials.gov](https://clinicaltrials.gov), about 18 applications for studying (*S*)-ketamine's antidepressant effect in patients with depression have been uploaded as of April 1, 2019. Some clinical trials have been completed, while others are currently recruiting patients. The route of administration in these clinical trials is mainly intranasal injection, for evaluating the efficacy and safety in patients with MDD or TRD. Therapeutic regimens in these clinical trials also include single and repeated administration. Singh et al. (2016) found in a double-blind, multicenter, randomized, placebo-controlled trial involving patients with TRD that 67% and 64% of the patients, respectively, responded to (*S*)-ketamine given at a single dose of 0.2 mg/kg or 0.4 mg/kg over 40 min within 1 day. Another clinical trial of a head-to-head study compared the antidepressant actions of (*S*)-ketamine and (*R,S*)-ketamine in 96 individuals with TRD given a single dose of (*S*)-ketamine (0.25 mg/kg) or (*R,S*)-ketamine (0.5 mg/kg) over 40 min (Correia-Melo et al. 2018). The authors considered their study as the best way to evaluate the efficacy and safety of (*S*)-ketamine and (*R,S*)-ketamine, as adverse psychotomimetic effects between the two compounds may be different (Correia-Melo et al.



2018). Clinical trials still need to provide more powerful evidence to assist the clinical application of (*S*)-ketamine in depression or TRD.

Other research on (*S*)-ketamine's antidepressant effects mainly involves combination therapy. Bartova et al. (2015) investigated combined intravenous therapy of (*S*)-ketamine and oral tranylcypromine in two patients with multi-treatment-resistant depression, showing a confusing outcome of evident antisuicidal effects but no detailed improvement in antidepressant effectiveness. Electroconvulsive therapy (ECT) plus (*S*)-ketamine has also been applied in three patients with TRD. Kallmunzer et al. (2016) reported that all subjects showed remission in terms of suicidal ideation and no serious side effects during treatment. In contrast, another clinical trial suggested that (*S*)-ketamine (0.4 mg/kg in a bolus) as adjuvant therapy with propofol made no contribution to the enhanced role of ECT in patients with resistance to antidepressants, even going as far as to cause adverse effects like posttreatment disorientation and restlessness (Jarventausta et al. 2013). Although ECT can help to remedy depression, there is still a lack of clear evidence (Read et al. 2019). Therefore, there is no valid data to prove the combination of (*S*)-ketamine and ECT is beneficial, especially given that the antidepressant effects of (*R,S*)-ketamine are more potent than those of ECT (Muller et al. 2016).

In humans, the idea of using (*S*)-ketamine as an antidepressant is relatively new and its intranasal treatment modality has recently been receiving a lot of attention. However, many challenges need to be faced in future study. For instance, how about its optimal dose and route of administration? How to solve its side effects during treatment? How long does it sustain antidepressant effects? More importantly, how does it work as an antidepressant? These questions remain without an answer at this time.

### **3.2 (*S*)-Ketamine's Antidepressant Effects in Rodents**

Animal experiments aimed at elucidating (*S*)-ketamine's antidepressant effect and its underlying mechanisms have also been conducted although no definitive answer was achieved. The current findings point out that (*S*)-ketamine works in a very complicated way, in that it can bind to multiple receptors in an organism, such as NMDAR, opioid receptors, monoamine receptors, adenosine receptors,  $\alpha$ -amino-3-hydroxy-5-methyl-4-isoxazolepropionic acid (AMPA) receptors, metabotropic glutamate receptors, L-type calcium channels, and other purinergic receptors (Kohrs and Durieux 1998; Trimmel et al. 2018). The prevailing view is that (*S*)-ketamine's antidepressant effect is related with the noncompetitive inhibition of NMDAR through binding to the phencyclidine (PCP) sites (Sinner and Graf 2008), due to its three- to fourfold higher affinity in comparison with (*R*)-ketamine (Domino 2010; Kohrs and Durieux 1998). Yet, (*S*)-ketamine dominates in the areas of anesthetic potency and undesirable psychotomimetic side effects over (*R*)-ketamine, in that seeing illusions, hearing and vision changes, and proprioception are related to

(*S*)-ketamine, while feelings of relaxation are connected with the actions of (*R*)-ketamine (Zanos et al. 2018).

Treccani et al. (2019) suggested that a single dose of (*S*)-ketamine (15 mg/kg) can induce acute antidepressant action in a rat model of depression, concluding first that dendritic spine density rapidly (<1 h) increases in brain structural changes and also that balancing the relationship between cofilin activity, homer3 levels, and the NMDAR subunits GluN2A and GluN2B plays a key role in the antidepressant effect. However, Ide et al. (2017), upon investigating the role of GluN2D in the antidepressant effects of ketamine enantiomers, suggested that such did not play a key role in the sustained antidepressant effects of (*R,S*)-ketamine and (*S*)-ketamine but rather in those of (*R*)-ketamine. Recent studies have indicated that (*S*)-ketamine elicits its acute and sustained antidepressant-like actions via a 5-hydroxytryptamine (5HT) receptor-dependent mechanism, which is confirmed via the forced swimming test by comparing the vortioxetine, fluoxetine, and (*S*)-ketamine in the serotonin system or by using the 5-HT<sub>1B</sub> receptor agonist CP94253 in a genetic rat model (du Jardin et al. 2016, 2017).

Other studies of note regarding the mechanisms of (*S*)-ketamine's antidepressant actions are as follows. In a rat depression model of maternal deprivation, it was suggested that a single dose of (*S*)-ketamine showed long-term antidepressant effects through acting against neural damage induced by oxidative stress (Reus et al. 2015). In a long-term corticosterone infusion rat model of depression, it was suggested that (*S*)-ketamine decreased depressive-like behaviors for at least 4 weeks, but not in a manner related with rapid maturity of the new hippocampal neurons (Soumier et al. 2016). In a rat hippocampus study, Ardalan et al. (2017) put forward the notion that a single injection (15 mg/kg) of (*S*)-ketamine improved the immobility behavior during the modified forced swim test within 24 h after treatment, proving that astrocyte plasticity in the hippocampus has a bearing on the (*S*)-ketamine antidepressant effect in a rat genetic animal model of depression.

## 4 (*R*)-Ketamine's Antidepressant Effects

### 4.1 *Summary of the Differences Between (R)-Ketamine and (S)-Ketamine*

With the deepening and development of research, the focus on antidepressant effects will be quickly shifted toward (*R*)-ketamine, because its advantages are becoming more and more obvious. As compared with (*S*)-ketamine, (*R*)-ketamine has been proven to be more potent and have longer-lasting antidepressant effects and was deemed to be free of psychotomimetic side effects in many studies on rodent models of depression (Chang et al. 2019a; Fukumoto et al. 2017; Yang et al. 2015, 2016b; Zhang et al. 2014), signifying that (*R*)-ketamine will be one of the most promising antidepressants.

(*R*)-Ketamine is an isomer of (*R,S*)-ketamine. (*R*)-ketamine is a left-handed molecule, while (*S*)-ketamine is a right-handed molecule, per the carbon connections in either one or the other direction of nonsuperimposable mirror images, prompting a difference in the body metabolism (Calvey 1995; Kharasch and Labroo 1992). As compared with (*S*)-ketamine, (*R*)-ketamine has a lower affinity to the PCP binding site of the NMDAR, with a lower anesthetic potency (Thomson et al. 1985; White et al. 1985; Zeilhofer et al. 1992). In addition, (*R*)-ketamine could also weakly bind to the sigma receptor sites, without (*S*)-ketamine binding to these sites (Vollenweider et al. 1997). Research on the side effects of the two isomers showed that (*R*)-ketamine produces a feeling of relaxation or “well-being,” while (*S*)-ketamine is mainly responsible for psychotomimetic effects, such as dissociations in hearing, vision, and proprioception (Hashimoto 2019; Vollenweider et al. 1997; Zanos et al. 2018). Moreover, Marietta et al. (1977) reported acute toxic effects of racemic ketamine and its two isomers at the dose of 40 mg/kg in male Sprague-Dawley rats based on median lethal dose values, indicating that (*R*)-ketamine is more secure than (*R,S*)-ketamine and (*S*)-ketamine, and its potential advantage is not a fatal drug according to the high dose and with less posthypnotic stimulation.

#### ***4.2 Different Antidepressant Effects Between (R)-Ketamine and (S)-Ketamine***

Our group reported that (*R*)-ketamine has a greater potency and longer-lasting antidepressant roles than (*S*)-ketamine in rodent models of depression (Yang et al. 2015; Zhang et al. 2014). In addition, it was suggested that ketamine’s side effects (e.g., psychotomimetic behaviors, neurotoxicity, abuse potential) may be associated with (*S*)-ketamine but not (*R*)-ketamine (Chang et al. 2019a; Hashimoto 2016a, b, c). Subsequently, different kinds of depression models with comparative objects and their relevant behavioral tests were employed to evaluate and identify the advantages of (*R*)-ketamine’s antidepressant effects. Fukumoto et al. (2017) reported that (*R*)-ketamine can elicit longer-lasting antidepressant effects than (*S*)-ketamine in forced swimming and tail suspension tests, and (*R*)-ketamine showed a sustained antidepressant effect in a treatment-refractory model while (*S*)-ketamine did not. Moreover, Fukumoto et al. (2017) also suggested that (*R*)-ketamine’s antidepressant effects may be related with AMPAR by testing the rats of a repeated corticosterone treatment model with an AMPAR antagonist, NBQX (Fukumoto et al. 2017). In a conscious positron-emission tomography study, a single infusion of (*S*)-ketamine but not (*R*)-ketamine caused dopamine release, indicating that (*S*)-ketamine-induced dopamine release may be associated with acute psychotomimetic and dissociative effects in humans (Hashimoto et al. 2017).

In addition, further research on the molecular mechanisms revealed more data about the differences between (*R*)-ketamine and (*S*)-ketamine. Specifically, the extracellular-signal-regulated kinase signaling pathway may play a role in

(*R*)-ketamine's antidepressant effects, while the mammalian target of rapamycin signaling pathway plays a role in the antidepressant effects of (*S*)-ketamine (Yang et al. 2018a). Nevertheless, glutamate is the primary excitatory neurotransmitter in the human brain in physiology (Jewett and Thapa 2019) and its participation in the role of ketamine's antidepressant effects should not be neglected in the following study, although we still cannot explain the real difference between (*R,S*)-ketamine and its two isomers (Zanos and Gould 2018). Even more important, the causes for the differences in antidepressant effects between (*R*)-ketamine and (*S*)-ketamine may be related with the gut microbiota–brain axis (Qu et al. 2017; Yang et al. 2017). As compared with (*S*)-ketamine, (*R*)-ketamine significantly attenuated the decrease in the levels of *Mollicutes* of susceptible mice in a CSDS model, and (*R*)-ketamine presented a stronger advantage than (*S*)-ketamine in reducing the levels of *Butyricimonas* (Yang et al. 2017).

### 4.3 (*R*)-Ketamine's Antidepressant Effects

(*R*)-ketamine has its own special features of antidepressant effects from the current study. As compared with the NMDAR partial agonist rapastinel, (*R*)-ketamine had longer-lasting antidepressant effects and significantly changed the brain-derived neurotrophic factor–TrkB signaling in a CSDS model (Yang et al. 2016a). Recent Ph3 data of rapastinel were negative (Hashimoto 2019).

In the light of the complex physiology and particularity that of NMDAR for regulating the electroneurographic signal in depression by voltage-gated ion channel influx, including calcium, sodium, and potassium (Cui et al. 2018; Yang et al. 2018b). Tian et al. (2018b) reported that the low-voltage-sensitive, T-type calcium channel blocker ethosuximide did not produce rapid or sustained antidepressant effects in a CSDS model, although (*R*)-ketamine showed rapid and sustained antidepressant effects in the same model (Tian et al. 2018b). Furthermore, Xiong et al. (2019) reported that the Kir4.1 inhibitors quinacrine and sertraline did not improve the depression-like behaviors during the tail suspension test and forced swimming test in a CSDS model, while (*R*)-ketamine produced rapid and sustained antidepressant effects in this model (Xiong et al. 2019).

Treatment with the 5-HT inhibitor para-chlorophenylalanine methyl ester hydrochloride also did not impact the antidepressant effects of (*R*)-ketamine in a CSDS model (Zhang et al. 2018). Furthermore, dopamine D<sub>1</sub> receptors may not play a major role in the antidepressant actions of (*R*)-ketamine, because pretreatment with the dopamine D<sub>1</sub> receptor antagonist SCH-23390 did not block the antidepressant effects of (*R*)-ketamine in the CSDS model (Chang et al. 2019b).

Given the role of gamma-aminobutyric acid receptors in depression (Zanos et al. 2017), both (*R*)-ketamine and MRK-016 (full inverse GABA<sub>A</sub> agonist) displayed rapid antidepressant effects, while only (*R*)-ketamine produced a longer-lasting antidepressant effect in a CSDS model (Xiong et al. 2018).

In addition, (*R*)-ketamine's antidepressant effects had regional differences in rat brains. A single bilateral infusion of (*R*)-ketamine was injected into the brain in a rat LH model of depression, showing that the infralimbic cortex of the medial prefrontal cortex (mPFC), dentate gyrus, and CA3 subregions of the hippocampus are related with (*R*)-ketamine's antidepressant effects as compared with other injection site areas including the mPFC subregion PrL, subregions of the shell and core in NAc, and BLA and CeA subregions of the amygdala, which had nothing to do with the antidepressant effects of (*R*)-ketamine (Shirayama and Hashimoto 2017). No toxicity was shown in the brain after repeated, intermittent administration with (*R*)-ketamine, with no loss in parvalbumin immunoreactivity in the brain region of mPFC and hippocampus observed, which was the opposite finding to those of (*S*)-ketamine (Yang et al. 2016b). Additionally, another interesting finding regarding neuropathological changes revealed that the neuronal injury marker heat shock protein HSP-70 was expressed in the rat retrosplenial cortex not because of (*R*)-ketamine but instead due to (*R,S*)-ketamine and (*S*)-ketamine (Tian et al. 2018a).

Based on the above findings, (*R*)-ketamine shows the rapid-acting and long-lasting antidepressant effects in rodents although its precise mechanism underlying these effects is still uncertain. A clinical trial of (*R*)-ketamine in humans is currently underway (Hashimoto 2019).

## 5 Conclusion

The discovery of the robust antidepressant actions of (*R,S*)-ketamine in depressed patients is serendipitous (Krystal et al. 2019). However, (*R,S*)-ketamine has not been approved by the US FDA for antidepressant treatment in clinical application because of a lack of patent. An (*S*)-ketamine nasal spray was approved by the FDA on March 5, 2019, although its side effects are known and it must be administered under supervision in a certified doctor's office or outpatient clinic after treatment. It seems that antidepressant effects of (*S*)-ketamine in patients with MDD are less potent than those related with (*R,S*)-ketamine in clinical studies. Although there is no clinical trial of (*R*)-ketamine in patients with MDD, many preclinical data show its more potent antidepressant effects without side effects, suggesting that (*R*)-ketamine could be a safer antidepressant alternative to (*R,S*)-ketamine and (*S*)-ketamine. Due to its lower adverse side effects, we are looking forward to seeing more data on (*R*)-ketamine's antidepressant effects in patients with MDD and other psychiatric disorders.

**Acknowledgments** This study was supported by grant from AMED, Japan (to K.H., JP19dm0107119). Dr. Lijia Chang was supported by the Japan China Sasakawa Medical Fellowship (Tokyo, Japan). Dr. Yan Wei (Southwest Medical University, China) was supported by the China Scholarship Council (China).

**Disclosure Statement:** Dr. Hashimoto is the inventor of filed patent applications on "The use of *R*-ketamine in the treatment of psychiatric diseases" by the Chiba University. Dr. Hashimoto also declares that he has received research support and consultant from Dainippon Sumitomo, Otsuka, and Taisho.

## References

- Abdallah CG et al (2019) Repeated ketamine infusions for antidepressant-resistant PTSD: methods of a multicenter, randomized, placebo-controlled clinical trial. *Contemp Clin Trials* 81:11–18. <https://doi.org/10.1016/j.cct.2019.04.009>
- Ajub E, Lacerda ALT (2018) Efficacy of esketamine in the treatment of depression with psychotic features: a case series. *Biol Psychiatry* 83:e15–e16. <https://doi.org/10.1016/j.biopsych.2017.06.011>
- Al Shirawi MI, Kennedy SH, Ho KT, Byrne R, Downar J (2017) Oral ketamine in treatment-resistant depression: a clinical effectiveness case series. *J Clin Psychopharmacol* 37:464–467. <https://doi.org/10.1097/JCP.0000000000000717>
- Andrade C (2017) Ketamine for depression, 4: in what dose, at what rate, by what route, for how long, and at what frequency? *J Clin Psychiatry* 78:e852–e857. <https://doi.org/10.4088/JCP.17f11738>
- Andrade C (2019) Oral ketamine for depression, 2: practical considerations. *J Clin Psychiatry* 80. <https://doi.org/10.4088/JCP.19f12838>
- Ardalan M, Rafati AH, Nyengaard JR, Wegener G (2017) Rapid antidepressant effect of ketamine correlates with astroglial plasticity in the hippocampus. *Br J Pharmacol* 174:483–492. <https://doi.org/10.1111/bph.13714>
- Bartoli F, Riboldi I, Crocarno C, Di Brita C, Clerici M, Carra G (2017) Ketamine as a rapid-acting agent for suicidal ideation: a meta-analysis. *Neurosci Biobehav Rev* 77:232–236. <https://doi.org/10.1016/j.neubiorev.2017.03.010>
- Bartova L, Vogl SE, Stamenkovic M, Praschak-Rieder N, Naderi-Heiden A, Kasper S, Willeit M (2015) Combination of intravenous S-ketamine and oral tranylcypromine in treatment-resistant depression: a report of two cases. *Eur Neuropsychopharmacol* 25:2183–2184. <https://doi.org/10.1016/j.euroneuro.2015.07.021>
- Becker A, Peters B, Schroeder H, Mann T, Huether G, Grecksch G (2003) Ketamine-induced changes in rat behaviour: a possible animal model of schizophrenia. *Prog Neuropsychopharmacol Biol Psychiatry* 27:687–700. [https://doi.org/10.1016/S0278-5846\(03\)00080-0](https://doi.org/10.1016/S0278-5846(03)00080-0)
- Berman RM, Cappiello A, Anand A, Oren DA, Heninger GR, Charney DS, Krystal JH (2000) Antidepressant effects of ketamine in depressed patients. *Biol Psychiatry* 47:351–354
- Bobo WV, Vande Voort JL, Croarkin PE, Leung JG, Tye SJ, Frye MA (2016) Ketamine for treatment-resistant unipolar and bipolar major depression: critical review and implications for clinical practice. *Depress Anxiety* 33:698–710. <https://doi.org/10.1002/da.22505>
- Calvey TN (1995) Isomerism and anaesthetic drugs. *Acta Anaesthesiol Scand Suppl* 106:83–90
- Canady VA (2019) Nasal spray treatment for adults with TRD approved by FDA. *Mental Health Wkly* 29:4–5
- Chan KW, Lee TM, Siu AM, Wong DP, Kam CM, Tsang SK, Chan CC (2013) Effects of chronic ketamine use on frontal and medial temporal cognition. *Addict Behav* 38:2128–2132. <https://doi.org/10.1016/j.addbeh.2013.01.014>
- Chang L et al (2019a) Comparison of antidepressant and side effects in mice after intranasal administration of (R,S)-ketamine, (R)-ketamine, and (S)-ketamine. *Pharmacol Biochem Behav* 181:53–59. <https://doi.org/10.1016/j.pbb.2019.04.008>
- Chang L et al (2019b) Lack of dopamine D1 receptors in the antidepressant actions of (R)-ketamine in a chronic social defeat stress model. *Eur Arch Psychiatry Clin Neurosci*. <https://doi.org/10.1007/s00406-019-01012-1>
- Chaturvedi HK, Chandra D, Bapna JS (1999) Interaction between N-methyl-D-aspartate receptor antagonists and imipramine in shock-induced depression. *Indian J Exp Biol* 37:952–958
- Cohen SP et al (2018) Consensus guidelines on the use of intravenous ketamine infusions for chronic pain from the American Society of Regional Anesthesia and Pain Medicine, the American Academy of Pain Medicine, and the American Society of Anesthesiologists. *Reg Anesth Pain Med* 43:521–546. <https://doi.org/10.1097/AAP.0000000000000808>

- Correia-Melo FS, Silva SS, Araujo-de-Freitas L, Quarantini LC (2017) S-(+)-ketamine-induced dissociative symptoms as a traumatic experience in patients with treatment-resistant depression. *Braz J Psychiatry* 39:188–189. <https://doi.org/10.1590/1516-4446-2016-2070>
- Correia-Melo FS et al (2018) Comparative study of esketamine and racemic ketamine in treatment-resistant depression: Protocol for a non-inferiority clinical trial. *Medicine (Baltimore)* 97:e12414. <https://doi.org/10.1097/MD.00000000000012414>
- Coyle CM, Laws KR (2015) The use of ketamine as an antidepressant: a systematic review and meta-analysis. *Hum Psychopharmacol* 30:152–163. <https://doi.org/10.1002/hup.2475>
- Cui Y et al (2018) Astroglial Kir4.1 in the lateral habenula drives neuronal bursts in depression. *Nature* 554:323–327. <https://doi.org/10.1038/nature25752>
- Cusin C (2019) Ketamine as a rapid antidepressant. In: *The Massachusetts General Hospital guide to depression*. Springer, Berlin, pp 139–145
- Domino EF (2010) Taming the ketamine tiger. 1965. *Anesthesiology* 113:678–684. <https://doi.org/10.1097/ALN.0b013e3181ed09a2>
- Donahue RJ, Muschamp JW, Russo SJ, Nestler EJ, Carlezon WA Jr (2014) Effects of striatal DeltaFosB overexpression and ketamine on social defeat stress-induced anhedonia in mice. *Biol Psychiatry* 76:550–558. <https://doi.org/10.1016/j.biopsych.2013.12.014>
- du Jardin KG, Liebenberg N, Muller HK, Elfving B, Sanchez C, Wegener G (2016) Differential interaction with the serotonin system by S-ketamine, vortioxetine, and fluoxetine in a genetic rat model of depression. *Psychopharmacology (Berl)* 233:2813–2825. <https://doi.org/10.1007/s00213-016-4327-5>
- du Jardin KG, Liebenberg N, Cajina M, Muller HK, Elfving B, Sanchez C, Wegener G (2017) S-ketamine mediates its acute and sustained antidepressant-like activity through a 5-HT1B receptor dependent mechanism in a genetic rat model of depression. *Front Pharmacol* 8:978. <https://doi.org/10.3389/fphar.2017.00978>
- Duman RS (2018) Ketamine and rapid-acting antidepressants: a new era in the battle against depression and suicide. *F1000Res* 7. <https://doi.org/10.12688/f1000research.14344.1>
- Esketamine (2006) *Drugs and lactation database (LactMed)*. National Library of Medicine (US), Bethesda, MD
- Fernando AB, Robbins TW (2011) Animal models of neuropsychiatric disorders. *Annu Rev Clin Psychol* 7:39–61. <https://doi.org/10.1146/annurev-clinpsy-032210-104454>
- Fukumoto K, Toki H, Iijima M, Hashihayata T, Yamaguchi JI, Hashimoto K, Chaki S (2017) Antidepressant potential of (R)-ketamine in rodent models: comparison with (S)-ketamine. *J Pharmacol Exp Ther* 361:9–16. <https://doi.org/10.1124/jpet.116.239228>
- Gao M, Rejaei D, Liu H (2016) Ketamine use in current clinical practice. *Acta Pharmacol Sin* 37:865–872. <https://doi.org/10.1038/aps.2016.5>
- Giorgetti R, Marcotulli D, Tagliabracci A, Schifano F (2015) Effects of ketamine on psychomotor, sensory and cognitive functions relevant for driving ability. *Forensic Sci Int* 252:127–142. <https://doi.org/10.1016/j.forsciint.2015.04.024>
- Gowda MR, Srinivasa P, Kumbar PS, Ramalingaiah VH, Muthyalappa C, Durgoji S (2016) Rapid resolution of grief with IV infusion of ketamine: a unique phenomenological experience. *Indian J Psychol Med* 38:62–64. <https://doi.org/10.4103/0253-7176.175121>
- Grunebaum MF et al (2018) Ketamine for rapid reduction of suicidal thoughts in major depression: a midazolam-controlled randomized clinical trial. *Am J Psychiatry* 175:327–335. <https://doi.org/10.1176/appi.ajp.2017.17060647>
- Hashimoto K (2016a) Detrimental side effects of repeated ketamine infusions in the brain. *Am J Psychiatry* 173:1044–1045. <https://doi.org/10.1176/appi.ajp.2016.16040411>
- Hashimoto K (2016b) Ketamine's antidepressant action: beyond NMDA receptor inhibition. *Expert Opin Ther Targets* 20:1389–1392. <https://doi.org/10.1080/14728222.2016.1238899>
- Hashimoto K (2016c) Letter to the Editor: R-ketamine: a rapid-onset and sustained antidepressant without risk of brain toxicity. *Psychol Med* 46:2449–2451. <https://doi.org/10.1017/S0033291716000969>

- Hashimoto K (2017) Rapid antidepressant activity of ketamine beyond NMDA receptor. In: The NMDA receptors. Springer, Berlin, pp 69–81
- Hashimoto K (2019) Rapid-acting antidepressant ketamine, its metabolites and other candidates: A historical overview and future perspective. *Psychiatry Clin Neurosci* 73(10):613–627. <https://doi.org/10.1111/pcn.12902>
- Hashimoto K, Kakiuchi T, Ohba H, Nishiyama S, Tsukada H (2017) Reduction of dopamine D<sub>2/3</sub> receptor binding in the striatum after a single administration of esketamine, but not *R*-ketamine: a PET study in conscious monkeys. *Eur Arch Psychiatry Clin Neurosci* 267:173–176
- Heal DJ, Gosden J, Smith SL (2018) Evaluating the abuse potential of psychedelic drugs as part of the safety pharmacology assessment for medical use in humans. *Neuropharmacology* 142:89–115. <https://doi.org/10.1016/j.neuropharm.2018.01.049>
- Hollis F, Kabbaj M (2014) Social defeat as an animal model for depression. *ILAR J* 55:221–232. <https://doi.org/10.1093/ilar/ilu002>
- Ide S, Ikekubo Y, Mishina M, Hashimoto K, Ikeda K (2017) Role of NMDA receptor GluN2D subunit in the antidepressant effects of enantiomers of ketamine. *J Pharmacol Sci* 135:138–140. <https://doi.org/10.1016/j.jphs.2017.11.001>
- Imre G, Salomons A, Jongasma M, Fokkema DS, Den Boer JA, Ter Horst GJ (2006) Effects of the mGluR2/3 agonist LY379268 on ketamine-evoked behaviours and neurochemical changes in the dentate gyrus of the rat. *Pharmacol Biochem Behav* 84:392–399. <https://doi.org/10.1016/j.pbb.2006.05.021>
- Ivan Ezquerro-Romano I, Lawn W, Krupitsky E, Morgan CJA (2018) Ketamine for the treatment of addiction: evidence and potential mechanisms. *Neuropharmacology* 142:72–82. <https://doi.org/10.1016/j.neuropharm.2018.01.017>
- Jarventausta K et al (2013) Effects of S-ketamine as an anesthetic adjuvant to propofol on treatment response to electroconvulsive therapy in treatment-resistant depression: a randomized pilot study. *J ECT* 29:158–161. <https://doi.org/10.1097/YCT.0b013e318283b7e9>
- Jewett BE, Thapa B (2019) Physiology, NMDA Receptor. In: StatPearls. StatPearls, Treasure Island, FL
- Ji M et al (2019) Acute ketamine administration attenuates lipopolysaccharide-induced depressive-like behavior by reversing abnormal regional homogeneity in the nucleus accumbens. *Neuroreport* 30:421–427. <https://doi.org/10.1097/WNR.0000000000001219>
- Kallmunzer B, Volbers B, Karthaus A, Tektas OY, Kornhuber J, Muller HH (2016) Treatment escalation in patients not responding to pharmacotherapy, psychotherapy, and electro-convulsive therapy: experiences from a novel regimen using intravenous S-ketamine as add-on therapy in treatment-resistant depression. *J Neural Transm (Vienna)* 123:549–552. <https://doi.org/10.1007/s00702-015-1500-7>
- Kharasch ED, Labroo R (1992) Metabolism of ketamine stereoisomers by human liver microsomes. *Anesthesiology* 77:1201–1207
- Kishimoto T, Chawla JM, Hagi K, Zarate CA, Kane JM, Bauer M, Correll CU (2016) Single-dose infusion ketamine and non-ketamine N-methyl-D-aspartate receptor antagonists for unipolar and bipolar depression: a meta-analysis of efficacy, safety and time trajectories. *Psychol Med* 46:1459–1472. <https://doi.org/10.1017/S0033291716000064>
- Kohrs R, Durieux ME (1998) Ketamine: teaching an old drug new tricks. *Anesth Analg* 87:1186–1193
- Koike H, Iijima M, Chaki S (2011) Involvement of AMPA receptor in both the rapid and sustained antidepressant-like effects of ketamine in animal models of depression. *Behav Brain Res* 224:107–111. <https://doi.org/10.1016/j.bbr.2011.05.035>
- Krishnan V, Nestler EJ (2011) Animal models of depression: molecular perspectives. *Curr Top Behav Neurosci* 7:121–147. [https://doi.org/10.1007/7854\\_2010\\_108](https://doi.org/10.1007/7854_2010_108)
- Krystal JH et al (1994) Subanesthetic effects of the noncompetitive NMDA antagonist, ketamine, in humans. Psychotomimetic, perceptual, cognitive, and neuroendocrine responses. *Arch Gen Psychiatry* 51:199–214. <https://doi.org/10.1001/archpsyc.1994.03950030035004>



- Krystal JH, Abdallah CG, Sanacora G, Charney DS, Duman RS (2019) Ketamine: a paradigm shift for depression research and treatment. *Neuron* 101:774–778. <https://doi.org/10.1016/j.neuron.2019.02.005>
- Kurdi MS, Theerth KA, Deva RS (2014) Ketamine: current applications in anesthesia, pain, and critical care. *Anesth Essays Res* 8:283–290. <https://doi.org/10.4103/0259-1162.143110>
- Lahti AC, Holcomb HH, Medoff DR, Tamminga CA (1995) Ketamine activates psychosis and alters limbic blood flow in schizophrenia. *Neuroreport* 6:869–872
- Lapidus KA et al (2014) A randomized controlled trial of intranasal ketamine in major depressive disorder. *Biol Psychiatry* 76:970–976. <https://doi.org/10.1016/j.biopsych.2014.03.026>
- Li L, Vlisides PE (2016) Ketamine: 50 years of modulating the mind. *Front Hum Neurosci* 10:612. <https://doi.org/10.3389/fnhum.2016.00612>
- Liao Y, Tang YI, Hao W (2017) Ketamine and international regulations. *Am J Drug Alcohol Abuse* 43:495–504
- Liriano F, Hatten C, Schwartz TL (2019) Ketamine as treatment for post-traumatic stress disorder: a review. *Drugs Context* 8:212305. <https://doi.org/10.7573/dic.212305>
- Luft A, Mendes FF (2005) Low S(+) ketamine doses: a review. *Rev Bras Anesthesiol* 55:460–469
- Ma J, Leung LS (2018) Involvement of posterior cingulate cortex in ketamine-induced psychosis relevant behaviors in rats. *Behav Brain Res* 338:17–27. <https://doi.org/10.1016/j.bbr.2017.09.051>
- Ma XC et al (2013) Long-lasting antidepressant action of ketamine, but not glycogen synthase kinase-3 inhibitor SB216763, in the chronic mild stress model of mice. *PLoS One* 8:e56053. <https://doi.org/10.1371/journal.pone.0056053>
- Marietta MP, Way WL, Castagnoli N Jr, Trevor AJ (1977) On the pharmacology of the ketamine enantiomorphs in the rat. *J Pharmacol Exp Ther* 202:157–165
- McCloud TL et al (2015) Ketamine and other glutamate receptor modulators for depression in bipolar disorder in adults. *Cochrane Database Syst Rev*:CD011611. <https://doi.org/10.1002/14651858.CD011611.pub2>
- Molero P, Ramos-Quiroga J, Martin-Santos R, Calvo-Sánchez E, Gutiérrez-Rojas L, Meana JJ (2018) Antidepressant efficacy and tolerability of ketamine and esketamine: a critical review. *CNS Drugs* 32:411–420
- Morgan CJA, Curran HV (2012) Ketamine use: a review. *Addiction* 107:27–38. <https://doi.org/10.1111/j.1360-0443.2011.03576.x>
- Muller J, Pentylala S, Dilger J, Pentylala S (2016) Ketamine enantiomers in the rapid and sustained antidepressant effects. *Ther Adv Psychopharmacol* 6:185–192. <https://doi.org/10.1177/2045125316631267>
- Murrough JW et al (2013a) Antidepressant efficacy of ketamine in treatment-resistant major depression: a two-site randomized controlled trial. *Am J Psychiatry* 170:1134–1142. <https://doi.org/10.1176/appi.ajp.2013.13030392>
- Murrough JW et al (2013b) Rapid and longer-term antidepressant effects of repeated ketamine infusions in treatment-resistant major depression. *Biol Psychiatry* 74:250–256. <https://doi.org/10.1016/j.biopsych.2012.06.022>
- Newport DJ et al (2015) Ketamine and other NMDA antagonists: early clinical trials and possible mechanisms in depression. *Am J Psychiatry* 172:950–966. <https://doi.org/10.1176/appi.ajp.2015.15040465>
- Papadimitropoulou K, Vossen C, Karabis A, Donatti C, Kubitz N (2017) Comparative efficacy and tolerability of pharmacological and somatic interventions in adult patients with treatment-resistant depression: a systematic review and network meta-analysis. *Curr Med Res Opin* 33:701–711. <https://doi.org/10.1080/03007995.2016.1277201>
- Parsaik AK, Singh B, Khosh-Chashm D, Mascarenhas SS (2015) Efficacy of ketamine in bipolar depression: systematic review and meta-analysis. *J Psychiatr Pract* 21:427–435. <https://doi.org/10.1097/PRA.000000000000106>

- Paslakis G, Gilles M, Meyer-Lindenberg A, Deuschle M (2010) Oral administration of the NMDA receptor antagonist S-ketamine as add-on therapy of depression: a case series. *Pharmacopsychiatry* 43:33–35. <https://doi.org/10.1055/s-0029-1237375>
- Paul R, Schaaff N, Padberg F, Moller HJ, Frodl T (2009) Comparison of racemic ketamine and S-ketamine in treatment-resistant major depression: report of two cases. *World J Biol Psychiatry* 10:241–244. <https://doi.org/10.1080/15622970701714370>
- Phillips JL et al (2019) Single, repeated, and maintenance ketamine infusions for treatment-resistant depression: a randomized controlled trial. *Am J Psychiatry* 176:401–409. <https://doi.org/10.1176/appi.ajp.2018.18070834>
- Pittenger C, Sanacora G, Krystal JH (2007) The NMDA receptor as a therapeutic target in major depressive disorder. *CNS Neurol Disord Drug Targets* 6:101–115
- Qu Y, Yang C, Ren Q, Ma M, Dong C, Hashimoto K (2017) Comparison of (R)-ketamine and lanicemine on depression-like phenotype and abnormal composition of gut microbiota in a social defeat stress model. *Sci Rep* 7:15725. <https://doi.org/10.1038/s41598-017-16060-7>
- Read J, Cunliffe S, Jauhar S, McLoughlin DM (2019) Should we stop using electroconvulsive therapy? *BMJ* 364:k5233. <https://doi.org/10.1136/bmj.k5233>
- Reinstatler L, Youssef NA (2015) Ketamine as a potential treatment for suicidal ideation: a systematic review of the literature. *Drugs R D* 15:37–43. <https://doi.org/10.1007/s40268-015-0081-0>
- Remus JL, Dantzer R (2016) Inflammation models of depression in rodents: relevance to psychotropic drug discovery. *Int J Neuropsychopharmacol* 19:pyw028. <https://doi.org/10.1093/ijnp/pyw028>
- Reus GZ et al (2015) A single dose of S-ketamine induces long-term antidepressant effects and decreases oxidative stress in adulthood rats following maternal deprivation. *Dev Neurobiol* 75:1268–1281. <https://doi.org/10.1002/dneu.22283>
- Reus GZ et al (2017) Ketamine potentiates oxidative stress and influences behavior and inflammation in response to lipopolysaccharide (LPS) exposure in early life. *Neuroscience* 353:17–25. <https://doi.org/10.1016/j.neuroscience.2017.04.016>
- Rosenblat JD, Carvalho AF, Li M, Lee Y, Subramaniepillai M, McIntyre RS (2019) Oral ketamine for depression: a systematic review. *J Clin Psychiatry* 80. <https://doi.org/10.4088/JCP.18r12475>
- Sanacora G et al (2017) A consensus statement on the use of ketamine in the treatment of mood disorders. *JAMA Psychiat* 74:399–405. <https://doi.org/10.1001/jamapsychiatry.2017.0080>
- Schwartz J, Murrough JW, Iosifescu DV (2016) Ketamine for treatment-resistant depression: recent developments and clinical applications. *Evid Based Ment Health* 19:35–38. <https://doi.org/10.1136/eb-2016-102355>
- Segmiller F et al (2013) Repeated S-ketamine infusions in therapy resistant depression: a case series. *J Clin Pharmacol* 53:996–998. <https://doi.org/10.1002/jcph.122>
- Serafini G, Howland RH, Rovedi F, Girardi P, Amore M (2014) The role of ketamine in treatment-resistant depression: a systematic review. *Curr Neuropharmacol* 12:444–461. <https://doi.org/10.2174/1570159x12666140619204251>
- Sheth MK, Brand A, Halterman J (2018) Ketamine-induced changes in blood pressure and heart rate in pre-hospital intubated patients. *Adv J Grad Res* 3:20–33
- Shirayama Y, Hashimoto K (2017) Effects of a single bilateral infusion of R-ketamine in the rat brain regions of a learned helplessness model of depression. *Eur Arch Psychiatry Clin Neurosci* 267:177–182. <https://doi.org/10.1007/s00406-016-0718-1>
- Short B, Fong J, Galvez V, Shelker W, Loo CK (2018) Side-effects associated with ketamine use in depression: a systematic review. *Lancet Psychiatry* 5:65–78. [https://doi.org/10.1016/S2215-0366\(17\)30272-9](https://doi.org/10.1016/S2215-0366(17)30272-9)
- Sihra N, Ockrim J, Wood D (2018) The effects of recreational ketamine cystitis on urinary tract reconstruction—a surgical challenge. *BJU Int* 121:458–465. <https://doi.org/10.1111/bju.14094>
- Singh JB et al (2016) Intravenous esketamine in adult treatment-resistant depression: a double-blind, double-randomization, placebo-controlled study. *Biol Psychiatry* 80:424–431. <https://doi.org/10.1016/j.biopsych.2015.10.018>

- Singh I, Morgan C, Curran V, Nutt D, Schlag A, McShane R (2017) Ketamine treatment for depression: opportunities for clinical innovation and ethical foresight. *Lancet Psychiatry* 4:419–426. [https://doi.org/10.1016/S2215-0366\(17\)30102-5](https://doi.org/10.1016/S2215-0366(17)30102-5)
- Sinner B, Graf BM (2008) Ketamine. *Handb Exp Pharmacol*:313–333. [https://doi.org/10.1007/978-3-540-74806-9\\_15](https://doi.org/10.1007/978-3-540-74806-9_15)
- Soumier A, Carter RM, Schoenfeld TJ, Cameron HA (2016) New hippocampal neurons mature rapidly in response to ketamine but are not required for its acute antidepressant effects on neophagia in rats. *eNeuro* 3. <https://doi.org/10.1523/ENEURO.0116-15.2016>
- Stevenson C (2005) Ketamine: a review. *Update Anaesth* 20:25–29
- Strong CE, Kabbaj M (2018) On the safety of repeated ketamine infusions for the treatment of depression: effects of sex and developmental periods. *Neurobiol Stress* 9:166–175. <https://doi.org/10.1016/j.ynstr.2018.09.001>
- Sun HL et al (2016) Role of hippocampal p11 in the sustained antidepressant effect of ketamine in the chronic unpredictable mild stress model. *Transl Psychiatry* 6:e741. <https://doi.org/10.1038/tp.2016.21>
- Szlachta M et al (2017) Effect of clozapine on ketamine-induced deficits in attentional set shift task in mice. *Psychopharmacology (Berl)* 234:2103–2112. <https://doi.org/10.1007/s00213-017-4613-x>
- Thomson AM, West DC, Lodge D (1985) An N-methylaspartate receptor-mediated synapse in rat cerebral cortex: a site of action of ketamine? *Nature* 313:479–481
- Tian Z, Dong C, Fujita A, Fujita Y, Hashimoto K (2018a) Expression of heat shock protein HSP-70 in the retrosplenial cortex of rat brain after administration of (R,S)-ketamine and (S)-ketamine, but not (R)-ketamine. *Pharmacol Biochem Behav* 172:17–21. <https://doi.org/10.1016/j.pbb.2018.07.003>
- Tian Z, Dong C, Zhang K, Chang L, Hashimoto K (2018b) Lack of antidepressant effects of low-voltage-sensitive T-type calcium channel blocker ethosuximide in a chronic social defeat stress model: comparison with (R)-ketamine. *Int J Neuropsychopharmacol* 21:1031–1036. <https://doi.org/10.1093/ijnp/pyy072>
- Tracy DK, Wood DM, Baumeister D (2017) Novel psychoactive substances: types, mechanisms of action, and effects. *BMJ* 356:i6848. <https://doi.org/10.1136/bmj.i6848>
- Treccani G et al (2019) S-ketamine reverses hippocampal dendritic spine deficits in flinders sensitive line rats within 1 h of administration. *Mol Neurobiol* 56(11):7368–7379. <https://doi.org/10.1007/s12035-019-1613-3>
- Trimmel H, Helbok R, Staudinger T, Jaksch W, Messerer B, Schochl H, Likar R (2018) S(+)-ketamine: Current trends in emergency and intensive care medicine. *Wien Klin Wochenschr* 130:356–366. <https://doi.org/10.1007/s00508-017-1299-3>
- US Food and Drug Administration (2019) FDA approves new nasal spray medication for treatment-resistant depression; available only at a certified doctor's office or clinic. [PressAnnouncements/ucm632761.htm](https://www.fda.gov/pressannouncements/ucm632761.htm)
- Veraart JKE, Smith-Apeldoorn SY, Trueman H, de Boer MK, Schoevers RA, McShane R (2018) Characteristics of patients expressing an interest in ketamine treatment: results of an online survey. *BJPsych Open* 4:389–392. <https://doi.org/10.1192/bjo.2018.51>
- Vollenweider FX, Leenders KL, Oye I, Hell D, Angst J (1997) Differential psychopathology and patterns of cerebral glucose utilisation produced by (S)- and (R)-ketamine in healthy volunteers using positron emission tomography (PET). *Eur Neuropsychopharmacol* 7:25–38
- White PF, Schuttler J, Shafer A, Stanski DR, Horai Y, Trevor AJ (1985) Comparative pharmacology of the ketamine isomers. Studies in volunteers. *Br J Anaesth* 57:197–203. <https://doi.org/10.1093/bja/57.2.197>
- Wilkinson ST et al (2018) The effect of a single dose of intravenous ketamine on suicidal ideation: a systematic review and individual participant data meta-analysis. *Am J Psychiatry* 175:150–158. <https://doi.org/10.1176/appi.ajp.2017.17040472>
- World Health Organization (2011) WHO model list of essential medicines: 17th list, March 2011

- World Health Organization (2017) Depression and other common mental disorders: global health estimates (No. WHO/MSD/MER/2017.2). World Health Organization
- Xiong Z, Zhang K, Ishima T, Ren Q, Chang L, Chen J, Hashimoto K (2018) Comparison of rapid and long-lasting antidepressant effects of negative modulators of  $\alpha_5$ -containing GABA<sub>A</sub> receptors and (*R*)-ketamine in a chronic social defeat stress model. *Pharmacol Biochem Behav* 175:139–145. <https://doi.org/10.1016/j.pbb.2018.10.005>
- Xiong Z et al (2019) Lack of rapid antidepressant effects of Kir4.1 channel inhibitors in a chronic social defeat stress model: Comparison with (*R*)-ketamine. *Pharmacol Biochem Behav* 176:57–62. <https://doi.org/10.1016/j.pbb.2018.11.010>
- Yang C et al (2015) *R*-ketamine: a rapid-onset and sustained antidepressant without psychotomimetic side effects. *Transl Psychiatry* 5:e632. <https://doi.org/10.1038/tp.2015.136>
- Yang B et al (2016a) Comparison of *R*-ketamine and rapastinel antidepressant effects in the social defeat stress model of depression. *Psychopharmacology (Berl)* 233:3647–3657. <https://doi.org/10.1007/s00213-016-4399-2>
- Yang C, Han M, Zhang JC, Ren Q, Hashimoto K (2016b) Loss of parvalbumin-immunoreactivity in mouse brain regions after repeated intermittent administration of esketamine, but not *R*-ketamine. *Psychiatry Res* 239:281–283. <https://doi.org/10.1016/j.psychres.2016.03.034>
- Yang C, Qu Y, Fujita Y, Ren Q, Ma M, Dong C, Hashimoto K (2017) Possible role of the gut microbiota-brain axis in the antidepressant effects of (*R*)-ketamine in a social defeat stress model. *Transl Psychiatry* 7:1294. <https://doi.org/10.1038/s41398-017-0031-4>
- Yang C, Ren Q, Qu Y, Zhang JC, Ma M, Dong C, Hashimoto K (2018a) Mechanistic target of rapamycin-independent antidepressant effects of (*R*)-ketamine in a social defeat stress model. *Biol Psychiatry* 83:18–28. <https://doi.org/10.1016/j.biopsych.2017.05.016>
- Yang Y, Cui Y, Sang K, Dong Y, Ni Z, Ma S, Hu H (2018b) Ketamine blocks bursting in the lateral habenula to rapidly relieve depression. *Nature* 554:317–322. <https://doi.org/10.1038/nature25509>
- Zanos P, Gould TD (2018) Intracellular signaling pathways involved in (*s*)- and (*r*)-ketamine antidepressant actions. *Biol Psychiatry* 83:2–4. <https://doi.org/10.1016/j.biopsych.2017.10.026>
- Zanos P, Nelson ME, Highland JN, Krimmel SR, Georgiou P, Gould TD, Thompson SM (2017) A negative allosteric modulator for  $\alpha_5$  subunit-containing GABA receptors exerts a rapid and persistent antidepressant-like action without the side effects of the NMDA receptor antagonist ketamine in mice. *eNeuro* 4. <https://doi.org/10.1523/ENEURO.0285-16.2017>
- Zanos P et al (2018) Ketamine and ketamine metabolite pharmacology: insights into therapeutic mechanisms. *Pharmacol Rev* 70:621–660. <https://doi.org/10.1124/pr.117.015198>
- Zarate CA Jr et al (2006) A randomized trial of an N-methyl-D-aspartate antagonist in treatment-resistant major depression. *Arch Gen Psychiatry* 63:856–864. <https://doi.org/10.1001/archpsyc.63.8.856>
- Zeilhofer HU, Swandulla D, Geisslinger G, Brune K (1992) Differential effects of ketamine enantiomers on NMDA receptor currents in cultured neurons. *Eur J Pharmacol* 213:155–158
- Zhan Y et al (2019) A preliminary study of anti-suicidal efficacy of repeated ketamine infusions in depression with suicidal ideation. *J Affect Disord* 251:205–212. <https://doi.org/10.1016/j.jad.2019.03.071>
- Zhang K, Hashimoto K (2019) An update on ketamine and its two enantiomers as rapid-acting antidepressants. *Expert Rev Neurother* 19:83–92. <https://doi.org/10.1080/14737175.2019.1554434>
- Zhang JC, Li SX, Hashimoto K (2014) *R* (-)-ketamine shows greater potency and longer lasting antidepressant effects than *S* (+)-ketamine. *Pharmacol Biochem Behav* 116:137–141. <https://doi.org/10.1016/j.pbb.2013.11.033>
- Zhang JC et al (2015) Comparison of ketamine, 7,8-dihydroxyflavone, and ANA-12 antidepressant effects in the social defeat stress model of depression. *Psychopharmacology (Berl)* 232:4325–4335. <https://doi.org/10.1007/s00213-015-4062-3>

- Zhang GF et al (2016) Acute single dose of ketamine relieves mechanical allodynia and consequent depression-like behaviors in a rat model. *Neurosci Lett* 631:7–12. <https://doi.org/10.1016/j.neulet.2016.08.006>
- Zhang K, Dong C, Fujita Y, Fujita A, Hashimoto K (2018) 5-hydroxytryptamine-independent antidepressant actions of (R)-ketamine in a chronic social defeat stress model. *Int J Neuropsychopharmacol* 21:157–163. <https://doi.org/10.1093/ijnp/pyx100>
- Zhao J, Wang Y, Wang D (2018) The effect of ketamine infusion in the treatment of complex regional pain syndrome: a systemic review and meta-analysis. *Curr Pain Headache Rep* 22:12. <https://doi.org/10.1007/s11916-018-0664-x>
- Zheng W et al (2018) Rapid and longer-term antidepressant effects of repeated-dose intravenous ketamine for patients with unipolar and bipolar depression. *J Psychiatr Res* 106:61–68. <https://doi.org/10.1016/j.jpsychires.2018.09.013>



Contents lists available at ScienceDirect

## Brain, Behavior, &amp; Immunity - Health

journal homepage: [www.editorialmanager.com/bbih/default.aspx](http://www.editorialmanager.com/bbih/default.aspx)

## Research Report

## Abnormalities of the composition of the gut microbiota and short-chain fatty acids in mice after splenectomy

Yan Wei<sup>a,b,1</sup>, Lijia Chang<sup>a</sup>, Tamaki Ishima<sup>a</sup>, Xiayun Wan<sup>a</sup>, Li Ma<sup>a</sup>, Gerile Wuyun<sup>a</sup>, Yaoyu Pu<sup>a</sup>, Kenji Hashimoto<sup>a,\*</sup><sup>a</sup> Division of Clinical Neuroscience, Chiba University Center for Forensic Mental Health, Chiba, 260-8670, Japan<sup>b</sup> Key Laboratory of Medical Electrophysiology of Ministry of Education and Medical Electrophysiological Key Laboratory of Sichuan Province, Collaborative Innovation Center for Prevention and Treatment of Cardiovascular Disease, Institute of Cardiovascular Research, Southwest Medical University, Luzhou, 646000, Sichuan, China

## ARTICLE INFO

## Keywords:

Gut microbiota  
Immune system  
Short-chain fatty acids  
Spleen  
Spleen–gut–microbiota axis  
Splenectomy

## ABSTRACT

The brain–gut–microbiota axis is a complex multi-organ bidirectional signaling system between the brain and microbiota that participates in the host immune system. The spleen, as the largest immune organ in the body, has a key role in the brain–gut–microbiota axis. Here, we investigated whether splenectomy could affect depression-like phenotypes and the composition of the gut microbiota in adult mice. In behavioral tests, splenectomy did not cause depression-like behaviors in mice. Conversely, splenectomy led to significant alterations in the diversity of gut microbes compared with the findings in control (no surgery) and sham-operated mice. In an unweighted UniFrac distance analysis, the boxplots representing the splenectomy group were distant from those representing the other two groups. We found differences in abundance for several bacteria in the splenectomy group at the taxonomic level compared with the other two groups. Finally, splenectomy induced significant changes in lactic acid and n-butyric acid levels compared with those in the other groups. Interestingly, there were significant correlations between the counts of certain bacteria and lactic acid (or n-butyric acid) levels in all groups. These data suggest that splenectomy leads to an abnormal composition of the gut microbiota. It is likely that the spleen–gut–microbiota axis plays a crucial role in the composition of the gut microbiota by regulating immune homeostasis.

## 1. Introduction

The brain–gut–microbiota axis is a complex multi-organ bidirectional signaling system between the brain and microbiota with an important role in host homeostasis (Cryan et al., 2019; Cusotto et al., 2018; Dinan and Cryan, 2017; Fung et al., 2017; Long-Smith et al., 2020). Accumulating evidence suggests that the immune system plays a key role in the brain–gut–microbiota axis (Cerf-Bensussan and Gaboriau-Routhiau, 2010; Cryan et al., 2019; Fung, 2020; Round and Mazmanian, 2009). The composition of the gut microbiota in patients with psychiatric disorders such as depression (Chen et al., 2020; Jiang et al., 2015; Lin et al., 2017; Liu et al., 2020; Wong et al., 2016; Zheng et al., 2016) and schizophrenia (Ma et al., 2020; Xu et al., 2020b; Zheng et al., 2019; Zhu et al., 2020a, Zhu et al., 2020b) is altered compared with that in healthy control subjects. Collectively, it is likely that abnormalities of the brain–gut–microbiota axis influence the pathogenesis of these

psychiatric disorders (Flux and Lowry, 2020). In addition, accumulating preclinical studies suggest that an abnormal gut microbiota composition could contribute to depression-like behaviors in rodents exposed to stress (Jianguo et al., 2019; Szyszkwicz et al., 2017; Wang et al., 2020a, 2020b; Yang et al., 2017b, 2019; Zhang et al., 2019a, 2020b).

The spleen is the largest secondary lymphoid organ in the body (Lewis et al., 2019). Accumulating evidence has identified a key role of the spleen in stress-related disorders (Bronte and Pittet, 2013; Lewis et al., 2019; Mebius and Kraal, 2005). For example, chronic stress (Bailey et al., 2007; McKim et al., 2018; Powell et al., 2009; Zhang et al., 2019b) or lipopolysaccharide (LPS)-induced stress (Zhang et al., 2020b) impairs splenic function in rodents. Collectively, it has been proposed that the brain–spleen axis plays a crucial role in stress-related psychiatric disorders (Hashimoto, 2020; Xu et al., 2020a; Yang et al., 2017a; Zhang et al., 2019b, 2020a, 2020b). Recently, Zhang et al. (2020c) demonstrated that splenic denervation in mice specifically compromises the formation of

\* Corresponding author.

E-mail address: [hashimoto@faculty.chiba-u.jp](mailto:hashimoto@faculty.chiba-u.jp) (K. Hashimoto).<sup>1</sup> Yan Wei and Lijia Chang contributed equally to this work.<https://doi.org/10.1016/j.bbih.2021.100198>

Received 30 December 2020; Accepted 31 December 2020

Available online 4 January 2021

2666-3546/© 2021 The Authors. Published by Elsevier Inc. This is an open access article under the CC BY-NC-ND license (<http://creativecommons.org/licenses/by-nc-nd/4.0/>).

plasma cells during T cell-dependent immune activity, indicating key roles of brain–spleen communication in antibody production and brain–body interactions in the adaptive immune system (Cathomas and Russo, 2020; Whalley, 2020). Despite the well-known effects of stress on the spleen, the precise molecular mechanisms underlying stress-induced changes in splenic function remain unknown. Moreover, no study had demonstrated the role of spleen in the brain–gut–microbiota axis in rodents.

Splenectomy is a surgical procedure that partially or completely removes the spleen as a treatment for a wide variety of disorders, although subjects can experience a number of serious complications after surgery (Weledji, 2014). Given the crucial role of the spleen in the immune system, the present study investigated whether splenectomy affects the composition of the gut microbiota in mice. Furthermore, we sought to clarify previous findings (Haile et al., 2016) indicating that splenectomy causes depression-like phenotypes in mice.

## 2. Materials and methods

### 2.1. Animals

Male C57BL/6 mice (8 weeks old, weighing 20–25 g,  $n = 25$ ) were purchased from Japan SLC Inc. (Hamamatsu, Shizuoka, Japan). Mice were housed (4 or 5 per cage) under a 12-h/12-h light/dark cycle (lights on 07:00 a.m.) under controlled conditions for temperature and humidity. Mice were granted access to food (CE-2; CLEA Japan, Inc., Tokyo, Japan) and water ad libitum. The experiment was approved by the Chiba University Institutional Animal Care and Use Committee (Permission number: 1–365). All efforts were made to minimize animal suffering.

### 2.2. Splenectomy

Splenectomy (or sham) surgery was performed under continuous isoflurane inhalation anesthesia. Briefly, the mice were anesthetized with 3% isoflurane through an inhalation anesthesia apparatus (KN-1071 NARCOBIT-E; Natsume Seisakusho, Tokyo, Japan). In the splenectomy group, each mouse was kept in a left lateral recumbent position, and an approximately 1-cm incision was made from the abdominal wall under the left costal margin. The skin was dissected, and subcutaneous, muscle, and fascia layers were removed individually until the spleen was exposed. The peripheral ligament of the spleen was separated, associated blood vessels and nerves were ligatured using 6-0 silk sutures, and the spleen removed by transecting the blood vessels distal to the ligature. Abdominal muscles and the skin incision were closed sequentially using 4-0 silk sutures. During sham surgery, the abdominal wall was similarly opened, and the wall was closed immediately after identifying the spleen.

### 2.3. Behavioral tests

The locomotion test (LMT), tail suspension test (TST), forced swimming test (FST), and 1% sucrose preference test (SPT) were performed as described previously (Chang et al., 2019; Wang et al., 2020a, 2020b). Behavioral tests were performed in a blind manner.

**LMT:** An automated animal movement analysis system (SCANET MV-40; MELQUEST Co., Ltd., Toyama, Japan) was used to measure the locomotor activity of mice. The cumulative ambulatory activity counts were recorded continuously over a period of 60 min after the mice were placed in the experimental cages (56 cm [length] × 56 cm [width] × 33 cm [height]). The cages were cleaned between the testing sessions.

**TST:** The TST was performed using a small piece of adhesive tape placed approximately 2 cm from the tip of the tail for each mouse. A single hole was punched in the tape, and mice were hung individually on hooks. The immobility time was recorded for 10 min. Mice were

considered immobile only when they hung passively and they were completely motionless.

**FST:** The FST was performed using an automated forced-swim apparatus (SCANET MV-40). The mice were individually placed into a cylinder (23 cm [diameter] × 31 cm [height]) with a water depth of 15 cm (water temperature,  $23 \pm 1$  °C). The immobility time was recorded and calculated by the analytical software of the apparatus throughout a 6 min observation time.

**SPT:** For the SPT, mice were exposed to both water and 1% sucrose solution for 48 h, followed by 4 h of water and food deprivation and a 1-h exposure to two identical bottles (water and 1% sucrose solution). The bottles containing water and sucrose were weighed before and after the exposure period. The sucrose preference was calculated as the percent sucrose solution consumption relative to the total liquid consumption.

### 2.4. Fecal sample DNA extraction

Fresh fecal samples of mice were collected before the behavioral tests. The fecal samples were placed into sterilized screw-cap microtubes immediately after defecation and stored at  $-80$  °C until use. DNA from the mouse fecal samples of the three different groups (control, sham, and splenectomy) was extracted using a NucleoSpin DNA stool kit (MACHEREY-NAGEL, Germany) according to the manufacturer's protocol. The DNA concentration was determined using a BioPhotometer® Plus system (Eppendorf, Germany). Purity was determined by analyzing the ratio of absorbance at 260 nm and 280 nm (OD 260/OD 280) and also monitored using 1% agarose gels. The DNA samples were stored at  $-80$  °C before further analysis.

### 2.5. 16 S rRNA analysis of fecal samples

The 16 S rRNA analyses of fecal samples were performed at Novogene Bioinformatics Technology Co. (Tianjin, China). PCR amplification was performed before sequencing, and a barcoded sequencing approach was used to study the bacterial composition of each fecal sample. The V3–V4 regions of the 16 S rRNA gene were amplified with the specific primers 341 F (CCTAYGGGRBGCASCAG) and 806 R (GGACTACNNGGGTATC-TAAT). Sequencing was performed on the Illumina NovaSeq 6000 platform.

Sequences analysis for operational taxonomy units (OTU) production was performed using Uparse software (version 7.0.1001, <http://drive5.com/uparse/>). Sequence reads were further processed to remove low-quality and short reads according to the Quantitative Insights Into Microbial Ecology (QIIME, version 1.7.0, <http://qiime.org/index.html>) and UCHIME algorithms [http://www.drive5.com/usearch/manual/uchime\\_algo.html](http://www.drive5.com/usearch/manual/uchime_algo.html)). Then, the effective tags were obtained according to the aforementioned data filtration. For species annotation, the remaining reads (46,218 reads) were clustered into OTUs at 97% identity using Mothur software against the SILVA Database (SILVA132, <http://www.arb-silva.de/>) at each taxonomic rank of kingdom, phylum, class, order, family, genus, and species (threshold value = 0.8–1). The OTU abundance bioinformation was normalized using the sequence number corresponding to the sample sequences for alpha and beta diversity.

Alpha diversity, defined as the gut microbiota richness (Rhoads et al., 2018), was used to analyze the complexity of species diversity for a sample through six indices, including the observed OTU, Chao 1, Shannon, Simpson, ACE, and Fisher indices. These indices were analyzed using QIIME (Kuczynski et al., 2012) and displayed using R software (version 2.15.3).

Beta diversity was used to determine the differences of species complexity among samples. The beta diversity of unweighted UniFrac and weighted UniFrac distances were analyzed using QIIME software (version 1.7.0). Unweighted pair group method of arithmetic means (UPGMA) clustering was used as a hierarchical clustering method to

interpret the distance matrix using the average linkage with QIIME software (version 1.7.0). Metastats (Duan et al., 2020) and R software were used to analyze the effects of splenectomy on the beta diversity of the gut microbiota at the taxonomic level as demonstrated using a heatmap, and significance was indicated by  $P < 0.05$  or  $P < 0.01$ . Differences in bacterial taxa between groups at the species or higher level (depending on the taxon annotation) were calculated via linear discriminant analysis (LDA) effect size (LEfSe) using LEfSe software (LDA score  $> 4.0$ ,  $P < 0.05$ ) (Segata et al., 2011).

## 2.6. Prediction of functional profiles of gut microbiota using PICRUSt

Based on the 16 S rRNA gene sequencing data and Kyoto Encyclopedia of Genes and Genome (KEGG) orthology, PICRUSt (Phylogenetic Investigation of Communities by Reconstruction of Unobserved States) analysis and Statistical Analysis of Metagenomic Profiles (STAMP) software package were applied for the functional prediction of gut microbiota (Langille et al., 2013; Parks et al., 2014).

## 2.7. Measurement of short-chain fatty acid (SCFA) levels in fecal samples

Determination of SCFAs (i.e., acetic acid, propionic acid, butyric acid, lactic acid, succinic acid) in fecal samples was performed at TechnoSuruga Laboratory, Co., Ltd. (Shizuoka, Japan), as reported previously (Wang et al., 2020a, 2020b; Zhang et al., 2019a). The concentrations of SCFAs were determined using gas chromatography with a flame ionization detector. The SCFA data were expressed as milligrams per gram of feces.

## 2.8. Statistical analysis

Data are expressed as the mean  $\pm$  standard error of the mean (S.E.M.). The body weight data were analyzed using repeated-measures one-way analysis of variance (ANOVA), followed by Fisher's least significant difference (LSD) test. Data for behavioral tests, and SCFA levels were analyzed using one-way ANOVA, followed by Fisher's LSD test. Data for alpha-diversity of the gut microbiota were analyzed using the

Kruskal–Wallis test, followed by the Dunn's test for *post-hoc* analysis. For beta-diversity of the gut microbiota, principal component analysis (PCA) of OUT level and the weighted UniFrac phylogenetic distance were performed using analysis of similarities (ANOSIM) by R package vegan (2.5.4) (Xia and Sun, 2017). The unweighted UniFrac phylogenetic distance was also calculated to estimate beta-diversity using ANOSIM by R package vegan (2.5.4). To compare gut microbiome structure among different groups for beta-diversity based on the unweighted UniFrac phylogenetic distance, we used a Wilcoxon-signed rank test. Metastats analysis was used to determine the differentially abundant genera between the two groups. Correlations between SCFAs and the relative bacterial abundance were analyzed using Spearman's correlation analysis.  $P < 0.05$  was considered statistically significant.

## 3. Results

### 3.1. Effects of splenectomy on depression-like phenotypes

A previous study found that splenectomy caused depression-like phenotype in mice (Haile et al., 2016). Therefore, we performed behavioral tests for depression-like behaviors in mice after splenectomy (Fig. 1A). Body weight did not differ before and 7 days after splenectomy among the three groups (Fig. 1B). No differences were noted in any behavioral tests, including the LMT (Fig. 1C), TST (Fig. 1D), FST (Fig. 1E), and SPT (Fig. 1F), among the three groups.

### 3.2. Effects of splenectomy on the OTU clustering of the evolutionary tree and taxon composition profile of the gut microbiota

To understand the distribution of gut bacteria after splenectomy at different taxonomic levels, the evolutionary tree of the 100 most abundant genera was constructed to observe the representative sequences of bacteria at the genus level with color-coding at the phylum level for the three groups (Fig. 2A). We identified different distributions of bacteria at the genus level in the splenectomy group. For example, the splenectomy group exhibited a lower abundance of *Lactobacillus* (Fig. 2A). Simultaneously, the taxon composition profile of gut bacteria was also presented

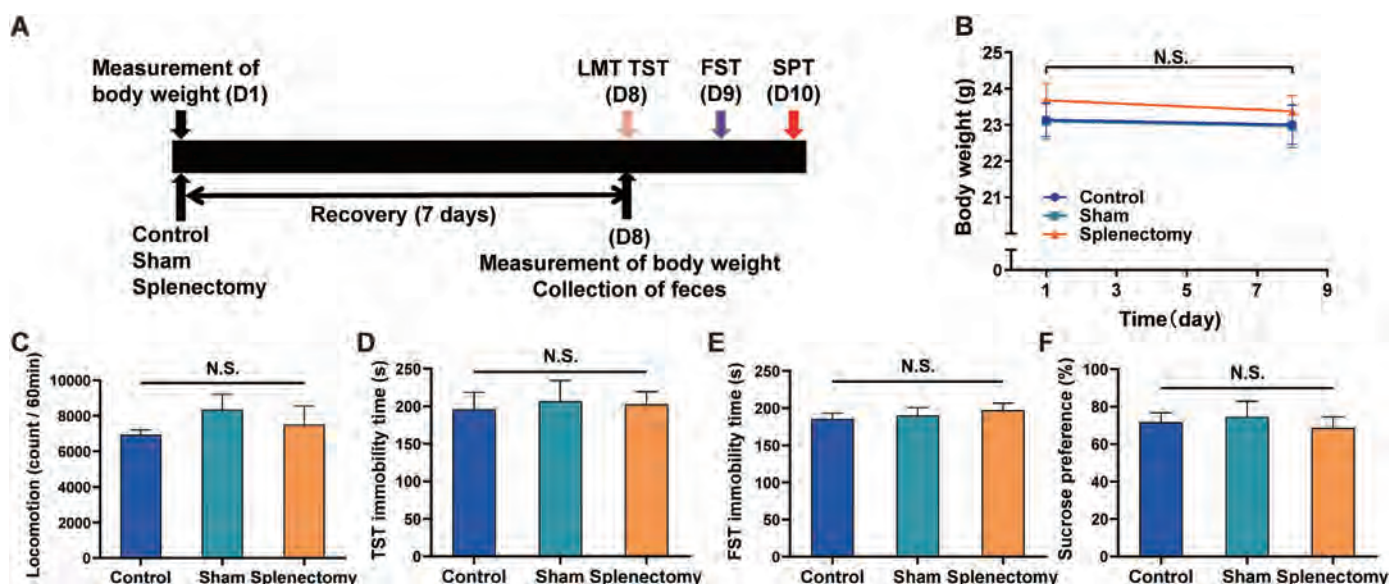


**Fig. 1. Schedule of splenectomy, collection of feces and behavioral tests**

(A): Splenectomy or sham surgery was performed on day 1. Collection of feces, locomotion test (LMT) and tail suspension test (TST) were performed on day 8. Forced swimming test (FST) and one % sucrose preference test (SPT) were performed on day 9 and day 10, respectively. (B): Body weight of three groups on day 1 and day 8 (repeated measure one-way ANOVA:  $F_{2,22} = 0.321$ ,  $P = 0.728$ ). (C): LMT (one-way ANOVA:  $F_{2,22} = 0.7135$ ,  $P = 0.5009$ ). (D): TST (one-way ANOVA:  $F_{2,22} = 0.0573$ ,  $P = 0.9444$ ). (E): FST (one-way ANOVA:  $F_{2,22} = 0.3959$ ,  $P = 0.6778$ ). (F): SPT (one-way ANOVA:  $F_{2,22} = 0.2038$ ,  $P = 0.8172$ ). The values represent the mean  $\pm$  S.E.M. ( $n = 8$  or  $9$ ). N.S.: not significant. LMT: locomotion test. TST: tail suspension test. FST: forced swimming test. SPT: 1% sucrose preference test.



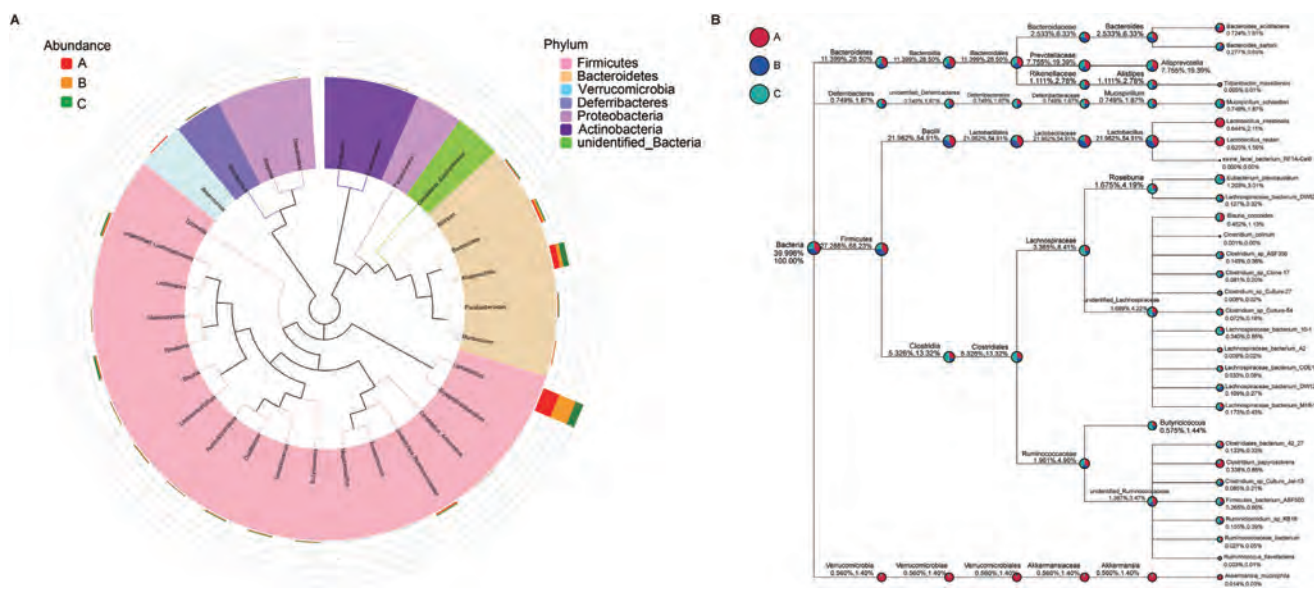


**Fig. 2. Effects of splenectomy on the OTU clustering of evolutionary tree and taxon composition profile of gut microbiota**  
 The evolutionary tree of top 100 abundant genera and taxonomy tree. (A): Circular phylogenetic tree at genus level. The inner band represents the genus taxonomy with color-coded by phylum level. Different colors of the branches represent different phylum. Relative abundance of each genus in each group was displayed outside the circle and different colors represent different groups. Red for control group, yellow for sham group, and green for splenectomy group. (B): Taxon composition profile of gut bacteria shown by taxonomy tree. Different colors represent different group of taxonomic ranks for the relative abundances in gut bacteria. Red for control group, blue for sham group, and green for splenectomy group. A, control (no surgery) group; B, sham group; C, splenectomy group. . (For interpretation of the references to color in this figure legend, the reader is referred to the Web version of this article.)

using a taxonomy tree among the three groups (Fig. 2B). For example, higher abundance was observed for *Clostridia* at the class level, *Clostridiales* at the order level, and *Lachnospiraceae* at the family level in the splenectomy group (Fig. 2B).

### 3.3. Effects of splenectomy on the composition diversity of the gut microbiota

The composition of the gut microbiota among the three groups was analyzed using alpha- and beta-diversity. Kruskal–Wallis test revealed significant differences in the observed OUT, fisher and ACE indices among the three groups. *Post-hoc* analysis of Dunn’s test showed that alpha-diversity was significantly higher in the splenectomy group than that in the control and sham groups (Fig. 3A–C). Regarding beta-diversity, PCA was applied to analyze the bacterial community composition of gut microbiota among three groups (Fig. 3D). PCA revealed significant separation in the community composition evaluated by ANOSIM ( $R = 0.3287$ ,  $P = 0.001$ ) (Fig. 3D) based on the OTU level. Furthermore, the UPGMA cluster analysis demonstrated that the splenectomy group was

different from the control and sham groups based on the unweighted UniFrac distance (Fig. 3E and F). Importantly, the unweighted UniFrac distance among the three groups was also calculated by the ANOSIM ( $R = 0.2462$ ,  $P = 0.001$ ), and unweighted UniFrac distance illustrated that the boxplots representing the splenectomy group were distant from those representing in the control group (Wilcox,  $P < 0.01$ ) and the sham group (Wilcox,  $P < 0.01$ ) (Fig. 3G). In addition, the ordination of weighted UniFrac distance by PCoA revealed separation of splenectomy group from other two groups using the ANOSIM ( $R = 0.1486$ ,  $P = 0.018$ ) (Fig. 3H). Moreover, the heatmap of beta-diversity displayed significantly difference in splenectomy group compared with other two groups based on weighted UniFrac distance (Fig. 3I).

### 3.4. Effects of splenectomy on the beta diversity of the gut microbiota at the taxonomic level

At the phylum level, *Proteobacteria* and *Deferribacteres* had the highest abundance in the splenectomy group (Fig. 4A). The abundance of *Proteobacteria* in the splenectomy group was significantly higher ( $P < 0.01$ )

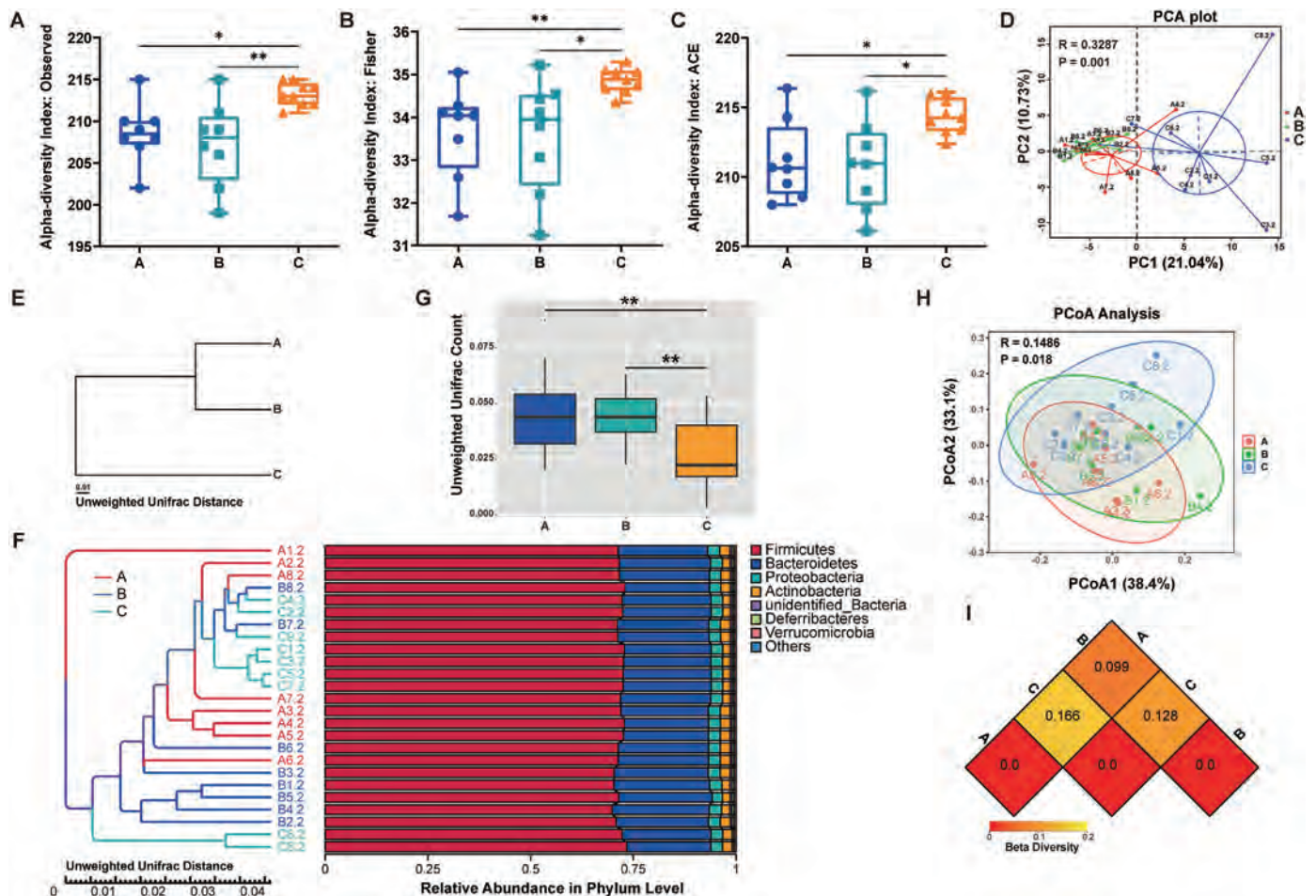


**Fig. 3. Effects of splenectomy on the composition of gut microbiota in alpha-diversity and beta-diversity**

(A): Alpha-diversity index of observed (Kruskal–Wallis test,  $\chi^2 = 10.085$ ,  $P = 0.006$ ). (B): Alpha-diversity index of fisher (Kruskal–Wallis test,  $\chi^2 = 10.125$ ,  $P = 0.006$ ). (C): Alpha-diversity index of ACE (Kruskal–Wallis test,  $\chi^2 = 6.801$ ,  $P = 0.033$ ). (D): Principal component analysis (PCA) of beta-diversity based on the OTU level, where each point represents a single sample colored by group circle, indicated by the second principal component of 10.73% on the Y-axis and the first principal component of 21.04% on the X-axis (ANOSIM ( $R = 0.3287$ ,  $P = 0.001$ )). (E) and (F): Unweighted UniFrac distance matrix was calculated by UPGMA cluster analysis. Splenectomy group was different with control and sham groups based on the Unweighted UniFrac distance. UPGMA hierarchical clustering results and the relative abundance of each sample at phylum level. (G): Boxplot of beta-diversity based on Unweighted UniFrac distance (ANOSIM,  $R = 0.2462$ ,  $P = 0.001$ ). Wilcox rank tests are performed for analysis of significance of difference between groups. (H): PCoA plot based upon weighted UniFrac distance (ANOSIM,  $R = 0.1486$ ,  $P = 0.015$ ). Each dot represents a single sample indicated by a principal component of 38.4% on the X-axis and another principal component of 33.1% on the Y-axis, contributing to discrepancy among the three groups. (I): Heatmap of beta-diversity based on weighted UniFrac distance. The values represent the mean  $\pm$  S.E.M. ( $n = 8$  or  $9$ ). \* $P < 0.05$ ; \*\* $P < 0.01$  \*\*\* $P < 0.001$ . A, control (no surgery) group; B, sham group; C, splenectomy group.

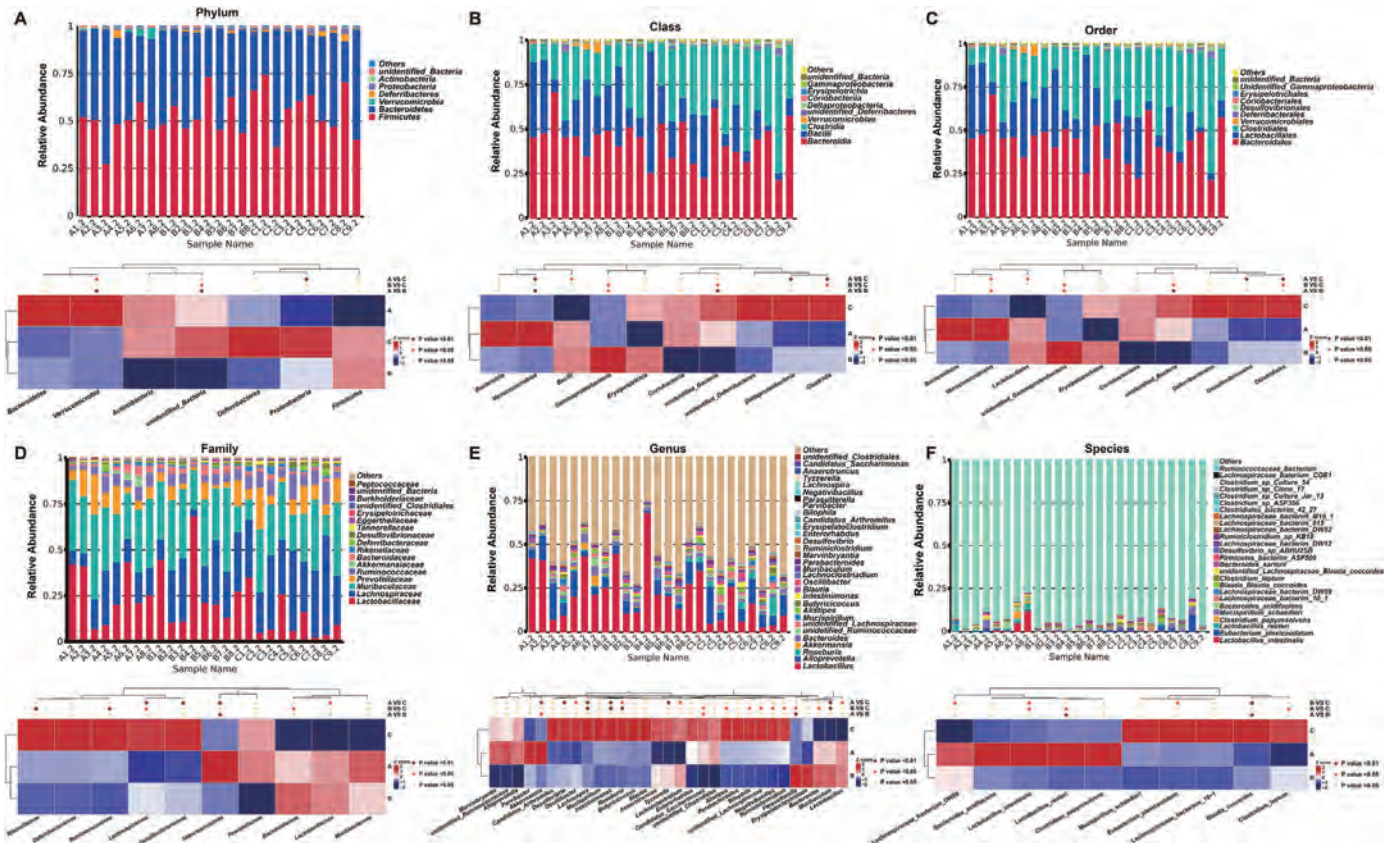


**Fig. 4.** Effects of splenectomy on the taxonomic level of gut microbiota in beta-diversity. Relative abundance distribution and comparison of relative taxon abundances at different taxonomic level. The taxonomic level includes phylum (A), class (B), order (C), family (D), genus (E) and species (F), displayed by histogram on each fecal sample among the three groups. Heat map showed the relative abundance of the significantly changed bacteria at different taxonomic level based on MetaStat method. Relative abundance from high to low of bacteria was indicated by Z score with the color from red to blue. P value ( $P < 0.01$ ,  $P < 0.05$  and  $P > 0.05$ ) was also shown in different color from red to yellow. A, control (no surgery) group; B, sham group; C, splenectomy group. (For interpretation of the references to color in this figure legend, the reader is referred to the Web version of this article.)

than that in the control group (Fig. 4A).

At the class level, *Deltaproteobacteria* and *Clostridia* had the highest abundance in the splenectomy group, whereas *Bacilli* had the lowest abundance (Fig. 4B). The abundance of *Deltaproteobacteria* was significantly higher ( $P < 0.01$ ) in the splenectomy group than in the control group, whereas that of *Bacilli* was significantly lower in the splenectomy group than in the control group ( $P < 0.05$ ) (Fig. 4B). In addition, the abundance of *Clostridia* was significantly higher in the splenectomy group than in the control ( $P < 0.01$ ) and sham groups ( $P < 0.05$ , Fig. 4B).

At the order level, *Deferribacterales*, *Desulfovibrionales*, and *Clostridiales* had the highest abundance in the splenectomy group, whereas *Lactobacillales* had the lowest abundance (Fig. 4C). The abundance of *Desulfovibrionales* was significantly higher ( $P < 0.01$ ) in the splenectomy group than in the control group, whereas that of *Lactobacillales* was significantly lower ( $P < 0.05$ , Fig. 4C). Moreover, the abundance of *Clostridiales* was significantly higher in the splenectomy group than in the control ( $P < 0.01$ ) and sham groups ( $P < 0.05$ ) (Fig. 4C).

At the family level, *Rikenellaceae*, *Deferribacteraceae*, *Ruminococcaceae*, *Lachnospiraceae*, and *Desulfovibrionaceae* had the highest abundance in the splenectomy group, whereas *Bacteroidaceae*, *Lactobacillaceae*, and *Muribaculaceae* had the lowest abundance (Fig. 4D). The abundance of *Lactobacillaceae* was significantly higher ( $P < 0.05$ ) in the splenectomy group than in the control group, whereas that of *Bacteroidaceae* was significantly lower in the splenectomy group ( $P < 0.05$ ) (Fig. 4D). Meanwhile, the abundance of *Desulfovibrionaceae* was significantly

higher ( $P < 0.01$ ) in the splenectomy group than in the control group, and those of *Rikenellaceae* and *Ruminococcaceae* were significantly higher ( $P < 0.01$ ) in the splenectomy group than in the sham group (Fig. 4D). More importantly, the abundance of *Lachnospiraceae* was significantly higher in the splenectomy group than in the control ( $P < 0.01$ ) and sham groups ( $P < 0.05$ , Fig. 4D).

At the genus level, the abundance of *Desulfovibrio*, *Oscillibacter*, *Lachnospira*, *Mucispirillum*, *Intestinimonas*, *Roseburia*, *Alistipes*, *Bilophila*, unidentified *Lachnospiraceae*, *Negativibacillus*, and *Ruminiclostridium* was elevated in the splenectomy group, whereas that of *Bacteroides*, *Muribaculum*, and *Lactobacillus* was decreased (Fig. 4E). Obviously, the abundance of *Desulfovibrio* ( $P < 0.01$ ) and *Oscillibacter* ( $P < 0.05$ ) was higher in the splenectomy group than in the control group, and that of *Lactobacillus* ( $P < 0.05$ ) was lower in the splenectomy group. Furthermore, the abundance of *Alistipes*, *Bilophila*, unidentified *Lachnospiraceae*, *Negativibacillus*, and *Ruminiclostridium* was significantly higher ( $P < 0.05$ ) in the splenectomy group than in the sham group, whereas that of *Bacteroides* was significantly lower ( $P < 0.05$ , Fig. 4E). More importantly, the abundance of *Lachnospira* ( $P < 0.01$  vs. control and sham), *Intestinimonas* ( $P < 0.01$  vs. control and sham), and *Roseburia* ( $P < 0.05$  vs. control and  $P < 0.01$  vs. sham) was significantly higher in the splenectomy group than in the control and sham groups (Fig. 4E). Contrarily, the abundance of *Muribaculum* was significantly lower ( $P < 0.01$ ) in the splenectomy group than in the control and sham groups (Fig. 4E).

The beta-diversity of the gut microbiota at the species level in the

three groups is presented in Fig. 4F. The abundance of *Clostridium leptum*, *Blautia coccoides*, *Lachnospiraceae bacterium 10-1*, *Eubacterium plexicaudatum*, and *Mucispirillum schaedleri* was increased in the splenectomy group, whereas that of *Clostridium papyrosolvans*, *Lactobacillus reuteri*, *Lactobacillus intestinalis*, *Bacteroides acidifaciens*, and *Lachnospiraceae bacterium DW59* was decreased (Fig. 4F). Importantly, the abundance of *Lactobacillus reuteri* was significantly lower ( $P < 0.05$ ) and that of *Clostridium leptum* was significantly higher ( $P < 0.05$ ) in the splenectomy group than in the control group (Fig. 4F). The abundance of *Lachnospiraceae bacterium DW59* was significantly lower ( $P < 0.05$ ) in the splenectomy group than in the sham group, whereas that of *Blautia coccoides* ( $P < 0.01$ ) and *Eubacterium plexicaudatum* ( $P < 0.05$ ) was significantly higher in the splenectomy group (Fig. 4F). Moreover, the abundance of

*Lactobacillus intestinalis* was significantly lower in the splenectomy group ( $P < 0.05$ ) than in the control and sham groups (Fig. 4F).

### 3.5. Effects of splenectomy on the LEfSe algorithm of gut microbiota

The gut microbiota changes of the abundant taxa among the three groups were analyzed using the LEfSe algorithm, which permits the identification of microbial markers that are more important in one group than in another group. The color differences illustrated differences in the abundant taxa among the groups (Kwak et al., 2020). As presented in Fig. 5A and C, a similar distribution for potential microbial markers was found between the control and splenectomy groups and between the sham and splenectomy groups. Six mixed-level phylotypes, including the

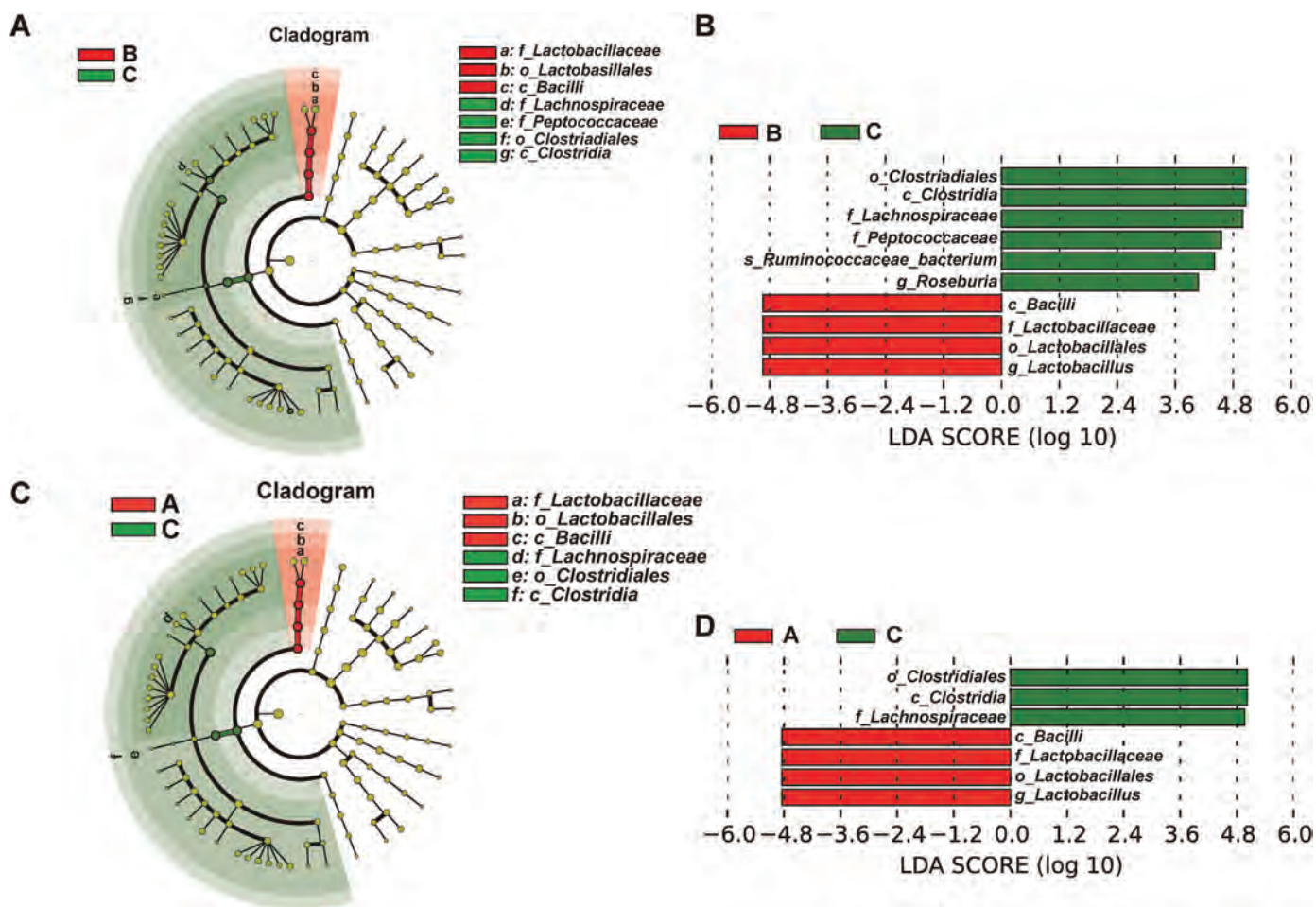


**Fig. 5. Effects of splenectomy on LEfSe algorithm of gut microbiota**

Linear discriminant analysis Effect Size (LEfSe) algorithm of gut microbiota changes in abundant taxa between the two groups. The colors showed that the group of abundant taxa was different with the other groups. (A): Cladogram (LDA score > 4.0,  $P < 0.05$ ) showed the taxonomic distribution difference between the sham group and splenectomy group, indicating with different color region. Each successive circle represents a differentially abundant taxonomic clades at phylum, class, order, family, genus and species level from the inner to outer rings. (B): Histograms of the different abundant taxa based on the cutoff value of LDA score (log10) > 4.0 and  $P < 0.05$  between the sham group and splenectomy group. The LDA scores of the sham group was negative, while those of the splenectomy group was positive. (C): Cladogram (LDA score > 4.0,  $P < 0.05$ ) showed the taxonomic distribution difference between the control group and splenectomy group indicated with different color region. Each successive circle represents a differentially abundant taxonomic clades at phylum, class, order, family, genus and species level from the inner to outer rings. (D): Histograms of the different abundant taxa based on the cutoff value of LDA score (log10) > 4.0 and  $P < 0.05$  between the control group and splenectomy group. The LDA scores of the control group was negative, while those of the splenectomy group was positive. A, control (no surgery) group; B, sham group; C, splenectomy group. (For interpretation of the references to color in this figure legend, the reader is referred to the Web version of this article.)

order *Clostridiales*, the class *Clostridia*, the families *Lachnospiraceae* and *Peptococcaceae*, the species *Ruminococcaceae bacterium*, and the genus *Roseburia*, were identified as potential microbial markers in the splenectomy group compared with the findings in the sham group (Fig. 5B, Table 1). Interestingly, three mixed-level phylotypes, including the order *Clostridiales*, class *Clostridia*, and family *Lachnospiraceae*, were also identified as potential microbial markers in the splenectomy group compared with the findings in the control group (Fig. 5D). As we expected, the same four mixed-level biomarkers, including the class *Bacilli*, family *Lactobacillaceae*, order *Lactobacillales*, and genus *Lactobacillus*, were found in both the control and sham groups compared with the results in the splenectomy group (Fig. 5B and D, Table 1).

### 3.6. Predictive functional metagenomes after splenectomy

The functional alterations of gut microbiota were predicted using the PICRUSt among the three groups. Predominant KEGG pathways involved in metabolism (Fig. 6A), including biosynthesis of other secondary metabolites, carbohydrate metabolism, lipid metabolism, metabolism of cofactors and vitamins, metabolism of terpenoids and polyketides, xenobiotics biodegradation and metabolism (Fig. 6B). Significant differences among the three groups were identified in 9 pathways on KEGG level 3, including beta-lactam resistance, penicillin and cephalosporin biosynthesis, amino sugar and nucleotide sugar metabolism, starch and sucrose metabolism, primary bile acid biosynthesis, secondary bile acid biosynthesis, ubiquinone and other terpenoid-quinone biosynthesis, biosynthesis of ansamycins and styrene degradation ( $P < 0.05$ ) (Fig. 6C). In addition, other pathways on KEGG level 3 were also different among the three groups, such as ubiquitin system, renal cell carcinoma, plant-pathogen interaction, germination, sporulation ( $P < 0.05$ ) (Fig. 6C), which related to genetic information processing (folding, sorting and degradation), human diseases (cancers), organismal systems (environmental adaptation) and cellular processes and signaling (Fig. 6A and B).

### 3.7. Measurement of SCFA content in fecal samples and correlations between the relative bacterial abundance and SCFA levels

SCFAs produced by microbiome play a role in brain-gut communication (Dallile et al., 2019; Silva et al., 2020; Wu et al., 2020). We

**Table 1**  
Linear discriminant analysis (LDA) score for gut microbiota.

Mix taxonomic level	Abundance	Group	LDA score	P value
A vs C				
c_Clostridia	5.636	C	5.019	0.002
o_Clostridiales	5.636	C	5.019	0.002
f_Lachnospiraceae	5.541	C	4.961	0.003
g_Lactobacillus	5.422	A	4.845	0.034
o_Lactobacillales	5.422	A	4.845	0.034
f_Lactobacillaceae	5.422	A	4.845	0.034
c_Bacilli	5.422	A	4.845	0.034
B vs C				
g_Lactobacillus	5.438	B	4.935	0.045
o_Lactobacillales	5.438	B	4.935	0.045
f_Lactobacillaceae	5.438	B	4.935	0.045
c_Bacilli	5.438	B	4.935	0.045
f_Peptococcaceae	2.627	C	4.548	0.036
g_Roseburia	4.511	C	4.073	0.032
s_Ruminococcaceae_bacterium	2.523	C	4.409	0.011
f_Lachnospiraceae	5.541	C	4.991	0.009
c_Clostridia	5.636	C	5.058	0.009
o_Clostridiales	5.636	C	5.058	0.009

p, phylum; c, class; o, order; f, family; g, genus; s, species.

The cutoff value of LDA score ( $\log_{10}$ )  $> 4.0$  and  $p < 0.05$  were considered as significant differences. A, control (no surgery) group; B, sham group; C, splenectomy group.

measured the concentrations of SCFAs in fecal samples because gut microbes produce SCFAs (Table 2). The levels of lactic acid were significantly lower in the splenectomy group than those in the sham groups, whereas those of n-butyric acid were significantly higher in the splenectomy group than those in the other two groups (Table 2 and Fig. 7A and B).

To explore the possible relationships between the relative bacterial abundance and SCFA levels in fecal samples, we performed logistic regression and correlation analyses. There were significant negative correlations of the relative abundance of *Clostridia* ( $r = -0.4558$ ,  $P = 0.0252$ ) at the class level (Fig. 7C), *Clostridiales* ( $r = -0.4558$ ,  $P = 0.0252$ ) at the order level (Fig. 7D), *Lachnospiraceae* ( $r = -0.4532$ ,  $P = 0.0261$ ) at the family level (Fig. 7E), *Lachnospira* ( $r = -0.6444$ ,  $P = 0.0007$ ) and *Intestinimonas* ( $r = -0.4110$ ,  $P = 0.0460$ ) at the genus level (Fig. 7F and G) and *Blautia Blautia\_coccoides* ( $r = -0.6155$ ,  $P = 0.0014$ ) at the species level (Fig. 7H) with the lactic acid content in all three groups.

Moreover, there was a significant negative correlation between the relative abundance of *Muribaculum* ( $r = -0.4005$ ,  $P = 0.0472$ ) at the genus level and n-butyric acid levels in all three groups (Fig. 7I). There was a significant positive correlation between the relative abundance of *Blautia Blautia\_coccoides* ( $r = 0.4925$ ,  $P = 0.0124$ ) at the species level and n-butyric acid levels in all three groups (Fig. 7K).

## 4. Discussion

The major findings of the current study were as follows. First, splenectomy did not induce depression-like phenotypes in mice, inconsistent with previous findings (Haile et al., 2016). Second, the OTU clustering of evolutionary trees revealed low abundance of the phylum *Lactobacillus* and higher abundance of the class *Clostridia*, the order *Clostridiales*, and the family *Lachnospiraceae* in the splenectomy group compared with the results in the other two groups. Third, splenectomy induced significant changes in the alpha- and beta-diversity of the host gut microbiota in adult mice. UPGMA cluster analysis indicated differences between the splenectomy group and the other two groups. Fourth, splenectomy altered the abundance of several bacteria at different taxonomic levels. Fifth, the LEfSe algorithm identified *Clostridiales*, *Clostridia*, *Lachnospiraceae*, *Peptococcaceae*, *Ruminococcaceae bacterium*, and *Roseburia* as important phylotypes in the splenectomy group. Sixth, predictive functional metagenomes using PICRUSt showed that splenectomy caused alterations in metabolisms, including biosynthesis of other secondary metabolites, carbohydrate metabolism, lipid metabolism, metabolism of cofactors and vitamins, metabolism of terpenoids and polyketides, xenobiotics biodegradation and metabolism. Finally, lactic acid levels were significantly lower in the splenectomy group than in other two groups, whereas n-butyric acid levels were significantly higher in the splenectomy group. Interestingly, there were significant correlations between the fecal levels of lactic acid (or n-butyric acid) and the abundance of several components of the microbiome in all groups. Taken together, the current data indicated that splenectomy alters the composition of the gut microbiota and SCFAs in the host without causing depression-like phenotypes.

A previous study demonstrated that splenectomy induced decreased sucrose preference in the SPT 5 days after surgery and that splenectomy caused neuroinflammation (i.e., microglial activation, reactive astrogliosis) in the brain (Haile et al., 2016). Conversely, using three behavioral tests (i.e., TST, FST, SPT), we did not detect depression-like phenotypes in mice 7–9 days after splenectomy. In addition, there were no differences in the blood levels of pro-inflammatory cytokines such as interleukin-6 and tumor necrosis factor-alpha among the three groups (data not shown), indicating that splenectomy did not cause systemic inflammation. The reasons underlying the discrepancy concerning depression-like behaviors are currently unclear. One possible cause was the use of different mouse strains (Swiss Webster for the study by Haile et al. (2016) vs. C57/B6 in our study). The second possibility is the timing of the SPT (5 days for the Haile study (Haile et al., 2016) vs. 7 days for our

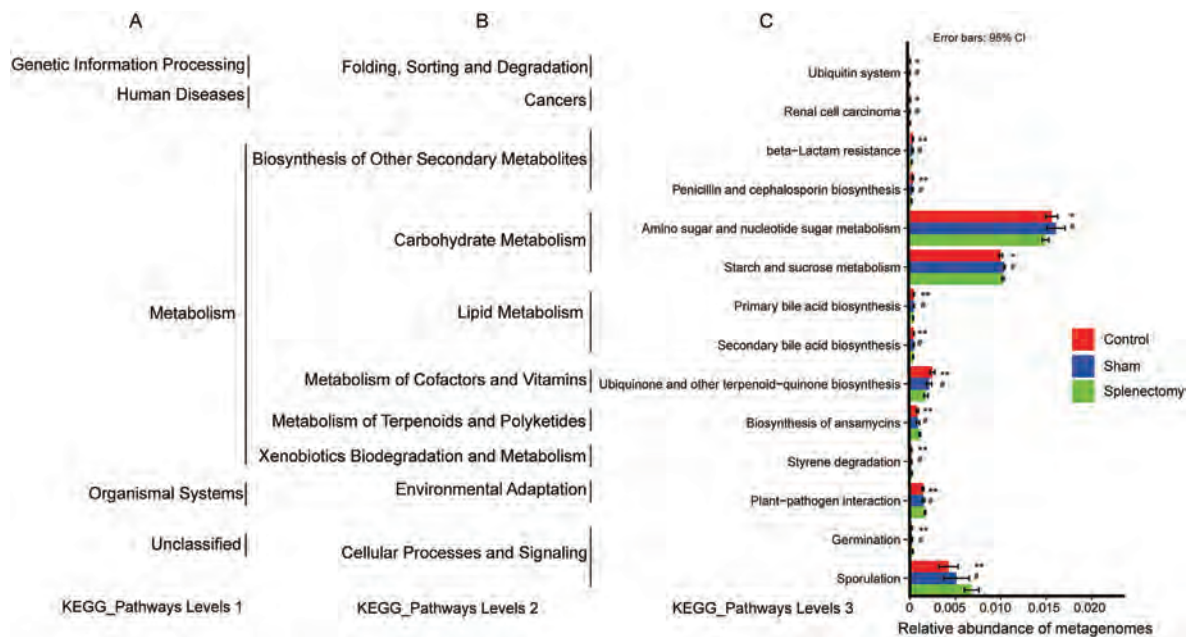


**Fig. 6. Relative abundance of KEGG pathways of functional categories.**

Functional predictions of the gut microbiota among the control, sham and splenectomy group generated from 16

S rRNA gene sequences using PICRUSt analysis. Significant differences of KEGG pathways at level 3 were determined by STAMP software based on the KEGG pathway database. \* $P < 0.05$ , \*\* $P < 0.01$  and # $P < 0.05$  vs splenectomy group.

**Table 2**

Levels of SCFAs in the fecal samples.

SCFAs (mg/g)	A: Control	B: Sham	C: Splenectomy	One-way ANOVA
Succinic acid	0.364 ± 0.097	0.305 ± 0.039	0.193 ± 0.039	$F_{2,22} = 1.975, P = 0.1626$
Lactic acid	0.540 ± 0.093	0.651 ± 0.134*	0.254 ± 0.086	$F_{2,21} = 3.705, P = 0.0419$
Acetic acid	1.165 ± 0.082	1.525 ± 0.216	1.722 ± 0.216	$F_{2,22} = 2.319, P = 0.1220$
Propionic acid	0.369 ± 0.033	0.431 ± 0.044	0.454 ± 0.077	$F_{2,22} = 0.604, P = 0.5556$
n-butyric acid	0.349 ± 0.029**	0.523 ± 0.088*	0.854 ± 0.130	$F_{2,22} = 7.366, P = 0.0036$

The values are the mean ± SEM (n = 8 or 9). \* $P < 0.05$ , \*\* $P < 0.01$  vs C group. One data of C group was under the limitation (0.05 mg/g).

study), as the recovery time after surgery may affect the results of behavioral tests such as the SPT. A third possibility was the changes in locomotor activity after surgery. Haile et al. (2016) reported decreased locomotor activity in mice after splenectomy. However, we did not find such changes. Thus, it is likely that reduced locomotor activity in the splenectomy group affects the results of SPT in mice. Therefore, further study on the effects of splenectomy on depression-like phenotypes is needed.

In this study, we found that splenectomy altered the abundance of several bacteria at different taxonomic levels. *Clostridium leptum* is one of the dominant groups of fecal bacteria in adult humans, constituting 16%–25% of the fecal microbiota (Lay et al., 2005). Prior research found that the abundance of *Clostridium leptum* and *Blautia coccoides* was negatively correlated with depression-like behaviors in mice (Tian et al., 2019), supporting the findings that splenectomized mice did not exhibit depression-like phenotypes in this study. *Eubacterium plexicaudatum* is a butyrate-producing bacterium (Breyner et al., 2019). The increase in n-butyric acid levels in the splenectomy group may be attributable to the higher abundance of *Eubacterium plexicaudatum*, although further study is needed. *Mucispirillum schaedleri*, a member of the phylum *Deferribacteres*, is a key antagonist of *Salmonella enterica* serovar Typhimurium colitis

(Herp et al., 2019). Furthermore, a recent study indicated that neutralization using anti-mouse IL-1 alpha exerts anti-inflammatory effects in a mouse model of inflammatory bowel disease by modulating gut microbes such as *Mucispirillum schaedleri* (Menghini et al., 2019). Considering the anti-inflammatory actions of *Mucispirillum schaedleri*, it is likely that increases in the abundance of bacteria may reflect a compensatory response in the host after splenectomy. Nonetheless, further research is needed to investigate the mechanisms underlying increases in the counts of these bacteria after splenectomy.

Meanwhile, *Clostridium papyrosolvens* produce a wide variety of carbohydrate-active enzymes including extracellular multi-enzyme complexes termed cellulosomes with different specificities for enhanced cellulosic biomass degradation (Ren et al., 2019). The reduced abundance of *Lactobacillus reuteri* and *Lactobacillus intestinalis* in the splenectomy group may explain the reduced levels of lactic acid in splenectomized mice because lactobacilli ferment lactose into lactic acid (Fine et al., 2020). Furthermore, *Lactobacillus reuteri* is known to have several beneficial effects on anti-microbial activity, the host immune system, and microbial translocation (Fine et al., 2020; Mu et al., 2018). Furthermore, *Lactobacillus reuteri* is also known to produce the anti-microbial compound reuterin (Fine et al., 2020). Thus, it is possible that splenectomy affected the anti-microbial activity of reuterin in the host, although we did not measure reuterin levels in the same samples. Recently, we reported that *Lactobacillus intestinalis* and *Lactobacillus reuteri* may be responsible for the anhedonia-like phenotype in antibiotic-treated mice after fecal microbiome transplantation from mice with depression-like phenotypes (Wang et al., 2020a). Thus, the current data may support the findings that splenectomized mice did not exhibit depression-like phenotypes. *Bacteroides acidifaciens* was the most abundant *Bacteroidetes* species in mice. It has been reported that the levels of immunoglobulin A (IgA) in the gut were associated with the relative abundance of *Bacteroides fragilis* group species such as *Bacteroides acidifaciens* (Nakajima et al., 2020). Given the essential role of IgA in the defense of the intestinal mucosa against harmful pathogens, it appears that reduced counts of *Bacteroides fragilis* may be associated with inflammatory diseases induced by harmful pathogens. The functions of *Lachnospiraceae* bacterium DW59 are unknown. Although the precise

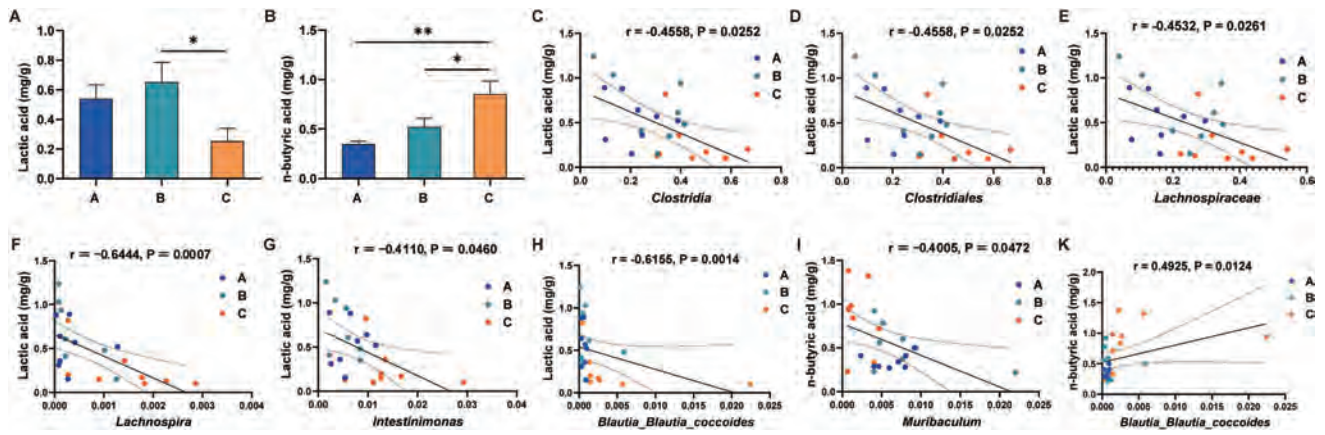


Fig. 7. Levels of SCFAs in the fecal samples and correlations between bacterial relative abundance and SCFAs

(A): Levels of lactic acid in fecal samples among the three groups (one-way ANOVA,  $F_{2,21} = 3.705, P = 0.0419$ ). One data of C group was under the limitation (0.05 mg/g). (B): Levels of n-butyric acid in the fecal samples among the three groups (one-way ANOVA,  $F_{2,22} = 7.366, P = 0.0036$ ). (C): There was a significant negative correlation between the relative abundance of the class *Clostridia* and lactic acid in the all groups. (D): There was a significant negative correlation between the relative abundance of the order *Clostridiales* and lactic acid in the all groups. (E): There was a significant negative correlation between the relative abundance of the family *Lachnospiraceae* and lactic acid in the all groups. (F): There was a significant negative correlation between the relative abundance of the genus *Lachnospira* and lactic acid in the all groups. (G): There was a significant negative correlation between the relative abundance of the genus *Intestinimonas* and lactic acid in the all groups. (H): There was a significant negative correlation between the relative abundance of the species *Blautia\_Blautia\_coccoides* and lactic acid in the all groups. (I): There was a significant negative correlation between the relative abundance of the genus *Muribaculum* and n-butyric acid the all three groups. (K): There was a significant positive correlation between the relative abundance of the species *Blautia\_Blautia\_coccoides* and n-butyric acid the all three groups. The values represent the mean  $\pm$  S.E.M. (n = 8 or 9). \* $P < 0.05$ ; \*\* $P < 0.01$ . A, control (no surgery) group; B, sham group; C, splenectomy group.

mechanisms underlying the abnormal composition of the gastrointestinal microbiota after splenectomy are currently unknown, it is likely that the abnormal composition of the gut microbiota and subsequent abnormalities in the levels of metabolites such as SCFAs may contribute to short- and long-term complications after splenectomy.

The spleen plays a major role in hematological and immunological functions (Lewis et al., 2019). Subjects lacking a spleen have impaired immune activity because this organ is responsible for producing antibodies and removing bacteria and aged, antibody-coated, and damaged blood cells (Weledji, 2014). Splenectomy is a surgical procedure that partially or completely removes the spleen to treat a wide variety of disorders such as splenic trauma, splenic abscess (e.g., tuberculous infection), neoplasm, and aneurysm of splenic arteries (Weledji, 2014). However, there are a number of serious complications in the early (i.e., atelectasis, pulmonary embolism, bleeding) and late periods (i.e., pulmonary tuberculous, overwhelming postoperative infection) (Cadili and de Gara, 2008; Weledji, 2014). A recent study using the database of the Taiwan National Health Insurance Program found that splenectomy is associated with pyogenic liver abscess (Lai et al., 2015) and acute pancreatitis (Lai et al., 2016). In addition, it is reported that splenectomy may ameliorate altered composition of gut microbiota in patients with liver cirrhosis (Liu et al., 2018) and that altered composition of gut microbiota in splenectomized patients were associated with plasma LPS levels (Zhu et al., 2018). It is suggested that the immunological role and structure of the spleen of humans may be quite different from those of rodents (Steiniger, 2015). Nonetheless, these studies suggest that splenectomy can affect the composition of gut microbiota in humans although it is unknown how splenectomy could affect levels of SCFAs. Collectively, splenectomy should be performed only after carefully assessing the short- and long-term risks and potential benefits to the patient. Given the key role of the spleen in the immune system and gut microbiota, the abnormal composition of the gut microbiota after splenectomy should be considered when assessing outcomes of splenectomized patients.

To understand the role of altered composition of gut microbiota after splenectomy, we examined the predictable function of gut microbiota using PICRUSt based on the 16rRNA gene sequence. According to the level 3 functional prediction map of KEGG pathway, the current data indicated that splenectomy may contribute to the altered metabolism induced by gut microbiota. Altered levels of SCFAs produced by gut microbes might be related with the functional prediction of the altered metabolism. It is shown that the production of SCFAs is regulated by the interaction among the environmental, host and microbiological factors (den Besten et al., 2013; Macfarlane and Macfarlane, 2003). Considering the relationship among the SCFAs, metabolism alteration and spleen, it is likely that SCFAs produced by gut microbiota can initiate and maintain the immune responses, which involved in the carbon metabolism (Bachem et al., 2019; Kim et al., 2016). Collectively, the KEGG pathways predicting the function of gut microbiota provide a functional view for the understanding the gut microbiota that makes a differential expression profile.

In conclusion, this study revealed that splenectomy induced abnormal changes in the gut microbiota in adult mice without causing depression-like phenotypes. The role of the brain–gut–microbiota and brain–spleen axes in splenectomized subjects should be considered.

## 5. Data availability statement

The data that support the findings of this study are available from the corresponding author upon reasonable request.

## Declaration of competing interest

All authors report no biomedical financial interests or potential conflicts of interest.

## Acknowledgements

Dr. Yan Wei was supported by the China Scholarship Council (China). Dr. Lijia Chang was supported by the Japan China Sasakawa Medical Fellowship (Tokyo, Japan). This study was supported by the National Natural Science Foundation of China (NSFC), China (to Y.W., 31701009) and Japan Agency for Medical Research and Development (AMED), Japan (to K.H., JP20dm0107119).

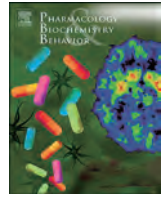
## References

- Bachem, A., Makhlof, C., Binger, K.J., de Souza, D.P., Tull, D., Hochheiser, K., Whitney, P.G., Fernandez-Ruiz, D., Dähling, S., Kastenmüller, W., Jönsson, J., Gressier, E., Lew, A.M., Perdomo, C., Kupz, A., Figgett, W., Mackay, F., Oleshansky, M., Russ, B.E., Parish, I.A., Kallies, A., McConville, M.J., Turner, S.J., Gebhardt, T., Bedoui, S., 2019. Microbiota derived short chain fatty acids promote the memory potential of antigen activated CD8<sup>+</sup> T Cells. *Immunity* 51, 285–297. <https://doi.org/10.1016/j.immuni.2019.06.002> e5.
- Bailey, M.T., Engler, H., Powell, N.D., Padgett, D.A., Sheridan, J.F., 2007. Repeated social defeat increases the bactericidal activity of splenic macrophages through a Toll-like receptor-dependent pathway. *Am. J. Physiol. Regul. Integr. Comp. Physiol.* 293, R1180–R1190. <https://doi.org/10.1152/ajpregu.00307.2007>.
- Breyner, N.M., Vilas Boas, P.B., Fernandes, G., de Carvalho, R.D., Rochat, T., Michel, M.L., Chain, F., Sokol, H., de Azevedo, M., Myiوشي, A., Azevedo, V.A., Langella, P., Barmudez-Humaran, L.G., Chatel, J.M., 2019. Oral delivery of pancreatitis-associated protein by *Lactococcus lactis* displays protective effects in dinitro-benzenesulfonic-acid-induced colitis model and is able to modulate the composition of the microbiota. *Environ. Microbiol.* 21, 4020–4031. <https://doi.org/10.1111/1462-2920.14748>.
- Bronte, V., Pittet, M.J., 2013. The spleen in local and systemic regulation of immunity. *Immunity* 39, 806–818. <https://doi.org/10.1016/j.immuni.2013.10.010>.
- Cadili, A., de Gara, C., 2008. Complications of splenectomy. *Am. J. Med.* 121, 371–375. <https://doi.org/10.1016/j.amjmed.2008.02.014>.
- Cathomas, F., Russo, S.J., 2020. Brain-spleen connection aids antibody production. *Nature* 581, 142–143. <https://doi.org/10.1038/d41586-020-01168-0>.
- Cerf-Bensussan, N., Gaboriau-Routhiau, V., 2010. The immune system and the gut microbiota: friends or foes? *Nat. Rev. Immunol.* 10, 735–744. <https://doi.org/10.1038/nri2850>.
- Chang, L., Zhang, K., Pu, Y., Qu, Y., Wang, S.M., Xiong, Z., Ren, Q., Dong, C., Fujita, Y., Hashimoto, K., 2019. Comparison of antidepressant and side effects in mice after intranasal administration of (R,S)-ketamine, (R)-ketamine, and (S)-ketamine. *Pharmacol. Biochem. Behav.* 181, 53–59. <https://doi.org/10.1016/j.pbb.2019.04.008>.
- Chen, J.J., He, S., Fang, L., Wang, B., Bai, S.J., Xie, J., Zhou, C.J., Wang, W., Xie, P., 2020. Age-specific differential changes on gut microbiota composition in patients with major depressive disorder. *Aging* 12, 2764–2776. <https://doi.org/10.18632/aging.102775>.
- Cryan, J.F., O'Riordan, K.J., Cowan, C.S.M., Sandhu, K.V., Bastiaansen, T.F.S., Boehme, M., Codagnone, M.G., Cusotto, S., Fulling, C., Golubeva, A.V., Guzzetta, K.E., Jaggard, M., Long-Smith, C.M., Lyte, J.M., Martin, J.A., Molinero-Perez, A., Moloney, G., Morelli, E., Morillas, E., O'Connor, R., Cruz-Pereira, J.S., Peterson, V.L., Rea, K., Ritz, N.L., Sherwin, E., Spichak, S., Teichman, E.M., van de Wouwe, M., Ventura-Silva, A.P., Wallace-Fitzsimons, S.E., Hyland, N., Clarke, G., Dinan, T.G., 2019. The microbiota-gut-brain axis. *Physiol. Rev.* 99, 1877–2013. <https://doi.org/10.1152/physrev.00018.2018>.
- Cusotto, S., Sandhu, K.V., Dinan, T.G., Cryan, J.F., 2018. The neuroendocrinology of the microbiota-gut-brain axis: a behavioural perspective. *Front. Neuroendocrinol.* 51, 80–101. <https://doi.org/10.1016/j.yfrne.2018.04.002>.
- Dalile, B., Van Oudenhove, L., Vervliet, B., Verbeke, K., 2019. The role of short-chain fatty acids in microbiota-gut-brain communication. *Nat. Rev. Gastroenterol. Hepatol.* 16, 461–478. <https://doi.org/10.1038/s41575-019-0157-3>.
- den Besten, G., van Eunen, K., Groen, A.K., Venema, K., Reijngoud, D.J., Bakker, B.M., 2013. The role of short chain fatty acids in the interplay between diet, gut microbiota, and host energy metabolism. *J. Lipid Res.* 54, 2325–2340. <https://doi.org/10.1194/jlr.R036012>.
- Dinan, T.G., Cryan, J.F., 2017. Brain-gut-microbiota axis and mental health. *Psychosom. Med.* 79, 920–926. <https://doi.org/10.1097/PSY.0000000000000519>.
- Duan, J., Meng, X., Liu, S., Zhou, P., Zeng, C., Fu, C., Dou, Q., Wu, A., Li, C., 2020. Gut microbiota composition associated with *Clostridium difficile*-Positive Diarrhea and *C. difficile* type in ICU patients. *Front. Cell. Infect. Microbiol.* 10, 190. <https://doi.org/10.3389/fcimb.2020.00190>.
- Fine, R.L., Mubiru, D.L., Krieger, M.A., 2020. Friend or foe? *Lactobacillus* in the context of autoimmune disease. *Adv. Immunol.* 146, 29–56. <https://doi.org/10.1016/bs.ai.2020.02.002>.
- Flux, M.C., Lowry, C.A., 2020. Finding intestinal fortitude: integrating the microbiome into a holistic view of depression mechanisms, treatment, and resilience. *Neurobiol. Dis.* 135, 104578. <https://doi.org/10.1016/j.nbd.2019.104578>.
- Fung, T.C., 2020. The microbiota-immune axis as a central mediator of gut-brain communication. *Neurobiol. Dis.* 136, 104714. <https://doi.org/10.1016/j.nbd.2019.104714>.
- Fung, T.C., Olson, C.A., Hsiao, E.Y., 2017. Interactions between the microbiota, immune and nervous systems in health and disease. *Nat. Neurosci.* 20, 145–155. <https://doi.org/10.1038/nn.4476>.



- Haile, M., Boutajangout, A., Chung, K., Chan, J., Stolper, T., Vincent, N., Batchan, M., D'Urso, J., Lin, Y., Kline, R., Yaghoor, F., Jahfal, S., Kamal, R., Aljohani, W., Blanck, T., Bekker, A., Wisniewski, T., 2016. The cox-2 inhibitor meloxicam ameliorates neuroinflammation and depressive behavior in adult mice after splenectomy. *J. Neurophysiol. Neurol. Disord.* 3, 101.
- Hashimoto, K., 2020. Molecular mechanisms of the rapid-acting and long-lasting antidepressant actions of (R)-ketamine. *Biochem. Pharmacol.* 177, 113935. <https://doi.org/10.1016/j.bcp.2020.113935>.
- Herp, S., Brugioux, S., Garzetti, D., Ring, D., Jochum, L.M., Beutler, M., Eberl, C., Hussain, S., Walter, S., Gerlach, R.G., Ruscheweyh, H.J., Huson, D., Sellin, M.E., Slack, E., Hanson, B., Loy, A., Baines, J.F., Rausch, P., Basic, M., Bleich, A., Berry, D., Stecher, B., 2019. *Mucispirillum schaedleri* antagonizes *Salmonella* Virulence to protect mice against colitis. *Cell Host Microbe* 25, 681–694. <https://doi.org/10.1016/j.chom.2019.03.004> e688.
- Jiang, H., Ling, Z., Zhang, Y., Mao, H., Ma, Z., Yin, Y., Wang, W., Tang, W., Tan, Z., Shi, J., Li, L., Ruan, B., 2015. Altered fecal microbiota composition in patients with major depressive disorder. *Brain Behav. Immun.* 48, 186–194. <https://doi.org/10.1016/j.bb.2015.03.016>.
- Jianguo, L., Xueyang, J., Cui, W., Changxin, W., Xuemei, Q., 2019. Altered gut metabolome contributes to depression-like behaviors in rats exposed to chronic unpredictable mild stress. *Transl. Psychiatry* 9, 40. <https://doi.org/10.1038/s41398-019-0391-z>.
- Kim, M., Qie, Y., Park, J., Kim, C.H., 2016. Gut microbial metabolites fuel host antibody responses. *Cell Host Microbe* 20, 202–214. <https://doi.org/10.1016/j.chom.2016.07.001>.
- Kuczynski, J., Stombaugh, J., Walters, W.A., González, A., Caporaso, J.G., Knight, R., 2012. Using QIIME to analyze 16S rRNA gene sequences from microbial communities. *Curr. Protoc. Microbiol.* 27. <https://doi.org/10.1002/9780471729259.mc01e05s27> (Chapter 1):Unit-1E.5.
- Kwak, M.S., Cha, J.M., Shin, H.P., Jeon, J.W., Yoon, J.Y., 2020. Development of a novel metagenomic biomarker for prediction of upper gastrointestinal tract involvement in patients with Crohn's disease. *Front. Microbiol.* 11, 1162. <https://doi.org/10.3389/fmicb.2020.01162>.
- Lai, S.W., Lai, H.C., Lin, C.L., Liao, K.F., 2015. Splenectomy correlates with increased risk of pyogenic liver abscess: a nationwide cohort study in Taiwan. *J. Epidemiol.* 25, 561–566. <https://doi.org/10.2188/jea.JE20140267>.
- Lai, S.W., Lin, C.L., Liao, K.F., 2016. Splenectomy correlates with increased risk of acute pancreatitis: a case-control study in Taiwan. *J. Epidemiol.* 26, 488–492. <https://doi.org/10.2188/jea.JE20150214>.
- Langille, M.G., Zaneveld, J., Caporaso, J.G., McDonald, D., Knights, D., Reyes, J.A., Clemente, J.C., Burkepile, D.E., Vega Thurber, R.L., Knight, R., Beiko, R.G., Huttenhower, C., 2013. Predictive functional profiling of microbial communities using 16S rRNA marker gene sequences. *Nat. Biotechnol.* 31, 814–821. <https://doi.org/10.1038/nbt.2676>.
- Lay, C., Rigottier-Gois, L., Holmstrom, K., Rajilic, M., Vaughan, E.E., de Vos, W.M., Collins, M.D., Thiel, R., Namsolleck, P., Blaut, M., Dore, J., 2005. Colonic microbiota signatures across five northern European countries. *Appl. Environ. Microbiol.* 71, 4153–4155. <https://doi.org/10.1128/AEM.71.7.4153-4155.2005>.
- Lewis, S.M., Williams, A., Eisenbarth, S.C., 2019. Structure and function of the immune system in the spleen. *Sci. Immunol.* 4, eaau6085 <https://doi.org/10.1126/sciimmunol.aau6085>.
- Lin, P., Ding, B., Feng, C., Yin, S., Zhang, T., Qi, X., Lv, H., Guo, X., Dong, K., Zhu, Y., Li, Q., 2017. *Prevotella* and *Klebsiella* proportions in fecal microbial communities are potential characteristic parameters for patients with major depressive disorder. *J. Affect. Disord.* 207, 300–304. <https://doi.org/10.1016/j.jad.2016.09.051>.
- Liu, R.T., Rowan-Nash, A.D., Sheehan, A.E., Walsh, R.F.L., Sanzari, C.M., Korry, B.J., Belenky, P., 2020. Reductions in anti-inflammatory gut bacteria are associated with depression in a sample of young adults. *Brain Behav. Immun.* 88, 308–324. <https://doi.org/10.1016/j.bb.2020.03.026>.
- Liu, Y., Li, J., Jin, Y., Zhao, L., Zhao, F., Feng, J., Li, A., Wei, Y., 2018. Splenectomy leads to amelioration of altered gut microbiota and metabolome in liver cirrhosis patients. *Front. Microbiol.* 9, 963. <https://doi.org/10.3389/fmicb.2018.00963>.
- Long-Smith, C., O'Riordan, K.J., Clarke, G., Stanton, C., Dinan, T.G., Cryan, J.F., 2020. Microbiota-gut-brain axis: new therapeutic opportunities. *Annu. Rev. Pharmacol. Toxicol.* 60, 477–502. <https://doi.org/10.1146/annurev-pharmtox-010919-023628>.
- Ma, X., Asif, H., Dai, L., He, Y., Zheng, W., Wang, D., Ren, H., Tang, J., Li, C., Jin, K., Li, Z., Chen, X., 2020. Alteration of the gut microbiome in first-episode drug-naive and chronic medicated schizophrenia correlate with regional brain volumes. *J. Psychiatr. Res.* 123, 136–144. <https://doi.org/10.1016/j.jpsychires.2020.02.005>.
- Macfarlane, S., Macfarlane, G.T., 2003. Regulation of short chain fatty acid production. *Proc. Nutr. Soc.* 62, 67–72. <https://doi.org/10.1079/PNS2002207>.
- McKim, D.B., Yin, W., Wang, Y., Cole, S.W., Godbout, J.P., Sheridan, J.F., 2018. Social stress mobilizes hematopoietic stem cells to establish persistent splenic myelopoiesis. *Cell Rep.* 25, 2552–2562. <https://doi.org/10.1016/j.celrep.2018.10.102> e2553.
- Mebius, R.E., Kraal, G., 2005. Structure and function of the spleen. *Nat. Rev. Immunol.* 5, 606–616. <https://doi.org/10.1038/nri1669>.
- Menghini, P., Corridoni, D., Butto, L.F., Osme, A., Shivaswamy, S., Lam, M., Bamias, G., Pizarro, T.T., Rodriguez-Palacios, A., Dinarello, C.A., Cominelli, F., 2019. Neutralization of IL-1 $\alpha$  ameliorates Crohn's disease-like ileitis by functional alterations of the gut microbiome. *Proc. Natl. Acad. Sci. U.S.A.* 116, 26717. <https://doi.org/10.1073/pnas.1915043116>.
- Mu, Q., Tavella, V.J., Luo, X.M., 2018. Role of *Lactobacillus reuteri* in human health and diseases. *Front. Microbiol.* 9, 757. <https://doi.org/10.3389/fmicb.2018.00757>.
- Nakajima, A., Sasaki, T., Itoh, K., Kitahara, T., Takema, Y., Hiramatsu, K., Ishikawa, D., Shibuya, T., Kobayashi, O., Osada, T., Watanabe, S., Nagahara, A., 2020. A soluble fiber diet increases *Bacteroides fragilis* group abundance and immunoglobulin A production in the gut. *Appl. Environ. Microbiol.* 86 <https://doi.org/10.1128/AEM.00405-20>.
- Parks, D.H., Tyson, G.W., Hugenholtz, P., Beiko, R.G., 2014. STAMP: statistical analysis of taxonomic and functional profiles. *Bioinformatics* 30, 3123–3124. <https://doi.org/10.1093/bioinformatics/btu494>.
- Powell, N.D., Bailey, M.T., Mays, J.W., Stiner-Jones, L.M., Hanke, M.L., Padgett, D.A., Sheridan, J.F., 2009. Repeated social defeat activates dendritic cells and enhances Toll-like receptor dependent cytokine secretion. *Brain Behav. Immun.* 23, 225–231. <https://doi.org/10.1016/j.bbi.2008.09.010>.
- Ren, Z., You, W., Wu, S., Poetsch, A., Xu, C., 2019. Secretomic analyses of *Ruminiclostridium papyrosolvans* reveal its enzymatic basis for lignocellulose degradation. *Biotechnol. Biofuels* 12, 183. <https://doi.org/10.1186/s13068-019-1522-8>.
- Rhoads, J.M., Collins, J., Fatheree, N.Y., Hashmi, S.S., Taylor, C.M., Luo, M., Hoang, T.K., Gleason, W.A., Van Arsdall, M.R., Navarro, F., Liu, Y., 2018. Infant colic represents gut inflammation and dysbiosis. *J. Pediatr.* 203, 55–61. <https://doi.org/10.1016/j.jpeds.2018.07.042> e53.
- Round, J.L., Mazmanian, S.K., 2009. The gut microbiota shapes intestinal immune responses during health and disease. *Nat. Rev. Immunol.* 9, 313–323. <https://doi.org/10.1038/nri2515>.
- Segata, N., Izard, J., Waldron, L., Gevers, D., Miropolsky, L., Garrett, W.S., Huttenhower, C., 2011. Metagenomic biomarker discovery and explanation. *Genome Biol.* 12, R60. <https://doi.org/10.1186/gb-2011-12-6-r60>.
- Silva, Y.P., Bernardi, A., Frozza, R.L., 2020. The role of short-chain fatty acids from gut microbiota in gut-brain communication. *Front. Endocrinol.* 11, 25. <https://doi.org/10.3389/fendo.2020.00025>.
- Steiniger, B.S., 2015. Human spleen microanatomy: why mice do not suffice. *Immunology* 145, 334–346. <https://doi.org/10.1111/imm.12469>.
- Szyszkowicz, J.K., Wong, A., Anisman, H., Merali, Z., Audet, M.C., 2017. Implications of the gut microbiota in vulnerability to the social avoidance effects of chronic social defeat in male mice. *Brain Behav. Immun.* 66, 45–55. <https://doi.org/10.1016/j.bbi.2017.06.009>.
- Tian, T., Xu, B., Qin, Y., Fan, L., Chen, J., Zheng, P., Gong, X., Wang, H., Bai, M., Pu, J., Lu, J., Zhou, W., Zhao, L., Yang, D., Xie, P., 2019. *Clostridium butyricum* miyairi 588 has preventive effects on chronic social defeat stress-induced depressive-like behaviour and modulates microglial activation in mice. *Biochem. Biophys. Res. Commun.* 516, 430–436. <https://doi.org/10.1016/j.bbrc.2019.06.053>.
- Wang, S., Ishima, T., Zhang, J., Qu, Y., Chang, L., Pu, Y., Fujita, Y., Tan, Y., Wang, X., Hashimoto, K., 2020a. Ingestion of *Lactobacillus intestinalis* and *Lactobacillus reuteri* causes depression- and anhedonia-like phenotypes in antibiotic-treated mice via the vagus nerve. *J. Neuroinflammation* 17, 241. <https://doi.org/10.1186/s12974-020-01916-z>.
- Wang, S., Qu, Y., Chang, L., Pu, Y., Zhang, K., Hashimoto, K., 2020b. Antibiotic-induced microbiome depletion is associated with resilience in mice after chronic social defeat stress. *J. Affect. Disord.* 260, 448–457. <https://doi.org/10.1016/j.jad.2019.09.064>.
- Weledji, E.P., 2014. Benefits and risks of splenectomy. *Int. J. Surg.* 12, 113–119. <https://doi.org/10.1016/j.ijsu.2013.11.017>.
- Whalley, K., 2020. Brain-spleen link tunes immunity. *Nat. Rev. Immunol.* 20, 406–407. <https://doi.org/10.1038/s41577-020-0347-9>.
- Wong, M.L., Insera, A., Lewis, M.D., Mastrorandi, C.A., Leong, L., Choo, J., Kentish, S., Xie, P., Morrison, M., Wesselingh, S.L., Rogers, G.B., Licinio, J., 2016. Inflammation signaling affects anxiety- and depressive-like behavior and gut microbiome composition. *Mol. Psychiatr.* 21, 797–805. <https://doi.org/10.1038/mp.2016.46>.
- Wu, M., Tian, T., Mao, Q., Zou, T., Zhou, C.J., Xie, J., Chen, J.J., 2020. Associations between disordered gut microbiota and changes of neurotransmitters and short-chain fatty acids in depressed mice. *Transl. Psychiatry* 10, 350. <https://doi.org/10.1038/s41398-020-01038-3>.
- Xia, Y., Sun, J., 2017. Hypothesis testing and statistical analysis of microbiome. *Genes Dis* 4, 138–148. <https://doi.org/10.1016/j.gendis.2017.06.001>.
- Xu, D., Zhang, Y., Xie, B., Yao, H., Yuan, Y., Yuan, S., Zhang, J., 2020a. The spleen mediates chronic sleep restriction-mediated enhancement of LPS-induced neuroinflammation, cognitive deficits, and anxiety-like behavior. *Aging* 12. <https://doi.org/10.18632/aging.103659>, 2020 Aug 3.
- Xu, R., Wu, B., Liang, J., He, F., Gu, W., Li, K., Luo, Y., Chen, J., Gao, Y., Wu, Z., Wang, Y., Zhou, W., Wang, M., 2020b. Altered gut microbiota and mucosal immunity in patients with schizophrenia. *Brain Behav. Immun.* 85, 120–127. <https://doi.org/10.1016/j.bbi.2019.06.039>.
- Yang, B., Ren, Q., Zhang, J.C., Chen, Q.X., Hashimoto, K., 2017a. Altered expression of BDNF, BDNF pro-peptide and their precursor proBDNF in brain and liver tissues from psychiatric disorders: rethinking the brain-liver axis. *Transl. Psychiatry* 7, e1128. <https://doi.org/10.1038/tp.2017.95>.
- Yang, C., Fang, X., Zhan, G., Huang, N., Li, S., Bi, J., Jiang, R., Yang, L., Miao, L., Zhu, B., Luo, A., Hashimoto, K., 2019. Key role of gut microbiota in anhedonia-like phenotype in rodents with neuropathic pain. *Transl. Psychiatry* 9, 57. <https://doi.org/10.1038/s41398-019-0379-8>.
- Yang, C., Fujita, Y., Ren, Q., Ma, M., Dong, C., Hashimoto, K., 2017b. *Bifidobacterium* in the gut microbiota confer resilience to chronic social defeat stress in mice. *Sci. Rep.* 7, 45942. <https://doi.org/10.1038/srep45942>.
- Zhang, J., Chang, L., Pu, Y., Hashimoto, K., 2020a. Abnormal expression of colony stimulating factor 1 receptor (CSF1R) and transcription factor PU.1 (SPI1) in the spleen from patients with major psychiatric disorders: a role of brain-spleen axis. *J. Affect. Disord.* 272, 110–115. <https://doi.org/10.1016/j.jad.2020.03.128>.
- Zhang, J., Ma, L., Chang, L., Pu, Y., Qu, Y., Hashimoto, K., 2020b. A key role of the subdiaphragmatic vagus nerve in the depression-like phenotype and abnormal composition of gut microbiota in mice after lipopolysaccharide administration. *Transl. Psychiatry* 10, 186. <https://doi.org/10.1038/s41398-020-00878-3>.

- Zhang, K., Fujita, Y., Chang, L., Qu, Y., Pu, Y., Wang, S., Shirayama, Y., Hashimoto, K., 2019a. Abnormal composition of gut microbiota is associated with resilience versus susceptibility to inescapable electric stress. *Transl. Psychiatry* 9, 231. <https://doi.org/10.1038/s41398-019-0571-x>.
- Zhang, K., et al., 2019b. Splenic NKG2D confers resilience versus susceptibility in mice after chronic social defeat stress: beneficial effects of (R)-ketamine. *Eur. Arch. Psychiatr. Clin. Neurosci.* <https://doi.org/10.1007/s00406-019-01092-z>.
- Zhang, X., Lei, B., Yuan, Y., Zhang, L., Hu, L., Jin, S., Kang, B., Liao, X., Sun, W., Xu, F., Zhong, Y., Hu, J., Qi, H., 2020c. Brain control of humoral immune responses amenable to behavioural modulation. *Nature* 581, 204–208. <https://doi.org/10.1038/s41586-020-2235-7>.
- Zheng, P., Zeng, B., Liu, M., Chen, J., Pan, J., Han, Y., Liu, Y., Cheng, K., Zhou, C., Wang, H., Zhou, X., Gui, S., Perry, S.W., Wong, M., Licinio, J., Wei, H., Xie, P., 2019. The gut microbiome from patients with schizophrenia modulates the glutamate-glutamine-GABA cycle and schizophrenia-relevant behaviors in mice. *Sci. Adv.* 5, eaau8317. <https://doi.org/10.1126/sciadv.aau8317>.
- Zheng, P., Zeng, B., Zhou, C., Liu, M., Fang, Z., Xu, X., Zeng, L., Chen, J., Fan, S., Du, X., Zhang, X., Yang, D., Yang, Y., Meng, H., Li, W., Melgiri, N.D., Licinio, J., Wei, H., Xie, P., 2016. Gut microbiome remodeling induces depressive-like behaviors through a pathway mediated by the host's metabolism. *Mol. Psychiatr.* 21, 786–796. <https://doi.org/10.1038/mp.2016.44>.
- Zhu, F., Guo, R., Wang, W., Ju, Y., Wang, Q., Ma, Q., Sun, Q., Fan, Y., Xie, Y., Yang, Z., Jie, Z., Zhao, B., Xiao, L., Yang, L., Zhang, T., Liu, B., Guo, L., He, X., Chen, Y., Chen, C., Gao, C., Xu, X., Yang, H., Wang, J., Dang, Y., Madsen, L., Brix, S., Kristiansen, K., Jia, H., Ma, X., 2020a. Transplantation of microbiota from drug-free patients with schizophrenia causes schizophrenia-like abnormal behaviors and dysregulated kynurenine metabolism in mice. *Mol. Psychiatry* 25, 2905–2918. <https://doi.org/10.1038/s41380-019-0475-4>.
- Zhu, F., Ju, Y., Wang, W., Wang, Q., Guo, R., Ma, Q., Sun, Q., Fan, Y., Xie, Y., Yang, Z., Jie, Z., Zhao, B., Xiao, L., Yang, L., Zhang, T., Feng, J., Guo, L., He, X., Chen, Y., Chen, C., Gao, C., Xu, X., Yang, H., Wang, J., Dang, Y., Madsen, L., Brix, S., Kristiansen, K., Jia, H., Ma, X., 2020b. Metagenome-wide association of gut microbiome features for schizophrenia. *Nat. Commun.* 11, 1612. <https://doi.org/10.1038/s41467-020-15457-9>.
- Zhu, H., Liu, Y., Li, S., Jin, Y., Zhao, L., Zhao, F., Feng, J., Yan, W., Wei, Y., 2018. Altered gut microbiota after traumatic splenectomy is associated with endotoxemia. *Emerg. Microb. Infect.* 7, 197. <https://doi.org/10.1038/s41426-018-0202-2>.



## Review

## A historical review of antidepressant effects of ketamine and its enantiomers

Yan Wei<sup>a,b</sup>, Lijia Chang<sup>a</sup>, Kenji Hashimoto<sup>a,\*</sup><sup>a</sup> Division of Clinical Neuroscience, Chiba University Center for Forensic Mental Health, Chiba 260-8670, Japan<sup>b</sup> Key Laboratory of Medical Electrophysiology of Ministry of Education and Medical Electrophysiological Key Laboratory of Sichuan Province, Collaborative Innovation Center for Prevention and Treatment of Cardiovascular Disease, Institute of Cardiovascular Research, Southwest Medical University, Luzhou 646000, Sichuan, China.

## ARTICLE INFO

## Keywords:

Antidepressant  
Arketamine  
Enantiomer  
Esketamine  
Ketamine

## ABSTRACT

The robust antidepressant effects of (*R,S*)-ketamine are among the most important discoveries in mood research over the last half century. Off-label use of (*R,S*)-ketamine, which is an equal mixture of (*R*)-ketamine and (*S*)-ketamine, has become especially popular in the United States (US) for treatment-resistant depression. On March 5, 2019, the US Food and Drug Administration approved an (*S*)-ketamine nasal spray for use in treatment-resistant depression, though its use has been limited to certified medical offices or clinics. On December 19, 2019, (*S*)-ketamine nasal spray was approved for the same indication in Europe. However, despite its potential for benefit, there are several concerns about the efficacy of (*S*)-ketamine nasal spray. Accumulating evidence from preclinical studies show that (*R*)-ketamine has greater potency and longer lasting antidepressant effects than (*S*)-ketamine in animal models of depression, and that (*R*)-ketamine has fewer detrimental side effects than either (*R,S*)-ketamine or (*S*)-ketamine. As such, clinical studies of (*R*)-ketamine in humans are now underway by Perception Neuroscience Ltd. In this article, we review the brief history of (*R,S*)-ketamine and its two enantiomers as novel antidepressants. We also discuss the mechanisms of ketamine's antidepressant actions.

## 1. Introduction

More than 300 million people of all ages suffer from depression, which is a major contributor to the overall global burden of disease (WHO, 2017). Approximately one-third of depressed patients have a treatment-resistant form of depression after trialing typical antidepressants such as selective serotonin reuptake inhibitors (SSRIs) and serotonin and norepinephrine reuptake inhibitors (SNRIs). Moreover, these antidepressants have proven ineffective in the treatment of suicide ideation in patients with severe depression. Novel therapeutic agents are therefore required to meet these unmet needs. In recent decades, (*R,S*)-ketamine (Fig. 1) has come to the attention of neuroscientists and psychiatrists worldwide because it produces robust antidepressant effects in patients with treatment-resistant depression (Duman, 2018; Gould et al., 2019; Hashimoto, 2016a; Hashimoto, 2016b; Hashimoto, 2017; Hashimoto, 2019a; Krystal et al., 2019; Murrough et al., 2017; Witkin et al., 2018; Zhang and Hashimoto, 2019b).

In this article, we offer a review of the brief history of (*R,S*)-ketamine and its two enantiomers as novel antidepressants. Furthermore, we discuss the mechanisms of action for ketamine's antidepressant effects.

## 2. Brief history of ketamine

The discovery of ketamine's antidepressant effects is among the most important discoveries of the last half century. Not originally developed as an antidepressant, it took a long and fascinating journey for clinicians and researchers to discover its rapid-acting antidepressant effects (Fig. 2). The history of ketamine can be traced back to 1956 when phencyclidine (PCP) was first synthesized as a general anesthetic by the pharmaceutical company Parke-Davis (Maddox et al., 1965). It had an inhibitory constant (*K<sub>i</sub>*) of 0.06 μM at the *N*-methyl-D-aspartate receptor (NMDAR) (Fig. 1) (Domino and Luby, 2012; Mion, 2017). However, subsequent studies in humans revealed that PCP could cause a high rate of side effects, including hallucinations, postoperative delirium, and confusion (Bush, 2013; Domino and Luby, 2012; Hoiseth et al., 2005), resulting in its medical use in humans being terminated in 1965 (Morris and Wallach, 2014).

In efforts to identify an alternative to PCP without the serious psychotomimetic side effects, but that retained the excellent anesthetic effects (Mion, 2017), the original form of ketamine (CI-581) was synthesized as short half-life derivative of PCP by Parke-Davis (Fig. 2) (Domino, 2010). In 1964, Dr., Edward Domino and Dr. Guenter Corsen performed the first study of the anesthetic effects of CI-581 in healthy prisoners (Domino, 2010). Shortly thereafter, in 1965, ketamine was

\* Corresponding author.

E-mail address: [hashimoto@faculty.chiba-u.jp](mailto:hashimoto@faculty.chiba-u.jp) (K. Hashimoto).<https://doi.org/10.1016/j.pbb.2020.172870>

Received 15 January 2020; Received in revised form 30 January 2020; Accepted 4 February 2020

Available online 05 February 2020

0091-3057/ © 2020 The Authors. Published by Elsevier Inc. This is an open access article under the CC BY license

(http://creativecommons.org/licenses/by/4.0/).

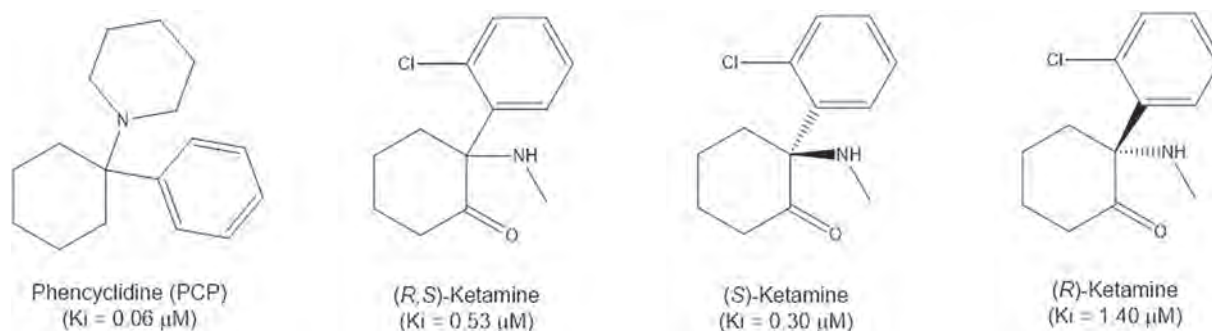


Fig. 1. Chemical structure of phencyclidine (PCP), (R,S)-ketamine and its enantiomers. Ki values for NMDAR are presented in parenthesis (Ebert et al., 1997).

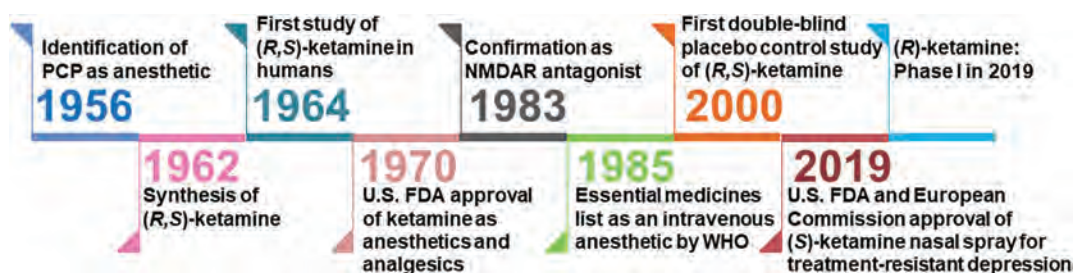


Fig. 2. Brief history of (R,S)-ketamine and two enantiomers from anesthetic to antidepressant.

confirmed to be an effective analgesic and anesthetic (Domino et al., 1965). In the first clinical study of ketamine among 130 patients who underwent surgical procedures it was reported to induce a unique state of altered consciousness, described as being disconnected (Corssen and Domino, 1966). Ketamine was later approved in 1970 for anesthetic use by the US Food Drug Administration (FDA) (Fig. 2) (Dong et al., 2015; Mion, 2017; Stevenson, 2005). However, due to its euphoric effects, ketamine became a popular recreational drug in the US and Europe in subsequent decades (Lankenau, 2016; Wolff, 2016). Ketamine remains a commonly abused illicit drug worldwide (Y. Liu et al., 2016).

Contemporaneous reports since the 1970s have shown that ketamine hydrochloride (Ketalar<sup>®</sup>) received much attention, with researchers exploring its pharmacokinetics and mechanism of anesthetic and analgesic action for therapeutic purposes (Li and Vlissides, 2016; Lodge and Mercier, 2015; Tyler et al., 2017). As part of this history, it is worth noting that ketamine was shown to be an NMDAR antagonist in 1983 (Fig. 2) (Anis et al., 1983). Given ketamine's unique properties in pain relief and sedation (Gao et al., 2016), ketamine was added to the WHO's essential medicines list as an intravenous anesthetic in 1985 (Fig. 2) (Gowda et al., 2016; WHO, 2011). Although it has now been used for more than 50 years, not only as an anesthetic and analgesic agent but also as a drug of abuse, its use remains limited due to its undesirable psychotomimetic effects.

### 3. Antidepressant-like effects of (R,S)-ketamine and NMDAR antagonists in rodents

In 1975, (R,S)-ketamine was reported to show antidepressant-like effects in animal models. For example, it was associated with the reversal of tetrabenazine-induced ptosis in mice, reversal of reserpine-induced hypothermia in rats, enhancement of yohimbine toxicity in mice, and inhibition of oxotremorine-induced tremors in mice (Sofia and Harakal, 1975). In these models, however, the antidepressant-like activity of ketamine was substantially less than that of imipramine (Sofia and Harakal, 1975).

As already mentioned, ketamine was identified to be an NMDAR antagonist in 1983 (Fig. 2) (Anis et al., 1983). In 1990 it was reported that NMDAR antagonists like AP-7 and (+)-MK-801 had

antidepressant-like effects in rodents (Trullas and Skolnick, 1990). In a chronic mild stress model, (+)-MK-801 showed anti-anhedonia-like effects in rats (Papp and Moryl, 1993). Several animal studies soon documented that NMDAR antagonists, such as MK-801, CGP 37849, and eliprodil, may have the antidepressant-like effects in animal model of depression (Autry et al., 2011; Layer et al., 1995; Maj et al., 1992; Meloni et al., 1993; Papp and Moryl, 1994; Petrie et al., 2000; Skolnick et al., 1996; Wedzony et al., 1995; B. Yang et al., 2016). Importantly, (+)-MK-801 did not show ketamine-like long-lasting antidepressant effects in susceptible mice after chronic social defeat stress (CSDS), but it did produce rapid-acting antidepressant effects in CSDS-susceptible mice (B. Yang et al., 2016). Thus, available evidence indicated that NMDAR antagonists could alleviate depression-like behaviors in rodents, which led to several pharmaceutical companies developing NMDAR antagonists as novel antidepressants (Hashimoto, 2019a).

In a shock-induced depression model, Chaturvedi et al. (1999) reported that the antidepressant effects of (R,S)-ketamine at the dose of 5 and 10 mg/kg respectively significantly increased ambulation and rearing in the open field test and attenuated the increased immobility time in forced swimming test. In a rat learned helplessness (LH) model, Koike et al. (2011) reported that (R,S)-ketamine (10 mg/kg) exerted rapid antidepressant-like effects that were sustained for at least 72 h after a single dose. In a model of chronic unpredictable mild stress (CUMS), a single dose of (R,S)-ketamine (10 mg/kg) elicited rapid-onset persistent antidepressant effects in rodents (W.X. Liu et al., 2016; Ma et al., 2013; Sun et al., 2016). Comparable to tropomyosin receptor kinase B (TrkB) agonists and antagonists (7,8-dihydroxyflavone and ANA-12, respectively), it was reported that (R,S)-ketamine showed rapid-acting and longer lasting antidepressant effects in CSDS-susceptible mice (Zhang et al., 2015). It also showed antidepressant-like effects of (R,S)-ketamine in inflammation-induced depression models (Huang et al., 2019; Lindqvist et al., 2017; Remus and Dantzer, 2016; Yamaguchi et al., 2018; Zhang et al., 2016; Zhang and Hashimoto, 2019b).

Unfortunately, the potential psychotomimetic and other unwanted side effects of (R,S)-ketamine have also been well-documented in rodents. These include hyperlocomotion, prepulse inhibition (PPI) deficits, conditioned place preference, schizophrenia-like psychotic

symptoms, and cognitive deficits (Becker and Grecksch, 2004; Chan et al., 2013; Chang et al., 2019; Giorgetti et al., 2015; Imre et al., 2006; Lahti et al., 1995; Yang et al., 2015). These have limited interest in its use in humans.

#### 4. Brief history of (R,S)-ketamine's antidepressant effects in humans

The discovery of (R,S)-ketamine's antidepressant effects in humans began in the 1970s (Fig. 2). As described in Edward Domino's review article, some PCP (or ketamine) abusers had used (R,S)-ketamine to improve depressive symptoms rapidly when usual antidepressants were not effective (Domino, 2010). However, he conducted no further study because of concerns that PCP and (R,S)-ketamine were illicit drugs (Domino, 2010). It was therefore a major advancement when (R,S)-ketamine's antidepressant effects were later acknowledged and the agent was introduced for the treatment of severe depression. Berman et al. (2000) had already demonstrated the rapid-acting and sustained antidepressant effects of (R,S)-ketamine in patients with depression, and these findings were replicated by Zarate Jr. et al. (2006) in treatment-resistant patients with major depressive disorder (MDD). Since then, many studies have confirmed the antidepressant effects of (R,S)-ketamine for treatment-resistant patients with MDD, bipolar disorder, and suicidal ideation (Bobo et al., 2016; Grunebaum et al., 2018; Kishimoto et al., 2016; Murrugh et al., 2013; Newport et al., 2015; Singh et al., 2016b).

In clinical trials, interventional studies have sought to evaluate the beneficial effects of (R,S)-ketamine. Several randomized single- and double-blind placebo- or drug-controlled studies have replicated the antidepressant effects of (R,S)-ketamine in both MDD and bipolar disorder, even after a single intravenous dose of 0.5 mg/kg (Berman et al., 2000; Zarate Jr. et al., 2006). Another cross-over double-blind study indicated that many patients with treatment-resistant bipolar disorder (71%) showed significant improvements (Diazgranados et al., 2010). Zarate Jr. et al. (2012) also evidenced that depressive symptoms and suicidal ideation improved within 40 min of patients with bipolar disorder receiving a single infusion of (R,S)-ketamine. Furthermore, in a dose-ranging trial of intravenous (R,S)-ketamine, Fava et al. (2018) suggested that there was evidence to support the validity of single dose therapy at either 0.5 mg/kg or 1.0 mg/kg in patients with treatment-resistant depression.

In two midazolam-controlled randomized clinical trials, (R,S)-ketamine caused rapid reductions in suicidal ideation and depressive symptoms within 24 h (Grunebaum et al., 2018; Murrugh et al., 2013). Moreover, (R,S)-ketamine was shown to have potent anti-suicidal effects in depressed patients with suicidal ideation (Bartoli et al., 2017; Reinstatler and Youssef, 2015; Wilkinson et al., 2018). These studies indicate that (R,S)-ketamine is a promising antidepressant for the treatment of severe depressed patients with suicide ideation.

Repeated ketamine infusion is important for maintenance therapy in patients with treatment-resistant depression (Phillips et al., 2019; Strong and Kabbaj, 2018). In a double-blind, randomized, placebo-controlled study, Singh et al., 2016b suggested that twice- or thrice-weekly administration of (R,S)-ketamine (0.5 mg/kg) was sufficient to maintain antidepressant efficacy over 15 days in patients with treatment-resistant depression. At present, there is a lack of long-term data on the long-term safety and efficacy of (R,S)-ketamine for patients with treatment-resistant depression. This is important given the potential for severe side effects.

#### 5. Antidepressant-like effects of ketamine enantiomers in rodents

(R,S)-ketamine ( $K_i = 0.53 \mu\text{M}$  for NMDAR) comprises a racemic mixture of (R)-ketamine ( $K_i = 1.4 \mu\text{M}$  for NMDAR) and (S)-ketamine ( $K_i = 0.30 \mu\text{M}$  for NMDAR) in equal measure (Fig. 1) (Ebert et al., 1997). In 2014, Zhang et al. (2014) first reported that (R)-ketamine had

greater potency and longer lasting antidepressant effects than (S)-ketamine in a neonatal dexamethasone-treated model of depression. In 2015, they further reported that (R)-ketamine had greater potency and longer lasting antidepressant effects than (S)-ketamine in CSDS and LH models of depression (Yang et al., 2015). Subsequently, the superiority of (R)-ketamine over (S)-ketamine was reported in rodents (Chang et al., 2019; Fukumoto et al., 2017; Zanos et al., 2016). Importantly, (R)-ketamine also has fewer detrimental side effects than either (R,S)-ketamine or (S)-ketamine in rodents and monkey (Chang et al., 2019; Fukumoto et al., 2017; Hashimoto, 2017; Hashimoto et al., 2017; Tian et al., 2018a; Yang et al., 2015; B. Yang et al., 2016a; C. Yang et al., 2016). However, in 2019, Masaki et al. (2019) demonstrated that the functional MRI (fMRI) responses in the brains of conscious rats after a single injection of (S)-ketamine, (R,S)-ketamine, or (+)-MK-801 were different from the fMRI responses after a single injection of (R)-ketamine. Their results indicated that NMDAR inhibition was unlikely to play a role in the pharmacological effects of (R)-ketamine in rat brains (Masaki et al., 2019).

#### 6. Antidepressant-like effects of ketamine metabolites in rodents

In 2016, a group led by Dr. Todd Gould (University of Maryland) reported that the metabolism of (R,S)-ketamine to (2R,6R)-hydroxynorketamine (HNK) (Fig. 3) was essential for the antidepressant-like effects of the parent compound in rodents (Zanos et al., 2016). Although (2R,6R)-HNK is a minor metabolite of (R)-ketamine, the dose necessary to achieve antidepressant-like effects was similar to that for (R,S)-ketamine (Zanos et al., 2016). Unfortunately, our group was unable to replicate the antidepressant-like effects of (2R,6R)-HNK in rodents with depression-like phenotypes (Chaki, 2018; Chang et al., 2018; Hashimoto and Shirayama, 2018; Shirayama and Hashimoto, 2018; Xiong et al., 2019; Yamaguchi et al., 2018; Zhang et al., 2018b; Zhang et al., 2018c).

In a study using cytochrome P450 inhibitors, it was shown that metabolism to (2R,6R)-HNK was unnecessary for the antidepressant-like effects of (R)-ketamine, and that (R)-ketamine itself may be responsible for the observed antidepressant-like actions (Yamaguchi et al., 2018). Clinical study of (2R,6R)-HNK in humans is to be started by the US National Institute of Mental Health. A double-blind randomized study of (R)-ketamine versus (2R,6R)-HNK would be of great interest in depressed patients.

Finally, (S)-ketamine is metabolized to (S)-norketamine (Fig. 3). In 2018, Yang et al. (2018a) reported that (S)-norketamine produced rapid and sustained antidepressant-like effects in a CSDS model. Importantly, unlike to (S)-ketamine, (S)-norketamine did not produce the expected side effects in rodents (Yang et al., 2018a). Therefore, (S)-norketamine could be an alternative to (S)-ketamine, potentially offering antidepressant efficacy with fewer side effects (Hashimoto, 2019a; Hashimoto, 2019b; Hashimoto and Yang, 2018).

#### 7. Effects of ketamine enantiomers in humans

Vollenweider et al. (1997) reported on the psychological state and cerebral glucose metabolism produced after injecting either (S)-ketamine or (R)-ketamine. Although (S)-ketamine produced psychotic reactions, including depersonalization and hallucinations, (R)-ketamine did not produce any psychotic symptoms in the same subjects at the same dose (Vollenweider et al., 1997). Positron emission tomography showed that (S)-ketamine led to markedly increased glucose utilization in the frontal cortex and thalamus, whereas (R)-ketamine suppressed glucose metabolism in several brain areas (Vollenweider et al., 1997). Collectively, these results suggested that (S)-ketamine contributed to the acute side effects of ketamine, whereas (R)-ketamine may be free of these side effects (Hashimoto, 2019a; Zanos et al., 2018).

In the US, Janssen Pharmaceutical developed (S)-ketamine nasal spray for use in treatment-resistant depression. This was based on the

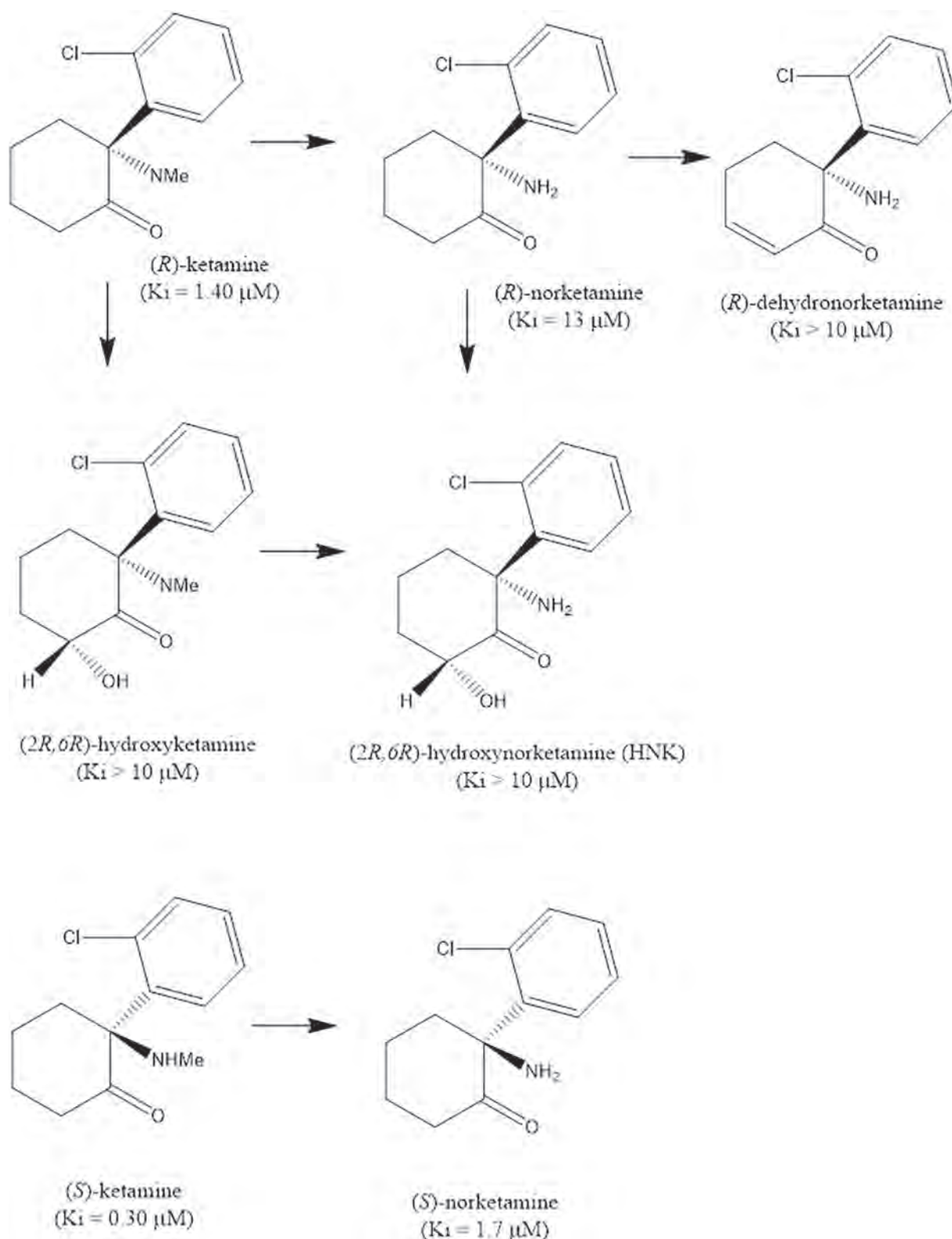


**Fig. 3.** Chemical structure of metabolites (2R,6R)-HNK and (S)-norketamine of (R)-ketamine and (S)-ketamine.  $K_i$  values for NMDAR are presented in parenthesis (Ebert et al., 1997; Zanos et al., 2016).

results of a double-blind, multicenter, randomized, placebo-controlled trial (Singh et al., 2016a) in which it was reported that (S)-ketamine (0.2 and 0.40 mg/kg by intravenous infusion) showed a rapid and robust antidepressant effect (within 2 h) in patients with treatment-resistant depression. The most common treatment-emergent adverse

events were headache, nausea, and dissociation (Singh et al., 2016a). A recent head-to-head study of (S)-ketamine (0.25 mg/kg by intravenous infusion) and (R,S)-ketamine (0.5 mg/kg by intravenous infusion) demonstrated that (S)-ketamine produced similar antidepressant effects to those of (R,S)-ketamine in treatment-resistant patients with depression

(Correia-Melo et al., 2019), indicating the non-inferiority of (S)-ketamine (0.25 mg/kg) to (R,S)-ketamine (0.5 mg/kg) 24 h after a single infusion. Interestingly, however, the antidepressant effects of (R,S)-ketamine (0.5 mg/kg) by 7 days after a single injection were more potent than for (S)-ketamine, albeit without statistical significance ( $P = 0.08$ ) (Correia-Melo et al., 2019). In contrast, based on the pre-clinical findings (Yang et al., 2015; Yang et al., 2018a; Zhang et al., 2014), it is likely that (R)-ketamine plays a role in the long-lasting antidepressant effects of (R,S)-ketamine. Double-blind, randomized trials of (R)-ketamine versus (S)-ketamine are therefore urgently needed to assess their relative efficacies in patients with depression.

Only two of the five phase III trials performed by Janssen Pharmaceutical showed positive results for (S)-ketamine. Nevertheless, on March 5, 2019, the US FDA approved the use of (S)-ketamine nasal spray (esketamine) for treatment-resistant depression in conjunction with an oral antidepressant (Fig. 2). Because of the risk of serious adverse effects, it is only available through a restricted distribution system, under the Risk Evaluation and Mitigation Strategy. On December 19, 2019, (S)-ketamine nasal spray was approved for use in treatment-resistant depression in Europe (Fig. 2) (Mahase, 2019). However, there are many concerns about the efficacy of esketamine nasal spray (Kaur et al., 2019; Turner, 2019; Zimmermann et al., 2020).

A recent pilot study in Brazil demonstrated that intravenous infusion of (R)-ketamine (0.5 mg/kg for 40-min) elicited rapid-acting and sustained antidepressant actions in treatment-resistant patients with MDD, and that side effects such as dissociation were low (Leal et al., 2020). At present, a clinical trial of (R)-ketamine by Perception Neuroscience Ltd. is underway for use in depressed patients (Hashimoto, 2019a).

## 8. Mechanisms of ketamine's antidepressant actions

### 8.1. NMDAR inhibition and AMPAR activation

It is widely acknowledged that the rapid antidepressant actions of ketamine occur via blockade of NMDARs located at inhibitory interneurons. This blockade causes the disinhibition of pyramidal cells that result in a burst of glutamatergic transmission (Duman, 2018; Krystal et al., 2019). Subsequently, activation of the AMPAR ( $\alpha$ -amino-3-hydroxy-5-methyl-4-isoxazolepropionic acid receptor) is required for ketamine's antidepressant effects. This was demonstrated by research showing that pretreatment with an AMPAR antagonist blocked ketamine's antidepressant effects in rodents (Maeng et al., 2008). In addition, the role of AMPAR activation in the antidepressant effects of ketamine and its two enantiomers has been replicated (Autry et al., 2011; Yang et al., 2015).

Unfortunately, other NMDAR antagonists (e.g., memantine, lanicemine, rapastinel, and AV-101) do not show ketamine-like robust antidepressant actions in patients with depression (Hashimoto, 2019a; Kishimoto et al., 2016; Newport et al., 2015; Sanacora et al., 2017; Yang et al., 2019b; Zarate Jr. et al., 2006). Preclinical data using the two ketamine enantiomers has indicated that NMDAR inhibition may not be central to the antidepressant effects of ketamine in rodents (Hashimoto, 2019a; Yang et al., 2015, 2019b). Therefore, we must now reconsider the role of NMDAR inhibition in the antidepressant effects of ketamine and its enantiomers (Yang et al., 2019b). In addition, there are some questions that remain to be explored although role of NMDAR in ketamine's antidepressant effects is supported by convergent pre-clinical data. Nonetheless, a full picture of the multiple mechanistic pieces linking ketamine to antidepressant actions is still under experimental scrutiny.

### 8.2. Monoaminergic system

It has long been established that 5-hydroxytryptamine (5-HT) plays a key role in the mechanisms of action of SSRIs and SNRIs. Research also

indicates that AMPAR-dependent 5-HT release in the medial prefrontal cortex may be involved in the antidepressant effects of (R,S)-ketamine in rodents without depression-like phenotypes (Chaki and Fukumoto, 2019; Fukumoto et al., 2016), though it is considered unlikely that 5-HT plays a role in the antidepressant effects of either (R,S)-ketamine or (R)-ketamine in rodents with a depression-like phenotype (Gigliucci et al., 2013; Zhang et al., 2018a). Therefore, further detailed studies are needed on the role of 5-HT in the antidepressant effects of (R,S)-ketamine and its enantiomers in animals with depression-like phenotypes.

It has also been suggested that the dopamine system plays a role in depression. A recent study demonstrated that disruption of the dopamine D<sub>1</sub> receptor encoded by the *Drd1* in the medial prefrontal cortex blocked the rapid antidepressant effects of (R,S)-ketamine in control mice (Hare et al., 2019). This finding suggested that activation of dopamine D<sub>1</sub> receptors in the medial prefrontal cortex was necessary for the rapid antidepressant actions of (R,S)-ketamine. By contrast, Li et al. (2015) reported that the dopamine D<sub>1</sub> receptor antagonist SCH-23390 did not block the antidepressant-like effects of (R,S)-ketamine in control mice. It has also been shown that pretreatment with SCH-23390 failed to block the antidepressant effects of (R)-ketamine in CSDS-susceptible mice (Chang et al., 2020). A recent study also demonstrated that (S)-ketamine caused a robust increase in dopamine release in the prefrontal cortex compared with (R)-ketamine (Ago et al., 2019), but that its antidepressant effects were less potent than those of (R)-ketamine in animal models of depression. Therefore, although it is unlikely that dopamine D<sub>1</sub> receptors play a major role in the antidepressant actions of (R,S)-ketamine or (R)-ketamine, the dopamine system may contribute to some of the observed pharmacological actions (Chang et al., 2020).

### 8.3. BDNF-TrkB system

In 2011, Autry et al. (2011) demonstrated that the rapid-acting antidepressant effects of (R,S)-ketamine were dependent on the rapid synthesis of brain-derived neurotrophic factor (BDNF); this was based on the finding that (R,S)-ketamine did not cause antidepressant-like effects in inducible *Bdnf*-knockout mice. Subsequent studies have replicated the role of the BDNF-TrkB cascade in the antidepressant effects of (R,S)-ketamine (Yang et al., 2013; Zhou et al., 2014). The TrkB inhibitor ANA-12 has also been shown to block the rapid and long-lasting antidepressant effects of (R)-ketamine and (S)-ketamine in CSDS-susceptible mice (Yang et al., 2015). Regulation of glutamate transporter 1 on astrocytes, through the activation of TrkB, also appears to play a role in the beneficial effects of (R,S)-ketamine on behavioral abnormalities and in the morphological changes seen in the hippocampi of rats exposed to CUMS (W.X. Liu et al., 2016a). Collectively, it is likely that prolonged activation of the BDNF-TrkB cascade in the prefrontal cortex and hippocampus is responsible for the long-lasting antidepressant effects of (R,S)-ketamine and its enantiomers.

### 8.4. mTORC1 and ERK

In 2010, Dr. Ronald Duman (Yale University) and colleagues demonstrated that rapamycin, an mTOR inhibitor, blocked the antidepressant-like effects of (R,S)-ketamine in rodents (Li et al., 2010). By contrast, Autry et al. (2011) later showed that the level of phosphorylated mTOR was not altered in the hippocampi of control and *Bdnf*-knockout mice after injecting (R,S)-ketamine. The antidepressant-like effects of (R,S)-ketamine were not affected by rapamycin in wild-type mice. Furthermore, it was shown that (R,S)-ketamine did not alter the levels of phosphorylated mTOR in the hippocampi and prefrontal cortexes of mice, but that the levels of phosphorylated eukaryotic elongation factor 2 and BDNF were significantly increased in the hippocampi (Zanos et al., 2016). Interestingly, a CSDS model indicated that mTORC1 plays a major role in the antidepressant effects of (S)-ketamine, but not in those of (R)-ketamine, (Yang et al., 2018b). Instead, the antidepressant effects of (R)-ketamine may be mediated by ERK

activation, based on evidence that pretreatment with SL327 (an ERK inhibitor) inhibited its antidepressant effects (Yang et al., 2018b).

A recent randomized, placebo-controlled clinical study demonstrated that rapamycin did not alter the acute effects of (*R,S*)-ketamine in treatment-resistant patients with depression, but that combination therapy led to prolonged antidepressant effects (Abdallah et al., 2018). As such, the role of mTORC1 in the antidepressant effect of (*R,S*)-ketamine has not been confirmed in treatment-resistant patients with depression. Further investigation using a larger sample should help to confirm the role of mTORC1 in the antidepressant effects of (*R,S*)-ketamine and its enantiomers in clinically depressed patients.

### 8.5. Low-voltage-sensitive T-type calcium channel

In 2018, a group of Dr. Hailan Hu (Zhejiang University) demonstrated that blockade of NMDAR-dependent bursting activity in the lateral habenula was induced by (*R,S*)-ketamine. Further, they showed that this lateral habenula bursting promoted rapid-acting antidepressant effects in rodents and that it required both NMDARs and low-voltage-sensitive T-type calcium channels (Y. Yang et al., 2018). Giving ethosuximide (200 mg/kg), a T-type calcium channel inhibitor, resulted in rapid antidepressant effects in rodents (Y. Yang et al., 2018). However, giving ethosuximide (100, 200, 400 mg/kg) did not produce any antidepressant actions in CSDS-susceptible mice, whereas (*R*)-ketamine did, in the same model (Tian et al., 2018b). A recent double-blind, placebo-controlled study demonstrated that ethosuximide did not produce antidepressant actions in medication-free patients with depression (Zhang et al., 2020b).

Overall, existing research indicates that T-type calcium channel inhibitors are unlikely to exert ketamine-like robust antidepressant actions in depressed patients. Further study is needed to confirm the antidepressant action of ethosuximide. At present, a randomized clinical trial is underway at Zhejiang University in China to assess the effects of ethosuximide in treatment-resistant patients with depression (Jiang et al., 2019).

### 8.6. Opioid system

It is well known that ketamine interacts with opioid receptors, with (*S*)-ketamine binding to mu and kappa receptors being 2- to 4-fold stronger than that of (*R*)-ketamine (Domino, 2010; Hirota and Lambert, 1996). Pretreatment with the opiate receptor antagonist naltrexone (50 mg) significantly blocked the antidepressant and anti-suicidal effects of (*R,S*)-ketamine in treatment-resistant patients with depression, suggesting that activation of the opioid system was necessary to produce the rapid-acting antidepressant effects of (*R,S*)-ketamine (Williams et al., 2019; Williams et al., 2018). Other research has shown that pretreatment with naltrexone did not alter the antidepressant effects of (*R,S*)-ketamine in depressed patients with alcohol use disorder (Yoon et al., 2019). Furthermore, (*R,S*)-ketamine still produced antidepressant effects in patients concurrently receiving a high-affinity mu opioid receptor agonists (i.e., buprenorphine, methadone, or naltrexone) (Marton et al., 2019). Thus, the role of the opioid system in the antidepressant effects of (*R,S*)-ketamine remains controversial in humans.

In CSDS and inflammation-induced models of depression, naltrexone pretreatment did not block the antidepressant-like effects of (*R,S*)-ketamine, suggesting that the opioid system may not facilitate the antidepressant-like effects of (*R,S*)-ketamine (Zhang and Hashimoto, 2019a). However, a recent study showed that NMDAR and opioid receptors were required for (*R,S*)-ketamine to reduce the depression-like and lateral habenula hyperactive cellular phenotypes in congenital LH rats (Klein et al., 2020). Both the behavioral and cellular effects of (*R,S*)-ketamine were blocked by naltrexone in congenital LH rats (Klein et al., 2020). The authors concluded that (*R,S*)-ketamine likely does not act as an opiate at antidepressant doses, with its cellular and behavioral effects instead primarily mediated through the NMDAR (Klein et al.,

2020). Further study with each ketamine enantiomer is needed to confirm the role of the opioid system in the antidepressant actions of (*R,S*)-ketamine.

### 8.7. Transforming growth factor $\beta$ 1 system

The molecular mechanisms underpinning (*R*)-ketamine's antidepressant effects remain unclear, especially compared with our understanding of (*S*)-ketamine. However, based on RNA sequencing analysis, we demonstrated that transforming growth factor (TGF)- $\beta$ 1 in the microglia plays a role in the antidepressant effects of (*R*)-ketamine (Zhang et al., 2020a). Of even greater interest, TGF- $\beta$ 1 was shown to elicit rapid-acting and long-lasting antidepressant effects in CSDS, LH, and inflammation models (Zhang et al., 2020a). As such, it is likely that TGF- $\beta$ 1 could be a novel therapeutic target for depression.

### 8.8. Brain-gut-microbiota axis

Multiple lines of evidence suggest a possible role of the brain-gut-microbiota axis in the stress-induced depression-like phenotype and in the antidepressant-like effects of certain compounds (Carlessi et al., 2019; Wang et al., 2020; Yang et al., 2017a; Yang et al., 2019a; Zhang et al., 2017; Zhang et al., 2019). (*R,S*)-ketamine is shown to improve abnormal composition of gut microbiota in rodents with depression-like phenotype (Huang et al., 2019). Furthermore, (*R*)-ketamine ameliorated abnormal composition of gut microbiota in the CSDS susceptible mice (Yang et al., 2017b; Qu et al., 2017). Taken together, the brain-gut-microbiota axis may, in part, play a role in the antidepressant actions of (*R*)-ketamine [or (*R,S*)-ketamine], although further studies are needed.

## 9. Concluding remarks

The discovery that (*R,S*)-ketamine had robust antidepressant actions in depressed patients was certainly serendipitous (Krystal et al., 2019), and has so far led to the esketamine nasal spray being approved for use in treatment-resistant depression in both the US and Europe, despite several concerns about its efficacy and side effects. By contrast, there are no therapeutic options for (*R*)-ketamine, although clinical research is underway in humans. From the preclinical and clinical findings, it seems that safety profile of (*R*)-ketamine in humans is better than (*R,S*)-ketamine and (*S*)-ketamine (Hashimoto, 2019a, 2019b, 2020). This is of great importance because there is accumulating preclinical data to show that (*R*)-ketamine has greater antidepressant potency and elicits longer lasting effects than either (*R,S*)-ketamine or (*S*)-ketamine. Collectively, existing data indicate that (*R*)-ketamine could be a safer antidepressant, necessitating that the research community conduct double-blind randomized study comparing (*R*)-ketamine with (*S*)-ketamine in depressed patients. As mentioned, non-ketamine NMDAR antagonists fail to produce robust ketamine-like antidepressant effects in patients with depression (Hashimoto, 2019a), suggesting that mechanisms other than NMDAR inhibition play a role in the antidepressant effects of (*R,S*)-ketamine (Hashimoto, 2019a; Yang et al., 2019b). Further detailed study is therefore needed to identify the primary target of (*R,S*)-ketamine's antidepressant actions.

## Acknowledgements

This study was supported by Japan Agency for Medical Research and Development, AMED (to K.H., JP19dm0107119). Dr. Yan Wei (Southwest Medical University, China) was supported by the China Scholarship Council (China). Dr. Lijia Chang was supported by the Japan China Sasakawa Medical Fellowship (Tokyo, Japan).



## Declaration of competing interest

Dr. Hashimoto is an inventor on a filed patent application on “The use of (R)-ketamine in the treatment of psychiatric diseases”, “(S)-norketamine and salt thereof as pharmaceutical”, and “transforming growth factor- $\beta$ 1 in the treatment of depression” by Chiba University. Dr. Hashimoto has received research support from Dainippon-Sumitomo, Otsuka, and Taisho (Japan). Other authors declare no conflict of interest.

## References

- Abdallah, C.G., Averill, L.A., Gueorguieva, R., Goktas, S., Purohit, P., Ranganathan, M., D'Souza, D.C., Formica, R., Southwick, S.M., Duman, R.S., Sanacora, G., Krystal, J.H., 2018. Rapamycin, an immunosuppressant and mTORC1 inhibitor, triples the antidepressant response rate of ketamine at 2 weeks following treatment: A double-blind, placebo-controlled, cross-over, randomized clinical trial. *bioRxiv*, 500959.
- Ago, Y., Tanabe, W., Higuchi, M., Tsukada, S., Tanaka, T., Yamaguchi, T., Igarashi, H., Yokoyama, R., Seiriki, K., Kasai, A., Nakazawa, T., Nakagawa, S., Hashimoto, K., Hashimoto, H., 2019. (R)-ketamine induces a greater increase in prefrontal 5-HT release than (S)-ketamine and ketamine metabolites via an AMPA receptor-independent mechanism. *Int. J. Neuropsychopharmacol.* 22 (10), 665–674.
- Anis, N.A., Berry, S.C., Burton, N.R., Lodge, D., 1983. The dissociative anaesthetics, ketamine and phencyclidine, selectively reduce excitation of central mammalian neurons by *N*-methyl-aspartate. *Br. J. Pharmacol.* 79 (2), 565–575.
- Autry, A.E., Adachi, M., Nosyreva, E., Na, E.S., Los, M.F., Cheng, P.-f., Kavalali, E.T., Monteggia, L.M., 2011. NMDA receptor blockade at rest triggers rapid behavioural antidepressant responses. *Nature* 475 (7354), 91–95.
- Bartoli, F., Riboldi, I., Crocamo, C., Di Brita, C., Clerici, M., Carra, G., 2017. Ketamine as a rapid-acting agent for suicidal ideation: a meta-analysis. *Neurosci. Biobehav. Rev.* 77, 232–236.
- Becker, A., Grecksch, G., 2004. Ketamine-induced changes in rat behaviour: a possible animal model of schizophrenia. Test of predictive validity. *Prog. Neuro-Psychopharmacol. Biol. Psychiatry* 28 (8), 1267–1277.
- Berman, R.M., Cappiello, A., Anand, A., Oren, D.A., Heninger, G.R., Charney, D.S., Krystal, J.H., 2000. Antidepressant effects of ketamine in depressed patients. *Biol. Psychiatry* 47 (4), 351–354.
- Bobo, W.V., Vande Voort, J.L., Croarkin, P.E., Leung, J.G., Tye, S.J., Frye, M.A., 2016. Ketamine for treatment-resistant unipolar and bipolar major depression: critical review and implications for clinical practice. *Depress. Anxiety* 33 (8), 698–710.
- Bush, D.M., 2013. Emergency department visits involving phencyclidine (PCP). In: *The CBHSQ Report*, pp. 1–8 Rockville (MD).
- Carlessi, A.S., Borba, L.A., Zugno, A.L., Quevedo, J., Reus, G.Z., 2019. Gut microbiota-brain axis in depression: the role of neuroinflammation. *Eur. J. Neurosci.* <https://doi.org/10.1111/ejn.14631>. 2019 Nov. 30.
- Chaki, S., 2018. Is metabolism of (R)-ketamine essential for the antidepressant effects? *Int. J. Neuropsychopharmacol.* 21 (2), 154–156.
- Chaki, S., Fukumoto, K., 2019. Role of serotonergic system in the antidepressant actions of mGlu<sub>2/3</sub> receptor antagonists: similarity to ketamine. *Int. J. Mol. Sci.* 20 (6), 1270.
- Chan, K.W., Lee, T.M., Siu, A.M., Wong, D.P., Kam, C.M., Tsang, S.K., Chan, C.C., 2013. Effects of chronic ketamine use on frontal and medial temporal cognition. *Addict. Behav.* 38 (5), 2128–2132.
- Chang, L., Toki, H., Qu, Y., Fujita, Y., Mizuno-Yasuhira, A., Yamaguchi, J.I., Chaki, S., Hashimoto, K., 2018. No sex-specific differences in the acute antidepressant actions of (R)-ketamine in an inflammation model. *Int. J. Neuropsychopharmacol.* 21 (10), 932–937.
- Chang, L., Zhang, K., Pu, Y., Qu, Y., Wang, S.M., Xiong, Z., Ren, Q., Dong, C., Fujita, Y., Hashimoto, K., 2019. Comparison of antidepressant and side effects in mice after intranasal administration of (R,S)-ketamine, (R)-ketamine, and (S)-ketamine. *Pharmacol. Biochem. Behav.* 181, 53–59.
- Chang, L., Zhang, K., Pu, Y., Qu, Y., Wang, S.-m., Xiong, Z., Shirayama, Y., Hashimoto, K., 2020. Lack of dopamine D<sub>1</sub> receptors in the antidepressant actions of (R)-ketamine in a chronic social defeat stress model. *Eur. Arch. Psych. Clin. Neurosci.* <https://doi.org/10.1007/s00406-019-01012-1>. press.
- Chaturvedi, H.K., Chandra, D., Bapna, J.S., 1999. Interaction between *N*-methyl-D-aspartate receptor antagonists and imipramine in shock-induced depression. *Indian J. Exp. Biol.* 37 (10), 952–958.
- Correia-Melo, F.S., Leal, G.C., Vieira, F., Jesus-Nunes, A.P., Mello, R.P., Magnavita, G., Caliman-Fontes, A.T., Echeagaray, M.V.F., Bandeira, I.D., Silva, S.S., Cavalcanti, D.E., Araújo-de-Freitas, L., Sarin, L.M., Tuena, M.A., Nakahira, C., Sampaio, A.S., Del-Porto, J.A., Turecki, G., Loo, C., Lacerda, A.L.T., Quarantini, L.C., 2019. Efficacy and safety of adjunctive therapy using esketamine or racemic ketamine for adult treatment-resistant depression: a randomized, double-blind, non-inferiority study. *J. Affect. Disord.* <https://doi.org/10.1016/j.jad.2019.11.086>.
- Corssen, G., Domino, E.F., 1966. Dissociative anesthesia: further pharmacologic studies and first clinical experience with the phencyclidine derivative CI-581. *Anesth. Analg.* 45 (1), 29–40.
- Diazgranados, N., Ibrahim, L., Brutsche, N.E., Newberg, A., Kronstein, P., Khalife, S., Kammerer, W.A., Quezado, Z., Luckenbaugh, D.A., Salvatore, G., Machado-Vieira, R., Manji, H.K., Zarate Jr., C.A., 2010. A randomized add-on trial of an *N*-methyl-D-aspartate antagonist in treatment-resistant bipolar depression. *Arch. Gen. Psychiatry* 67 (8), 793–802.
- Domino, E.F., 2010. Taming the ketamine tiger. *Anesthesiology* 113 (3), 678–684.
- Domino, E.F., Luby, E.D., 2012. Phencyclidine/schizophrenia: one view toward the past, the other to the future. *Schizophr. Bull.* 38 (5), 914–919.
- Domino, E.F., Chodoff, P., Corssen, G., 1965. Pharmacologic effects of CI-581, a new dissociative anesthetic in man. *Clin. Pharmacol. Ther.* 6, 279–291.
- Dong, T.T., Mellin-Olsen, J., Gelb, A.W., 2015. Ketamine: a growing global health-care need. *Br. J. Anaesth.* 115 (4), 491–493.
- Duman, R.S., 2018. Ketamine and rapid-acting antidepressants: a new era in the battle against depression and suicide. *F1000Res* 7 (F1000 Faculty Rev), 659.
- Ebert, B., Mikkelsen, S., Thorkildsen, C., Borgbjerg, F.M., 1997. Norketamine, the main metabolite of ketamine, is a non-competitive NMDA receptor antagonist in the rat cortex and spinal cord. *Eur. J. Pharmacol.* 333 (1), 99–104.
- Fava, M., Freeman, M.P., Flynn, M., Judge, H., Hoepfner, B.B., Cusin, C., Ionescu, D.F., Mathew, S.J., Chang, L.C., Iosifescu, D.V., Murrough, J., DeBattista, C., Schatzberg, A.F., Trivedi, M.H., Jha, M.K., Sanacora, G., Wilkinson, S.T., Papakostas, G.I., 2018. Double-blind, placebo-controlled, dose-ranging trial of intravenous ketamine as adjunctive therapy in treatment-resistant depression (TRD). *Mol. Psychiatry.* <https://doi.org/10.1038/s41380-018-0256-5>.
- Fukumoto, K., Iijima, M., Chaki, S., 2016. The antidepressant effects of an mGlu<sub>2/3</sub> receptor antagonist and ketamine require AMPA receptor stimulation in the mPFC and subsequent activation of the 5-HT neurons in the DRN. *Neuropsychopharmacology* 41 (4), 1046–1056.
- Fukumoto, K., Toki, H., Iijima, M., Hashihayata, T., Yamaguchi, J.I., Hashimoto, K., Chaki, S., 2017. Antidepressant potential of (R)-ketamine in rodent models: comparison with (S)-ketamine. *J. Pharmacol. Exp. Ther.* 361 (1), 9–16.
- Gao, M., Rejazi, D., Liu, H., 2016. Ketamine use in current clinical practice. *Acta Pharmacol. Sin.* 37 (7), 865–872.
- Gigliucci, V., O'Dowd, G., Casey, S., Egan, D., Gibney, S., Harkin, A., 2013. Ketamine elicits sustained antidepressant-like activity via a serotonin-dependent mechanism. *Psychopharmacology* 228 (1), 157–166.
- Giorgetti, R., Marcotulli, D., Tagliabracchi, A., Schifano, F., 2015. Effects of ketamine on psychomotor, sensory and cognitive functions relevant for driving ability. *Forensic Sci. Int.* 252, 127–142.
- Gould, T.D., Z. Jr., C.A., Thompson, S.M., 2019. Molecular pharmacology and neurobiology of rapid-acting antidepressants. *Annu. Rev. Pharmacol. Toxicol.* 59 (1), 213–236.
- Gowda, M.R., Srinivasa, P., Kumbar, P.S., Ramalingaiah, V.H., Muthyalappa, C., Durgoji, S., 2016. Rapid resolution of grief with IV infusion of ketamine: a unique phenomenological experience. *Indian J. Psychol. Med.* 38 (1), 62–64.
- Grunebaum, M.F., Galfalvy, H.C., Choo, T.H., Keilp, J.G., Moitra, V.K., Parris, M.S., Marver, J.E., Burke, A.K., Milak, M.S., Sublette, M.E., Oquendo, M.A., Mann, J.J., 2018. Ketamine for rapid reduction of suicidal thoughts in major depression: a midazolam-controlled randomized clinical trial. *Am. J. Psychiatry* 175 (4), 327–335.
- Hare, B.D., Shinohara, R., Liu, R.J., Pothula, S., DiLeone, R.J., Duman, R.S., 2019. Optogenetic stimulation of medial prefrontal cortex Drd1 neurons produces rapid and long-lasting antidepressant effects. *Nat. Commun.* 10 (1), 223.
- Hashimoto, K., 2016a. Detrimental side effects of repeated ketamine infusions in the brain. *Am. J. Psychiatry* 173 (10), 1044–1045.
- Hashimoto, K., 2016b. Ketamine's antidepressant action: beyond NMDA receptor inhibition. *Expert Opin. Ther. Targets* 20 (11), 1389–1392.
- Hashimoto, K., 2017. Rapid Antidepressant Activity of Ketamine Beyond NMDA Receptor, the NMDA Receptors. *Humana Press*, Cham, pp. 69–81.
- Hashimoto, K., 2019a. Rapid-acting antidepressant ketamine, its metabolites and other candidates: a historical overview and future perspective. *Psychiatry Clin. Neurosci.* 73 (10), 613–627.
- Hashimoto, K., 2019b. Mood, psychomotor, and cognitive function in major depressive disorder: from biomarkers to rapid-acting antidepressants. *Eur. Arch. Psychiatry Clin. Neurosci.* 269, 759–760.
- Hashimoto, K., 2020. Impact of age on optimal dose of antidepressants. *EClinicalMedicine* 18, 100233.
- Hashimoto, K., Kakiuchi, T., Ohba, H., Nishiyama, S., Tsukada, H., 2017. Reduction of dopamine D<sub>2/3</sub> receptor binding in the striatum after a single administration of esketamine, but not R-ketamine: a PET study in conscious monkeys. *Eur. Arch. Psychiatry Clin. Neurosci.* 267 (2), 173–176.
- Hashimoto, K., Shirayama, Y., 2018. What are the causes for discrepancies of antidepressant actions of (2R,6R)-hydroxynorketamine? *Biol. Psychiatry* 84 (1), e7–e8.
- Hashimoto, K., Yang, C., 2018. Is (S)-norketamine an alternative antidepressant for esketamine? *Eur. Arch. Psych. Clin. Neurosci.* 269 (7), 867–868.
- Hirota, K., Lambert, D.G., 1996. Ketamine: its mechanism(s) of action and unusual clinical uses. *Br. J. Anaesth.* 77 (4), 441–444.
- Hoiseth, G., Hjelmeland, K., Bachs, L., 2005. Phencyclidine-angel dust. *Tidsskr. Nor. Lægeforen.* 125 (20), 2775–2776.
- Huang, N., Hua, D., Zhan, G., Li, S., Zhu, B., Jiang, R., Yang, L., Bi, J., Xu, H., Hashimoto, K., Luo, A., Yang, C., 2019. Role of *Actinobacteria* and *Coriobacteria* in the antidepressant effects of ketamine in an inflammation model of depression. *Pharmacol. Biochem. Behav.* 176, 93–100.
- Imre, G., Fokkema, D.S., Den Boer, J.A., Ter Horst, G.J., 2006. Dose-response characteristics of ketamine effect on locomotion, cognitive function and central neuronal activity. *Brain Res. Bull.* 69 (3), 338–345.
- Jiang, J., Wang, Z., Dong, Y., Yang, Y., Ng, C.H., Ma, S., Xu, Y., Hu, H., Hu, S., 2019. A statistical analysis plan for a randomized clinical trial to evaluate the efficacy and safety of ethosuximide in patients with treatment-resistant depression. *Medicine* 98 (31), e16674-e16674.
- Kaur, U., Pathak, B.K., Singh, A., Chakrabarti, S.S., 2019. Esketamine: a glimmer of hope in treatment-resistant depression. *Eur. Arch. Psych. Clin. Neurosci.* <https://doi.org/>

- 10.1007/s00406-019-01084-z.
- Kishimoto, T., Chawla, J.M., Hagi, K., Zarate, C.A., Kane, J.M., Bauer, M., Correll, C.U., 2016. Single-dose infusion ketamine and non-ketamine *N*-methyl-*D*-aspartate receptor antagonists for unipolar and bipolar depression: a meta-analysis of efficacy, safety and time trajectories. *Psychol. Med.* 46 (7), 1459–1472.
- Klein, M.E., Chandra, J., Sheriff, S., Malinow, R., 2020. Opioid system is necessary but not sufficient for antidepressant actions of ketamine in rodents. *Proc. Natl. Acad. Sci. U. S. A.* 117 (5), 2656–2662.
- Koike, H., Iijima, M., Chaki, S., 2011. Involvement of AMPA receptor in both the rapid and sustained antidepressant-like effects of ketamine in animal models of depression. *Behav. Brain Res.* 224 (1), 107–111.
- Krystal, J.H., Abdallah, C.G., Sanacora, G., Charney, D.S., Duman, R.S., 2019. Ketamine: a paradigm shift for depression research and treatment. *Neuron* 101 (5), 774–778.
- Lahti, A.C., Koffel, B., LaPorte, D., Tamminga, C.A., 1995. Subanesthetic doses of ketamine stimulate psychosis in schizophrenia. *Neuropsychopharmacology* 13 (1), 9–19.
- Lankenau, S.E., 2016. On ketamine: in and out of the K hole. In: *Drugs, Clubs and Young People*. Routledge, pp. 91–101.
- Layer, R.T., Popik, P., Olds, T., Skolnick, P., 1995. Antidepressant-like actions of the polyamine site NMDA antagonist, eliprodil (SL-82.0715). *Pharmacol. Biochem. Behav.* 52 (3), 621–627.
- Leal, G.C., Bandeira, I.D., Correia-Melo, F.S., Telles, M., Mello, R.P., Vieira, F., Lima, C.S., Jesus-Nunes, A.P., Guerreiro-Costa, L.N.F., Marback, R.F., Caliman-Fontes, A.T., Marques, B.L.S., Bezerra, M.L.O., Dias-Neto, A.L., Silva, S.S., Sampaio, A.S., Sanacora, G., Turecki, G., Loo, C., Lacerda, A.L.T., Quarantini, L.C., 2020. Intravenous esketamine for treatment-resistant depression: open-label pilot study. *Eur. Arch. Psych. Clin. Neurosci.* <https://doi.org/10.1007/s00406-020-01110-5>. In press.
- Li, L., Vlissides, P.E., 2016. Ketamine: 50 years of modulating the mind. *Front. Hum. Neurosci.* 10, 612.
- Li, N., Lee, B., Liu, R.J., Banasr, M., Dwyer, J.M., Iwata, M., Li, X.Y., Aghajanian, G., Duman, R.S., 2010. mTOR-dependent synapse formation underlies the rapid antidepressant effects of NMDA antagonists. *Science* 329 (5994), 959–964.
- Li, Y., Zhu, Z.R., Ou, B.C., Wang, Y.Q., Tan, Z.B., Deng, C.M., Gao, Y.Y., Tang, M., So, J.H., Mu, Y.L., Zhang, L.Q., 2015. Dopamine D<sub>2/3</sub> but not dopamine D<sub>1</sub> receptors are involved in the rapid antidepressant-like effects of ketamine in the forced swim test. *Behav. Brain Res.* 279, 100–105.
- Lindqvist, D., Dhabhar, F.S., James, S.J., Hough, C.M., Jain, F.A., Bersani, F.S., Reus, V.I., Verhoeven, J.E., Epel, E.S., Mahan, L., Rosser, R., Wolkowitz, O.M., Mellon, S.H., 2017. Oxidative stress, inflammation and treatment response in major depression. *Psychoneuroendocrinology* 76, 197–205.
- Liu, W.X., Wang, J., Xie, Z.M., Xu, N., Zhang, G.F., Jia, M., Zhou, Z.Q., Hashimoto, K., Yang, J.J., 2016a. Regulation of glutamate transporter 1 via BDNF-TrkB signaling plays a role in the anti-apoptotic and antidepressant effects of ketamine in chronic unpredictable stress model of depression. *Psychopharmacology* 233 (3), 405–415.
- Liu, Y., Lin, D., Wu, B., Zhou, W., 2016b. Ketamine abuse potential and use disorder. *Brain Res. Bull.* 126 (Pt 1), 68–73.
- Lodge, D., Mercier, M.S., 2015. Ketamine and phencyclidine: the good, the bad and the unexpected. *Br. J. Pharmacol.* 172 (17), 4254–4276.
- Ma, X.C., Dang, Y.H., Jia, M., Ma, R., Wang, F., Wu, J., Gao, C.G., Hashimoto, K., 2013. Long-lasting antidepressant action of ketamine, but not glycogen synthase kinase-3 inhibitor SB216763, in the chronic mild stress model of mice. *PLoS One* 8 (2), e56053.
- Maddox, V.H., Godefroi, E.F., Parcell, R.F., 1965. The synthesis of phencyclidine and other 1-arylcyclohexylamines. *J. Med. Chem.* 8, 230–235.
- Maeng, S., Zarate, C.A., Du, J., Schloesser, R.J., McCammon, J., Chen, G., Manji, H.K., 2008. Cellular mechanisms underlying the antidepressant effects of ketamine: role of  $\alpha$ -amino-3-hydroxy-5-methylisoxazole-4-propionic acid receptors. *Biol. Psychiatry* 63 (4), 349–352.
- Mahase, E., 2019. Measles cases rise 300% globally in first few months of 2019. *Br. Med. J.* 365, 11810.
- Maj, J., Rogoz, Z., Skuza, G., Sowinska, H., 1992. Effects of MK-801 and antidepressant drugs in the forced swimming test in rats. *Eur. Neuropsychopharmacol.* 2 (1), 37–41.
- Marton, T., Barnes, D.E., Wallace, A., Woolley, J.D., 2019. Concurrent use of buprenorphine, methadone, or naltrexone does not inhibit ketamine's antidepressant activity. *Biol. Psychiatry* 85 (12), e75–e76.
- Masaki, Y., Kashiwagi, Y., Watabe, H., Abe, K., 2019. (*R*-) and (*S*-) ketamine induce differential fMRI responses in conscious rats. *Synapse* 73 (12), e22126.
- Meloni, D., Gambarana, C., De Montis, M.G., Dal Pra, P., Taddei, I., Tagliamonte, A., 1993. Dizocilpine antagonizes the effect of chronic imipramine on learned helplessness in rats. *Pharmacol. Biochem. Behav.* 46 (2), 423–426.
- Mion, G., 2017. History of anaesthesia: the ketamine story - past, present and future. *Eur. J. Anaesthesiol.* 34 (9), 571–575.
- Morris, H., Wallach, J., 2014. From PCP to MXE: a comprehensive review of the non-medical use of dissociative drugs. *Drug Test. Anal.* 6 (7–8), 614–632.
- Murrough, J.W., Iosifescu, D.V., Chang, L.C., Al Jurdi, R.K., Green, C.E., Perez, A.M., Iqbal, S., Pillemer, S., Foulkes, A., Shah, A., Charney, D.S., Mathew, S.J., 2013. Antidepressant efficacy of ketamine in treatment-resistant major depression: a two-site randomized controlled trial. *Am. J. Psychiatry* 170 (10), 1134–1142.
- Murrough, J.W., Abdallah, C.G., Mathew, S.J., 2017. Targeting glutamate signalling in depression: progress and prospects. *Nat. Rev. Drug Discov.* 16 (7), 472–486.
- Newport, D.J., Carpenter, L.L., McDonald, W.M., Potash, J.B., Tohen, M., Nemeroff, C.B., Biomarkers, A.P.A.C.o.R.T.F.o.N., Treatments, 2015. Ketamine and other NMDA antagonists: early clinical trials and possible mechanisms in depression. *Am. J. Psychiatry* 172 (10), 950–966.
- Papp, M., Moryl, E., 1993. New evidence for the antidepressant activity of MK-801, a non-competitive antagonist of NMDA receptors. *Pol. J. Pharmacol.* 45 (5–6), 549–553.
- Papp, M., Moryl, E., 1994. Antidepressant activity of non-competitive and competitive NMDA receptor antagonists in a chronic mild stress model of depression. *Eur. J. Pharmacol.* 263 (1–2), 1–7.
- Petrie, R.X., Reid, I.C., Stewart, C.A., 2000. The *N*-methyl-*D*-aspartate receptor, synaptic plasticity, and depressive disorder. A critical review. *Pharmacol. Ther.* 87 (1), 11–25.
- Phillips, J.L., Norris, S., Talbot, J., Birmingham, M., Hatchard, T., Ortiz, A., Owoeye, O., Batten, L.A., Blier, P., 2019. Single, repeated, and maintenance ketamine infusions for treatment-resistant depression: a randomized controlled trial. *Am. J. Psychiatry* 176 (5), 401–409.
- Qu, Y., Yang, C., Ren, Q., Ma, M., Dong, C., Hashimoto, K., 2017. Comparison of (*R*-) ketamine and lanicemine on depression-like phenotype and abnormal composition of gut microbiota in a social defeat stress model. *Sci. Rep.* 7 (1), 15725.
- Reinstatler, L., Youssef, N.A., 2015. Ketamine as a potential treatment for suicidal ideation: a systematic review of the literature. *Drugs R&D* 15 (1), 37–43.
- Remus, J.L., Dantzer, R., 2016. Inflammation models of depression in rodents: relevance to psychotropic drug discovery. *Int. J. Neuropsychopharmacol.* 19 (9).
- Sanacora, G., Heimer, H., Hartman, D., Mathew, S.J., Frye, M., Nemeroff, C., Robinson Beale, R., 2017. Balancing the promise and risks of ketamine treatment for mood disorders. *Neuropsychopharmacology* 42 (6), 1179–1181.
- Shirayama, Y., Hashimoto, K., 2018. Lack of antidepressant effects of (*2R,6R*)-hydroxynorketamine in a rat learned helplessness model: comparison with (*R*-) ketamine. *Int. J. Neuropsychopharmacol.* 21 (1), 84–88.
- Singh, J.B., Fedgchin, M., Daly, E.J., De Boer, P., Cooper, K., Lim, P., Pinter, C., Murrough, J.W., Sanacora, G., Shelton, R.C., Kurian, B., Winokur, A., Fava, M., Manji, H., Drevets, W.C., Van Nueten, L., 2016a. A double-blind, randomized, placebo-controlled, dose-frequency study of intravenous ketamine in patients with treatment-resistant depression. *Am. J. Psychiatry* 173 (8), 816–826.
- Singh, J.B., Fedgchin, M., Daly, E., Xi, L., Melman, C., De Bruecker, G., Tadic, A., Sienaert, P., Wiegand, F., Manji, H., Drevets, W.C., Van Nueten, L., 2016b. Intravenous esketamine in adult treatment-resistant depression: a double-blind, double-randomization, placebo-controlled study. *Biol. Psychiatry* 80 (6), 424–431.
- Skolnick, P., Layer, R.T., Popik, P., Nowak, G., Paul, I.A., Trullas, R., 1996. Adaptation of *N*-methyl-*D*-aspartate (NMDA) receptors following antidepressant treatment: implications for the pharmacotherapy of depression. *Pharmacopsychiatry* 29 (1), 23–26.
- Sofia, R.D., Harakal, J.J., 1975. Evaluation of ketamine HCl for anti-depressant activity. *Arch. Int. Pharmacodyn. Ther.* 214 (1), 68–74.
- Stevenson, C., 2005. Ketamine: a review. *Update in Anaesthesia* 20 (20), 25–29.
- Strong, C.E., Kabbaj, M., 2018. On the safety of repeated ketamine infusions for the treatment of depression: effects of sex and developmental periods. *Neurobiol. Stress* 9, 166–175.
- Sun, H.L., Zhou, Z.Q., Zhang, G.F., Yang, C., Wang, X.M., Shen, J.C., Hashimoto, K., Yang, J.J., 2016. Role of hippocampal p11 in the sustained antidepressant effect of ketamine in the chronic unpredictable mild stress model. *Transl. Psychiatry* 6, e741.
- Tian, Z., Dong, C., Fujita, A., Fujita, Y., Hashimoto, K., 2018a. Expression of heat shock protein HSP-70 in the retrosplenial cortex of rat brain after administration of (*R,S*)-ketamine and (*S*-) ketamine, but not (*R*-) ketamine. *Pharmacol. Biochem. Behav.* 172, 17–21.
- Tian, Z., Dong, C., Zhang, K., Chang, L., Hashimoto, K., 2018b. Lack of antidepressant effects of low-voltage-sensitive T-type calcium channel blocker ethosuximide in a chronic social defeat stress model: comparison with (*R*-) ketamine. *Int. J. Neuropsychopharmacol.* 21 (11), 1031–1036.
- Trullas, R., Skolnick, P., 1990. Functional antagonists at the NMDA receptor complex exhibit antidepressant actions. *Eur. J. Pharmacol.* 185 (1), 1–10.
- Turner, E.H., 2019. Esketamine for treatment-resistant depression: seven concerns about efficacy and FDA approval. *Lancet Psychiatry* 6 (12), 977–979.
- Tyler, M.W., Yourish, H.B., Ionescu, D.F., Haggarty, S.J., 2017. Classics in chemical neuroscience: ketamine. *ACS Chem. Neurosci.* 8 (6), 1122–1134.
- Vollenweider, F.X., Leenders, K.L., Oye, I., Hell, D., Angst, J., 1997. Differential psychopathology and patterns of cerebral glucose utilisation produced by (*S*-) and (*R*-) ketamine in healthy volunteers using positron emission tomography (PET). *Eur. Neuropsychopharmacol.* 7 (1), 25–38.
- Wang, S., Qu, Y., Chang, L., Pu, Y., Zhang, K., Hashimoto, K., 2020. Antibiotic-induced microbiome depletion is associated with resilience in mice after chronic social defeat stress. *J. Affect. Disord.* 260, 448–457.
- Wedzony, K., Klimek, V., Nowak, G., 1995. Rapid down-regulation of beta-adrenergic receptors evoked by combined forced swimming test and CGP 37849—a competitive antagonist of NMDA receptors. *Pol. J. Pharmacol.* 47 (6), 537–540.
- WHO, 2011. WHO Model List of Essential Medicines: 17th List. (March 2011).
- WHO, 2017. Depression and Other Common Mental Disorders: Global Health Estimates. World Health Organization.
- Wilkinson, S.T., Ballard, E.D., Bloch, M.H., Mathew, S.J., Murrough, J.W., Feder, A., Sos, P., Wang, G., Zarate Jr., C.A., Sanacora, G., 2018. The effect of a single dose of intravenous ketamine on suicidal ideation: a systematic review and individual participant data meta-analysis. *Am. J. Psychiatry* 175 (2), 150–158.
- Williams, N.R., Heifets, B.D., Blasey, C., Sudheimer, K., Pannu, J., Pankow, H., Hawkins, J., Birnbaum, J., Lyons, D.M., Rodriguez, C.I., Schatzberg, A.F., 2018. Attenuation of antidepressant effects of ketamine by opioid receptor antagonism. *Am. J. Psychiatry* 175 (12), 1205–1215.
- Williams, N.R., Heifets, B.D., Bentzley, B.S., Blasey, C., Sudheimer, K.D., Hawkins, J., Lyons, D.M., Schatzberg, A.F., 2019. Attenuation of antidepressant and antisuicidal effects of ketamine by opioid receptor antagonism. *Mol. Psychiatry* 24 (12), 1779–1786.
- Witkin, J.M., Knutson, D.E., Rodriguez, G.J., Shi, S., 2018. Rapid-acting antidepressants. *Curr. Pharm. Des.* 24 (22), 2556–2563.
- Wolff, K., 2016. Ketamine: The pharmacokinetics and pharmacodynamics in misusing populations. In: *The SAGE Handbook of Drug & Alcohol Studies: Biological Approaches*, pp. 177.

- Xiong, Z., Fujita, Y., Zhang, K., Pu, Y., Chang, L., Ma, M., Chen, J., Hashimoto, K., 2019. Beneficial effects of (R)-ketamine, but not its metabolite (2R,6R)-hydroxynorketamine, in the depression-like phenotype, inflammatory bone markers, and bone mineral density in a chronic social defeat stress model. *Behav. Brain Res.* 368, 111904.
- Yamaguchi, J.I., Toki, H., Qu, Y., Yang, C., Koike, H., Hashimoto, K., Mizuno-Yasuhiro, A., Chaki, S., 2018. (2R,6R)-hydroxynorketamine is not essential for the antidepressant actions of (R)-ketamine in mice. *Neuropsychopharmacology* 43 (9), 1900–1907.
- Yang, C., Hu, Y.-M., Zhou, Z.-Q., Zhang, G.-F., Yang, J.-J., 2013. Acute administration of ketamine in rats increases hippocampal BDNF and mTOR levels during forced swimming test. *Ups. J. Med. Sci.* 118 (1), 3–8.
- Yang, C., Shirayama, Y., Zhang, J.C., Ren, Q., Yao, W., Ma, M., Dong, C., Hashimoto, K., 2015. R-ketamine: a rapid-onset and sustained antidepressant without psychotomimetic side effects. *Transl. Psychiatry* 5, e632.
- Yang, B., Ren, Q., Ma, M., Chen, Q.X., Hashimoto, K., 2016a. Antidepressant effects of (+)-MK-801 and (–)-MK-801 in the social defeat stress model. *Int. J. Neuropsychopharmacol.* 19 (12), pyw080.
- Yang, C., Han, M., Zhang, J.C., Ren, Q., Hashimoto, K., 2016b. Loss of parvalbumin-immunoreactivity in mouse brain regions after repeated intermittent administration of esketamine, but not R-ketamine. *Psychiatry Res.* 239, 281–283.
- Yang, C., Fujita, Y., Ren, Q., Ma, M., Dong, C., Hashimoto, K., 2017a. *Bifidobacterium* in the gut microbiota confer resilience to chronic social defeat stress in mice. *Sci. Rep.* 7, 45942.
- Yang, C., Qu, Y., Fujita, Y., Ren, Q., Ma, M., Dong, C., Hashimoto, K., 2017b. Possible role of gut-microbiota in the antidepressant effects of (R)-ketamine in a social defeat stress model. *Transl. Psychiatry* 7, 1294.
- Yang, C., Kobayashi, S., Nakao, K., Dong, C., Han, M., Qu, Y., Ren, Q., Zhang, J.C., Ma, M., Toki, H., Yamaguchi, J.I., Chaki, S., Shirayama, Y., Nakazawa, K., Manabe, T., Hashimoto, K., 2018a. AMPA receptor activation-independent antidepressant actions of ketamine metabolite (S)-norketamine. *Biol. Psychiatry* 84 (8), 591–600.
- Yang, C., Ren, Q., Qu, Y., Zhang, J.-C., Ma, M., Dong, C., Hashimoto, K., 2018b. Mechanistic target of rapamycin-independent antidepressant effects of (R)-ketamine in a social defeat stress model. *Biol. Psychiatry* 83 (1), 18–28.
- Yang, Y., Cui, Y., Sang, K., Dong, Y., Ni, Z., Ma, S., Hu, H., 2018c. Ketamine blocks bursting in the lateral habenula to rapidly relieve depression. *Nature* 554 (7692), 317–322.
- Yang, C., Fang, X., Zhan, G., Huang, N., Li, S., Bi, J., Jiang, R., Yang, L., Miao, L., Zhu, B., Luo, A., Hashimoto, K., 2019a. Key role of gut microbiota in anhedonia-like phenotype in rodents with neuropathic pain. *Transl. Psychiatry* 9, 57.
- Yang, C., Yang, J., Luo, A., Hashimoto, K., 2019b. Molecular and cellular mechanisms underlying the antidepressant effects of ketamine enantiomers and its metabolites. *Transl. Psychiatry* 9 (1), 280.
- Yoon, G., Petrakis, I.L., Krystal, J.H., 2019. Association of combined naltrexone and ketamine with depressive symptoms in a case series of patients with depression and alcohol use disorder. *JAMA Psychiatry* 76 (3), 337–338.
- Zanos, P., Moaddel, R., Morris, P.J., Georgiou, P., Fischell, J., Elmer, G.I., Alkondon, M., Yuan, P., Pribut, H.J., Singh, N.S., Dossou, K.S., Fang, Y., Huang, X.P., Mayo, C.L., Wainer, I.W., Albuquerque, E.X., Thompson, S.M., Thomas, C.J., Zarate Jr., C.A., Gould, T.D., 2016. NMDAR inhibition-independent antidepressant actions of ketamine metabolites. *Nature* 533 (7604), 481–486.
- Zanos, P., Moaddel, R., Morris, P.J., Riggs, L.M., Highland, J.N., Georgiou, P., Pereira, E.F.R., Albuquerque, E.X., Thomas, C.J., Zarate, C.A., Gould, T.D., 2018. Ketamine and ketamine metabolite pharmacology: insights into therapeutic mechanisms. *Pharmacol. Rev.* 70 (3), 621–660.
- Zarate Jr., C.A., Singh, J.B., Carlson, P.J., Brutsche, N.E., Ameli, R., Luckenbaugh, D.A., Charney, D.S., Manji, H.K., 2006. A randomized trial of an N-methyl-D-aspartate antagonist in treatment-resistant major depression. *Arch. Gen. Psychiatry* 63 (8), 856–864.
- Zarate Jr., C.A., Brutsche, N.E., Ibrahim, L., Franco-Chaves, J., Diazgranados, N., Cravchik, A., Selter, J., Marquardt, C.A., Liberty, V., Luckenbaugh, D.A., 2012. Replication of ketamine's antidepressant efficacy in bipolar depression: a randomized controlled add-on trial. *Biol. Psychiatry* 71 (11), 939–946.
- Zhang, K., Hashimoto, K., 2019a. Lack of opioid system in the antidepressant actions of ketamine. *Biol. Psychiatry* 85 (6), e25–e27.
- Zhang, K., Hashimoto, K., 2019b. An update on ketamine and its two enantiomers as rapid-acting antidepressants. *Expert. Rev. Neurother.* 19 (1), 83–92.
- Zhang, K., Jia, G., Xia, L., Du, J., Gai, G., Wang, Z., Cao, L., Zhang, F., Tao, R., Liu, H., Hashimoto, K., Wang, G., 2020b. Efficacy of anticonvulsant ethosuximide for major depressive disorder: a randomized, placebo-control clinical trial. *Eur. Arch. Psych. Clin. Neurosci.* <https://doi.org/10.1007/s00406-020-01103-4>.
- Zhang, J.C., Li, S.X., Hashimoto, K., 2014. R (–)-ketamine shows greater potency and longer lasting antidepressant effects than S (+)-ketamine. *Pharmacol. Biochem. Behav.* 116, 137–141.
- Zhang, K., Yang, C., Chang, L., Sakamoto, A., Suzuki, T., Fujita, Y., Qu, Y., Wang, S., Pu, Y., Tan, Y., Wang, X., Ishima, T., Shirayama, Y., Hatano, M., Tanaka, K.F., Hashimoto, K., 2020a. Essential role of microglial transforming growth factor- $\beta$ 1 in antidepressant actions of (R)-ketamine and the novel antidepressant TGF- $\beta$ 1. *Transl. Psychiatry* 10, 32.
- Zhang, J.C., Yao, W., Dong, C., Yang, C., Ren, Q., Ma, M., Han, M., Hashimoto, K., 2015. Comparison of ketamine, 7,8-dihydroxyflavone, and ANA-12 antidepressant effects in the social defeat stress model of depression. *Psychopharmacology* 232 (23), 4325–4335.
- Zhang, J.C., Yao, W., Hashimoto, K., 2016. Brain-derived neurotrophic factor (BDNF)-TrkB signaling in inflammation-related depression and potential therapeutic targets. *Curr. Neuropharmacol.* 14 (7), 721–731.
- Zhang, J.C., Yao, W., Dong, C., Yang, C., Ren, Q., Ma, M., Hashimoto, K., 2017. Blockade of interleukin-6 receptor in the periphery promotes rapid and sustained antidepressant actions: a possible role of gut-microbiota-brain axis. *Transl. Psychiatry* 7, e1138.
- Zhang, K., Dong, C., Fujita, Y., Fujita, A., Hashimoto, K., 2018a. 5-hydroxytryptamine-independent antidepressant actions of (R)-ketamine in a chronic social defeat stress model. *Int. J. Neuropsychopharmacol.* 21 (2), 157–163.
- Zhang, K., Fujita, Y., Hashimoto, K., 2018b. Lack of metabolism in (R)-ketamine's antidepressant actions in a chronic social defeat stress model. *Sci. Rep.* 8 (1), 4007.
- Zhang, K., Toki, H., Fujita, Y., Ma, M., Chang, L., Qu, Y., Harada, S., Nemoto, T., Mizuno-Yasuhiro, A., Yamaguchi, J.I., Chaki, S., Hashimoto, K., 2018c. Lack of deuterium isotope effects in the antidepressant effects of (R)-ketamine in a chronic social defeat stress model. *Psychopharmacology* 235 (11), 3177–3185.
- Zhang, K., Fujita, Y., Chang, L., Qu, Y., Pu, Y., Wang, S., Shirayama, Y., Hashimoto, K., 2019. Abnormal composition of gut microbiota is associated with resilience versus susceptibility to inescapable electric stress. *Transl. Psychiatry* 9, 231.
- Zhou, W., Wang, N., Yang, C., Li, X.M., Zhou, Z.Q., Yang, J.J., 2014. Ketamine-induced antidepressant effects are associated with AMPA receptors-mediated upregulation of mTOR and BDNF in rat hippocampus and prefrontal cortex. *Eur. Psychiatry* 29 (7), 419–423.
- Zimmermann, K.S., Ricvhardson, R., Baker, K.D., 2020. Esketamine as a treatment for paediatric depression: questions of safety and efficacy. *Lancet Psychiatry.* [https://doi.org/10.1016/S2215-0366\(19\)30521-8](https://doi.org/10.1016/S2215-0366(19)30521-8). 2020 Jan. 14.

# Antibiotic-induced microbiome depletion protects against MPTP-induced dopaminergic neurotoxicity in the brain

Yaoyu Pu<sup>1</sup>, Lijia Chang<sup>1</sup>, Youge Qu<sup>1</sup>, Siming Wang<sup>1</sup>, Kai Zhang<sup>1</sup>, Kenji Hashimoto<sup>1</sup>

<sup>1</sup>Division of Clinical Neuroscience, Chiba University Center for Forensic Mental Health, Chiba 260-8670, Japan

**Correspondence to:** Kenji Hashimoto; email: [hashimoto@faculty.chiba-u.jp](mailto:hashimoto@faculty.chiba-u.jp)

**Keywords:** antibiotic, dopamine, gut microbiota, MPTP, neurotoxicity

**Received:** July 30, 2019

**Accepted:** August 13, 2019

**Published:** September 3, 2019

**Copyright:** Pu et al. This is an open-access article distributed under the terms of the Creative Commons Attribution License (CC BY 3.0), which permits unrestricted use, distribution, and reproduction in any medium, provided the original author and source are credited.

## ABSTRACT

Although the brain–gut axis appears to play a role in the pathogenesis of Parkinson’s disease, the precise mechanisms underlying the actions of gut microbiota in this disease are unknown. This study was undertaken to investigate whether antibiotic-induced microbiome depletion affects dopaminergic neurotoxicity in the mouse brain after administration of 1-methyl-4-phenyl-1,2,3,6-tetrahydropyridine (MPTP). MPTP significantly decreased dopamine transporter (DAT) immunoreactivity in the striatum and tyrosine hydroxylase (TH) immunoreactivity in the substantia nigra of water-treated mice. However, MPTP did not decrease DAT or TH immunoreactivity in the brains of mice treated with an antibiotic cocktail. Furthermore, antibiotic treatment significantly decreased the diversity and altered the composition of the host gut microbiota at the genus and species levels. Interestingly, MPTP also altered microbiome composition in antibiotic-treated mice. These findings suggest that antibiotic-induced microbiome depletion might protect against MPTP-induced dopaminergic neurotoxicity in the brain via the brain–gut axis.

## INTRODUCTION

Parkinson’s disease (PD) is a common and progressive neurodegenerative disease that predominately affects dopaminergic neurons in the striatum and substantia nigra (SNr) [1, 2]. There is also evidence that loss of dopamine at extrastriatal sites in the basal ganglia, thalamus, or cortex contributes to PD pathology [3]. Although the precise mechanisms underlying PD pathology remain largely unknown, evidence suggests that the brain–gut axis plays a crucial role [4–13]. For example, alterations in bowel function, mainly in the form of constipation, can precede the onset of the prototypical motor symptoms of PD [14].

Over the past two decades, it has become apparent that gut microbiota is a fundamental factor in host physiology and pathology. The brain–gut axis is a complex, multi–organ, bidirectional signaling system involving the gut microbiota and the brain [6, 15–23]. Moreover, although antibiotics are crucial, their overuse plays a role in the pathogenesis of several diseases

associated with microbiota impairment [24, 25]. Antibiotic cocktail-induced microbiome depletion has been used to investigate the role of gut microbiota in some pathological conditions [26–35]. In addition, Sampson et al. [36] reported that gut microbiota are necessary for motor deficits induced by  $\alpha$ -synuclein overexpression in mice. Interestingly, antibiotic treatment ameliorated these deficits, while microbial re-colonization promoted PD pathology in mice. Remarkably, colonization of  $\alpha$ -synuclein overexpressing mice with microbiota from PD patients enhanced physical impairments compared to microbiota transplants from healthy control subjects. Collectively, these findings suggest that the effects of the brain–gut axis in the pathology of PD are mediated at least in part by the gut microbiota. However, the effects of antibiotic-induced microbiome depletion on dopaminergic neurotoxicity in the brains of PD model mice are unknown.

In this study, we investigated whether antibiotic-induced microbiome depletion affects MPTP (1-methyl-4-

phenyl-1,2,3,6-tetrahydropyridine)-induced dopaminergic neurotoxicity, which is widely used as an animal model of PD [37], in the mouse brain.

## RESULTS

### Effects of the antibiotic cocktail on body weight

A repeated measures two-way ANOVA revealed that treatment with an antibiotic cocktail for 14 days reduced mouse body weights (antibiotic:  $F_{1,36} = 20.549$ ,  $P < 0.001$ ; MPTP:  $F_{1,36} = 0.005$ ,  $P = 0.994$ ; interaction (antibiotic  $\times$  MPTP):  $F_{1,36} = 0.045$ ,  $P = 0.833$ ; Figure 1B). On day 22, antibiotic + saline group body weights, but not antibiotic + MPTP group weights, remained lower than those of mice that did not receive antibiotics (Figure 1B). Thus, antibiotic + MPTP group body weights recovered gradually after treatment, while antibiotic + saline group weights did not.

### Antibiotic treatment protected against MPTP-induced neurotoxicity in the mouse brain

DAT immunohistochemistry revealed that MPTP reduced DAT levels in the striatum of the water-treated group, but not the antibiotic-treated group (Figure 1C). A two-way ANOVA revealed significant differences in DAT immunoreactivity among the four groups (antibiotic:  $F_{1,36} = 11.30$ ,  $P = 0.002$ ; MPTP:  $F_{1,36} = 20.46$ ,  $P < 0.001$ ; interaction (antibiotic  $\times$  MPTP):  $F_{1,36} = 15.32$ ,  $P < 0.001$ ; Figure 1D). TH immunohistochemistry revealed that MPTP reduced TH immunoreactivity in the SNr of the water-treated group, but not the antibiotic-treated group (Figure 1E). A two-way ANOVA revealed significant differences in TH immunoreactivity among the four groups (antibiotic:  $F_{1,36} = 11.48$ ,  $P = 0.002$ ; MPTP:  $F_{1,36} = 10.19$ ,  $P = 0.003$ ; interaction (antibiotic  $\times$  MPTP):  $F_{1,36} = 11.75$ ,  $P = 0.002$ ; Figure 1F). Collectively, these results indicate that treatment with an antibiotic cocktail for 14 days protected against MPTP-induced dopaminergic neurotoxicity in the striatum and SNr.

### Gut microbiota composition

Next, we investigated the composition of the gut microbiota, which can be altered by antibiotic cocktail treatment [33–35], in the four experimental groups.  $\alpha$ -diversity is defined as the richness of gut microbiota and can be measured using different indices. Two-way ANOVAs revealed a significant difference in the Chao1 (antibiotic:  $F_{1,36} = 15.928$ ,  $P < 0.001$ ; MPTP:  $F_{1,36} = 37.541$ ,  $P < 0.001$ ; interaction (antibiotic  $\times$  MPTP):  $F_{1,36} = 20.587$ ,  $P < 0.001$ ; Figure 2A) and Ace (antibiotic:  $F_{1,36} = 12.968$ ,  $P < 0.001$ ; MPTP:  $F_{1,36} = 43.032$ ,  $P < 0.001$ ; interaction (antibiotic  $\times$  MPTP):  $F_{1,36} = 22.827$ ,  $P < 0.001$ ; Figure 2B) indices among the four groups.

Specifically, Chao 1 and Ace indices were higher in the water + MPTP group than in both the water + saline and antibiotic + MPTP groups ( $P < 0.001$ ). Interestingly, antibiotic cocktail treatment attenuated the MPTP-induced increase in the Chao 1 and Ace indices. A two-way ANOVA also revealed significant differences in the Shannon index among the four groups (antibiotic:  $F_{1,36} = 8.942$ ,  $P = 0.005$ ; MPTP:  $F_{1,36} = 0.593$ ,  $P = 0.446$ ; interaction (antibiotic  $\times$  MPTP):  $F_{1,36} = 3.427$ ,  $P = 0.072$ ; Figure 2C). The Shannon index in the antibiotic + MPTP group was lower than that of the water + MPTP group. In an unweighted UniFrac PCoA dot map, dots representing the antibiotic-treated groups were far away from dots representing the water-treated groups (Figure 2D). Interestingly, dots representing the antibiotic + MPTP group were isolated from dots representing the other three groups (Figure 2D).

At the phylum level, *Firmicutes* were the most abundant phylum in the water + saline group microbiota (Figure 3A and 3B). The abundance of *Firmicutes* was lower in the antibiotic + MPTP group than in the water + MPTP and antibiotic + saline groups ( $P < 0.001$ , Figure 3B). In contrast, the most dominant phylum in the antibiotic + MPTP group, *Bacteroidetes*, was less abundant in the water + MPTP and antibiotic + saline groups ( $P < 0.001$ , Figure 3C). *Proteobacteria* levels were higher after treatment with the antibiotic cocktail compared to the two water-treated groups (Figure 3D), while *Deferribacteres* and *TM7* levels decreased after treatment with the antibiotic cocktail or with MPTP (Figure 3E, 3F).

Antibiotic and MPTP treatment also altered the composition of fecal microbiota at the genus level (Figure 4A). *Lactobacillus*, *Mucispirillum*, and *Candidatus Arthromitus* levels decreased after treatment with the antibiotic cocktail (Figure 4B–4D). In contrast, *Parasutterella*, *Blautia*, *Robinsoniella*, *Escherichia*, *Dorea*, and *Eubacterium* levels increased after treatment with antibiotic cocktail (Figure 4E–4J). Interestingly, *Asaccharobacter* levels increased in the antibiotic + MPTP group compared to the other three groups (Figure 4K). *Clostridium*, which was the most dominant genus in control mice, decreased after MPTP injections and antibiotic cocktail treatment (Figure 4L). Furthermore, the antibiotic + MPTP group had a higher abundance of *Parabacteroides* than the other three groups (Figure 4M). Finally, MPTP treatment attenuated the antibiotic-induced increase in the abundance of *Bacteroides* and *Enterococcus* (Figure 4N, 4O).

Gut microbiota composition at the species level in the four experimental groups is shown in Figure 5A. *Lactobacillus murinus*, *Lactobacillus johnsonii*, *Mucispirillum schaedleri*, and *Candidatus Arthromitus sp. SFB-mouse*

decreased after antibiotic cocktail treatment (Figure 5B–5E). In contrast, *Escherichia coli*, *Blautia sp. Ser8*, and *Robinsoniella peoriensis* increased after antibiotic treatment (Figure 5F–5H). *Clostridium sp. Clone-27*, the most abundant species in control water + saline group

mice, decreased in all other groups (Figure 5I). On the other hand, *Blautia sp. canine oral taxon 143*, *Parabacteroides distasonis*, *Blautia coccoides*, *Clostridium sp. HGF2*, and *Clostridium bolteae* increased in the antibiotic + MPTP group (Figure 5J–5N).

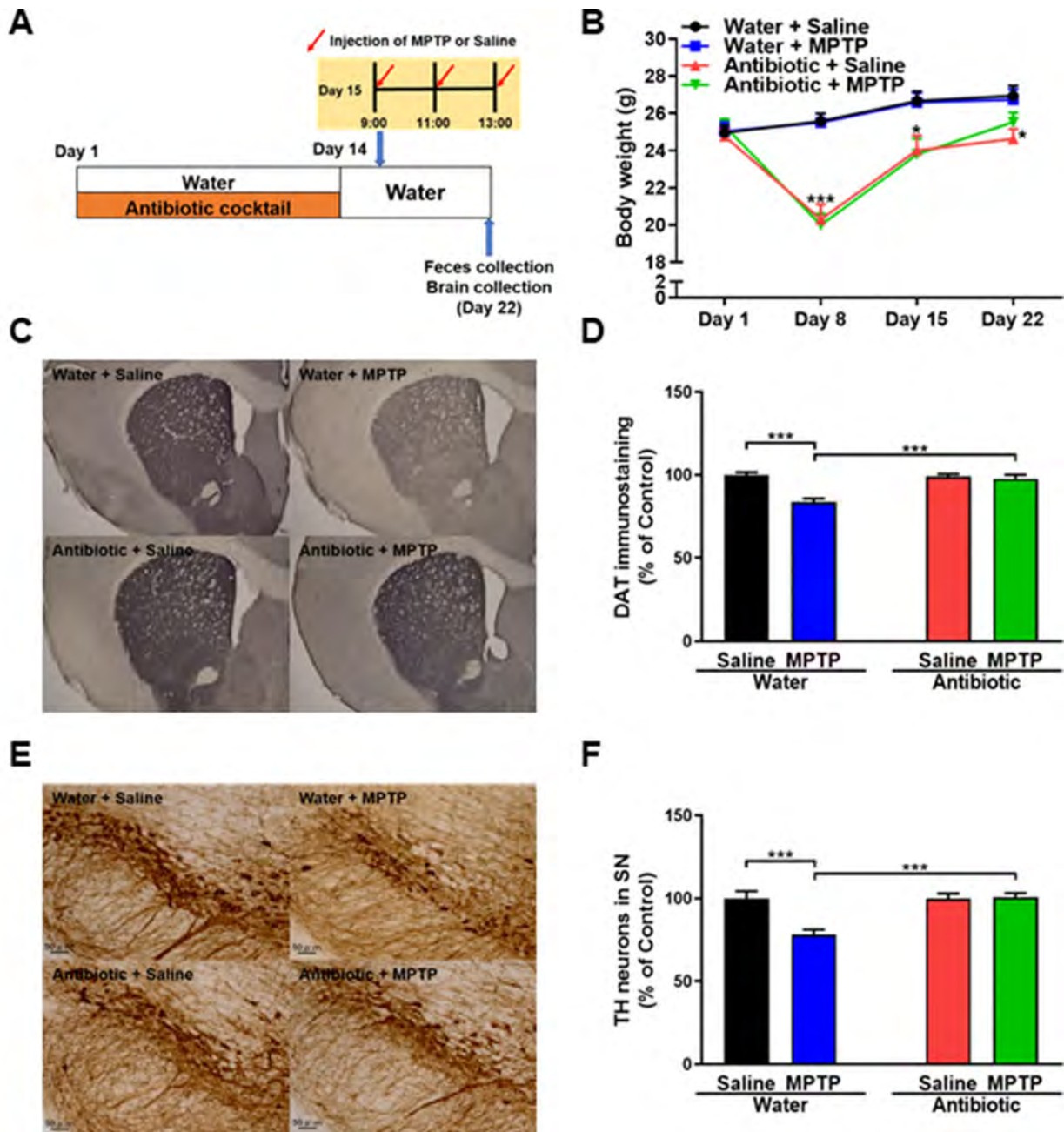


**Figure 1. Effects of antibiotic treatment on gut microbiota diversity.** (A) Treatment schedule. Adult mice received drinking water with or without antibiotic cocktail from day 1 to day 14. On day 15, MPTP or saline injections were administered. On day 22, fresh feces were collected. Mice were then perfused for immunohistochemistry. (B) Body weights in the different groups (repeated two-way ANOVA, antibiotic:  $F_{1,36} = 20.549$ ,  $P < 0.001$ ; MPTP:  $F_{1,36} = 0.005$ ,  $P = 0.994$ ; interaction (antibiotic  $\times$  MPTP):  $F_{1,36} = 0.045$ ,  $P = 0.833$ ). (C) Representative images of DAT immunohistochemistry in the water + saline, water + MPTP, antibiotic + saline, and antibiotic + MPTP groups. (D) Striatal DAT immunoreactivity data. (E) Representative images of TH immunohistochemistry in the water + saline, water + MPTP, antibiotic + saline, and antibiotic + MPTP groups. (F) SNr TH immunoreactivity data. Data are shown as mean  $\pm$  S.E.M. ( $n = 10$ ). \*\*\* $P < 0.001$ . Bar = 50  $\mu$ m.

In addition, *Lactobacillus intestinalis* and *Lactobacillus reuteri*, which increased in the water + MPTP group compared to the water + saline group, were markedly reduced after antibiotic treatment (Figure 5O and 5P). Interestingly, DAT immunoreactivity was negatively correlated with levels of *Lactobacillus intestinalis* ( $r = -0.38$ ,  $P = 0.01$ ) and *Lactobacillus reuteri* ( $r = -0.39$ ,  $P = 0.01$ ; Figure 5U and 5V). The antibiotic-induced increase in the abundance of *Bacteroides acidifaciens*, [*Clostridium*] *cocleatum*, and *Enterococcus casseliflavus* was largely reversed after MPTP administration (Figure 5Q–5S). In addition, MPTP restored *Bacteroides sp. TP-5* to control levels after it had been reduced by antibiotic treatment (Figure 5T).

## DISCUSSION

In this study, we examined the effects of treatment with an antibiotic cocktail on gut microbiota in a mouse model of PD. We found that MPTP markedly reduced DAT immunoreactivity in the striatum and TH immunoreactivity in the SNr of the water-treated group,

but not the antibiotic-treated group. Second, antibiotic cocktail treatment caused substantial alterations in host gut microbiota composition compared to the water-treated group. In an unweighted UniFrac PCoA, dots representing the two unantibiotic-treated groups were located far away from dots representing the two water-treated groups. Interestingly, dots representing the antibiotic + MPTP group were also far from the dots of the other three groups. At the phylum level, *Proteobacteria* was markedly increased, while *Deferribacteres*, and *TM7* were markedly decreased, in the gut of antibiotic-treated mice. Antibiotic treatment was also associated with substantial microbiome alterations at the genus and species levels. Overall, 14 days of treatment with an antibiotic cocktail caused significant changes in the diversity and composition of the host gut microbiota, which is consistent with previous reports [33–35]. Taken together, these results suggest that antibiotic-induced microbiome depletion might protect against MPTP-induced dopaminergic neurotoxicity in the mouse brain via the brain–gut microbiota axis.

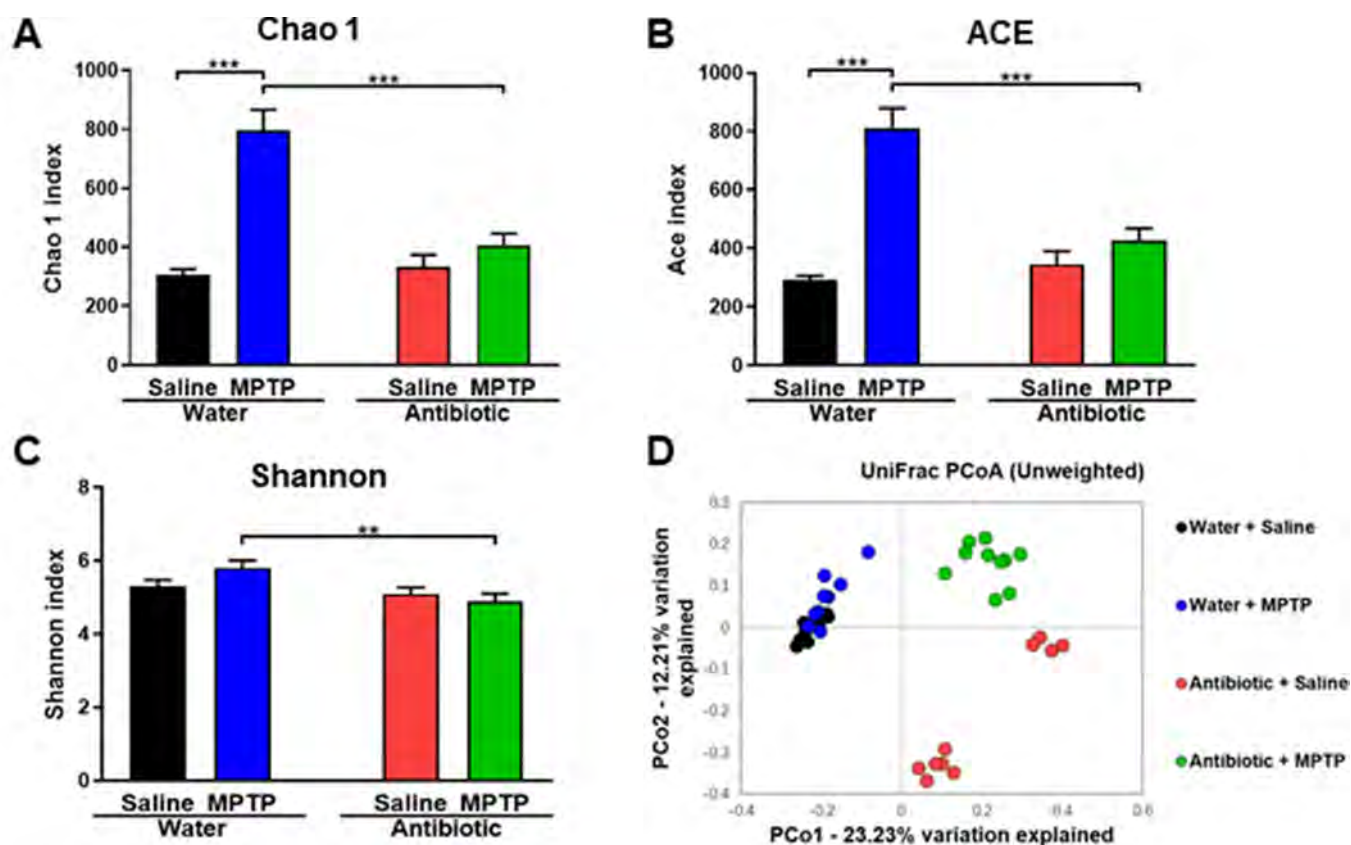


**Figure 2.  $\alpha$ -diversity and  $\beta$ -diversity in gut microbiota.** Diversity index values for the four groups. (A) *Chao 1* index (two-way ANOVA, antibiotic:  $F_{1,36} = 15.928$ ,  $P < 0.001$ ; MPTP:  $F_{1,36} = 37.541$ ,  $P < 0.001$ ; interaction (antibiotic  $\times$  MPTP):  $F_{1,36} = 20.587$ ,  $P < 0.001$ ). (B) *ACE* index (two-way ANOVA, antibiotic:  $F_{1,36} = 12.968$ ,  $P < 0.001$ ; MPTP:  $F_{1,36} = 43.032$ ,  $P < 0.001$ ; interaction (antibiotic  $\times$  MPTP):  $F_{1,36} = 22.827$ ,  $P < 0.001$ ). (C) *Shannon* index (two-way ANOVA, antibiotic:  $F_{1,36} = 8.942$ ,  $P = 0.005$ ; MPTP:  $F_{1,36} = 0.593$ ,  $P = 0.446$ ; interaction (antibiotic  $\times$  MPTP):  $F_{1,36} = 3.427$ ,  $P = 0.072$ ). (D) PCoA analysis of gut bacteria data (Bray–Curtis dissimilarity).

In another recent study, we reported that 14 days of antibiotic treatment increases levels of bacteria from the phylum *Proteobacteria* and decreases levels of the major bacterial phyla *Bacteroidetes* and *Firmicutes* in the mouse gut microbiota (Wang et al., submitted); similar results have also been observed in other studies [26, 31, 32]. Here, we found that the relative abundance of *Proteobacteria* increased in the antibiotic-treated groups compared to the water-treated groups. In contrast, the relative abundance of *Firmicutes* and *Bacteroidetes* was

similar in the antibiotic + saline and water + saline groups, indicating that spontaneous recovery of these bacteria occurred. The mechanisms underlying the increased relative abundance of *Proteobacteria* after antibiotic cocktail treatment are currently unknown. Interestingly, MPTP significantly altered the relative abundance of *Firmicutes* and *Bacteroidetes* in the antibiotic-treated group, but not in the water-treated group. Thus, MPTP might further alter gut microbiome composition after antibiotic-induced microbiome depletion.

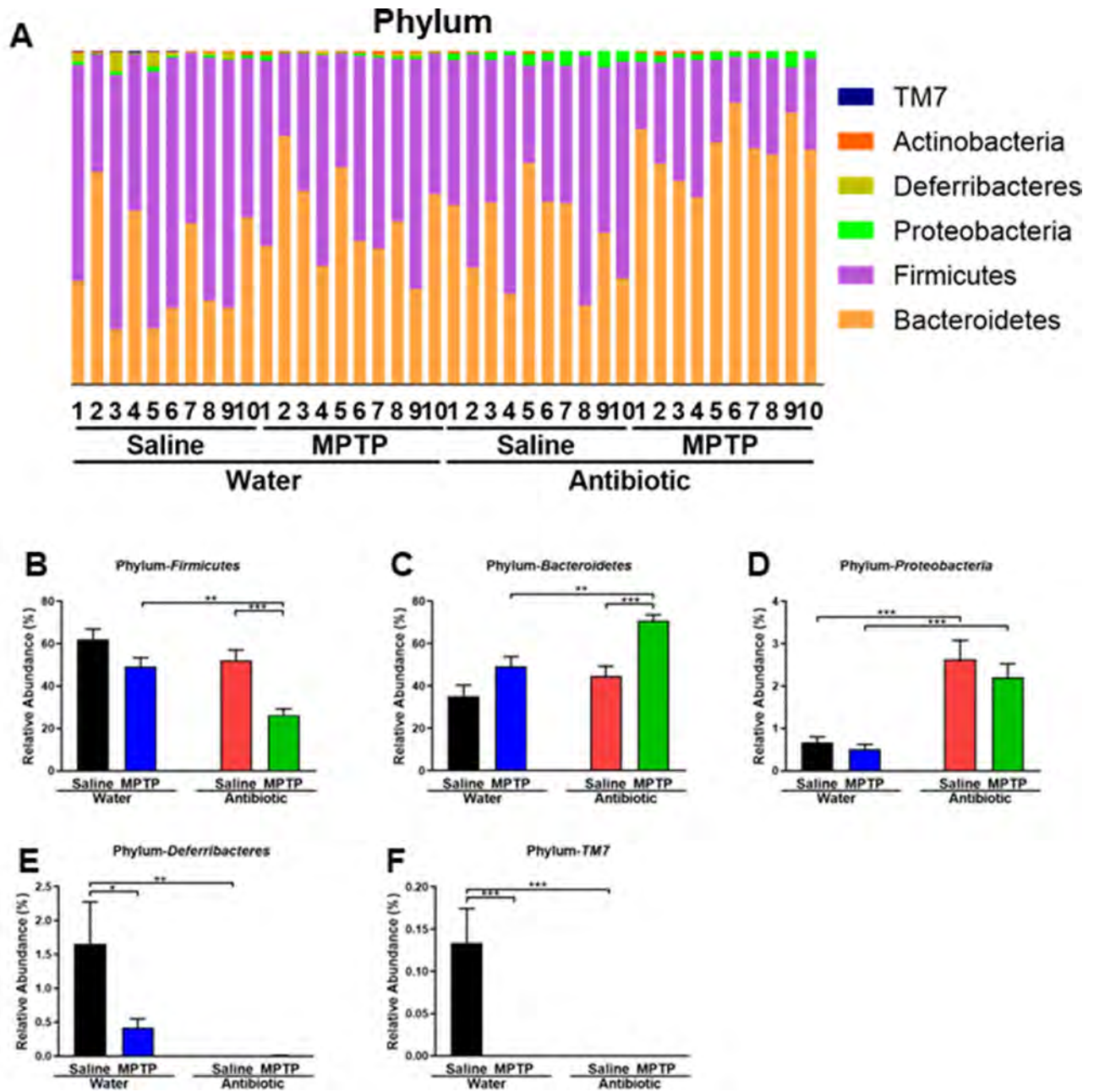


**Figure 3. Altered gut bacteria composition at the phylum level.** (A) Relative abundance at the phylum level. (B) *Bacteroidetes*. (C) *Firmicutes*. (D) *Proteobacteria*. (E) *Deferribacteres*. (F) *TM7*. Data are shown as mean  $\pm$  S.E.M. (n = 10). \*\*P < 0.01, \*\*\*P < 0.001. See the Supplementary Table 1 for detailed statistical analysis.



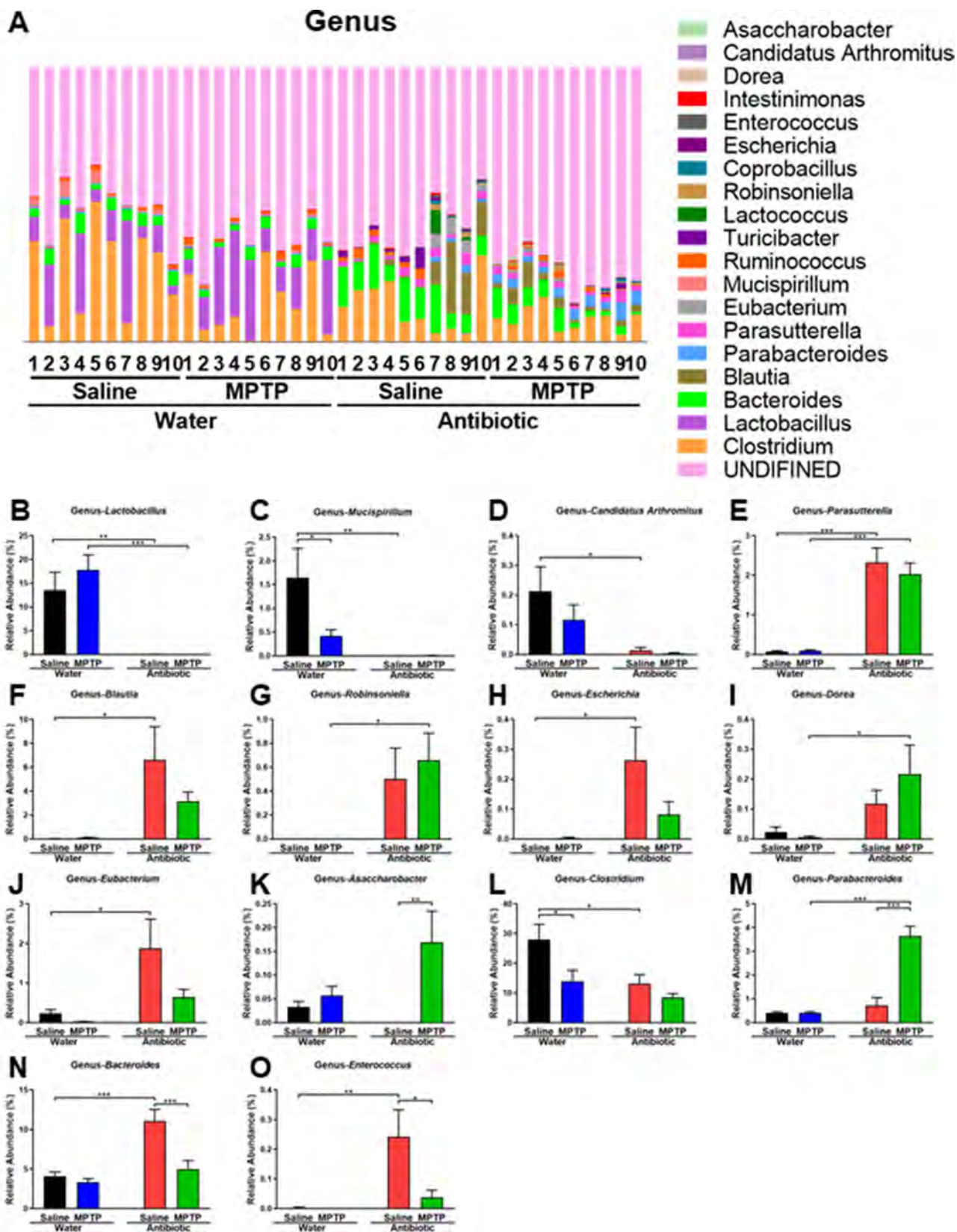


**Figure 4. Altered gut bacteria composition at the genus level.** (A) Relative abundance at the genus level. (B) *Lactobacillus*. (C) *Mucispirillum*. (D) *Candidatus Arthromitus*. (E) *Parasutterella*. (F) *Blautia*. (G) *Robinsoniella*. (H) *Escherichia*. (I) *Dorea*. (J) *Eubacterium*. (K) *Asaccharobacter*. (L) *Clostridium*. (M) *Parabacteroides*. (N) *Bacteroides*. (O) *Enterococcus*. Data are shown as mean  $\pm$  S.E.M. (n = 10). \*\*P < 0.01, \*\*\*P < 0.001. See the Supplementary Table 2 for detailed statistical analysis.

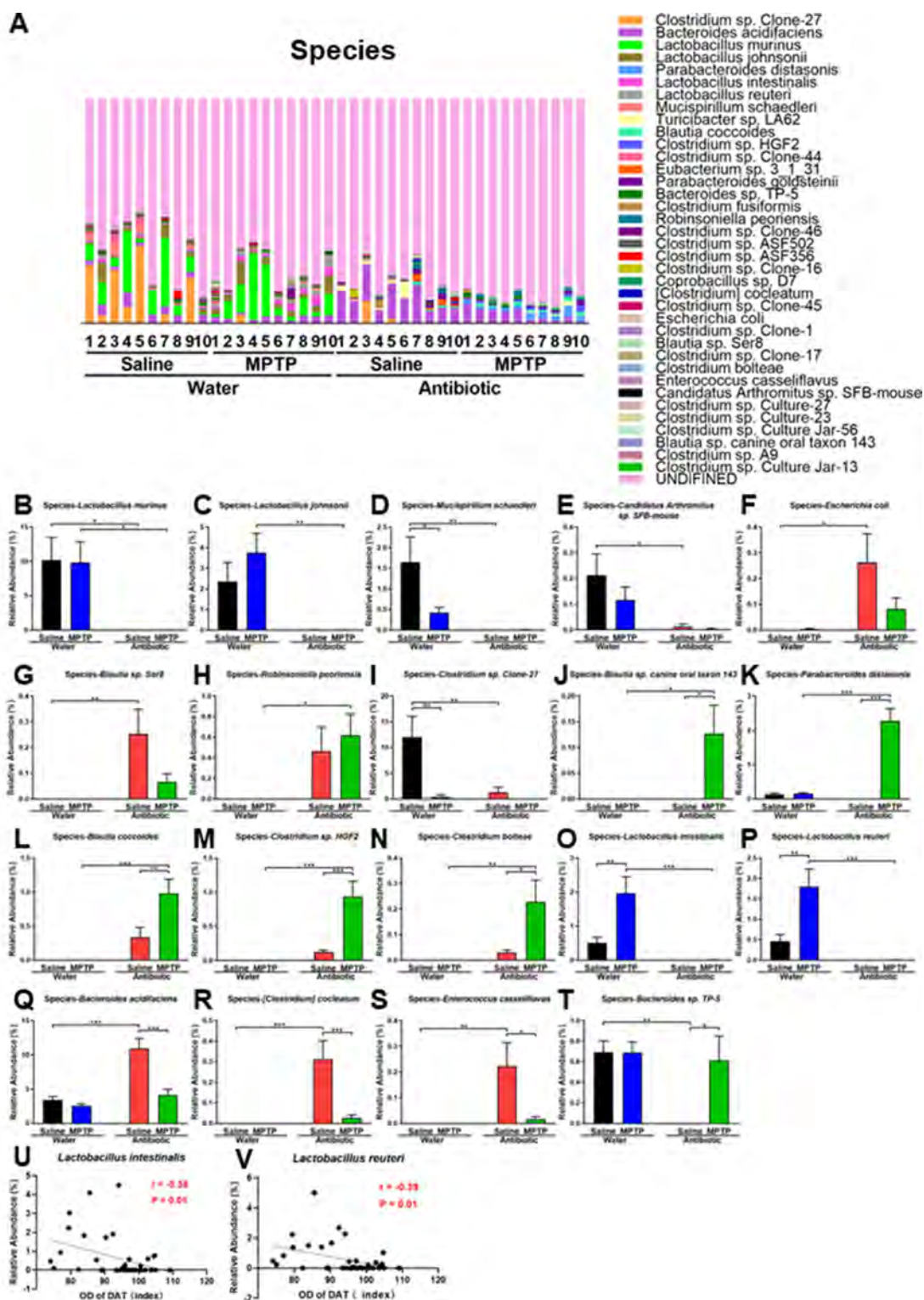


**Figure 5. Altered gut bacteria composition at the species level.** (A) Relative abundance at the species level. (B) *Lactobacillus murinus*. (C) *Lactobacillus johnsonii*. (D) *Mucispirillum schaedleri*. (E) *Candidatus Arthromitus sp. SFB-mouse*. (F) *Escherichia coli*. (G) *Blautia sp. Ser8*. (H) *Robinsoniella peoriensis*. (I) *Clostridium sp. Clone-27*. (J) *Blautia sp. canine oral taxon 143*. (K) *Parabacteroides distasonis*. (L) *Blautia coccoides*. (M) *Clostridium sp. HGF2*. (N) *Clostridium boltae*. (O) *Lactobacillus intestinalis*. (P) *Lactobacillus reuteri*. (Q) *Bacteroides acidifaciens*. (R) [*Clostridium*] *cocleatum*. (S) *Enterococcus casseliflavus*. (T) *Bacteroides sp. TP-5*. (U) Negative correlation ( $r = -0.38$ ,  $P = 0.01$ ) between *Lactobacillus intestinalis* and DAT immunoreactivity. (V) Negative correlation ( $r = -0.39$ ,  $P = 0.01$ ) between *Lactobacillus reuteri* and DAT immunoreactivity. Data are shown as mean  $\pm$  S.E.M. ( $n = 10$ ). \* $P < 0.05$ , \*\* $P < 0.01$ , \*\*\* $P < 0.001$ . See the Supplementary Table 3 for detailed statistical analysis.

MPTP specifically increased levels of the following bacterial species in the guts of antibiotic-treated mice: *Blautia sp. Canine oral taxon 143*, *Parabacteroides distasonis*, *Blautia coccoides*, *Clostridium sp. HGF2*, *Clostridium bolteae*, and *Bacteroides sp. TP-5*. A recent study demonstrated that *Parabacteroides distasonis* alleviated obesity and metabolic dysfunction via production of succinate and secondary bile acids [38]. In addition, *Parabacteroides distasonis* reduced the severity of intestinal inflammation in murine models of acute and chronic colitis induced by dextran sulphate sodium, suggesting that *Parabacteroides distasonis* may be useful for treating inflammatory bowel diseases [39]. *Blautia coccoides* produce hydrogen [13], which might have beneficial effects in the MPTP mouse model [40]. Interestingly, *Clostridium sp. HGF2* plays an important role in the metabolism of mannitol [41], which could attenuate behavioral abnormalities and aggregations of  $\alpha$ -synuclein in the rodent brain [42, 43]. Among the bacteria increased by MPTP, *Bacteroides sp. TP-5* is particularly noteworthy due to its ability to modulate immune system function [44]. Furthermore, a recent study demonstrated that fecal microbiota transplantation protected against MPTP-induced neurotoxicity by suppressing neuroinflammation [45]. The effects of supplementation with *Bacteroides sp. TP-5* on dopaminergic neurotoxicity in mouse MPTP model should be investigated further.

MPTP treatment also decreased levels of the *Bacteroides acidifaciens*, *[Clostridium] cocleatum*, and *Enterococcus casseliflavus* bacterial species. *Bacteroides acidifaciens* are important for promoting IgA production in the large intestine [46]. Interestingly, *Bacteroides acidifaciens* levels were increased in the feces of *Atg7<sup>ACD11c</sup>* mice with a lean phenotype compared to those of control *Atg7<sup>fl</sup>* mice, and wild-type C57BL/6 mice fed with a diet including *Bacteroides acidifaciens* gained less weight and fat mass than mice fed control food [47]. Those results suggest that *Bacteroides acidifaciens* might be a potential treatment for metabolic diseases such as obesity [47]. The functional roles of *[Clostridium] cocleatum* and *Enterococcus casseliflavus* are unclear, and the mechanisms underlying the recovery of the three bacterial species that increased in the gut microbiome of antibiotic-treated mice after MPTP administration in this study are currently unknown. Regardless, it is likely that interactions between the brain–gut axis and these microbiomes play a role in MPTP-induced neurotoxicity, and the relationship between neuroprotection, the immune system, and the brain–gut axis warrants further investigation.

In this study, we found that DAT immunoreactivity was negatively correlated with *Lactobacillus intestinalis* and *Lactobacillus reuteri* levels despite the marked decrease observed in these species after antibiotic treatment. Both

of these bacteria produce lactic acid, which was more abundant in the striatum of MPTP-treated mice [48]. Furthermore, treatment with *Lactobacillus reuteri* selectively rescues social deficits in genetic, environmental, and idiopathic autism spectrum disorder (ASD) models, suggesting that this species may be a promising non-invasive microbial-based therapy for ASD-related social dysfunctions [49]. Additionally, short-chain fatty acids promote proliferation of *Lactobacillus reuteri* [50]; this effect should be investigated further. It is possible that *Lactobacillus intestinalis*, *Lactobacillus reuteri*, and lactic acid might affect the dopaminergic neurotoxicity of MPTP in the brain. Furthermore, antibiotic-induced microbiome depletion might enhance or counteract MPTP-induced dopaminergic neurotoxicity in mouse brain, although the specific microbes that might be involved in these effects were not identified in this study. Additional studies are needed to confirm the relationship between MPTP-induced dopaminergic neurotoxicity and the gut microbiome.

Accumulating evidence suggests that abnormal gut microbiota composition might affect neuroprotection [8, 51, 52]. Choi et al. [53] identified dramatic and widespread increases in levels of *Enterobacteriaceae*, and particularly of *Proteus mirabilis*, in the mouse MPTP model. Administration of *Proteus mirabilis* isolated from MPTP-treated mice produced motor deficits, dopaminergic neuronal damage, and inflammation in the striatum and SNr, suggesting that *Proteus mirabilis* promotes PD pathology in the brain. Furthermore, Srivastav et al. [54] reported neuroprotective effects of a probiotic cocktail containing *Lactobacillus rhamnosus GG*, *Bifidobacterium animalis lactis*, and *Lactobacillus acidophilus* in MPTP-treated mice. Together, these results indicate that altered gut microbiota composition likely plays a role in dopaminergic neurotoxicity related to PD.

In conclusion, the present study suggests that antibiotic-induced microbiome depletion might protect against MPTP-induced dopaminergic neurotoxicity in the mouse brain, and that MPTP might improve the diversity and composition of gut microbiota in antibiotic-treated mice. These results indicate that the brain–gut axis plays a key role in the pathology of PD.

## MATERIALS AND METHODS

### Animals

Male adult C57BL/6 mice (8 weeks old) weighting 20–25 g were purchased from SLC (Inc., Hamamatsu, Japan). Animals were housed under controlled temperatures and 12-hour light/dark cycles (lights on between 07:00–19:00) with ad libitum food (CE-2; CLEA Japan, Inc., Tokyo,

Japan) and water. All experiments were carried out according to the Guide for Animal Experimentation of Chiba University. The experimental protocol was approved by the Chiba University Institutional Animal Care and Use Committee.

### **Preparation of antibiotics and MPTP**

As described in previous reports [33–35], broad-spectrum antibiotics (ampicillin 1 g/L, neomycin sulfate 1 g/L, metronidazole 1 g/L, Sigma-Aldrich Co., Ltd, St Louis, MO, USA) were dissolved in drinking water. This antibiotic cocktail, which was prepared fresh every other day, was administered to adult C57BL/6 mice for 14 continuous days. 1-Methyl-4-phenyl-1,2,3,6-tetrahydropyridine (MPTP: Tokyo Chemical Industry CO., Ltd., Tokyo, Japan) was dissolved in saline. Other compounds were purchased commercially.

### **Schedule of treatment and collection of fecal and brain samples**

The procedure for establishing MPTP-induced neurotoxicity was performed as previously reported [55, 56]. Forty mice (8 weeks old) were divided among the following four groups: water + saline; water + MPTP; antibiotic cocktail + saline; antibiotic cocktail + MPTP. Mice were given drinking water with or without the antibiotic cocktail from day 1 to day 14 (Figure 1A). All mice were given water without antibiotics from day 15 to day 22. On day 15, mice received intraperitoneal injections of MPTP (10 mg/kg x 3, 2-hr interval) or saline (5 mL/kg x 3, 2-hr interval; Figure 1A). One week after MPTP or saline injection, fresh fecal samples were collected and stored at -80°C until use. Subsequently, the mice were anesthetized with 5% isoflurane and sodium pentobarbital (50 mg/kg) for brain collection. Mice were perfused transcardially with 10 mL of isotonic saline followed by 30 mL of ice-cold 4% paraformaldehyde in 0.1 M phosphate buffer (pH 7.4). Brains were removed, post-fixed overnight at 4°C, and then used for immunohistochemical staining of dopamine transporter (DAT) and tyrosine hydroxylase (TH).

### **DAT and TH Immunohistochemistry**

Immunohistochemical staining of DAT and TH was performed as reported previously [55, 56]. Consecutive 50 µm-thick coronal brain sections (bregma 0.86–1.54 mm and -2.92–3.88 mm) were cut in ice-cold 10 mM phosphate buffered saline (pH 7.5) using a vibrating blade microtome (VT1000s, Leica Microsystems AG, Wetzlar, Germany). Free-floating sections were treated with 0.3% H<sub>2</sub>O<sub>2</sub> in 50 mM Tris-HCL saline (TBS) for 30 min and blocked in 0.2% Triton X-100 TBS (TBST) with 1.5% normal serum for 1 hour at room temperature.

Samples were then incubated for 36 hours at 4°C with rat anti-DAT antibody (1:10,000, Merck Millipore, Burlington, MA, USA) or rabbit anti-TH antibody (1:500, Sigma-Aldrich, St Louis, MO, USA). The sections were then washed three times in TBS and processed according to the avidin-biotin-peroxidase method (Vectastain Elite ABC, Vector Laboratories, Inc., Burlingame, CA, USA). Sections were then incubated with 0.15 mg/mL diaminobenzidine and 0.01% H<sub>2</sub>O<sub>2</sub> for 5 minutes; the staining solution for DAT only also contained 0.06% NiCl<sub>2</sub>. The sections were then mounted on gelatinized slides, dehydrated, cleared, and coverslipped with Permount® (Fisher Scientific, Fair Lawn, NJ, USA). Images were taken and DAT and TH immunoreactivity staining intensity in the anterior region (0.25 mm<sup>2</sup>) of the striatum as well as the number of TH-positive cells in SNr region (0.36 mm<sup>2</sup>) were analyzed using a Keyence BZ-9000 Generation microscope (Keyence Co., Ltd, Osaka, Japan). Eight data points (four brain slides) from each mouse were used for the quantitative analyses of DAT and TH immunoreactivity.

### **16S rRNA analysis**

DNA was extracted from fecal samples and 16S rRNA analyses were performed as previously described [57] by MyMetagenome Co., Ltd. (Tokyo, Japan). Briefly, PCR was performed using 27Fmod 5'-AGRGTTTGATYMTGGCTCAG-3' and 338R 5'-TGCTGCCTCCCGTAGGAGT-3' primers to amplify the V1–V2 region of the bacterial 16S rRNA gene. The amplified DNA (~330bp) was purified using AMPure XP (Beckman Coulter) and quantified using a Quant-iT Picogreen dsDNA assay kit (Invitrogen) and a TBS-380 Mini-Fluorometer (Turner Biosystems). The 16S amplicons were then sequenced using a MiSeq according to the Illumina protocol. The paired-end reads were merged using the fastq-join program based on overlapping sequences. Reads with an average quality value of <25 and inexact matches to both universal primers were filtered out. Filter-passed reads were analyzed further after trimming off both primer sequences. For each sample, 3,000 high-quality filter-passed reads were rearranged in descending order according to quality value and then clustered into operational taxonomic units (OTUs) with a 97% pairwise-identity cutoff using the UCLUST program version 5.2.32 (<https://www.drive5.com>). Taxonomic assignments of OTUs were performed based on similarity searches against the Ribosomal Database Project and the National Center for Biotechnology Information genome database using the GLSEARCH program [58].

### **Statistical analysis**

Animal experiment data are presented as the mean ± standard error of the mean (S.E.M.). Statistical analyses

were performed using SPSS Statistics 20 (SPSS, Tokyo, Japan). Body weight data were analyzed using repeated two-way analysis of variance (ANOVA) followed by *post-hoc* Tukey's multiple comparison tests. DAT and TH immunohistochemistry and 16S rDNA data were analyzed using two-way ANOVAs followed by *post-hoc* Tukey's multiple comparison tests. *P* values of less than 0.05 were considered statistically significant.

## CONFLICTS OF INTEREST

The authors have no conflicts of interest to declare.

## FUNDING

This study was supported by Smoking Research Foundation, Japan (to K.H.), and AMED, Japan (to K.H., JP19dm0107119). Ms. Siming Wang was supported by TAKASE Scholarship Foundation (Tokyo, Japan). Dr. Lijia Chang was supported by the Japan China Sasakawa Medical Fellowship (Tokyo, Japan).

## REFERENCES

1. Ascherio A, Schwarzschild MA. The epidemiology of Parkinson's disease: risk factors and prevention. *Lancet Neurol.* 2016; 15:1257–72. [https://doi.org/10.1016/S1474-4422\(16\)30230-7](https://doi.org/10.1016/S1474-4422(16)30230-7) PMID:[27751556](https://pubmed.ncbi.nlm.nih.gov/27751556/)
2. Kalia LV, Lang AE. Parkinson's disease. *Lancet.* 2015; 386:896–912. [https://doi.org/10.1016/S0140-6736\(14\)61393-3](https://doi.org/10.1016/S0140-6736(14)61393-3) PMID:[25904081](https://pubmed.ncbi.nlm.nih.gov/25904081/)
3. Wichmann T. Changing views of the pathophysiology of Parkinsonism. *Mov Disord.* 2019; 34:1130–43. <https://doi.org/10.1002/mds.27741> PMID:[31216379](https://pubmed.ncbi.nlm.nih.gov/31216379/)
4. Aho VT, Pereira PA, Voutilainen S, Paulin L, Pekkonen E, Auvinen P, Scheperjans F. Gut microbiota in Parkinson's disease: temporal stability and relations to disease progression. *EBioMedicine.* 2019; 44:691–707. <https://doi.org/10.1016/j.ebiom.2019.05.064> PMID:[31221587](https://pubmed.ncbi.nlm.nih.gov/31221587/)
5. Chiang HL, Lin CH. Altered Gut Microbiome and Intestinal Pathology in Parkinson's Disease. *J Mov Disord.* 2019; 12:67–83. <https://doi.org/10.14802/jmd.18067> PMID:[31158941](https://pubmed.ncbi.nlm.nih.gov/31158941/)
6. Dinan TG, Cryan JF. Gut instincts: microbiota as a key regulator of brain development, ageing and neurodegeneration. *J Physiol.* 2017; 595:489–503. <https://doi.org/10.1113/JP273106> PMID:[27641441](https://pubmed.ncbi.nlm.nih.gov/27641441/)
7. Felice VD, Quigley EM, Sullivan AM, O'Keefe GW, O'Mahony SM. Microbiota-gut-brain signalling in Parkinson's disease: implications for non-motor symptoms. *Parkinsonism Relat Disord.* 2016; 27:1–8. <https://doi.org/10.1016/j.parkreldis.2016.03.012> PMID:[27013171](https://pubmed.ncbi.nlm.nih.gov/27013171/)
8. Girolamo F, Coppola C, Ribatti D. Immunoregulatory effect of mast cells influenced by microbes in neurodegenerative diseases. *Brain Behav Immun.* 2017; 65:68–89. <https://doi.org/10.1016/j.bbi.2017.06.017> PMID:[28676349](https://pubmed.ncbi.nlm.nih.gov/28676349/)
9. Mulak A, Bonaz B. Brain-gut-microbiota axis in Parkinson's disease. *World J Gastroenterol.* 2015; 21:10609–20. <https://doi.org/10.3748/wjg.v21.i37.10609> PMID:[26457021](https://pubmed.ncbi.nlm.nih.gov/26457021/)
10. Parashar A, Udayabanu M. Gut microbiota: implications in Parkinson's disease. *Parkinsonism Relat Disord.* 2017; 38:1–7. <https://doi.org/10.1016/j.parkreldis.2017.02.002> PMID:[28202372](https://pubmed.ncbi.nlm.nih.gov/28202372/)
11. Scheperjans F, Aho V, Pereira PA, Koskinen K, Paulin L, Pekkonen E, Haapaniemi E, Kaakkola S, Eerola-Rautio J, Pohja M, Kinnunen E, Murros K, Auvinen P. Gut microbiota are related to Parkinson's disease and clinical phenotype. *Mov Disord.* 2015; 30:350–58. <https://doi.org/10.1002/mds.26069> PMID:[25476529](https://pubmed.ncbi.nlm.nih.gov/25476529/)
12. Scheperjans F. Gut microbiota, 1013 new pieces in the Parkinson's disease puzzle. *Curr Opin Neurol.* 2016; 29:773–80. <https://doi.org/10.1097/WCO.0000000000000389> PMID:[27653288](https://pubmed.ncbi.nlm.nih.gov/27653288/)
13. Suzuki A, Ito M, Hamaguchi T, Mori H, Takeda Y, Baba R, Watanabe T, Kurokawa K, Asakawa S, Hirayama M, Ohno K. Quantification of hydrogen production by intestinal bacteria that are specifically dysregulated in Parkinson's disease. *PLoS One.* 2018; 13:e0208313. <https://doi.org/10.1371/journal.pone.0208313> PMID:[30586410](https://pubmed.ncbi.nlm.nih.gov/30586410/)
14. Adams-Carr KL, Bestwick JP, Shribman S, Lees A, Schrag A, Noyce AJ. Constipation preceding Parkinson's disease: a systematic review and meta-analysis. *J Neurol Neurosurg Psychiatry.* 2016; 87:710–16. <https://doi.org/10.1136/jnnp-2015-311680> PMID:[26345189](https://pubmed.ncbi.nlm.nih.gov/26345189/)
15. Cusotto S, Clarke G, Dinan TG, Cryan JF. Psychotropics and the Microbiome: a Chamber of Secrets... *Psychopharmacology (Berl).* 2019; 236:1411–32. <https://doi.org/10.1007/s00213-019-5185-8> PMID:[30806744](https://pubmed.ncbi.nlm.nih.gov/30806744/)
16. Cusotto S, Sandhu KV, Dinan TG, Cryan JF. The Neuroendocrinology of the Microbiota-Gut-Brain Axis: A Behavioural Perspective. *Front Neuroendocrinol.* 2018; 51:80–101.

- <https://doi.org/10.1016/j.yfrne.2018.04.002>  
PMID:29753796
17. Cusotto S, Strain CR, Fouhy F, Strain RG, Peterson VL, Clarke G, Stanton C, Dinan TG, Cryan JF. Differential effects of psychotropic drugs on microbiome composition and gastrointestinal function. *Psychopharmacology (Berl)*. 2019; 236:1671–85.  
<https://doi.org/10.1007/s00213-018-5006-5>  
PMID:30155748
  18. Forsythe P, Kunze W, Bienenstock J. Moody microbes or fecal phrenology: what do we know about the microbiota-gut-brain axis? *BMC Med*. 2016; 14:58.  
<https://doi.org/10.1186/s12916-016-0604-8>  
PMID:27090095
  19. Fung TC, Olson CA, Hsiao EY. Interactions between the microbiota, immune and nervous systems in health and disease. *Nat Neurosci*. 2017; 20:145–55.  
<https://doi.org/10.1038/nn.4476>  
PMID:28092661
  20. Kelly JR, Clarke G, Cryan JF, Dinan TG. Brain-gut-microbiota axis: challenges for translation in psychiatry. *Ann Epidemiol*. 2016; 26:366–72.  
<https://doi.org/10.1016/j.annepidem.2016.02.008>  
PMID:27005587
  21. Ma Q, Xing C, Long W, Wang HY, Liu Q, Wang RF. Impact of microbiota on central nervous system and neurological diseases: the gut-brain axis. *J Neuroinflammation*. 2019; 16:53.  
<https://doi.org/10.1186/s12974-019-1434-3>  
PMID:30823925
  22. Molina-Torres G, Rodriguez-Arrastia M, Roman P, Sanchez-Labraca N, Cardona D. Stress and the gut microbiota-brain axis. *Behav Pharmacol*. 2019; 30:187–200.  
<https://doi.org/10.1097/FBP.0000000000000478>  
PMID:30844962
  23. Round JL, Mazmanian SK. The gut microbiota shapes intestinal immune responses during health and disease. *Nat Rev Immunol*. 2009; 9:313–23.  
<https://doi.org/10.1038/nri2515>  
PMID:19343057
  24. Champagne-Jorgensen K, Kunze WA, Forsythe P, Bienenstock J, McVey Neufeld KA. Antibiotics and the nervous system: more than just the microbes? *Brain Behav Immun*. 2019; 77:7–15.  
<https://doi.org/10.1016/j.bbi.2018.12.014>  
PMID:30582961
  25. Ianiro G, Tilg H, Gasbarrini A. Antibiotics as deep modulators of gut microbiota: between good and evil. *Gut*. 2016; 65:1906–15.  
<https://doi.org/10.1136/gutjnl-2016-312297>  
PMID:27531828
  26. Antonopoulos DA, Huse SM, Morrison HG, Schmidt TM, Sogin ML, Young VB. Reproducible community dynamics of the gastrointestinal microbiota following antibiotic perturbation. *Infect Immun*. 2009; 77:2367–75.  
<https://doi.org/10.1128/IAI.01520-08>  
PMID:19307217
  27. Becattini S, Taur Y, Pamer EG. Antibiotic-Induced Changes in the Intestinal Microbiota and Disease. *Trends Mol Med*. 2016; 22:458–78.  
<https://doi.org/10.1016/j.molmed.2016.04.003>  
PMID:27178527
  28. Davey KJ, Cotter PD, O’Sullivan O, Crispie F, Dinan TG, Cryan JF, O’Mahony SM. Antipsychotics and the gut microbiome: olanzapine-induced metabolic dysfunction is attenuated by antibiotic administration in the rat. *Transl Psychiatry*. 2013; 3:e309.  
<https://doi.org/10.1038/tp.2013.83>  
PMID:24084940
  29. Jernberg C, Löfmark S, Edlund C, Jansson JK. Long-term ecological impacts of antibiotic administration on the human intestinal microbiota. *ISME J*. 2007; 1:56–66.  
<https://doi.org/10.1038/ismej.2007.3>  
PMID:18043614
  30. Kim S, Covington A, Pamer EG. The intestinal microbiota: Antibiotics, colonization resistance, and enteric pathogens. *Immunol Rev*. 2017; 279:90–105.  
<https://doi.org/10.1111/imr.12563>  
PMID:28856737
  31. Young VB, Schmidt TM. Antibiotic-associated diarrhea accompanied by large-scale alterations in the composition of the fecal microbiota. *J Clin Microbiol*. 2004; 42:1203–06.  
<https://doi.org/10.1128/JCM.42.3.1203-1206.2004>  
PMID:15004076
  32. Zarrinpar A, Chaix A, Xu ZZ, Chang MW, Marotz CA, Saghatelian A, Knight R, Panda S. Antibiotic-induced microbiome depletion alters metabolic homeostasis by affecting gut signaling and colonic metabolism. *Nat Commun*. 2018; 9:2872.  
<https://doi.org/10.1038/s41467-018-05336-9>  
PMID:30030441
  33. Yang C, Fang X, Zhan G, Huang N, Li S, Bi J, Jiang R, Yang L, Miao L, Zhu B, Luo A, Hashimoto K. Key role of gut microbiota in anhedonia-like phenotype in rodents with neuropathic pain. *Transl Psychiatry*. 2019; 9:57.  
<https://doi.org/10.1038/s41398-019-0379-8>  
PMID:30705252
  34. Zhan G, Yang N, Li S, Huang N, Fang X, Zhang J, Zhu B, Yang L, Yang C, Luo A. Abnormal gut microbiota composition contributes to cognitive dysfunction in

- SAMP8 mice. Aging (Albany NY). 2018; 10:1257–67.  
<https://doi.org/10.18632/aging.101464>  
PMID:29886457
35. Zhang J, Bi JJ, Guo GJ, Yang L, Zhu B, Zhan GF, Li S, Huang NN, Hashimoto K, Yang C, Luo AL. Abnormal composition of gut microbiota contributes to delirium-like behaviors after abdominal surgery in mice. CNS Neurosci Ther. 2019; 25:685–96.  
<https://doi.org/10.1111/cns.13103> PMID:30680947
36. Sampson TR, Debelius JW, Thron T, Janssen S, Shastri GG, Ilhan ZE, Challis C, Schretter CE, Rocha S, Gradinaru V, Chesselet MF, Keshavarzian A, Shannon KM, et al. Gut Microbiota Regulate Motor Deficits and Neuroinflammation in a Model of Parkinson's Disease. Cell. 2016; 167:1469–1480.e12.  
<https://doi.org/10.1016/j.cell.2016.11.018>  
PMID:27912057
37. Jackson-Lewis V, Przedborski S. Protocol for the MPTP mouse model of Parkinson's disease. Nat Protoc. 2007; 2:141–51.  
<https://doi.org/10.1038/nprot.2006.342>  
PMID:17401348
38. Wang K, Liao M, Zhou N, Bao L, Ma K, Zheng Z, Wang Y, Liu C, Wang W, Wang J, Liu SJ, Liu H. Parabacteroides distasonis Alleviates Obesity and Metabolic Dysfunctions via Production of Succinate and Secondary Bile Acids. Cell Rep. 2019; 26:222–235.e5.  
<https://doi.org/10.1016/j.celrep.2018.12.028>  
PMID:30605678
39. Kverka M, Zakostelska Z, Klimesova K, Sokol D, Hudcovic T, Hrcir T, Rossmann P, Mrazek J, Kopečný J, Verdu EF, Tlaskalova-Hogenova H. Oral administration of Parabacteroides distasonis antigens attenuates experimental murine colitis through modulation of immunity and microbiota composition. Clin Exp Immunol. 2011; 163:250–59.  
<https://doi.org/10.1111/j.1365-2249.2010.04286.x>  
PMID:21087444
40. Fujita K, Seike T, Yutsudo N, Ohno M, Yamada H, Yamaguchi H, Sakumi K, Yamakawa Y, Kido MA, Takaki A, Katafuchi T, Tanaka Y, Nakabeppu Y, Noda M. Hydrogen in drinking water reduces dopaminergic neuronal loss in the 1-methyl-4-phenyl-1,2,3,6-tetrahydropyridine mouse model of Parkinson's disease. PLoS One. 2009; 4:e7247.  
<https://doi.org/10.1371/journal.pone.0007247>  
PMID:19789628
41. Feng Q, Liu Z, Zhong S, Li R, Xia H, Jie Z, Wen B, Chen X, Yan W, Fan Y, Guo Z, Meng N, Chen J, et al. Integrated metabolomics and metagenomics analysis of plasma and urine identified microbial metabolites associated with coronary heart disease. Sci Rep. 2016; 6:22525.  
<https://doi.org/10.1038/srep22525>  
PMID:26932197
42. Shaltiel-Karyo R, Frenkel-Pinter M, Rockenstein E, Patrick C, Levy-Sakin M, Schiller A, Egoz-Matia N, Masliah E, Segal D, Gazit E. A blood-brain barrier (BBB) disrupter is also a potent  $\alpha$ -synuclein ( $\alpha$ -syn) aggregation inhibitor: a novel dual mechanism of mannitol for the treatment of Parkinson disease (PD). J Biol Chem. 2013; 288:17579–88.  
<https://doi.org/10.1074/jbc.M112.434787>  
PMID:23637226
43. Paul A, Zhang BD, Mohapatra S, Li G, Li YM, Gazit E, Segal D. Novel Mannitol-Based Small Molecules for Inhibiting Aggregation of  $\alpha$ -Synuclein Amyloids in Parkinson's Disease. Front Mol Biosci. 2019; 6:16.  
<https://doi.org/10.3389/fmolb.2019.00016>  
PMID:30968030
44. Lazar V, Ditu LM, Pircalabioru GG, Gheorghe I, Curutiu C, Holban AM, Picu A, Petcu L, Chifiriuc MC. Aspects of Gut Microbiota and Immune System Interactions in Infectious Diseases, Immunopathology, and Cancer. Front Immunol. 2018; 9:1830.  
<https://doi.org/10.3389/fimmu.2018.01830>  
PMID:30158926
45. Sun MF, Zhu YL, Zhou ZL, Jia XB, Xu YD, Yang Q, Cui C, Shen YQ. Neuroprotective effects of fecal microbiota transplantation on MPTP-induced Parkinson's disease mice: gut microbiota, glial reaction and TLR4/TNF- $\alpha$  signaling pathway. Brain Behav Immun. 2018; 70:48–60.  
<https://doi.org/10.1016/j.bbi.2018.02.005>  
PMID:29471030
46. Yanagibashi T, Hosono A, Oyama A, Tsuda M, Suzuki A, Hachimura S, Takahashi Y, Momose Y, Itoh K, Hirayama K, Takahashi K, Kaminogawa S. IgA production in the large intestine is modulated by a different mechanism than in the small intestine: bacteroides acidifaciens promotes IgA production in the large intestine by inducing germinal center formation and increasing the number of IgA+ B cells. Immunobiology. 2013; 218:645–51.  
<https://doi.org/10.1016/j.imbio.2012.07.033>  
PMID:22940255
47. Yang JY, Lee YS, Kim Y, Lee SH, Ryu S, Fukuda S, Hase K, Yang CS, Lim HS, Kim MS, Kim HM, Ahn SH, Kwon BE, et al. Gut commensal Bacteroides acidifaciens prevents obesity and improves insulin sensitivity in mice. Mucosal Immunol. 2017; 10:104–16.  
<https://doi.org/10.1038/mi.2016.42>  
PMID:27118489
48. Koga K, Mori A, Ohashi S, Kurihara N, Kitagawa H, Ishikawa M, Mitsumoto Y, Nakai M. H MRS identifies lactate rise in the striatum of MPTP-treated C57BL/6 mice. Eur J Neurosci. 2006; 23:1077–81.

- <https://doi.org/10.1111/j.1460-9568.2006.04610.x>  
PMID:[16519673](https://pubmed.ncbi.nlm.nih.gov/16519673/)
49. Sgritta M, Dooling SW, Buffington SA, Momin EN, Francis MB, Britton RA, Costa-Mattioli M. Mechanisms underlying microbial-mediated changes in social behavior in mouse models of autism spectrum disorder. *Neuron*. 2019; 101:246–259.e6.  
<https://doi.org/10.1016/j.neuron.2018.11.018>  
PMID:[30522820](https://pubmed.ncbi.nlm.nih.gov/30522820/)
50. Oh JH, Alexander LM, Pan M, Schueler KL, Keller MP, Attie AD, Walter J, van Pijkeren JP. Dietary fructose and microbiota-derived short-chain fatty acids promote bacteriophage production in the gut symbiont *Lactobacillus reuteri*. *Cell Host Microbe*. 2019; 25:273–284.e6.  
<https://doi.org/10.1016/j.chom.2018.11.016>  
PMID:[30658906](https://pubmed.ncbi.nlm.nih.gov/30658906/)
51. Kigerl KA, Hall JC, Wang L, Mo X, Yu Z, Popovich PG. Gut dysbiosis impairs recovery after spinal cord injury. *J Exp Med*. 2016; 213:2603–20.  
<https://doi.org/10.1084/jem.20151345>  
PMID:[27810921](https://pubmed.ncbi.nlm.nih.gov/27810921/)
52. Zhu CS, Grandhi R, Patterson TT, Nicholson SE. A Review of Traumatic Brain Injury and the Gut Microbiome: Insights into Novel Mechanisms of Secondary Brain Injury and Promising Targets for Neuroprotection. *Brain Sci*. 2018; 8:E113.  
<https://doi.org/10.3390/brainsci8060113>  
PMID:[29921825](https://pubmed.ncbi.nlm.nih.gov/29921825/)
53. Choi JG, Kim N, Ju IG, Eo H, Lim SM, Jang SE, Kim DH, Oh MS. Oral administration of *Proteus mirabilis* damages dopaminergic neurons and motor functions in mice. *Sci Rep*. 2018; 8:1275.  
<https://doi.org/10.1038/s41598-018-19646-x>  
PMID:[29352191](https://pubmed.ncbi.nlm.nih.gov/29352191/)
54. Srivastav S, Neupane S, Bhurtel S, Katila N, Maharjan S, Choi H, Hong JT, Choi DY. Probiotics mixture increases butyrate, and subsequently rescues the nigral dopaminergic neurons from MPTP and rotenone-induced neurotoxicity. *J Nutr Biochem*. 2019; 69:73–86.  
<https://doi.org/10.1016/j.jnutbio.2019.03.021>  
PMID:[31063918](https://pubmed.ncbi.nlm.nih.gov/31063918/)
55. Pu Y, Qu Y, Chang L, Wang SM, Zhang K, Ushida Y, Saganuma H, Hashimoto K. Dietary intake of glucoraphanin prevents the reduction of dopamine transporter in the mouse striatum after repeated administration of MPTP. *Neuropsychopharmacol Rep*. 2019. [Epub ahead of print].  
<https://doi.org/10.1002/npr2.12060> PMID:[31132231](https://pubmed.ncbi.nlm.nih.gov/31132231/)
56. Ren Q, Ma M, Yang J, Nonaka R, Yamaguchi A, Ishikawa KI, Kobayashi K, Murayama S, Hwang SH, Saiki S, Akamatsu W, Hattori N, Hammock BD, Hashimoto K. Soluble epoxide hydrolase plays a key role in the pathogenesis of Parkinson's disease. *Proc Natl Acad Sci USA*. 2018; 115:E5815–23.  
<https://doi.org/10.1073/pnas.1802179115>  
PMID:[29735655](https://pubmed.ncbi.nlm.nih.gov/29735655/)
57. Kim SW, Suda W, Kim S, Oshima K, Fukuda S, Ohno H, Morita H, Hattori M. Robustness of gut microbiota of healthy adults in response to probiotic intervention revealed by high-throughput pyrosequencing. *DNA Res*. 2013; 20:241–53.  
<https://doi.org/10.1093/dnares/dst006>  
PMID:[23571675](https://pubmed.ncbi.nlm.nih.gov/23571675/)
58. Tanoue T, Morita S, Plichta DR, Skelly AN, Suda W, Sugiura Y, Narushima S, Vlamakis H, Motoo I, Sugita K, Shiota A, Takeshita K, Yasuma-Mitobe K, et al. A defined commensal consortium elicits CD8 T cells and anti-cancer immunity. *Nature*. 2019; 565:600–05.  
<https://doi.org/10.1038/s41586-019-0878-z>  
PMID:[30675064](https://pubmed.ncbi.nlm.nih.gov/30675064/)



## SUPPLEMENTARY MATERIALS

### Supplementary Tables

**Supplementary Table 1. Statistical analysis data of gut microbiota data at phylum.**

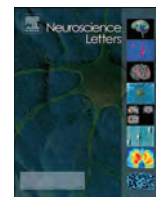
<b>Graph</b>	<b>Factor effect (Antibiotic)</b>	<b>Factor effect (MPTP)</b>	<b>Interaction effect (Antibiotic × MPTP)</b>
<i>Bacteroidetes</i>	$F_{(1,36)} = 12.695, P = 0.001$	$F_{(1,36)} = 21.180, P < 0.001$	$F_{(1,36)} = 1.806, P = 0.187$
<i>Firmicutes</i>	$F_{(1,36)} = 14.284, P = 0.001$	$F_{(1,36)} = 20.353, P < 0.001$	$F_{(1,36)} = 2.272, P = 0.140$
<i>Proteobacteria</i>	$F_{(1,36)} = 40.495, P < 0.001$	$F_{(1,36)} = 1.034, P = 0.316$	$F_{(1,36)} = 0.190, P = 0.665$
<i>Deferribacteres</i>	$F_{(1,36)} = 10.911, P = 0.002$	$F_{(1,36)} = 3.872, P = 0.057$	$F_{(1,36)} = 3.948, P = 0.055$
<i>TM7</i>	$F_{(1,36)} = 10.916, P = 0.002$	$F_{(1,36)} = 10.916, P = 0.002$	$F_{(1,36)} = 10.916, P = 0.002$

**Supplementary Table 2. Statistical analysis data of gut microbiota data at genus.**

<b>Graph</b>	<b>Factor effect (Antibiotic)</b>	<b>Factor effect (MPTP)</b>	<b>Interaction effect (Antibiotic × MPTP)</b>
<i>Lactobacillus</i>	$F_{(1,36)} = 40.826, P < 0.001$	$F_{(1,36)} = 0.743, P = 0.394$	$F_{(1,36)} = 0.744, P = 0.394$
<i>Mucispirillum</i>	$F_{(1,36)} = 10.835, P = 0.002$	$F_{(1,36)} = 3.818, P = 0.059$	$F_{(1,36)} = 3.893, P = 0.056$
<i>Candidatus Arthromitus</i>	$F_{(1,36)} = 10.302, P = 0.003$	$F_{(1,36)} = 1.204, P = 0.280$	$F_{(1,36)} = 0.796, P = 0.378$
<i>Parasutterella</i>	$F_{(1,36)} = 81.500, P < 0.001$	$F_{(1,36)} = 0.344, P = 0.561$	$F_{(1,36)} = 0.495, P = 0.486$
<i>Blautia</i>	$F_{(1,36)} = 11.239, P = 0.002$	$F_{(1,36)} = 1.430, P = 0.240$	$F_{(1,36)} = 1.542, P = 0.222$
<i>Robinsoniella</i>	$F_{(1,36)} = 11.589, P = 0.002$	$F_{(1,36)} = 0.211, P = 0.649$	$F_{(1,36)} = 0.211, P = 0.649$
<i>Escherichia</i>	$F_{(1,36)} = 8.289, P = 0.007$	$F_{(1,36)} = 2.245, P = 0.143$	$F_{(1,36)} = 2.399, P = 0.130$
<i>Dorea</i>	$F_{(1,36)} = 7.766, P = 0.008$	$F_{(1,36)} = 0.548, P = 0.464$	$F_{(1,36)} = 1.104, P = 0.300$
<i>Eubacterium</i>	$F_{(1,36)} = 8.529, P = 0.006$	$F_{(1,36)} = 3.508, P = 0.069$	$F_{(1,36)} = 1.747, P = 0.195$
<i>Asaccharobacter</i>	$F_{(1,36)} = 1.292, P = 0.263$	$F_{(1,36)} = 7.712, P = 0.009$	$F_{(1,36)} = 4.353, P = 0.044$
<i>Clostridium</i>	$F_{(1,36)} = 7.982, P = 0.008$	$F_{(1,36)} = 6.757, P = 0.013$	$F_{(1,36)} = 1.664, P = 0.205$
<i>Parabacteroides</i>	$F_{(1,36)} = 43.663, P < 0.001$	$F_{(1,36)} = 29.742, P < 0.001$	$F_{(1,36)} = 29.742, P < 0.001$
<i>Bacteroides</i>	$F_{(1,36)} = 19.018, P < 0.001$	$F_{(1,36)} = 12.176, P = 0.001$	$F_{(1,36)} = 7.447, P = 0.010$
<i>Enterococcus</i>	$F_{(1,36)} = 8.910, P = 0.005$	$F_{(1,36)} = 4.904, P = 0.033$	$F_{(1,36)} = 4.624, P = 0.038$

**Supplementary Table 3. Statistical analysis data of gut microbiota data at species.**

<b>Graph</b>	<b>Factor effect (Antibiotic)</b>	<b>Factor effect (MPTP)</b>	<b>Interaction effect (Antibiotic × MPTP)</b>
<i>Lactobacillus murinus</i>	F <sub>(1,36)</sub> = 19.973, P < 0.001	F <sub>(1,36)</sub> = 0.007, P = 0.935	F <sub>(1,36)</sub> = 0.006, P = 0.936
<i>Lactobacillus johnsonii</i>	F <sub>(1,36)</sub> = 21.666, P < 0.001	F <sub>(1,36)</sub> = 1.126, P = 0.296	F <sub>(1,36)</sub> = 1.126, P = 0.296
<i>Mucispirillum schaedleri</i>	F <sub>(1,36)</sub> = 10.803, P = 0.002	F <sub>(1,36)</sub> = 3.836, P = 0.058	F <sub>(1,36)</sub> = 3.912, P = 0.056
<i>Candidatus Arthromitus sp. SFB-mouse</i>	F <sub>(1,36)</sub> = 10.302, P = 0.003	F <sub>(1,36)</sub> = 1.204, P = 0.280	F <sub>(1,36)</sub> = 0.796, P = 0.378
<i>Escherichia coli</i>	F <sub>(1,36)</sub> = 8.289, P = 0.007	F <sub>(1,36)</sub> = 2.245, P = 0.143	F <sub>(1,36)</sub> = 2.399, P = 0.130
<i>Blautia sp. Ser8</i>	F <sub>(1,36)</sub> = 10.059, P = 0.003	F <sub>(1,36)</sub> = 3.457, P = 0.071	F <sub>(1,36)</sub> = 3.457, P = 0.071
<i>Robinsoniella peoriensis</i>	F <sub>(1,36)</sub> = 11.921, P = 0.001	F <sub>(1,36)</sub> = 0.239, P = 0.628	F <sub>(1,36)</sub> = 0.239, P = 0.628
<i>Clostridium sp. Clone-27</i>	F <sub>(1,36)</sub> = 6.957, P = 0.012	F <sub>(1,36)</sub> = 9.366, P = 0.004	F <sub>(1,36)</sub> = 6.036, P = 0.019
<i>Blautia sp. canine oral taxon 143</i>	F <sub>(1,36)</sub> = 5.309, P = 0.027	F <sub>(1,36)</sub> = 5.309, P = 0.027	F <sub>(1,36)</sub> = 5.309, P = 0.027
<i>Parabacteroides distasonis</i>	F <sub>(1,36)</sub> = 30.573, P < 0.001	F <sub>(1,36)</sub> = 40.561, P < 0.001	F <sub>(1,36)</sub> = 39.576, P < 0.001
<i>Blautia coccoides</i>	F <sub>(1,36)</sub> = 26.794, P < 0.001	F <sub>(1,36)</sub> = 6.406, P = 0.016	F <sub>(1,36)</sub> = 6.406, P = 0.016
<i>Clostridium sp. HGF2</i>	F <sub>(1,36)</sub> = 21.898, P < 0.001	F <sub>(1,36)</sub> = 12.850, P = 0.001	F <sub>(1,36)</sub> = 12.850, P = 0.001
<i>Clostridium bolteae</i>	F <sub>(1,36)</sub> = 8.670, P = 0.006	F <sub>(1,36)</sub> = 5.094, P = 0.030	F <sub>(1,36)</sub> = 5.094, P = 0.030
<i>Lactobacillus intestinalis</i>	F <sub>(1,36)</sub> = 23.328, P < 0.001	F <sub>(1,36)</sub> = 8.172, P = 0.007	F <sub>(1,36)</sub> = 8.105, P = 0.007
<i>Lactobacillus reuteri</i>	F <sub>(1,36)</sub> = 23.676, P < 0.001	F <sub>(1,36)</sub> = 8.288, P = 0.007	F <sub>(1,36)</sub> = 8.214, P = 0.007
<i>Bacteroides acidifaciens</i>	F <sub>(1,36)</sub> = 26.102, P < 0.001	F <sub>(1,36)</sub> = 18.528, P < 0.001	F <sub>(1,36)</sub> = 11.141, P = 0.002
<i>[Clostridium] cocleatum</i>	F <sub>(1,36)</sub> = 14.097, P = 0.001	F <sub>(1,36)</sub> = 9.975, P = 0.003	F <sub>(1,36)</sub> = 9.975, P = 0.003
<i>Enterococcus casseliflavus</i>	F <sub>(1,36)</sub> = 6.743, P = 0.014	F <sub>(1,36)</sub> = 5.058, P = 0.031	F <sub>(1,36)</sub> = 5.058, P = 0.031
<i>Bacteroides sp. TP-5</i>	F <sub>(1,36)</sub> = 7.426, P = 0.010	F <sub>(1,36)</sub> = 4.685, P = 0.037	F <sub>(1,36)</sub> = 4.747, P = 0.036



## Research article

# Glyphosate exposure exacerbates the dopaminergic neurotoxicity in the mouse brain after repeated administration of MPTP



Yaoyu Pu, Lijia Chang, Youge Qu, Siming Wang, Yunfei Tan, Xingming Wang, Jiancheng Zhang, Kenji Hashimoto\*

Division of Clinical Neuroscience, Chiba University Center for Forensic Mental Health, Chiba, 260-8670, Japan

## ARTICLE INFO

## Keywords:

Dopamine transporter  
Glyphosate  
Tyrosine hydroxylase  
Parkinson disease

## ABSTRACT

Parkinson's disease (PD) is a chronic and progressive neurodegenerative disorder. Epidemiological studies suggest that the exposure of the herbicide glyphosate may influence the development of PD in humans. In this study, we examined whether the exposure of glyphosate can affect the reduction of dopamine transporter (DAT) in the striatum and tyrosine hydroxylase (TH) in the substantia nigra (SNr) of mouse brain after repeated administration of 1-methyl-4-phenyl-1,2,3,6-tetrahydropyridine (MPTP). Repeated injections of MPTP (10 mg/kg  $\times$  3, 2-h interval) significantly decreased the density of DAT-immunoreactivity in the striatum and the number of TH-immunoreactivity in the SNr. Glyphosate exposure for 14 days significantly potentiated MPTP-induced dopaminergic neurotoxicity in the striatum and SNr of mouse brain. This study suggests that glyphosate exposure might exacerbate MPTP-induced dopaminergic neurotoxicity in the striatum and SNr of adult mice. It is likely that exposure of glyphosate may be an environmental risk factor for PD since glyphosate has been used widely in the world.

## 1. Introduction

Parkinson's disease (PD) is the common neurodegenerative disorder that affects predominately dopaminergic neurons in the substantia nigra (SNr) [1,11]. Although the molecular mechanisms underlying PD pathology are unclear, the agrochemicals such as the pesticide rotenone and the herbicide paraquat may be involved in the pathology of PD [12]. For example, a meta-analysis showed a high association between paraquat exposure and PD (odds ratio = 1.64) [20].

Glyphosate [*N*-(phosphonomethyl)glycine], the world's most heavily applied herbicide, is an active ingredient in Roundup®. It is reported that people exposed to glyphosate had 33% higher odds (odds ratio = 1.33) of premature mortality from PD than those that were not exposed [3]. In contrast, exposure to other agrochemicals such as paraquat, atrazine, or diazinon was not associated with premature mortality from PD [3]. Furthermore, there are some cases who developed PD after ingesting glyphosate [2,6,24]. However, there are no reports investigating the effects of glyphosate exposure in the animal models of PD.

This study was undertaken to investigate whether the exposure of glyphosate could affect the dopaminergic neurotoxicity in the striatum and SNr of mouse brain after the repeated administration of 1-methyl-4-

phenyl-1,2,3,6-tetrahydropyridine (MPTP) since MPTP-induced dopaminergic neurotoxicity has been widely used as animal model of PD [10].

## 2. Methods and materials

## 2.1. Animals

Male adult C57BL/6 mice (10 weeks old, body weight 20–25 g, Japan SLC, Inc., Hamamatsu, Japan) were used. Mice were housed in room temperature (23  $\pm$  1 °C), humidity (55  $\pm$  5%) and 12-h light/dark cycles (lights on between 07:00–19:00) with *ad libitum* food and water. The experimental protocol of this study was approved by the Chiba University Institutional Animal Care and Use Committee (permission number: 2-314).

## 2.2. Exposure of glyphosate

In this study, we used commercially available Roundup® Maxload [48% (w/v) glyphosate (*N*-phosphonomethylglycine) potassium salt, 52% other ingredients such as water and surfactant. Lot number: 11946898. Nissan Chemical Corporation, Tokyo, Japan], as previously

\* Corresponding author.

E-mail address: [hashimoto@faculty.chiba-u.jp](mailto:hashimoto@faculty.chiba-u.jp) (K. Hashimoto).

<https://doi.org/10.1016/j.neulet.2020.135032>

Received 20 April 2020; Received in revised form 28 April 2020; Accepted 1 May 2020

Available online 07 May 2020

0304-3940/ © 2020 Elsevier B.V. All rights reserved.

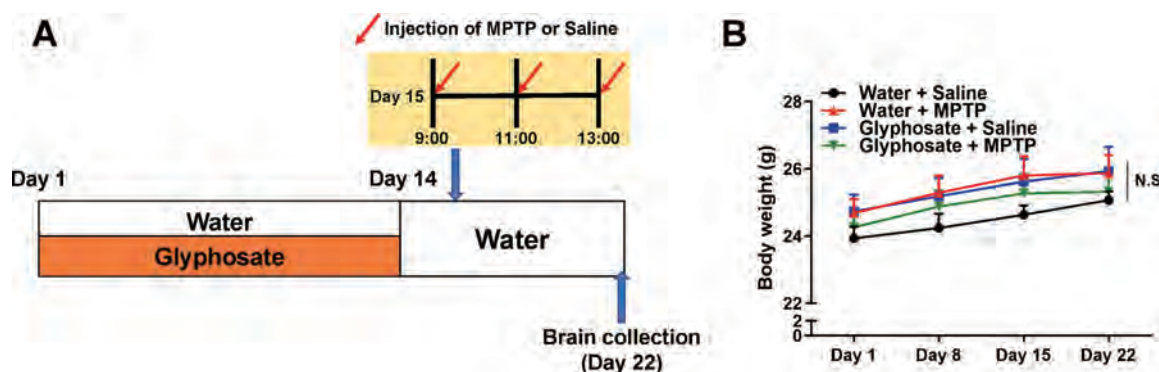


Fig. 1. Schedule of drinking water including glyphosate and MPTP treatment.

(A): Water or water including 0.098% formulated glyphosate was given to male mice (10 week old) (day 1–day 14). On day 15, mice received three injections of MPTP (10 mg/kg at 9:00, 11:00, 13:00, i.p.) or saline (5 ml/kg at 9:00, 11:00 and 13:00). Mice were perfused 7 days after the administration of MPTP (day 22). (B): Time course of body weight. There were no statistical changes among the four groups. Each value is the mean  $\pm$  SEM ( $n = 8$ –10 per group). N.S.: not significant.

reported [15]. Water or formulated glyphosate [or 0.098% Roundup<sup>®</sup>] was given to the adult mice for 14 days (day 1–day 14) as drinking water (Fig. 1). The concentration of formulated glyphosate (0.098%) was used as previously reported [15].

### 2.3. Dopaminergic neurotoxicity after MPTP administration

The protocol of MPTP-induced dopaminergic neurotoxicity was used as previously reported [7,16–18]. Male mice (10 weeks old) were divided into the following four groups: water + saline (5 mL/kg  $\times$  3, 2-hr interval) group; water + MPTP (10 mg/kg  $\times$  3, 2-hr interval, Tokyo Chemical Industry CO., Ltd., Tokyo, Japan) group; glyphosate + saline group; glyphosate + MPTP group (Fig. 1). MPTP or saline was injected intraperitoneally into mice on day 15. Seven days (day 22) after administration of MPTP, mice were anesthetized with 5% isoflurane and sodium pentobarbital (50 mg/kg), and perfused transcardially with 10 mL of isotonic saline, followed by 30 mL of ice-cold 4% paraformaldehyde in 0.1 M phosphate buffer (pH 7.4). Brains were removed from the skulls and postfixed overnight at 4 °C. Subsequently, brain was used for immunohistochemistry of dopamine transporter (DAT) and tyrosine hydrolase (TH).

### 2.4. DAT and TH immunohistochemistry

Immunohistochemistry of DAT and TH was performed as reported previously [16–18]. The free-floating mouse brain sections (bregma 0.86–1.54 mm and  $-2.92$  to  $-3.88$  mm) were put in 0.3% H<sub>2</sub>O<sub>2</sub> in 0.05 M Tris–HCl saline (TBS) for 30 min and blocked in 0.2% Triton X-100 TBS (TBST) with 1.5% normal serum for 1 h, at room temperature. Samples were then incubated for 36 h at 4 °C, with rat anti-DAT antibody (1:10,000, Merck Millipore, Burlington, MA, USA) or rabbit anti-TH antibody (1:500, Sigma-Aldrich, St Louis, MO, USA). The sections were processed according to the avidin-biotin-peroxidase method (Vectastain Elite ABC, Vector Laboratories, Inc., Burlingame, CA, USA). Sections were then reacted with 0.15 mg/mL diaminobenzidine, containing 0.01% H<sub>2</sub>O<sub>2</sub> for 5 min; the staining solution for DAT only also contained 0.06% NiCl<sub>2</sub>. Then the sections were mounted on gelatinized slides, dehydrated, cleared, and coverslipped under Permount<sup>®</sup> (Fisher Scientific, Fair Lawn, NJ, USA). Next, sections were imaged, and the staining intensity of DAT immunoreactivity in the anterior regions (0.25 mm<sup>2</sup>) of the striatum as well as the number of TH-positive cells in SNr region (0.36 mm<sup>2</sup>) were analyzed using a light microscope equipped with a CCD camera (Olympus IX70) and the SCION IMAGE software package. Eight sections from each mouse were used for the quantitative analyses of DAT and TH immunoreactivity.

### 2.5. Statistical analysis

The animal experiment data was expressed as the mean  $\pm$  standard error of the mean (S.E.M.). The statistical analysis was performed using SPSS Statistics 20 (SPSS, Tokyo, Japan). Data were analyzed using two-way analyses of variance (ANOVA), followed *post-hoc* Tukey's multiple comparison test. The *P* values of less than 0.05 were considered statistically significant.

## 3. Results

There were no changes in body weight among the four groups (Fig. 1B). Repeated administration of MPTP (10 mg/kg  $\times$  3, 2-h interval) significantly decreased the density of DAT-immunoreactivity in the mouse striatum (Fig. 2A). Two-way ANOVA revealed statistical differences among the four groups [MPTP:  $F_{1,30} = 70.88$ ,  $P < 0.001$ , glyphosate:  $F_{1,30} = 6.407$ ,  $P = 0.017$ , interaction (MPTP  $\times$  glyphosate),  $F_{1,30} = 3.596$ ,  $P = 0.068$ ] (Fig. 2A). *Post-hoc* test revealed that MPTP significantly ( $P < 0.001$ ) reduced the density of DAT-immunoreactivity in the striatum. Furthermore, DAT-immunoreactivity in the striatum of glyphosate + MPTP group was significantly lower than that of water + MPTP group (Fig. 2A).

Repeated administration of MPTP (10 mg/kg  $\times$  3, 2-h interval) significantly reduced the number of TH-positive cells in the mouse SNr (Fig. 2B). Two-way ANOVA revealed statistical differences among the four groups [MPTP:  $F_{1,30} = 144.5$ ,  $P < 0.001$ , glyphosate:  $F_{1,30} = 12.33$ ,  $P = 0.001$ , interaction (MPTP  $\times$  glyphosate),  $F_{1,30} = 14.37$ ,  $P < 0.001$ ] (Fig. 2B). *Post-hoc* test showed that MPTP significantly ( $P < 0.001$ ) decreased the number of TH-positive cells in the SNr. Furthermore, the number of TH-positive cells in the NAc of glyphosate + MPTP group was significantly lower than that of water + MPTP group (Fig. 2B).

## 4. Discussion

Here, we found that drinking water of glyphosate for 14 days exacerbated the reduction of DAT-immunoreactivity in the mouse striatum and the reduced number of TH-positive cells in the SNr after repeated MPTP administration. We recently reported that maternal glyphosate exposure caused autism-like behavioral abnormalities in offspring through inflammation [15]. Therefore, it is possible that glyphosate exposure may increase the risk for PD in adulthood.

Glyphosate is the most commonly and intensively used herbicide worldwide. The widespread application of glyphosate has spurred the spread of the tolerant and resistant weeds in the USA and worldwide. Humans might be exposed to glyphosate through several routes such as drinking water and food [8,14]. A study in Washington State, USA

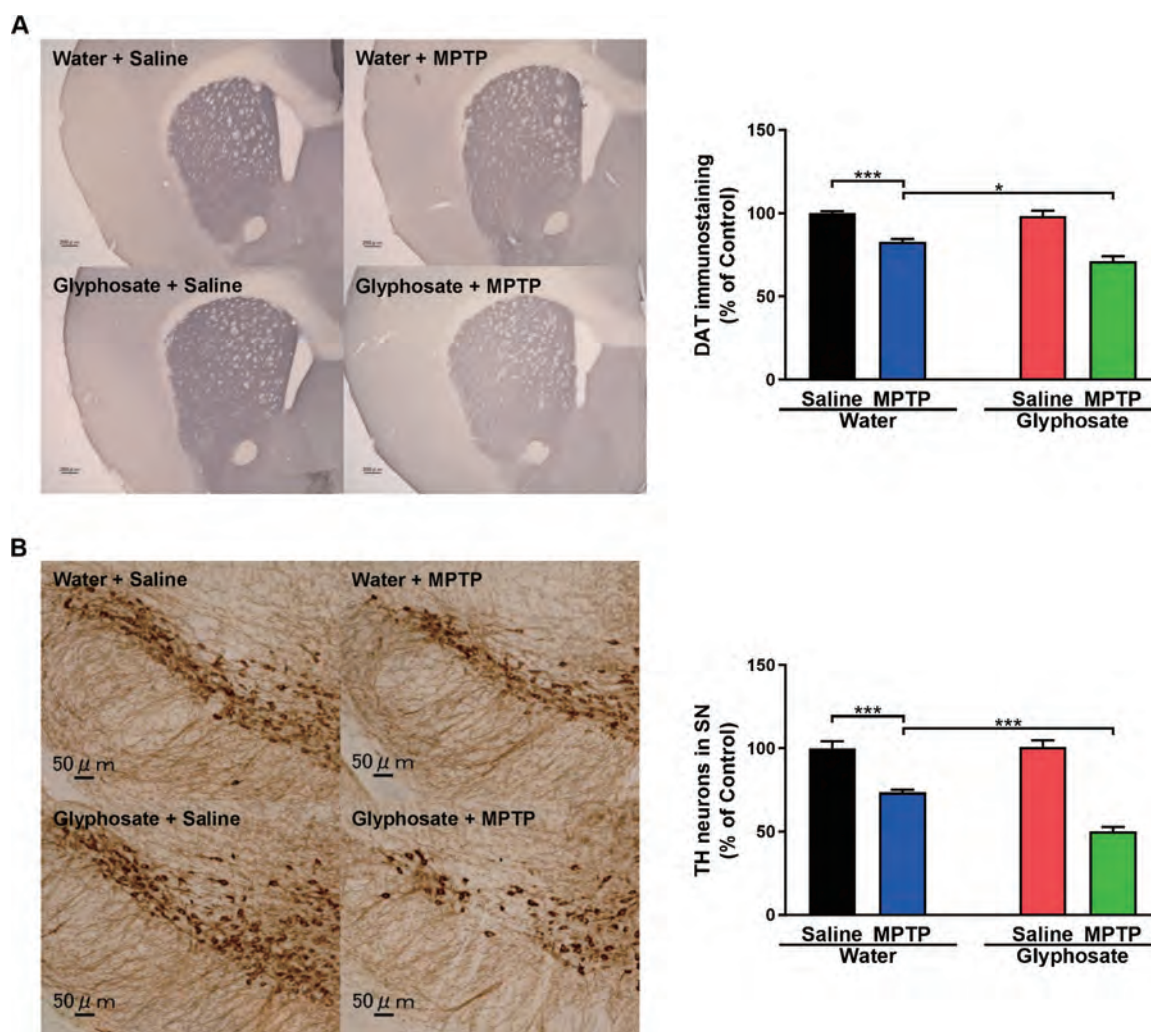


**Fig. 2.** Effects of glyphosate exposure on the dopaminergic neurotoxicity in the mouse brain after the repeated administration of MPTP. (A): DAT immunohistochemistry in the striatum: Left: Representative photomicrographs showing the DAT-immunoreactivity in the striatum of mice. Right: The mean value for DAT-immunoreactivity staining was determined for each group, and was expressed as a percentage of that of control mice. (B): TH immunohistochemistry in the SNr: Left: Representative photomicrographs showing the TH-immunoreactivity in the SNr of mice. Right: The mean value for TH-positive cells was determined for each group, and was expressed as a percentage of that of control mice. Each value is the mean  $\pm$  SEM ( $n = 8-10$  per group). \* $P < 0.05$ , \*\*\* $P < 0.001$  as compared with water + MPTP group.

showed that glyphosate exposure was associated with premature mortality from PD [3]. Exposure of 0.36% glyphosate from E5 to P15 caused oxidative stress and glutamate excitotoxicity in offspring [5]. Although the precise mechanisms underlying glyphosate-induced potentiation of MPTP-induced neurotoxicity remain determined, it is likely that oxidative stress and glutamatergic excitotoxicity may play a role in the potentiation of MPTP-induced dopaminergic neurotoxicity in the brain. It is known that the acute toxic effects of glyphosate and its breakdown product aminomethyl phosphonic acid on mammals are low. However, there are accumulating data indicating the possibility of health effects associated with chronic, ultra-low doses related to accumulation of these compounds in the environment [21]. Given the growing and widespread use of glyphosate in the world, it is likely that glyphosate exposure may increase a risk of the onset of PD in later life. Therefore, we must pay attention to glyphosate exposure in adults.

We previously reported that dietary intake of glucoraphanin (a precursor of anti-inflammatory compound sulforaphane) attenuated MPTP-induced dopaminergic neurotoxicity in the mouse brain [17]. Furthermore, dietary intake of glucoraphanin could produce protective effects in several rodent models such as depression [22,23] and schizophrenia [13,19]. Therefore, it is possible that dietary intake of anti-

inflammatory nutrition such as sulforaphane and its precursor GF may attenuate the onset of PD after glyphosate exposure [4,9,17].

In conclusion, the present data suggest that glyphosate exposure might exacerbate MPTP-induced dopaminergic neurotoxicity in the adult mouse brain. Therefore, it is likely that glyphosate exposure may be an environmental risk factor for PD in later life although further study is needed.

#### CRediT authorship contribution statement

**Yaoyu Pu:** Investigation, Writing - original draft. **Lijia Chang:** Investigation. **Younge Qu:** Investigation. **Siming Wang:** . **Yunfei Tan:** Investigation. **Xingming Wang:** Investigation. **Jiancheng Zhang:** Investigation. **Kenji Hashimoto:** Conceptualization, Funding acquisition, Supervision, Writing - original draft, Writing - review & editing.

#### Declaration of competing interest

The authors declare that they have no known competing financial interests or personal relationships that could have appeared to influence the work reported in this paper.

## Acknowledgements

This study was partly supported by the Japan Society for the Promotion of Science (JSPS) KAKENHI (to K.H., 17H04243). Dr. Lijia Chang was supported by the NIPPON Foundation, The Japan China Medical Association (Tokyo, Japan). Ms. Siming Wang was supported by TAKASE Scholarship Foundation (Tokyo, Japan).

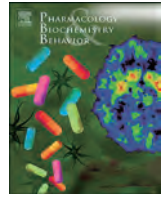
## References

- [1] A. Ascherio, M.A. Schwarzschild, The epidemiology of Parkinson's disease: risk factors and prevention, *Lancet Neurol.* 15 (2016) 1257–1272.
- [2] E.R. Barbosa, M.D. Leiros da Costa, L.A. Bacheschi, M. Scaff, C.C. Leite, Parkinsonism after glycine-derivate exposure, *Mov. Disord.* 16 (2001) 565–568.
- [3] M. Caballero, S. Amiri, J.T. Denney, P. Monsivais, P. Hystad, O. Amram, Estimated residential exposure to agricultural chemicals and premature mortality by parkinson's disease in Washington State, *Int. J. Environ. Res. Public Health* 15 (2018).
- [4] E. Cassani, M. Barichella, V. Ferri, G. Pinelli, L. Iorio, C. Bolliri, S. Caronni, S.A. Faierman, A. Mottolese, C. Pusani, F. Monajemi, M. Pasqua, A. Lubisco, E. Cereda, G. Frazzitta, M.L. Petroni, G. Pezzoli, Dietary habits in Parkinson's disease: adherence to Mediterranean diet, *Parkinsonism Relat. Disord.* 42 (2017) 40–46.
- [5] D. Cattani, P.A. Cesconetto, M.K. Tavares, E.B. Parisotto, P.A. De Oliveira, C.E.H. Rieg, M.C. Leite, R.D.S. Prediger, N.C. Wendt, G. Razzera, D.W. Filho, A. Zamoner, Herbicide and depressive-like behavior in adult offspring: implication of glutamate excitotoxicity and oxidative stress, *Toxicology* 387 (2017) 67–80.
- [6] M. Eriguchi, K. Iida, S. Ikeda, M. Osoegawa, K. Nishioka, N. Hattori, H. Nagayama, H. Hara, Parkinsonism relating to intoxication with glyphosate, *Intern. Med.* 58 (2019) 1935–1938.
- [7] A. Fujita, Y. Fujita, Y. Pu, L. Chang, K. Hashimoto, MPTP-induced dopaminergic neurotoxicity in mouse brain is attenuated after subsequent intranasal administration of (R)-ketamine: a role of TrkB signaling, *Psychopharmacology (Berl.)* 237 (2020) 83–92.
- [8] C. Gillezeau, M. van Gerwen, R.M. Shaffer, I. Rana, L. Zhang, L. Sheppard, E. Taioli, The evidence of human exposure to glyphosate: a review, *Environ. Health* 18 (2019) 2.
- [9] K. Hashimoto, Essential role of Keap1-Nrf2 signaling in mood disorders: overview and future perspective, *Front. Pharmacol.* 9 (2018) 1182.
- [10] V. Jackson-Lewis, S. Przedborski, Protocol for the MPTP mouse model of Parkinson's disease, *Nat. Protoc.* 2 (2007) 141–151.
- [11] L.V. Kalia, A.E. Lang, Parkinson's disease, *Lancet (London, England)* 386 (2015) 896–912.
- [12] E.A. Konnova, M. Swanberg, Animal models of parkinson's disease, in: T.B. Stoker, J.C. Greenland (Eds.), *Parkinson's Disease: Pathogenesis and Clinical Aspects*, Brisbane (AU), 2018.
- [13] A. Matsuura, T. Ishima, Y. Fujita, Y. Iwayama, S. Hasegawa, R. Kawahara-Miki, M. Maekawa, M. Toyoshima, Y. Ushida, H. Suganuma, S. Kida, T. Yoshikawa, M. Iyo, K. Hashimoto, Dietary glucoraphanin prevents the onset of psychosis in the adult offspring after maternal immune activation, *Sci. Rep.* 8 (2018) 2158.
- [14] J.P. Myers, M.N. Antoniou, B. Blumberg, L. Carroll, T. Colborn, L.G. Everett, M. Hansen, P.J. Landrigan, B.P. Lanphear, R. Mesnage, L.N. Vandenberg, F.S. vom Saal, W.V. Welshons, C.M. Benbrook, Concerns over use of glyphosate-based herbicides and risks associated with exposures: a consensus statement, *Environ. Health A Glob. Access Sci. Source* 15 (2016) 19.
- [15] Y. Pu, J. Yang, L. Chang, Y. Qu, S. Wang, K. Zhang, Z. Xiong, J. Zhang, Y. Tan, X. Wang, Y. Fujita, T. Ishima, D. Wan, S.H. Hwang, B.D. Hammock, K. Hashimoto, Maternal glyphosate exposure causes autism-like behaviors in offspring through increased expression of soluble epoxide hydrolase, *Proc. Natl. Acad. Sci. USA* (2020), <https://doi.org/10.1073/pnas.1922287117> in press.
- [16] Y. Pu, L. Chang, Y. Qu, S. Wang, K. Zhang, K. Hashimoto, Antibiotic-induced microbiome depletion protects against MPTP-induced dopaminergic neurotoxicity in the brain, *Aging (Albany NY)* 11 (2019) 6915–6929.
- [17] Y. Pu, Y. Qu, L. Chang, S.M. Wang, K. Zhang, Y. Ushida, H. Suganuma, K. Hashimoto, Dietary intake of glucoraphanin prevents the reduction of dopamine transporter in the mouse striatum after repeated administration of MPTP, *Neuropsychopharmacol. Rep.* 39 (2019) 247–251.
- [18] Q. Ren, M. Ma, J. Yang, R. Nonaka, A. Yamaguchi, K.I. Ishikawa, K. Kobayashi, S. Murayama, S.H. Hwang, S. Saiki, W. Akamatsu, N. Hattori, B.D. Hammock, K. Hashimoto, Soluble epoxide hydrolase plays a key role in the pathogenesis of Parkinson's disease, *Proc. Natl. Acad. Sci. USA* 115 (2018) E5815–E5823.
- [19] Y. Shirai, Y. Fujita, R. Hashimoto, K. Ohi, H. Yamamori, Y. Yasuda, T. Ishima, H. Suganuma, Y. Ushida, M. Takeda, K. Hashimoto, Dietary intake of sulforaphane-rich broccoli sprout extracts during juvenile and adolescence can prevent phencyclidine-induced cognitive deficits at adulthood, *PLoS One* 10 (2015) e0127244.
- [20] W. Tangamornsuksan, O. Lohitnavy, R. Srumsiri, N. Chaiyakunapruk, C. Norman Scholfield, B. Reisfeld, M. Lohitnavy, Paraquat exposure and Parkinson's disease: a systematic review and meta-analysis, *Arch. Environm. Occup. Health* 74 (2019) 225–238.
- [21] A.H.C. Van Bruggen, M.M. He, K. Shin, V. Mai, K.C. Jeong, M.R. Finckh, J.G. Morris Jr., Environmental and health effects of the herbicide glyphosate, *Sci. Total Environ.* 616–617 (2018) 255–268.
- [22] W. Yao, J.C. Zhang, T. Ishima, C. Dong, C. Yang, Q. Ren, M. Ma, M. Han, J. Wu, H. Suganuma, Y. Ushida, M. Yamamoto, K. Hashimoto, Role of Keap1-Nrf2 signaling in depression and dietary intake of glucoraphanin confers stress resilience in mice, *Sci. Rep.* 6 (2016) 30659.
- [23] J.C. Zhang, W. Yao, C. Dong, C. Yang, Q. Ren, M. Ma, M. Han, J. Wu, Y. Ushida, H. Suganuma, K. Hashimoto, Prophylactic effects of sulforaphane on depression-like behavior and dendritic changes in mice after inflammation, *J. Nutr. Biochem.* 39 (2017) 134–144.
- [24] Q. Zheng, J. Yin, L. Zhu, L. Jiao, Z. Xu, Reversible Parkinsonism induced by acute exposure glyphosate, *Parkinsonism Relat. Disord.* 50 (2018) 121.



Contents lists available at ScienceDirect

## Pharmacology, Biochemistry and Behavior

journal homepage: [www.elsevier.com/locate/pharmbiochembeh](http://www.elsevier.com/locate/pharmbiochembeh)

## Neuronal brain injury after cerebral ischemic stroke is ameliorated after subsequent administration of (R)-ketamine, but not (S)-ketamine

Zhongwei Xiong<sup>a,b</sup>, Lijia Chang<sup>a</sup>, Youge Qu<sup>a</sup>, Yaoyu Pu<sup>a</sup>, Siming Wang<sup>a</sup>, Yuko Fujita<sup>a</sup>, Tamaki Ishima<sup>a</sup>, Jincuo Chen<sup>b</sup>, Kenji Hashimoto<sup>a,\*</sup><sup>a</sup> Division of Clinical Neuroscience, Chiba University Center for Forensic Mental Health, Chiba 260-8670, Japan<sup>b</sup> Department of Neurosurgery, Zhongnan Hospital of Wuhan University, Wuhan University, Wuhan 430071, PR China.

## ARTICLE INFO

## Keywords:

Ischemia  
MCAO  
(R)-ketamine  
(S)-ketamine  
Neuroprotection

## ABSTRACT

Although stroke is the most common acute cerebrovascular disease, there are no currently effective therapeutic drugs for ischemic stroke. (R,S)-ketamine has been shown to protect against brain injury in rodents after middle cerebral artery occlusion (MCAO). Interestingly, we reported that (R)-ketamine has greater beneficial effects than (S)-ketamine in animal models of depression and Parkinson's disease. This study was undertaken whether two enantiomers of ketamine show neuroprotective effects in MCAO model. MCAO-induced brain injury and behavioral abnormalities in mice was attenuated by subsequent administration of (R)-ketamine (10 mg/kg, twice, 1 and 24 h after MCAO), but not (S)-ketamine (10 mg/kg, twice, 1 and 24 h after MCAO). Furthermore, the treatment with (R)-ketamine (10 mg/kg, twice, 30 min before and 24 h after MCAO) significantly protected against brain injury and behavioral abnormalities in mice after MCAO. These findings suggest that (R)-ketamine can protect against neuronal injury and behavioral abnormalities in mice after MCAO. Therefore, it is likely that (R)-ketamine could represent a therapeutic drug for ischemic stroke.

## 1. Introduction

Ischemic stroke, the most common acute cerebrovascular disease, has been recognized as one of the leading causes of mortality and disability in the world. At present, the recombinant tissue plasminogen activator (tPA) has been used to a small portion of patients with ischemic stroke. However, tPA has the narrow time window and the risk of hemorrhagic transformation, indicating limited advance for the clinical use (Wardlaw et al., 2012; Whiteley et al., 2012; Yaghi et al., 2014). Therefore, there is a significant unmet medical need to develop the new therapeutic drugs.

Middle cerebral artery occlusion (MCAO) is the most widely used as animal model of ischemic stroke. The common anesthetics including (R,S)-ketamine have been used during MCAO models (Chen et al., 2020). In contrast, these anesthetics are known to produce anti-inflammatory and neuroprotective properties (Guler et al., 2014; Liman et al., 2015; Xu et al., 2004). (R,S)-ketamine has been shown to produce neuroprotection against cerebral ischemic injury in rodents after MCAO (Chang et al., 2002; Ridenour et al., 1991; Shu et al., 2012). It is also reported that immediate administration of (R,S)-ketamine after an ischemia-reperfusion injury can alleviate pain and inflammation in the

chronic post-ischemia pain model (Liman et al., 2015). Collectively, it is likely that (R,S)-ketamine has anti-inflammatory and neuroprotective actions in rodents although the precise mechanisms underlying its beneficial effects remain unclear.

(R,S)-ketamine is a racemic mixture containing equal amount of (R)-ketamine (or arketamine) and (S)-ketamine (or esketamine). (S)-ketamine has an approximately 4-fold greater affinity for the N-methyl-D-aspartate receptor (NMDAR) than (R)-ketamine. (S)-ketamine has been used in some countries as anesthetic since (S)-ketamine produces 3–4 times greater anesthetic potency than (R)-ketamine (Domino, 2010). In contrast, (R)-ketamine has the beneficial effects compared with (S)-ketamine in several animal models such as depression (Chang et al., 2019; Fukumoto et al., 2017; Yang et al., 2015, 2017, 2018; Zanos et al., 2016; Zhang et al., 2014), stress-induced inflammatory bone markers (Xiong et al., 2019; Zhang et al., 2018) and Parkinson's disease (Fujita et al., 2020). Thus, it seems that (R)-ketamine has more potent anti-inflammatory and neuroprotective effects than (S)-ketamine in rodents. However, there are no reports examining the effects of two ketamine enantiomers in MCAO model.

This study was, therefore, undertaken to investigate whether two ketamine enantiomers could produce neuroprotective effects in the

\* Corresponding author.

E-mail address: [hashimoto@faculty.chiba-u.jp](mailto:hashimoto@faculty.chiba-u.jp) (K. Hashimoto).<https://doi.org/10.1016/j.pbb.2020.172904>

Received 11 February 2020; Received in revised form 4 March 2020; Accepted 6 March 2020

Available online 07 March 2020

0091-3057/ © 2020 Elsevier Inc. All rights reserved.

mouse brain injury after MCAO.

## 2. Methods and materials

### 2.1. Animals

Male adult C57BL/6 mice ( $n = 48$ ), aged 9 weeks (body weight 25–30 g, Japan SLC, Inc., Hamamatsu, Japan) were used. Animals were housed under controlled temperatures and 12-h light/dark cycles (lights on between 07:00–19:00 h), with ad libitum food (CE-2; CLEA Japan, Inc., Tokyo, Japan) and water. The protocol was approved by the Chiba University Institutional Animal Care and Use Committee (Permission number: 30-409). This study was carried out in strict accordance with the recommendations in the Guide for the Care and Use of Laboratory Animals of the National Institutes of Health, USA. Animals were deeply anesthetized with isoflurane before being killed by cervical dislocation. All efforts were made to minimize suffering.

### 2.2. Drugs and drug administration

(*R*)-ketamine hydrochloride and (*S*)-ketamine hydrochloride were prepared by recrystallization of (*R,S*)-ketamine (Ketalar®, ketamine hydrochloride, Daiichi Sankyo Pharmaceutical Ltd., Tokyo, Japan) and D-(–)-tartaric acid and L-(+)-tartaric acid, as described previously (Zhang et al., 2014). The dose (10 mg/kg) of (*R*)-ketamine and (*S*)-ketamine was used as previously reported (Fujita et al., 2020; Yang et al., 2015, 2017, 2018; Zhang et al., 2014). All compounds were dissolved in the physiological saline. Other reagents were purchased commercially. Saline (10 ml/kg), (*R*)-ketamine (10 mg/kg as hydrochloride salt) or (*S*)-ketamine (10 mg/kg as hydrochloride salt) was administered intraperitoneally (i.p.) into mice twice, 30 min before or after 1 h-MCAO and 24 h after 1 h-MCAO (Fig. 1A and 2A).

### 2.3. Animals experimental design

In this study, mice ( $n = 8$  per group) were randomly allocated into groups. First we examined the neuroprotective effects of (*R*)-ketamine (10 mg/kg) and (*S*)-ketamine (10 mg/kg) in 1 h MCAO model (Fig. 1A). There were 4 groups as follows: (1): Sham: saline (10 ml/kg) group (I/R + saline 0.5 h + saline 24 h), (2): Sham: saline (10 ml/kg) group (I/R + saline 0.5 h + saline 24 h), (3): MCAO: (*R*)-ketamine (10 mg/kg) treatment group (I/R + R-Ket 0.5 h + R-Ket 24 h), (4): MCAO: (*S*)-ketamine (10 mg/kg) treatment group (I/R + S-Ket 0.5 h + S-Ket 24 h).

Second, we examined the prophylactic effects of (*R*)-ketamine (10 mg/kg) in 1 h MCAO model (Fig. 2A). There were 3 groups as follows: (1): Sham: saline (10 ml/kg) group (I/R + saline 0.5 h before MCAO + saline 24 h after MCAO), (2): MCAO: saline (10 ml/kg) group (I/R + saline 0.5 h before MCAO + saline 24 h after MCAO), (3): MCAO: (*R*)-ketamine (10 mg/kg) pretreatment group (R-Ket 0.5 h before MCAO + I/R + R-Ket 24 h after MCAO). Behavioral tests and collection of tissue samples were performed at the indicated time point (Fig. 2A). All the procedures in the behavioral test were carried out in a blinded fashion.

### 2.4. MCAO model

The MCAO model was performed according to a previously published protocol (Chen et al., 2007). After mice were anesthetized with pentobarbital sodium (60 mg/kg, i.p.), the right common carotid artery and external carotid artery were exposed and ligated through a ventral midline incision. An arteriotomy was made in common carotid artery allowing the introduction of a monofilament suture (Doccol, 602356PK10) for 60 min. The filament was gently advanced into the internal carotid artery to a point approximately 12 mm distal to the carotid bifurcation until a mild resistance was felt, thereby occluding the origins of the middle cerebral artery. After 1 h of MCAO, filament

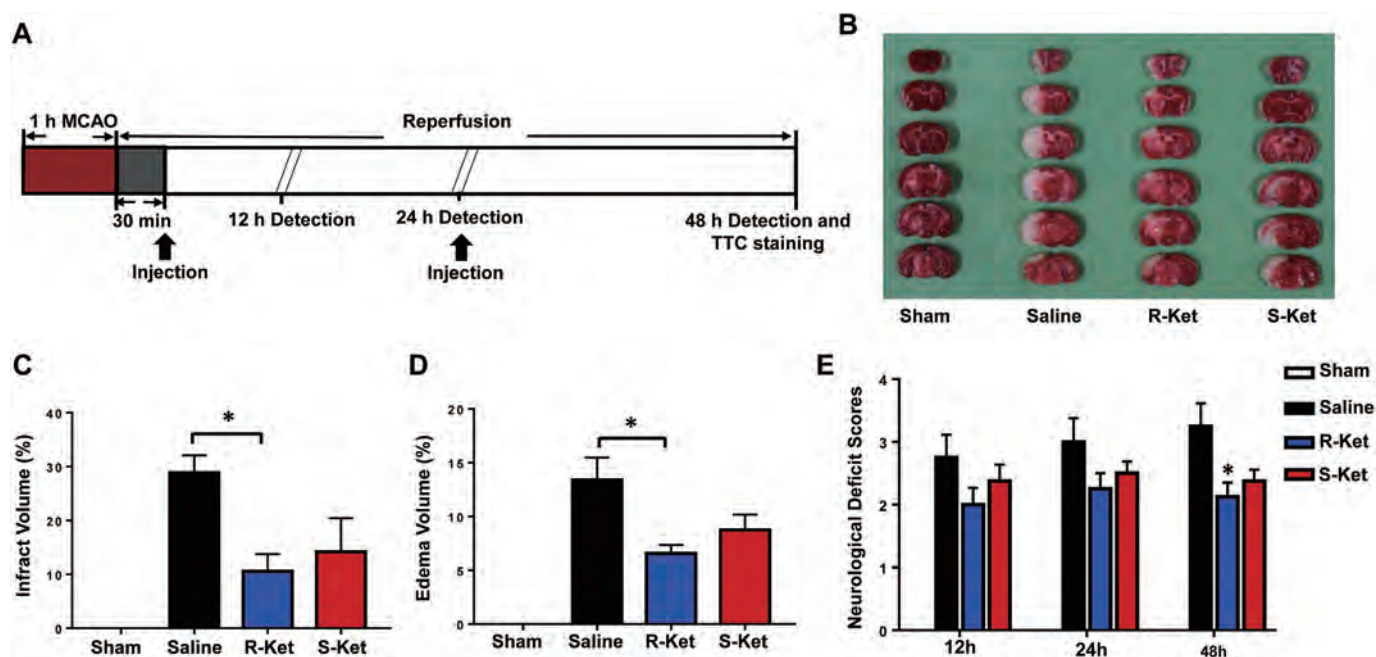


Fig. 1. Neuroprotection of MCAO-induced neuronal injury by (*R*)-ketamine, but not (*S*)-ketamine.

(A): Experimental schedule. Saline (10 ml/kg), (*R*)-ketamine (10 mg/kg), or (*S*)-ketamine (10 mg/kg) was administered i.p. twice 30 min and 24 h after 1 h MCAO. Neurological deficit scores were measured 12, 24, and 48 h after MCAO. Brain was removed for TTC staining 48 h after MCAO. (B): Representative samples of TTC-stained brain sections showed the infarcted areas in white. (C): The infarct volume was determined using image analysis and expressed as a percentage of the whole cerebral tissue. Data are presented as mean  $\pm$  S.E.M. ( $n = 8$ ). (D): Edema volume was determined as described in method. Data are presented as mean  $\pm$  S.E.M. ( $n = 8$ ). (E): Neurological deficit score was determined as described in method. Data are presented as mean  $\pm$  S.E.M. ( $n = 8$ ). \* $P < 0.05$  compared to saline + MCAO group.



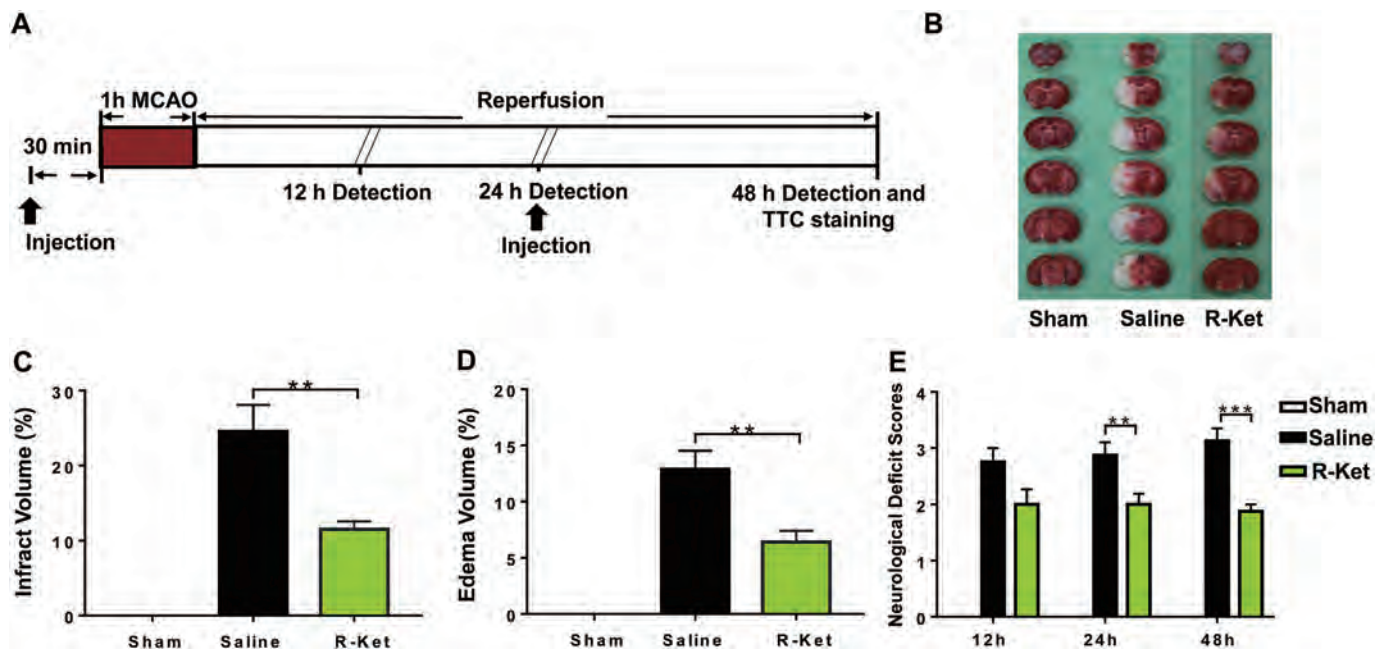


Fig. 2. Prophylactic effects of (*R*)-ketamine in MCAO-induced neuronal injury.

(A): Experimental schedule. Saline (10 ml/kg), or (*R*)-ketamine (10 mg/kg) was administered i.p. twice 30 min before and 24 h after 1 h MCAO. Neurological deficit scores were measured 12, 24, and 48 h after MCAO. Brain was removed for TTC staining 48 h after MCAO. (B): Representative samples of TTC-stained brain sections showed the infarcted areas in white. (C): The infarct volume was determined using image analysis and expressed as a percentage of the whole cerebral tissue. Data are presented as mean  $\pm$  S.E.M. ( $n = 8$ ). (D): Edema volume was determined as described in method. Data are presented as mean  $\pm$  S.E.M. ( $n = 8$ ). (E): Neurological deficit score was determined as described in method. Data are presented as mean  $\pm$  S.E.M. ( $n = 8$ ). \* $P < 0.05$ , \*\* $P < 0.01$ , \*\*\* $P < 0.001$  compared to saline + MCAO group.

was removal and reperfusion process performed after ischemia. In sham group, the mice received the same surgical exposure of carotid artery and ligation except for the insertion of an intraluminal filament. During the entire surgical procedure, the body temperature was continuously monitored with a rectal probe and maintained at  $37.0 \pm 0.5$  °C.

### 2.5. Neurological deficit scores

At 12 h, 24 h and 48 h after I/R, neurological deficits were evaluated by a 4-point scale, as previously described. 0 = no deficit; 1 = forelimb weakness; 2 = circling to affected side; 3 = partial paralysis on affected side; and 4 = no spontaneous motor activity.

### 2.6. Quantification of infarct volume

Mice ( $n = 8$  per group) were sacrificed by decapitation without any anesthetics 48 h after MCAO, and the brain was quickly removed and cut into 1.5 mm thick coronal sections. Brain sections were incubated for 20 min in a solution of 0.5% 2,3,5-triphenyltetrazolium chloride (TTC) in 0.01 M phosphate buffered saline at 37 °C, and then the slices were scanned into a computer. Cerebral infarct was determined by TTC staining of brain sections, and the images were analyzed using Image-Pro Plus 6.0 (Media Cybernetics, Bethesda, MD). The infarct volume (%) and edema volume (%) was calculated as follows: Infarct volume (Mokudai et al., 2000; Swanson et al., 1990) =  $(V_{\text{contralateral hemisphere}} - V_{\text{non-lesioned ipsilateral hemisphere}}) / V_{\text{contralateral hemisphere}}$ , edema (Hattori et al., 2000) =  $(V_{\text{ipsilateral hemisphere}} - V_{\text{contralateral hemisphere}}) / V_{\text{contralateral hemisphere}}$ .

### 2.7. Statistical analysis

The data show as the mean  $\pm$  standard error of the mean (S.E.M.). Analysis was performed using PASW Statistics 20 (formerly SPSS Statistics; SPSS, Tokyo, Japan). The data were analyzed using the one-

way ANOVA, followed by *post-hoc* Tukey test. The  $P$ -values of  $< 0.05$  were considered statistically significant.

## 3. Results

### 3.1. Effects of (*R*)-ketamine and (*S*)-ketamine on infarct volume, edema volume, neurological deficits of 1 h MCAO model

We examined the neuroprotective effects of (*R*)-ketamine (10 mg/kg) and (*S*)-ketamine (10 mg/kg) in 1 h MCAO model (Fig. 1A). Fig. 1B showed the typical results of TTC staining. One-way ANOVA of infarct volume data showed a statistical significance ( $F_{3,28} = 9.553$ ,  $P < 0.001$ ) among the four groups (Fig. 1C). *Post-hoc* tests showed that (*R*)-ketamine (10 mg/kg), but not (*S*)-ketamine (10 mg/kg), significantly attenuated the infarct volume in 1 h MCAO model (Fig. 1C).

One-way ANOVA of edema volume data showed a statistical significance ( $F_{3,28} = 18.133$ ,  $P < 0.001$ ) among the four groups (Fig. 1D). *Post-hoc* tests showed that (*R*)-ketamine (10 mg/kg), but not (*S*)-ketamine (10 mg/kg), significantly attenuated the edema volume in 1 h MCAO model (Fig. 1D). One-way ANOVA of 48 h neurological deficit scores data showed a statistical significance ( $F_{3,28} = 34.762$ ,  $P < 0.001$ ) among four groups (Fig. 1E). *Post-hoc* tests showed that 48 h neurological deficit scores of (*R*)-ketamine-treated group, but not (*S*)-ketamine-treated group, was significantly lower than saline treated group (Fig. 1E). These results suggest that (*R*)-ketamine shows greater potent neuroprotective effects than (*S*)-ketamine in 1 h MCAO model.

### 3.2. Effects of (*R*)-ketamine (10 mg/kg) pretreatment on infarct volume, edema volume, neurological deficits of 1 h MCAO model

We examined the neuroprotective effects of (*R*)-ketamine (10 mg/kg, 30 min before MCAO) pretreatment and posttreatment (10 mg/kg, 24 h after MCAO) in 1 h MCAO model (Fig. 2A). Fig. 2B showed the typical results of TTC staining. One-way ANOVA of infarct volume data

showed a statistical significance ( $F_{2,21} = 32.33$ ,  $P < 0.001$ ) among the three groups (Fig. 2C). *Post-hoc* tests showed that (R)-ketamine (10 mg/kg) significantly attenuated the infarct volume in 1 h MCAO model (Fig. 2C). One-way ANOVA of edema volume data showed a statistical significance ( $F_{2,21} = 32.91$ ,  $P < 0.001$ ) among the three groups (Fig. 2D). *Post-hoc* tests showed that (R)-ketamine (10 mg/kg) significantly attenuated the edema volume in 1 h MCAO model (Fig. 2D). One-way ANOVA of 24 h and 48 h neurological deficit scores data showed a statistical significance (24 h:  $F_{2,21} = 74.85$ ,  $P < 0.001$ ; 48 h:  $F_{2,21} = 110.8$ ,  $P < 0.001$ ) among three groups (Fig. 2E). *Post-hoc* tests showed that neurological deficit scores of (R)-ketamine (10 mg/kg)-treated group was significantly lower than saline-treated group (Fig. 2E). These results suggest that both pretreatment and posttreatment of (R)-ketamine (10 mg/kg) could produce potent neuroprotective effects in 1 h MCAO model.

#### 4. Discussion

The study suggests that (R)-ketamine would be a potential therapeutic drug for stroke. The major findings of the present study are as follows: First, MCAO-induced injury in the brain was significantly attenuated by subsequent (1 and 24 h after MCAO) administration of (R)-ketamine (10 mg/kg), but not (S)-ketamine (10 mg/kg). Second, MCAO-induced injury in the brain was also significantly attenuated by pretreatment (30 min before) and posttreatment (24 h after) with (R)-ketamine (10 mg/kg). Sustained neuroprotective effects of (R)-ketamine (10 mg/kg) in MCAO model are consistent with sustained antidepressant effects of (R)-ketamine (Shirayama and Hashimoto, 2018; Yang et al., 2015, 2017, 2018; Zhang et al., 2020). Collectively, these findings suggest that (R)-ketamine can protect against MCAO-induced neuronal injury in the brain. It is likely that (R)-ketamine would be a possible therapeutic drug for ischemic stroke since (R)-ketamine administration 1 h after MCAO elicited neuroprotective effects against MCAO-induced brain damages.

A previous report showed that (R,S)-ketamine (25 mg/kg, i.p. 30 min following MCAO), but not (R,S)-ketamine (50 and 100 mg/kg), reduced the infarct volume, edema ratio, and neurological deficits in mice after 6 h MCAO (Shu et al., 2012), indicating a lack of dose dependency. From the report (Shu et al., 2012) and our data, it seems that (R,S)-ketamine (25 mg/kg) and (R)-ketamine (10 mg/kg) may be optimal dose for MCAO model. It is likely that (R)-ketamine (10 mg/kg) is better than (R,S)-ketamine (25 mg/kg) since (R,S)-ketamine (25 mg/kg) can produce behavioral abnormalities in rodents (Fukumoto et al., 2017; Zanos et al., 2016; Yang et al., 2015).

It is reported that the pharmacokinetic profiles of two ketamine enantiomers are not different (Fukumoto et al., 2017; Zanos et al., 2016), suggesting that the differential protective effects for two enantiomers are not due to differences in their pharmacokinetic profiles. In addition, (S)-ketamine ( $K_i = 0.30 \mu\text{M}$ ) has an approximately 4-fold greater affinity for the NMDAR than (R)-ketamine ( $K_i = 1.40 \mu\text{M}$ ) (Ebert et al., 1997). It is therefore, unlikely that NMDAR inhibition plays a major role in the neuroprotective effects of (R)-ketamine in the brain injury after MCAO. Nonetheless, further detailed studies examining the precise mechanisms underlying the neuroprotective effects of (R)-ketamine are needed.

The detrimental side effects (i.e., psychotomimetic effects, dissociation, abuse liability) in humans after (R,S)-ketamine [or (S)-ketamine] infusion are well known (Liu et al., 2016; Sanacora et al., 2017; Short et al., 2018). Unlike (S)-ketamine, (R)-ketamine might not induce psychotomimetic side effects or exhibit abuse potential in rodents and monkey (Chang et al., 2019; Hashimoto et al., 2017; Tian et al., 2018; Yang et al., 2015, 2016). Interestingly, it is suggested that (S)-ketamine contributes to the acute psychotomimetic and dissociative effects of ketamine in humans, whereas (R)-ketamine may not be associated with these side effects (Vollenweider et al., 1997; Zanos et al., 2018). A recent pilot study demonstrated that (R)-ketamine (0.5 mg/kg,

intravenous infusion) produced rapid-acting and sustained antidepressant actions in treatment-resistant patients with depression (Leal et al., 2020). Importantly, side effects (i.e., dissociation) of (R)-ketamine (0.5 mg/kg, intravenous infusion) in these patients (Leal et al., 2020) were markedly lower than those of (S)-ketamine (0.2 and 0.4 mg/kg, intravenous infusion) (Singh et al., 2016). Taken all together, (R)-ketamine could be a safer antidepressant in humans than (R,S)-ketamine and (S)-ketamine (Hashimoto, 2016a, 2016b, 2019, 2020; Wei et al., 2020; Yang et al., 2019; Zhang and Hashimoto, 2019). Therefore, it is of great interest to investigate whether the faster treatment with (R)-ketamine in acute patients after ischemic stroke could prevent or delay the neuronal injury in the brain. Given the prevalence of depression in patients with stroke (Astrom et al., 1993; Wade et al., 1987), it is also of great interest to investigate whether (R)-ketamine has beneficial actions in patients with post-stroke depression.

(R,S)-ketamine is a short-acting agent with a rapid onset of action that does not produce systemic haemodynamics or respiratory drive (Oddo et al., 2016). Furthermore, (R,S)-ketamine was not associated with an increased risk of intracranial pressure (Himmelseher and Durieux, 2005). A retrospective and observational study showed that (R,S)-ketamine decreased the intracranial pressure, and is not associated with a higher rate of complications in patients with aneurysmal subarachnoid hemorrhage. Furthermore, the rate of cerebral infarction associated with delayed cerebral ischemia was lower in the ketamine group (Von der Brölie et al., 2017). Thus, it is likely that (R)-ketamine could be considered as the new therapeutic agent without side effects after acute brain injury.

In conclusion, this study shows that (R)-ketamine, but not (S)-ketamine, protects against neuronal injury in the mouse brain after MCAO. Therefore, (R)-ketamine appears to be a new therapeutic drug for ischemic stroke.

#### Declaration of competing interest

Dr. Hashimoto is an inventor on a filed patent application on “The use of (R)-ketamine in the treatment of psychiatric diseases” and “The use of (R)-ketamine in the treatment of neurodegenerative diseases” by Chiba University. Dr. Hashimoto has received research support from Dainippon-Sumitomo, Otsuka, and Taisho. Other authors declare no conflict of interest.

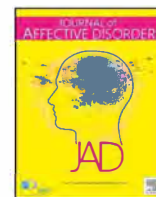
#### Acknowledgements

This study was supported by Japan Agency for Medical Research and Development, AMED (to K.H., JP19dm0107119). Dr. Zhongwei Xiong (Wuhan University, China) was supported by the China Scholarship Council.

#### References

- Astrom, M., Adolfsson, R., Asplund, K., 1993. Major depression in stroke patients. A 3-year longitudinal study. *Stroke* 24, 976–982.
- Chang, M.L., Yang, J., Kem, S., Klaidman, L., Sugawara, T., Chan, P.H., Adams Jr., J.D., 2002. Nicotinamide and ketamine reduce infarct volume and DNA fragmentation in rats after brain ischemia and reperfusion. *Neurosci. Lett.* 322, 137–140.
- Chang, L., Zhang, K., Pu, Y., Qu, Y., Wang, S.M., Xiong, Z., Ren, Q., Dong, C., Fujita, Y., Hashimoto, K., 2019. Comparison of antidepressant and side effects in mice after intranasal administration of (R,S)-ketamine, (R)-ketamine, and (S)-ketamine. *Pharmacol. Biochem. Behav.* 181, 53–59.
- Chen, A., Liao, W.P., Lu, Q., Wong, W.S., Wong, P.T., 2007. Upregulation of dihydropyrimidinase-related protein 2, spectrin alpha II chain, heat shock cognate protein 70 pseudogene 1 and tropomodulin 2 after focal cerebral ischemia in rats—a proteomics approach. *Neurochem. Int.* 50, 1078–1086.
- Chen, G., Kamat, P.K., Ahmad, A.S., Dore, S., 2020. Distinctive effect of anesthetics on the effects of limb remote ischemic preconditioning following ischemic stroke. *PLoS One* 15, e0227624.
- Domino, E.F., 2010. Taming the ketamine tiger. 1965. *Anesthesiology* 113, 678–684.
- Ebert, B., Mikkelsen, S., Thorkildsen, C., Borghjerg, F.M., 1997. Norketamine, the main metabolite of ketamine, is a non-competitive NMDA receptor antagonist in the rat cortex and spinal cord. *Eur. J. Pharmacol.* 333, 99–104.

- Fujita, A., Fujita, Y., Chang, L., Pu, Y., Hashimoto, K., 2020. MPTP-induced dopaminergic neurotoxicity in mouse brain is attenuated after subsequent intranasal administration of (R)-ketamine: a role of BDNF-TrkB signaling. *Psychopharmacology* 237, 83–92.
- Fukumoto, K., Toki, H., Iijima, M., Hashihayata, T., Yamaguchi, J.I., Hashimoto, K., Chaki, S., 2017. Antidepressant potential of (R)-ketamine in rodent models: comparison with (S)-ketamine. *J. Pharmacol. Exp. Ther.* 361, 9–16.
- Guler, L., Bozkirli, F., Bedirli, N., Unal, Y., Guler, A., Oztas, Y., Balta, S., Cakar, M., Demirkol, S., Arslan, Z., Unlu, M., 2014. Comparison of the effects of dexmedetomidine vs. ketamine in cardiac ischemia/reperfusion injury in rats – preliminary study. *Adv. Clin. Exp. Med.* 23, 683–689.
- Hashimoto, K., 2016a. R-ketamine: a rapid-onset and sustained antidepressant without risk of brain toxicity. *Psychol. Med.* 46, 2449–2451.
- Hashimoto, K., 2016b. Ketamine's antidepressant action: beyond NMDA receptor inhibition. *Expert Opin. Ther. Targets* 20, 1389–1392.
- Hashimoto, K., 2019. Rapid-acting antidepressant ketamine, its metabolites and other candidates: a historical overview and future perspective. *Psychiatry Clin. Neurosci.* 73, 613–627.
- Hashimoto, K., 2020. Impact of age on optimal dose of antidepressants. *EclinicalMedicine* 18, 100233.
- Hashimoto, K., Kakiuchi, T., Ohba, H., Nishiyama, S., Tsukada, H., 2017. Reduction of dopamine D<sub>2/3</sub> receptor binding in the striatum after a single administration of esketamine, but not R-ketamine: a PET study in conscious monkeys. *Eur. Arch. Psychiatry Clin. Neurosci.* 267, 173–176.
- Hattori, K., Lee, H., Hurn, P.D., Crain, B.J., Traystman, R.J., DeVries, A.C., 2000. Cognitive deficits after focal cerebral ischemia in mice. *Stroke* 31, 1939–1944.
- Himmelseher, S., Durieux, M.E., 2005. Revising a dogma: ketamine for patients with neurological injury? *Anesth. Analg.* 101, 524–534.
- Leal, G.C., Bandeira, I.D., Correia-Melo, F.S., Telles, M., Mello, R.P., Vieira, F., Lima, C.S., Jesus-Nunes, A.P., Guerreiro-Costa, L.N.F., Marback, R.F., Caliman-Fontes, A.T., Marques, B.L.S., Bezerra, M.L.O., Dias-Neto, A.L., Silva, S.S., Sampaio, A.S., Sanacora, G., Turecki, G., Loo, C., Lacerda, A.L.T., Quarantini, L.C., 2020. Intravenous arketamine for treatment-resistant depression: open-label pilot study. *Eur. Arch. Psych. Clin. Neurosci.* in press. <https://doi.org/10.1007/s00406-020-01110-5>.
- Liman, S., Cheung, C.W., Wong, K.L., Tai, W., Qiu, Q., Ng, K.F., Choi, S.W., Irwin, M., 2015. Preventive treatment with ketamine attenuates the ischaemia-reperfusion response in a chronic postschaemia pain model. *Oxidative Med. Cell. Longev.* 2015, 380403.
- Liu, Y., Lin, D., Wu, B., Zhou, W., 2016. Ketamine abuse potential and use disorder. *Brain Res. Bull.* 126, 68–73 Pt 1.
- Mokudai, T., Ayoub, I.A., Sakakibara, Y., Lee, E.J., Ogilvy, C.S., Maynard, K.I., 2000. Delayed treatment with nicotinamide (vitamin B(3)) improves neurological outcome and reduces infarct volume after transient focal cerebral ischemia in Wistar rats. *Stroke* 31, 1679–1685.
- Oddo, M., Crippa, I.A., Mehta, S., Menon, D., Payen, J.F., Taccone, F.S., Citerio, G., 2016. Optimizing sedation in patients with acute brain injury. *Crit. Care* 20, 128.
- Ridenour, T.R., Warner, D.S., Todd, M.M., Baker, M.T., 1991. Effects of ketamine on outcome from temporary middle cerebral artery occlusion in the spontaneously hypertensive rat. *Brain Res.* 565, 116–122.
- Sanacora, G., Frye, M.A., McDonald, W., Mathew, S.J., Turner, M.S., Schatzberg, A.F., Summergrad, P., Nemeroff, C.B., American Psychiatric Association (APA) Council of Research Task Force on Novel Biomarkers and Treatments, 2017. A consensus statement on the use of ketamine in the treatment of mood disorders. *JAMA Psychiatry* 74, 399–405.
- Shirayama, Y., Hashimoto, K., 2018. Lack of antidepressant effects of (2R,6R)-hydroxynorketamine in a rat learned helplessness model: comparison with (R)-ketamine. *Int. J. Neuropsychopharmacol.* 21, 84–88.
- Short, B., Fong, J., Galvez, V., Shelker, W., Loo, C.K., 2018. Side-effects associated with ketamine use in depression: a systematic review. *Lancet Psychiatry* 5, 65–78.
- Shu, L., Li, T., Han, S., Ji, F., Pan, C., Zhang, B., Li, J., 2012. Inhibition of neuron-specific CREB dephosphorylation is involved in propofol and ketamine-induced neuroprotection against cerebral ischemic injuries of mice. *Neurochem. Res.* 37, 49–58.
- Singh, J.B., Fedgchin, M., Daly, E., Xi, L., Melman, C., De Bruecker, G., Tadic, A., Sienaeert, P., Wiegand, F., Manji, H., Drevets, W.C., Van Nueten, L., 2016. Intravenous esketamine in adult treatment-resistant depression: a double-blind, double-randomization, placebo-controlled study. *Biol. Psychiatry* 80, 424–431.
- Swanson, R.A., Morton, M.T., Tsao-Wu, G., Savalos, R.A., Davidson, C., Sharp, F.R., 1990. A semiautomated method for measuring brain infarct volume. *J. Cereb. Blood Flow Metab.* 10, 290–293.
- Tian, Z., Dong, C., Fujita, A., Fujita, Y., Hashimoto, K., 2018. Expression of heat shock protein HSP-70 in the retrosplenial cortex of rat brain after administration of (R,S)-ketamine and (S)-ketamine, but not (R)-ketamine. *Pharmacol. Biochem. Behav.* 172, 17–21.
- Vollenweider, F.X., Leenders, K.L., Øye, I., Hell, D., Angst, J., 1997. Differential psychopathology and patterns of cerebral glucose utilization produced by (S)- and (R)-ketamine in healthy volunteers using positron emission tomography (PET). *Eur. Neuropsychopharmacol.* 7, 25–38.
- Von der Bröle, C., Seifert, M., Rot, S., Tittel, A., Sanfi, C., Meier, U., Lemcke, J., 2017. Sedation of patients with acute aneurysmal subarachnoid hemorrhage with ketamine is safe and might influence the occurrence of cerebral infarctions associated with delayed cerebral ischemia. *World Neurosurg* 97, 374–382.
- Wade, D.T., Legh-Smith, J., Hewer, R.A., 1987. Depressed mood after stroke: a community study of its frequency. *Br. J. Psychiatry* 151, 200–205.
- Wardlaw, J.M., Murray, V., Berge, E., del Zoppo, G., Sandercock, P., Lindley, R.L., Cohen, G., 2012. Recombinant tissue plasminogen activator for acute ischaemic stroke: an update systematic review and meta-analysis. *Lancet* 379, 2364–2372.
- Wei, Y., Chang, L., Hashimoto, K., 2020. A historical review of antidepressant effects of ketamine and its enantiomers. *Pharmacol. Biochem. Behav.* in press. <https://doi.org/10.1016/j.pbb.2020.172870>.
- Whiteley, W.N., Slot, K.B., Fernandes, P., Sandercock, P., Wardlaw, J., 2012. Risk factors for intracranial hemorrhage in acute ischemic stroke patients treated with recombinant tissue plasminogen activator: a systemic review and meta-analysis of 55 studies. *Stroke* 43, 2904–2909.
- Xiong, Z., Fujita, Y., Zhang, K., Pu, Y., Chang, L., Ma, M., Chen, J., Hashimoto, K., 2019. Beneficial effects of (R)-ketamine, but not its metabolite (2R,6R)-hydroxynorketamine, in the depression-like phenotype, inflammatory bone markers, and bone mineral density in a chronic social defeat stress model. *Behav. Brain Res.* 368, 111904.
- Xu, Q.S., Yu, B.W., Wang, Z.J., Chen, H.Z., 2004. Effects of ketamine, midazolam, thio-pental, and propofol on brain ischemia injury in rat cerebral cortical slices. *Acta Pharmacol. Sin.* 25, 115–120.
- Yaghi, S., Eisenberger, A., Willey, J.Z., 2014. Symptomatic intracerebral hemorrhage in acute ischemic stroke after thrombolysis with intravenous recombinant tissue plasminogen activator: a review of natural history and treatment. *JAMA Neurol* 71, 1181–1185.
- Yang, C., Shirayama, Y., Zhang, J.C., Ren, Q., Yao, W., Ma, M., Hashimoto, K., 2015. R-ketamine: a rapid-onset and sustained antidepressant without psychotomimetic side effects. *Transl. Psychiatry* 5, e632.
- Yang, C., Han, M., Zhang, J.C., Ren, Q., Hashimoto, K., 2016. Loss of parvalbumin-immunoreactivity in mouse brain regions after repeated intermittent administration of esketamine, but not R-ketamine. *Psychiatry Res.* 239, 281–283.
- Yang, C., Qu, Y., Fujita, Y., Ren, Q., Ma, M., Dong, C., Hashimoto, K., 2017. Possible role of the gut microbiota-brain axis in the antidepressant effects of (R)-ketamine in a social defeat stress model. *Transl. Psychiatry* 7, 1294.
- Yang, C., Ren, Q., Qu, Y., Zhang, J.C., Ma, M., Dong, C., Hashimoto, K., 2018. Mechanistic target of rapamycin-independent antidepressant effects of (R)-ketamine in a social defeat stress model. *Biol. Psychiatry* 83, 18–28.
- Yang, C., Yang, J., Luo, A., Hashimoto, K., 2019. Molecular and cellular mechanisms underlying the antidepressant effects of ketamine enantiomers and its metabolites. *Transl. Psychiatry* 9, 280.
- Zanos, P., Moaddel, R., Morris, P.J., Georgiou, P., Fischell, J., Elmer, G.I., Alkondon, M., Yuan, P., Pribut, H.J., Singh, N.S., Dossou, K.S., Fang, Y., Huang, X.P., Mayo, C.L., Wainer, I.W., Albuquerque, E.X., Thompson, S.M., Thomas, C.J., Zarate Jr., C.A., Gould, T.D., 2016. NMDAR inhibition-independent antidepressant actions of ketamine metabolites. *Nature* 533, 481–486.
- Zanos, P., Moaddel, R., Morris, P.J., Riggs, L.M., Highland, J.N., Georgiou, P., Pereira, E.F.R., Albuquerque, E.X., Thomas, C.J., Zarate Jr., C.A., Gould, T.D., 2018. Ketamine and ketamine metabolite pharmacology: insights into therapeutic mechanisms. *Pharmacol. Rev.* 70, 621–660.
- Zhang, K., Hashimoto, K., 2019. An update on ketamine and its two enantiomers as rapid-acting antidepressants. *Expert. Rev. Neurother.* 19, 83–92.
- Zhang, J.C., Li, S.X., Hashimoto, K., 2014. R(-)-ketamine shows greater potency and longer lasting antidepressant effects than S(+)-ketamine. *Pharmacol. Biochem. Behav.* 116, 137–141.
- Zhang, K., Ma, M., Dong, C., Hashimoto, K., 2018. Role of inflammatory bone markers in the antidepressant actions of (R)-ketamine in a chronic social defeat stress model. *Int. J. Neuropsychopharmacol.* 21, 1025–1030.
- Zhang, K., Yang, C., Chang, L., Sakamoto, A., Suzuki, T., Fujita, Y., Qu, Y., Wang, S., Pu, Y., Tan, Y., Wang, X., Ishima, T., Shirayama, Y., Hatano, M., Tanaka, K.F., Hashimoto, K., 2020. Essential role of microglial transforming growth factor- $\beta$ 1 in antidepressant actions of (R)-ketamine and the novel antidepressant TGF- $\beta$ 1. *Transl. Psychiatry* 10, 32.



## Research paper

# Abnormal expression of colony stimulating factor 1 receptor (CSF1R) and transcription factor PU.1 (SPI1) in the spleen from patients with major psychiatric disorders: A role of brain–spleen axis



Jiancheng Zhang<sup>a,b</sup>, Lijia Chang<sup>a</sup>, Yaoyu Pu<sup>a</sup>, Kenji Hashimoto<sup>a,\*</sup>

<sup>a</sup> Division of Clinical Neuroscience, Chiba University Center for Forensic Mental Health, Chiba, 260-8670, Japan

<sup>b</sup> Department of Critical Care Medicine (Dr. Zhang), Union Hospital, Tongji Medical College, Huazhong University of Science and Technology, Wuhan, 430022, P.R. China

## ARTICLE INFO

## Keywords:

Brain–spleen axis  
CSF1R  
Postmortem brain  
SPI1  
Spleen

## ABSTRACT

**Background:** The colony stimulating factor 1 receptor (CSF1R) regulates microglia/macrophage proliferation, differentiation and survival; however, the precise role of this protein in psychiatric disorders is unknown. CSF1R is also known to interact with the transcription factor PU.1 (SPI1). Here we studied whether the expressions of CSF1R and SPI1 are altered in the postmortem samples (parietal cortex, cerebellum, spleen) from patients with major psychiatric disorders.

**Methods:** Protein expression of CSF1R and SPI1 in the parietal cortex, cerebellum and spleen from control, major depressive disorder (MDD), schizophrenia (SZ), and bipolar disorder (BD) groups was measured.

**Results:** Levels of CSF1R in the spleen, but not cerebellum and parietal cortex, from MDD and SZ groups were significantly lower than the control group. There was a positive correlation between CSF1R levels in the spleen and CSF1R levels in the parietal cortex in the all subjects from four groups. Furthermore, levels of SPI1 in the cerebellum and spleen from MDD and SZ groups were significantly higher than the control group. Levels of SPI1 in the parietal cortex were not different among the four groups. Interestingly, there was a negative correlation between CSF1R and SPI1 levels in the spleen of the all subjects from four groups. There was also a negative correlation between CSF1R and SPI1 levels in the spleen of MDD group.

**Limitations:** The small number in each group may limit our interpretation.

**Conclusions:** Abnormalities in CSF1R and SPI1 in the brain–spleen axis might, in part, play a role in the pathophysiology of MDD.

## 1. Introduction

Major depressive disorder (MDD), schizophrenia (SZ), and bipolar disorder (BD) are major psychiatric disorders with complex etiologies. Postmortem brain samples from patients with these disorders might provide useful information for these psychiatric disorders (Harrison, 2011; Lewis, 2002; Kim and Webster, 2009; McCullumsmith et al., 2011, 2013; Meana et al., 2014; Mechawar and Savitz, 2016). Furthermore, there are some reports using postmortem peripheral tissues such as liver and spleen from patients with psychiatric disorders (Yang et al., 2017; Zhang et al., 2020a, Zhang et al., 2020b), suggesting a possible link between brain and peripheral organs.

Accumulating evidence suggests that abnormalities in immune system such as microglial function play a role in the pathophysiology of major psychiatric disorders (Frick et al., 2013; Hashimoto, 2009; Kato et al., 2013; Mondelli et al., 2017; Monji et al., 2009; Prinz and

Priller, 2014; Sperner-Unterweger, 2005; Trépanier et al., 2016; Yirmiya et al., 2015; van Kesteren et al., 2017). Microglia are dependent on colony-stimulating factor 1 receptor (CSF1R) signaling for their survival since the loss of the *Csf1r* gene blocks the normal population of resident microglia in the brain (Elmore et al., 2014). It is suggested that microglia in the adult brain are physiologically dependent upon CSF1R signaling (Priller and Prinz, 2019). It is reported that CSF1R interacts with the E26 transformation-specific (ETS) family transcription factor PU.1 (SPI1) (Sato et al., 2014), suggesting an association between CSF1R and SPI1. High expressions of CSF1R and SPI1 in human brain and spleen were reported at The Human Protein Atlas. Given the role of immune system in major psychiatric disorders, it is of interest to study the role of CSF1R and SPI1 in the postmortem samples from the major psychiatric disorders.

Spleen is the largest organ that plays a key role in the immune system. Furthermore, the spleen plays multiple roles in the immune

\* Corresponding author.

E-mail address: [hashimoto@faculty.chiba-u.jp](mailto:hashimoto@faculty.chiba-u.jp) (K. Hashimoto).

<https://doi.org/10.1016/j.jad.2020.03.128>

Received 2 January 2020; Received in revised form 10 February 2020; Accepted 29 March 2020

Available online 29 April 2020

0165-0327/ © 2020 Elsevier B.V. All rights reserved.

**Table 1**  
Characteristics of the postmortem samples from Neuropathology Consortium of the Stanley Medical Research Institute.

Characteristics	Control (n = 15)	MDD (n = 15)	SZ (n = 15)	BD (n = 15)	P value
Age at death (years)	48.1 ± 10.7 (29–68)	46.5 ± 9.3 (30–65)	44.5 ± 13.1 (25–62)	42.3 ± 11.7 (25–61)	0.540 <sup>a</sup>
Gender (male/female)	9/6	9/6	9/6	9/6	
PMI (hrs)	23.7 ± 9.95	27.5 ± 10.7	33.7 ± 14.6	32.5 ± 16.1	0.147 <sup>a</sup>
Brain pH	6.27 ± 0.24	6.18 ± 0.21	6.16 ± 0.26	6.18 ± 0.23	0.616 <sup>c</sup>
Brain hemispheres (right/left)	7/8	6/9	6/9	8/7	0.864 <sup>b</sup>
Brain weight (g)	1501.0 ± 164.1	1462.0 ± 142.1	1471.7 ± 108.2	1441.2 ± 171.5	0.740 <sup>a</sup>
Storage days	338.2 ± 234.2	434.0 ± 290.0	621.1 ± 233.1	620.5 ± 172.3	0.003 <sup>a</sup>
Age of onset (years)		33.9 ± 13.3	23.2 ± 8.0	21.5 ± 8.4	0.003 <sup>a</sup>
Duration of disease (years)		12.7 ± 11.1	21.3 ± 11.4	20.1 ± 9.7	0.068 <sup>a</sup>
History of Psychosis			15	11 with (4 without)	0.100 <sup>c</sup>
Fluphenazine equivalent (mg)			52,267 ± 62,062 (1 never)	20,827 ± 24,016 (3 never)	0.084 <sup>d</sup>

The data are shown the mean ± SD. MDD: major depressive disorder, SZ: schizophrenia, BD: bipolar disorder. PMI: postmortem interval.

<sup>a</sup> One-way ANOVA.

<sup>b</sup>  $\chi^2$  test for independence.

<sup>c</sup> Fisher's exact probability test.

<sup>d</sup> Unpaired *t*-test.

system of the body which might play a role in pathogenesis of psychiatric disorders. In the present study, we investigated whether protein expression of CSF1R and SPI1 in postmortem samples (parietal cortex, cerebellum, and spleen) from groups with three major psychiatric disorders showed differences when compared with control group.

## 2. Materials and methods

### 2.1. Postmortem human samples

Human postmortem parietal cortex (Brodmann area 7), cerebellum, and spleen from normal controls ( $N = 15$ ), as well as patients with major depressive disorder (MDD) ( $N = 15$ ), bipolar disorder (BD) ( $N = 15$ ) and schizophrenia (SZ) ( $N = 15$ ) were obtained from the Stanley Foundation Brain Collection (Bethesda, MD, USA) (Table 1). The spleen samples from three SZ patients and one MDD patient were not included. The specimens are collected by medical examiners. Permission from the next of kin was obtained in all the cases. The demographic, clinical and storage information for cases has been previously published (Torrey et al., 2000). Each diagnostic group was matched according to several parameters, including age at death, gender, post-mortem interval (PMI), brain pH and brain weight (Hashimoto et al., 2007; Yang et al., 2017; Ren et al., 2016; Xiong et al., 2019; Zhang et al., 2018, Zhang et al., 2020b). This study was approved by the Research Ethics Committee of the Graduate School of Medicine, Chiba University.

### 2.2. Western blot analysis

Western blot analysis was performed by one observer who was blinded to the four groups. Human brain samples were stored at  $-80\text{ }^{\circ}\text{C}$  until biochemical analyses. Tissue samples were homogenized in Laemmli lysis buffer, then centrifuged at  $3000 \times g$  at  $4\text{ }^{\circ}\text{C}$ , for 10 min to obtain the supernatants. Protein concentrations were determined using a BCA method assay kit (Bio-Rad, Hercules, CA), then samples were incubated for 5 min at  $95\text{ }^{\circ}\text{C}$ , with an equal volume of 125 mM Tris/HCl, pH 6.8, 20% glycerol, 0.1% bromophenol blue, 10%  $\beta$ -mercaptoethanol and 4% sodium dodecyl sulfate. Proteins were separated using sodium dodecyl sulfate-polyacrylamide gel electrophoresis (SDS-PAGE), on 10% mini-gels (Mini-PROTEAN<sup>®</sup> TGX<sup>™</sup> Precast Gel; Bio-Rad). Separated proteins were then transferred onto polyvinylidene difluoride (PVDF) membranes using a Trans Blot Mini Cell (Bio-Rad). For immunodetection, blots were blocked with 5% skim milk in TBST (TBS + 0.1% Tween-20) for 1 h at room temperature (RT), then incubated with primary antibodies overnight, at  $4\text{ }^{\circ}\text{C}$ . The following primary antibodies were used: CSF1R monoclonal antibody (1:1000,

Bioss, Inc., Woburn, MA; bsm-51303 M), SPI1 monoclonal antibody (1:3000, Abcam, Cambridge, MA, USA; ab76543) and  $\beta$ -actin (1:10,000, Sigma-Aldrich Co., Ltd., St Louis, MO, USA). The next day, blots were washed three times in TBST and incubated with horseradish peroxidase conjugated anti-rabbit or anti-mouse antibody (1:5000) for 1 h, at RT. After three washes in TBST, bands were detected using enhanced chemiluminescence (ECL) plus the Western Blotting Detection system (GE Healthcare Bioscience) and captured by ChemiDoc<sup>™</sup> Imaging System (170–01,401; Bio-Rad Laboratories, Hercules, CA). Image data were analyzed using Image Lab<sup>™</sup> 3.0 software (Bio-Rad Laboratories).

### 2.3. Statistical analysis

The data were shown as the mean ± standard error of the mean (S.E.M.). The analysis was performed using PASW Statistics 20 (formerly SPSS statistics; SPSS, Tokyo, Japan). Analyses of covariance (ANCOVAs) were performed on normalized spot volumes, for each spot in each region, with brain pH, age of disease onset, gender, duration of disease, postmortem interval, frozen brain hemisphere side, lifetime neuroleptic drug use, severity of substance abuse, severity of alcohol abuse and/or frozen storage time. If ANCOVA reached significance, we performed the post hoc least significance difference test to identify group comparisons. Correlation was determined by Pearson or non-parametric Spearman correlations. A *P*-value less than 0.05 was considered to be statistically significant.

## 3. Results

Since the postmortem samples have many parameters, the ANCOVA has been used for statistical analyses of the data. The ANCOVA of the data of CSF1R protein from the cerebellum ( $F_{3,56} = 0.950$ ,  $P = 0.423$ ; Fig. 1A) and parietal cortex ( $F_{3,56} = 0.687$ ,  $P = 0.564$ ; Fig. 1B) showed no statistical difference among the four groups. The ANCOVA of the data of CSF1R protein from the spleen showed the statistical difference ( $F_{3,52} = 3.901$ ,  $P = 0.030$ ) among the four groups. A *post-hoc* analysis showed that expression of CSF1R in MDD and SZ groups was significantly lower than that in the control group (Fig. 1C). The expression of CSF1R in BD group was not different from the control group (Fig. 1C).

Next, we analyzed the correlation between CSF1R expression in the brain and spleen. There was a positive correlation ( $r = 0.283$ ,  $P = 0.034$ ) between CSF1R in the parietal cortex and CSF1R in the spleen in the all subjects from the four groups (Fig. 1D). Moreover, we found a positive correlation ( $r = 0.584$ ,  $P = 0.022$ ) between CSF1R in the parietal cortex and CSF1R in the spleen of the subjects from BD

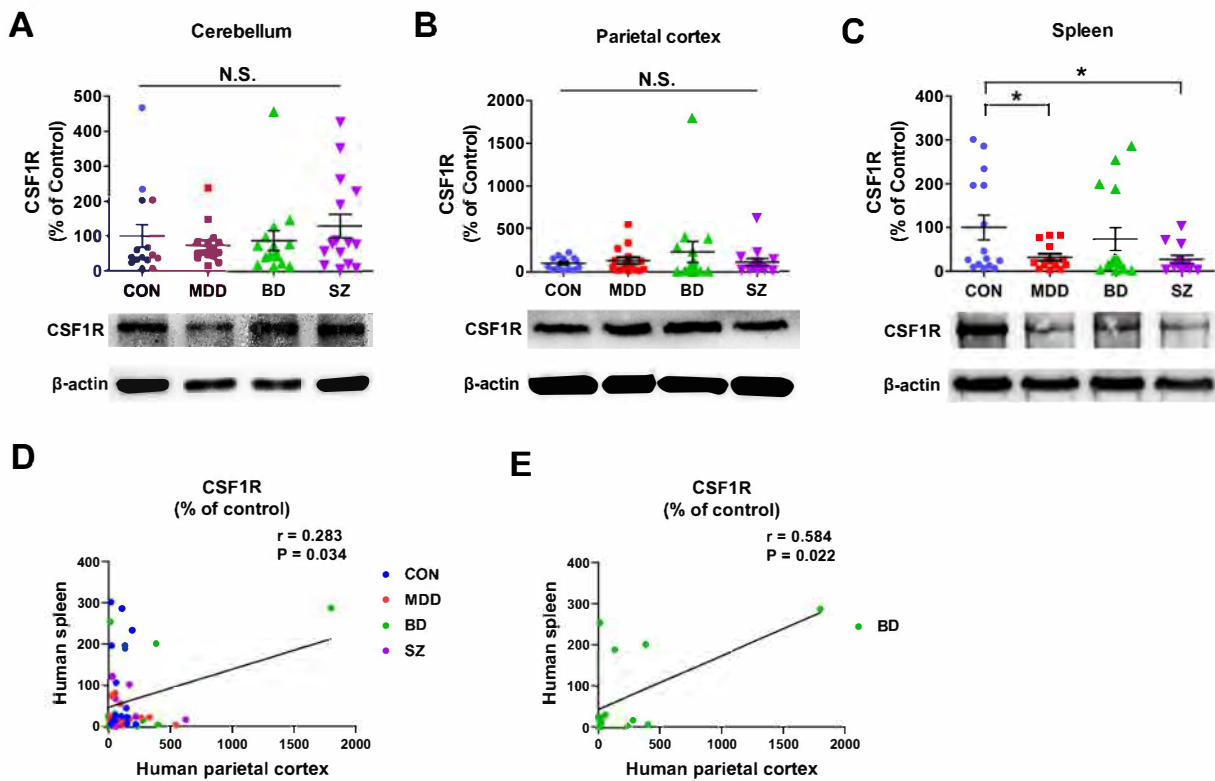


**Fig. 1.** Levels of CSF1R in the cerebellum, parietal cortex and spleen from control, MDD, BD and SZ groups. (A): Western blot analysis of CSF1R and  $\beta$ -actin in the cerebellum of control ( $n = 15$ ), MDD ( $n = 15$ ), BD ( $n = 15$ ) and SZ ( $n = 15$ ) groups was performed. (B): Western blot analysis of CSF1R and  $\beta$ -actin in the parietal cortex of control ( $n = 15$ ), MDD ( $n = 15$ ), BD ( $n = 15$ ) and SZ ( $n = 15$ ) groups was performed. (C): Western blot analysis of CSF1R and  $\beta$ -actin in the spleen of control ( $n = 15$ ), MDD ( $n = 14$ ), BD ( $n = 15$ ) and SZ ( $n = 12$ ) groups was performed. The data are expressed as a percentage of control group values. The data are shown as mean  $\pm$  S.E.M. \* $P < 0.05$  compared to the control group. (D): There was a positive correlation ( $r = 0.283$ ,  $P = 0.034$ ) between CSF1R in the parietal cortex and CSF1R in the spleen of the all subjects from the four groups ( $N = 56$ ). (E): There was a positive correlation ( $r = 0.584$ ,  $P = 0.022$ ) between CSF1R in the parietal cortex and CSF1R in the spleen of the subjects from BD group ( $N = 30$ ). BD, bipolar disorder; CON, control; CSF1R, colony stimulating factor 1 receptor; MDD, major depressive disorder; SZ, schizophrenia.

group (Fig. 1E).

Furthermore, the ANCOVA of the data of SPI1 protein from the cerebellum showed the statistical difference ( $F_{3,56} = 3.474$ ,  $P = 0.023$ ) among the four groups. A *post-hoc* analysis showed that expression of SPI1 in MDD, BD and SZ groups was significantly higher than that in the control group (Fig. 2A). However, the ANCOVA of the data of SPI1 protein in the parietal cortex showed no statistical difference among the four groups ( $F_{3,56} = 1.642$ ,  $P = 0.192$ ; Fig. 2B). The ANCOVA of the data of SPI1 protein in the spleen showed the statistical difference ( $F_{3,52} = 3.231$ ,  $P = 0.031$ ) among the four groups. A *post-hoc* analysis showed that expression of SPI1 in MDD and SZ groups was significantly higher than that in the control group (Fig. 2C). The expression of SPI1 in BD group was not different from the control group (Fig. 2C).

Further analysis of the correlation between SPI1 expression in the brain and spleen showed a positive correlation ( $r = 0.365$ ,  $P = 0.006$ ) between SPI1 in the cerebellum and SPI1 in the spleen in the all subjects from the four groups (Fig. 2D). There was also a positive correlation ( $r = 0.311$ ,  $P = 0.020$ ) between SPI1 in the parietal cortex and SPI1 in the spleen of the all subjects from the four groups (Fig. 2E). Moreover, we found a positive correlation between SPI1 in the parietal cortex and SPI1 in the spleen of the subjects from BD group ( $r = 0.902$ ,  $P = 0.000$ ; Figure F) and SZ group ( $r = 0.591$ ,  $P = 0.043$ ; Figure G).

Furthermore, the analysis of the correlation between CSF1R expression in the spleen and SPI1 expression in the spleen revealed a negative correlation ( $r = -0.337$ ,  $P = 0.011$ ) in the all subjects from the four groups (Fig. 3A). Interestingly, there was a negative correlation ( $r = -0.535$ ,  $P = 0.049$ ) between CSF1R expression in the spleen and SPI1 expression in the spleen of the subjects from MDD group (Fig. 3B).

#### 4. Discussion

The major findings of this study are as follows. First, tissue levels of CSF1R in the spleen from MDD group and SZ group, but not BD group, were significantly lower than those of the control group although there were no different for CSF1R in the brain samples among the all subjects from the four groups. There was a positive correlation between CSF1R in the parietal cortex and CSF1R in the spleen in the all subjects from the four groups. Second, tissue levels of SPI1 in the cerebellum from MDD, SZ, and BD groups were significantly higher than those of the control group. Furthermore, tissue levels of SPI1 in the spleen from MDD and SZ, but not BD group, were significantly higher than those of the control group. Interestingly, there was a positive correlation between SPI1 levels in the brain and spleen, suggesting a possible link between brain and spleen. Finally, there were negative correlations between CSF1R and SPI1 in the spleen in the all subjects from the four groups or in MDD group, suggesting a possible link between CSF1R and SPI1 in the spleen. Taken together, it is likely that abnormalities in the expression of CSF1R and SPI1 in the spleen may, in part, play a role in the pathophysiology of MDD and SZ.

Microglia are the only cell type that express CSF1R. *Csf1r* knockout mice are devoid of microglia in the brain, indicating a crucial role of CSF1R in microglia function (Erblich et al., 2011). Furthermore, *Csf1r* knockout mice show multiple defects in macrophage development, reproduction and tissue remodeling, indicating that CSF1R is the major regulator of tissue macrophage development and maintenance (Chiu and Stanley, 2017). In this study, we found the decreased expression of CSF1R in the spleen of MDD and SZ patients although there were no changes in the two brain regions among the four groups.

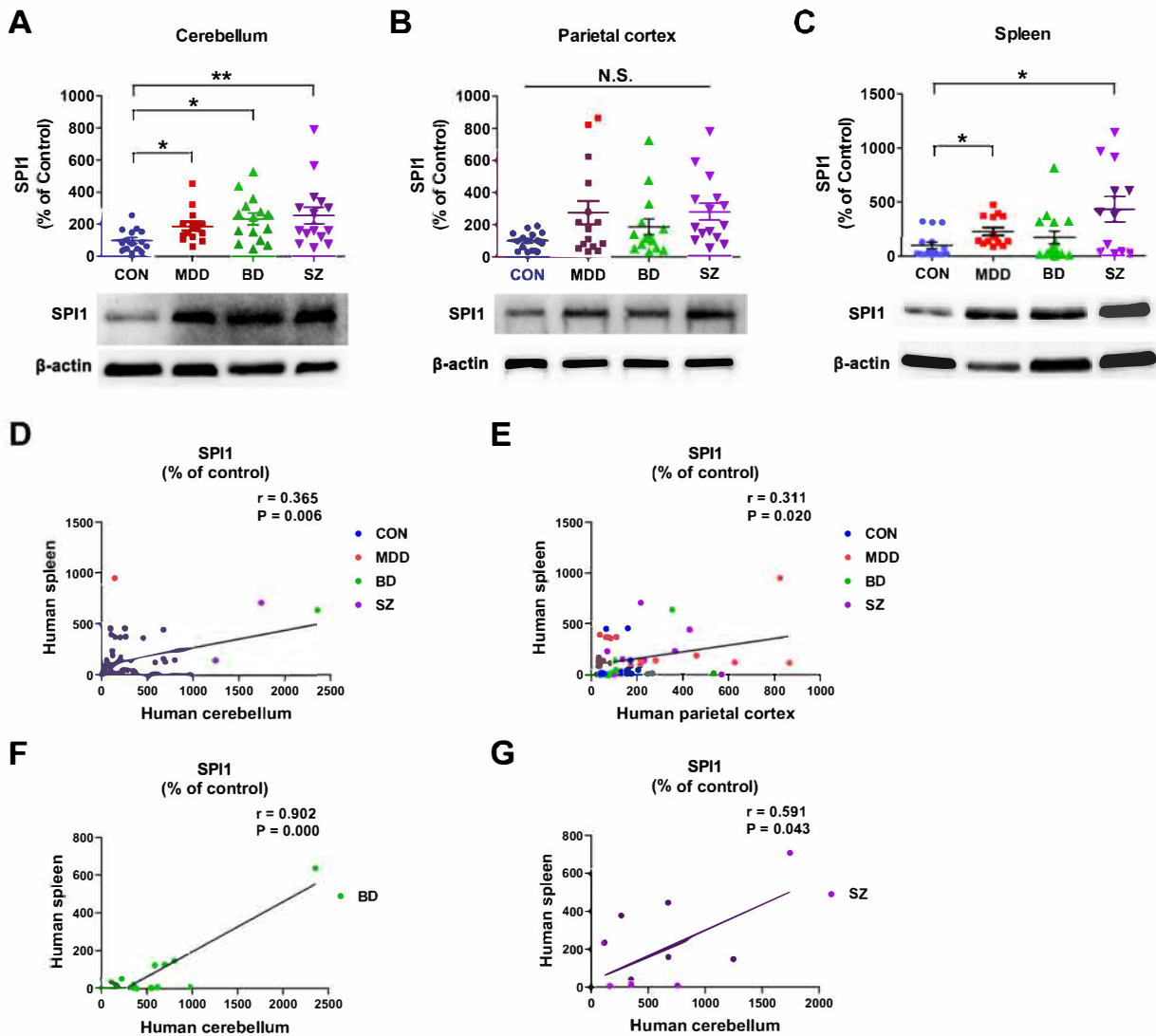


**Fig. 2.** Levels of SPI1 in the cerebellum, parietal cortex and spleen from control, MDD, BD and SZ groups. (A): Western blot analysis of SPI1 and  $\beta$ -actin in the cerebellum of control ( $n = 15$ ), MDD ( $n = 15$ ), BD ( $n = 15$ ) and SZ ( $n = 15$ ) groups was performed. (B): Western blot analysis of SPI1 and  $\beta$ -actin in the parietal cortex of control ( $n = 15$ ), MDD ( $n = 15$ ), BD ( $n = 15$ ) and SZ ( $n = 15$ ) groups was performed. (C): Western blot analysis of SPI1 and  $\beta$ -actin in the spleen of control ( $n = 15$ ), MDD ( $n = 14$ ), BD ( $n = 15$ ) and SZ ( $n = 12$ ) groups was performed. The data are expressed as a percentage of control group values. The data are shown as mean  $\pm$  S.E.M. \* $P < 0.05$  and \*\* $P < 0.01$  compared to the control group. (D): There was a positive correlation ( $r = 0.365$ ,  $P = 0.006$ ) between SPI1 in the cerebellum and SPI1 in the spleen of the all subjects from the four groups ( $N = 56$ ). (E): There was a positive correlation ( $r = 0.311$ ,  $P = 0.020$ ) between SPI1 in the parietal cortex and SPI1 in the spleen of the all subjects from the four groups ( $N = 56$ ). (F): There was a positive correlation ( $r = 0.902$ ,  $P < 0.001$ ) between SPI1 in the cerebellum and SPI1 in the spleen of the subjects from BD group ( $N = 30$ ). (G): There was a positive correlation ( $r = 0.591$ ,  $P = 0.043$ ) between SPI1 in the cerebellum and SPI1 in the spleen of the subjects from SZ group ( $N = 24$ ). BD, bipolar disorder; CON, control; MDD, major depressive disorder; SZ, schizophrenia.

Furthermore, we found a positive correlation between CSF1R protein in the parietal cortex and CSF1R protein in the spleen in the all subject from the four groups or MDD patients. Collectively, it is possible that abnormalities in the immune system by lower expression of CSF1R in the spleen may, in part, play a role in the pathology of MDD and SZ although further study is needed.

SPI1 plays a crucial role in regulation of the genes relevant to specialized functions of microglia (Satoh et al., 2014). In this study, we found increased expression of SPI1 in the cerebellum, but not parietal cortex, from MDD, SZ, and BD groups. Considering the role of cerebellum in psychiatric disorders (Phillips et al., 2015), the increased expression of SPI1 in the cerebellum from major psychiatric disorders is of interest. Furthermore, we also found increased expression of SPI1 in the spleen from MDD and SZ groups. Interestingly, there were positive correlations between SPI1 protein in the brain regions and spleen in the all groups, BD group, or SZ group, suggesting a possible link between brain and spleen. Collectively, it is likely that increased expression of

SPI1 in the brain and spleen may play a role in the pathology of psychiatric disorders such as MDD.

In this study, we found negative correlation between CSF1R protein and SPI1 protein in the spleen of the all subjects from all groups or MDD group. It is possible that abnormalities in the interaction of CSF1R and SPI1 in the spleen may cause abnormal function of macrophage in the spleen, resulting in the development of these psychiatric disorders. Nonetheless, further study on the role of CSF1R and SPI1 in the spleen is needed.

Spleen is a large immune system that plays a key role in the immune system. Very recently, we reported that NKG2D (natural killer group 2, member D) expression in the spleen of susceptible mice after chronic social defeat stress (CSDS) was higher than that in control mice and CSDS-resilient mice (Zhang et al., 2020a), suggesting a novel role of splenic NKG2D in stress susceptibility versus resilience in mice subjected to CSDS. In addition, NKG2D expression in the spleen of MDD group was significantly higher than that of control group (Zhang et al.,

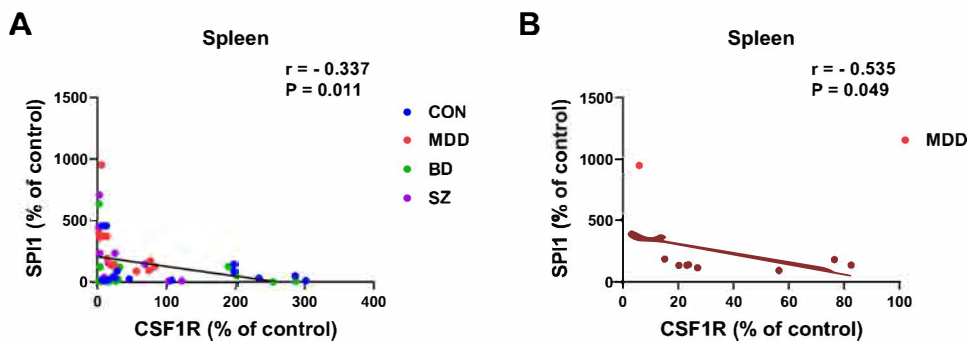


**Fig. 3. Correlation between CSF1R in the spleen and SPI1 in the spleen.** (A): There was a negative correlation ( $r = -0.337$ ,  $P = 0.011$ ) between CSF1R in the spleen and SPI1 in the spleen of the all subjects from the four groups ( $N = 56$ ). (B): There was a negative correlation ( $r = -0.535$ ,  $P = 0.049$ ) between CSF1R in the spleen and SPI1 in the spleen of the subjects from MDD group ( $N = 28$ ). BD, bipolar disorder; CON, control; CSF1R, colony stimulating factor 1 receptor; MDD, major depressive disorder; SZ, schizophrenia.

2020a). In addition, splenic functions and gene expression in mice with depression-like phenotype were markedly impaired (Zhan et al., 2017). Furthermore, we reported correlations between pro-peptide of brain-derived neurotrophic factor levels in the spleen and brain (Yang et al., 2017). In this study, we found alterations in the expression of CSF1R and SPI1 in the brain and spleen from psychiatric disorders. Taken all together, it is likely that abnormalities in the brain–spleen axis may, in part, play a role in the psychiatric disorders such as MDD and SZ.

This study has some limitation. First, sample size is small. Second, positive correlations of CSF1R between spleen and brain may be driven by one significant outlier. A further study using large sample size is needed. Third, we used the postmortem tissues from the Stanley Medical Research Foundation. Further study using postmortem tissues from other brain banks is needed to confirm brain–spleen axis in psychiatric disorders.

In conclusion, this study suggests that abnormal expression of CSF1R and SPI1 in the spleen as well as brain may, in part, play a role in the development of psychiatric disorders such as MDD. Further detailed investigations on the role of brain–spleen axis in the pathology of psychiatric disorders are warranted.

#### Contributors

Dr. Hashimoto conceptualized the study. Dr. Zhang performed the experiments. Dr. Zhang and Dr. Hashimoto had access to all data and take responsibility for the accuracy of the data analysis. Dr. Zhang performed the data analysis and interpreted the results. Dr. Chang and Dr. Pu discussed with all authors about the data. All authors contributed to and approve of the final manuscript.

#### Role of funding source

This study was supported by the grants from the Japan Agency for Medical Research and Development (AMED) (to K.H., JP19dm0107119) and the Grant-in-Aid for Scientific Research on Innovative Areas from the MEXT, Japan (to K.H., 19H05203).

#### CRediT authorship contribution statement

**Jiancheng Zhang:** Conceptualization, Data curation, Formal analysis, Methodology, Writing - original draft, Writing - review & editing.  
**Lijia Chang:** Data curation, Methodology, Writing - review & editing.  
**Yaoyu Pu:** Data curation, Methodology, Writing - review & editing.  
**Kenji Hashimoto:** Conceptualization, Funding acquisition, Supervision, Writing - original draft, Writing - review & editing.

#### Declaration of Competing Interest

All authors report no biomedical financial interests or potential conflicts of interest.

#### Acknowledgments

We thank to The Stanley Medical Research Institution (MD, USA) for providing the postmortem tissue samples from psychiatric disorders.

#### Supplementary materials

Supplementary material associated with this article can be found, in the online version, at [doi:10.1016/j.jad.2020.03.128](https://doi.org/10.1016/j.jad.2020.03.128).

#### References

- Chitu, V., Stanley, E.R., 2017. Regulation of embryonic and postnatal development by the CSF-1 receptor. *Curr. Top. Dev. Biol.* 123, 229–275.
- Elmore, M.R., Najafi, A.R., Koike, M.A., Dagher, N.N., Spangenberg, E.E., Rice, R.A., Kitazawa, M., Matusow, B., Nguyen, H., West, B.L., Green, K.N., 2014. Colony-stimulating factor 1 receptor signaling is necessary for microglia viability, unmasking a microglia progenitor cell in the adult brain. *Neuron* 82, 380–397.
- Erblich, B., Zhu, L., Etgen, A.M., Dobrenis, K., Pollard, J.W., 2011. Absence of colony stimulation factor-1 receptor results in loss of microglia, disrupted brain development and olfactory deficits. *PLoS ONE* 6 e26317.
- Frick, L.R., Williams, K., Pittenger, C., 2013. Microglial dysregulation in psychiatric disease. *Clin. Dev. Immunol.* 2013 608654.
- Harrison, P.J., 2011. Using our brains: the findings, flaws, and future of postmortem studies of psychiatric disorders. *Biol. Psychiatry* 69, 102–103.
- Hashimoto, K., 2009. Emerging role of glutamate in the pathophysiology of major depressive disorder. *Brain Res. Rev.* 61, 105–123.
- Hashimoto, K., Sawa, A., Iyo, M., 2007. Increased levels of glutamate in brains from patients with mood disorders. *Biol. Psychiatry* 62, 1310–1316.
- Kato, T.A., Watabe, M., Kanba, S., 2013. Neuron-glia interaction as a possible glue to translate the mind-brain gap: a novel multi-dimensional approach toward psychology and psychiatry. *Front. Psychiatry* 4, 139.
- Kim, S., Webster, M.J., 2009. Postmortem brain tissue for drug discovery in psychiatric research. *Schizophr. Bull.* 35, 1031–1033.
- Lewis, D.A., 2002. The human brain revisited: opportunities and challenges in postmortem studies of psychiatric disorders. *Neuropsychopharmacology* 26, 143–154.
- McCullumsmith, R.E., Hammond, J.H., Shan, D., Meador-Woodruff, J.H., 2013. Postmortem brain: an underutilized substrate for studying severe mental illness. *Neuropsychopharmacology* 39, 65–87.
- McCullumsmith, R.E., Meador-Woodruff, J.H., 2011. Novel approaches to the study of postmortem brain in psychiatric illness: old limitations and new challenges. *Biol. Psychiatry* 69, 127–133.
- Meana, J.J., Callado, L.F., Morentin, B., 2014. Do post-mortem brain studies provide useful information for psychiatry? *Rev. Psiquiatr. Salud. Ment. (Barc.)* 7, 101–103.
- Mechawar, N., Savitz, J., 2016. Neuropathology of mood disorders: do we see the stigmata of inflammation? *Transl. Psychiatry* 6, e946.
- Mondelli, V., Vernon, A.C., Turkheimer, F., Dazzan, P., Pariante, C.M., 2017. Brain microglia in psychiatric disorders. *Lancet Psychiatry* 4, 563–572.
- Monji, A., Kato, T., Kanba, S., 2009. Cytokines and schizophrenia: microglia hypothesis of schizophrenia. *Psychiatry Clin. Neurosci.* 63, 257–265.
- Phillips, J.R., Hewedi, D.H., Eissa, A.M., Moustafa, A.A., 2015. The cerebellum and psychiatric disorders. *Front. Public Health* 3, 66.
- Priller, J., Prinz, M., 2019. Targeting microglia in brain disorders. *Science* 365, 32–33.
- Prinz, M., Priller, J., 2014. Microglia and brain macrophages in the molecular age: from origin and neuropsychiatric disease. *Nat. Rev. Neurosci.* 15, 300–312.
- Ren, Q., Ma, M., Ishima, T., Morisseau, C., Yang, J., Wagner, K.M., Zhang, J.C., Yang, C., Yao, W., Dong, C., Han, M., Hammock, B.D., Hashimoto, K., 2016. Gene deficiency and pharmacological inhibition of soluble epoxide hydrolase confers resilience to repeated social defeat stress. *Proc. Natl. Acad. Sci. U S A* 113 E1944–52.
- Satoh, J.J., Asahina, N., Kitano, S., Kino, Y., 2014. A comprehensive profile of ChIP-Seq-based PU.1/Spi1 target genes in microglia. *Gene. Regul. Syst. Bio.* 8, 127–139.
- Sperner-Unterwiesing, B., 2005. Immunological aetiology of major psychiatric disorders: evidence and therapeutic implications. *Drugs* 65, 1493–1520.
- Torrey, E.F., Webster, M., Knable, M., Johnston, N., Yolken, R.H., 2000. The stanley




- foundation brain collection and neuropathology consortium. *Schizophr. Res.* 44, 151–155.
- Trépanier, M.O., Hopperton, K.E., Mizrahi, R., Mechawar, N., Bazinet, R.P., 2016. Postmortem evidence of cerebral inflammation in schizophrenia: a systematic review. *Mol. Psychiatry* 21, 1009–1026.
- van Kesteren, C.F., Gremmels, H., de Witte, L.D., Hol, E.M., Van Gool, A.R., Falkai, P.G., Kahn, R.S., Sommer, I.E., 2017. Immune involvement in the pathogenesis of schizophrenia: a meta-analysis on postmortem brain studies. *Transl. Psychiatry* 7 e1075.
- Xiong, Z., Zhang, K., Ren, Q., Chang, L., Chen, J., Hashimoto, K., 2019. Increased expression of inwardly rectifying Kir4.1 channel in the parietal cortex from patients with major depressive disorder. *J. Affect. Disord.* 245, 265–269.
- Yang, B., Ren, Q., Zhang, J.C., Chen, Q.X., Hashimoto, K., 2017. Altered expression of BDNF, BDNF pro-peptide and their precursor proBDNF in brain and liver tissues from psychiatric disorders: rethinking the brain-liver axis. *Transl. Psychiatry* 7 e1128.
- Yirmiya, R., Rimmerman, N., Reshef, R., 2015. Depression as a microglial disease. *Trend. Neurosci.* 38, 637–658.
- Zhan, H., Huang, F., Yan, F., Zhao, Z., Zhang, J., Cui, T., Yang, F., Hai, G., Jia, X., Shi, Y., 2017. Alterations in splenic function and gene expression in mice with depression-like behavior induced by exposure to corticosterone. *Int. J. Mol. Med.* 39, 327–336.
- Zhang, K., Sakamoto, A., Chang, L., Qu, Y., Wang, S., Pu, Y., Tan, Y., Wang, X., Fujita, Y., Ishima, T., Hatano, M., Hashimoto, K., 2020. Splenic NKG2D confers resilience versus susceptibility in mice after chronic social defeat stress: beneficial effects of (R)-ketamine. *Eur. Arch. Psychiatry Clin. Neurosci.* <https://doi.org/10.1007/s00406-019-01092-z>.
- Zhang, J., Tan, Y., Chang, L., Hammock, B.D., Hashimoto, K., 2020b. Increased expression of soluble epoxide hydrolase in the brain and liver from patients with major psychiatric disorders: a role of brain - liver axis. *J. Affect. Disord.* 270, 131–134 revision.
- Zhang, J.C., Yao, W., Dong, C., Han, M., Shirayama, Y., Hashimoto, K., 2018. Keap1-Nrf2 signaling pathway confers resilience versus susceptibility to inescapable electric stress. *Eur. Arch. psychiatry Clin. Neurosci.* 268, 865–870.

ARTICLE

Open Access

# Abnormal composition of gut microbiota is associated with resilience versus susceptibility to inescapable electric stress

Kai Zhang<sup>1,2</sup>, Yuko Fujita<sup>1</sup>, Lijia Chang<sup>1</sup>, Youge Qu<sup>1</sup>, Yaoyu Pu<sup>1</sup>, Siming Wang<sup>1</sup>, Yukihiko Shirayama<sup>1,3</sup> and Kenji Hashimoto<sup>1</sup> 

## Abstract

Increasing evidence indicates that abnormalities in the composition of gut microbiota might play a role in stress-related disorders. In the learned helplessness (LH) paradigm, ~60–70% rats are susceptible to LH in the face of inescapable electric stress. The role of gut microbiota in susceptibility in the LH paradigm is unknown. In this study, male rats were exposed to inescapable electric stress under the LH paradigm. The compositions of gut microbiota and short-chain fatty acids were assessed in fecal samples from control rats, non-LH (resilient) rats, and LH (susceptible) rats. Members of the order *Lactobacillales* were present at significantly higher levels in the susceptible rats than in control and resilient rats. At the family level, the number of *Lactobacillaceae* in the susceptible rats was significantly higher than in control and resilient rats. At the genus level, the numbers of *Lactobacillus*, *Clostridium* cluster III, and *Anaerofustis* in susceptible rats were significantly higher than in control and resilient rats. Levels of acetic acid and propionic acid in the feces of susceptible rats were lower than in those of control and resilient rats; however, the levels of lactic acid in the susceptible rats were higher than those of control and resilient rats. There was a positive correlation between lactic acid and *Lactobacillus* levels among these three groups. These findings suggest that abnormal composition of the gut microbiota, including organisms such as *Lactobacillus*, contributes to susceptibility versus resilience to LH in rats subjected to inescapable electric foot shock. Therefore, it appears likely that brain–gut axis plays a role in stress susceptibility in the LH paradigm.

## Introduction

Resilience is adaptation in the face of stress and adversity. It is well known that humans display wide variability in their responses to stress. Increasing amounts of evidence show that resilience might be mediated by adaptive changes in several neural circuits, including numerous molecular and cellular pathways<sup>1–11</sup>. An understanding of the molecular and cellular mechanisms underlying resilience will facilitate the discovery of new therapeutic drugs for stress-related psychiatric disorders,

but the detailed mechanisms underlying resilience and susceptibility remain unclear.

The brain–gut–microbiome axis is a complex, bidirectional signaling system between the brain and the gut microbiota<sup>12–16</sup>. Accumulating studies suggest that an abnormal composition of the gut microbiota contributes to the pathophysiology of depression<sup>17–21</sup> and the antidepressant effects of certain potential compounds<sup>22–29</sup>. Previously, we reported that the presence of *Bifidobacterium* in the gut microbiome confers stress resilience in a chronic social defeat stress (CSDS) model<sup>30</sup>. It has been shown that ~30–40% of rats are resilient to inescapable electric stress in the learned helplessness (LH) paradigm<sup>31–34</sup>; however, the role of gut microbiota in the production of this resilience has not yet been investigated. Microbes in the gut can produce short-chain fatty acids.

Correspondence: Kenji Hashimoto ([hashimoto@faculty.chiba-u.jp](mailto:hashimoto@faculty.chiba-u.jp))

<sup>1</sup>Division of Clinical Neuroscience, Chiba University Center for Forensic Mental Health, Chiba 260-8670, Japan

<sup>2</sup>Department of Psychiatry, Chaohu Hospital of Anhui Medical University, 238000 Hefei, China

Full list of author information is available at the end of the article.

© The Author(s) 2019



**Open Access** This article is licensed under a Creative Commons Attribution 4.0 International License, which permits use, sharing, adaptation, distribution and reproduction in any medium or format, as long as you give appropriate credit to the original author(s) and the source, provide a link to the Creative Commons license, and indicate if changes were made. The images or other third party material in this article are included in the article's Creative Commons license, unless indicated otherwise in a credit line to the material. If material is not included in the article's Creative Commons license and your intended use is not permitted by statutory regulation or exceeds the permitted use, you will need to obtain permission directly from the copyright holder. To view a copy of this license, visit <http://creativecommons.org/licenses/by/4.0/>.

The presence and abundance of such acids could possibly be used as an indicator of the types of bacteria present in the gut. However, it is also currently unknown how the altered composition of the gut microbiota affects the concentration of short-chain fatty acids in fecal samples.

The purpose of this study was to investigate the role of gut microbiota on stress resilience using a rat LH paradigm. First, we investigated whether the composition of the gut microbiota was altered in fecal samples from LH (susceptible) and non-LH (resilient) rats compared with control rats. Then we examined whether the levels of short-chain fatty acids—acetic acid, propionic acid, butyric acid, lactic acid, and succinic acid—in the fecal samples from susceptible and resilient rats were altered compared with control rats, since these short-chain fatty acids can be produced by the gut microbiota<sup>23</sup>.

## Materials and methods

### Animals

Male Sprague-Dawley rats ( $n = 25$ , 200–230 g; 7 weeks, Charles River Japan, Co., Tokyo, Japan) were used. The animals were housed under a 12-h light/dark cycle with ad libitum access to food and water. The experimental procedures were approved by the Chiba University Institutional Animal Care and Use Committee (Permission number: 31-341).

### Stress paradigm (LH model) and collection of fecal sample

The LH paradigm was performed as previously reported<sup>6–8,11,31–34</sup>. Animals were initially exposed to uncontrollable stress to create LH rats. When the rats were later placed in a situation in which the shock is controllable; that is, the animal could escape it, an animal exhibiting LH not only fails to acquire an escape response but also often makes no effort to escape the shock at all.

We used the Gemini Avoidance System (San Diego Instruments, San Diego, CA) for LH paradigm. This apparatus has two compartments by a retractable door. On day 1 and day 2, rats were subjected to 30 inescapable electric foot shocks (0.65 mA, 30 s duration, at random intervals averaging 18–42 s). On day 3, a post-shock test using a two-way conditioned avoidance test was performed to determine whether the rats would exhibit the predicted escape deficits (Fig. 1a). This session consisted of 30 trials, in which electric foot shocks (0.65 mA, 6 s duration, at random intervals with a mean of 30 s) were preceded by a 3-s conditioned stimulus tone that remained on until the shock was terminated. The numbers of escape failures and the latency to escape in each of the 30 trials were counted. Animals with more than 25 escape failures in the 30 trials were regarded as having met the criterion for LH rats (susceptible). Animals with fewer than 24 failures were defined as non-LH rats

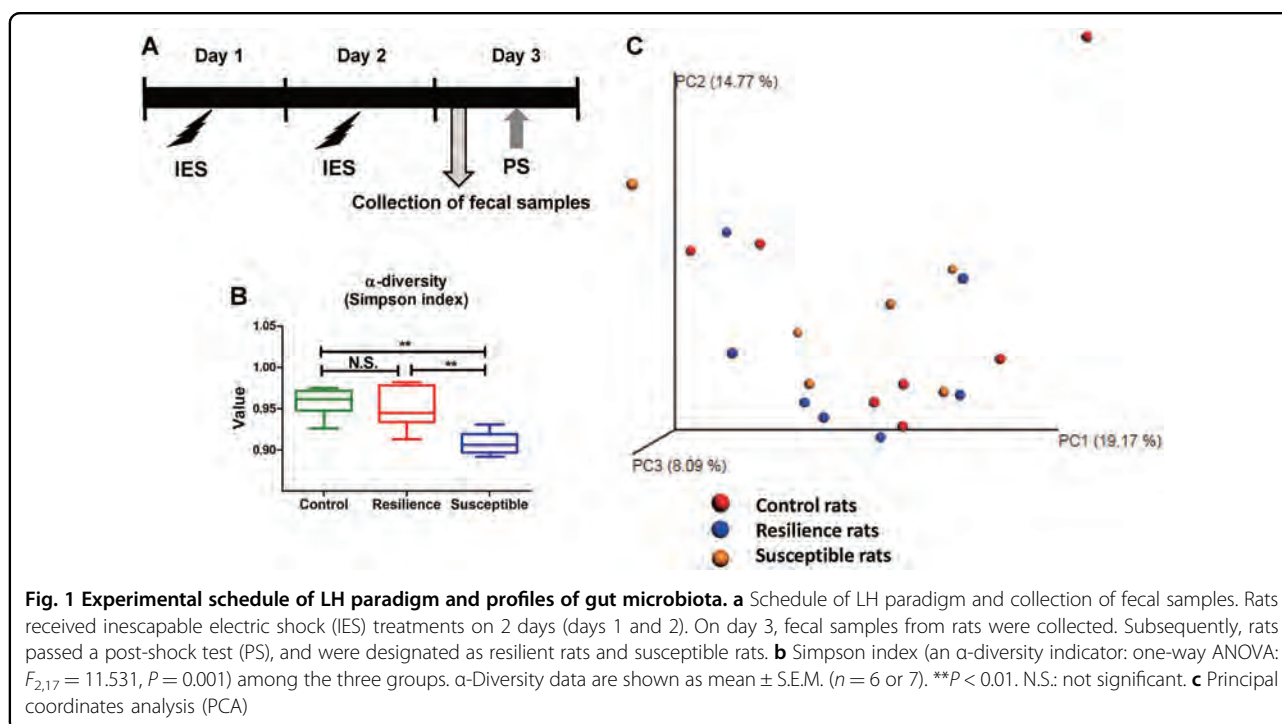
(resilient)<sup>31–34</sup>. Fresh fecal samples were collected in a blind manner before post-shock stress on day 4, and stored at  $-80^{\circ}\text{C}$  until use (Fig. 1A).

### 16S rDNA analysis

DNA extraction from fecal samples and the 16S rDNA analysis were performed at the TechnoSuruga Laboratory, Co., Ltd. (Shizuoka, Japan), as reported previously<sup>35</sup>. Briefly, the samples were suspended in a buffer containing 4 M guanidium thiocyanate, 100 mM Tris-HCl (pH 9.0) and 40 mM EDTA and broken up in the presence of zirconia beads using the FastPrep-24 5G homogenizer (MP Biomedicals, Irvine, CA). Then, DNA was extracted using GENE PREP STAR PI-480 (KURABO, Japan). The final concentration (10 ng/ $\mu\text{L}$ ) of the DNA sample was used. Briefly, the V3-V4 hypervariable regions of the 16S rRNA were amplified from microbial genomic DNA using PCR with the bacterial universal primers (341F/R806)<sup>35</sup> and the dual-index method<sup>36</sup>. For bioinformatics analysis, the overlapping paired-end reads were merged using the fastq-join program with default settings<sup>37</sup>. The reads were processed for quality and chimera filtering as follows. Only reads with quality value scores of 20 for >99% of the sequence were extracted, and chimeric sequences were removed using the program usearch6.1<sup>38</sup>. Non-chimeric reads were submitted for 16S rDNA-based taxonomic analysis using the Ribosomal Database Project (RDP) Multiclassifier tool<sup>39</sup>. Reads obtained in the Multi-FASTA format were assigned to genus or phylum levels with an 80% confidence threshold. Principal component analysis (PCA) was performed using Metagenome@KIN software (World Fusion Co., Ltd., Tokyo, Japan) based on data obtained from the bacterial family using the RDP taxonomic analysis software.

### Measurement of fecal short-chain fatty acids

Measurement of short-chain fatty acids—acetic acid, propionic acid, butyric acid, lactic acid, and succinic acid—in fecal samples was performed at the TechnoSuruga Laboratory, Co., Ltd. (Shizuoka, Japan). For the determination of these short-chain fatty acids, feces were suspended in distilled water, heated at  $85^{\circ}\text{C}$  for 15 min to inactivate viruses, and then centrifuged according to previously reported methods<sup>40,41</sup>. The concentrations of these short-chain fatty acids in feces were measured using a high-performance liquid chromatography organic acid analysis system with a Prominence CDD-10A conductivity detector (Shimadzu, Kyoto, Japan), two tandemly arranged Shim-pack SCR-102(H) columns [300 mm  $\times$  8 mm inner diameter (ID)], and a Shim-pack SCR-102(H) guard column (50 mm  $\times$  6 mm ID)<sup>40,41</sup>. The HPLC calibration curves for the measurement of the short-chain fatty acids were created using prepared standard solutions.



## Statistical analysis

The data are presented as the mean  $\pm$  standard error of the mean (S.E.M.). Analysis was performed using the PASW Statistics 20 software (now SPSS statistics; SPSS, Tokyo, Japan). Comparisons between groups were performed using one-way analysis of variance, followed by post hoc Fisher's Least Significant Difference test. A  $P$  value  $< 0.05$  was considered statistically significant.

## Results

### Composition of gut microbiota in control, resilient, and susceptible rats

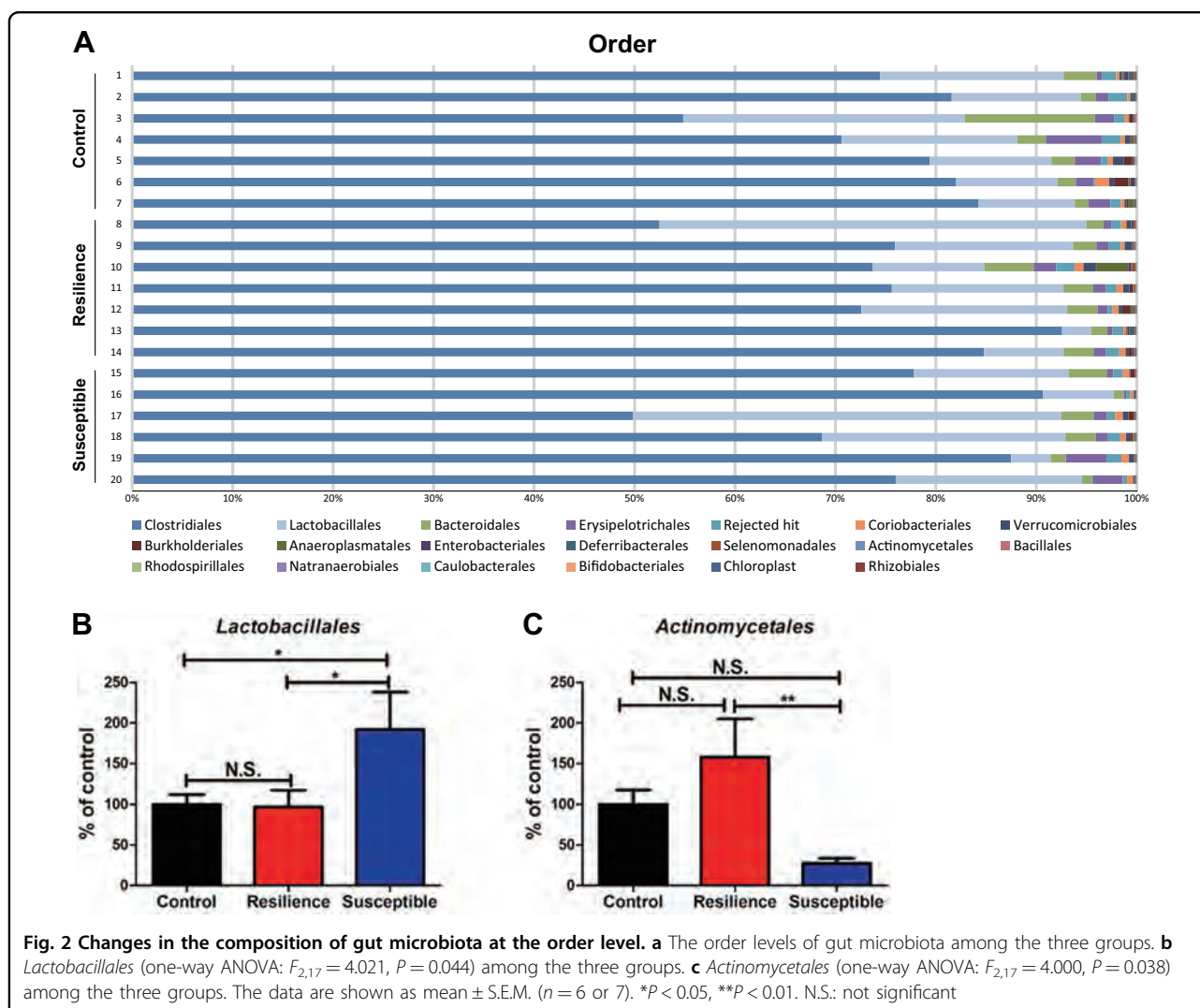
We used 16S rDNA gene sequencing to determine differences in the gut microbiota composition among the three groups of rats.  $\alpha$ -diversity refers to the diversity of bacteria or species within a community or habitat. The susceptible rats showed a significant decrease in the  $\alpha$ -diversity value compared with control rats or resilient rats (Fig. 1b). In the three-dimensional PCoA data, the measurements from susceptible rats were well separated from those of control rats and resilient rats. Four measurements from the susceptible group were close to those of the sham group, whereas the other three measurements were close to those of the resilient group (Fig. 1c).

*Firmicutes* were the most dominant phylum, comprising  $>85\%$  of the total sequences. There were no significant differences in the levels of this phylum among the three groups. The order levels of gut bacterium in control rats, resilient rats, and susceptible rats were identified (Fig. 2a).

*Clostridiales* and *Lactobacillales* were the most dominant orders, with  $>80\%$  of total sequences. The number of *Lactobacillales* was significantly increased in the susceptible rats compared with that in control and resilient rats (Fig. 2b). In contrast, the number of *Lactobacillales* in the resilient rats was similar to that in the control rats (Fig. 2b). The number of *Actinomycetales* in the susceptible rats was significantly lower than that in the resilient rats (Fig. 2c). Although the number of *Actinomycetales* in the resilient rats was higher than that in the control rats, the difference did not reach statistical significance.

The families of the gut bacteria in control, resilient, and susceptible rats are shown (Fig. 3a). *Lactobacillaceae* were significantly more highly represented in the susceptible rats than in the control and resilient rats, although the number of *Lactobacillaceae* in the resilient rats was similar to that in the control rats (Fig. 3b). In contrast, the number of *Corynebacteriaceae* was significantly lower in the susceptible rats than that in the resilient rats, although these two did not significantly differ from the control rats (Fig. 3c).

The genera of gut bacteria in the control, resilient, and susceptible rats are shown (Fig. 4a). *Lactobacillus*, *Clostridium* cluster III, and *Anaerofustis* numbers were significantly higher in the susceptible rats than in the control and resilient rats (Fig. 4b, c, e). *Corynebacterium* numbers were significantly lower in the susceptible rats than in the resilient rats, although these two groups were not significantly altered compared with the control rats (Fig. 4d).



### Measurement of short-chain fatty acids in fecal samples

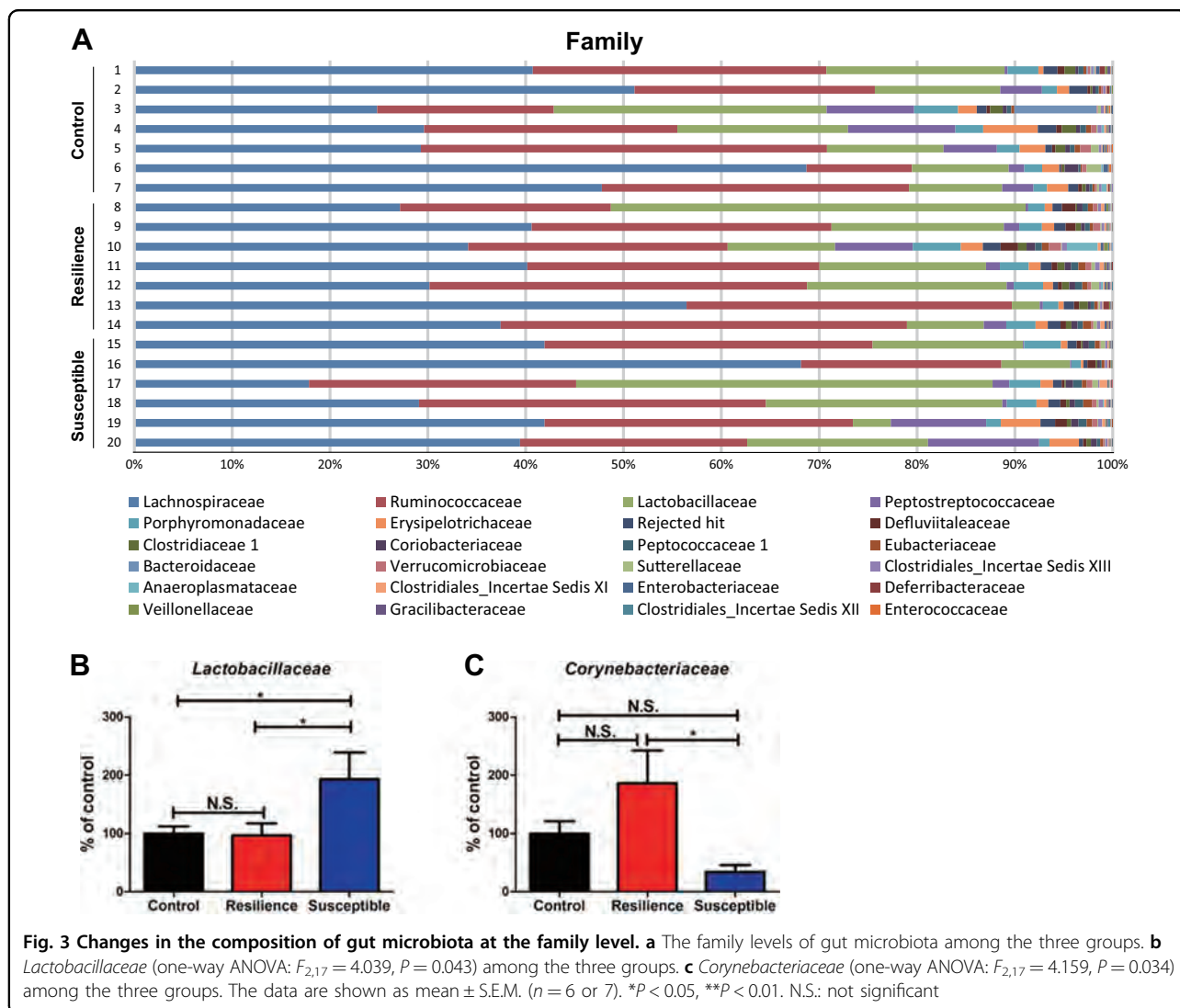
Levels of acetic acid and propionic acid in the susceptible rats were significantly lower than those in control rats and resilient rats, and there were no significant differences between control rats and resilient rats (Fig. 5a, b). There were no changes in butyric acid and succinic acid among the three groups (Fig. 5c, e). In contrast, levels of lactic acid in the susceptible rats were significantly higher than those of control rats and resilient rats, although there were no changes between control rats and resilient rats (Fig. 5d). There was a positive correlation ( $r = 0.461$ ,  $P = 0.041$ ) between lactic acid and *Lactobacillus* levels among three groups (Fig. 5f). There were no correlations between other short-chain fatty acids and the microbiome composition among the three experimental groups.

### Discussion

The major findings of this study are as follows. At the order level, susceptibility to LH in rats exposed to

inescapable shock might be associated with an increase of *Lactobacillales* and a decrease of *Actinomycetales* in the host gut. At the family level, stress susceptibility might be associated with an increase in *Lactobacillaceae* and decrease of *Corynebacteriaceae* in the host gut. At the gene level, stress susceptibility might be associated with the increase of *Lactobacillus*, *Clostridium* cluster III and *Anaerofustis*, and the decrease of *Corynebacterium* in the host gut. Levels of acetic acid and propionic acid in the feces from susceptible rats were lower than those in the feces of control and resilient rats, whereas levels of lactic acid in the susceptible rats were higher than those of control and resilient rats. There was a positive correlation between lactic acid and *Lactobacillus* levels among these three groups. These findings suggest that alterations in the composition of these microbiota contribute to susceptibility versus resilience in rats in the LH situation.

In this study, we found an increase in the abundance of members of the order *Lactobacillales* and the family

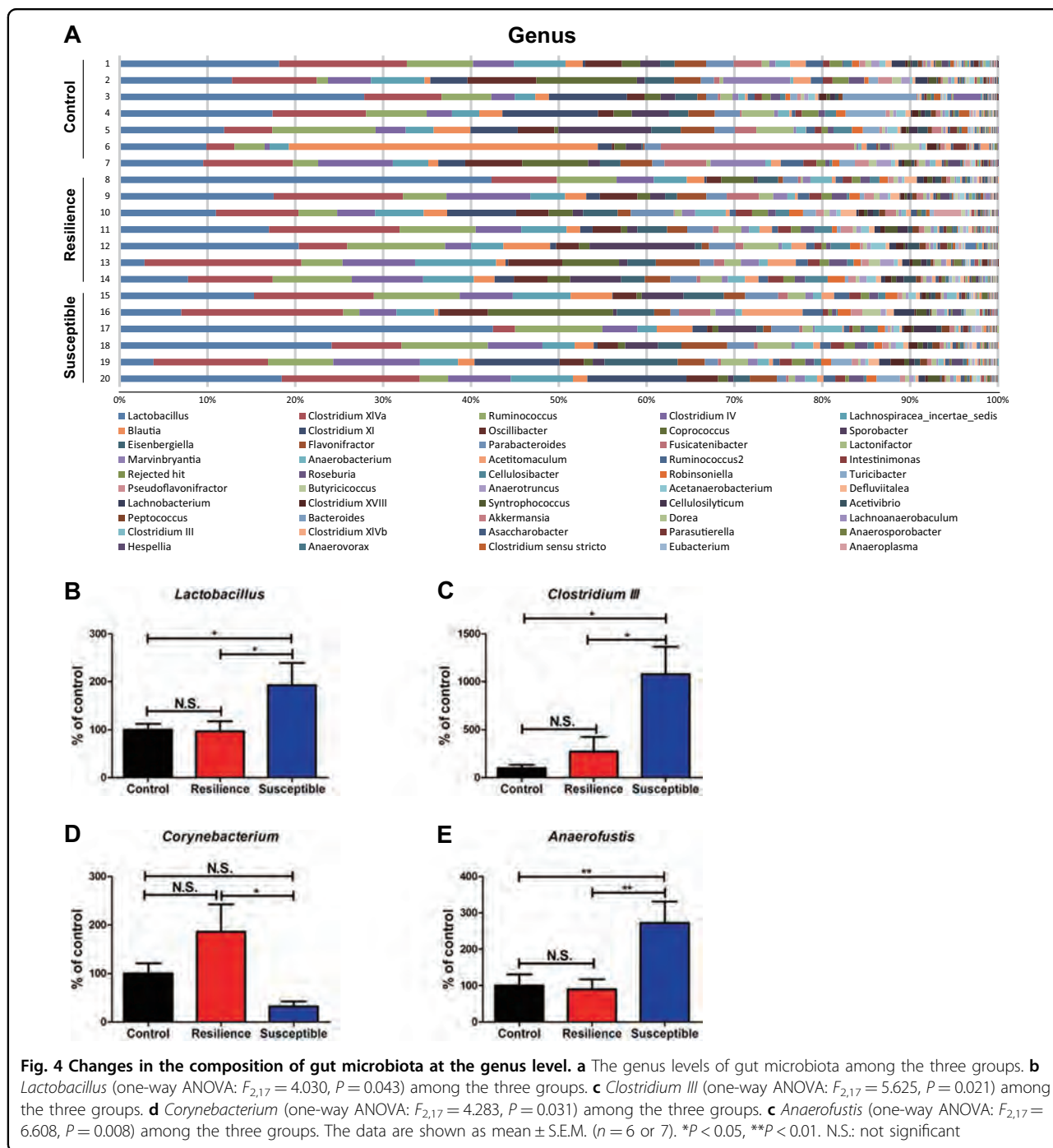


*Lactobacillaceae* in susceptible rats, in comparison with control and resilient rats. It is possible that increased abundance of members of the *Lactobacillales* order and *Lactobacillaceae* family might play a role in susceptibility versus resilience of rats to LH after inescapable electric stress.

At the genus level, susceptibility in rats exposed to inescapable shock might be associated with an increase in *Lactobacillus*, *Clostridium* cluster III, and *Anaerofustis* and a decrease of *Corynebacterium* in the host gut. *Clostridium*, a genus of Gram-positive bacteria, includes several significant human pathogens, such as the causative agent of botulism. High levels of members of the genus *Clostridium* have been reported in patients with major depressive disorder (MDD) compared with controls<sup>42,43</sup>, suggesting that increased levels of *Clostridium* play a role in depression. We reported that susceptible mice after CSDS have higher levels of *Clostridium*, and that the

novel antidepressant candidate (*R*)-ketamine attenuated the increased levels of *Clostridium* in susceptible mice<sup>25</sup>. This study shows that the antidepressant effects of (*R*)-ketamine might be partly mediated by the restoration of altered composition of the gut microbiota in the CSDS susceptible mice. Although the role of members of *Clostridium* cluster III in depression is currently unclear, it appears that *Clostridium* cluster III may contribute to susceptibility in rats subjected to inescapable electric stress.

*Anaerofustis* is a strictly anaerobic, Gram-positive, rod-shaped, non-spore-forming bacterial genus of the family *Eubacteriaceae*<sup>44</sup>. In this study, we found decreased levels of *Anaerofustis* in the susceptible rats compared with the control and resilient rats. At present, there have been no reports showing alterations in *Anaerofustis* in patients with MDD, or in rodents with depression-like phenotypes. Therefore, it is unclear how decreased levels of

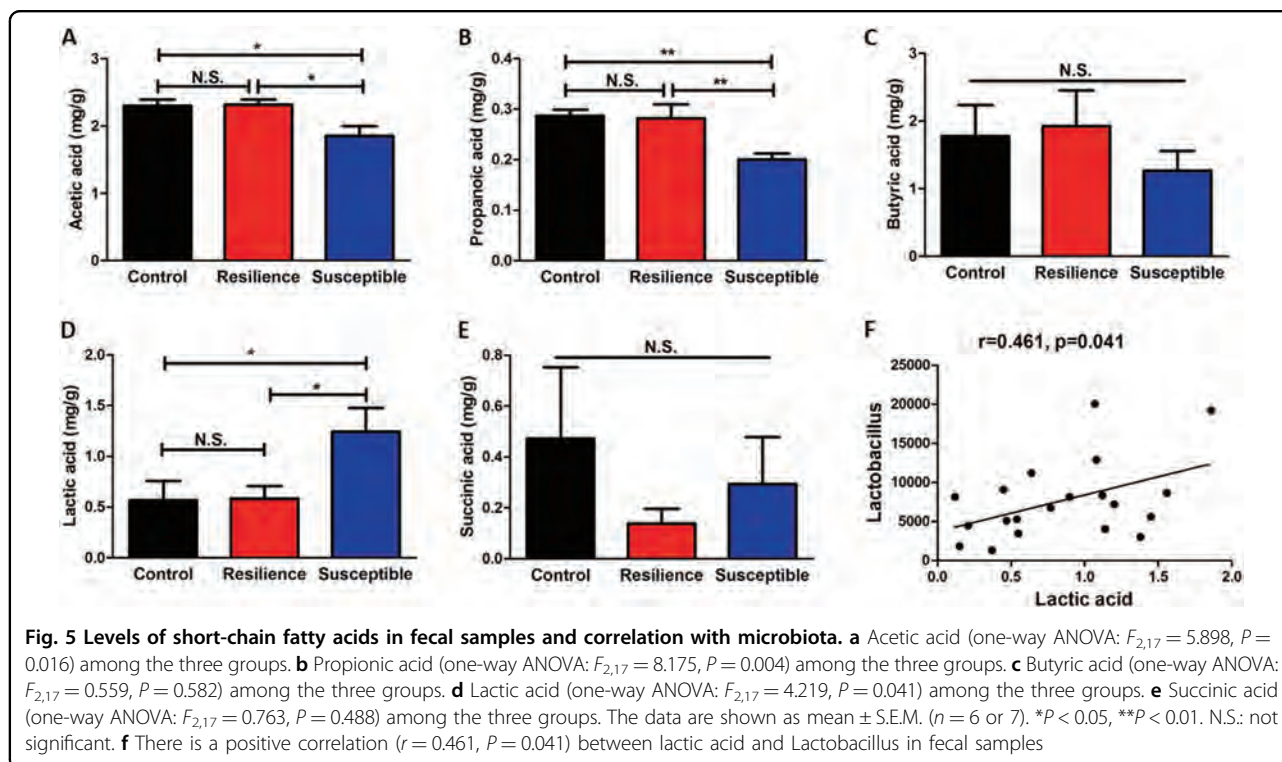


*Anaerofustis* play a role in susceptibility to LH. Further study into the role of *Anaerofustis* in depression is needed.

In this study, we found lower levels of *Corynebacterium* in the susceptible rats compared with control and resilient rats. It has been reported that sub-chronic and chronic exposure to glyphosate-based herbicides decreases the composition of microbiota, such as *Corynebacterium*, resulting in behavioral abnormalities including depression and anxiety<sup>45</sup>. Low levels of *Corynebacterium* were also

reported in a chronic variable stress-induced rat model of depression<sup>46</sup>. It appears likely that lowered levels of *Corynebacterium* might play a role in a depression-like phenotype in rodents, although further study into the role of *Corynebacterium* in depression is needed.

Short-chain fatty acids—acetic acid, propionic acid, butyric acid, lactic acid, and succinic acid—are generated as the end products of the degradation and fermentation of indigestible carbohydrates by the gut microbiota<sup>47</sup>.



Measurement of these short-chain fatty acids could therefore serve as an indirect method for the analysis of microbiota composition. These organic acids have specific anti-microbial activities<sup>48</sup>. It has been reported that levels of acetic acid and propionic acid in feces from women with depression are lower than those in control subjects, and that there are negative correlations between acetic acid or propionic acid and depression scores<sup>49</sup>. In this study, we found decreased levels of acetic acid and propionic acid in rats susceptible to LH, compared with control and resilient rats, consistent with the results from a recent clinical study<sup>49</sup>. We also found decreased levels of butyric acid in the susceptible rats, although the difference did not reach statistical significance. Three short-chain fatty acids containing C2–C4, acetic acid, propionic acid, and butyric acid, account for over 95% of the pool of short-chain fatty acids<sup>23</sup>. It is likely that decreased levels of acetic acid and propionic acid in feces may be associated with susceptibility to LH, and with depression in patients with MDD.

Elevated levels of lactic acid in the blood, cerebrospinal fluid and brain have been reported in patients with MDD<sup>50–52</sup>. Higher levels of lactic acid in rodents with depression-like behaviors have also been reported<sup>53</sup>. In contrast, peripheral administration of lactic acid produced antidepressant-like effects in different models of depression<sup>54</sup>. In this research we found higher levels of lactic acid in feces from susceptible rats compared with those from control and resilient rats. We found a positive

correlation between *Lactobacillus*, microbes which produce lactic acid, and the amounts of lactic acid in fecal samples. It appears likely that the increased levels of lactic acid produced by *Lactobacillus* might contribute to susceptibility to inescapable electric stress, although further study is needed.

The crosstalk between the brain and the gut is predominantly influenced by the gut bacteria<sup>55</sup>. Imbalance of gut microbiota has been found to cause abnormalities in the brain–gut axis in several neurological and psychiatric diseases<sup>13,55</sup>. Multiple lines of evidence suggest that an abnormal composition of the gut microbiota contributes to the resilience or susceptibility to LH in rodents after repeated stress<sup>30,56–59</sup>. It is well recognized that gut microbiota plays a role in animal behaviors<sup>14,60–62</sup>, although the precise mechanisms underlying the microbiome-mediated behaviors are currently unknown. For example, it has been reported that the vagus nerve plays a major role in modulating the constitutive communication pathway between the brain and the bacteria in the gut<sup>63,64</sup>. It is likely that altered composition of microbiota might play a key role in the stress-induced disorders although further study is needed.

This research has some limitations. In this study, we did not identify the specific microbiome which can affect susceptibility or resilience in the LH experiments. Therefore, from the present data, we do not know how the specific microbiome can affect behaviors under the LH paradigm. In the future, it will be necessary to identify



the specific microbiome, using approaches such as shotgun metagenomics sequencing. It will also be of interest to investigate the way in which specific microbiomes affect behaviors related to LH.

In conclusion, the present study suggests that an altered composition of the gut microbiota, including organisms, such as *Lactobacillus*, *Clostridium* cluster III, *Anaerofus-tis*, and *Corynebacterium*, contributes to resilience and susceptibility to learned helplessness in rats subjected to inescapable electric foot shock.

#### Acknowledgements

This study was supported by SENSHIN Medical Research Foundation, Japan (to K.Z.), Smoking Research Foundation, Japan (to K.H.), and AMED, Japan (to K.H., JP19dm0107119). L.C. was supported by Japan China Sasakawa Medical Fellowship (Tokyo, Japan). S.W. was supported by TAKASE Scholarship Foundation (Tokyo, Japan).

#### Author details

<sup>1</sup>Division of Clinical Neuroscience, Chiba University Center for Forensic Mental Health, Chiba 260-8670, Japan. <sup>2</sup>Department of Psychiatry, Chaohu Hospital of Anhui Medical University, 238000 Hefei, China. <sup>3</sup>Department of Psychiatry, Teikyo University Chiba Medical Center, Ichihara, Chiba 299-0111, Japan

#### Conflict of interest

K.H. has received research support from Dainippon-Sumitomo, Otsuka, and Taisho. The remaining authors declare that they have no conflict of interest.

#### Publisher's note

Springer Nature remains neutral with regard to jurisdictional claims in published maps and institutional affiliations.

Received: 10 May 2019 Revised: 29 June 2019 Accepted: 30 July 2019


Published online: 17 September 2019

#### References

- Southwick, S. M., Vythilingam, M. & Charney, D. S. The psychobiology of depression and resilience to stress: implications for prevention and treatment. *Ann. Rev. Clin. Psychol.* **1**, 255–291 (2005).
- Feder, A., Nestler, E. J. & Charney, D. S. Psychobiology and molecular genetics of resilience. *Nat. Rev. Neurosci.* **10**, 446–457 (2009).
- Franklin, T. B., Saab, B. J. & Mansuy, I. M. Neural mechanisms of stress resilience and vulnerability. *Neuron* **75**, 747–761 (2012).
- Russo, S. J., Murrugh, J. W., Han, M. H., Charney, D. S. & Nestler, E. J. Neurobiology of resilience. *Nat. Neurosci.* **15**, 1475–1484 (2012).
- Taliaz, D. et al. Resilience to chronic stress is mediated by hippocampal brain-derived neurotrophic factor. *J. Neurosci.* **31**, 4475–4483 (2012).
- Yang, C., Shirayama, Y., Zhang, J. C., Ren, Q. & Hashimoto, K. Regional differences in brain-derived neurotrophic factor levels and dendritic spine density confer resilience to inescapable stress. *Int. J. Neuropsychopharmacol.* **18**, pyu121 (2015).
- Yang, C., Shirayama, Y., Zhang, J. C., Ren, Q. & Hashimoto, K. Peripheral interleukin-6 promotes resilience versus susceptibility to inescapable electric stress. *Acta Neuropsychiatr.* **27**, 312–316 (2015).
- Yang, B. et al. Regional differences in the expression of brain-derived neurotrophic factor (BDNF) pro-peptide, proBDNF and preproBDNF in the brain confer stress resilience. *Eur. Arch. Psychiatry Clin. Neurosci.* **266**, 765–769 (2016).
- Dantzer, R., Cohen, S., Russo, S. J. & Dinan, T. G. Resilience and immunity. *Brain Behav. Immun.* **74**, 28–42 (2018).
- Qu, Y. et al. Regional differences in dendritic spine density confer resilience to chronic social defeat stress. *Acta Neuropsychiatr.* **30**, 117–122 (2018).
- Zhang, J. C. et al. Keap1-Nrf2 signaling pathway confers resilience versus susceptibility to inescapable electric stress. *Eur. Arch. Psychiatry Clin. Neurosci.* **268**, 865–870 (2018).
- Dinan, T. G. & Cryan, J. F. Brain-gut-microbiota axis and mental health. *Psychosom. Med.* **79**, 920–926 (2017).
- Fung, T. C., Olson, C. A. & Hsiao, E. Y. Interactions between the microbiota, immune and nervous systems in health and disease. *Nat. Neurosci.* **20**, 145–155 (2017).
- Cusotto, S., Sandhu, K. V., Dinan, T. G. & Cryan, J. F. The neuroendocrinology of the microbiota-gut-brain axis: a behavioural perspective. *Front. Neuroendocrinol.* **51**, 80–101 (2018).
- Molina-Torres, G., Rodriguez-Arastia, M., Roman, P., Sanchez-Labraca, N. & Cardona, D. Stress and the gut microbiota-brain axis. *Behav. Pharmacol.* **30**(2 and 3 Special Issue), 187–202 (2019).
- Cusotto S., et al. Differential effects of psychotropic drugs on microbiome composition and gastrointestinal function. *Psychopharmacology (Berl)*. <https://doi.org/10.1007/s00213-018-5006-5> (2018).
- Jiang, H. et al. Altered fecal microbiota composition in patients with major depressive disorder. *Brain Behav. Immun.* **48**, 186–194 (2015).
- Zheng, P. et al. Gut microbiome remodeling induces depressive-like behaviors through a pathway mediated by the host's metabolism. *Mol. Psychiatry* **21**, 786–796 (2016).
- Wong, M. L. et al. Inflammasome signaling affects anxiety- and depressive-like behavior and gut microbiome composition. *Mol. Psychiatry* **21**, 797–805 (2016).
- Huang, T. T. et al. Current understanding of gut microbiota in mood disorders: an update of human studies. *Front. Genet.* **10**, 98 (2019).
- Yang, C. et al. Key role of gut microbiota in anhedonia-like phenotype in rodents with neuropathic pain. *Transl. Psychiatry* **9**, 57 (2019).
- Burokas, A. et al. Targeting the microbiota-gut-brain axis: prebiotics have anxiolytic and antidepressant-like effects and reverse the impact of chronic stress in mice. *Biol. Psychiatry* **82**, 472–487 (2017).
- den Besten, G. et al. The role of short-chain fatty acids in the interplay between diet, gut microbiota, and host energy metabolism. *J. Lipid Res.* **54**, 2325–2340 (2013).
- Ho, P. & Ross, D. A. More than a gut feeling: the implications of the gut microbiota in psychiatry. *Biol. Psychiatry* **81**, e35–e37 (2017).
- Qu, Y. et al. Comparison of (R)-ketamine and lanicemine on depression-like phenotype and abnormal composition of gut microbiota in a social defeat stress model. *Sci. Rep.* **7**, 15725 (2017).
- Yang, C. et al. Possible role of the gut microbiota-brain axis in the antidepressant effects of (R)-ketamine in a social defeat stress model. *Transl. Psychiatry* **7**, 1294 (2017).
- Zhang, J. C. et al. Blockade of interleukin-6 receptor in the periphery promotes rapid and sustained antidepressant actions: a possible role of gut-microbiota-brain axis. *Transl. Psychiatry* **7**, e1138 (2017).
- Huang, N. et al. Role of *Actinobacteria* and *Coriobacteria* in the antidepressant effects of ketamine in an inflammation model of depression. *Pharmacol. Biochem. Behav.* **176**, 93–100 (2019).
- Lukić, I. et al. Antidepressants affect gut microbiota and *Ruminococcus flavefaciens* is able to abolish their effects on depressive-like behavior. *Transl. Psychiatry* **9**, 133 (2019).
- Yang, C. et al. *Bifidobacterium* in the gut microbiota confer resilience to chronic social defeat stress in mice. *Sci. Rep.* **7**, 45942 (2017).
- Muneoka, K., Shirayama, Y., Horio, M., Iyo, M. & Hashimoto, K. Differential levels of brain amino acids in rat models presenting learned helplessness or non-learned helplessness. *Psychopharmacol. (Berl.)* **226**, 63–71 (2013).
- Shirayama, Y. et al. Alterations in brain-derived neurotrophic factor (BDNF) and its precursor proBDNF in the brain regions of a learned helplessness rat model and the antidepressant effects of a TrkB agonist and antagonist. *Eur. Neuropsychopharmacol.* **25**, 2449–2458 (2015).
- Shirayama, Y. & Hashimoto, K. Effects of a single bilateral infusion of R-ketamine in the rat brain regions of a learned helplessness model of depression. *Eur. Arch. Psychiatry Clin. Neurosci.* **267**, 177–182 (2017).
- Shirayama, Y. & Hashimoto, K. Lack of antidepressant effects of (2R,6R)-hydroxynorketamine in a rat learned helplessness model: Comparison with (R)-ketamine. *Int. J. Neuropsychopharmacol.* **21**, 84–88 (2018).
- Takahashi, S., Tomita, J., Nishioka, K., Hisada, T. & Nishijima, M. Development of a prokaryotic universal primer for simultaneous analysis of *Bacteria* and *Archaea* using next-generation sequencing. *PLoS ONE* **9**, e105592 (2014).

36. Hisada, T., Endoh, K. & Kuriki, K. Inter- and intra-individual variations in seasonal and daily stabilities of the human gut microbiota in Japanese. *Arch. Microbiol.* **197**, 919–934 (2015).
37. Erik A. ea-utils “Command-line tools for processing biological sequencing data”. <http://code.google.com/p/ea-utils> (2011).
38. Edgar, R. C., Haas, B. J., Clemente, J. C., Quince, C. & Knight, R. UCHIME improves sensitivity and speed of chimera detection. *Bioinformatics* **27**, 2194–2200 (2011).
39. Wang, Q., Garrity, G. M., Tiedje, J. M. & Cole, J. R. Naïve Bayesian classifier for rapid assignment of rRNA sequences into the new bacterial taxonomy. *Appl. Environ. Microbiol.* **72**, 5261–5267 (2007).
40. Higashimura, Y. et al. Protective effect of agaro-oligosaccharides on gut dysbiosis and colon tumorigenesis in high-fat diet-fed mice. *Am. J. Physiol. Gastrointest. Liver Physiol.* **310**, G367–G375 (2016).
41. Aoe, S., Nakamura, F. & Fujiwara, S. Effect of wheat bran on fecal butyrate-producing bacteria and wheat bran combined with barley on *Bacteroides* abundance in Japanese healthy adults. *Nutrients* **10**, 1980 (2018).
42. Lin, P. et al. *Prevotella* and *Klebsiella* proportions in fecal microbial communities are potential characteristic parameters for patients with major depressive disorder. *J. Affect. Disord.* **207**, 300–304 (2017).
43. Rong, H. et al. Similarly in depression, nuances of gut microbiota: Evidences from a shotgun metagenomics sequencing study on major depressive disorder versus bipolar disorder with current major depressive episode patients. *J. Psychiatr. Res.* **113**, 90–99 (2019).
44. Finegold, S. M. et al. *Anaerofustis stercorihominis* gen. nov., sp. nov., from human feces. *Anaerobe* **10**, 41–45 (2004).
45. Aitbali, Y. et al. Glyphosate based- herbicide exposure affects gut microbiota, anxiety and depression-like behaviors in mice. *Neurotoxicol. Teratol.* **67**, 44–49 (2018).
46. Yu, M. et al. Variations in gut microbiota and fecal metabolic phenotype associated with depression by 16S rRNA gene sequencing and LC/MS-based metabolomics. *J. Pharm. Biomed. Anal.* **138**, 231–239 (2017).
47. Koh, A., De Vadder, F., Kovatcheva-Datchary, P. & Backhed, F. From dietary fiber to host physiology: short-chain fatty acids as key bacterial metabolites. *Cell* **165**, 1332–1345 (2016).
48. Dibner, J. J. & Buttin, P. Use of organic acids as a model to study the impact of gut microflora on nutrition and metabolism. *J. Appl. Poult. Res.* **11**, 453–463 (2002).
49. Skonieczna-Żydecka, K. et al. Faecal short chain fatty acids profile is changed in Polish depressive women. *Nutrients* **10**, E1939 (2018).
50. Levine, J., Panchalingam, K., McClure, R. J., Gershon, S. & Pettegrew, J. W. Stability of CSF metabolites measured by proton NMR. *J. Neural Transm. (Vienna)*. **107**, 843–848 (2000).
51. Regenold, W. T. et al. Elevated cerebrospinal fluid lactate concentrations in patients with bipolar disorder and schizophrenia: implications for the mitochondrial dysfunction hypothesis. *Biol. Psychiatry* **65**, 489–494 (2009).
52. Ernst, J. et al. Increased pregenual anterior cingulate glucose and lactate concentrations in major depressive disorder. *Mol. Psychiatry* **22**, 113–119 (2017).
53. Shi, B. et al. A <sup>1</sup>H-NMR plasma metabolomic study of acute and chronic stress models of depression in rats. *Behav. Brain. Res.* **241**, 86–91 (2013).
54. Carrard, A. et al. Peripheral administration of lactate produces antidepressant-like effects. *Mol. Psychiatry* **23**, 392–399 (2018).
55. Kelly, J. R., Clarke, G., Cryan, J. F. & Dinan, T. G. Brain-gut-microbiota axis: challenges for translation in psychiatry. *Ann. Epidemiol.* **26**, 366–372 (2016).
56. Szyzkowicz, J. K., Wong, A., Anisman, H., Merali, Z. & Audet, M. C. Implications of the gut microbiota in vulnerability to the social avoidance effects of chronic social defeat in male mice. *Brain Behav. Immun.* **66**, 45–55 (2017).
57. Hao, Z., Wang, W., Guo, R. & Liu, H. *Faecalibacterium prausnitzii* (ATCC 27766) has preventive and therapeutic effects on chronic unpredictable mild stress-induced depression-like and anxiety-like behavior in rats. *Psychoneuroendocrinology* **104**, 132–142 (2019).
58. Kentner, A. C., Cryan, J. F. & Brummelte, S. Resilience priming: Translational models for understanding resiliency and adaptation to early life adversity. *Dev. Psychobiol.* **61**, 350–375 (2019).
59. Gururajan, A. et al. Resilience to chronic stress is associated with specific neurobiological, neuroendocrine and immune responses. *Brain Behav. Immun.* <https://doi.org/10.1016/j.bbi.2019.05.004> (2019).
60. Ezewa, V. O., Gerardo, N. M., Inouye, D. W., Medina, M. & Xavier, J. B. Animal behavior and microbiome. *Science* **338**, 198–199 (2012).
61. Borre, Y. E., Moloney, R. D., Clarke, G., Dinan, T. G. & Cryan, J. F. The impact of microbiota on brain and behavior: mechanisms & therapeutic potential. *Adv. Exp. Med. Biol.* **817**, 373–403 (2014).
62. Jianguo, L., Xueyang, J., Cui, W., Changxin, W. & Xuemei, Q. Altered gut metabolome contributes to depression-like behaviors in rats exposed to chronic unpredictable mild stress. *Transl. Psychiatry* **9**, 40 (2019).
63. Bravo, J. A. et al. Ingestion of *Lactobacillus* strain regulates emotional behavior and central GABA receptor expression in a mouse via the vagus nerve. *Proc. Natl Acad. Sci. USA* **108**, 16050–16055 (2011).
64. Dinan, T. G. & Cryan, J. F. Gut microbiomes and depression: still waiting for godot. *Brain Behav. Immun.* **79**, 1–2 (2019).

# Dietary intake of glucoraphanin prevents the reduction of dopamine transporter in the mouse striatum after repeated administration of MPTP

Yaoyu Pu<sup>1</sup> | Youge Qu<sup>1</sup> | Lijia Chang<sup>1</sup> | Si-ming Wang<sup>1</sup> | Kai Zhang<sup>1</sup> |  
Yusuke Ushida<sup>2</sup> | Hiroyuki Suganuma<sup>2</sup> | Kenji Hashimoto<sup>1</sup> 

<sup>1</sup>Division of Clinical Neuroscience, Chiba University Center for Forensic Mental Health, Chiba, Japan

<sup>2</sup>Innovation Division, Kagome Co., Ltd., Tochigi, Japan

## Correspondence

Kenji Hashimoto, Division of Clinical Neuroscience, Chiba University Center for Forensic Mental Health, Chiba 260-8670, Japan.

Email: hashimoto@faculty.chiba-u.jp

## Funding information

Japan Society for the Promotion of Science, Grant/Award Number: 17H04243

## Abstract

**Aims:** Parkinson's disease (PD) is a chronic and progressive neurodegenerative disorder. Although diet may influence the development of PD, the precise mechanisms underlying relationship between diet and PD pathology are unknown. Here, we examined whether dietary intake of glucoraphanin (GF), the precursor of a natural antioxidant sulforaphane in cruciferous vegetables, can affect the reduction of dopamine transporter (DAT) in the mouse striatum after repeated administration of MPTP (1-methyl-4-phenyl-1,2,3,6-tetrahydropyridine).

**Methods:** Normal food pellet or 0.1% GF food pellet was given into male mice for 28 days from 8-week-old. Subsequently, saline (5 mL/kg × 3, 2-hour interval) or MPTP (10 mg/kg × 3, 2-hour interval) was injected into mice. Immunohistochemistry of DAT in the striatum was performed 7 days after MPTP injection.

**Results:** Repeated injections of MPTP significantly decreased the density of DAT-immunoreactivity in the mouse striatum. In contrast, dietary intake of 0.1% GF food pellet significantly protected against MPTP-induced reduction of DAT-immunoreactivity in the striatum.

**Conclusion:** This study suggests that dietary intake of GF food pellet could prevent MPTP-induced dopaminergic neurotoxicity in the striatum of adult mice. Therefore, dietary intake of GF-rich cruciferous vegetables may have beneficial effects on prevention for development of PD.

## KEYWORDS

dopamine transporter, glucoraphanin, nutrition, Parkinson disease, sulforaphane

## 1 | INTRODUCTION

Parkinson's disease (PD) is a common and progressive neurodegenerative disease that affects predominately dopamine-producing

neurons in the striatum.<sup>1,2</sup> Although the precise mechanisms underlying PD pathology are unknown, environmental factors play a role in the pathology of PD. Importantly, diet is an excellent first step for reducing the risk for PD.<sup>3,4</sup> For example, a high intake of fresh

This is an open access article under the terms of the Creative Commons Attribution-NonCommercial-NoDerivs License, which permits use and distribution in any medium, provided the original work is properly cited, the use is non-commercial and no modifications or adaptations are made.

© 2019 The Authors. *Neuropsychopharmacology Reports* published by John Wiley & Sons Australia, Ltd on behalf of The Japanese Society of Neuropsychopharmacology

vegetables, fruits, nuts and seeds, fish, olive oil, coconut oil, fresh herbs, and spices is associated with a reduced risk of PD development and slower disease progression.<sup>5,6</sup>

Accumulating evidence suggests that the transcription factor Kelch-like erythroid cell-derived protein with CNC homology (ECH)-associated protein 1 (Keap1)-Nuclear factor (erythroid-derived 2)-like 2 (Nrf2) system plays a key role in inflammation which is involved in a number of neurological and psychiatric disorders.<sup>7-11</sup> Multiple lines of evidence suggest a key role of Nrf2 in the pathology of PD.<sup>12-14</sup> Jazwa et al<sup>15</sup> reported that sulforaphane (SFN), a potent Nrf2 activator, protects against dopaminergic neurotoxicity in mice after administration of MPTP (1-methyl-4-phenyl-1,2,3,6-tetrahydropyridine). Furthermore, SFN did not protect MPTP-induced neurotoxicity in Nrf2 knock-out (KO) mice.<sup>15</sup> Furthermore, Zhou et al<sup>16</sup> reported that SFN protected against rotenone-induced neurotoxicity model of PD. Collectively, it is likely that SFN can exert neuroprotective effects in animal models of PD through Nrf2 activation.

Glucoraphanin (GF), which found in cruciferous vegetables, such as broccoli sprout, is a glucosinolate precursor of SFN.<sup>17</sup> Previously, we reported that dietary intake of 0.1% GF food pellet could prevent the onset of psychiatric disorders such as depression and psychosis in rodents,<sup>18-21</sup> suggesting that dietary intake of GF has prophylactic effects for development of psychiatric disorders.<sup>9</sup>

This study was undertaken to investigate whether dietary intake of 0.1% GF food pellet could prevent MPTP-induced dopaminergic neurotoxicity in the mouse striatum since MPTP-induced dopaminergic neurotoxicity is widely used as animal model of PD.<sup>22</sup>

## 2 | METHODS AND MATERIALS

### 2.1 | Animals

Eight weeks old of male adult C57BL/6 mice (body weight 20-25 g, Japan SLC, Inc) were used in experiments. Animals were housed in 23°C ± 1°C room temperature, 55% ± 5% humidity, and 12-hour light/dark cycles (lights on between 07:00-19:00) with libitum food and water. All experiments were done according to the Guide for

Animal Experimentation of Chiba University. The experimental protocol was approved by the Chiba University Institutional Animal Care and Use Committee.

### 2.2 | Preparation of 0.1% glucoraphanin (GF) diet

Glucoraphanin food pellets were prepared as previously reported.<sup>18-21</sup> Food pellets (CE-2; Japan CLEA, Ltd.) containing 0.1% glucoraphanin (GF) were prepared as follows. Broccoli sprout extract powder containing SFN precursor GF was industrially produced by KAGOME CO., LTD. In brief, broccoli sprout was grown from specially selected seeds (Brassica Protection Products LLC.) for 1 day after the germination. The 1-day broccoli sprout was plunged into boiling water and maintained at 95°C for 30 minutes, and the sprout residues were removed by filtration. The boiling water extract was mixed with a waxy corn starch dextrin and then spray dried to yield the broccoli sprout extract powder containing 135 mg (approx. 0.31 mmol) of GF per gram. For preparing the animal diet containing 0.1% GF (approx. 2.3 mmol GF per 1-kg diet), the extract powder was mixed with a basal diet CE-2, and then pelleted at a processing facility (Oriental Yeast Co., Ltd.). The GF content in the diet was determined by high-performance liquid chromatography as previously described.<sup>23,24</sup>

### 2.3 | MPTP-induced neurotoxicity

The protocol of MPTP-induced neurotoxicity was used as previously reported.<sup>25,26</sup> Thirty-nine male mice (8 weeks old) were divided into the following four groups: a normal food + saline (5 mL/kg × 3, 2-hour interval) group; a normal food pellet + MPTP (10 mg/kg × 3, 2-hour interval. Tokyo Chemical Industry CO., Ltd.) group; a 0.1% GF food pellet + saline group; a 0.1% GF food pellet + MPTP group. 0.1% GF food was given from day 1 to day 28 (Figure 1A). Normal food was given to all groups from day 29 to day 36. MPTP or saline was injected into mice on day 29. Seven days (day 36) after administration of MPTP, mice were anesthetized with 5% isoflurane and sodium pentobarbital (50 mg/kg), and perfused transcardially with 10 mL of isotonic saline, followed by 30 mL of ice-cold 4% paraformaldehyde in 0.1 M phosphate buffer

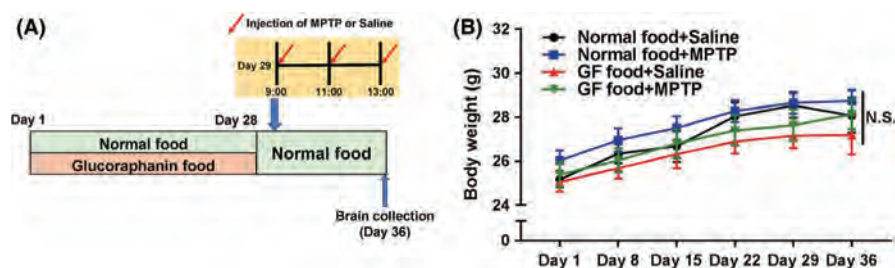


**FIGURE 1** Schedule of dietary intake of 0.1% GF food pellet and MPTP treatment. A, Normal food pellet or 0.1% GF food pellet was given to male mice (8-week-old) (day 1-day 28). Subsequently, normal food pellet was given to all mice (day 29-day 36). Mice received three injections of MPTP (10 mg/kg at 9:00, 11:00, 13:00, ip) or saline (5 mL/kg at 9:00, 11:00 and 13:00) (day 29). Mice were perfused 7 days after the administration of MPTP (day 36). B, Time course of body weight. There were no statistical changes among the four groups. Each value is the mean ± SEM (n = 9-11 per group). NS, not significant

(pH 7.4). Brains were removed from the skulls and postfixed overnight at 4°C, then brain was used for immunohistochemistry of dopamine transporter (DAT).

## 2.4 | DAT-immunohistochemistry

Immunohistochemistry of DAT was performed as reported previously.<sup>25,26</sup> The free-floating mouse brain sections (bregma 0.86–1.54 mm) were put in 0.3% H<sub>2</sub>O<sub>2</sub> in 0.05 M Tris-HCl saline (TBS) for 30 minutes and blocked in 0.2% Triton X-100 TBS (TBST) with 1.5% normal serum for 1 hour, at room temperature. Samples were then incubated for 36 hours at 4°C, with rat anti-DAT antibody (1:10 000, Cat. No: MAB 369, Chemicon International Inc). The sections were then washed three times in TBS and processed according to the avidin-biotin-peroxidase method (Vectastain Elite ABC, Vector Laboratories, Inc). Sections were then reacted with 0.15 mg/mL diaminobenzidine, containing 0.06% NiCl and 0.01% H<sub>2</sub>O<sub>2</sub> for 5 minutes. Then, the sections were mounted on gelatinized slides, dehydrated, cleared, and coverslipped under Permount® (Fisher Scientific). Next, sections were imaged, and the staining intensity of DAT-immunoreactivity in the anterior regions (0.25 mm<sup>2</sup>) of the striatum was analyzed using a light microscope equipped with a CCD camera (Olympus IX70) and the SCION IMAGE software package. Eight sections from each mouse were used for the quantitative analyses of DAT-immunoreactivity.

## 2.5 | Statistical analysis

The animal experiment data were expressed as the mean ± standard error of the mean (SEM). The statistical analysis was performed using SPSS Statistics 20 (SPSS). Data of body weight were analyzed using repeated two-way analyses of variance (ANOVA). Data of DAT were analyzed using two-way ANOVA, followed post hoc Tukey's multiple comparison test. The *P* values of less than 0.05 were considered statistically significant.

## 3 | RESULTS

Repeated two-way ANOVA revealed no statistical difference of body weight among the four groups [MPTP:  $F_{(1,35)} = 1.122$ ,  $P = 0.297$ , 0.1% GF:  $F_{(1,35)} = 2.203$ ,  $P = 0.147$ , interaction (MPTP × 0.1% GF),  $F_{(1,35)} = 0.021$ ,  $P = 0.88$ ] (Figure 1B). Repeated dosing with MPTP (10 mg/kg × 3, 2-hour interval) markedly decreased the density of DAT-immunoreactivity in the mouse striatum (Figure 2A–D). Two-way ANOVA revealed statistical differences among the four groups [MPTP:  $F_{(1,35)} = 16.73$ ,  $P < 0.001$ , 0.1% GF:  $F_{(1,35)} = 34.34$ ,  $P < 0.001$ , interaction (MPTP × 0.1% GF),  $F_{(1,35)} = 7.234$ ,  $P = 0.011$ ] (Figure 2E). Post hoc test showed that MPTP significantly ( $P < 0.001$ ) decreased the density of DAT-immunoreactivity in the striatum. Furthermore, dietary intake of 0.1% GF significantly ( $P < 0.001$ ) prevented the MPTP-induced reduction of DAT-immunoreactivity in the striatum.

## 4 | DISCUSSION

In this study, we found that dietary intake of 0.1% GF food pellets for 28 days prevented the reduction of DAT-immunoreactivity in the striatum after repeated administration of MPTP in adult mice, suggesting the potent protective effects of GF for MPTP-induced neurotoxicity. SFN increased Nrf2 protein levels in the striatum and led to upregulation of phase II antioxidant enzymes heme oxygenase-1 (HO-1) and NAD(P)H quinone oxidoreductase (NQO1).<sup>15</sup> In addition, SFN protected against MPTP-induced dopaminergic neurotoxicity in the mouse brain, suggesting that SFN can offer a neuroprotective effect for PD pathology. SFN is a compound derived from a glucosinolate precursor GF found in cruciferous vegetables, such as broccoli sprout.<sup>17</sup> Therefore, it is likely that GF-rich vegetables have prophylactic effects for the development of PD in adulthood.

We found neuroprotective effects of 0.1% GF supplementation for MPTP-induced neurotoxicity although 0.1% GF food pellet was not given for 7 days after MPTP injection (Figure 1A). Previously, we reported that dietary intake of 0.1% GF food pellet for 28 days could

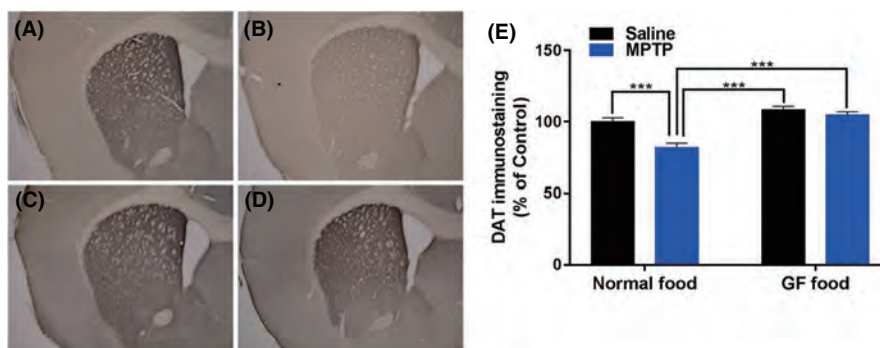


**FIGURE 2** Effects of dietary intake of 0.1% GF on the reduction in the DAT density in the striatum after the repeated administration of MPTP. A, Control food pellet + Saline, B, Control food pellet + MPTP, C, 0.1% GF food pellet + Saline, D, 0.1% GF food pellet + MPTP. Representative photomicrographs showing the DAT-immunoreactivity in the striatum of mice (A–D). The mean value for DAT-immunoreactivity staining was determined for each group and was expressed as a percentage of that of control mice (E). Each value is the mean ± SEM ( $n = 9$ –11 per group). \*\*\* $P < 0.001$  as compared with the normal food + MPTP group



prevent the onset of cognitive deficits and reduction of parvalbumin (PV)-immunoreactivity in the prefrontal cortex of mouse brain after repeated administration of phencyclidine.<sup>18</sup> Furthermore, dietary intake of 0.1% GF food pellet for 28 days prevented the onset of depression-like phenotypes in mice after chronic social defeat stress<sup>19</sup> or inflammation.<sup>20</sup> Moreover, dietary intake of 0.1% GF food pellet during juvenile and adolescent stages (P28-P56) prevented behavioral abnormalities in adult offspring (<P70) after maternal immune activation.<sup>21</sup> Collectively, it seems that dietary intake of 0.1% GF food pellet for 28 days has long-lasting beneficial effects despite 0.1% GF food pellet was not given at the behavioral evaluation. Interestingly, it is known that foods such as fresh vegetables are associated with the reduced rate of PD progression.<sup>3,6</sup> Therefore, it is likely that dietary intake of GF-rich cruciferous vegetables might play a role in preventing the onset of neuropsychiatric disorders in later life. In addition, the natural antioxidants (ie, the polyphenol-rich aqueous walnut extract, an extract of *Juglandis Semen* and *pigallocatechin gallate*, a major polyphenol in green tea) could protect against MPTP-induced dopaminergic neurotoxicity in mouse striatum.<sup>27,28</sup> It seems that the natural antioxidants may have beneficial effects in an animal model of PD.

This paper has some limitations. First, we did not measure concentration of SFN in the brain after dietary intake of 0.1% GF food pellet. However, it is reported that dietary intake of 0.1% GF increased levels of SFN in the mouse brain<sup>17</sup> and that SFN prepared from 0.1% GF could produce the gene expression of a number of oxidative stress genes through Nrf2 activation.<sup>29</sup> It is also reported that SFN could protect against MPTP-induced neurotoxicity in the mouse brain. Collectively, it is likely that dietary intake of 0.1% GF might have prophylactic effects in MPTP model of PD. Second, we did not confirm specific genes which can contribute to beneficial effects of SFN in this model. It is known that SFN can stimulate the gene expression of a number of ARE (antioxidant response element)-regulated genes (ie, HO-1 and NQO1) related with oxidative stress. It is currently unclear whether specific antioxidant genes play a role in the beneficial effects of 0.1% GF food pellet.

In conclusion, the present data suggest that dietary intake of 0.1% GF food pellet for 28 days could prevent the onset of MPTP-induced reduction of DAT in the striatum of adult mice. Therefore, it is likely that dietary intake of GF-rich cruciferous vegetables may prevent neurodegenerative disorders such as PD in later life.

## ACKNOWLEDGEMENTS

This study was partly supported by the Japan Society for the Promotion of Science (JSPS) KAKENHI (to K.H., 17H04243). Dr. Lijia Chang was supported by The Japan-China Sasakawa Medical Fellowship (Tokyo, Japan).

## CONFLICT OF INTEREST

Dr Ushida and Dr Suganuma are employee of KAGOME which produce SFN supplement. The other authors declare no conflict of interest.

## AUTHOR CONTRIBUTION

KH is responsible for the design of the research and experiment and supervised the experimental analyses. YP and KH wrote the paper. YP, YQ, CL, SW, and KZ performed behavioral experiments. YP analyzed the data. YU and HS provided 0.1% GF food pellet. All authors read and approved this paper.

## DATA REPOSITORY

All relevant data are included in Supporting Information.

## ANIMAL STUDIES

All animal experiments were approved by the Animal Care and Use Committee of Chiba University.

## ORCID

Kenji Hashimoto  <https://orcid.org/0000-0002-8892-0439>

## REFERENCES

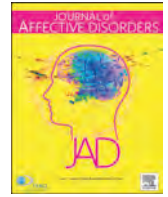
- Kalia LV, Lang AE. Parkinson's disease. *Lancet*. 2015;386:896–912.
- Ascherio PA, Schwarzschild MA. The epidemiology of Parkinson's disease: risk factors and prevention. *Lancet Neurol*. 2016;15:1257–72.
- Archer T, Kostrzewa RM. Exercise and nutritional benefits in PD: rodent models and clinical settings. *Curr Top Behav Neurosci*. 2016;29:333–51.
- Cassani E, Barichella M, Ferri V, Pinelli G, Iorio L, Bolliri C, et al. Dietary habits in Parkinson's disease: adherence to Mediterranean diet. *Parkinsonism Relat Disord*. 2017;42:40–6.
- Gao X, Chen H, Fung TT, Logroscino G, Schwarzschild MA, Hu FB, et al. Prospective study of dietary pattern and risk of Parkinson disease. *Am J Clin Nutr*. 2007;86:1486–94.
- Mischley LK, Lau RC, Bennett RD. Role of diet and nutritional supplements in Parkinson's disease progression. *Oxid Med Cell Longev*. 2017;2017:6405278.
- Deshmukh P, Unni S, Krishnappa G, Padmanabhan B. The Keap1-Nrf2 pathway: promising therapeutic target to counteract ROS-mediated damage in cancers and neurodegenerative diseases. *Biophys Rev*. 2017;9:41–56.
- Yamamoto M, Kensler TW, Motohashi H. The KEAP1-NRF2 system: a thiol-based sensor-effector apparatus for maintaining redox homeostasis. *Physiol Rev*. 2018;98:1169–203.
- Hashimoto K. Essential role of Keap1-Nrf2 signaling in mood disorders: overview and future perspective. *Front Pharmacol*. 2018;9:1182.
- Zhang JC, Yao W, Dong C, Han M, Shirayama Y, Hashimoto K. Keap1-Nrf2 signaling pathway confers resilience versus susceptibility to inescapable electric stress. *Eur Arch Psychiatry Clin Neurosci*. 2018;268:865–70.
- Vasconcelos AR, Dos Santos NB, Scavone C, Munhoz CD. Nrf2/ARE pathway modulation by dietary energy regulation in neurological disorders. *Front Pharmacol*. 2019;10:33.
- Innamorato NG, Jazwa A, Rojo AI, García C, Fernández-Ruiz J, Grochot-Przeczek A, et al. Different susceptibility to the Parkinson's toxin MPTP in mice lacking the redox master regulator Nrf2 or its target gene heme oxygenase-1. *PLoS ONE*. 2010;5:e11838.

13. Kaidery NA, Banerjee R, Yang L, Smirnova NA, Hushpalian DM, Liby KT, et al. Targeting Nrf2-mediated gene transcription by extremely potent synthetic triterpenoids attenuate dopaminergic neurotoxicity in the MPTP mouse model of Parkinson's disease. *Antioxid Redox Signal*. 2013;18:139–57.
14. Todorovic M, Wood SA, Mellick GD. Nrf2: a modulator of Parkinson's disease? *J Neural Transm (Vienna)*. 2016;123:611–9.
15. Jazwa A, Rojo AI, Innamorato NG, Hesse M, Fernández-Ruiz J, Cuadrado A. Pharmacological targeting of the transcription factor Nrf2 at the basal ganglia provides disease modifying therapy for experimental parkinsonism. *Antioxid Redox Signal*. 2011;14:2347–60.
16. Zhou Q, Chen B, Wang X, Wu L, Yang Y, Cheng X, et al. Sulforaphane protects against rotenone-induced neurotoxicity in vivo: involvement of the mTOR, Nrf2, and autophagy pathways. *Sci Rep*. 2016;6:32206.
17. Fahey JW, Holtzclaw WD, Wehage SL, Wade KL, Stephenson KK, Talalay P. Sulforaphane bioavailability from glucoraphanin-rich broccoli: control by active endogenous myrosinase. *PLoS ONE*. 2015;10:e0140963.
18. Shirai Y, Fujita Y, Hashimoto R, Ohi K, Yamamori H, Yasuda Y, et al. Dietary intake of sulforaphane-rich broccoli sprout extracts during juvenile and adolescence can prevent phencyclidine-induced cognitive deficits at adulthood. *PLoS ONE*. 2015;10:e0127244.
19. Yao W, Zhang J-C, Ishima T, Dong C, Yang C, Ren Q, et al. Role of Keap1-Nrf2 signaling in depression and dietary intake of glucoraphanin confers stress resilience in mice. *Sci Rep*. 2016;6:30659.
20. Zhang J-C, Yao W, Dong C, Yang C, Ren Q, Ma M, et al. Prophylactic effects of sulforaphane on depression-like behavior and dendritic changes in mice after inflammation. *J Nutr Biochem*. 2017;39:134–44.
21. Matsuura A, Ishima T, Fujita Y, Iwayama Y, Hasegawa S, Kawahara-Miki R, et al. Dietary glucoraphanin prevents the onset of psychosis in the adult offspring after maternal immune activation. *Sci Rep*. 2018;8:2158.
22. Jackson-Lewis V, Przedborski S. Protocol for the MPTP mouse model of Parkinson's disease. *Nat Protoc*. 2007;2:141–51.
23. Bennett RN, Mellon FA, Rosa EA, Perkins L, Kroon PA. Profiling glucosinolates, flavonoids, alkaloids, and other secondary metabolites in tissues of *Azima tetraacantha* L. (*Salvadoraceae*). *J Agric Food Chem*. 2004;52:5856–62.
24. West LG, Meyer KA, Balch BA, Rossi FJ, Schultz MR, Haas GW. Glucoraphanin and 4-hydroxyglucobrassicin contents in seeds of 59 cultivars of broccoli, raab, kohlrabi, radish, cauliflower, brussels sprouts, kale, and cabbage. *J Agric Food Chem*. 2004;52:916–26.
25. Ren Q, Ma M, Yang J, Nonaka R, Yamaguchi A, Ishikawa K-I, et al. Soluble epoxide hydrolase plays a key role in the pathogenesis of Parkinson's disease. *Proc Natl Acad Sci USA*. 2018;115:E5815–E5823.
26. Ren Q, Zhang JC, Ma M, Fujita Y, Wu J, Hashimoto K. 7,8-Dihydroxyflavone, a TrkB agonist, attenuates behavioral abnormalities and neurotoxicity in mice after administration of methamphetamine. *Psychopharmacology*. 2014;231:159–66.
27. Choi JG, Park G, Kim HG, Oh DS, Kim H, Oh MS. *In vitro* and *in vivo* neuroprotective effects of Walnut (*Juglandis Semen*) in models of Parkinson's disease. *Int J Mol Sci*. 2016;17:E108.
28. Xu Q, Langley M, Kanthasamy AG, Reddy MB. *Epigallocatechin gallate* has a neurorescue effect in a mouse model of Parkinson disease. *J Nutr*. 2017;147:1926–31.
29. Clarke JD, Hsu A, Williams DE, Dashwood RH, Stevens JF, Yamamoto M, et al. Metabolism and tissue distribution of sulforaphane in Nrf2 knockout and wild-type mice. *Pharm Res*. 2011;28:3171–9.

#### SUPPORTING INFORMATION

Additional supporting information may be found online in the Supporting Information section at the end of the article.

**How to cite this article:** Pu Y, Qu Y, Chang L, et al. Dietary intake of glucoraphanin prevents the reduction of dopamine transporter in the mouse striatum after repeated administration of MPTP. *Neuropsychopharmacol Rep*. 2019;39:247–251. <https://doi.org/10.1002/npr2.12060>



## Research paper

## Antibiotic-induced microbiome depletion is associated with resilience in mice after chronic social defeat stress



Siming Wang, Youge Qu, Lijia Chang, Yaoyu Pu, Kai Zhang, Kenji Hashimoto\*

Division of Clinical Neuroscience, Chiba University Center for Forensic Mental Health, Chiba 260-8670, Japan

## ARTICLE INFO

## Keywords:

Anhedonia  
Antibiotic  
Chronic social defeat stress  
Gut microbiota  
Resilience  
Susceptibility

## ABSTRACT

**Background:** The brain–gut axis plays a role in the pathogenesis of stress-related disorders such as depression. However, the role of brain–gut axis in the resilience versus susceptibility after stress remains unclear. Here, we examined the effects of antibiotic-induced microbiome depletion on an anhedonia-like phenotype in adult mice subjected to chronic social defeat stress (CSDS).

**Methods:** Using CSDS paradigm, we investigated the effects of antibiotic-induced microbiome depletion on the resilience versus susceptibility in mice.

**Results:** Treatment with an antibiotic cocktail for 14 days significantly decreased the diversity and composition of the microbiota in the host gut. *Proteobacteria* were markedly increased after treatment with the antibiotic cocktail. At the genus and species levels, the antibiotic-treated group exhibited marked alterations in the microbiota compared with a control group. CSDS was shown to significantly improve the abnormal composition of gut microbiota in the antibiotic-treated group. CSDS did not produce an anhedonia-like phenotype in the antibiotic-treated mice, but did induce an anhedonia-like phenotype in control mice, suggesting that gut bacteria are essential for the development of CSDS-induced anhedonia. CSDS treatment did not alter the plasma levels of interleukin-6 or the expression of synaptic proteins, such as PSD-95 and GluA1, in the prefrontal cortex of antibiotic-treated mice.

**Limitations:** Specific microbiome were not determined.

**Conclusions:** These findings suggest that antibiotic-induced microbiome depletion contributed to resilience to anhedonia in mice subjected to CSDS. Therefore, it is likely that the brain–gut axis plays a role in resilience versus susceptibility to stress.

## 1. Introduction

In the past two decades, the gut microbiota has been recognized as a fundamental player in host physiology and pathology. The gut microbiota is prominently involved in the development and education of the immune system (Becattini et al., 2016; Cerf-Bensussan and Gaboriau-Routhiau, 2010; Round and Mazmanian, 2009). The brain–gut axis is a complex multi-organ bidirectional signaling system involving the gut microbiota and the brain, and plays a fundamental role in host physiology, homeostasis, development, and metabolism (Cusotto et al., 2018, 2019; Dinan and Cryan, 2017; Forsythe et al., 2016; Fung et al., 2017; Kelly et al., 2016; Ma et al., 2019; Molina-Torres et al., 2019; Zhu et al., 2019). Multiple lines of evidence suggest that an abnormal composition of microbiota in the host gut may contribute to the pathogenesis of stress-related diseases such as depression (Huang et al., 2019b; Jiang et al., 2015; Wong et al., 2016; Yang et al., 2019;

Zheng et al., 2016) and may affect the antidepressant actions of certain compounds (Burokas et al., 2017; Ho and Ross, 2017; Huang et al., 2019a; Lukic et al., 2019; Qu et al., 2017; Yang et al., 2017b; Zhang et al., 2017). Gut microbiota may also contribute to resilience versus susceptibility to anhedonia in rodents after repeated stress (Bailey et al., 2011; Hao et al., 2019; Szyszkwicz et al., 2017; Yang et al., 2017a). We found higher levels of *Bifidobacterium* in resilient mice compared with susceptible mice after chronic social defeat stress (CSDS), and supplementation with *Bifidobacterium* produced resilience in mice after CSDS, suggesting a role for *Bifidobacterium* in stress resilience (Yang et al., 2017a). It has also been reported that specific clusters of bacterial communities in the cecum may be linked to vulnerability to CSDS (Szyszkwicz et al., 2017).

Antibiotics are often beneficial, but can also be potentially harmful drugs. The abuse of antibiotics plays a role in the pathogenesis of several diseases associated with the impairment of microbiota

\* Corresponding author.

E-mail address: [hashimoto@faculty.chiba-u.jp](mailto:hashimoto@faculty.chiba-u.jp) (K. Hashimoto).<https://doi.org/10.1016/j.jad.2019.09.064>

Received 15 August 2019; Received in revised form 4 September 2019; Accepted 13 September 2019

Available online 13 September 2019

0165-0327/ © 2019 Elsevier B.V. All rights reserved.



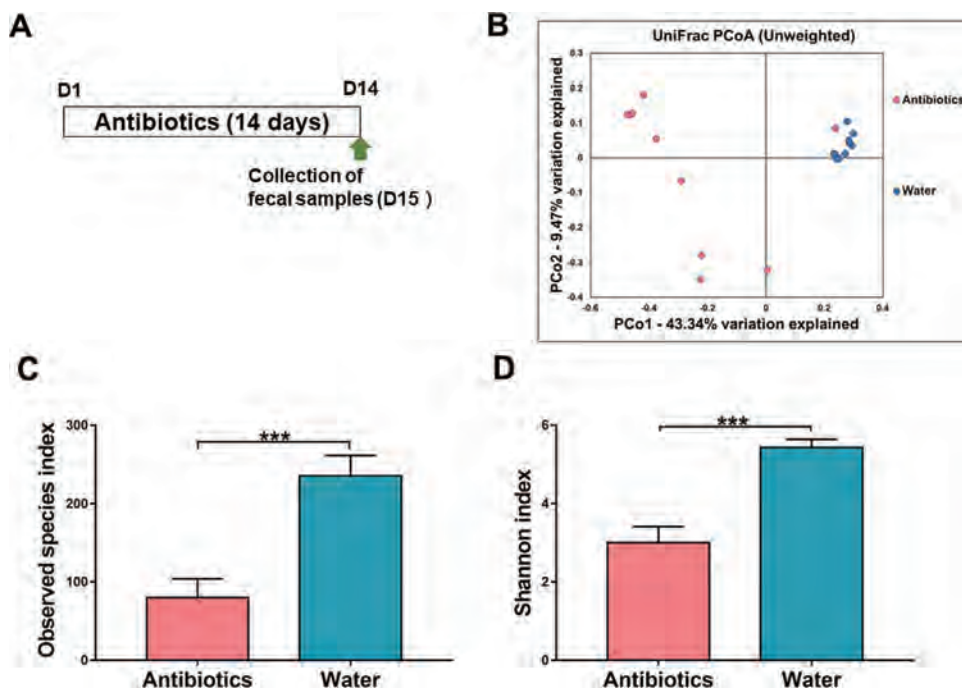


**Fig. 1.** Effects of antibiotic cocktail in the diversity of gut microbiota. (A): The schedule of drinking water in antibiotic cocktail and feces collection. Drinking water including antibiotic cocktail or water was given to adult mice from day 1 to day 14. On day 15, feces were collected. (B): UniFrac PCoA of gut bacteria data. (C): Observed species index. (D): Shannon index. Data are shown as mean  $\pm$  S.E.M. ( $n = 10$ ). \*\*\* $P < 0.001$ . NS: not significant.

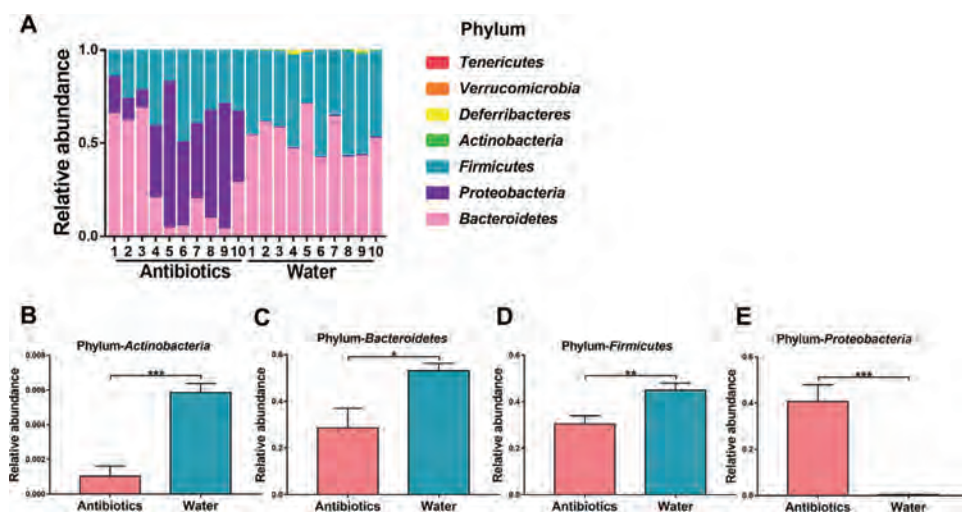


**Fig. 2.** Altered composition in the gut bacteria at the phylum level. (A): The relative abundances of microbiome at phylum level in fecal samples of the two groups after repeated treatment with antibiotics for 14 days. (B): *Actinobacteria*. (C): *Bacteroidetes*. (D): *Firmicutes*. (E): *Proteobacteria*. Data are shown as mean  $\pm$  S.E.M. ( $n = 10$ ). \* $P < 0.05$ , \*\* $P < 0.01$ , \*\*\* $P < 0.001$ . NS: not significant.

(Champagne-Jorgensen et al., 2019; Ianiro et al., 2016). Instead of germ-free mice, antibiotic cocktail-induced microbiome depletion has been used to investigate the role of gut microbiota in some pathological conditions (Hernandez-Chirlaque et al., 2016; Pu et al., 2019; Sampson et al., 2016; Zhan et al., 2018; Zhang et al., 2019). For example, dextran sulfate sodium (DSS) has been shown to cause colitis in mice, although mice treated with an antibiotic cocktail did not show DSS-induced colitis, suggesting that enteric bacteria are essential for the development of DSS-induced colitis (Hernandez-Chirlaque et al., 2016). Yang et al. (2019) reported that transplantation of fecal microbiota from rats with an anhedonia-like phenotype aggravated depression-like and anhedonia-like phenotypes in mice treated with an antibiotic cocktail. It appears likely that gut microbiota play a key role in the pathology of inflammation-related diseases such as colitis and depression. However, the effects of antibiotic-induced microbiome depletion on inflammation and anhedonia-like phenotype in rodents subjected to CSDS are unknown.

Anhedonia (loss of pleasure) is a core symptom of major depressive disorder. The neurobiological mechanisms of anhedonia remain poorly understood (Treadway and Zald, 2011). Therefore, we hypothesized

that antibiotic-induced microbiome depletion may affect the resilience of mice to anhedonia after CSDS. The purpose of this study was, therefore, to investigate the role of gut microbiota in anhedonia-like phenotypes in mice after CSDS. First, we examined whether repeated administration of an antibiotic cocktail for 14 days affected the diversity and composition of gut microbiota in mouse feces. Then, we examined whether antibiotic-induced microbiome depletion could affect the anhedonia-like phenotype, inflammation, and synaptic proteins in mice after CSDS, since CSDS causes an anhedonia-like phenotype through inflammation in the periphery (Zhang et al., 2017).

## 2. Materials and methods

### 2.1. Animals

Male adult C57BL/6 mice ( $n = 40$ ), aged 8 weeks with a body weight of 20–25 g and male adult CD1 (ICR) mice ( $n = 20$ ), aged 13–15 weeks with a body weight  $> 40$  g (Japan SLC, Inc., Hamamatsu, Japan) were used. Animals were housed under controlled temperatures with 12 h light/dark cycles (lights on between 07:00 and 19:00), with ad

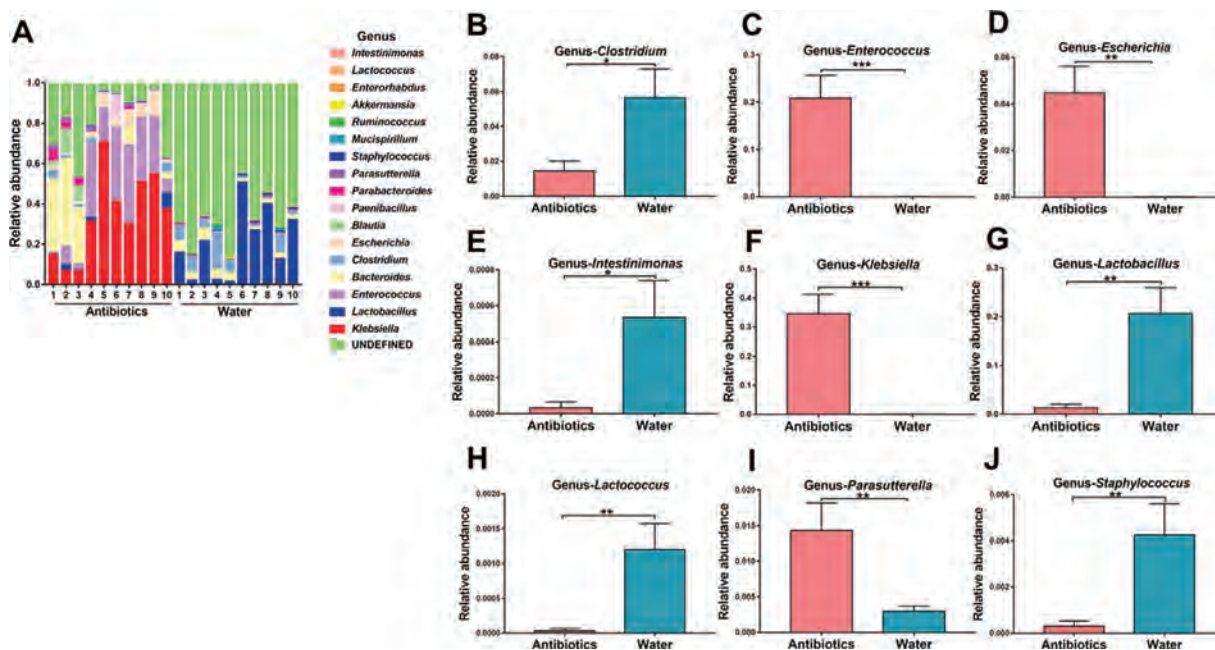


**Fig. 3.** Altered composition in the gut bacteria at the genus level. (A): The relative abundances of microbiome at genus level in fecal samples of the two groups after repeated treatment with antibiotics for 14 days. (B): *Clostridium*. (C): *Enterococcus*. (D): *Escherichia*. (E): *Intestinimonas*. (F): *Klebsiella*. (G): *Lactobacillus*. (H): *Lactococcus*. (I): *Parasutterella*. (J): *Staphylococcus*. Data are shown as mean ± S.E.M. (n = 10). \**P* < 0.05, \*\**P* < 0.01, \*\*\**P* < 0.001. NS: not significant.

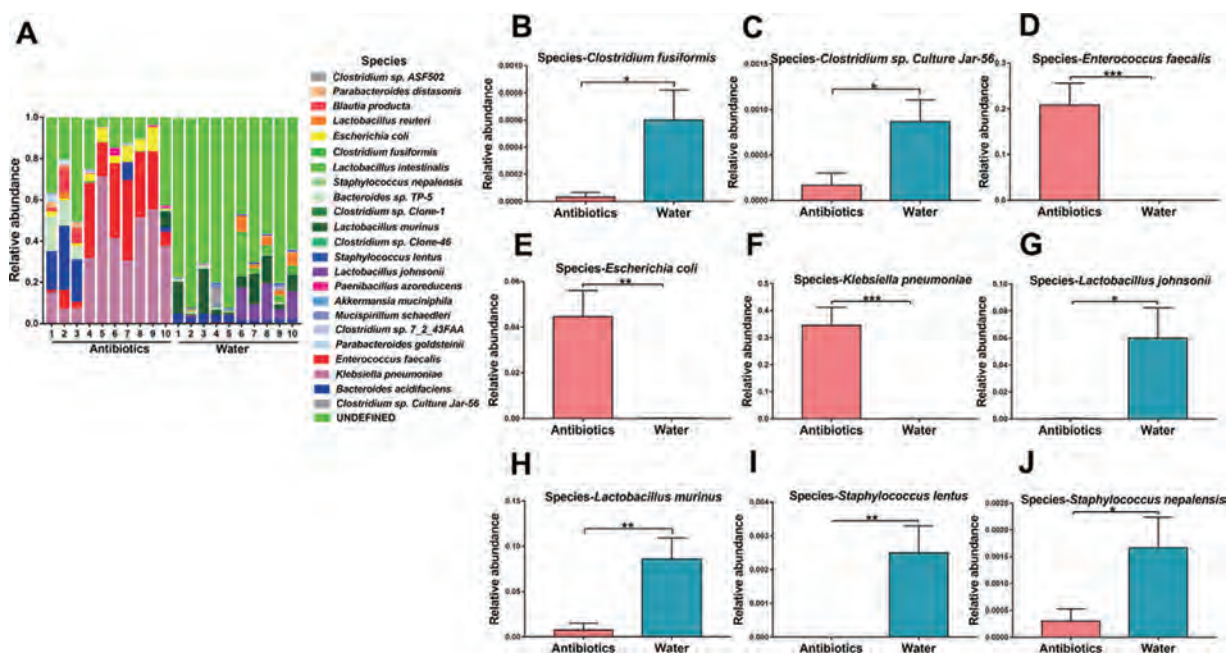


**Fig. 4.** Altered composition in the gut bacteria at the species level. (A): The relative abundances of microbiome at species level in fecal samples of the two groups after repeated treatment with antibiotics for 14 days. (B): *Clostridium fusiformis*. (C): *Clostridium sp. Culture Jar-56*. (D): *Enterococcus faecalis*. (E): *Escherichia coli*. (F): *Klebsiella pneumoniae*. (G): *Lactobacillus johnsonii*. (H): *Lactobacillus murinus*. (I): *Staphylococcus lentus*. (J): *Staphylococcus nepalensis*. Data are shown as mean ± S.E.M. (n = 10). \**P* < 0.05, \*\**P* < 0.01, \*\*\**P* < 0.001. NS: not significant.

libitum access to food (CE-2; CLEA Japan, Inc., Tokyo, Japan) and water. The protocol was approved by the Chiba University Institutional Animal Care and Use Committee (Permission number: 30–399). This study was carried out in strict accordance with the recommendations in the Guide for the Care and Use of Laboratory Animals of the National Institutes of Health, USA. Animals were deeply anesthetized with isoflurane before being killed by cervical dislocation. All efforts were made to minimize suffering. CSDS was performed from 13:00 to 17:00,

and one percent sucrose preference tests (SPT) were performed from 17:00 to 18:00.

2.2. Treatment with antibiotic cocktail, CSDS and behavioral tests

Based upon previous reports (Pu et al., 2019; Yang et al., 2019; Zhan et al., 2018; Zhang et al., 2019b), broad-spectrum antibiotics (ampicillin 1g/L, neomycin sulfate 1g/L, and metronidazole 1g/L,

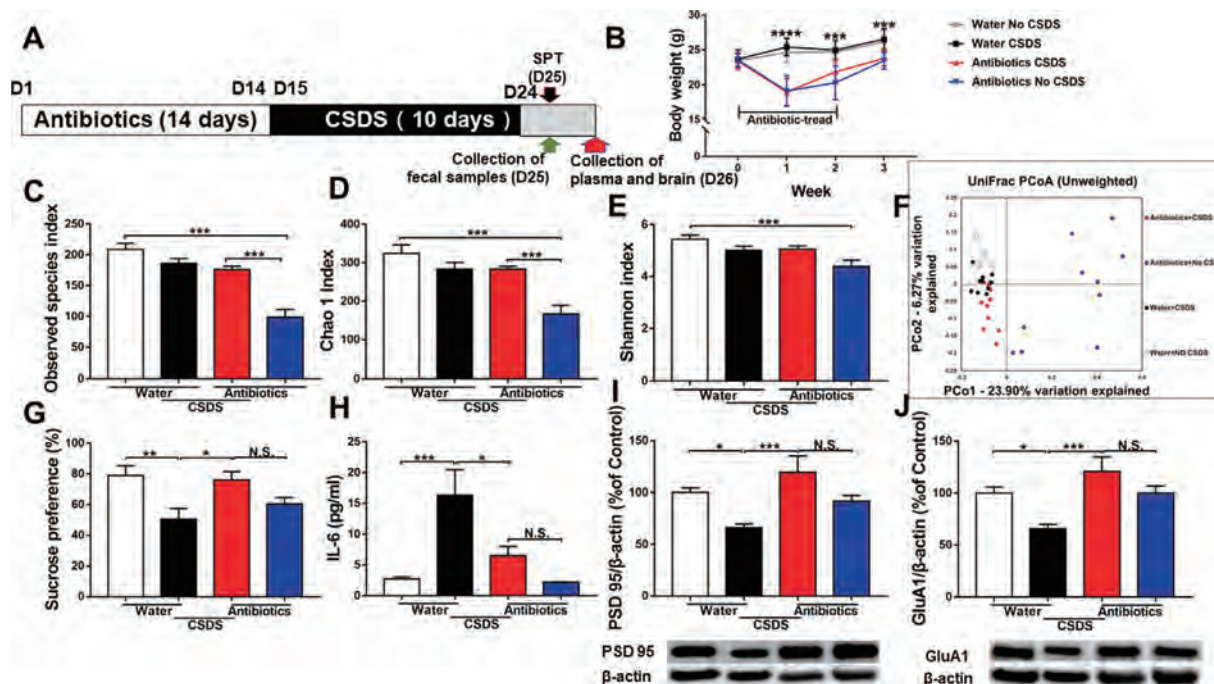


Fig. 5. Effects of antibiotics in the anhedonia-like phenotype in mice after CSDS.

(A): The schedule of antibiotics treatment, CSDS model, sucrose preference test and feces collection. Antibiotic cocktail or water in drinking water was given to mice for 14 days. Subsequently, CSDS was performed for 10 days from day 14 to day 24, and 1% sucrose preference test (SPT) was performed on day 25. On day 25, fresh feces were collected. On day 26, plasma and PFC were collected. (B): Body weight (repeated two-way ANOVA, antibiotics:  $F_{1,36} = 52.436$ ,  $P < 0.001$ , CSDS:  $F_{1,36} = 1.267$ ,  $P = 0.268$ , interaction:  $F_{1,36} = 0.21$ ,  $P = 0.885$ ). (C): Observed species index (two-way ANOVA, antibiotics:  $F_{1,36} = 41.206$ ,  $P < 0.001$ , CSDS:  $F_{1,36} = 8.378$ ,  $P = 0.006$ , interaction:  $F_{1,36} = 28.863$ ,  $P < 0.001$ ). (D): Chao 1 index (two-way ANOVA, antibiotics:  $F_{1,36} = 18.192$ ,  $P < 0.001$ , CSDS:  $F_{1,36} = 4302$ ,  $P = 0.045$ , interaction:  $F_{1,36} = 183.528$ ,  $P < 0.001$ ). (E): Shannon index (two-way ANOVA, antibiotics:  $F_{1,36} = 8.111$ ,  $P = 0.007$ , CSDS:  $F_{1,36} = 0.448$ ,  $P = 0.508$ , interaction:  $F_{1,36} = 9.493$ ,  $P = 0.004$ ). (F): PCoA analysis of gut bacteria data. (G) Sucrose preference test (two-way ANOVA, antibiotics:  $F_{1,36} = 0.357$ ,  $P = 0.554$ , CSDS:  $F_{1,36} = 1.157$ ,  $P = 0.289$ , interaction:  $F_{1,36} = 14.108$ ,  $P = 0.001$ ). (H): Plasma IL-6 (two-way ANOVA, antibiotics:  $F_{1,36} = 5.072$ ,  $P = 0.031$ , CSDS:  $F_{1,36} = 16.133$ ,  $P < 0.001$ , interaction:  $F_{1,36} = 4.322$ ,  $P = 0.045$ ). (I): PSD 95 (two-way ANOVA, antibiotics:  $F_{1,36} = 6.613$ ,  $P = 0.014$ , CSDS:  $F_{1,36} = 0.114$ ,  $P = 0.737$ , interaction:  $F_{1,36} = 12.465$ ,  $P = 0.001$ ). (J): GluA1 (two-way ANOVA, antibiotics:  $F_{1,36} = 10.163$ ,  $P = 0.003$ , CSDS:  $F_{1,36} = 0.604$ ,  $P = 0.442$ , interaction:  $F_{1,36} = 10.267$ ,  $P = 0.003$ ). Data are shown as mean  $\pm$  S.E.M. ( $n = 10$ ). \* $P < 0.05$ , \*\* $P < 0.01$ , \*\*\* $P < 0.001$ . NS: not significant.

Sigma-Aldrich Co. Ltd, MO, USA) dissolved in drinking water were provided ad libitum to male C57BL/6 mice for 14 consecutive days, as reported previously (Pu et al., 2019; Yang et al., 2019; Zhan et al., 2018; Zhang et al., 2019b). The drinking solution was renewed every 2 days. Fresh fecal samples were collected on day 15 before CSDS. We collected fresh fecal samples from each mouse at around 10:00 in order to avoid circadian effects on the microbiome. We also collected fecal samples when each mouse was placed in a new, clean cage. The fecal samples were put into a sterilized screw cap microtube immediately after defecation, and these samples were stored at  $-80^{\circ}\text{C}$  until use.

Mice were divided into four groups: water + no CSDS; water + CSDS; antibiotics + no CSDS; and antibiotics + CSDS. The CSDS procedure was performed as previously reported (Golden et al., 2011; Qu et al., 2017; Yang et al., 2016, 2017b, 2015; Zhang et al., 2015, 2017). The C57BL/6 mice were exposed to a different CD1 aggressor mouse for 10 min per day for 10 consecutive days (day 15 to day 24). When the social defeat session ended, the resident CD1 mouse and the intruder mouse were housed in opposite sides of the cage, separated by a perforated Plexiglas divider to allow visual, olfactory, and auditory contact for the remainder of the 24-h period. At 24 h after the last session, all mice were housed individually. Control C57BL/6 mice without exposure to CSDS were housed in the cage before the behavioral tests.

On day 25, 1% SPTs were performed from 17:00 to 18:00, to identify anhedonia-like phenotypes. Mice were exposed to water and 1% sucrose solution for 48 h, followed by 4 h of water and food deprivation and a 1-h exposure to two identical bottles containing either water or a 1% sucrose solution. The bottles containing water and

sucrose were weighed before and at the end of this period. The sucrose preference was calculated as the ratio of sucrose solution consumption to total liquid consumption.

On day 25 (before SPT), fresh fecal samples were collected as described above, and stored at  $-80^{\circ}\text{C}$  until use. On day 26, plasma and brain samples from the prefrontal cortex (PFC) were collected after anesthesia with 5% isoflurane. Tissues from the PFC were dissected from the brains on ice using a Leica microscope S9E (Leica Microsystems, Tokyo, Japan). We selected the PFC because the expression of synaptic proteins such as PSD-95 and GluA1 was significantly reduced in the PFC of CSDS-susceptible mice (Yang et al., 2016, 2015; Zhang et al., 2015). Plasma and PFC were stored at  $-80^{\circ}\text{C}$  until use.

### 2.3. ELISA measurement of pro-inflammatory cytokine IL-6

Plasma levels of interleukin-6 (IL-6) were measured, because we previously found an increase in blood IL-6 in the CSDS model (Zhang et al., 2017). The plasma IL-6 levels were measured using the ELISA kit (Invitrogen, cat#: 88-7064-22) according to the manufacturer's instructions.

### 2.4. Western blot analysis

The PFC tissues were homogenized in Laemmli lysis buffer. The protein levels of 10  $\mu\text{g}$  aliquots were measured using DC protein assay kits (Bio-Rad, Hercules, CA, USA) and incubated for 5 min at  $95^{\circ}\text{C}$ , with an equal volume of 125 mM Tris/HCl (pH 6.8), 20% glycerol, 0.1%

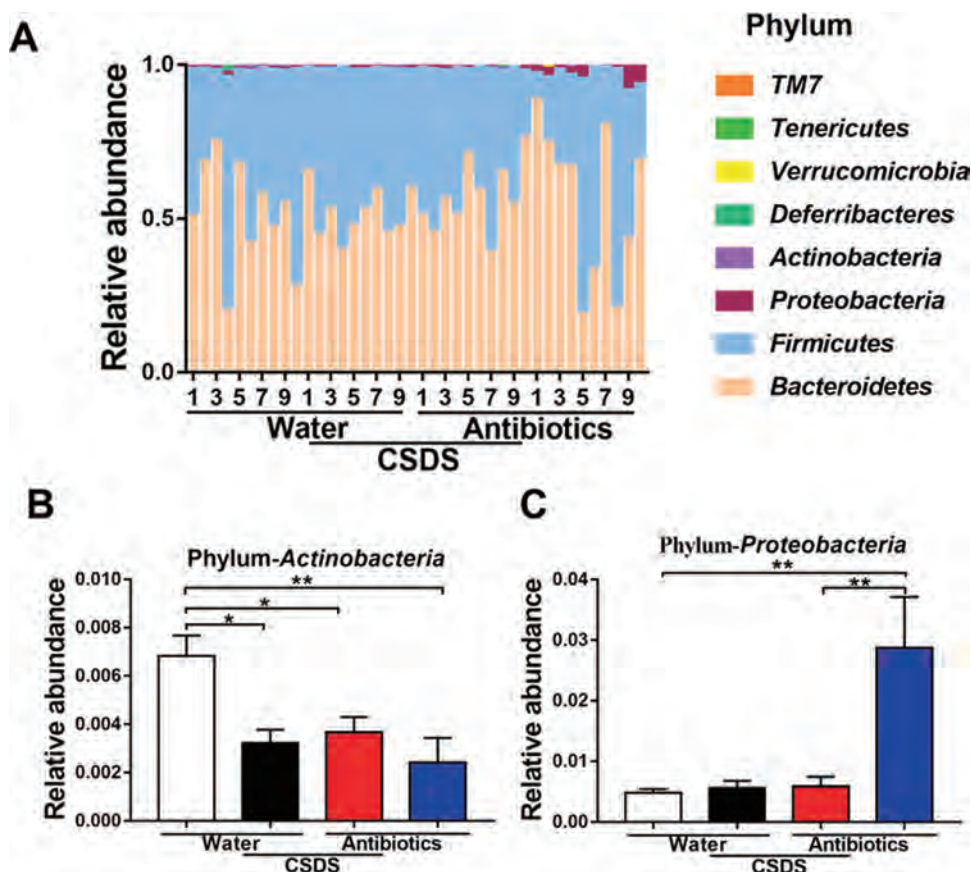


**Fig. 6.** Altered composition in the gut bacteria at the phylum level.

(A): The relative abundances of phylum in fecal samples of the four groups 24 hrs after CSDS. (B): *Actinobacteria* (two-way ANOVA, antibiotics:  $F_{1,36} = 6.560$ ,  $P = 0.015$ , CSDS:  $F_{1,36} = 2.335$ ,  $P = 0.135$ , interaction:  $F_{1,36} = 9.740$ ,  $P = 0.004$ ). (C): *Proteobacteria* (two-way ANOVA, antibiotics:  $F_{1,36} = 7.943$ ,  $P = 0.008$ , CSDS:  $F_{1,36} = 6.646$ ,  $P = 0.014$ , interaction:  $F_{1,36} = 7.555$ ,  $P = 0.009$ ). Data are shown as mean  $\pm$  S.E.M. ( $n = 10$ ). \* $P < 0.05$ , \*\* $P < 0.01$ , \*\*\* $P < 0.001$ . NS: not significant.

bromophenol blue, 10%  $\beta$ -mercaptoethanol, and 4% sodium dodecyl sulfate, and subjected to sodium dodecyl sulfate polyacrylamide gel electrophoresis using 10% mini-gels (Mini-PROTEAN TGX™ Precast Gel; Bio-Rad). Proteins were transferred onto polyvinylidene difluoride membranes using a Trans Blot Mini Cell (Bio-Rad). For immunodetection, the blots were blocked with 2% bovine serum albumin in TBST (TBS + 0.1% Tween-20) for 1 h at room temperature and incubated with primary antibodies overnight at 4 °C. The primary antibody used was postsynaptic density protein 95 (PSD-95; 1  $\mu$ g/ml Invitrogen, Carlsbad, CA, USA). The next day, blots were washed thrice in TBST and incubated with horseradish peroxidase conjugated anti-rabbit antibody (1:5000) for 1 h at room temperature. After three final washes with TBST, bands were detected using enhanced chemiluminescence plus the Western Blotting Detection system (GE Healthcare Bioscience). The blots then were incubated in stripping buffer (2% sodium dodecyl sulfate, 100 mM  $\beta$ -mercaptoethanol, and 62.5 mM Tris-HCl, pH 6.8) for 30 min at 60 °C and then washed thrice with TBST. The stripped blots were kept in blocking solution for 1 h and incubated with a primary antibody directed against  $\alpha$ -amino-3-hydroxy-5-methyl-4-isoxazolepropionic acid receptor (AMPA) 1 (GluA1; 1  $\mu$ g/ml Abcam, Cambridge, MA) and  $\beta$ -actin. Images were captured with a Fuji LAS3000-mini imaging system (Fujifilm, Tokyo, Japan), and immunoreactive bands were quantified.

## 2.5. 16S rRNA analysis

DNA extraction from mouse feces and 16S rRNA analysis of fecal samples were performed by MyMetagenome Co, Ltd. (Tokyo, Japan). The analysis of 16S rRNA from fecal samples was performed as previously described (Kim et al., 2013). Briefly, PCR was performed using 27Fmod 5'-AGRGTGGATYMTGGCTCAG-3' and 338R 5'-TGCTGCCTCCGTAGGAGT-3' to amplify the V1–V2 region of the bacterial 16S rRNA gene. The amplified DNA (~330 bp) was purified using AMPure

XP (Beckman Coulter), and quantified using a Quant-iT Picogreen dsDNA assay kit (Invitrogen) and a TBS-380 Mini-Fluorometer (Turner Biosystems). The 16S amplicons were then sequenced using MiSeq according to the Illumina protocol. The paired-end reads were merged using the fastq-join program based on overlapping sequences. Reads with an average quality value of  $< 25$  and inexact matches to both universal primers were filtered out. Filter-passed reads were used for further analysis after trimming off both primer sequences. For each sample, 3000 high-quality filter-passed reads were rearranged in descending order according to the quality value and then clustered into operational taxonomic units (OTUs) with a 97% pairwise-identity cutoff, using the UCLUST program version 5.2.32 (<https://www.drive5.com>). Taxonomic assignment of OTUs was made by similarity searches against the Ribosomal Database Project and the National Center for Biotechnology Information genome database using the GLSEARCH program (Tanoue et al., 2019).

## 2.6. Statistical analysis

The data are shown as the mean  $\pm$  standard error of the mean (S.E.M.). Analysis was carried out using PASW Statistics 20 (now SPSS statistics; SPSS, Tokyo, Japan). Comparisons between groups were performed using Student t-tests and two-way analysis of variance (ANOVA), followed by *post hoc* Tukey test. The data of body weight were analyzed using repeated two-way ANOVA, followed by *post hoc* Tukey test.  $P$  values of less than 0.05 were considered to be statistically significant.

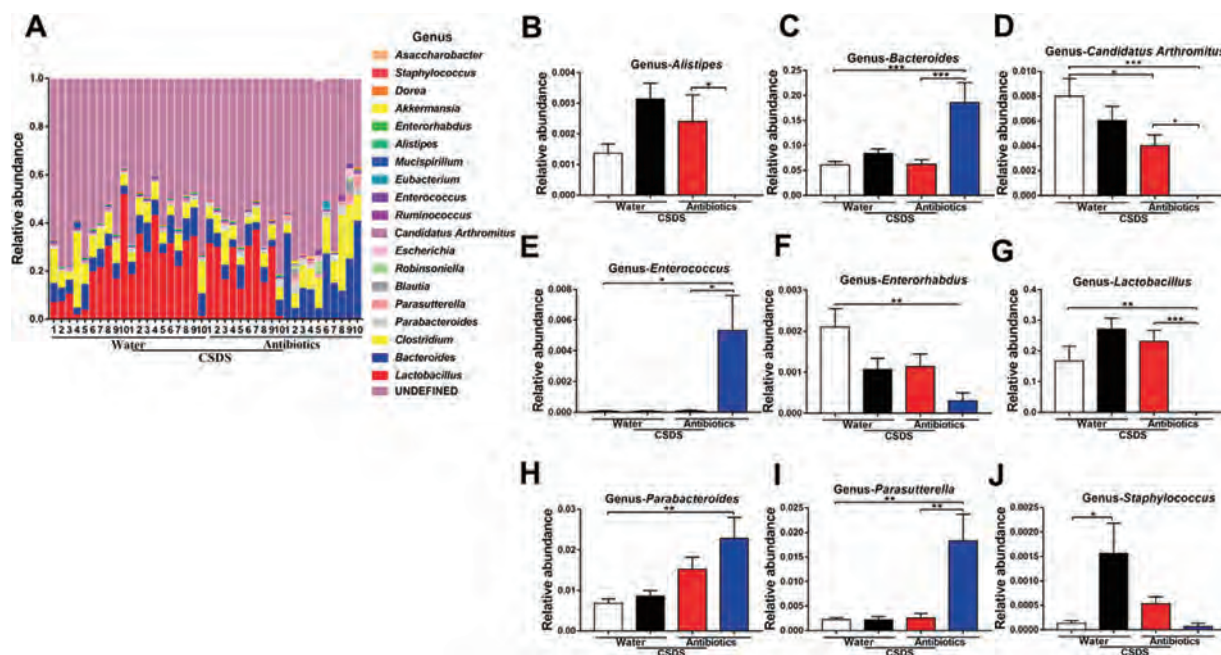


**Fig. 7.** Altered composition in the gut bacteria at the genus level.

(A): The relative abundances of genus in fecal samples of the four groups 24 days after drink antibiotics and CSDS. (B): *Alistipes* (two-way ANOVA, antibiotics:  $F_{1,36} = 3.922$ ,  $P = 0.055$ , CSDS:  $F_{1,36} = 15.438$ ,  $P < 0.001$ , interaction:  $F_{1,36} = 0.357$ ,  $P = 0.554$ ). (C): *Bacteroides* (two-way ANOVA, antibiotics:  $F_{1,36} = 5.959$ ,  $P = 0.020$ , CSDS:  $F_{1,36} = 5.567$ ,  $P = 0.024$ , interaction:  $F_{1,36} = 11.801$ ,  $P = 0.002$ ). (D): *Candidatus Arthromitus* (two-way ANOVA, antibiotics:  $F_{1,36} = 24.682$ ,  $P < 0.001$ , CSDS:  $F_{1,36} = 1.054$ ,  $P = 0.311$ , interaction:  $F_{1,36} = 8.885$ ,  $P = 0.005$ ). (E): *Enterococcus* (two-way ANOVA, antibiotics:  $F_{1,36} = 5.457$ ,  $P = 0.025$ , CSDS:  $F_{1,36} = 5.321$ ,  $P = 0.027$ , interaction:  $F_{1,36} = 5.321$ ,  $P = 0.027$ ). (F): *Enterorhabdus* (two-way ANOVA, antibiotics:  $F_{1,36} = 7.308$ ,  $P = 0.010$ , CSDS:  $F_{1,36} = 0.097$ ,  $P = 0.757$ , interaction:  $F_{1,36} = 8.476$ ,  $P = 0.006$ ). (G): *Lactobacillus* (two-way ANOVA, antibiotics:  $F_{1,36} = 8.701$ ,  $P = 0.006$ , CSDS:  $F_{1,36} = 22.717$ ,  $P < 0.001$ , interaction:  $F_{1,36} = 3.312$ ,  $P = 0.077$ ). (H): *Parabacteroides* (two-way ANOVA, antibiotics:  $F_{1,36} = 13.509$ ,  $P = 0.001$ , CSDS:  $F_{1,36} = 0.926$ ,  $P = 0.342$ , interaction:  $F_{1,36} = 2.323$ ,  $P = 0.136$ ). (I): *Parasutterella* (two-way ANOVA, antibiotics:  $F_{1,36} = 8.645$ ,  $P = 0.006$ , CSDS:  $F_{1,36} = 8.092$ ,  $P = 0.007$ , interaction:  $F_{1,36} = 7.889$ ,  $P = 0.008$ ). (J): *Staphylococcus* (two-way ANOVA, antibiotics:  $F_{1,36} = 2.948$ ,  $P = 0.095$ , CSDS:  $F_{1,36} = 8.794$ ,  $P = 0.005$ , interaction:  $F_{1,36} = 2.276$ ,  $P = 0.140$ ). Data are shown as mean  $\pm$  S.E.M. ( $n = 10$ ). \* $P < 0.05$ , \*\* $P < 0.01$ , \*\*\* $P < 0.001$ . NS: not significant.

### 3. Results

#### 3.1. Treatment with antibiotics caused significant differences in the diversity of gut microbiota

An antibiotic cocktail or water was given to mice for 14 days (Fig. 1A). Un-weighted UniFrac-based principal coordinate analysis (PCoA), based on the relative abundance of taxa in the gut microbiota of mice showed a significant difference between the two groups (Fig. 1B). There was a significant decrease in the observed species index in the antibiotic-treated group compared with the water-treated group (Fig. 1C). Shannon indices are commonly used to evaluate the  $\alpha$ -diversity of gut microbiota. There was a significant decrease in the Shannon index of the antibiotic-treated group compared with that of the water-treated group (Fig. 1D).

#### 3.2. Altered composition in gut bacteria at the phylum level

Analysis of 16S rRNA was used to identify differences in the composition of gut microbiota between the antibiotic-treated mice and the water-treated mice. The phylum level composition of gut bacterium was identified (Fig. 2A). *Bacteroidetes* and *Firmicutes* were the most abundant phyla in the water-treated group (Fig. 2A). At the phylum level, *Actinobacteria*, *Bacteroidetes*, and *Firmicutes* were present at significantly lower levels in the antibiotic-treated group than in the water-treated group (Fig. 2B–D). In contrast, *Proteobacteria* levels were markedly increased after treatment with the antibiotic cocktail (Fig. 2E).

#### 3.3. Altered composition in gut bacteria at the genus level

The genus levels of gut bacteria were investigated (Fig. 3A). Five

genera of bacteria (*Clostridium*, *Intestinimonas*, *Lactobacillus*, *Lactococcus*, and *Staphylococcus*) were present at significantly lower levels in the antibiotic-treated group compared with the water-treated group (Figs. 3B, E, G, H, J). In contrast, four bacteria (*Enterococcus*, *Escherichia*, *Klebsiella*, and *Parasutterella*) were present at significantly higher levels in the antibiotic-treated group than those in the water-treated group (Figs. 3B, D, F, I).

#### 3.4. Altered composition of gut bacteria at the species level

The genus levels of gut bacterium were identified (Fig. 4A). Three bacteria (*Enterococcus faecalis*, *Escherichia coli*, and *Klebsiella pneumoniae*) were present at significantly higher levels in the antibiotic-treated group than those in the water-treated group (Figs. 4D, E, F). In contrast, six bacteria (*Clostridium fusiformis*, *Clostridium* sp. *Culture Ja-56*, *Lactobacillus johnsonii*, *Lactobacillus murinus*, *Staphylococcus lentus*, and *Staphylococcus nepaiensis*) was present at significantly lower levels in the antibiotic-treated group than those in the water-treated group (Figs. 4B, C, G, H, I, J).

#### 3.5. An antibiotic cocktail produced resilience in mice after csds

An antibiotic cocktail or water was provided as drinking water for 14 days, then CSDS was performed for 10 days (D15–D24) (Fig. 5A). The time course of the body weight of the mice was recorded (Fig. 5B). Treatment with an antibiotic cocktail significantly decreased body weight in the mice. CSDS did not alter body weight in the mice (Fig. 5B). There were significant differences in the  $\alpha$ -diversity of microbiota among the four groups. CSDS significantly improved the reduced diversity of microbiota in the antibiotic-treated group (Figs. 5C, D, E). Un-weighted UniFrac-based PCoA showed significant differences

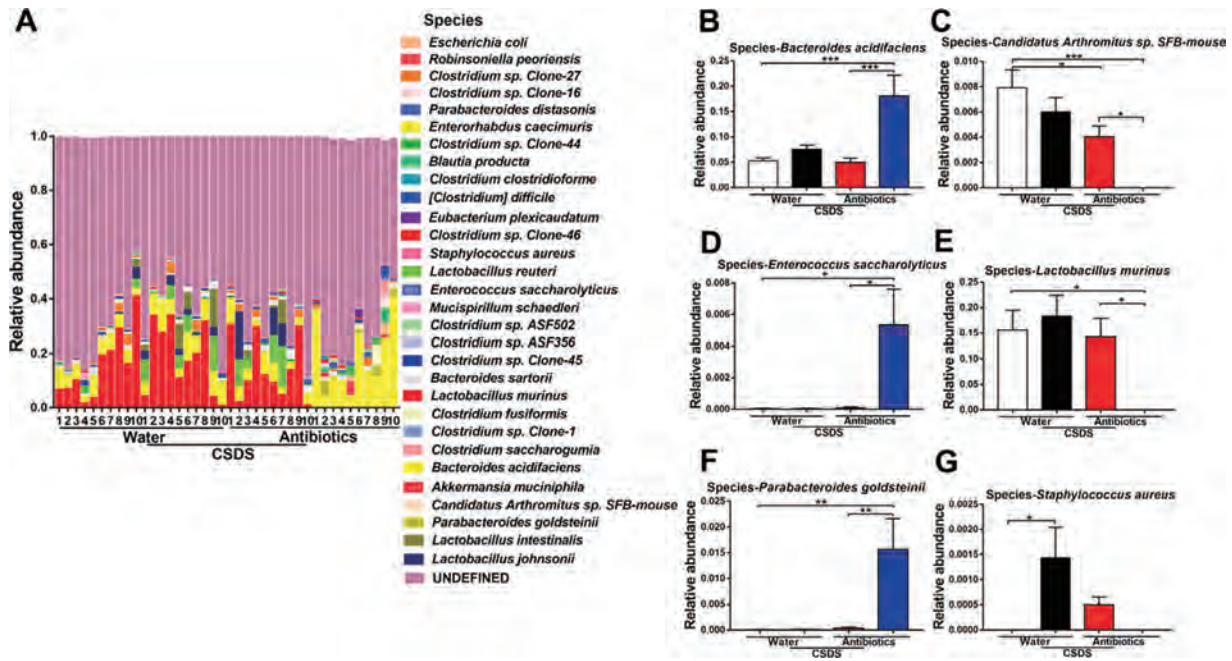


Fig. 8. Altered composition in the gut bacteria at the species level.

(A): The relative abundances of species in fecal samples of the four groups 24 days after drink antibiotics and CSDS. (B): *Bacteroides acidifaciens* (two-way ANOVA, antibiotics:  $F_{1,36} = 5.757, P = 0.022$ , CSDS:  $F_{1,36} = 6.434, P = 0.016$ , interaction:  $F_{1,36} = 12.957, P = 0.001$ ). (C): *Candidatus Arthromitus sp. SFB-mouse* (two-way ANOVA, antibiotics:  $F_{1,36} = 24.529, P < 0.001$ , CSDS:  $F_{1,36} = 1.104, P = 0.300$ , interaction:  $F_{1,36} = 8.910, P = 0.005$ ). (D): *Enterococcus saccharolyticus* (two-way ANOVA, antibiotics:  $F_{1,36} = 5.597, P = 0.023$ , CSDS:  $F_{1,36} = 5.323, P = 0.027$ , interaction:  $F_{1,36} = 5.323, P = 0.027$ ). (E): *Lactobacillus murinus* (two-way ANOVA, antibiotics:  $F_{1,36} = 8.450, P = 0.006$ , CSDS:  $F_{1,36} = 6.335, P = 0.016$ , interaction:  $F_{1,36} = 2.860, P = 0.099$ ). (F): *Parabacteroides goldsteinii* (two-way ANOVA, antibiotics:  $F_{1,36} = 6.997, P = 0.012$ , CSDS:  $F_{1,36} = 6.422, P = 0.016$ , interaction:  $F_{1,36} = 6.478, P = 0.015$ ). (G): *Staphylococcus aureus* (two-way ANOVA, antibiotics:  $F_{1,36} = 2.215, P = 0.145$ , CSDS:  $F_{1,36} = 9.503, P = 0.004$ , interaction:  $F_{1,36} = 2.215, P = 0.145$ ). Data are shown as mean  $\pm$  S.E.M. (n = 10). \* $P < 0.05$ , \*\* $P < 0.01$ , \*\*\* $P < 0.001$ . NS: not significant.

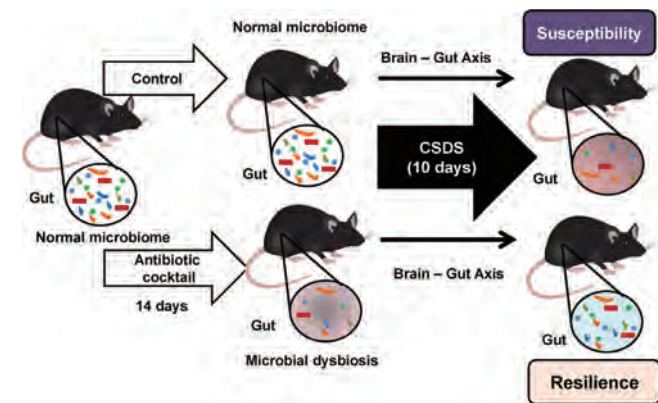


Fig. 9. Proposed scheme of brain-gut axis in resilience and susceptibility after repeated stress. Treatment of an antibiotic cocktail for 14 days caused microbial dysbiosis in mice by microbiome depletion. Subsequently, chronic social defeat stress was performed 10 days. Water-treated control mice showed the susceptibility after CSDS. In contrast, antibiotic cocktail treated mice showed the resilience after CSDS. Brain-gut axis may play a role in the susceptibility versus resilience in mice after CSDS.

among the four groups (Fig. 5F).

In SPT, CSDS caused significant reduction in sucrose preference in the water-treated group, but not in the antibiotic-treated group (Fig. 5G). There was no significant difference between the antibiotic-treated non-CSDS group and the water-treated non-CSDS group (Fig. 5G). CSDS treatment significantly increased plasma levels of IL-6 in the water-treated group, whereas CSDS treatment did not alter plasma IL-6 levels in the antibiotic-treated group (Fig. 5H). CSDS significantly decreased the expression of PSD-95 and GluA1 in the PFC of

water-treated group, but not in the antibiotic-treated group (Figs. 5I, J).

Overall, the antibiotic-treated group appeared to be protected against the CSDS-induced anhedonia-like phenotype, inflammation, and decreased synaptogenesis in the PFC.

### 3.6. Effects of CSDS on altered composition in the gut bacteria

The effects of CSDS on the composition of the microbiome of antibiotic-treated mice were investigated. The phyla of gut bacteria were identified (Fig. 6A). At the phylum level, the antibiotic-treated group showed significant reduction in *Actinobacteria* compared with the water-treated group (Fig. 6B). CSDS significantly decreased *Actinobacteria* in the water-treated group, but not in the antibiotic-treated group (Fig. 6B). The antibiotic-treated group showed significantly higher levels of *Proteobacteria* compared with the water-treated group (Fig. 6C). CSDS also significantly decreased the levels of *Proteobacteria* in the antibiotic-treated group, but not in the water-treated group (Fig. 6C).

The genus levels of gut bacterium were also identified (Fig. 7A). CSDS significantly altered the levels of six genera (*Alistipes*, *Bacteroides*, *Candidatus Arthromitus*, *Enterococcus*, *Lactobacillus*, and *Parasutterella*) in the antibiotic-treated group, but not in the water-treated group (Figs. 7B–I). In contrast, CSDS significantly increased levels of *Staphylococcus* in the water-treated group, but not in the antibiotic-treated group (Fig. 7J).

The species of gut bacterium were identified (Fig. 8A). CSDS significantly altered the levels of five microbes (*Bacteroides acidifaciens*, *Candidatus Arthromitus sp. SFB-mouse*, *Enterococcus saccharolyticus*, *Lactobacillus murinus*, and *Parabacteroides goldsteinii*) in the antibiotic-treated group, but not in the water-treated group (Figs. 8B–F). In contrast, CSDS significantly increased levels of *Staphylococcus aureus* in the water-treated group, but not in the antibiotic-treated group (Fig. 8G).

#### 4. Discussion

The major findings of this study are as follows. Treatment with an antibiotic cocktail in drinking water for 14 days caused marked reduction in the  $\alpha$ -diversity of microbiota in the host gut compared with the water-treated group. At the phylum level, the antibiotic-treated group showed a marked increase in *Proteobacteria* in the host gut, whereas the levels of three bacteria (*Actinobacteria*, *Bacteroidetes*, and *Firmicutes*) were decreased after treatment with the antibiotic cocktail. At the genus and species levels, the antibiotic-treated group showed marked alterations in several bacteria. Overall, treatment with an antibiotic cocktail for 14 days caused significant changes in the diversity and composition of microbiota in the host gut, consistent with previous reports (Hernandez-Chirlaque et al., 2016; Sampson et al., 2016; Zarrinpar et al., 2018; Zhan et al., 2018; Zhang et al., 2019a).

We performed CSDS for 10 days after treatment with an antibiotic cocktail for 14 days. The UniFrac-based PCoA showed significant differences among the four groups. CSDS significantly improved the abnormal diversity of microbiota in the antibiotic-treated group. In particular, CSDS significantly decreased levels of bacteria from the phylum *Proteobacteria*, genus *Bacteroides*, genus *Enterococcus*, genus *Parasutterella*, species *Bacteroides acidifaciens*, species *Enterococcus saccharolyticus*, and species *Parabacteroides goldsteinii* in the antibiotic-treated mice. A study reported that supplementation with rhubarb extract changed the microbial ecosystem in favor of *Parabacteroides goldsteinii* (Neyrinck et al., 2017). It seems that *Parabacteroides goldsteinii* may contribute to resilience to stress although a further study is needed.

In contrast, CSDS significantly increased the levels of genus *Alistipes*, genus *Candidatus Arthromitus*, genus *Lactobacillus*, species *Candidatus Arthromitus* sp. *SFB-mouse*, species *Lactobacillus murinus*. A recent study showed that CSDS-induced depression-like phenotypes were correlated with *Candidatus Arthromitus* sp. *SFB-mouse* (Tian et al., 2019). The mechanisms underlying CSDS-induced recovery of the composition of the microbiota in the host gut of antibiotic-treated mice are currently unknown. Previously, Bailey et al. (2011) reported that the exposure to a social stressor called social disruption failed to increase blood IL-6 in antibiotic-treated mice, although the same stress caused increases in levels of IL-6 in the blood of control mice, suggesting that the microbiota are necessary for stress-induced increases in circulating cytokines. Furthermore, the restraint stress was able to disrupt both the mucosa-associated and lumenally-associated colonic microbiota by causing changes in the relative abundances of multiple groups of bacteria, suggesting that stress can have distinct effects upon the colonic microbiota of the mucosal epithelium as compared with the luminal-associated microbiota (Galley et al., 2014). Given the role of immune system in resilience (Cathomas et al., 2019; Dantzer et al., 2008), it is likely that modulation of the bidirectional relationship between resilience and immunity by the gut microbiota plays a role in the recovery from CSDS. In addition, we reported the role of the brain–gut axis in the resilience versus susceptibility in rats exposed to inescapable electric stress (Zhang et al., 2019b). Further detailed study on the relationship between resilience and immunity via the brain–gut axis is needed.

In this study, we found marked increases in organisms from the phylum *Proteobacteria* after antibiotic treatment, whereas levels of bacteria from two major phyla (*Bacteroidetes* and *Firmicutes*) were decreased after antibiotic treatment (Fig. 2). Previous studies (Antonopoulos et al., 2009; Young and Schmidt, 2004; Zarrinpar et al., 2018) have shown that the microbiome of antibiotic-treated mice had a compositional shift to *Proteobacteria* from the major microbiota (*Bacteroidetes*, *Firmicutes*), consistent with our current data. Although *Proteobacteria* are natural inhabitants of the intestine, they normally comprise a minority of the healthy homeostatic microbiota. It has been suggested that an increased prevalence of *Proteobacteria* in the microbial community can serve as a potential diagnostic signature of dysbiosis and risk of disease (Kim et al., 2017; Shin et al., 2015). It is also

well known that treatment with a broad antibiotic cocktail causes a dramatic loss in diversity, as well as in representation of specific taxa, insurgence of antibiotic resistant strains, and up-regulation of antibiotic resistance genes (Becattini et al., 2016; Jernberg et al., 2007). In this study, we found an increase in the relative abundance of *Proteobacteria* in the antibiotic-treated group compared with the water-only group. However, the precise mechanisms underlying the increase in the relative abundance of *Proteobacteria* after treatment of antibiotic cocktail is currently unknown. The proportions of several genera and species were altered after repeated treatment with the antibiotic cocktail. Thus, antibiotic-induced microbiome depletion could be useful to study the role of the gut microbiota in pathological conditions.

We also found that CSDS decreased the sucrose preference of SPT in the water-treated group, although CSDS did not decrease the sucrose preference of SPT in the antibiotic-treated group. CSDS also significantly increased the plasma levels of IL-6 in the water-treated group, but not in the antibiotic-treated group, suggesting anti-inflammatory effects in antibiotic-treated mice. It has been reported that CSDS resilient mice had lower blood levels of IL-6 than susceptible mice in response to acute stress (Hodes et al., 2014). CSDS significantly decreased the expression of the synaptic proteins PSD-95 and GluA1 in the PFC from the water-treated group, but not the antibiotic-treated group. These findings suggest that antibiotic-induced microbiome depletion may contribute to stress resilience in mice after CSDS via the brain–gut–microbiome axis. It has also been reported that treatment with DSS caused colitis in control mice, although antibiotic-induced microbiome depletion did not produce DSS-induced colitis in the mice, suggesting that enteric bacteria are essential for the development of DSS-induced colitis (Hernandez-Chirlaque et al., 2016). These data suggest that microbiome reduction by antibiotic cocktail treatment may play a role in the development of susceptibility in mice after CSDS, although the specific microbes were not identified in this study. It is also possible that a complex interaction of these manipulations—the antibiotic cocktail treatment and CSDS—may contribute to the current data. Further detailed study is needed to confirm the relationship between stress resilience and the microbiome.

The crosstalk between brain and gut is predominately influenced by the gut bacteria (Kelly et al., 2016). Imbalance of gut microbiota is well established as causing abnormal brain–gut axes in several neurological and psychiatric diseases (Fung et al., 2017; Kelly et al., 2016). Accumulating evidence suggests that an abnormal composition of gut microbiota may contribute to resilience versus susceptibility in rodents after repeated stress (Bailey et al., 2011; Hao et al., 2019; Szyzkowicz et al., 2017; Yang et al., 2017a) (Fig. 9). It is likely that an altered composition of gut microbiota may play a role in stress-induced disorders. In contrast, it is reported that antibiotic cocktail treatment for 14 days caused depression-like phenotype in mice, and subsequent administration of *Lactobacillus casei* DG for 7 days countered most of these gut inflammatory, behavioral and functional alterations (Guida et al., 2018). Therefore, further detailed study on relationship between antibiotic-induced microbiome depletion and behavioral abnormalities are needed.

This study has some limitations. In this study, we did not identify the specific microbiota, which plays a role in resilience after CSDS. We do not know whether the microbiome in the fecal samples reflects the microbiome in the gut. Additionally, we did not produce conclusive evidence that the improvement in the density of the microbiota is mainly due to CSDS. The control mice that did not receive CSDS were not exposed to a non-aggressive resident CD1 mouse. It is possible that exposure to an aggressive CD1 mouse may be the cause of the improvement in the abnormal composition of microbiota in the antibiotic-treated mice, although further study is needed. Furthermore, we did not measure short-chain fatty acids (SCFAs) in the fecal samples although the microbiome can produce SCFAs which play a role in the several pathological conditions (Sudo, 2019; Tan et al., 2014; Zaiss et al., 2019). Finally, treatment with the antibiotic cocktail significantly

decreased the body weight, which may affect the susceptibility and reaction to CSDS. Further detailed study is needed to resolve the above limitations.

In conclusion, the present study suggests that antibiotic-induced microbiome depletion may contribute to resilience versus susceptibility in mice subjected to CSDS, and that CSDS may improve the diversity and composition of gut microbiota in mice treated with an antibiotic cocktail. It is likely that the brain–gut axis plays a role in susceptibility to stress-related disorders.

#### CRedit authorship contribution statement

**Siming Wang:** Conceptualization, Data curation, Methodology, Formal analysis, Writing - original draft, Writing - review & editing. **Younge Qu:** Data curation, Methodology, Writing - review & editing. **Lijia Chang:** Data curation, Methodology, Writing - review & editing. **Yaoyu Pu:** Data curation, Methodology, Writing - review & editing. **Kai Zhang:** Data curation, Methodology, Writing - review & editing. **Kenji Hashimoto:** Conceptualization, Funding acquisition, Supervision, Writing - original draft, Writing - review & editing.

#### Declaration of Competing Interest

All authors report no biomedical financial interests or potential conflicts of interest.

#### Acknowledgements

This study was supported by Smoking Research Foundation, Japan (to K.H.), and AMED, Japan (to K.H., JP19dm0107119). Dr. Lijia Chang was supported by Japan China Sasakawa Medical Fellowship (Tokyo, Japan). Ms. Siming Wang was supported by TAKASE Scholarship Foundation (Tokyo, Japan).

#### Supplementary materials

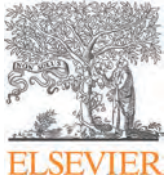
Supplementary material associated with this article can be found, in the online version, at [doi:10.1016/j.jad.2019.09.064](https://doi.org/10.1016/j.jad.2019.09.064).

#### References

- Antonopoulos, D.A., Huse, S.M., Morrison, H.G., Schmidt, T.M., Sogin, M.L., Young, V.B., 2009. Reproducible community dynamics of the gastrointestinal microbiota following antibiotic perturbation. *Infect. Immun.* 77, 2367–2375.
- Bailey, M.T., Dowd, S.E., Galley, J.D., Hufnagle, A.R., Allen, R.G., Lyte, M., 2011. Exposure to a social stressor alters the structure of the intestinal microbiota: implications for stressor-induced immunomodulation. *Brain Behav. Immun.* 25, 397–407.
- Becattini, S., Taur, Y., Pamer, E.G., 2016. Antibiotic-induced changes in the intestinal microbiota and disease. *Trends Mol. Med.* 22, 458–478.
- Burokas, A., Arbolea, S., Moloney, R.D., Peterson, V.L., Murphy, K., Clarke, G., Stanton, C., Dinan, T.G., Cryan, J.F., 2017. Targeting the microbiota-gut-brain axis: prebiotics have anxiolytic and antidepressant-like effects and reverse the impact of chronic stress in mice. *Biol. Psychiatry* 82, 472–487.
- Cathomas, F., Murrrough, J.W., Nestler, E.J., Han, M.H., Russo, S.J., 2019. Neurobiology of resilience: interface between mind and body. *Biol. Psychiatry*.
- Cerf-Bennussan, N., Gaboriau-Routhiau, V., 2010. The immune system and the gut microbiota: friends or foes? *Nat. Rev. Immunol.* 10, 735–744.
- Champagne-Jorgensen, K., Kunze, W.A., Forsythe, P., Bienenstock, J., Neufeld, K.A.M., 2019. Antibiotics and the nervous system: more than just the microbes? *Brain Behav. Immun.* 77, 7–15.
- Cusotto, S., Sandhu, K.V., Dinan, T.G., Cryan, J.F., 2018. The neuroendocrinology of the microbiota-gut-brain axis: a behavioural perspective. *Front Neuroendocrinol.* 51, 80–101.
- Cusotto, S., Strain, C.R., Fouhy, F., Strain, R.G., Peterson, V.L., Clarke, G., Stanton, C., Dinan, T.G., Cryan, J.F., 2019. Differential effects of psychotropic drugs on microbiome composition and gastrointestinal function. *Psychopharmacology (Berl)* 236, 1671–1685.
- Dantzer, R., Cohen, S., Russo, S.J., Dinan, T.G., 2008. Resilience and immunity. *Brain Behav. Immun.* 74, 28–42.
- Dinan, T.G., Cryan, J.F., 2017. Brain-gut-microbiota axis and mental health. *Psychosom. Med.* 79, 920–926.
- Forsythe, P., Kunze, W., Bienenstock, J., 2016. Moody microbes or fecal phrenology: what do we know about the microbiota-gut-brain axis? *BMC Med.* 14, 58.
- Fung, T.C., Olson, C.A., Hsiao, E.Y., 2017. Interactions between the microbiota, immune and nervous systems in health and disease. *Nat. Neurosci.* 20, 145–155.
- Galley, J.D., Yu, Z.T., Kumar, P., Dowd, S.E., Lyte, M., Bailey, M.T., 2014. The structures of the colonic mucosa-associated and luminal microbial communities are distinct and differentially affected by a prolonged murine stressor. *Gut Microbes* 5, 748–760.
- Golden, S.A., Covington 3rd, H.E., Berton, O., Russo, S.J., 2011. A standardized protocol for repeated social defeat stress in mice. *Nat. Protoc.* 6, 1183–1191.
- Guida, F., Turco, F., Iannotta, M., De Gregorio, D., Palumbo, I., Sarnelli, G., Furiano, A., Napolitano, F., Boccella, S., Luongo, L., Mazzitelli, M., Usiello, A., De Filippis, F., Iannotti, F.A., Piscitelli, F., Ercolini, D., de Novellis, V., Di Marzo, V., Cuomo, R., Maione, S., 2018. Antibiotic-induced microbiota perturbation causes gut endocannabinoidome changes, hippocampal neuroglial reorganization and depression in mice. *Brain Behav. Immun.* 67, 230–245.
- Hao, Z.K., Wang, W., Guo, R., Liu, H., 2019. *Faecalibacterium prausnitzii* (ATCC 27766) has preventive and therapeutic effects on chronic unpredictable mild stress-induced depression-like and anxiety-like behavior in rats. *Psychoneuroendocrinol.* 104, 132–142.
- Hernandez-Chirlaque, C., Aranda, C.J., Ocon, B., Capitan-Canadas, F., Ortega-Gonzalez, M., Carrero, J.J., Suarez, M.D., Zarzuelo, A., de Medina, F.S., Martinez-Augustin, O., 2016. Germ-free and antibiotic-treated mice are highly susceptible to epithelial injury in dss colitis. *J. Crohns. Colitis* 10, 1324–1335.
- Ho, P., Ross, D.A., 2017. More than a gut feeling: the implications of the gut microbiota in psychiatry. *Biol. Psychiatry* 81, E35–E37.
- Hodes, G.E., Pfau, M.L., Leboeuf, M., Golden, S.A., Christoffel, D.J., Bregman, D., Rebusi, N., Heshmati, M., Aleyasin, H., Warren, B.L., Lebonite, B., Horn, S., Lapidus, K.A., Stelzhammer, V., Wong, E.H.F., Bahn, S., Krishnan, V., Bolanos-Guzman, C.A., Murrrough, J.W., Merad, M., Russo, S.J., 2014. Individual differences in the peripheral immune system promote resilience versus susceptibility to social stress. *Proc. Natl. Acad. Sci. USA* 111, 16136–16141.
- Huang, N.N., Hua, D.Y., Zhan, G.F., Li, S., Zhu, B., Jiang, R.Y., Yang, L., Bi, J.J., Xu, H., Hashimoto, K., Luo, A.L., Yang, C., 2019a. Role of actinobacteria and coriobacteriia in the antidepressant effects of ketamine in an inflammation model of depression. *Pharmacol. Biochem. Behav.* 176, 93–100.
- Huang, T.T., Lai, J.B., Du, Y.L., Xu, Y., Ruan, L.M., Hu, S.H., 2019b. Current understanding of gut microbiota in mood disorders: an update of human studies. *Front Genet.* 10, 98.
- Ianiro, G., Tilg, H., Gasbarrini, A., 2016. Antibiotics as deep modulators of gut microbiota: between good and evil. *Gut.* 65, 1906–1915.
- Jernberg, C., Lofmark, S., Edlund, C., Jansson, J.K., 2007. Long-term ecological impacts of antibiotic administration on the human intestinal microbiota. *ISME J.* 1, 56–66.
- Jiang, H.Y., Ling, Z.X., Zhang, Y.H., Mao, H.J., Ma, Z.P., Yin, Y., Wang, W.H., Tang, W.X., Tan, Z.L., Shi, J.F., Li, L.J., Ruan, B., 2015. Altered fecal microbiota composition in patients with major depressive disorder. *Brain Behav. Immun.* 48, 186–194.
- Kelly, J.R., Clarke, G., Cryan, J.F., Dinan, T.G., 2016. Brain-gut-microbiota axis: challenges for translation in psychiatry. *Ann. Epidemiol.* 26, 366–372.
- Kim, S., Covington, A., Pamer, E.G., 2017. The intestinal microbiota: antibiotics, colonization resistance, and enteric pathogens. *Immunol. Rev.* 279, 90–105.
- Kim, S.W., Suda, W., Kim, S., Oshima, K., Fukuda, S., Ohno, H., Morita, H., Hattori, M., 2013. Robustness of gut microbiota of healthy adults in response to probiotic intervention revealed by high-throughput pyrosequencing. *DNA Res.* 20, 241–253.
- Lukic, I., Getselter, D., Ziv, O., Oron, O., Reuveni, E., Koren, O., Elliott, E., 2019. Antidepressants affect gut microbiota and *ruminococcus flavefaciens* is able to abolish their effects on depressive-like behavior. *Transl. Psychiatry* 9, 133.
- Ma, Q.Q., Xing, C.S., Long, W.Y., Wang, H.Y., Liu, Q., Wang, R.F., 2019. Impact of microbiota on central nervous system and neurological diseases: the gut-brain axis. *J. Neuroinflammation* 16, 53.
- Molina-Torres, G., Rodriguez-Arrastia, M., Roman, P., Sanchez-Labraca, N., Cardona, D., 2019. Stress and the gut microbiota-brain axis. *Behav. Pharmacol.* 30, 187–200.
- Neyrinck, A.M., Exteberria, U., Taminiau, B., Daube, G., Van Hul, M., Everard, A., Cani, P.D., Bindels, L.B., Delzenne, N.M., 2017. Rhubarb extract prevents hepatic inflammation induced by acute alcohol intake, an effect related to the modulation of the gut microbiota. *Mol. Nutr. Food Res.* 61, 150899.
- Pu, Y., Chang, L., Qu, Y., Wang, S., Zhang, K., Hashimoto, K., 2019. Antibiotic-induced microbiome depletion protects against MPTP-induced dopaminergic neurotoxicity in the brain. *Aging* 11, 6915–6929. <https://doi.org/10.18632/aging.102221>.
- Qu, Y.G., Yang, C., Ren, Q., Ma, M., Dong, C., Hashimoto, K., 2017. Comparison of (R)-ketamine and lanicemine on depression-like phenotype and abnormal composition of gut microbiota in a social defeat stress model. *Sci. Rep.* 7, 15725.
- Round, J.L., Mazmanian, S.K., 2009. The gut microbiota shapes intestinal immune responses during health and disease. *Nat. Rev. Immunol.* 9, 313–323.
- Sampson, T.R., Debelius, J.W., Thron, T., Janssen, S., Shastri, G.G., Ilhan, Z.E., Challis, C., Schretter, C.E., Rocha, S., Gradinaru, V., Chesselet, M.F., Keshavarzian, A., Shannon, K.M., Krajmalnik-Brown, R., Wittung-Stafshede, P., Knight, R., Mazmanian, S.K., 2016. Gut microbiota regulate motor deficits and neuroinflammation in a model of Parkinson's disease. *Cell* 167, 1469–1480.
- Shin, N.R., Whon, T.W., Bae, J.W., 2015. Proteobacteria: microbial signature of dysbiosis in gut microbiota. *Trends Biotechnol.* 33, 496–503.
- Sudo, N., 2019. Role of gut microbiota in brain function and stress-related pathology. *Biosci. Microbiota Food Health* 38, 75–80.
- Szyszkowicz, J.K., Wong, A., Anisman, H., Merali, Z., Audet, M.C., 2017. Implications of the gut microbiota in vulnerability to the social avoidance effects of chronic social defeat in male mice. *Brain Behav. Immun.* 66, 45–55.
- Tan, J., McKenzie, C., Potamitis, M., Thorburn, A.N., MacKay, C.R., Macia, L., 2014. The role of short-chain fatty acids in health and disease. *Adv. Immunol.* 121, 91–119.
- Tian, T., Xu, B., Qin, Y., Fan, L., Chen, J., Zheng, P., Gong, X., Wang, H., Bai, M., Pu, J., Lu, J., Zhou, W., Zhao, L., Yang, D., Xie, P., 2019. *Clostridium butyricum* miyairi 588



- has preventive effects on chronic social defeat stress-induced depressive-like behaviour and modulates microglial activation in mice. *Brain Behav. Immun.* 516, 430–436.
- Tanoue, T., Morita, S., Plichta, D.R., Skelly, A.N., Suda, W., Sugiura, Y., Narushima, S., Vlamakis, H., Motoo, I., Sugita, K., Shiota, A., Takeshita, K., Yasuma-Mitobe, K., Riethmacher, D., Kaisho, T., Norman, J.M., Mucida, D., Suematsu, M., Yaguchi, T., Bucci, V., Inoue, T., Kawakami, Y., Olle, B., Roberts, B., Hattori, M., Xavier, R.J., Atarashi, K., Honda, K., 2019. A defined commensal consortium elicits CD8 t cells and anti-cancer immunity. *Nature* 565, 600–605.
- Treadway, M.T., Zald, D.H., 2011. Reconsidering anhedonia in depression: lessons from translational neuroscience. *Neurosci. Biobehav. Rev.* 35, 537–555.
- Wong, M.L., Insera, A., Lewis, M.D., Mastronardi, C.A., Leong, L., Choo, J., Kentish, S., Xie, P., Morrison, M., Wesselingh, S.L., Rogers, G.B., Licinio, J., 2016. Inflammasome signaling affects anxiety- and depressive-like behavior and gut microbiome composition. *Mol. Psychiatry* 21, 797–805.
- Yang, B., Zhang, J.C., Han, M., Yao, W., Yang, C., Ren, Q., Ma, M., Chen, Q.X., Hashimoto, K., 2016. Comparison of *R*-ketamine and rapastinel antidepressant effects in the social defeat stress model of depression. *Psychopharmacology (Berl.)* 233, 3647–3657.
- Yang, C., Fang, X., Zhan, G.F., Huang, N.N., Li, S., Bi, J.J., Jiang, R.Y., Yang, L., Miao, L.Y., Zhu, B., Luo, A.L., Hashimoto, K., 2019. Key role of gut microbiota in anhedonia-like phenotype in rodents with neuropathic pain. *Transl. Psychiatry* 9, 57.
- Yang, C., Fujita, Y., Ren, Q., Ma, M., Dong, C., Hashimoto, K., 2017a. *Bifidobacterium* in the gut microbiota confer resilience to chronic social defeat stress in mice. *Sci. Rep.* 7, 45942.
- Yang, C., Qu, Y.G., Fujita, Y., Ren, Q., Ma, M., Dong, C., Hashimoto, K., 2017b. Possible role of the gut microbiota-brain axis in the antidepressant effects of (*R*)-ketamine in a social defeat stress model. *Transl. Psychiatry* 7, 15725.
- Yang, C., Shirayama, Y., Zhang, J.C., Ren, Q., Yao, W., Ma, M., Dong, C., Hashimoto, K., 2015. *R*-ketamine: a rapid-onset and sustained antidepressant without psychotomimetic side effects. *Transl. Psychiatry* 5, e632.
- Young, V.B., Schmidt, T.M., 2004. Antibiotic-associated diarrhea accompanied by large-scale alterations in the composition of the fecal microbiota. *J. Clin. Microbiol.* 42, 1203–1206.
- Zaiss, M.M., Jones, R.M., Schett, G., Pacifici, R., 2019. The gut-bone axis: how bacterial metabolites bridge the distance. *J. Clin. Invest.* 129, 3018–3028.
- Zarrinpar, A., Chaix, A., Xu, Z.J.Z., Chang, M.W., Marotz, C.A., Saghatelian, A., Knight, R., Panda, S., 2018. Antibiotic-induced microbiome depletion alters metabolic homeostasis by affecting gut signaling and colonic metabolism. *Nat. Commun.* 9, 2872.
- Zhan, G.F., Yang, N., Li, S., Huang, N.N., Fang, X., Zhang, J., Zhu, B., Yang, L., Yang, C., Luo, A.L., 2018. Abnormal gut microbiota composition contributes to cognitive dysfunction in SAMP8 mice. *Aging* 10, 1257–1267.
- Zhang, J., Bi, J.J., Guo, G.J., Yang, L., Zhu, B., Zhan, G.F., Li, S., Huang, N.N., Hashimoto, K., Yang, C., Luo, A.L., 2019a. Abnormal composition of gut microbiota contributes to delirium-like behaviors after abdominal surgery in mice. *CNS Neurosci. Ther.* 25, 685–696.
- Zhang, J.C., Yao, W., Dong, C., Yang, C., Ren, Q., Ma, M., Han, M., Hashimoto, K., 2015. Comparison of ketamine, 7,8-dihydroxyflavone, and ANA-12 antidepressant effects in the social defeat stress model of depression. *Psychopharmacology (Berl.)* 232, 4325–4335.
- Zhang, J.C., Yao, W., Dong, C., Yang, C., Ren, Q., Ma, M., Hashimoto, K., 2017. Blockade of interleukin-6 receptor in the periphery promotes rapid and sustained antidepressant actions: a possible role of gut-microbiota-brain axis. *Transl. Psychiatry* 7, e1138.
- Zhang, K., Fujita, Y., Chang, J., Qu, Y., Pu, Y., Wang, S., Shirayama, Y., Hashimoto, K., 2019b. Abnormal composition of gut microbiota is associated with resilience versus susceptibility to inescapable electric stress. *Transl. Psychiatry*. <https://doi.org/10.1038/s41398-019-0571-x>. In press.
- Zheng, P., Zeng, B., Zhou, C., Liu, M., Fang, Z., Xu, X., Zeng, L., Chen, J., Fan, S., Du, X., Zhang, X., Yang, D., Yang, Y., Meng, H., Li, W., Melgiri, N.D., Licinio, J., Wei, H., Xie, P., 2016. Gut microbiome remodeling induces depressive-like behaviors through a pathway mediated by the host's metabolism. *Mol. Psychiatry* 21, 786–796.
- Zhu, F., Guo, R., Wang, W., Ju, Y., Wang, Q., Ma, Q., Sun, Q., Fan, Y., Xie, Y., Yang, Z., Jie, Z., Zhao, B., Xiao, L., Yang, L., Zhang, T., Liu, B., Guo, L., He, X., Chen, Y., Chen, C., Gao, C., Xu, X., Yang, H., Wang, J., Dang, Y., Madsen, L., Brix, S., Kristiansen, K., Jia, H., Ma, X., 2019. Transplantation of microbiota from drug-free patients with schizophrenia causes schizophrenia-like abnormal behaviors and dysregulated kynurenine metabolism in mice. *Mol. Psychiatry*. <https://doi.org/10.1038/s41380-019-0475-4>. 2019 Aug 7.



Contents lists available at ScienceDirect

## Pharmacology, Biochemistry and Behavior

journal homepage: [www.elsevier.com/locate/pharmbiochembeh](http://www.elsevier.com/locate/pharmbiochembeh)

# Phencyclidine-induced cognitive deficits in mice are ameliorated by subsequent repeated intermittent administration of (R)-ketamine, but not (S)-ketamine: Role of BDNF-TrkB signaling

Yunfei Tan, Yuko Fujita, Youge Qu, Lijia Chang, Yaoyu Pu, Siming Wang, Xingming Wang, Kenji Hashimoto\*

Division of Clinical Neuroscience, Chiba University Center for Forensic Mental Health, Chiba, Japan

## ARTICLE INFO

**Keywords:**  
BDNF  
Cognition  
(R)-ketamine  
(S)-ketamine  
TrkB

## ABSTRACT

The *N*-methyl-D-aspartate receptor (NMDAR) antagonists including phencyclidine (PCP) and ketamine produce cognitive deficits in rodents and humans. We previously reported that (R)-ketamine produced the beneficial effects compared to (S)-ketamine in several animal models including depression. Here we compared the effects of two enantiomers of ketamine on cognitive deficits in mice after repeated administration of PCP. PCP (10 mg/kg/day for 10 days)-induced cognitive deficits were ameliorated by subsequent repeated intermittent administration of (R)-ketamine (10 mg/kg/day, twice weekly for 2-weeks), but not (S)-ketamine. Western blot analysis showed decreased levels of brain-derived neurotrophic factor (BDNF) and decreased ratio of phosphorylated-TrkB (p-TrkB) to TrkB in the prefrontal cortex (PFC) and hippocampus of PCP-treated mice. Furthermore, PCP-induced reduction of BDNF and p-TrkB/TrkB ratio in the PFC and hippocampus of PCP-treated mice was ameliorated by subsequent intermittent administration of (R)-ketamine. Interestingly, the beneficial effects of (R)-ketamine were blocked by pretreatment with TrkB inhibitor ANA-12. These findings suggest that (R)-ketamine could ameliorate PCP-induced cognitive deficits *via* activation of BDNF-TrkB signaling in the brain. Therefore, (R)-ketamine could be a potential therapeutic drug for cognitive impairment in patients with schizophrenia.

## 1. Introduction

Cognitive impairment is a core symptom in patients with schizophrenia; however, there are no therapeutic drugs for cognitive impairment in these patients (Goff et al., 2011; Green, 1996; Hashimoto, 2019a). Multiple lines of evidence suggest that the *N*-methyl-D-aspartate receptor (NMDAR) hypofunction might be involved in the several symptoms including cognitive impairment in schizophrenia (Coyle, 2017; Hashimoto et al., 2013; Hashimoto, 2014; Javitt and Zukin, 1991; Lin et al., 2019; Lin and Lane, 2019; Nakazawa and Sapkota, 2019). The NMDAR antagonist phencyclidine (PCP) is known to induce schizophrenia-like symptoms including cognitive impairment in healthy subjects (Javitt and Zukin, 1991; Domino and Luby, 2012; Javitt et al., 2012). Therefore, PCP-treated rodents have been used as an animal model of schizophrenia (Hashimoto et al., 2005, 2007; Hashimoto et al., 2008; Hida et al., 2015; Jentsch and Roth, 1999; Morris et al., 2005; Shirai et al., 2015; Yoshimi et al., 2014). Our study using the novel object recognition test (NORT) demonstrated that PCP-

induced cognitive deficits could be ameliorated by subsequent repeated administration of clozapine, but not haloperidol (Hashimoto et al., 2005). Thus, it is possible that the reversal of PCP-induced cognitive deficits might be a potential animal model of clozapine-like antipsychotic activity (Hashimoto et al., 2005).

The NMDAR antagonist (R,S)-ketamine is also known to produce schizophrenia-like symptoms including cognitive impairment in healthy subjects (Domino, 2010; Krystal et al., 1994). However, in the mood disorder research, (R,S)-ketamine is the most attractive antidepressant since (R,S)-ketamine produces rapid-acting and sustained antidepressant effects in treatment-resistant depressed patients (Chaki, 2017; Duman, 2018; Hashimoto, 2019b; Krystal et al., 2019; ; C. Yang et al., 2019; Zanos et al., 2018; Zhang and Hashimoto, 2019). (R,S)-ketamine is a racemic mixture containing equal amount of (R)-ketamine and (S)-ketamine. (S)-ketamine has an approximately 4-fold greater affinity for the NMDAR than (R)-ketamine (Domino, 2010; Hashimoto, 2019b). On March 5, 2019, the United State Food and Drug Administration approved (S)-ketamine nasal spray in conjunction with an oral

\* Corresponding author at: Division of Clinical Neuroscience, Chiba University Center for Forensic Mental Health, 1-8-1 Inohana, Chiba 260-8670, Japan.  
E-mail address: [hashimoto@faculty.chiba-u.jp](mailto:hashimoto@faculty.chiba-u.jp) (K. Hashimoto).

<https://doi.org/10.1016/j.pbb.2019.172839>

Received 29 November 2019; Received in revised form 17 December 2019; Accepted 17 December 2019

Available online 19 December 2019

0091-3057/ © 2019 Elsevier Inc. All rights reserved.

antidepressant for peoples with treatment-resistant depression. However, there are several concerns regarding the efficacy and the safety of (*S*)-ketamine (Jauhar and Morrison, 2019; Kaur et al., 2019; McShane et al., 2019; Turner, 2019).

In contrast, (*R*)-ketamine has the beneficial effects compared with (*S*)-ketamine in several animal models such as depression (Fukumoto et al., 2017; Yang et al., 2015, 2018; Zanos et al., 2016; Zhang et al., 2014) and Parkinson's disease (Fujita et al., 2019). Furthermore, brain-derived neurotrophic factor (BDNF) and its receptor tropomyosin kinase B (TrkB) signaling might play a role in the beneficial effects of (*R*)-ketamine (Fujita et al., 2019; Yang et al., 2015, 2018). However, there are no reports examining the effects of ketamine enantiomers in PCP-induced cognitive deficits in rodents.

In this study, using the NORT, we investigated the effects of subsequent repeated intermittent administration of two ketamine enantiomers on PCP-induced cognitive deficits in mice. Furthermore, we investigated the role of BDNF-TrkB signaling in the beneficial effects of (*R*)-ketamine in the PCP-induced model.

## 2. Methods

### 2.1. Animals

Male ICR mice (6 weeks old) weighing 25–30 g were purchased from SLC Japan (Hamamatsu, Shizuoka, Japan). Mice were housed in the clear polycarbonate cages (22.5 × 33.8 × 14.0 cm) and in groups of 5 or 6 mice under a controlled 12/12-h light–dark cycle (light from 7:00 AM to 7:00 PM), with room temperature at 23 ± 1 °C and humidity at 55 ± 5%. The mice were given free access to water and food pellets for mice. The experimental procedure was approved by the Animal Care and Use Committee of Chiba University Graduate School of Medicine (Permission number: 31-142).

### 2.2. Drugs

PCP hydrochloride was synthesized in our laboratory. (*R*)-ketamine hydrochloride and (*S*)-ketamine hydrochloride were also prepared in our laboratory, as previously reported (Zhang et al., 2014). The dose (10 mg/kg as hydrochloride) of PCP and ketamine enantiomers were dissolved in the saline, as previously reported (Hashimoto et al., 2005; Hashimoto et al., 2007, 2008; Shirai et al., 2015; Yoshimi et al., 2014; Yang et al., 2015, 2018). ANA-12 (*N*-[2-[[[Hexahydro-2-oxo-1*H*-azepin-3-yl]amino]carbonyl]phenyl]-benzo[*b*]thiophene-2-carboxamide: 0.5 mg/kg) (Sigma-Aldrich Japan, Tokyo, Japan) were dissolved in phosphate-buffered saline (PBS) containing 17% dimethylsulfoxide (DMSO), as previously reported (Cazorla et al., 2011; Ren et al., 2015; Yang et al., 2015; Zhang et al., 2015). Other reagents were purchased commercially.

### 2.3. Drug administration

The schedule of PCP-induced cognitive deficits model was used as previously reported (Hashimoto et al., 2005; Hashimoto et al., 2007, 2008; Shirai et al., 2015; Yoshimi et al., 2014). Saline (10 ml/kg) or PCP (10 mg/kg) were administered subcutaneously (s.c.) for 10 days (once daily on days 1–5, 8–12), and no treatment was on days 6, 7, 13 and 14. In the experiment of repeated intermittent treatment, 3 days (day 15) after a final administration of saline or PCP, saline (10 ml/kg) or (*R*)-ketamine (10 mg/kg)[or (*S*)-ketamine (10 mg/kg)], were administered i.p. for subsequent 2 weeks (twice weekly on days 15, 18, 22, 25) (Fig. 1A). In the experiment using a TrkB inhibitor ANA-12, vehicle or ANA-12 (0.5 mg/kg) were injected i.p. 30 min before saline (10 ml/kg) or (*R*)-ketamine (10 mg/kg) (Fig. 3A).

### 2.4. Novel object recognition test (NORT)

NORT was performed four days after the final administration of saline or (*R*)-ketamine [or (*S*)-ketamine] (Fig. 1A), as reported previously (Hashimoto et al., 2005; Hashimoto et al., 2007, 2008; Shirai et al., 2015; Yoshimi et al., 2014). The apparatus for this task consisted of a black open field box (50.8 × 50.8 × 25.4 cm). Before the test, mice were habituated in the box for 3 days. During a training session, two objects (various objects differing in their shape and color but similar in size) were placed in the box 35.5 cm apart (symmetrically) and each animal was allowed to explore in the box for 10 min (5 min × 2). The animals were considered to be exploring the object when the head of the animal was facing the object within an inch from the object or any part of the body, except for the tail, was touching the object. The time that mice spent exploring each object was recorded. After training, mice were immediately returned to their homecages, and the box and objects were cleaned with 75% ethanol to avoid any possible instinctive odorant cues. Retention tests were carried out at 1-day intervals following the respective training. During the retention test, each mouse was placed back into the same box, in which one of the objects used during training was replaced by a novel one. The mice were then allowed to freely explore for 5 min and the time spent exploring each object was recorded. Throughout the experiments, the objects were used in a counter-balanced manner in terms of their physical complexity. A preference index, a ratio of the amount of time spent exploring any one of the two objects (training session) or the novel one (retention test session) over the total time spent exploring respective to both objects, was used to measure memory performance.

### 2.5. Western blot analysis

One day after NORT, the brain samples of prefrontal cortex (PFC) and hippocampus were collected. Basically, tissue samples were homogenized in Laemmli lysis buffer. Aliquots (60 µg) of protein were measured using the DC protein assay kit (Bio-Rad, Hercules, CA) and incubated for 5 min at 95 °C, with an equal volume of 125 mM Tris/HCl, pH 6.8, 20% glycerol, 0.1% bromophenol blue, 10% β-mercaptoethanol, and 4% sodium dodecyl sulfate, and subjected to sodium dodecyl sulfate–polyacrylamide gel electrophoresis, using 10% minigels (Mini-PROTEAN® TGX™ Precast Gel; Bio-Rad, CA, USA). Proteins were transferred onto polyvinylidene difluoride (PVDF) membranes using a Trans Blot Mini Cell (Bio-Rad). For immunodetection, the blots were blocked with 3% non-fat dry milk (for BDNF), 3% BSA (for p-TrkB), 5% BSA (for TrkB) in Tris buffered saline (TBS) + 0.1% Tween 20 (TBST) for 1 h at room temperature (RT) and kept with primary antibodies overnight at 4 °C. The following primary antibodies were used: BDNF (1:1000, ABclonal, Inc., Tokyo, Japan), phosphorylated-TrkB (1:1000, ABclonal, Inc., Tokyo, Japan) and TrkB (80E3) (1:1000, Cell Signaling Technology, MA, USA). The next day, the blots were washed three times in TBST and incubated with horseradish peroxidase-conjugated anti-rabbit antibody (BDNF and p-TrkB: 1:10,000, TrkB: 1:1000) for 1 h at RT. After final three washes with TBST, the bands were detected using enhanced chemiluminescence (ECL) plus the Western Blotting Detection system (GE Healthcare Bioscience). The blots then were washed three times in TBST and incubated with the primary antibody directed against β-actin. Images were captured with a ChemiDoc™ Touch Imaging System (Bio-Rad, CA, USA), and immunoreactive bands were quantified.

### 2.6. Statistical analysis

Data were expressed as mean ± S.E.M. Statistical analysis was performed by using one-way analysis of variance (ANOVA) and *post hoc* Fisher's Least Significant Difference (LSD) test. The P values < 0.05 were considered statistically significant.

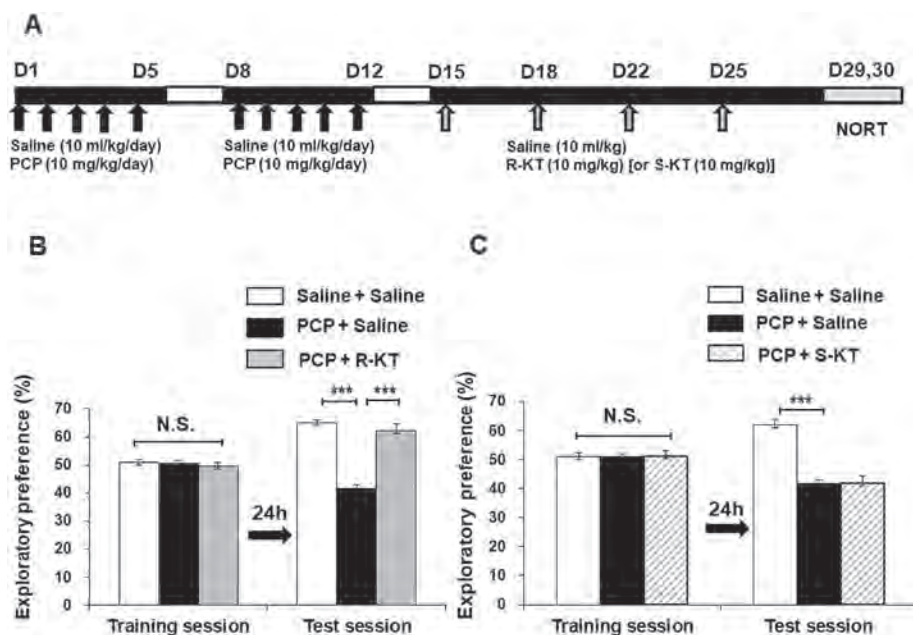


**Fig. 1.** Effects of two ketamine enantiomers on PCP-induced cognitive deficits in mice.

(A): Schedule of treatment and behavioral test. Saline (10 ml/kg/day) or PCP (10 mg/kg/day) were administered s.c. for 10 days (once daily on days 1–5, 8–12). Subsequently, vehicle (10 ml/kg; saline), or (R)-ketamine (10 mg/kg) [or (S)-ketamine (10 mg/kg)] was administered i.p. into mice on days 15, 18, 22, 25. Four days (days 29) after the last administration of vehicle or ketamine enantiomer, the training session of NORT was performed. The retention test session was performed 24 h after the training session. (B): NORT result of (R)-ketamine. (C): NORT result of (S)-ketamine. Values are the mean  $\pm$  S.E.M (n = 6–8). \*\*\*P < 0.001 as compared with PCP plus saline treated group. N.S.: not significant. R-KT: (R)-ketamine. S-KT: (S)-ketamine.

### 3. Results

#### 3.1. Effects of two ketamine enantiomers on PCP-induced cognitive deficits

In the NORT, repeated administration of PCP (10 mg/kg/day for 10 days) caused cognitive deficits in mice (Fig. 1B and C). In the training session, there were no significant differences [one-way ANOVA: (R)-ketamine:  $F_{2,18} = 0.577$ ,  $P = 0.572$ . (S)-ketamine:  $F_{2,21} = 0.011$ ,  $P = 0.989$ ] between the three groups (Fig. 1B and C). In the retention test, the repeated intermittent administration of (R)-ketamine significantly (one-way ANOVA:  $F_{2,18} = 26.36$ ,  $P < 0.001$ ) ameliorated the decreased exploratory preference in mice after repeated administration of PCP (Fig. 1B). In contrast, in the retention test, the repeated intermittent administration of (S)-ketamine did not improve the decreased exploratory preference in mice after repeated administration of PCP (one-way ANOVA:  $F_{2,21} = 34.21$ ,  $P < 0.001$ ) (Fig. 1C).

#### 3.2. Role of BDNF-TrkB signaling in the PFC and hippocampus

Western blot analyses of BDNF, TrkB, phosphorylated TrkB (p-TrkB) in PFC and hippocampus were performed. Repeated PCP administration significantly decreased the levels of BDNF protein in the PFC and hippocampus of mouse brain. One-way ANOVA showed a statistical significance in BDNF protein (PFC:  $F_{2,30} = 4.485$ ,  $P < 0.05$ ; hippocampus:  $F_{2,30} = 3.99$ ,  $P < 0.05$ ) among the three groups (Fig. 2A and B). Subsequent repeated intermittent administration of (R)-ketamine (10 mg/kg/day, twice weekly for 2-weeks) significantly attenuated the reduced levels of BDNF protein in the PFC and hippocampus of PCP-treated mice (Fig. 2A and B).

To examine the role of TrkB phosphorylation in the pharmacological effect of (R)-ketamine, we performed Western blot analyses of TrkB and p-TrkB (an activated form of TrkB) in the same brain regions. Repeated PCP administration significantly decreased the ratio of p-TrkB/TrkB in the PFC and hippocampus. Subsequent repeated intermittent administration of (R)-ketamine significantly attenuated the reduced ratio of p-TrkB/TrkB in the PFC and hippocampus of PCP-treated mice (Fig. 2A and B). One-way ANOVA revealed statistical significance in p-TrkB/TrkB (PFC:  $F_{2,30} = 4.206$ ,  $P < 0.05$ ; hippocampus:  $F_{2,30} = 4.329$ ,  $P < 0.05$ ) among the three groups (Fig. 2A and B). These findings suggest that BDNF-TrkB signaling in the PFC and

hippocampus might be involved in the beneficial effects of (R)-ketamine in PCP model.

#### 3.3. Effects of ANA-12 in the effects of (R)-ketamine in PCP-induced model

To examine the role of BDNF-TrkB in the mechanisms of action of (R)-ketamine, we investigated the effects of the TrkB inhibitor ANA-12 in the PCP-induced cognitive deficits (Fig. 3A). In the training session, there were no significant differences (one-way ANOVA:  $F_{4,32} = 5.96$ ,  $P = 0.668$ ) between the five groups (Fig. 3B). In the retention session, there were significant differences (one-way ANOVA:  $F_{4,32} = 7.77$ ,  $P < 0.001$ ) between the five groups (Fig. 3B). The pretreatment with ANA-12 significantly antagonized the beneficial effects of (R)-ketamine in PCP-induced cognitive deficits (Fig. 3B). In contrast, ANA-12 alone did not improve PCP-induced cognitive deficits (Fig. 3B).

### 4. Discussion

The major findings of this study are as follows: First, PCP-induced cognitive deficits could be ameliorated by subsequent repeated intermittent administration of (R)-ketamine, but not (S)-ketamine. Second, PCP-induced decreased BDNF-TrkB signaling in the PFC and hippocampus could be ameliorated by subsequent repeated intermittent administration of (R)-ketamine. Third, pretreatment with ANA-12 (a TrkB inhibitor) antagonized the beneficial effects of (R)-ketamine in PCP-induced cognitive deficits. These findings suggest that (R)-ketamine can ameliorate PCP-induced cognitive deficits through BDNF-TrkB activation in the PFC and hippocampus. Therefore, it is likely that (R)-ketamine could be a potential therapeutic drug for cognitive impairment in patients with schizophrenia.

The pharmacokinetic profiles for (R)-ketamine and (S)-ketamine are similar (Fukumoto et al., 2017; Zanos et al., 2016), suggesting that the differential effects between two ketamine enantiomers are not due to differences in their pharmacokinetic profiles. In addition, (S)-ketamine has an approximately 4-fold greater affinity for the NMDAR than the (R)-ketamine (Domino, 2010; Hashimoto, 2019b). Using a functional magnetic resonance imaging (fMRI) study in conscious rats, Masaki et al. (2019) reported that, similar to the potent NMDAR antagonist (+)-MK-801, (R,S)-ketamine (10 mg/kg) and (S)-ketamine (10 mg/kg) produced a significant positive response in the brain whereas (R)-ketamine (10 mg/kg) produced negative response in the brain. This study

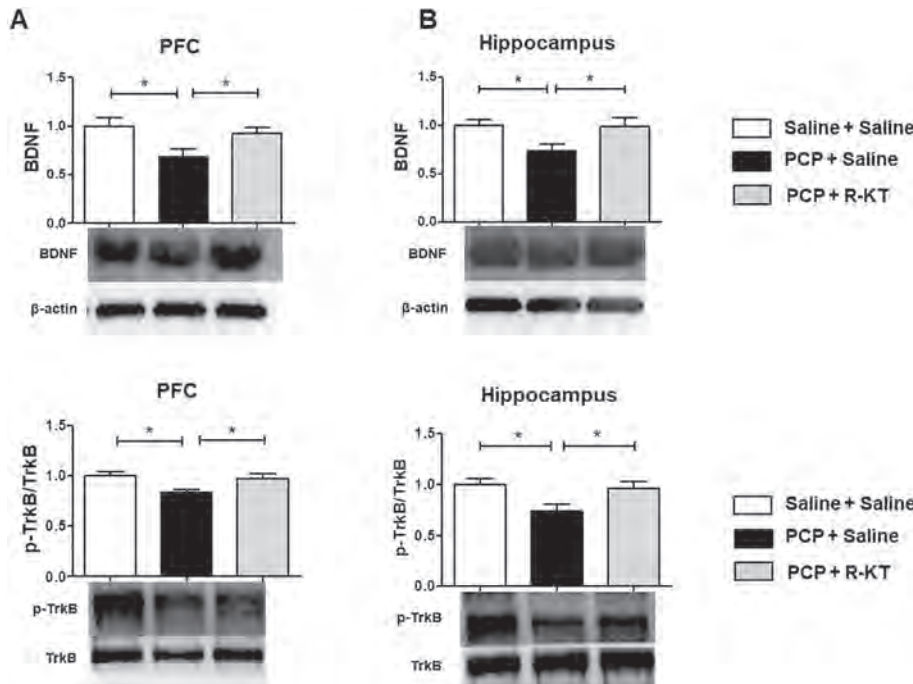


**Fig. 2.** Effects of (R)-ketamine on the BDNF and TrkB phosphorylation in the PFC and hippocampus of PCP-treated mice.

(A): Expression of BDNF and the ratio of p-TrkB to total TrkB in the PFC. (B): Expression of BDNF and the ratio of p-TrkB to total TrkB in the hippocampus. The value was expressed as a percentage of that of control mice. Values are the mean ± S.E.M (n = 10–12). \*P < 0.05 as compared with PCP plus saline treated group. R-KT: (R)-ketamine.

suggests that NMDAR inhibition is not involved in the (R)-ketamine-induced fMRI pattern in conscious rat brain. It is, therefore, unlikely that NMDAR inhibition may play a crucial role in the beneficial effects of (R)-ketamine in PCP-induced cognitive deficits.

In this study, we found the reduction of BDNF in the PFC and hippocampus of PCP-treated mice, consistent with previous reports (Snigdha et al., 2011; Li et al., 2018). Previously, we reported that (R)-ketamine could attenuate reduced BDNF level in the PFC and hippocampus in susceptible mice after chronic social defeat stress (CSDS), and ANA-12 blocked the antidepressant-like effects of (R)-ketamine, indicating a crucial role for BDNF-TrkB cascade in (R)-ketamine's antidepressant-like actions (Yang et al., 2015). Recently, we reported that (R)-ketamine protected against MPTP (1-methyl-4-phenyl-1,2,3,6-tetrahydropyridine)-induced neurotoxicity through TrkB activation (Fujita

et al., 2019). In this study, we found that BDNF-TrkB signaling might play a role in the beneficial effects of (R)-ketamine in PCP-induced cognitive deficits. Collectively, it is likely that (R)-ketamine can exert beneficial effects by activating BDNF-TrkB signaling in the brain, although further detailed studies underlying the role of BDNF-TrkB signaling in the beneficial effects of (R)-ketamine are necessary.

PCP-induced cognitive deficits in mice were ameliorated by subsequent repeated administration of clozapine, but not haloperidol (Hashimoto et al., 2005). Here, we demonstrated that repeated intermittent (twice weekly for two weeks) administration of (R)-ketamine can improve PCP-induced cognitive deficits. Clinical trial of (R)-ketamine in humans is underway (Hashimoto, 2019b). Interestingly, there are associations between peripheral BDNF levels and cognitive impairment in patients with schizophrenia (Man et al., 2018; Y. Yang

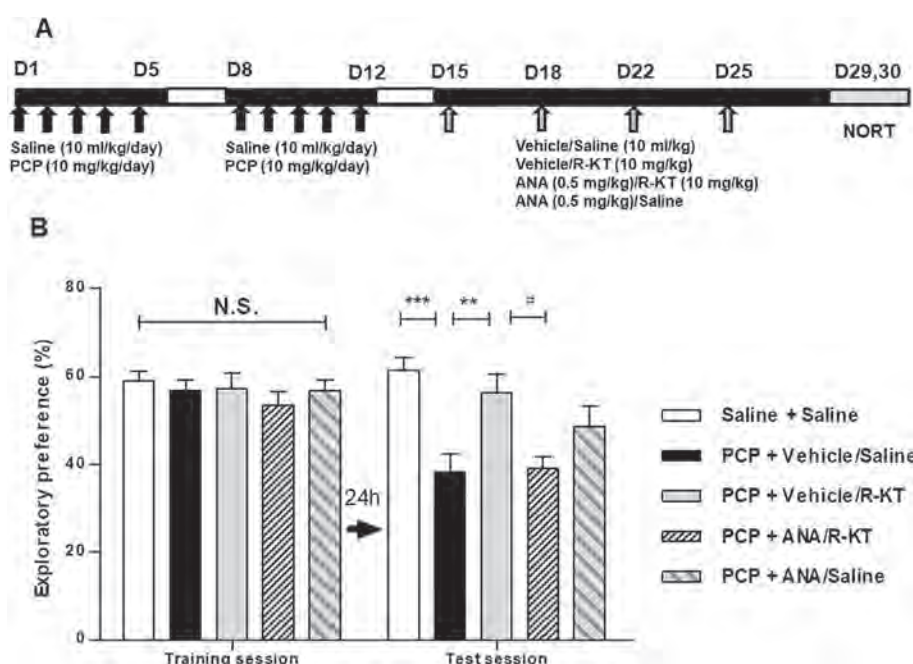


**Fig. 3.** Effects of ANA-12 in the beneficial effects of (R)-ketamine in PCP model.

(A): Schedule of treatment and behavioral test. Saline (10 ml/kg/day) or PCP (10 mg/kg/day) were administered s.c. for 10 days (once daily on days 1–5, 8–12). Subsequently, vehicle (10 ml/kg; 17% DMSO in PBS) + Saline, vehicle (10 ml/kg)/(R)-ketamine (10 mg/kg), ANA-12 (0.5 mg/kg)/(R)-ketamine (10 mg/kg), or ANA-12 (0.5 mg/kg)/saline (10 ml/kg) was administered i.p. into mice on days 15, 18, 22, 25. Vehicle or ANA-12 was administered i.p. 30 min before injection of saline or (R)-ketamine. Four days (days 29) after the last administration of vehicle or (R)-ketamine, the training session of NORT was performed. The retention test session was performed 24 h after the training session. (B): NORT. Values are the mean ± S.E.M (n = 10–12). \*\*\*P < 0.01, \*\*\*\*P < 0.001 as compared with PCP plus saline treated group. #P < 0.05 as compared with PCP plus vehicle/(R)-ketamine group. ANA: ANA-12. R-KT: (R)-ketamine.

et al., 2019; Zhang et al., 2012; Zhang et al., 2018). Therefore, it is of great interest to investigate whether (R)-ketamine could improve cognitive impairment in patients with schizophrenia.

The side effects such as psychotomimetic effects and dissociation in humans after (R,S)-ketamine injection are well known (Sanacora et al., 2017; Singh et al., 2017; Zhu et al., 2016). Unlike (S)-ketamine, (R)-ketamine might not produce psychotomimetic side effects or exhibit abuse potential in rodents and monkeys (Chang et al., 2019; Hashimoto et al., 2017; Tian et al., 2018; Yang et al., 2015, 2016). Importantly, the previous data from human studies suggest that (S)-ketamine could contribute to the acute side effects of (R,S)-ketamine, whereas (R)-ketamine may not be associated with these side effects (Vollenweider et al., 1997; Zanos et al., 2018). Collectively, (R)-ketamine would be a safer drug in humans than (R,S)-ketamine and (S)-ketamine (Hashimoto, 2016a, 2016b, 2019b; C. Yang et al., 2019; Zhang and Hashimoto, 2019).

In conclusion, these findings show that PCP-induced cognitive deficits could be ameliorated after subsequent repeated intermittent (twice weekly for 2-weeks) administration of (R)-ketamine, but not (S)-ketamine, and that TrkB inhibitor blocked the beneficial effects of (R)-ketamine. Therefore, (R)-ketamine would be a new therapeutic drug for cognitive impairment in patients with schizophrenia.

### Acknowledgements

This study was supported by Japan Agency for Medical Research and Development (AMED) (to K.H., JP19dm0107119). Dr. Lijia Chang was supported by the Japan China Sasakawa Medical Fellowship (Tokyo, Japan). Ms. Siming Wang was supported by TAKASE Scholarship Foundation (Tokyo, Japan).

### Declaration of competing interest

Dr. Hashimoto is an inventor on a filed patent application on “The use of (R)-ketamine in the treatment of psychiatric diseases” by Chiba University. Dr. Hashimoto has received research support from Dainippon-Sumitomo, Otsuka, and Taisho. Other authors declare no conflict of interest.

### References

- Cazorla, M., Prémont, J., Mann, A., Girard, N., Kellendonk, C., Rognan, D., 2011. Identification of a low-molecular weight TrkB antagonist with anxiolytic and antidepressant activity in mice. *J. Clin. Invest.* 121, 1846–1857.
- Chaki, S., 2017. Beyond ketamine: new approaches to the development of safer antidepressants. *Curr. Neuropharmacol.* 15, 963–976.
- Chang, L., Zhang, K., Pu, Y., Qu, Y., Wang, S.M., Xiong, Z., Ren, Q., Dong, C., Fujita, Y., Hashimoto, K., 2019. Comparison of antidepressant and side effects in mice after intranasal administration of (R,S)-ketamine, (R)-ketamine, and (S)-ketamine. *Pharmacol. Biochem. Behav.* 181, 53–59.
- Coyle, J.T., 2017. Schizophrenia: basic and clinical. *Adv. Neurobiol.* 15, 255–280.
- Domino, E.F., 2010. Taming the ketamine tiger. 1965. *Anesthesiology* 113, 678–684.
- Domino, E.F., Luby, E.D., 2012. Phencyclidine/schizophrenia: one view toward the past, the other to the future. *Schizophr. Bull.* 38, 914–919.
- Duman, R.S., 2018. Ketamine and Rapid-acting Antidepressants: A New Era in the Battle Against Depression and Suicide. *F1000Res.* 7, Rev-659.
- Fujita, A., Fujita, Y., Pu, Y., Chang, L., Hashimoto, K., 2019. MPTP-induced dopaminergic neurotoxicity in mouse striatum is attenuated after subsequent intranasal administration of (R)-ketamine: a role of TrkB signaling. *Psychopharmacology*. <https://doi.org/10.1007/s00213-019-05346-5>. 2019 Aug 15.
- Fukumoto, K., Toki, H., Iijima, M., Hashihayata, T., Yamaguchi, J., Hashimoto, K., Chaki, S., 2017. Antidepressant potential of (R)-ketamine in rodent models: comparison with (S)-ketamine. *J. Pharmacol. Exp. Ther.* 361, 9–16.
- Goff, D.C., Hill, M., Barch, D., 2011. The treatment of cognitive impairment in schizophrenia. *Pharmacol. Biochem. Behav.* 99, 245–253.
- Green, M., 1996. What are the functional consequences of neurocognitive deficits in schizophrenia? *Am. J. Psychiatry* 153, 321–330.
- Hashimoto, K., 2014. Targeting of NMDA receptors in new treatments for schizophrenia. *Expert Opin. Ther. Targets* 18, 1049–1063.
- Hashimoto, K., 2016a. R-ketamine: a rapid-onset and sustained antidepressant without risk of brain toxicity. *Psychol. Med.* 46, 2449–2451.
- Hashimoto, K., 2016b. Ketamine's antidepressant action: beyond NMDA receptor inhibition. *Expert Opin. Ther. Targets* 20, 1389–1392.
- Hashimoto, K., 2019a. Recent advances in the early intervention in schizophrenia: future direction from preclinical findings. *Curr. Psychiatr. Rev.* 21, 75.
- Hashimoto, K., 2019b. Rapid-acting antidepressant ketamine, its metabolites and other candidates: a historical overview and future perspective. *Psychiatry Clin. Neurosci.* 73, 613–627.
- Hashimoto, K., Fujita, Y., Iyo, M., 2007. Phencyclidine-induced cognitive deficits in mice are improved by subsequent subchronic administration of fluvoxamine: role of sigma-1 receptors. *Neuropsychopharmacology* 32, 514–521.
- Hashimoto, K., Fujita, Y., Shimizu, E., Iyo, M., 2005. Phencyclidine-induced cognitive deficits in mice are improved by subsequent subchronic administration of clozapine, but not haloperidol. *Eur. J. Pharmacol.* 519, 114–117.
- Hashimoto, K., Ishima, T., Fujita, Y., Matsuo, M., Kobashi, T., Takahagi, M., Tsukada, H., Iyo, M., 2008. Phencyclidine-induced cognitive deficits in mice are improved by subsequent subchronic administration of the novel selective  $\alpha 7$  nicotinic receptor agonist SSR180711. *Biol. Psychiatry* 63, 92–97.
- Hashimoto, K., Malchow, B., Falkai, P., Schmitt, A., 2013. Glutamate modulators as potential therapeutic drugs in schizophrenia and affective disorders. *Eur. Arch. Psychiatry Clin. Neurosci.* 263, 367–377.
- Hashimoto, K., Kakiuchi, T., Ohba, H., Nishiyama, S., Tsukada, H., 2017. Reduction of dopamine D<sub>2/3</sub> receptor binding in the striatum after a single administration of esketamine, but not R-ketamine: a PET study in conscious monkeys. *Eur. Arch. Psychiatry Clin. Neurosci.* 267, 173–176.
- Hida, H., Mouri, A., Mori, K., Matsumoto, Y., Seki, T., Taniguchi, M., Yamada, K., Iwamoto, K., Ozaki, N., Nabeshima, N., Noda, Y., 2015. Blonanserin ameliorates phencyclidine-induced visual-recognition memory deficits: the complex mechanism of blonanserin action involving D<sub>3</sub>-5-HT<sub>2A</sub> and D<sub>1</sub>-NMDA receptors in the mPFC. *Neuropsychopharmacology* 40, 601–613.
- Jauhar, S., Morrison, P., 2019. Esketamine for treatment resistant depression. *BMJ* 366, 15572.
- Javitt, D.C., Zukin, S.R., 1991. Recent advances in the phencyclidine model of schizophrenia. *Am. J. Psychiatry* 148, 1301–1308.
- Javitt, D.C., Zukin, S.R., Heresco-Levy, U., Umbricht, D., 2012. Has an angel shown the way? Etiological and therapeutic implications of the PCP/NMDA model of schizophrenia. *Schizophr. Bull.* 38, 958–966.
- Jentsch, J.D., Roth, R.H., 1999. The neuropsychopharmacology of phencyclidine: from NMDA receptor hypofunction to the dopamine hypothesis of schizophrenia. *Neuropsychopharmacology* 20, 201–225.
- Kaur, U., Pathak, B.K., Singh, A., Chakrabarti, S.S., 2019. Esketamine: a glimmer of hope in treatment-resistant depression. *Eur. Arch. Psychiatry Clin. Neurosci.* <https://doi.org/10.1007/s00406-019-01084-z>. 2019 Nov 19.
- Krystal, J.H., Kaepfer, L.P., Seibyl, J.P., Freeman, G.K., Delaney, R., Bremner, J.D., Heninger, G.R., Bowers Jr., M.B., Charney, D.S., 1994. Subanesthetic effects of the noncompetitive NMDA antagonist, ketamine, in humans. Psychotomimetic, perceptual, cognitive, and neuroendocrine responses. *Arch. Gen. Psychiatry* 51, 199–214.
- Krystal, J.H., Abdallah, C.G., Sanacora, G., Charney, D.S., Duman, R.S., 2019. Ketamine: a paradigm shift for depression research and treatment. *Neuron* 101, 774–778.
- Li, Y.X., Ye, Z.H., Chen, T., Jia, X.F., He, L., 2018. The effects of donepezil on phencyclidine-induced cognitive deficits in a mouse model of schizophrenia. *Pharmacol. Biochem. Behav.* 175, 69–76.
- Lin, C.H., Lane, H.Y., 2019. Early identification and intervention of schizophrenia: insight from hypotheses of glutamate dysfunction and oxidative stress. *Front. Psych.* 10, 93.
- Lin, C.H., Chen, Y.M., Lane, H.Y., 2019. Novel treatment for the hardest-to-treat schizophrenia: dual action of NMDA receptor and antioxidant. *Curr. Drug Targets*. <https://doi.org/10.2174/1389450120666191011163539>. 2019 Oct 11.
- Man, L., Lv, X., Du, X.D., Yin, G., Zhu, X., Zhang, Y., Soares, J.C., Yang, X.N., Chen, X., Zhang, X.Y., 2018. Cognitive impairments and low BDNF serum levels in first-episode drug-naïve patients with schizophrenia. *Psychiatry Res.* 263, 1–6.
- Masaki, Y., Kashiwagi, Y., Watabe, H., Abe, K., 2019. (R)- and (S)-ketamine induce differential fMRI responses in conscious rats. *Synapse* 73, e22126.
- McShane, R., Baldwin, D.S., McAllister-Williams, R.H., Stone, J.M., Taylor, D., Winstock, A.R., Young, A.H., 2019. Esketamine and the need for a new type of registry for drugs with abuse potential. *Am. J. Psychiatry* 176, 966.
- Morris, B.J., Cochran, S.M., Pratt, J.A., 2005. PCP: from pharmacology to modelling schizophrenia. *Curr. Opin. Pharmacol.* 5, 101–106.
- Nakazawa, K., Sapkota, K., 2019. The origin of NMDA receptor hypofunction in schizophrenia. *Pharmacol. Ther.* <https://doi.org/10.1016/j.pharmthera.2019.107426>. 2019 Oct 16:107426.
- Ren, Q., Ma, M., Yang, C., Zhang, J.C., Yao, W., Hashimoto, K., 2015. BDNF-TrkB signaling in the nucleus accumbens shell of mice has key role in methamphetamine withdrawal symptoms. *Transl. Psychiatry* 5, e666.
- Sanacora, G., Frye, M.A., McDonald, W., Mathew, S.J., Turner, M.S., Schatzberg, A.F., Summergrad, P., Nemeroff, C.B., American Psychiatric Association (APA) Council of Research Task Force on Novel Biomarkers and Treatments, 2017. A consensus statement on the use of ketamine in the treatment of mood disorders. *JAMA Psychiatr.* 74, 399–405.
- Shirai, Y., Fujita, Y., Hashimoto, R., Ohi, K., Yamamori, H., Yasuda, Y., Ishima, T., Suganuma, H., Ushida, Y., Takeda, M., Hashimoto, K., 2015. Dietary intake of sulfuraphane-rich broccoli sprout extracts during juvenile and adolescence can prevent phencyclidine-induced cognitive deficits at adulthood. *PLoS One* 10, e0127144.
- Singh, I., Morgan, C., Curran, V., Nutt, D., Schlag, A., McShane, R., 2017. Ketamine treatment for depression: opportunities for clinical innovation and ethica foresight. *Lancet Psychiatry* 4, 419–426.
- Snigdha, S., Neill, J.C., McLean, S.L., Shemar, G.K., Cruise, L., Shahid, M., Henry, B., 2011. Phencyclidine (PCP)-induced disruption in cognitive performance is gender-specific and associated with a reduction in brain-derived neurotrophic factor (BDNF) in specific regions of the female rat brain. *J. Mol. Neurosci.* 43, 337–345.

- Tian, Z., Dong, C., Fujita, A., Fujita, Y., Hashimoto, K., 2018. Expression of heat shock protein HSP-70 in the retrosplenial cortex of rat brain after administration of (R,S)-ketamine and (S)-ketamine, but not (R)-ketamine. *Pharmacol. Biochem. Behav.* 172, 17–21.
- Turner, E.H., 2019. Esketamine for treatment-resistant depression: seven concerns about efficacy and FDA approval. *Lancet Psychiatry* 6, 977–979.
- Yang, C., Shirayama, Y., Zhang, J.C., Ren, R., Yao, W., Ma, M., Dong, C., Hashimoto, K., 2015. R-ketamine: a rapid-onset and sustained antidepressant without psychotomimetic side effects. *Transl. Psychiatry* 5, e632.
- Vollenweider, F.X., Leenders, X.L., Øye, I., Hell, D., Angst, J., 1997. Differential psychopathology and patterns of cerebral glucose utilization produced by (S)- and (R)-ketamine in healthy volunteers using positron emission tomography (PET). *Eur. Neuropsychopharmacol.* 7, 25–38.
- Yang, C., Han, M., Zhang, J.C., Ren, Q., Hashimoto, K., 2016. Loss of parvalbumin-immunoreactivity in mouse brain regions after repeated intermittent administration of esketamine, but not R-ketamine. *Psychiatry Res.* 239, 281–283.
- Yang, C., Ren, Q., Qu, Y., Zhang, J.C., Ma, M., Dong, C., Hashimoto, K., 2018. Mechanistic target of rapamycin-independent antidepressant effects of (R)-ketamine in a social defeat stress model. *Biol. Psychiatry* 83, 18–28.
- Yang, Y., Liu, Y., Wang, G., Hei, G., Wang, X., Li, R., Li, L., Wu, R., Zhao, J., 2019a. Brain-derived neurotrophic factor is associated with cognitive impairments in first-episode and chronic schizophrenia. *Psychiatry Res.* 273, 528–536.
- Yang, C., Yang, J., Luo, A., Hashimoto, K., 2019b. Molecular and cellular mechanisms underlying the antidepressant effects of ketamine enantiomers and its metabolites. *Transl. Psychiatry* 9, 280.
- Yoshimi, N., Fujita, Y., Ohgi, Y., Futamura, T., Kikuchi, T., Hashimoto, K., 2014. Effects of brexpiprazole, a novel serotonin-dopamine activity modulator, on phencyclidine-induced cognitive deficits in mice: a role for serotonin 5-HT<sub>1A</sub> receptors. *Pharmacol. Biochem. Behav.* 124, 245–249.
- Zanos, P., Moaddel, R., Morris, P.J., Georgiou, P., Fischell, J., Elmer, G.I., Alkondon, M., Yuan, P., Pribut, H.J., Singh, N.S., Dossou, K.S., Fang, Y., Huang, X.P., Mayo, C.L., Wainer, I.W., Albuquerque, E.X., Thompson, S.M., Thomas, C.J., Zarate Jr., C.A., Gould, T.D., 2016. NMDAR inhibition-independent antidepressant actions of ketamine metabolites. *Nature* 533, 481–486.
- Zanos, P., Moaddel, R., Morris, P.J., Riggs, L.M., Highland, J.N., Georgiou, P., Pereira, E.F.R., Albuquerque, E.X., Thomas, C.J., Zarate Jr., C.A., Gould, T.D., 2018. Ketamine and ketamine metabolites pharmacology: insights into therapeutic mechanisms. *Pharmacol. Rev.* 70, 621–660.
- Zhang, K., Hashimoto, K., 2019. An update on ketamine and its two enantiomers as rapid-acting antidepressants. *Expert. Rev. Neurother.* 19, 83–92.
- Zhang, X.Y., Liang, J., Chen, D.C., Xiu, M.H., Yang, F.D., Kosten, T.A., Kosten, T.R., 2012. Low BDNF is associated with cognitive impairment in chronic patients with schizophrenia. *Psychopharmacology* 222, 277–284.
- Zhang, J.C., Li, S.X., Hashimoto, K., 2014. R (–)-ketamine shows greater potency and longer lasting antidepressant effects than S (+)-ketamine. *Pharmacol. Biochem. Behav.* 116, 137–141.
- Zhang, J.C., Yao, W., Dong, C., Yang, C., Ren, Q., Ma, M., Han, M., Hashimoto, K., 2015. Comparison of ketamine, 7, 8-dihydroxyflavone, and ANA-12 antidepressant effects in the social defeat stress model of depression. *Psychopharmacology* 232, 4325–4335.
- Zhang, Y., Fang, X., Fan, W., Tang, W., Cai, J., Song, L., Zhang, C., 2018. Brain-derived neurotrophic factor as a biomarker for cognitive recovery in acute schizophrenia: 12-week results from a prospective longitudinal study. *Psychopharmacology* 235, 1191–1198.
- Zhu, W., Ding, Z., Zhang, Y., Shi, J., Hashimoto, K., Lu, L., 2016. Risks associated with misuse of ketamine as a rapid-acting antidepressant. *Neurosci. Bull.* 32, 557–564.